DR-1173

MASTER

FAST
BURST
REACTORS

DISCLAIMER

DISCLAIMER

Portions of this document may be illegible in electronic image products. Images are produced from the best available original document.

FAST

BURST

REACTORS

Proceedings of the National Topical Meeting
on Fast Burst Reactors held at
The University of New Mexico, Albuquerque,
January 28– 30, 1969

Sponsored by
The University of New Mexico
American Nuclear Society

Technical Coordinators

Robert L. Long
Paul D. O'Brien

December 1969

This document is
PUBLICLY RELEASABLE

Hugh Kinser

Authorizing Official
11/2 8/06

U. S. ATOMIC ENERGY COMMISSION Division of Technical Information

DISTRIBUTION OF THIS DOCUMENT IS UNLIMITED

PREFACE

In the past several years, significant advances have been made in the field of fast burst and repetitively pulsed reactor design and analysis. Several new reactors have been designed, built, and tested, including the Army Pulse Radiation Facility Reactor at Aberdeen Proving Ground, Sandia Pulsed Reactor II in Albuquerque, Godiva IV at Los Alamos, VIPER in the United Kingdom, and the SORA test assembly at Oak Ridge. During this time Sandia Corporation sponsored two informal meetings, the last of which was a one-day meeting in the fall of 1965. These meetings provided an opportunity for the attendees to discuss the then-current developments in fast burst reactor technology. Much of the information presented at the informal meetings was unpublished, and, as developments continued, the need for a well-documented record of the many years' experience with burst reactors became evident. We believe that this volume provides such a record.

The papers herein were presented at the National Topical Meeting on Fast Burst Reactors held at the University of New Mexico, Albuquerque, Jan. 28–30, 1969. The meeting was sponsored by the Nuclear Engineering Department of the University of New Mexico, the Trinity Section of the American Nuclear Society and the Reactor Physics Division of the American Nuclear Society. About 175 persons attended the meeting, including speakers from the United States, the United Kingdom, the Soviet Union, the Federal Republic of Germany, and EURATOM. Also included in this volume are four papers from a Conference on the Use of Fast Burst Reactors in University Programs, held on Jan. 31, 1969, and sponsored by the Nuclear

iii

PREFACE

Engineering Department of the University of New Mexico, the Associated Western Universities, and the AEC Division of Nuclear Education and Training.

Although we hesitate to single out anyone from the fine list of speakers, the keynote address by Professor Otto Frisch, the "father of pulsed reactors," and the paper by Professor Di Blokhintsev of the USSR were highlights that added greatly to the international flavor and enthusiastic exchange of ideas which characterized the meeting.

It is evident in reading the papers that there are still many interesting and challenging problems remaining to be solved. The possibilities for higher yields from future burst reactors and the many interesting applications of repetitively pulsed reactors should stimulate a continuing interest in this field.

We want to thank the authors and session chairmen for their contributions. We are also grateful for the efforts of the organizing committee in planning, arranging, and scheduling the meeting. Finally, a word of special appreciation must go to Mrs. Glenda Epting of the AEC Division of Technical Information Extension, Oak Ridge, for all her effort in preparing this volume for publication.

<div style="text-align: right">

ROBERT L. LONG
University of New Mexico

PAUL D. O'BRIEN
Sandia Corporation

</div>

Albuquerque, New Mexico
October 1969

ORGANIZING COMMITTEE

General Chairman: G. R. Keepin
Technical Program Cochairmen: R. L. Long and P. D. O'Brien
Administration Chairman: D. R. Smith
Arrangements Chairman: G. A. Whan
Finance Chairman: W. L. Everett
Registration Chairman: D. P. Wood
Tours Chairman: R. M. Jefferson

CONTENTS

CONTENTS

Session 3   Repetitively Pulsed Reactors
            Chairman J. A. Larrimore

CONTENTS

vii

CONTENTS

CONTENTS

THE DRAGON EXPERIMENT:
Keynote Address

PROFESSOR OTTO R. FRISCH
Cavendish Laboratory, University of Cambridge, Cambridge, England

Just about 8 months ago my wife brought me a letter. I had overslept and was still rather sleepy, and I stared at the letter from the American Nuclear Society, National Topical Meeting, Fast Burst Reactors. And I said, "Do the Americans run a topical meeting on a nationwide scale because their reactors burst so fast?" After that I realized that I was being honored as the father, or I feel more like the grandfather, of pulsed reactors, having arranged the experiment which for the first time established a short-lasting harmless fast-fission reaction that did not depend on delayed neutrons.

A group of no less than 17 people worked on this first controlled fission experiment known as the Dragon experiment, and I want to tell you how it came about.

The purpose of Los Alamos was to assemble part of the scientists who were needed to develop an atomic bomb. In particular, we mea-sured the cross sections, time constants, and so on, which would make it possible to design a bomb with a reasonable degree of efficiency and safety. One of the most difficult things was to determine that the fast reaction would really work as fast as the theory predicted. Nuclear theory, of course, said that once a neutron hits a uranium nucleus, fission follows almost instantaneously, if it follows at all. But electronic methods at that time were not really fast enough to decide whether it happens with the sort of subnanosecond speed which was theoretically foreseen and needed if the bomb was to be an effective explosive.

So a number of ingenious experiments were devised to test the speed of the fission reaction, and the limit was pushed fairly well toward the point where we wanted it. But even so, I for one thought it would be very

nice to go one step nearer to a real atomic explosion. It is a bit like the curiosity of the explorer who has climbed a volcano and wants to take one step nearer to look down into the crater but not fall in! That chance came when we learned that around the beginning of 1945 some amounts of separated ^{235}U were to arrive. These shipments were meant mainly for us to carry out critical experiments to check the calculations of the theoreticians. The theoreticians, of course, had taken all the cross-section measurements—fission cross sections, elastic, inelastic, everything that we could produce for them—and from these, by complicated integrations, had worked out the critical size. However, experimental confirmation was desirable.

It was clear that we would not be able to test with a critical assembly of metallic ^{235}U or metallic plutonium because once such a quantity had been produced the military would want to use it immediately. Instead, the first amount of ^{235}U that came out of the mass separators was made into hydride, UH^3, and combined with a plastic binder into bricks of the approximate composition UH^{10}. You may ask why use that material; it would never make a useful bomb. That is quite true; but it enabled us to carry out critical measurements and compare them with calculations the theoreticians had performed for the same material. This comparison gave the theoreticians at least an idea about how reliable their calculations were and by how much and in which direction they might have to be corrected.

A large number of critical measurements were made, indeed, and the theoreticians were very pleased to have this corroboration of their calculations. In addition, I felt that here was a chance of looking a bit closer at the occurrence of a fast reaction, a reaction not limited by thermal neutrons, and I made the proposal that we should make an assembly with a hole in the middle, and that the missing portion should then be allowed to drop through the assembly under such conditions that for a few milliseconds the whole assembly would be critical with respect to prompt neutrons. I did a few simple calculations to be sure that this would be feasible, then sent this proposal to the coordinating council. Of course, I was not present when the proposal was discussed, but it was accepted; it was said that Enrico Fermi nodded his head in a pleased manner and said this was a nice experiment that we ought to try, and I was told that Dick Feinman, who was present, started to chuckle and to say that this is just like tickling the tail of a sleeping dragon. That is how the experiment was named.

When the ^{235}U arrived, we built the equipment for the experiment, and Fig. 1 roughly shows what this equipment looked like. It looks, crudely speaking, like an oil derrick, but it was only something like 6 m high. Near the bottom the uranium assembly was set upon a steel table. The material was available in the form of little bricks; I believe
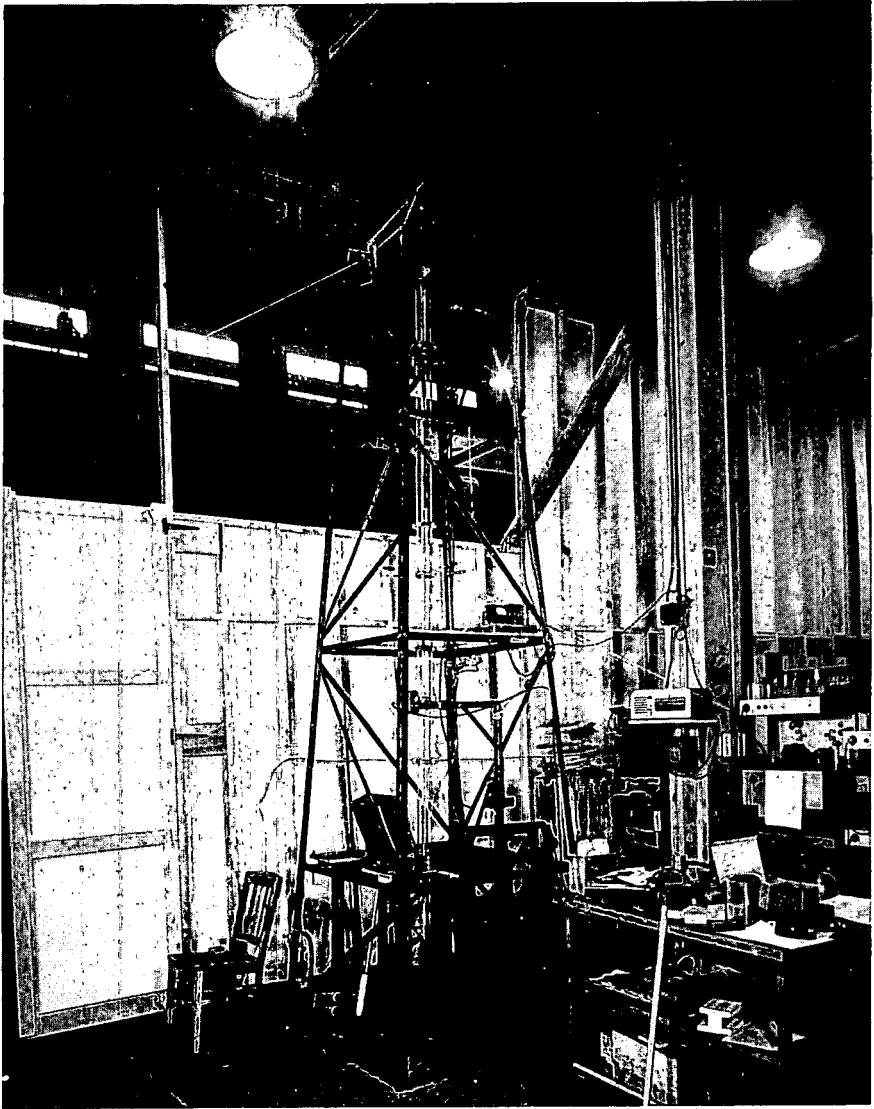
Fig. 1 — The Dragon reactor.

they were 1 in. by ½ in. by ½ in. and very accurately made. (It was a joy to build little skyscrapers out of uranium hydride and other materials like that!) A slightly askew box that contained part of the assembly was mounted on a hydraulic pusher rod so it could be released and lowered—deliberately, rather slowly. The guides for the falling slug can also be seen.

Everybody, of course, asked me what if the slug gets stuck — you all blow up. We could not all be blown up. The material became only very slightly supercritical. It would have been a bomb of extremely low efficiency, and probably we would have been quite well protected by our 5-ft concrete wall, although it would have been wise to clear out fast if the slug had stuck.

The top of the derrick contained a fairly elaborate device for holding the slug until everything was ready for the drop because we were aware that a danger much greater than the slug's getting stuck was the danger of the slug's falling before the supercriticality had been correctly adjusted. We made quite sure that the slug could only be dropped after the operator had checked a certain number of things and was convinced that they were okay. In the end, of course, a great responsibility did fall on the operator.

The steel table (about a centimeter thick) was placed so that material could rest firmly against the fuel box, which in actual use would be pushed up until it would be leaning against the guides or almost touching them. The gadgets attached to the guides measured the speed of the slug. You may say there is no reason to measure the speed if by some bad chance extra friction stops or slows the slug. The purpose of the measuring, however, was to do a few dummy drops before beginning the day's work to make sure the slug was dropping according to Galileo's law. In fact it never did. It was always about 1% slower owing to friction. It did not fall freely in the guide; in fact, we deliberately leaned the whole tower a little to one side so that the slug was sliding down the guides rather than falling through them. This development was important because a very small sideways movement changed the multiplication constant and made a very big difference in the size of burst produced.

Much of the top of the assembly was crude and primitive. Parts were held together by ordinary mechanics clamps and there was a rope going up over several pulleys and holding an electromagnet that hauled up the slug. The electromagnet could not be switched off until after everything else was straightened out. I will not bore you with the safety precautions; they are completely out of date. What I really wanted to impress upon you is the rather primitive setup. This entire reactor was built in a matter of a few weeks, and all the experiments were performed during, I believe, three short periods in three weeks, each lasting only a few days. The reason we worked so fast was that the chemists were waiting for us to return the material so that together with further ^{235}U it could be turned into metal and this metal into bombs as soon as possible.

With the very first material that arrived, we made a number of drops to make sure the device worked, and the first pulses were ob-

tained just at this time of year 24 years ago. Then we replaced the
material with a somewhat bigger assembly and performed a number of
drops to test the theory, and they all came out as we expected. The
pulses were of the duration that we had approximately predicted from
nuclear data. Figure 2 shows the outcome obtained by having a boron
chamber close to the arrangement, which was connected to a cathode-
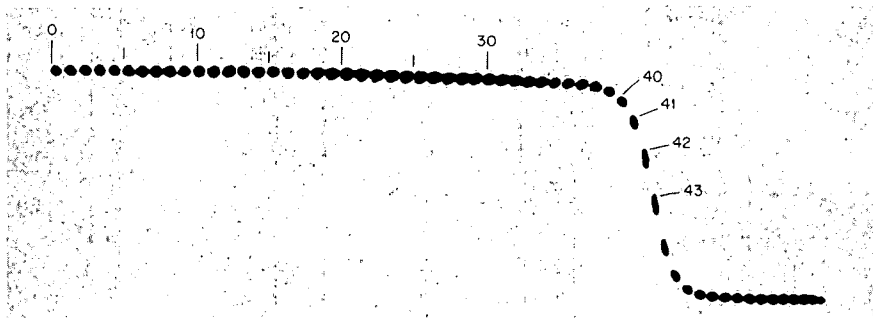
Fig. 2—Integrated-pulse reading.

ray oscilloscope, and simply integrated the amount of charge deposited.
The figure reads from left to right in units of 6 msec, the rate at which
the oscilloscope was pulsed. The charge suddenly begins to increase,
increase more rapidly, and then straighten out once again; this is the
integrated pulse. This result could be compared with the theory, and
the agreement was very good.

Well, so much for the Dragon. It was dismantled a few weeks after
it had been built, and the whole group dispersed. And there, as far as
I am concerned, the matter rests. I have never tried to build another
one although I have speculated about things like rotating wheels and so
on, which I now hear to my great pleasure our Russian colleagues have
realized.

We did perform a few Dragon-type experiments of the more modern
variety unintentionally and with tragic results. Two men who worked
on the Dragon experiment were killed within a few months after this
experiment. Harry Daghlian, working by himself one night, which was
breaking the rules, did not know how slippery the large blocks of
tungsten carbide reflecting material were. While trying to put on one
more block, he realized that the reaction was going up much too fast;
he tried to pull the block away again, but it slipped out of his hands.
What then happened can only be reconstructed by theory; no one else
was present. He saw a blue flash, and about 10 days later he died in
the hospital from radiation damage. He had received well over a fatal
dose. Probably what happened is that the material expanded thermally

and thereby switched itself off, but the amount of radiation it had given off in that short time was enough.

Later I left Los Alamos, and Louis Slotin took over the group working on critical assemblies. He told me that Fermi warned him, "You know that in this sort of work you have perhaps an even chance to survive your work here." Slotin was rather shaken about it. Even so, he did use something makeshift — some people say it was a pencil, some people say it was a screwdriver — to separate two lumps of the active material which he knew would give a fast reaction if that separating material was removed. The screwdriver slipped out, and he was killed.

So you see, some of the fundamental experiments which led to the present very lively developments in fast burst reactors were indeed started in those old days in Los Alamos in a makeshift building at the bottom of Omega Canyon. I have no idea what goes on there now, but I am hoping to go to Los Alamos in a few days' time and see for myself. Anyhow, I have at least told you something about the old days.

Fast Burst Reactor Analysis Techniques

Session 1

1-1 COMPARISON OF FAST PULSED REACTOR CALCULATIONS WITH EXPERIMENT

J. T. MIHALCZO
Union Carbide Corporation, Nuclear Division, Y-12 Plant, Oak Ridge, Tennessee

ABSTRACT

Various methods of solution of the Boltzmann transport equation have been used to predict the properties of fast burst reactors. This paper reviews these methods and their application to the calculation of some properties of some fast burst reactors and associated critical experiments. The calculations of criticality, prompt-neutron decay constant, neutron lifetime, fission-density distribution, and reactivity effects are compared with experiment.

Various methods of solution of the Boltzmann transport equation have been used to predict the properties of fast burst reactors. This paper reviews these methods and their application to the calculation of some properties of some fast burst reactors and associated critical experiments. Most of the fast burst reactors, except the IBR,[1] have used uranium or uranium – molybdenum alloy for fuel. This paper describes the calculations of an unreflected uranium sphere, Godiva I,[2] of some critical experiments with uranium – molybdenum alloy,[3] of the HPRR,[4] of the APRFR,[5] and of the mockup of the SORA reactor used in the critical experiments at Oak Ridge.[6] The uranium in all these experiments is enriched to approximately 93 wt.% in the ^{235}U isotope. The calculations of criticality, prompt-neutron decay constant, neutron lifetime, fission-density distribution, and reactivity effects are compared with experiment.

The most widely used method of calculation applicable to this type of reactor is the S_n transport theory method of Carlson.[7] Present versions of this method are limited to two space coordinates. The major difficulty therefore is the inability of this method to correctly represent the geometry of some fast burst reactors. Synthesis methods[8] can adequately treat the other space coordinate but as yet have

9

not been applied to these systems. The generality of the geometry routines used in the Monte Carlo method[9] permits calculations with the geometry treated exactly. This method has recently been used in the design of a fast pulsed reactor,[10] and it has also been a useful method of calculating the multiplication factor for many critical assemblies.[11] Both these methods are sufficiently good solutions of the Boltzmann equation to accurately predict most of the static properties of fast pulsed reactors. Diffusion theory has been used in some of the survey calculations for the design of the pulsed reactor VIPER,[12] but it is a poor approximation to the Boltzmann equation for most of these systems and therefore will not be discussed further.

CRITICALITY

In support of the design of the Health Physics Research Reactor (HPRR), the first fast burst reactor of uranium–molybdenum alloy, some clean critical experiments with a 10-wt.% molybdenum alloy were performed. A solid alloy cylinder, an alloy annulus with an axial hole filled with stainless steel and left empty, and an alloy assembly with various conditions of reflection were studied. Results of these experiments and their comparison with calculation are given in Table 1. The calculations were performed with the computer codes TDC[7] and DDK,[13] which are two-dimensional S_n programs in (r,z) geometry. The DDK code differed from TDC in that it permits linearly anisotropic scattering in the laboratory. The S_8 approximation was used throughout with the 6- or 16-group uranium cross sections of Hansen and Roach,[14] except for molybdenum, whose cross sections are given by Connolly.[15] The uranium cross sections of this set satisfactorily computed the criticality of Godiva I. The TDC code with six neutron-energy groups was used to calculate the unreflected systems. The Plexiglas-reflected assemblies were calculated with DDK since they required the anisotropic scattering to handle the hydrogen in the reflectors. Sixteen energy groups were used. The calculated multiplication factor for the uranium–molybdenum experiments agrees very well with the experimental since the experiments are cylindrically symmetric and the geometry can be treated accurately by S_n methods.

Consider the geometry of the Army Pulse Radiation Facility Reactor (APRFR) shown in Fig. 1. The approximation to the geometry of this reactor used in S_6 transport theory calculations with the DOT code[16] is shown in Fig. 2. In this figure the glory hole filler, safety tube, safety cage, and coolant shroud are omitted since they were not used in the experiments at Oak Ridge. The calculated multiplication factor for the delayed critical experiment was 1.003, in good agreement

Table 1

DIMENSIONS AND MULTIPLICATION FACTORS OF URANIUM-MOLYBDENUM ALLOY ASSEMBLIES

Reflector conditions*	Height of radial increment of uranium, in.			Mass, kg of ^{235}U	Center region material	Reactivity, ¢	Multiplication factor	
	0-1	1-1.75	1.72-4				Measured	Calculated
None	5.71	5.78	5.78	68.265		-3.1	1.000	0.998
None		7.75	7.75	85.715	Void	3.8	1.000	0.997
None		7.38	7.37	81.558	Stainless steel	-14.8	0.999	0.996
1 in. Plexiglas		6.78	6.78	67.361	Void	-6.1	1.000	1.005
		5.50	5.50	53.185	Plexiglas	28.0	1.002	0.999

*Reflector completely covered top and sides.

REGULATING ROD

SAFETY ANNULUS HANGER

CORE SUPPORT RING

PULSE ROD

CORE SUPPORT FINGER

AIR SUPPLY LINE (THREE PROVIDED)

MASS ADJUSTMENT ROD

THERMOCOUPLE

CORE BOLT

SAFETY ANNULUS

COOLANT SHROUD

GLORY HOLE FILLER

SAFETY CAGE

SAFETY TUBE
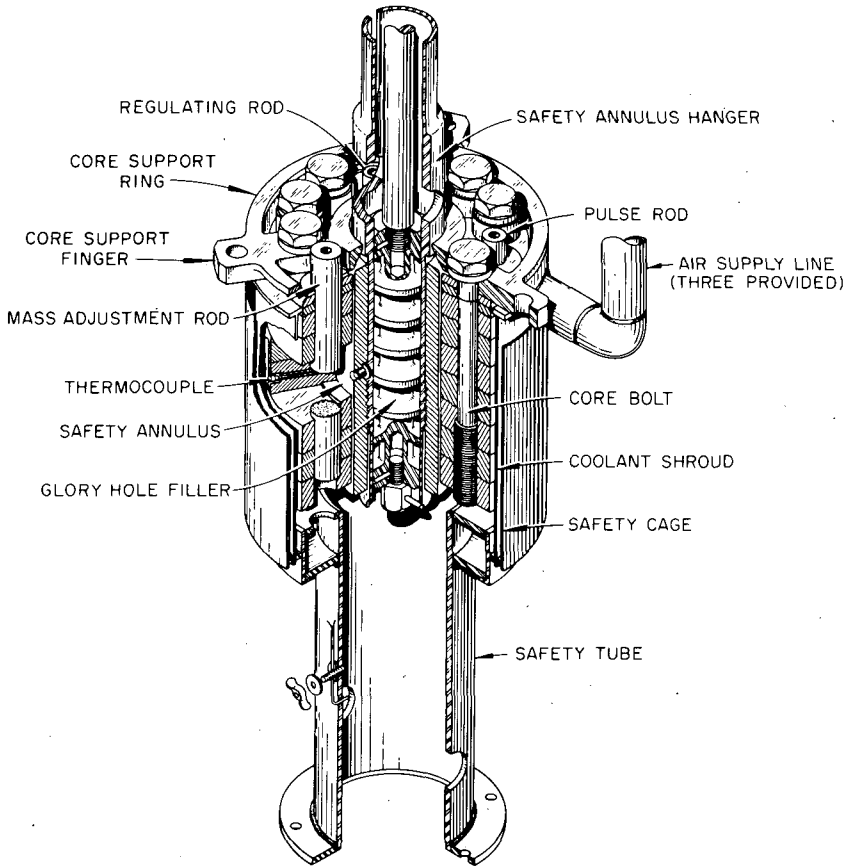
Fig. 1 — Cutaway of APRFR.

with the experimental. A cross section of a typical assembly used in the critical experiments for the SORA reactor at Oak Ridge is shown in Fig. 3. The neutron multiplication factor of the assembly with all reflector components of iron has been calculated by the 05R Monte Carlo neutron transport code.[9] The generality of the geometry routine in this code allowed an exact specification of the geometry of the SORA assembly. Each of the approximately 85 uranium fuel rods in the core was treated as a separate region. The uranium cross sections were those that have been adjusted to satisfactorily predict the properties of unmoderated and unreflected uranium metal assemblies.[17] The iron cross sections were those that Alter[18] used to successfully predict the neutron age in iron−water mixtures. The calculated multiplication factor was within 1% of the experimental value with a standard deviation of 1%.

Recent Monte Carlo calculation of a uranium sphere using the recommended ENDF-B[19] cross sections for ^{233}U and ^{238}U, as the cross

REGION   REMARKS CONCERNING REGION
NO.

1   STAINLESS STEEL
2   U – Mo ALLOY
3   U – Mo ALLOY DENSITY WAS REDUCED
     TO ACCOUNT FOR THE VOID AROUND
     THE BOLTS AND RODS. VOID DISTRI-
     BUTED UNIFORMLY IN THIS REGION.
4   REDUCED-DENSITY STAINLESS STEEL
     REPRESENTING THE CORE SUPPORT RING
5   REDUCED DENSITY U – Mo REPRESENTING
     THE PROTRUSION OF THE BOLT SHANK
     OUT OF THE TOP OF THE CORE
6   REDUCED-DENSITY U – Mo REPRESENTING
     THE BOLT HEADS
7   VOID
8   HOMOGENEOUS MIXTURE WITH VOLUME
     FRACTION OF 0.4 FOR U – Mo, 0.4 FOR
     STAINLESS STEEL, 0.2 VOID
9   IRON REPRESENTING THE DISPLACEMENT
     GAUGE MOUNTING PLATE

Fig. 2—Sketch of the APRFR used in transport theory calculations.

sections are received from the National Neutron Cross Section Center at Brookhaven National Laboratory without any reduction to group average cross sections, predicted a multiplication factor 2.3% above the experimental. A set of cross sections used for the calculation of un-moderated and unreflected assemblies at Oak Ridge, in which the ^{235}U

BORON CARBIDE

BERYLLIUM

IRON OF FIXED REFLECTOR

CORE

POLYETHYLENE

CONTROL RODS INDICATED
BY NOS. 1, 2a, 2b, 3a, 3b, AND 5

MOVABLE
REFLECTOR

DIMENSIONS IN CM
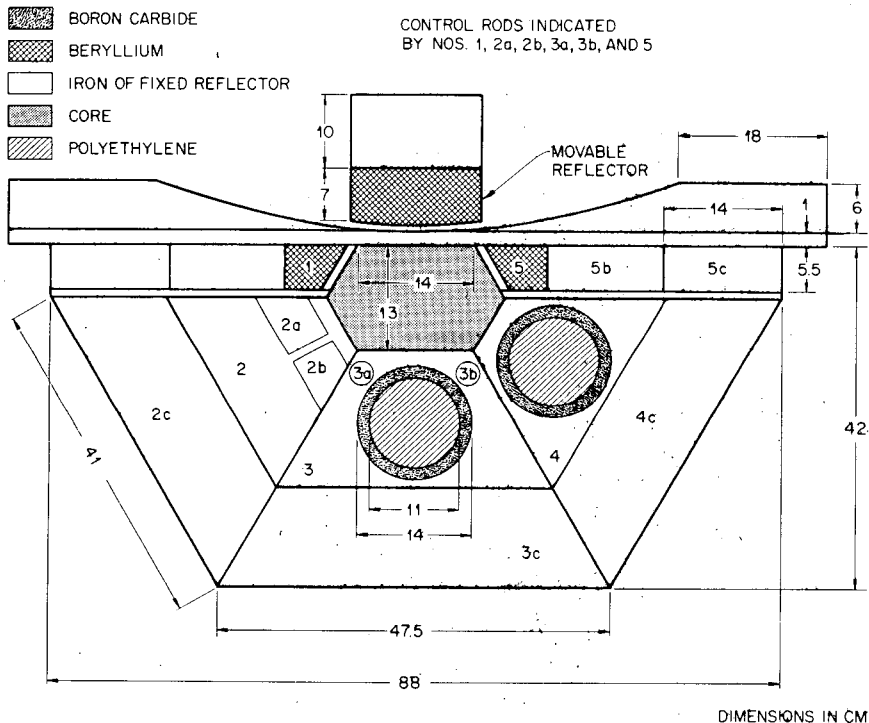
Fig. 3— Cross section of a typical SORA critical assembly.

fission cross section is lower than that recommended in the ENDF-B file, predicted a multiplication factor of 0.995. The statistical error in both these calculations is ~0.3%. The basic difference between these cross sections is shown in Fig. 4 where the fission cross sections are plotted as a function of energy. Table 2 lists these adjusted fission cross sections as a function of energy.

Both the S_n transport theory and the Monte Carlo method are adequate for predicting the criticality of fast burst reactors. If the geometry is extremely complicated, the Monte Carlo method can be used as long as a desired accuracy of ~0.5% in the multiplication factor is adequate. The use of the recommended fission cross sections of ^{235}U results in an overestimate of the multiplication factor, which suggests that the recommended values of the fission cross sections may be too high.

Fission-Density Distribution

Fission-density distributions measured in several assemblies have been compared with the results of transport theory calculations. This
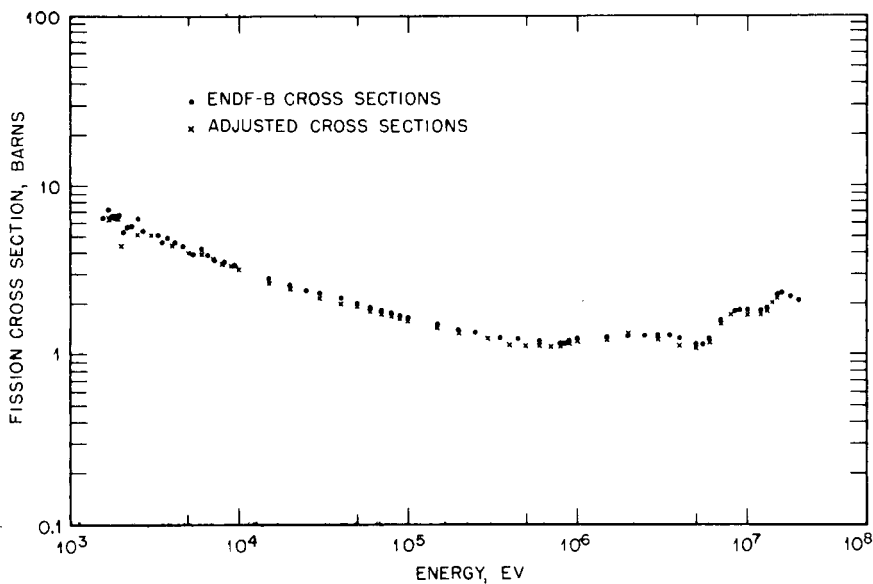
Fig. 4 — Fission cross section of ^{235}U as a function of energy.

Table 2

ADJUSTED ^{235}U FISSION CROSS SECTIONS

Energy, Mev	σ_f, barns	Energy, Mev	σ_f, barns
15.0	2.19	1.0	1.21
14.0	2.09	0.7	1.17
13.0	1.85	0.8	1.13
12.0	1.76	0.7	1.12
11.0	1.76	0.6	1.12
10.0	1.77	0.5	1.13
9.0	1.80	0.4	1.16
8.0	1.72	0.3	1.23
7.0	1.53	0.2	1.35
6.5	1.33	0.15	1.43
6.0	1.17	0.10	1.60
5.0	1.10	0.08	1.70
4.0	1.15	0.06	1.85
3.0	1.24	0.04	2.00
2.0	1.32	0.02	2.42
1.5	1.25	0.01	3.25

comparison is made in Fig. 5 for a solid uranium—molybdenum cylinder and in Fig. 6 for a uranium—molybdenum annulus. The axial fission-density distribution in the glory hole of the HPRR is compared with experimental results in Fig. 7, and comparisons of measurements and calculations for the APRFR are given in Figs. 8 and 9. The agreement between experiment and theory is good except for the axial distribution along the bolt surface of the APRFR. This disagreement is due to the inability of the S_n codes to correctly represent the
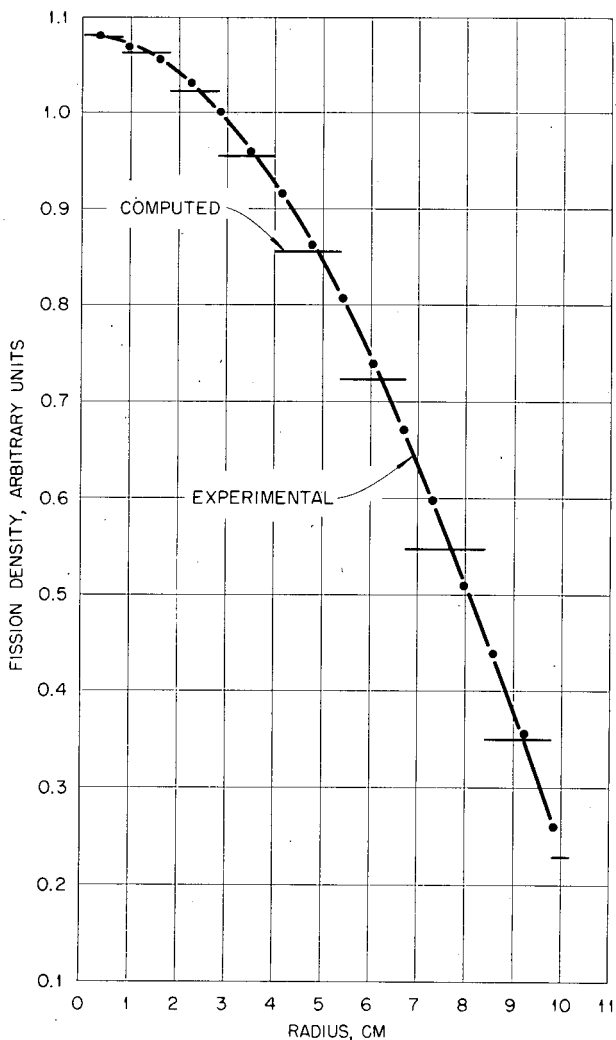
Fig. 5—Midplane fission density as a function of radius for a U—Mo cylinder.

geometry of the bolt in the bolt-head region. Thus fission-density distributions can be calculated quite accurately by transport theory provided the reactor geometry can be described within the two-dimensional limitations of the transport theory codes. The Monte Carlo method has been used to calculate fission-density distributions[20] but at present is not capable of calculating them in sufficient detail in reasonable computing time to be of very practical use in the design of fast burst reactors.
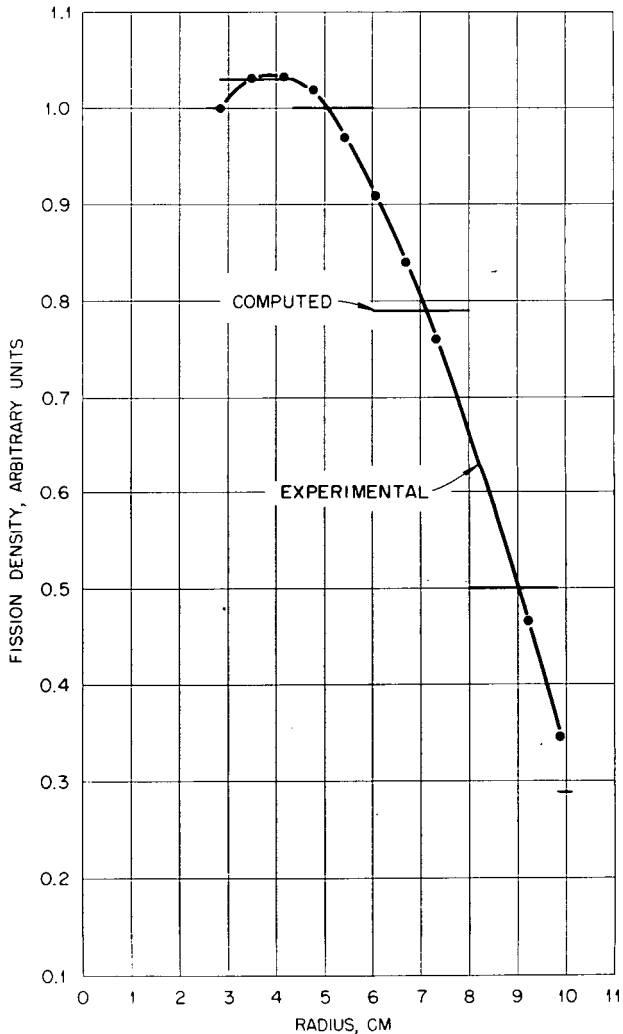
Fig. 6 — *Midplane fission density as a function of radius for a U—Mo annulus.*
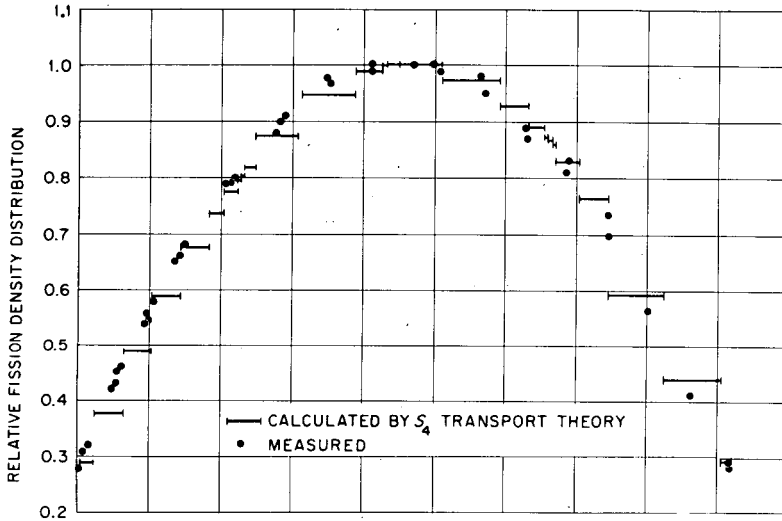
Fig. 7—Axial fission-density distribution in the irradiation hole of the HPRR.
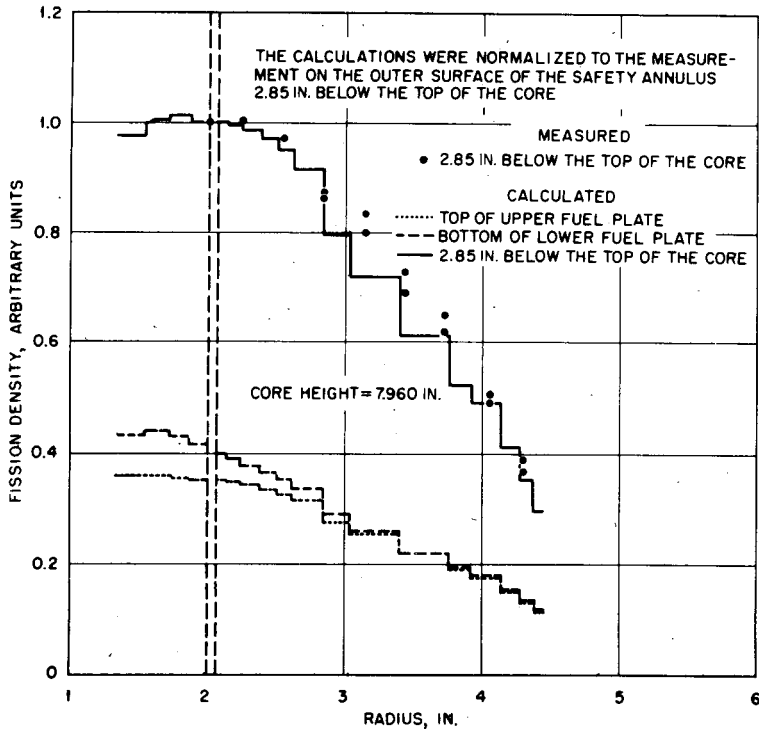
Fig. 8—Radial fission-density distribution in the APRFR.

Reactivity Effects

Both transport theory and the Monte Carlo method have been used successfully for calculating reactivity effects in fast burst reactors. For very small changes in the reactor, perturbation theory is a very accurate means of calculating the reactivity effect, as shown by Hansen and Maier.[21] Their calculations of the reactivity coefficients of ^{235}U, ^{238}U, H, and D as a function of radius in Godiva I were all within ~5% of the experimental values. In the critical experiments with uranium — molybdenum alloy, the change in reactivity as a result of the introduction of small voids was measured; the results are compared in Table 3 with those of first-order perturbation theory using forward and adjoint angular fluxes obtained from the transport theory calculations. The agreement between calculation and experiment is good.
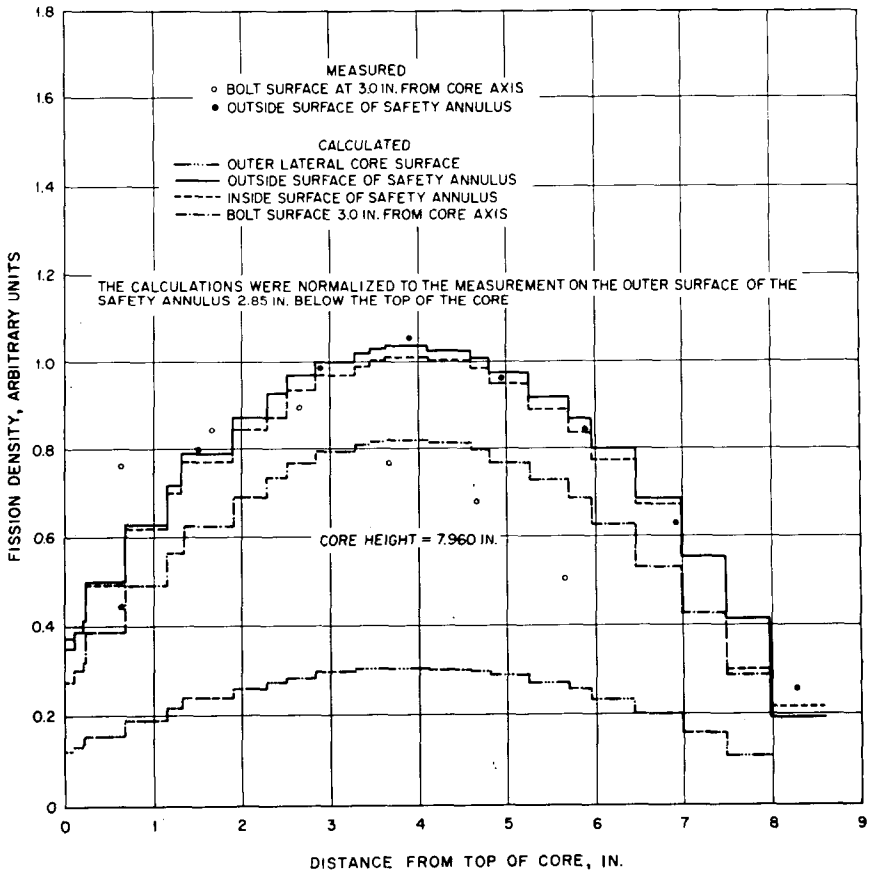
Fig. 9 — *Axial fission-density distribution in the APRFR.*

The ability of transport theory calculation to correctly predict the fission-density distribution and the accuracy of perturbation theory in predicting small reactivity effects provide a means of calculating the dynamic temperature coefficient for these reactors in the non-inertial case if the thermal-expansion properties of the fuel are known.

For large reactivity effects, such as the removal of the safety annulus of the APRFR or the rotating reflector of the SORA assembly, other methods must be used. Since the safety annulus of the APRFR is cylindrically symmetric, the reactivity effects of its removal can be calculated by the transport theory codes. The calculated multiplication factor with the annulus lowered 5 in. and 11.5 in. was 0.927 and 0.873, respectively. With a value of 0.0068 for the effective delayed-neutron fraction, these multiplication factors correspond to reactivities

Table 3

VOID COEFFICIENT MEASUREMENTS IN
UNREFLECTED URANIUM – MOLYBDENUM
CYLINDERS 20.32 CM IN DIAMETER

| Radial position of void,* cm | Void coefficient, $\rlap{c}/$ /cm³† | |
	Measured	Computed (perturbation theory)
Midplane of U–Mo annulus with steel in center		
2.86	4.62	4.58
3.49	4.72	4.76
4.13	4.80	
4.76	4.78	
5.40	4.43	4.57
6.61	3.75	3.57
7.94	3.26	
9.21	2.27	2.28
9.84	2.03	
13.33 cm above the base of the U–Mo annulus with steel in the center		
2.86	3.71	3.60
3.49	3.86	3.70
Midplane of U–Mo cylinder		
0.00	7.40	7.90
Midplane of U–Mo annulus		
2.86	4.15	4.20
4.13	4.54	4.55
9.84	1.81	1.65

*Center of void located at position given. Voids were cylindrical holes 0.927 cm in diameter and 0.635 cm long.
†Magnitude of the reduction in reactivity as a result of addition of the void.

of $11.6 and $21.4. The values of reactivity obtained from measurements of the prompt-neutron decay constant by the pulsed-neutron technique for the two conditions of safety-annulus withdrawal are $11.9 and $18.8, in fair agreement with the calculations.

The Monte Carlo method, in which a correlated sampling technique is used, has successfully predicted the reactivity effects measured in the critical experiments for SORA.[23] The neutrons are marked after they enter the perturbed region; secondary neutrons, which are produced by the marked neutrons, are accumulated separately. The sampling values obtained from these marked neutrons allow the estimation of differential quantities like Δk. Comparison of the results of the method with the experiments is given in Table 4. The agreement with experiment is quite good, and the statistical accuracy of this calculation is adequate for most reactor design purposes.

Table 4

CALCULATION OF THE REACTIVITY OF COMPONENTS OF
THE SORA CRITICAL EXPERIMENT BY A CORRELATED
SAMPLING TECHNIQUE

Material		Reactivity,* $	
		Measured	Calculated
Moving reflector			
Beryllium	11.0 cm wide	6.1	6.1 ± 0.3
	16.2 cm wide	12.0	12.0 ± 0.5
Iron	11.0 cm wide	3.7	3.9 ± 0.2
	21.0 cm wide	6.5	6.2 ± 0.3
Safety rod			
Beryllium		1.81	1.90 ± 0.10
Tungsten		1.54	1.66 ± 0.10
Central fuel rod		1.75	1.74 ● 0.05

*Magnitude of the reduction in reactivity as a result of removal of the material.

Prompt-Neutron Decay Constant, Delayed-Neutron Fraction, and Prompt-Neutron Lifetime

The long-standing discrepancy[24] between the calculated prompt-neutron lifetime and decay constants and the values obtained from measurements is the result of errors either in the measurements or in the calculations. Measurements at delayed criticality have been made by Orndoff[25] with Godiva I and have been made at Oak Ridge[26] with a sphere and with five cylinders of diameters varying from 7 to 15 in. The measured prompt-neutron decay constants for all the solid uranium (~93 wt.% ^{235}U) metal assemblies are between 1.063 and 1.10 μsec^{-1}. The error is about 0.005 to 0.010 μsec^{-1} for measurements

at Oak Ridge and about 0.02 μsec^{-1} for the early measurements at Los Alamos. The prompt-neutron lifetime can be obtained from these measurements since at delayed criticality the prompt-neutron decay constant equals the effective delayed-neutron fraction divided by the prompt-neutron lifetime.

The effective delayed-neutron fraction for the ith delayed-neutron group is defined by Gross and Marable[27] as

$$\beta_{i(\text{eff})} = \beta_i(\varphi_s^+, \ f_i F \varphi_d)/(\varphi_s^+ f_s F \varphi_d)$$

where the static adjoint and the dynamic forward angular fluxes are obtained from transport theory calculation. The total effective delayed-neutron fraction is the sum over the delayed-neutron groups. A calculated value within about 0.1% of this for these systems can be obtained from the difference in the multiplication factor calculated first with the normal fission-neutron spectrum and then with the spectrum modified by subtracting the delayed neutrons out of the calculation. This modification included subtracting delayed neutrons from fast fission in ^{238}U. The fraction of fissions arising in ^{238}U was obtained from the transport calculations. For calculating β_{eff} half the fissions in ^{234}U and ^{236}U were assumed to be ^{235}U fissions, and the other half were assumed to be ^{238}U fissions. The prompt-neutron lifetime obtained from the measured decay constants for the cylinder and the calculated values of β_{eff} was between 6.21 and 6.28 nsec with an average value of 6.25 ± 0.03 nsec. The value of the neutron lifetime obtained in the same way from the measurements of Godiva I is 6.2 ± 0.1 nsec. The very close agreement between the measurements at two different laboratories and their interpretation, which shows that the neutron lifetime is independent of geometry as long as the assemblies do not contain voids, suggests that the source of the discrepancy may be errors in the calculation of the decay constant and neutron lifetime.

Four possible sources of error in the calculations are the value of the delayed-neutron fraction for ^{235}U, the cross sections, the fission spectrum at low energy, and the energy distribution of neutrons emerging from inelastic scattering by ^{235}U. The value of β for ^{235}U is well known and is consistent with the interpretation of central reactivity coefficient measurements for ^{235}U in Godiva I. The change in the cross sections required to resolve the discrepancy would be large.[28] More neutrons at lower energy in the fission spectrum would lead to a larger neutron lifetime. The fission spectrum has not been measured at low energy, and the energy distribution of the neutrons emitted in inelastic scattering by ^{235}U has not been measured in any detail. Two difficulties in the latter measurement are the number of levels involved and the separation of these neutrons from the fission neutrons.

For this paper I have assumed that the inelastically scattered neutron spectrum is the difficulty and therefore have adjusted the energy distribution of neutrons from inelastic scattering until the neutron generation time calculated by the Monte Carlo method is equal to ~6.25 nsec. This adjustment results in a nuclear temperature for the evaporation spectrum of the neutrons emitted in inelastic scattering with ^{235}U of ~0.2 Mev for an incident-neutron energy of 1 Mev. The energy distribution of the neutrons before collision in the central region of a uranium sphere using the adjusted set of cross sections is softer than the distribution calculated with ENDF-B cross section as shown in Fig. 10. The energy distribution of the neutrons leaking out
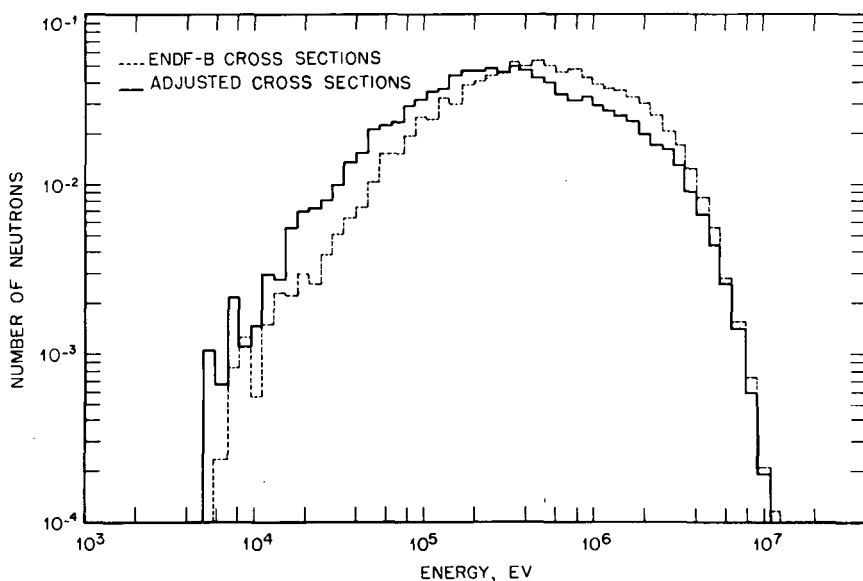
Fig. 10—Neutron collision spectrum in the center of a uranium-metal sphere.

of the sphere surface is not as dependent on the treatment of inelastic scattering. The neutron spectrum from the Monte Carlo calculations and the adjusted cross sections were used to calculate a set of six-group cross sections, given in Table 5, for use in S_n transport theory calculations. The transfer cross sections are compared with the Hansen—Roach values. The downscattering cross sections are slightly larger than those of Hansen. The results of transport theory calculation of the prompt-neutron decay constant, using this set of six-group cross sections derived from the adjusted set and the neutron energy distribution in the uranium sphere, are given in Table 6 for some uranium assemblies[29] and the APRFR. The calculated values of this decay constant agree very

Table 5

SIX-GROUP MICROSCOPIC TRANSFER CROSS SECTIONS FOR ^{235}U

	Group 1	Group 2	Group 3	Group 4	Group 5	Group 6
			Averaged by Monte Carlo			
$\sigma g \rightarrow g$	1.04	1.67	2.21	3.30	6.57	10.13
$\sigma g - 1 \rightarrow g$	0	0.26	0.25	0.51	0.69	0.22
$\sigma g - 2 \rightarrow g$	0	0	0.36	0.72	0.72	0.19
$\sigma g - 3 \rightarrow g$	0	0	0	0.76	0.71	0.13
$\sigma g - 4 \rightarrow g$	0	0	0	0	0.51	0.11
$\sigma g - 5 \rightarrow g$	0	0	0	0	0	0.06
			Hansen—Roach set			
$\sigma g \rightarrow g$	1.20	1.77	2.30	3.42	6.16	9.06
$\sigma g - 1 \rightarrow g$	0	0.27	0.24	0.55	0.35	0.08
$\sigma g - 2 \rightarrow g$	0	0	0.37	0.67	0.40	0.08
$\sigma g - 3 \rightarrow g$	0	0	0	0.65	0.45	0.07
$\sigma g - 4 \rightarrow g$	0	0	0	0	0.44	0.07
$\sigma g - 5 \rightarrow g$	0	0	0	0	0	0.06

Table 6

COMPARISON OF MEASURED AND CALCULATED PROMPT-
NEUTRON DECAY CONSTANT

	Prompt-neutron decay constant, μsec^{-1}	
System description	Measured	Calculated
Uranium sphere	1.10	1.10
Uranium cylinders		
7.0 in. diam.	1.082	1.075
9.0 in. diam.	1.088	1.093
11.0 in. diam.	1.076	1.062
13.0 in. diam.	1.071	1.073
15.0 in. diam.	1.063	1.064
APRFR		
Safety annulus		
inserted	0.675	0.66
Safety annulus		
out 5.0 in.*	7.97	7.52
Safety annulus		
out 11.5 in.*	11.87	12.15

*These systems were subcritical. All others in this table are
at delayed criticality.

well with the measured values. Prompt-neutron decay constants for fast pulse reactors can also be calculated by Monte Carlo methods.

CONCLUSIONS

In conclusion, the present transport theory and Monte Carlo methods are adequate for predicting the criticality, fission-density distribution, temperature coefficients, reactivity effects, and prompt-neutron decay constants or lifetimes of fast pulse reactors. The calculation of the criticality of these systems indicates that the ^{235}U fission cross sections are too high. The energy spectrum of neutrons inelastically scattered by ^{235}U is not known well enough for the accurate prediction of the prompt-neutron decay constants. In this case it is not the inadequacy of the methods of calculation but rather it is the deficiency in the basic nuclear data used as input to the calculations that prevents the accurate calculation of criticality and of quantities that depend on the energy spectrum, such as the prompt-neutron lifetime.

REFERENCES

1. G. E. Blokhin et al., Fast-Neutron Pulse Reactor, *Atom. Energ. (USSR)*, 10: 430 (1961).
2. R. E. Peterson and G. A. Newby, An Unreflected U-235 Critical Assembly, *Nucl. Sci. Eng.*, 1: 112 (1956).
3. W. E. Kinney and J. T. Mihalczo, ORNL Fast Burst Reactor: Critical Experiments and Calculations, Report ORNL CF-61-8-71, Oak Ridge National Laboratory, 1961.
4. J. T. Mihalczo, Super Prompt-Critical Behavior of an Unmoderated, Unreflected Uranium—Molybdenum Alloy Reactor, *Nucl. Sci. Eng.*, 16: 291-298 (1963).
5. J. T. Mihalczo, Static and Dynamic Measurements with the Army Pulse Radiation Facility Reactor, USAEC Report ORNL-TM-2330, Oak Ridge National Laboratory, June 1969.
6. G. Kistner and J. T. Mihalczo, Critical Experiments for the Repetitively Pulsed Reactor SORA, *Nucl. Sci. Eng.*, 35: 27-44 (1969).
7. B. G. Carlson, C. E. Lee, and J. Worlton, The DSN and TDC Neutron Transport Codes, USAEC Report LAMS-2346, Los Alamos Scientific Laboratory, 1960.
8. J. E. Meyer, Synthesis of Three-dimensional Power Shapes—A Flux-weighting Synthesis Technique, in *Proceedings of the Second United Nations International Conference on the Peaceful Uses of Atomic Energy, Geneva, 1958*, Vol. 11, p. 519, United Nations, New York, *1958;* and S. Kaplan, Some New Methods of Flux Synthesis, *Nucl. Sci. Eng.*, 13: 22-31 (1962).
9. D. C. Irving, R. M. Freestone, Jr., and F. B. K. Kam, 05R, A General-Purpose Monte Carlo Neutron Transport Code, USAEC Report ORNL-3622, Oak Ridge National Laboratory, 1965; and G. E. Whitesides and N. F. Cross, KENO-A, Multigroup Monte Carlo Criticality Program, Report CTC 5, Computer Technology Center, in preparation; T. C. Longworth, The Gem 4 Code, British Report AHSB(S) R 146, 1968.
10. H. Rief, H. Kschwendt, and R. Jaarsma, Reactivity Calculations for a Periodically Pulsed Fast Reactor by the TIMOC Code, *Proceedings of the*

International Conference on Research Reactor Utilization and Reactor Mathematics, Mexico City, Mexico, May 2−4, 1967, American Nuclear Society, Hinsdale, Ill., in preparation.

11. J. T. Mihalczo, Monte Carlo Calculations of Thick Graphite-Reflected Uranium Metal Critical Assemblies, *Trans. Amer. Nucl. Soc.,* 11: 385 (1968).

12. A. Brickstock and A. R. Davies, SWAN—A Multi-Group One-Dimension Diffusion Code for the IBM-7030, British Report AWRE 0-99/65, 1966.

13. W. J. Worlton and B. G. Carlson, Los Alamos Scientific Laboratory, private communication to E. Whitesides, Computing Technology Center, Oak Ridge, 1962.

14. G. E. Hansen and W. H. Roach, Six and Sixteen Group Cross Sections for Fast and Intermediate Critical Assemblies, USAEC Report LAMS-2543, Los Alamos Scientific Laboratory, 1961.

15. Lucie D. Connolly, Los Alamos Group-Averaged Cross Sections, USAEC Report LAMS-2941, Los Alamos Scientific Laboratory, 1963.

16. F. R. Mynatt, A Users Manual for DOT, A Two-Dimensional Discrete Ordinates Transport Code with Anisotropic Scattering, USAEC Report K-1694, Oak Ridge Computing Technology Center, 1968.

17. R. Q. Wright, ENDF-B Data File, Element No. 1098, 1099, Oak Ridge National Laboratory.

18. H. Alter, The Age of Fission Neutrons to Indium Resonance Energy in Iron-Water Mixtures. 2. Theory, *J. Nucl. Energy, Parts A and B,* 20: 37 (1966).

19. ENDF-B Tape No. 116, issued 10/26/67, revised 7/1/68, National Neutron Cross Section Center, Brookhaven National Laboratory.

20. J. T. Mihalczo, Monte Carlo Calculations of Two Core Delayed Critical Assemblies, *Trans. Amer. Nucl. Soc.,* 11: 603 (1968).

21. Gordon E. Hansen and Clifford Maier, Perturbation Theory of Reactivity Coefficients for Fast Neutron Critical Systems, *Nucl. Sci. Eng.,* 8: 532-542 (1960).

22. H. Kahn, Applications of Monte Carlo, USAEC Report AECU-3259, RAND Corp., 1956.

23. H. Rief, The Application of Monte Carlo to Neutron Transport and Reactor Analysis Problems at the Euratom Research Center, Ispra, Proceedings of the Special Sessions on Resonance Cross Sections in the Unresolved Resonance Region and Application of Monte Carlo Techniques to Reactor Physics, Presented at the 1968 Summer Meeting of the American Nuclear Society and the Canadian Nuclear Association, Toronto, Canada, June 10, 1968, USAEC Report ANS-RFD-1, American Nuclear Society, 1968.

24. G. E. Hansen, Status of Computational and Experimental Correlations for Los Alamos Fast-Neutron Critical Assemblies, in *Physics of Fast and Intermediate Reactors,* Symposium Proceedings, Vienna, 1961, Vol. I, p. 453, International Atomic Energy Agency, Vienna, 1962 (STI/PUB/49).

25. J. Orndoff, Prompt Neutron Periods of Metal Critical Assemblies, *Nucl. Sci. Eng.,* 2: 450 (1957).

26. J. T. Mihalczo, Prompt Neutron Lifetime in Critical Enriched-Uranium Metal Cylinders and Annuli, *Nucl. Sci. Eng.,* 20: 60-65 (1964).

27. E. E. Gross and J. H. Marable, Static and Dynamic Multiplication Factors and Their Relation to the Inhour Equation, *Nucl. Sci. Eng.,* 7: 281 (1960).

28. J. T. Mihalczo, Sensitivity of Neutron Spectrum-Dependent Quantities in Uranium (93.2% ^{235}U) Metal Assemblies to Inelastic Scattering Models for ^{235}U, *Trans. Amer. Nucl. Soc.,* 9: 489 (1966).

29. G. W. Morrison, J. R. Knight, and D. C. Irving, Prompt Neutron Delay Constants Calculated in Highly Enriched-Uranium Metal Assemblies, *Trans. Amer. Nucl. Soc.,* 10: 223 (1967).

DISCUSSION

McTAGGART: I would like to ask if you have any reaction-rate ratio measurements in these systems with which to compare your calculations.

MIHALCZO: I have made these calculations in the past for the reaction-rate measurements in Godiva, but I have not done them with these recent calculations. This will probably be done.

McTAGGART: I think if one is going to make adjustments of ^{235}U fission cross sections as you have described to get the criticality right, one must at the same time be sure that these adjustments do not upset the fission ratio measurements between plutonium and ^{235}U or ^{238}U and ^{235}U. This was the reason for my question.

MILEY: Have you compared the various calculation techniques that you mentioned — Monte Carlo, S_n, and multigroup diffusion theory — for a single problem that is representative of these small fast burst reactors?

MIHALCZO: You mean for a single system?

MILEY: Right. The same system and the same cross sections.

MIHALCZO: I have made these comparisons for the transport theory and the Monte Carlo method but not for the diffusion theory. If you use the six-group cross sections, which you get by averaging the cross sections used for the Monte Carlo calculations with the spectrum computed by Monte Carlo, the S_n method predicts criticality that agrees with the Monte Carlo method and gives decay constants that agree with experiment. We have not computed the decay constants by Monte Carlo, but we are now working on the codes to do this.

MILEY: Could you comment on the time required for calculations by different methods?

MIHALCZO: In a bare system like Godiva you can do a calculation on a 360-75 computer (with the statistical accuracies quoted here) in about 30 min with the O5R code. There are other Monte Carlo codes at Oak Ridge, for instance, the KENO code, which is a multigroup Monte Carlo, essentially does just what transport theory calculations do. KENO handles slowing down by a transfer matrix. The only feature that makes it different from transport theory is that it handles the geometry exactly. You can do calculations with this code, for instance, on a uranium-metal cylinder with 18 in. of graphite around it, in roughly a factor of 20 less computing time than you can by S_n transport theory if a statistical error of ~0.5% on the multiplication constant is satisfactory. Part of the reason for the long time on the transport theory calculations is that you have to worry about convergence, you have to worry about the order of S_n, and you have to worry about the number of spatial mesh intervals, particularly near the thermal

reflector – fast core boundary. This increases the calculating time to something like $1\frac{1}{2}$ hr or 2 hr, and the KENO code using adjoint biasing in the reflector can run a calculation like this in about 5 min.

FOELL: I was interested in the very close agreement you have obtained between your measured and calculated reactivity coefficients in central worth measurements or void measurements. In the fast criticals that have been done at Argonne National Laboratory and other places, in general, there is not very good agreement between the measured and calculated reactivity coefficients, particularly for some of the lighter materials. I think this occurs partially because there is a cancellation between the various components — the moderation, the fission, and the capture components. Would you comment on the reason for the very good agreement in your calculations.

MIHALCZO: In these systems the energy spectrum is harder than in those at Argonne. Also, I think in this particular case, the model which is being used in the calculations (for instance, the Monte Carlo model of Rief in the case of the SORA experiment) correctly represents the change geometry-wise and is a very accurate representation of the system from a calculational standpoint. The reactivity coefficients that have been calculated, e.g., the removal of a fissionable rod from the center, the removal of a beryllium control rod, or an iron reflector block, are maybe not as complicated as the competing reactivity effects in the Argonne experiments. Also, the Argonne experiments are not simple geometry experiments but I understand are computed by reactor codes which have simple geometry capability. There may be some problem in correctly representing the changes in the code.

SHAFTMAN: Are you proposing to use a single set of cross sections for a rather large number of different systems instead of attempting to tailor cross sections to the particular composition?

MIHALCZO: I have just been concerned with 93% enriched-uranium-metal systems, and I feel I have a set of cross sections that will predict criticality and neutron lifetime, and these are only good now down to energies of ~1 kv. If you have a system that has many neutrons below 1 kv, you cannot use the cross sections I have compiled.

SHAFTMAN: Except you have iron, molybdenum, and other materials in them.

MIHALCZO: The iron cross sections I used in the Monte Carlo calculations very satisfactorily predicted the age in iron – water mixtures. The cross sections that were used in the transport theory codes are cross sections which were compiled by Gordon Hansen over the years for use in the calculations of a wide variety of integral experiments. I think there have been measurements at Los Alamos of the integral quantities that are used for these calculations.

SHAFTMAN: This was done at Argonne too, except that there were enough differences that cross sections more specific to the particular system were developed.

MIHALCZO: You have two problems at Argonne; you do not necessarily know what the cross sections are and your models for the complicated geometries you have are not exact. In the cases that I have calculated, I could take the Monte Carlo method and compute the system and because of the accuracy of the model know that if there was a disagreement with experiment it was due to the cross sections. You can get a set of adjusted cross sections which would be fine for the geometry approximations you have made to get the problem on the computer. If you change the geometry, the same set of cross sections may not give you the agreement between experiment and calculation.

NELSON: Could you briefly describe how you carried out the lifetime calculations? In particular, I would like to know whether you are using a mean destruct time, a mean time to fission, or something else.

MIHALCZO: The Monte Carlo method calculated the mean time to production. The S_n calculations were used to obtain an effective-delayed-neutron fraction which allowed the determination of a lifetime from the prompt-neutron decay constant measurement at delayed criticality. The lifetime calculation as calculated by S_n would be the usual ratio of integrals as appears, for instance, in articles by Henry and others where you use the static adjoint and dynamic forward angular fluxes to do the calculation of the integrals. (See A. F. Henry, *Nuc. Sci. Eng.*, 3: 52 (1958) and L. N. Ussachoff, Equation for the Importance of Neutrons, Reactor Kinetics, and the Theory of Perturbations, in *Proceedings of the International Conference on the Peaceful Uses of Atomic Energy, Geneva, 1955,* Vol. 5, p. 503, United Nations, New York, 1956.)

1-2 FAST BURST REACTOR KINETICS

M. H. McTAGGART
Atomic Weapons Research Establishment, Aldermaston,
Berkshire, United Kingdom

ABSTRACT

The simple transient response equation of reactor kinetics is the basis of more-sophisticated methods of calculating the behavior of fast burst reactors. The need to stretch burst reactor designs to their ultimate capability, however, has forced designers to extend the simple model. This paper reviews these extensions and examines their range of validity. Many reactivity-feedback coefficients are nonlinear, e.g., the Doppler effect used in VIPER. In systems with short prompt-neutron lifetimes, such as Godiva and Super KUKLA, inertia effects become important, and the kinetics problem consists in solving coupled kinetics equations that take account of the elastic waves set up in the fuel by the rapid heating.

The delayed-neutron fraction and prompt lifetime, which govern the prompt kinetics in many systems, are not well determined at present. Ways of adjusting delayed-neutron parameters to fit the observed reactor behavior are outlined, and experiments suggesting that certain delayed fractions may be in error are discussed.

Simple models that predict the general features of a prompt burst were at one time a satisfactory basis for design.[1,2] Now that the demand is for higher yields and shorter bursts, burst reactor designs are being stretched to their ultimate capability, and more-sophisticated models are required. Nevertheless, from the viewpoint of designing and operating burst reactors to produce a large number of pulses without serious damage, relatively straightforward extensions to the simple model, with a proper appreciation of the range of validity, are generally adequate. The calculation techniques described are concerned primarily with observable quantities, such as reactor period, pulse shape, and yield, and can be applied to future designs provided their reliability and accuracy can be established for existing systems.

This paper reviews methods of deriving reactivity feedback in terms of a one-point model with separable time and space dependence. Some discussion of inertia effects, which can usually be represented by a simple single-frequency oscillator model of the system, leads to useful approximate relations for yield vs. reactivity. A realistic model must allow for the lag in system feedback due to fuel inertia and may have to consider nonlinear processes, such as the Doppler effect. For assessing the design limitations ideally, the model should also describe the stress pattern throughout the system.

The kinetic behavior above prompt critical is governed by the neutron lifetime and the reactivity. In practice the reactivity scale is usually established by means of the delayed-neutron fraction. When a burst reactor is used as an irradiation device, the presence of experiments in or near the core can alter the effective neutron life-time. Experiments with the Sandia Pulsed Reactor (SPR) show that for moderating reflectors this alteration is due to the slowing down time and transit time of those neutrons which travel from the core to the reflector, are scattered there, and return to the core as low-energy neutrons. Practical ways of accounting for these effects are needed to predict reactor performance with a variety of irradiation experiments if the reactor is to continue operating safely and reliably.

Delayed-neutron parameters, such as effective group fractions, can also be affected by the presence of irradiation experiments. Even the basic data calculated using multigroup effectiveness values do not describe adequately the variation of period with reactivity between delayed and prompt critical. From the operators' point of view, a consistent set of delayed-neutron parameters is very useful. Empirical adjustments can usually be made to provide such a set.

The operator also needs an accurate value of the total delayed-neutron fraction if only to connect effects calculated on an absolute reactivity scale to those he is measuring (which are usually based on a dollar reactivity scale). The possibility of revised values for certain isotopes should not be ruled out.

BURST REACTOR KINETIC THEORY

According to Keepin[3] the basic problem is solving the transient response equation

$$\frac{dn}{dt} = \frac{n(t)}{\tau} \left[k(t)(1 - \gamma\beta) - 1 \right]$$

$$+ \int_{-\infty}^{t} \frac{n(t')}{\tau} k(t') \sum \lambda_i \gamma_i \beta_i \exp\left[-\lambda_i(t - t') \right] dt' \quad (1)$$

for an arbitrary reactivity variation k(t). The simplest case of a compensated response is when k(t) takes the form

$$k(t) = k(o) - A \int_0^t n(t') \, dt' \tag{2}$$

where the negative sign signifies negative feedback. The kinetic behavior is governed by three things, the most important of which is the feedback term in the equation for k(t), the form and quantitative expression for $A \int_0^t n(t') \, dt'$. This expression determines the amount by which the reactivity has to exceed prompt critical for a given burst yield. Next in importance is the neutron lifetime τ which dictates the initial prompt period (usually referred to in the form of its reciprocal α). The third governing factor, the delayed-neutron contribution, is negligible if the reactor is super-prompt critical and the neutron population is growing rapidly and becomes most important when the system is between delayed and prompt critical.

The well-known simple solution obtained when A is constant predicts a linear relation between energy yield and excess prompt reactivity

$$E_{total} = 2 \, \frac{\delta k_p}{B_\epsilon} \tag{3}$$

where B_ϵ is a generalized shutdown coefficient expressed as reactivity change per unit energy. The pulse shape and energy are given by

$$\dot{E}(t) = \frac{2\delta k_p \alpha}{B_\epsilon} \, \frac{\exp \alpha t}{[1 + \exp \alpha t]^2} \tag{4}$$

and

$$E(t) = \frac{2\delta k_p}{B_\epsilon} \, \frac{\exp \alpha t}{1 + \exp \alpha t} \tag{5}$$

which gives a power pulse with width at half peak power of $W_{\frac{1}{2}} = 3.52/\alpha$. After the prompt pulse when the delayed neutrons can no longer be ignored, the plateau level is given by

$$\left(\frac{dE}{dt} \right)_{plateau} = \frac{2 \Sigma \lambda_i \beta_i}{B_\epsilon} \tag{6}$$

In this simple solution the plateau power level (1) is the same for all sizes of pulse, (2) is independent of the prompt lifetime, and (3) is inversely proportional to the shutdown coefficient.

Reactivity Feedback

The simple proportionality between reactivity feedback and energy can be justified by considering the effect of rapid fission heating of the fuel during a prompt transient. For example, if thermal expansion results in a displacement $\xi(r, t)$ proportional to the temperature rise, the resulting reactivity change can be expressed in first-order perturbation theory by

$$k(t) = \int_{core} \xi(r,t) \frac{\partial w}{\partial r} \, dv \tag{7}$$

where w is the worth of fuel and $\partial w/\partial r$ is the gradient in the direction of the displacement. Since the temperature rise up to time t is proportional to the number of fissions that have occurred up to that time and the fission rate is proportional to the neutron population, this reactivity change can be separated into time- and spatial-dependent components:

$$k(t) = \int_0^t n(t) \, dt \int g(r) \, dr \tag{8}$$

where g(r) represents the space-dependent part of Eq. 7.

Departures from this simple proportionality arise for a number of reasons:

1. For slow pulses heat transfer during the pulse may have to be considered. For most fast-pulsed reactors, heat loss during the pulse can be neglected.

2. Some materials have neither constant specific heat nor constant expansion coefficient. This leads to minor departures from linearity which can generally be accommodated by choosing a suitable averaged value.

3. Some feedback mechanisms, notably the Doppler effect, have a well-established nonlinear temperature relation. Typically $\partial k/\partial T$ (Doppler) varies as $T^{-3/2}$, where T is absolute fuel temperature. This variance affects the pulse shape and alters the yield−reactivity relation.

4. In very rapid heating quasi-static expansion is inhibited by the fuel inertia, and expansion lags behind the fission energy release. The feedback term is thus delayed with respect to the fission heating, and the yield is larger than predicted by the simple-model theory.

In practicable fast burst reactors, the pulse widths vary from a few tens of microseconds to a few milliseconds, and heat transfer during the pulse is negligible. Variations in specific heat and expansion coefficient with temperature are generally less than 5% for a

single-phase material over the operating range of most pulsed reac-
tors. These variations, along with such effects as the Doppler coeffi-
cient, are not easily incorporated in an analytical solution. If relations
between temperature rise and fission energy or reactivity change and
temperature are added to the response equations, numerical solutions
for pulse shape, yield, etc., can be obtained for a particular reactor.

Inertia effects can be included in the compensated-response
calculation if the reactivity changes associated with the constrained
expansion can be expressed as a function of time. This is generally
done by constructing a dynamic displacement equation for the average
expansion and assuming that the reactivity change is proportional to
the expansion.

Calculation of Temperature Coefficients for VIPER

As an example of the simple model, the temperature coefficient
for the VIPER reactor (the comparatively slow pulse of VIPER allows
inertia effects to be neglected) was calculated[4,5] in two parts. The
expansion contribution was obtained by calculating fuel displacements
as a function of position and by performing a numerical integration
over the core cylinder volume of the reactor. The result was a tem-
perature coefficient of $(0.70 \pm 0.09) \times 10^{-5}$ of average fuel-temperature
rise. The Doppler coefficient was calculated by using Doppler-broad-
ened resonance data for 300, 600, and 900°K. Although the temperature
is not uniform throughout the real core, it is a reasonable approxima-
tion to assume a uniform temperature equal to the core average. For
each temperature the criticality of the core was calculated using a
diffusion theory program with allowance for heterogeneity. The results
were fitted to an expression of the form $AT^{-\frac{1}{2}}$ between the 300 and
600°K points. The curve passes within 6% of the 900°K point. The
initial slope of this function is $(0.88 \pm 0.13) \times 10^{-5}/°C$, and the average
slope from 300 to 600°K is $(0.58 \pm 0.09) \times 10^{-5}/°C$. Combining this
last result with the expansion coefficient, the overall coefficient is
$(1.28 \pm 0.15) \times 10^{-5}$.

The observed slope of the yield vs. reactivity curve, which in
the simple model is proportional to the temperature coefficient, is
$(1.08 \pm 0.07) \times 10^{-5}/°C$ average fuel temperature. Within the experi-
mental accuracy and with allowance for the uncertainty in the calcu-
lated values, the measure of agreement between this coefficient and
the calculated value is satisfactory.

Following a suggestion by J. Randles, and in an attempt to deter-
mine the relative proportions of Doppler and expansion coefficient,
the full feedback equation was solved using the RKSF point reactor
kinetics code[6] and the DOPPELAS code,[7] both of which can accommo-
date a nonlinear temperature coefficient. These calculations are

summarized in Table 1 and Fig. 1. Because it is a point kinetics code, the calculated temperature is simply the fission energy divided by the heat capacity of the core. The results show that with a coefficient comprised of equal expansion and Doppler effects the following occur:

1. The pulse yield vs. reactivity becomes slightly nonlinear.

2. The relation between width and reciprocal initial period changes from 3.52, as in the simple model, to a number which varies from 3.7 to 3.9, depending on the size of pulse.

3. The post-pulse plateau, which in the simple theory is constant, also increases with pulse size.

The effect of varying the relative proportions of Doppler and expansion is illustrated by the last four entries in Table 1. If we assume that expansion contributes between 50 and 70% of the total coefficient, a better value for the average coefficient from ambient to 320°C is $(1.19 \pm 0.07) \times 10^{-5}{}^\circ C^{-1}$. This is closer to the calculated value of $(1.28 \pm 0.15) \times 10^{-5}{}^\circ C^{-1}$.

Because the deviation from linearity is small in relation to the experimental errors, the proportions of linear and nonlinear temperature coefficients cannot be determined solely from the dependence of yield on reactivity insertion. Although in VIPER it is difficult to measure the pulse shape accurately, there is evidence that the plateau power level is higher after large pulses than after small ones.

Calculation Methods for Inertia Effects

Because of its importance to Godiva systems, the inertia effect has received much attention. Various models have been used, but essentially they are all attempts to treat realistically a coupled neutronics−dynamics system of equations in terms of a few parameters. An exact solution within the one-point kinetics model would be obtained by solving point by point the equations of motion of the heated fuel, calculating displacements and thus the reactivity change, and substituting this value in the response equation to produce a further temperature rise. It is clearly a gross simplification to represent the expanding fuel by a single displacement parameter, such as the vibration amplitude of a single-frequency oscillator. Nevertheless, this procedure has been followed using suitably averaged values, and the results are in good agreement with the observed variation of yield vs. reactivity.

Formally we still may represent the displacement by $\xi(r,t)$ and the reactivity change by the integral

$$\int_{core} \xi(r,t) \frac{\partial w}{\partial r}$$

Table 1

CALCULATED VIPER PULSE KINETICS INCLUDING $T^{-\frac{3}{2}}$
TEMPERATURE-DEPENDENT DOPPLER COEFFICIENT

Reactivity insertion, ¢	Temperature coefficient ($\times 10^{-5}$ °C^{-1})		Ratio of width to period		Prompt temperature rise, °C		Plateau heating, RKSF, °C/msec
	Doppler*	Expansion	DOPPELAS	RKSF	DOPPELAS	RKSF	
2	0.54	0.54	3.56	3.68	20	22	0.45
5	0.54	0.54	3.61	3.65	51	53	0.52
10	0.54	0.54	3.70	3.71	108	109	0.60
15	0.54	0.54	3.76	3.78	170	170	0.66
20	0.54	0.54	3.82	3.87	237	237	0.71
23.5	0.54	0.54	3.86	3.90	286	286	0.75
23.5	0	1.08	3.43	3.53	316	317	0.70
23.5	0.69	0.39	3.96	3.99	277	277	0.76
23.5	0.39	0.69	3.75	3.80	294	295	0.74
23.5	1.08	0	4.17		252		

*Doppler coefficient expressed as the reactivity change from ambient to maximum (25°C to 345°C) divided by the temperature difference.
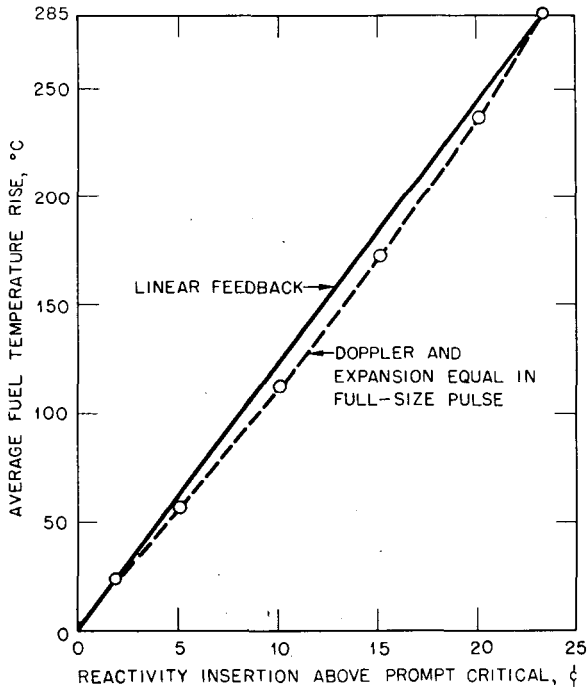
Fig. 1 — RKSF calculations of VIPER yield vs. reactivity, including nonlinear Doppler reactivity-feedback term.

In this instance, ξ is not readily separable into spatial- and time-dependent functions. The equations of motion which determine ξ are readily derived in the one-dimensional case.

The stress equation is

$$p = -E\frac{\partial \xi}{\partial x} + E\phi T \tag{9}$$

where E is Young's modulus and ϕ is the expansion coefficient of the fuel of density ρ.

The equation of motion is

$$\frac{\partial p}{\partial x} = -\rho\frac{\partial^2 \xi}{\partial t^2} \tag{10}$$

Eliminating the stress, the displacement equation becomes

$$\frac{\rho}{E}\frac{\partial^2 \xi}{\partial t^2} - \frac{\partial^2 \xi}{\partial x^2} = -\phi\frac{\partial T}{\partial x} \tag{11}$$

This is obviously a wave equation with wave velocity $\sqrt{(E/\rho)}$ and a source term that depends on the temperature profile. With appropriate boundary conditions this equation can be used to generate numerical solutions for ξ. In practice simplifying assumptions are generally made before even numerical solutions are attempted.

The earliest solutions[1] produced bounds to the yield of the form

$$\begin{aligned} E^1 &< 2(1 + \alpha^2 t_0^2)E \\ E^1 &> (1 + \alpha^2 t_0^2)E \end{aligned} \tag{12}$$

where E is the yield given by the simple theory, α is the inverse initial period, and t_0 is an inertial time constant associated with the transit time of a stress wave across the system. To a first approximation the yield is given by the lower bound, i.e., it increases by a factor $(1 + \alpha^2 t_0^2)$ over the simple theory. The pulse width reduces from $3.52/\alpha$ to a lower limit of $2.44/\alpha$.

CONEC[8] is a one-dimensional neutronic elastic code capable of dealing with solid spheres or spherical shells. It resembles the neutronics—hydrodynamics codes used for accident studies in that it calculates reactivity feedback by repeating the neutronics calculation at intervals throughout the pulse but uses an elastic equation of state. Applied to Godiva it appears to predict a ringing period in agreement with a corresponding analytical value of 58 μsec. In predicting the yield vs. reactivity (or reciprocal initial period α), it

gives values which exceed the experimental ones for $\alpha < 0.06 \times 10^6$ sec^{-1} and which are less than the experimental ones for $\alpha > 0.06 \times 10^6$ sec^{-1}, though over the entire range the curves agree within the experimental uncertainty.

In solving these equations for a spherical system, Kolesov[9,10] uses the perturbation equation to calculate reactivity feedback but derives solutions for the displacements in terms of eigenfunctions, which involve the characteristic vibration frequencies of the components. Numerical calculations were performed for two variants: (1) a solid sphere (20.5 cm in diameter) and (2) a sphere divided into four parts (a solid center 8.2 cm in diameter and three shells 8.6 to 12.7 cm in diameter, 12.7 to 16.7 cm in diameter, and 16.7 to 20.5 cm in diameter. Only the first term of the eigenfunction expansion was used in the quoted results although other calculations were done using the first two terms, and Kolesov states that the results obtained were practically identical. Comparing this with Godiva, which may be regarded as a sphere 17.5 cm in diameter, the yield−reactivity relation is similar and shows the same departure from linearity for initial periods shorter than 25 μsec. The free-oscillation period of the 20.5-cm sphere is 75 μsec compared with the CONEC value for Godiva of 55 μsec.

Kurstedt and Kazi[11] have published numerical solutions of a similar set of equations which treat the Army Pulse Radiation Facility Reactor (APRFR) as a thin shell. The cylindrical core is represented by a shell with an effective radius equal to the radius of gyration of the core disks. Allowance is also made for temperature dependence of the specific heat, and provision is made for Doppler feedback terms. In the results quoted the feedback due to expansion is not calculated from the properties of the assembly but is fitted empirically to the largest experimental pulse.

Direct measurements[12,13] of the displacement of the outer surface of SPR II provide a comparison with the thermoelastic equation applied to a simplified model of the core, neglecting the presence of holes and other irregularities. Predicted displacements of the outer surface were 10% greater than the measured expansion of 21 mils, and the inner surface moved 20% further than predicted. The observed vibrational period was 160 μsec compared with the theoretical value of 130 μsec.

In the DOPPELAS program which is written for rod-type cores, such as SORA and VIPER, Randles[7,14] adopts a slightly different approach. Although intended for use in accident calculations, this program can be used to calculate the effect of inertia on both yield and pulse width. The numerical solution is simplified by assuming that (1) the worth of fuel varies linearly with height above the core

center plane, and (2) the core is uniformly heated. The feedback reactivity equation reduces to

$$\epsilon_{elastic}(t) = A \int_0^t T(bt') Q(t - t') dt'$$

$$\epsilon_{Doppler}(t) = B[Q(t)]$$

(13)

where ϵ is the feedback reactivity, $T(\theta)$ is a triangular wave of unit amplitude, b is a time constant associated with the time taken for pressure waves to travel from one end of a fuel pin to the other, and Q(t) is the energy input.

Some DOPPELAS calculations for VIPER are shown in Fig. 2, where the neutron lifetime is varied for a fixed set of other parameters
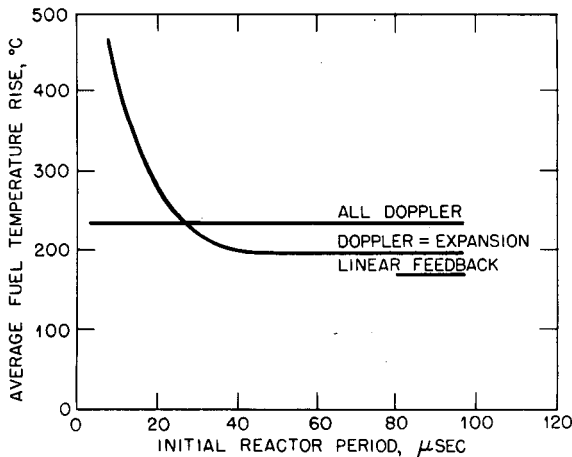
Fig. 2—DOPPELAS calculations of VIPER yield, illustrating inertial effects by artificially varying neutron lifetime.

corresponding to a 240°C VIPER pulse. The yield is constant until the period becomes comparable with 56 μsec, which corresponds to the time taken for a pressure wave to traverse half the length of a fuel rod (analogous to the "inertia time constant"). This shows that the effect of inertia on yield in VIPER is probably negligible though it does not mean that the fuel is not stressed during a pulse.

Although all these methods appear to describe the inertia effects qualitatively within the elastic range, there is room for improvement in (1) making more detailed quantitative comparisons and (2) examining the validity of some of the simplifying assumptions. One important material property is the modulus of elasticity. First, the modulus is usually assumed to be constant, though in most materials it decreases with temperature and may vary by as much as 25% between ambient

and the peak reactor operating temperature, and, second, its dynamic value may differ from the quasi-static one. Mechanical complexity is also difficult to incorporate. Few Godiva-type systems can be treated as solid assemblies. All have holes for control and burst rods, etc., and most are bolted together by nonfissile materials. It is difficult to represent the notch in the fuel pin adequately in a stress calculation. Attempts have been made to represent the stress conditions in more detail, using a temperature profile derived by one of the simplified methods previously described. For accident analysis, of course, treatments should be extended beyond the elastic range.

PROMPT KINETICS

Above prompt critical the initial exponential period of a transient is simply related to the reactivity insertion. Equation 1 reduces to

$$\alpha = \frac{\beta}{\tau} \rho \qquad (14)$$

where α is the reciprocal of the initial period and the reactivity ρ is measured in dollars. Except very close to prompt critical, the slope of the linear relation between α and ρ gives the experimental value of β/τ.

Direct measurement[4,5] of this ratio in VIPER gives a value of $(4.36 \pm 0.05) \times 10^4$ sec^{-1} for the basic core. The slope increases significantly when an experiment is included. For example, when a small cavity is created near the core, the core loading has to be increased to accommodate the change in criticality, and the value of β/τ becomes $(4.65 \pm 0.10) \times 10^4$ sec^{-1}.

Similar measurements[14,15] with other systems, such as SPR II, also show a nearly linear variation of α vs. ρ except that for small reactivity insertions above prompt critical some curvature is observed which can be attributed to room-reflected neutrons. Similarly, changes in the location and type of reflector cause the slope to decrease. This decrease is due to an increase in the effective lifetime which is caused by neutrons that leave the core being moderated in the reflector and then returning to the core sometime later. Both the moderation time and the return transit time have to be considered. These measurements are discussed in Session 4, Paper 4.

Rossi-alpha, pulsed-alpha, and variance-to-mean methods have been used extensively, both in pulsed reactors and in other fast critical reactors.[16,17,18] These techniques provide a means of checking β/τ experimentally before reaching prompt critical since the prompt decay constant at delayed critical in the one-point kinetics model is

also the ratio β/τ. For simple systems a single exponential decay constant is usually easy to establish, but it is clear from measurements with reflected systems that the simple model is not adequate. Attempts have been made to devise two-region models and calculate the time dependence of the neutron population in the system as a whole.

Omitting systems where it is clearly necessary to represent the prompt decay by more than a single exponential, Table 2 summarizes values of β/τ for a range of systems, including pulsed reactors VIPER, Godiva, and Jezebel, and the zero-energy reactors FRO, VERA, and Zebra.[20] It is noteworthy that the value of β/τ at delayed critical for VIPER obtained from Rossi-alpha measurements, $(4.05 \pm 0.05) \times 10^4$ sec^{-1}, is 7% less than the ratio derived from super-prompt pulses.

If the appropriate value of the effective delayed-neutron fraction is used, the prompt-neutron lifetime corresponding to the measured ratio can be derived for comparison with the prompt lifetime directly calculated using multigroup methods. This comparison provides a test of neutron cross-section data and methods which is different from the comparison of calculated and experimental critical sizes. In most examples the calculated lifetime is shorter than the experimental value. The exceptions are either very simple systems, such as the Los Alamos assemblies, or ones, such as VERA 5A and 7A, in which great effort has been made to include heterogeneity effects and thus improve the low-energy spectrum. In the case of VIPER, the difference, although significant, between the experimental values of β/τ derived from Rossi-alpha measurements and from super-prompt pulses is much less than the discrepancy between calculated and experimental lifetime.

DELAYED-NEUTRON DATA FOR PULSED REACTORS

Although control rods can be calibrated conveniently in a pulsed reactor in terms of the delayed fraction, i.e., in dollar units, there is a need for accurate delayed-neutron data for two reasons. First, the prompt kinetics depends on the total delayed fraction as well as the lifetime, and, second, the prediction of prompt criticality from control-rod and pulse-rod calibrations near delayed critical depends on the relative abundances through the inhour equation

$$\rho = \frac{\tau}{(\tau + T)\beta} + \frac{T}{\tau + T} \sum_i \frac{a_i}{1 + \lambda_i T} \tag{15}$$

where T is the reactor period and a_i, $i = 1, \ldots, k$ are the relative abundances of the delayed-neutron groups. In VIPER a method[5] has

Table 2

COMPARISON BETWEEN CALCULATED AND EXPERIMENTAL VALUES
OF THE RATIO β/τ AND NEUTRON LIFETIME

Reactor	Measurement	Experimental value of β/τ ($\times 10^4$ sec^{-1})	Calculated values		Experimental value of lifetime, μsec	Ref.
			β, %	Lifetime, μsec		
VIPER 1	Super-prompt pulses	4.36 ± 0.05	0.728	0.133	0.167	5
VIPER 1	Rossi α	4.05 ± 0.05	0.728	0.133	0.180	5
Godiva	Rossi α	1.10×10^2	0.69	0.0057 0.0051†	0.0060*	19
^{239}Pu sphere	Rossi α	0.65×10^2	0.20	0.0031	0.0030*	19
FRO core 2	Rossi α	Decay fitted	0.784	0.074	0.107	17
FRO core 3	Rossi α	to a two-region kinetics model	Not quoted	0.123	0.146	17
Zebra core 1	Rossi α	10.3 ● 0.3	0.734	0.057	0.071	20
Zebra core 3	Rossi α	8.63 ± 0.09	0.434	0.05	0.05	20
VERA core 1B	Rossi α and pulsed α	6.9 ± 0.1	0.73	0.095	0.106	21
VERA core 5A	Rossi α and pulsed α	2.6 ± 0.1	0.75	0.288	0.288	21
VERA core 7A	Rossi α and pulsed α	3.2 ± 0.1	0.67	0.220	0.209	21

*Reference 19 gives an "experimental" value of β. This was used in converting the experimental β/τ ratio into an experimental lifetime.

†Calculation at AWRE using 13 energy groups.[23]

been devised for adjusting these abundances to fit the observed relation between period and reactivity. This method is useful, practical, and expedient; in practice the adjustments are within the uncertainties of the calculated parameters.

Delayed-neutron data used for the initial analyses were calculated from the basic data[3] for ^{235}U and ^{238}U, making allowance for the delayed-neutron spectra and the core fission distribution. The pulse rod was calibrated in terms of a control rod (CRA) whose worth per unit length did not vary by more than 2% over its position range from 4 to 8 in. The standard reactivity unit was taken as the worth of CRA movement from 6 to 7 in. The measured period for this movement was 67.15 sec, and, if we use the effective data, this is equivalent to 12.35 ± 0.1¢/in. On the basis of this calibration, the required insertion for prompt criticality is 8.097 in. CRA, and the predicted variation of period with reactivity increment up to prompt critical is shown as curve 1 in Fig. 3. The corresponding measured variation is shown as curve 2. The object of the adjustment exercise is to find a set of delayed-neutron data which makes these curves coincide. In Fig. 3 the predicted critical point is clearly 0.2 in., i.e., 2.4¢ below the observed one. For reactor periods greater than a few milliseconds, the first term in the inhour equation is negligible. The contribution to the second term from each group varies most in the range from $T \simeq 1/5\lambda_i$ to $T \simeq 5/\lambda_i$. For $T < 1/5\lambda_i$ the ith group contribution is virtually constant between $0.8a_i$ and a_i. For $T > 5/\lambda_i$ the contribution is less than $0.2a_i$ and rapidly decreasing. By inspecting ways in which the difference between the two curves varies with the period T, we can easily decide which group abundances require adjustment and by how much. Agreement was obtained by adding 0.7% to group 4 and 1% each to groups 5 and 6. Table 3 lists the original data and the adjusted set.

For a period of 67.15 sec, corresponding to a 1-in. movement of CRA from the 6- to the 7-in. position, the reactivity change given by the adjusted set is 12.06¢, and it predicts prompt criticality at 8.292 standard inches of CRA.

A similar technique can be applied to the adjustment of delayed-neutron data, adding extra delayed groups if needed, in any system where there is a need to predict the period variation between delayed and prompt critical. Often, as with VIPER or Super KUKLA, the inclusion of experiments will alter the flux pattern and the adjoint spectrum in the core and thus change the relative effectiveness of the delayed-neutron groups. The absolute delayed fraction cannot be checked from reactor period measurements alone.

A knowledge of this fraction is essential to the comparison of directly calculated reactivity effects and measured ones, which are generally based on control-rod calibrations using delayed-neutron

CURVE 1. PREDICTION BASED ON
         EFFECTIVE SET (KEEPIN DATA)

CURVE 2. OBSERVED

REACTOR PERIOD, SEC

REACTIVITY INCREMENT (IN. CRA.)
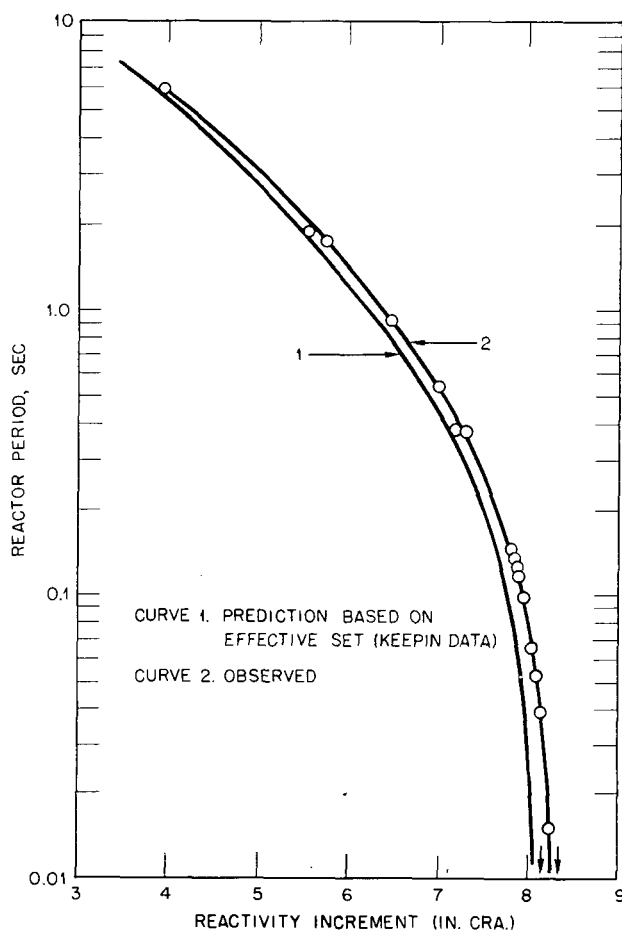
Fig. 3—VIPER period vs. reactivity up to prompt critical.

parameters to convert from period to reactivity. Both Rossi-alpha
and variance-to-mean methods are, in principle, capable of providing
a direct measure of the effective absolute delayed-neutron fraction.
The Rossi-alpha method has been used for VIPER and gives the
result $\beta = (0.03 \pm 0.04)\%$. This is somewhat lower than the calculated
value, and, although it reduces the discrepancy between measured and
calculated lifetime, it does not remove it. Measurements have been
made in other fast reactors, notably some recent work with FRO.[17]
Generally, in ^{235}U-fueled systems the agreement is within a few
percent.

The validity of the basic data, particularly for ^{239}Pu and ^{235}U,
has been tested in the Los Alamos fast criticals where the reactivity

Table 3

DELAYED-NEUTRON DATA FOR VIPER 1

Group No.	Group decay constant, sec^{-1}	Effective set based on Keepin data[3]*	Adjusted set for VIPER 1
1	0.0127 ± 0.0002	0.000253 ± 0.000020	0.000246
2	0.0317 ± 0.0008	0.001449 ± 0.000070	0.001411
3	0.1150 ± 0.003	0.001340 ± 0.000140	0.001305
4	0.3110 ± 0.008	0.002928 ± 0.000060	0.002903
5	1.400 ± 0.081	0.001057 ± 0.000060	0.001100
6	3.870 ● 0.369	0.000253 ± 0.000030	0.000315
	Total	0.00728	0.00728

*Errors quoted are based on errors given by Keepin for relative abundances of ^{235}U delayed neutrons. Additional errors, ~5%, introduced by the effectiveness calculation are not included.

increment between delayed and prompt critical is compared with the corresponding surface increment. This, in turn, can be expressed in terms of absolute reactivity by criticality calculations. The agreement is within 10%.[19] In more-complex systems the perturbation effect based on delayed-neutron-calibrated control rods of a small sample at the core center may be compared with the calculated value. The uncertainty of this calculation can be reduced to a few per cent by choosing a fissile sample, preferably the same fissile material as the core, and using cross-section data, which allows the criticality of the system to be correctly calculated. For a range of Zebra cores, this comparison as given in Table 4 shows that there is a discrepancy, especially in cores in which the main fissile component is ^{239}Pu. Because of its small delayed-neutron fraction, the effective delayed-neutron fraction for the system depends crucially on the value for ^{238}U, which is currently nearly six times the ^{239}Pu value. Table 4 shows that the revised

Table 4

CENTRAL PERTURBATION VALUES IN ZEBRA ASSEMBLIES[20]

Zebra core	Main fissile material	Ratio*	
		Keepin[3] delayed-neutron data	Revised[22] delayed-neutron data
1	^{235}U	1.21	1.10
2	^{235}U	1.25	1.15
3	^{239}Pu	1.33	1.15
6A	^{239}Pu	1.34	1.18

*Ratio of the calculated worth of ^{239}Pu sample at the core center to the observed worth based on control rods calibrated by period measurements.

delayed-neutron data[22] could help to reduce this discrepancy. The increase could be due to the higher energy of neutrons producing fission in this revised data.

A change of this magnitude also affects the value of β used in deriving the prompt lifetime for the Zebra cores from the measured decay constant by the Rossi-alpha method. For example, the quoted value for core 3 in Table 2 is 0.43%. If this were to be increased in the same ratio, i.e., to 0.525%, the experimental lifetime for Zebra core 3 would become 0.06 μsec, showing the same trend as observed with the other systems, namely, that the experimental lifetime is longer than the calculated lifetime.

CONCLUSIONS

The overall kinetic behavior of pulsed reactors is well represented by the point kinetics model though it is often necessary to simplify more-complex parameters by converting them to an equivalent point kinetics version. The usual assumption of nearly linear temperature coefficient is inadequate if a high proportion of the feedback is Doppler. Nevertheless, in a system such as VIPER, relatively simple basic calculations of the expected temperature coefficient which is partly expansion and partly Doppler agree with the experimentally observed coefficient to within 10 to 15%.

When the pulse is very fast, inertial effects must be considered. Relatively simple single-oscillator models appear to predict qualitatively the variation of overall yield in a burst with reactivity insertion. Although yield calculations can be made to fit the observed behavior by suitably choosing the inertial time constant, few direct comparisons of the precise stress and displacement patterns with realistic elastic models have been made. Using the approximate expression for the yield increase due to inertia $(1 + \alpha^2 t_0^2)$, the effect of a 10% change in time constant corresponds to a 20% increase in yield when the inertia effect is large (typically, the maximum value of $1 + \alpha^2 t_0^2$ is 7 to 8). Stress calculations which ultimately set a limit to the burst yield require a much more detailed treatment of the mechanical features of the core geometry, and, though yield calculations may be accurate to within 20 to 30%, it is not valid to assume equal accuracy of stress calculation in these much simplified models.

Although calculation methods for prompt kinetics are in general satisfactory, detailed comparisons suggest that many calculations of neutron lifetime tend to predict shorter lifetimes than are observed, in some cases by as much as 30%. Minor but significant differences appear between the one-point kinetics parameter β/τ derived (1) from super-prompt pulses and (2) from Rossi-alpha and pulsed-alpha

measurements near delayed critical. The treatment of low-energy neutrons, which has little effect on the critical size, does affect lifetime calculations but is not tested by comparing measured with calculated critical masses. The point reactor model, which is known to be an inadequate representation of certain reflected-core systems from Rossi-alpha and pulsed-alpha measurements, may also be unrealistic in describing prompt kinetics.

Finally, indications are that the satisfactory agreement in basic delayed-neutron data for small ^{235}U- and ^{239}Pu-fueled systems, such as the Los Alamos critical reactors, applies also to other burst reactors though minor adjustments may be necessary to obtain a satisfactory set of parameters to use in the inhour equations. However, new measurements of the delayed fraction in ^{238}U, though not claiming high accuracy, are 20% higher than previous values, and this larger value gives better consistency in predicting the reactivity scale in systems particularly sensitive to delayed neutrons from ^{238}U.

REFERENCES

1. T. F. Wimett and J. D. Orndoff, Applications of Godiva II Neutron Pulses, in *Proceedings of the Second United Nations International Conference on the Peaceful Uses of Atomic Energy, Geneva, 1958,* Vol. 10, pp. 449-460, United Nations, New York, 1958.
2. T. F. Wimett, R. H. White, W. R. Stratton, and D. P. Wood, Godiva II Unmoderated Pulse Irradiation Reactor, *Nucl. Sci. Eng.,* 8: 691-708 (1960).
3. G. R. Keepin, *Physics of Nuclear Kinetics,* Addison–Wesley Publishing Company, Inc., Reading, Mass., 1965.
4. J. W. Weale, H. Goodfellow, M. H. McTaggart, and E. G. Warnke, The Fast Pulsed Reactor VIPER. Part I–General Description, *J. Brit. Nucl. Energy Soc.,* 7(4): 313-327 (1968).
5. M. H. McTaggart, H. Goodfellow, W. B. McCormick, and J. W. Weale, The Fast Pulsed Reactor VIPER. Part II–Reactor Physics Measurements and Analysis, *J. Brit. Nucl. Energy Soc.,* 7(4): 328-342 (1968).
6. A. Brickstock and A. R. Davies, RKSF — A Reactor Kinetics Code for the IBM 7030, British Report AWRE-0-4/66, 1966.
7. J. Randles, Accident and Self-Regulation Studies of Pulsed Fast Reactors, *J. Nucl. Energy, Parts A and B,* 20: 713-728 (1966).
8. O. C. Kolar and N. Pruvost, CONEC — A Coupled Neutronic-Elasticity Theory Code and Its Application to Pulsed Fast Reactors, USAEC Report UCRL 6798, Lawrence Radiation Laboratory, 1962.
9. V. F. Kolesov, The Dynamics of a Spherically Symmetric Pulsed Fast Reactor, *At. Energ. (USSR),* 14(3): 273-280 (1963).
10. V. F. Kolesov, *Inzh.-Fiz. Zh,* 14: 134-137 (1968).
11. H. A. Kurstedt, Jr., and A. H. Kazi, Analysis of the Inertial Effect on Fast Pulse Reactor Behavior, *Trans. Amer. Nucl. Soc.,* 11(1): 219 (1968).
12. J. A. Reuscher, Dynamic Mechanical Characteristics of the Sandia Pulsed Reactor II, *Trans. Amer. Nucl. Soc.,* 11(1): 220-221 (1968).
13. R. L. Coats and P. D. O'Brien, Pulse Characteristics of Sandia Pulsed Reactor II, *Trans. Amer. Nucl. Soc.,* 11(1): 219-220 (1968).
14. J. Randles, Feedback Due to Elastic Waves and Doppler Coefficient During the Excursions of a Pulsed Fast Reactor, *J. Nucl. Energy, Parts A and B,* 20: 1-16 (1966).

15. R. L. Coats, Neutron Kinetics of a Reflected Fast Burst Reactor, USAEC Report SC-RR-67-802, Sandia Corporation, 1967.
16. J. W. Weale, W. J. Paterson, H. Goodfellow, and M. H. McTaggart, Measurements of the Prompt Neutron Decay Constant of the VERA Reactor Using the Pulsed Source Methods, in *Pulsed Neutron Research*, Symposium Proceedings, Karlsruhe, 1965, pp. 759-774, International Atomic Energy Agency, Vienna, 1965 (STI/PUB/104).
17. A. Bergstroem, B. Brunfelter, J. Kockum, and S. Soederberg, Pulsed-Source, Rossi-α, and Variance-to-mean Measurements Performed at the FRO Reactor, in *Proceedings of the International Conference on Fast Critical Experiments and Their Analysis*, Argonne National Laboratory, Oct. 10-13, 1966, USAEC Report ANL-7320, pp. 694-704, 1966.
18. G. S. Brunson and R. J. Huber, Precision Pulsed Measurements with Reflected Fast Critical Assemblies, in *Proceedings of the International Conference on Fast Critical Experiments and Their Analysis*, Argonne National Laboratory, Oct. 10-13, 1966, USAEC Report ANL-7320, pp. 706-713, 1966.
19. G. E. Hansen, Status of Computational and Experimental Correlations for Los Alamos Fast-Neutron Critical Assemblies. in *Physics of Fast and Intermediate Reactors*, Symposium Proceedings, Vienna, 1961, Vol. 1, pp. 445-455, International Atomic Energy Agency, Vienna, 1962 (STI/PUB/49).
20. J. Codd, Atomic Energy Establishment, Winfrith, private communication, 1968.
21. M. H. McTaggart, H. Goodfellow, W. J. Paterson, and J. W. Weale, Uranium-Fueled VERA Reactor Experiments, British Report AWRE-R-5/66, 1966.
22. C. F. Masters, M. M. Thorpe, and D. B. Smith, Measurement of Absolute Delayed-Neutron Yields from 14-MeV Fission, *Trans. Amer. Nucl. Soc.*, 11(1): 179 (1968).
23. E. D. Pendlebury, Atomic Weapons Research Establishment, Aldermaston, private communication, 1968.

DISCUSSION

KEEPIN: There are, of course, the neutron importance or effectiveness factors which must be multiplied by delayed-neutron yields or delayed-neutron fraction values entering into kinetics calculations or reactivity-worth calculations. Due to uncertainties in delayed-neutron-group spectra, cross sections, etc., this is still a significant source of error, not large perhaps, but until it is resolved, I do not know that we can make as detailed a comparison as we would like to in the case of Mr. McTaggart's very fine work.

McTAGGART: Perhaps I could just say that some work has been done in this field by Mr. Codd at Winfrith. The effects of differing delayed-neutron spectra have been looked into, and changes of the order of 5% can be produced by rather extreme variations in the spectra. In our view this is not sufficient to explain these 20 or 30% changes, but I agree there is need for improved spectra.

BRUNSON: You showed a table listing various critical assemblies, and until we reached the last three entries, we had a rather consistent

variation between the calculated and the measured lifetimes; but for VERA 1B the discrepancy was much smaller, for VERA 5A there was no discrepancy at all, and for VERA 7A the discrepancy was in the other direction. How do you account for this? We have looked at a number of assemblies, too, and we have seen what you were seeing on the first entries in the table.

McTAGGART: We included these VERA assemblies because these are recent results. The agreement there is good because we have altered the method of using some low-energy nuclear data to force agreement between the measured spectra and the calculated spectra in these systems at low energies. These measurements are recent time-of-flight results. I hesitate to give too much importance to this data because what we have done in these calculations is not entirely justified. We have used methods of heterogeneity correction, which are valid at very low energies, up to much higher neutron energy. This produces more low-energy neutrons. When the calculation agrees with our measured spectra, we have used it to calculate lifetimes. In these cases, as you pointed out, the agreement is quite good.

BRUNSON: Is there a difference in the reflector between the 1B, the 5A, and the 7A?

McTAGGART: VERA core 1B is a fairly fast system consisting of a ^{235}U graphite core and a natural-uranium reflector. Cores 5A and 7A are also ^{235}U fueled but both contain hydrogen. Core 7A contains ^{238}U, but 5A does not. They all have a natural-uranium reflector.

1·3 THERMOMECHANICAL ANALYSIS
OF FAST BURST REACTORS

J. A. REUSCHER
Sandia Laboratories, Sandia Corporation, Albuquerque, New Mexico

ABSTRACT

Various methods for calculating the thermomechanical effects of rapid heating on the core of a fast burst reactor are reviewed, and some comparisons between theory and experiment are provided. The narrow power pulse causes the temperature of the core to rise faster than the fuel material can respond by thermal expansion. A small portion of the thermal energy becomes kinetic energy, causing the core to vibrate and inducing large dynamic stresses in the fuel material. In addition to the determination of stresses for evaluating fuel integrity, it is important to calculate displacements since the movement of the core surfaces determines the burst characteristics of the reactor.

Both one- and two-dimensional calculational techniques based on linear thermoelasticity are discussed and compared with experimental measurements.

The operational mode of a fast burst reactor induces severe stresses on the fuel material. The energy generated during the narrow power pulse causes the temperature of the core to rise faster than the fuel material can respond by thermal expansion. A small portion of the thermal energy is converted into kinetic energy, causing the core to vibrate; this vibration, in turn, creates dynamic stresses. The motion imparted to the core can be simply explained by the following arguments. The lag in expansion during the temperature rise initially causes compression of the fuel. Since the fuel mass is unrestrained over the majority of its surface, the initial compression, together with the increasing temperature, causes the core to expand. After termination of the burst, the total temperature rise is achieved, and the core expansion reaches its maximum value. The dynamic expansion of the core exceeds the static expansion that would result if the fuel were heated slowly; the elastic properties of the fuel material cause the core to contract to a minimum expansion which is below

51

the static value. Expansion and contraction continue at the natural vibrational frequency of the core until material damping eliminates the oscillations, and the final magnitude of the expansions is the static value. These dynamic effects disappear within a few milliseconds after the burst, during which time heat transfer within the core is negligible.

The oscillations of the core produce large dynamic stresses in the fuel components. In several instances these induced stresses have been of sufficient magnitude to cause fuel-component damage and even reactor disassembly.[1-3,14] Conventional thermal-stress analysis cannot be used to calculate the stresses induced in a fast burst reactor core because the time to achieve the temperature rise is of the same order of magnitude as the natural vibrational period of the core. This means that the effect of mass inertia must be included in the calculations. In addition to the determination of stresses for evaluation of fuel integrity, it is important to calculate the displacements since the movement of the core surfaces determines the burst characteristics of the reactor.

SURVEY OF CALCULATIONAL TECHNIQUES

Techniques for calculating dynamic thermoelasticity must include the effect of mass inertia; however, heat transfer in the core can be neglected because the dynamic effects of interest occur before any appreciable conduction can change the initial temperature distribution. The dynamic thermoelastic equations must also be coupled with the neutron kinetic equations to describe properly the time history of the power and therefore the time dependence of the temperature rise in the fuel. In this paper the neutron kinetic problem will be ignored, and attention will be fixed on the methods for calculating the displacements and stresses using a temperature-rise function which approximates the time-dependent integral of the pulse profile. Thermal-stress analysis for fast burst reactors can be divided into two general categories according to the number of spatial directions that are included in the analysis.

One-Dimensional Analyses

Burgreen[4-6] has written several papers concerned with the thermoelastic dynamics of fast burst reactor components. His method treats the reactor core as a rod and replaces the temperature-induced stresses with equivalent body forces, surface tractions, and internal pressures. The temperature is assumed uniform; so no temperature gradients exist, and internal points of stress-wave initiation are thus eliminated. Plane-wave propagation starts only at the free ends of the

rod. Burgreen[4] also analyzes the behavior of thin cylindrical and spherical shells and solid spheres. By applying the method of equivalent loads to a segmented rod, Burgreen[5,6] derived expressions for the velocity of separation of the various axial segments and an expression for the peak bolt stress.

An analysis of a bolted fuel assembly using a mass-spring model shows good agreement with the equivalent-load method. Austin[7] studied the dynamic response of thin nested spherical shells subjected to rapid and uniform heating. This analysis provided for heating of only the innermost shell; a plastic outer shell with an elastic inner shell was also considered. The work of both Burgreen and Austin showed that the amplitude of the dynamic stress in a rapidly heated body is dependent upon the ratio of the heating time to the natural vibrational period and also upon the magnitude of the temperature rise. This can be illustrated by Burgreen's results for a spherical or cylindrical shell[4] as shown in Fig. 1.
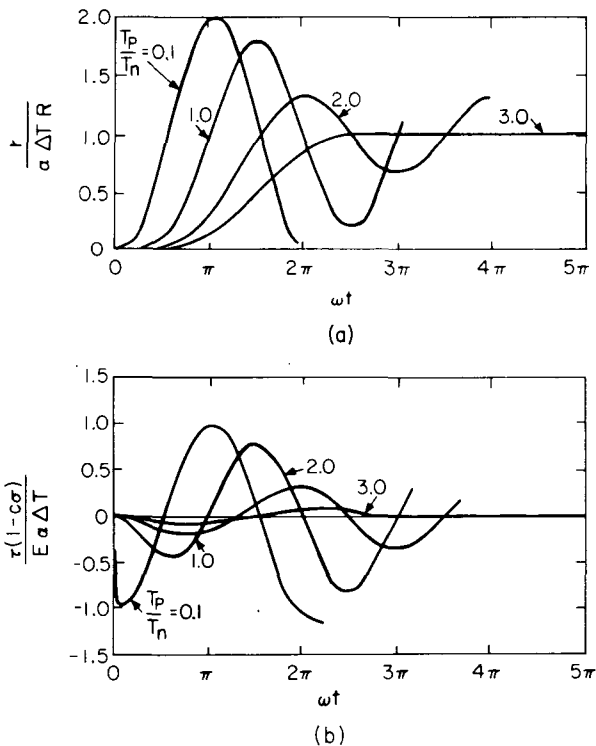

Fig. 1—Effect of rapid and uniform heating on a cylindrical or spherical shell. (a) Radial expansion of spherical or cylindrical shell. (b) Stress oscillation in shell.

The upper curve shows the normalized radial displacement of the shell, $r/\alpha \, \Delta T \, R$, where r = radial displacement, α = thermal expansion coefficient, ΔT = temperature increase, and R = mean radius, plotted as a function of ωt, where t = time and ω = vibrational frequency defined by

$$\omega = \frac{1}{R} \sqrt{\frac{E}{\rho}} \qquad \text{for a cylindrical shell}$$

and

$$\omega = \frac{1}{R} \sqrt{\frac{2E}{(1 - \sigma)\rho}} \qquad \text{for a spherical shell}$$

The symbol E = modulus of elasticity, ρ = density, and σ = Poisson's ratio. The ratio of heating time to vibrational period, T_p/T_n, is given as a parameter and determines the magnitude of the displacement oscillations. The curves oscillate about the static expansion where $r/\alpha \, \Delta T \, R = 1.0$; and for $T_p/T_n = 3$ there are no dynamic effects. The lower curve shows the normalized stress in the shell, $T(1 - c\sigma)/E\alpha \, \Delta T$, where T = stress, $c = 0$ for a cylindrical shell, and $c = 1$ for a spherical shell, for the same ratios of T_p/T_n. The stress shows initial compression and then oscillates into tension, the magnitudes depending upon T_p/T_n. For a ratio of $T_p/T_n = 3$, there is very little stress in the shell.

One-dimensional calculational techniques employed at Sandia Laboratories use a numerical solution of the dynamic thermoelastic displacement equation in cylindrical, spherical, and slab geometry. For an infinite cylinder with the temperature rise a function of radius and time, the displacement equation is

$$\frac{\partial^2 u}{\partial r^2} + \frac{1}{r} \frac{\partial u}{\partial r} - \frac{u}{r^2} - \frac{(1 + \sigma)}{(1 - \sigma)} \alpha \frac{\partial T}{\partial r} = \frac{1}{c^2} \frac{\partial^2 u}{\partial t^2} \tag{1}$$

where $u = u(r,t)$ = radial displacement component
   r = radial coordinate
   t = time coordinate
   c = speed of sound
   $c^2 = E(1 - \sigma)/[(1 + \sigma)(1 - 2\sigma)\rho]$
   σ = Poisson's ratio
   E = Young's modulus
   ρ = density
   α = thermal expansion coefficient
   $T = T(r,t)$ = temperature rise

This equation assumes that the elastic properties are time and temperature independent and that motion is restricted to the radial direction only. After this equation has been solved for the radial displacement component for a specified time and spatial variation of temperature, the stress components across the cylinder are calculated from

$$\tau_{rr}(r,t) = (2\mu + \lambda)\frac{\partial u}{\partial r} + \frac{\lambda u}{r} - (3\lambda + 2\mu)\ \alpha T(r,t) \tag{2}$$

$$\tau_{\theta\theta}(r,t) = \lambda\frac{\partial u}{\partial r} + (2\mu + \lambda)\frac{u}{r} - (3\lambda + 2\mu)\ \alpha T(r,t) \tag{3}$$

and

$$\tau_{zz}(r,t) = \lambda\left\{\frac{\partial u}{\partial r} + \frac{u}{r}\right\} - (3\lambda + 2\mu)\ \alpha T(r,t) \tag{4}$$

where τ_{rr} = radial stress component
$\tau_{\theta\theta}$ = tangential stress component
τ_{zz} = axial stress component
$\lambda = \sigma E/[(1 + \sigma)(1 - 2\sigma)]$
$\mu = E/[2(1 + \sigma)]$

The form of the displacement equation in spherical geometry with angular symmetry is

$$\frac{\partial^2 u}{\partial r^2} + \frac{2}{r}\frac{\partial u}{\partial r} - \frac{2u}{r^2} - \frac{(1 + \sigma)}{(1 - \sigma)}\ \alpha\frac{\partial T}{\partial r} = \frac{1}{c^2}\frac{\partial^2 u}{\partial t^2} \tag{5}$$

where the symbols are as defined previously. After this equation has been solved in the same manner as described for the cylindrical case, the stress components are found from

$$\tau_{rr}(r,t) = (2\mu + \lambda)\frac{\partial u}{\partial r} + \lambda\frac{u}{r} - (3\lambda + 2\mu)\ \alpha T(r,t) \tag{6}$$

$$\tau_{\theta\theta}(r,t) = \tau_{\phi\phi}(r,t)$$

$$= \lambda\frac{\partial u}{\partial r} + (2\mu + \lambda)\frac{u}{r} - (3\lambda + 2\mu)\ \alpha T(r,t) \tag{7}$$

where $\tau_{\theta\theta} = \tau_{\phi\phi}$ = tangential stress component.

Certain initial and boundary conditions must be used in the solution of Eqs. 1 and 5. The initial condition specifies that the body is at rest at zero time or that the displacement components across the body are all zero:

$$u(r,0) = 0 \qquad \text{for all } r \text{ at } t = 0$$

If the proper boundary conditions are chosen, Eqs. 1 and 5 can be solved either for a solid or a hollow cylinder or sphere. For a solid body the proper boundary conditions state that there is no movement or displacement of the center and the outer surface is free to expand, i.e., there is no pressure imposed on the outer surface:

$$u(0,t) = 0 \qquad \text{at the center of the body } (r = 0)$$

$$\tau_{rr}(R_o,t) = 0 \qquad \text{at the outer surface of the body } (r = R_o)$$

For a hollow body the boundary conditions consider both inside and outside boundaries as free surfaces; so no pressure is imposed on those surfaces:

$$\tau_{rr}(R_i,t) = 0 \qquad \text{at the inside surface } (r = R_i)$$

$$\tau_{rr}(R_o,t) = 0 \qquad \text{at the outside surface } (r = R_o)$$

The form of the displacement equation for rectangular geometry with only x-direction dependence is

$$\frac{\partial^2 u}{\partial x^2} - \frac{(1 + \sigma)}{(1 - \sigma)}\, \alpha\, \frac{\partial T}{\partial x} = \frac{1}{c^2}\frac{\partial^2 u}{\partial t^2} \tag{8}$$

where x is the rectangular coordinate and the other symbols are as previously defined. After this equation has been solved for the displacements, $u(x)$, the stress components are calculated from

$$\tau_{xx}(x,t) = (2\mu + \lambda)\,\frac{\partial u}{\partial x} - (3\lambda + 2\mu)\,\alpha T(x,t) \tag{9}$$

$$\tau_{zz}(x,t) = \tau_{yy}(x,t) = \lambda\,\frac{\partial u}{\partial x} - (3\lambda + 2\mu)\,\alpha T(x,t) \tag{10}$$

where τ_{xx} = x-stress component, τ_{yy} = y-stress component, and τ_{zz} = z-stress component.

Since the body is assumed to be initially at rest,

$$u(x,0) = 0 \qquad \text{for all x at t = 0}$$

The surfaces of the rectangular or slab body are free to expand; so the following boundary conditions must be used in the solution of Eq. 8:

$$\tau_{xx}(0,t) = 0 \qquad \text{at one free surface (x = 0)}$$

$$\tau_{xx}(L,t) = 0 \qquad \text{at the other free surface (x = L)}$$

The method used in the numerical solution of Eqs. 1, 5, and 8 employs an explicit finite-difference analog of these partial differential equations. The one-dimensional body is subdivided into space points, and the interior values of the displacements are determined explicitly. At the boundaries the displacements are calculated using the boundary conditions written in backward or forward differences, depending on whether the surface is an outside or inside boundary. After the displacements have been calculated across the body, the stress components are determined from finite-difference forms of Eqs. 2, 3, and 4; Eqs. 6 and 7; or Eqs. 9 and 10. Some results typical of these calculations are shown in Figs. 2 and 3 using Eq. 1 for a burst with a maximum temperature rise of 420°C and a width of 41μsec. The fuel component is a plate[12] in the Sandia Pulsed Reactor II (SPR II), and the material properties are those of uranium−10 wt.% molybdenum (see R. M. Jefferson, Session 2, Paper 3). The time and spatial variations of temperature are shown in Fig. 2, where the upper curve shows the time variation of the temperature rise at the glory hole and outer surfaces and the lower curve gives the spatial variation of the temperature which was inferred from the measured radial neutron-flux distribution. Figure 3 gives both the time variation of the glory hole and outer surface expansions and the dynamic hoop stresses at these surfaces. The one-dimensional theory shows quite clearly that the critical stress region is at the glory hole surface where the maximum dynamic tensile stress occurs. The plate oscillates with a natural vibrational period of 130 μsec, and expansion peaks correspond to peak tensile stresses. No damping is included in the calculations; so the magnitude of the oscillations does not diminish with time.

The magnitude of the calculated displacements and stresses is sensitive to the function used to describe the temperature rise. Several different functions have been suggested to approximate the temperature rise during a burst. The simplest function is a ramp temperature rise, where the time variation is given by two functions

$$T(t) = T_{max} \left(\frac{t}{T_p}\right) \qquad \text{for } 0 \leq t \leq T_p$$

(11)

$$T(t) = T_{max} \qquad \text{for } t > T_p$$

where T_{max} = maximum temperature rise, t = time, and T_p = heating time.

The ramp function gives too fast a temperature rise initially and toward the end of the burst and too slow a rise otherwise. A function
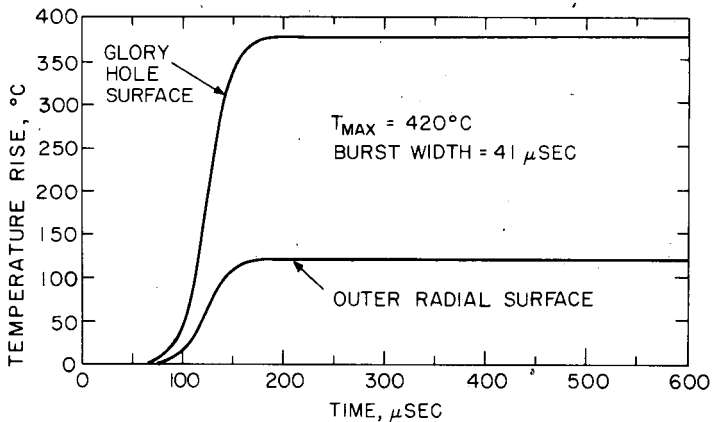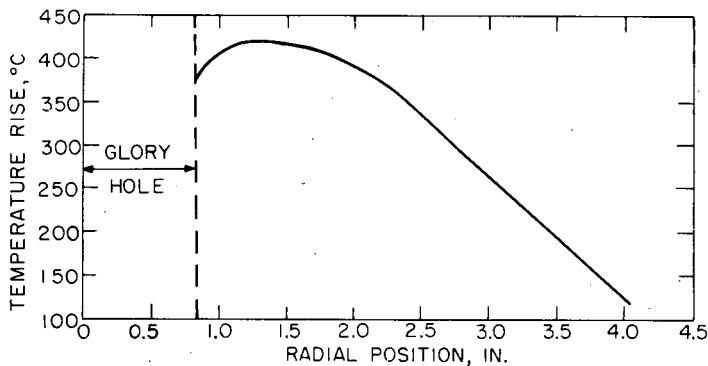
Fig. 2—Space and time variation of temperature for one-dimensional calculations. (a) Time variation of temperature rise. (b) Temperature distribution across SPR II plate.

that better approximates a burst is[4]

$$T(t) = \frac{T_{max}}{2}\left[1 - \cos\left(\frac{\pi t}{T_p}\right)\right] \qquad \text{for } 0 \le t \le T_p$$

$$T(t) = T_{max} \qquad \text{for } t > T_p$$

(12)

Since the proper temperature rise should be proportional to the integral of the power pulse, an even better function to describe the time variation of the temperature rise is

$$T(t) = \frac{T_{max}}{\exp\left[-\frac{3.52}{b}\left(t - \frac{T_p}{2}\right)\right] + 1}$$

(13)
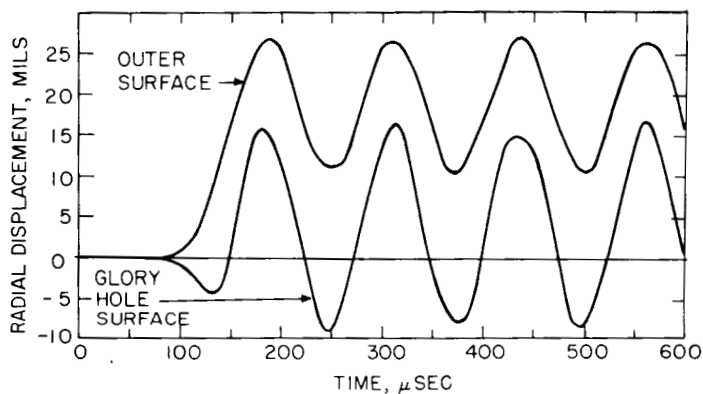
(a)
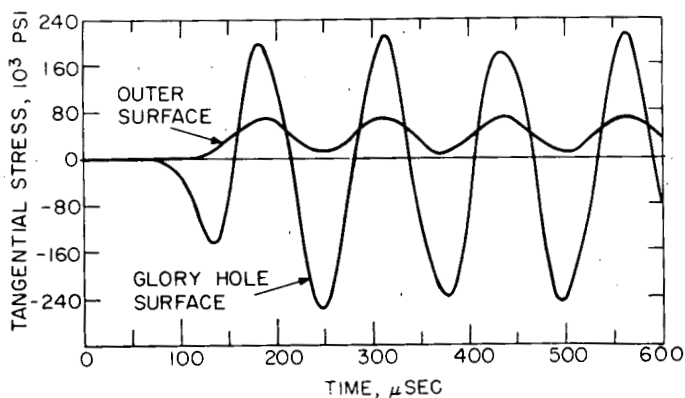
(b)

Fig. 3—Results of one-dimensional calculations for SPR II fuel plate.

for all values of time, where b = width of the pulse at one-half maximum power and the peak power is reached in time $T_p/2$. This last expression is an integration of the symmetric power pulse given by Wimett et al.,[8] normalized to the maximum temperature rise. These three functions are compared in Fig. 4, and the calculated displacements using these functions are compared in Fig. 5 for a SPR II plate
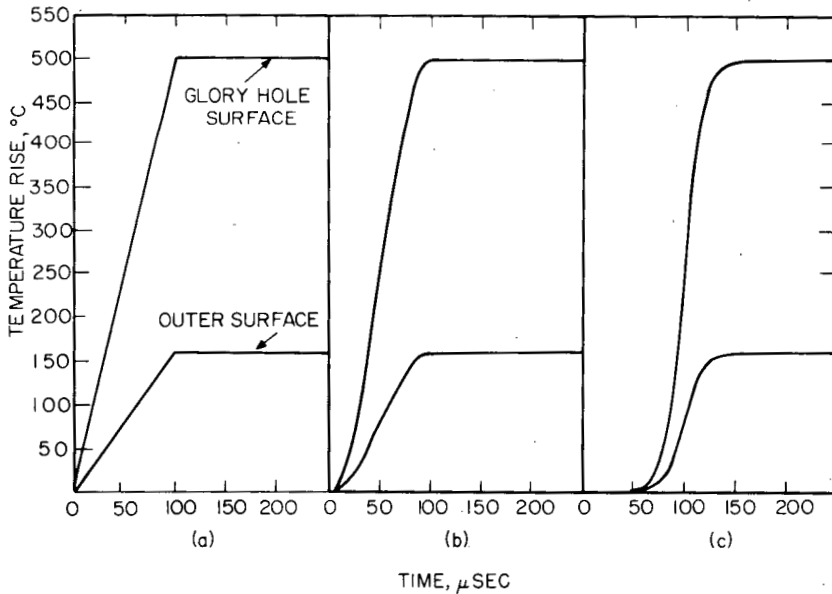
Fig. 4 — *Comparison of temperature-rise functions. (a) Ramp function. (b) Cosine function. (c) Burst integral function.*

with the spatial variation shown in Fig. 2. The displacements calculated using Eq. 13 are larger than those obtained using Eqs. 11 and 12. The calculated maximum values of tensile stress for these three functions are compared in Table 1.

Table 1 COMPARISON OF CALCULATED MAXIMUM TENSILE STRESS VALUES		
Temperature function	Glory hole surface, psi	Outer surface, psi
Ramp	85,000	70,000
Cosine	230,000	85,000
Burst integral	320,000	110,000
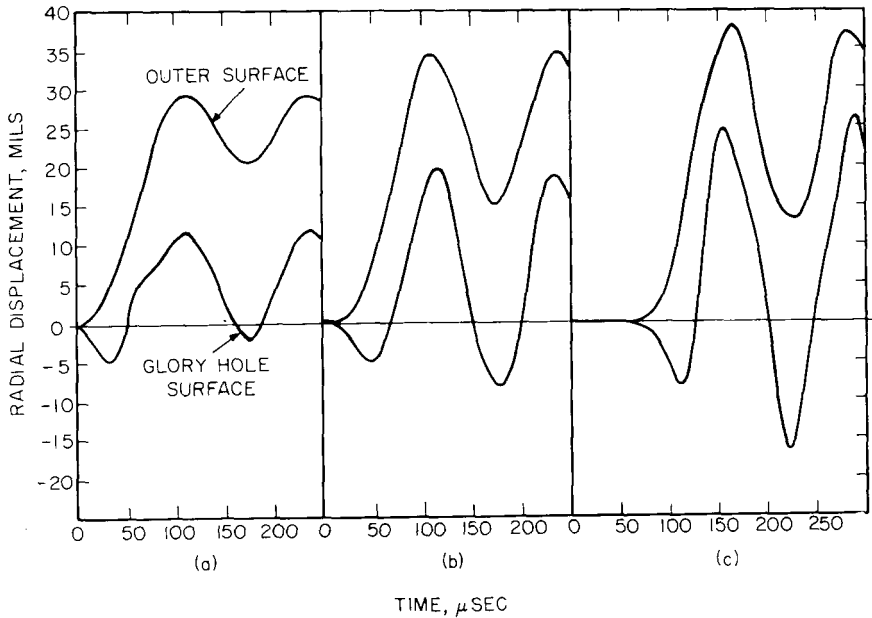
Fig. 5 — *Comparison of calculated displacements using three temperature-rise functions. (a) Ramp function. (b) Cosine function. (c) Burst integral function.*

The temperature rise calculated from Eq. 13 gives a greater rate of temperature rise and therefore larger dynamic stresses than the cosine function of the ramp function for the same maximum temperature rise and heating time. Experimental measurements and calculated values using one-dimensional analysis will be compared later in this paper.

Two-Dimensional Analyses

The one-dimensional calculations restrict expansion to a single direction and, as a consequence, tend to overestimate the magnitude of displacements and stresses. A two-dimensional calculation allows motion in two directions but is considerably more complicated than the one-dimensional analysis. Since fast burst reactors are generally cylindrical, the dynamic thermoelastic displacement equations in cylindrical geometry with angular symmetry are:

$$(2\mu + \lambda) \left(\frac{\partial^2 u}{\partial r^2} + \frac{1}{r} \frac{\partial u}{\partial r} - \frac{u}{r^2} \right) + \mu \frac{\partial^2 u}{\partial z^2} + (\lambda + \mu) \frac{\partial^2 v}{\partial r \partial z}$$

$$- (3\lambda + 2\mu) \alpha \frac{\partial T}{\partial r} = \rho \frac{\partial^2 u}{\partial t^2} \quad (14)$$

and

$$\mu\left(\frac{\partial^2 v}{\partial r^2} + \frac{1}{r}\frac{\partial v}{\partial r}\right) + (2\mu + \lambda)\frac{\partial^2 v}{\partial z^2} + (\lambda + \mu)\left(\frac{\partial^2 u}{\partial r \partial z} + \frac{1}{r}\frac{\partial u}{\partial z}\right)$$

$$- (3\lambda + 2\mu)\,\alpha\,\frac{\partial T}{\partial z} = \rho\,\frac{\partial^2 v}{\partial t^2} \qquad (15)$$

where u = radial displacement component, v = axial displacement component, z = axial coordinate, T = T(r,z,t) = temperature, and all other terms are as previously defined. After these equations have been solved for the displacements for a specified time and spatial variation of temperature, the stress components throughout the cylinder are

$$\tau_{rr} = (\lambda + 2\mu)\frac{\partial u}{\partial r} + \lambda\left(\frac{u}{r} + \frac{\partial v}{\partial z}\right) - (3\lambda + 2\mu)\alpha T \qquad (16)$$

$$\tau_{\theta\theta} = (\lambda + 2\mu)\frac{u}{r} + \lambda\left(\frac{\partial u}{\partial r} + \frac{\partial v}{\partial z}\right) - (3\lambda + 2\mu)\alpha T \qquad (17)$$

$$\tau_{zz} = (\lambda + 2\mu)\frac{\partial v}{\partial z} + \lambda\left(\frac{\partial u}{\partial r} + \frac{u}{r}\right) - (3\lambda + 2\mu)\alpha T \qquad (18)$$

$$\tau_{rz} = \mu\left(\frac{\partial u}{\partial z} + \frac{\partial v}{\partial r}\right) \qquad (19)$$

where these are the radial, tangential, axial, and shear-stress components, respectively.

The initial conditions for the solution of Eqs. 14 and 15 specify the cylinder to be at rest at zero time or the displacement components all to be zero:

$$u(r,z,0) = 0 \qquad \text{for all r and z at } t = 0$$

$$v(r,z,0) = 0 \qquad \text{for all r and z at } t = 0$$

The form of the boundary conditions used in solving Eqs. 14 and 15 determines whether the solution is for a hollow or solid finite cylinder. For a solid cylinder the following conditions must be satisfied:

$$u(0,z,t) = 0 \qquad \text{along the center of the cylinder } (r = 0)$$

$$\frac{\partial v(0,z,t)}{\partial r} = 0 \qquad \text{along the center of the cylinder } (r = 0)$$

$$\tau_{rr}(R_o,z,t) = 0 \qquad \text{along the outer radial boundary } (r = R_o)$$

$\tau_{rz}(R_o, z, t) = 0$ along the outer radial boundary $(r = R_o)$

$\tau_{zz}(r, 0, t) = \tau_{zz}(r, L, t) = 0$ along both axial boundaries $(z = 0; z = L)$

$\tau_{rz}(r, 0, t) = \tau_{rz}(r, L, t) = 0$ along both axial boundaries $(z = 0; z = L)$

For a hollow cylinder the first two boundary conditions are replaced by

$\tau_{rr}(R_i, z, t) = 0$ along inner radial boundary $(r = R_i)$

$\tau_{rz}(R_i, z, t) = 0$ along inner radial boundary $(r = R_i)$

and the other boundary conditions remain the same. These conditions specify that the cylinder surfaces have no imposed normal and shear stresses and are thus free to expand.

A finite-difference scheme[15] is used to solve Eqs. 14 and 15. An explicit-difference analog of these equations is used to obtain interior values of u and v and radial boundary values of the displacements. For satisfying radial boundary conditions, values of u and v are calculated at fictitious points outside the radial boundaries from a finite-difference form of Eqs. 16 and 19. For the axial boundaries or the ends of the cylinder, the displacements are determined from a simultaneous solution of finite-difference forms of Eqs. 17 and 18.

Two-dimensional analyses have been used for long solid rods in which the length is about 10 times the diameter and for hollow cylinders in which the length approximately equals the outside diameter. The rod calculations are theoretical support for a fuel-alloy study being conducted at Sandia Laboratories. The hollow-cylinder calculations simulate the behavior of the SPR II.

Results of a solid-cylinder calculation are shown in Fig. 6 for a uranium–10 wt.% molybdenum rod with a length of 10 in. and a diameter of 0.67 in. The temperature distribution for the rod is uniform across the radius and varies with rod length such that the maximum of 560°C occurs at the rod center $(z = 5$ in.$)$ and the minimum of 160°C occurs at the rod ends. The temperature rise is calculated using Eq. 13 with a burst width of 33 μsec, and the material properties are those of a uranium−10 wt.% molybdenum alloy. Figure 6 gives the axial expansion of both ends of the rod and the outer radial expansion at the center of the rod. The axial stress at the center of the rod is the maximum stress and is also shown in Fig. 6. Since the radial inertia is not important in the rod, the radial expansion follows the temperature rise, reaching a maximum first; and then the axial expansion reaches its maximum producing the peak tensile stress. The stress at the center oscillates between tension and compression as the rod expands and contracts.
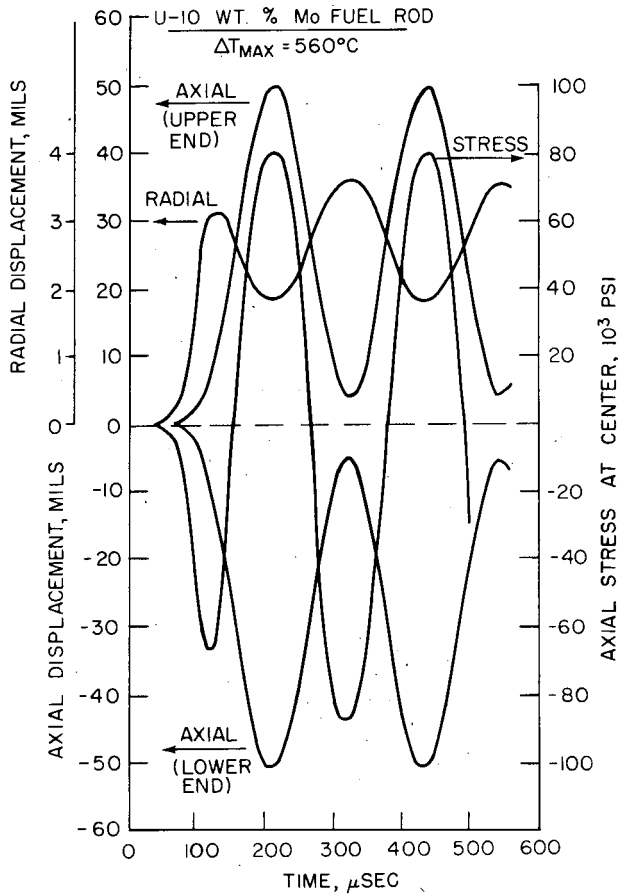
Fig. 6 — *Results of two-dimensional calculations for a solid cylinder.*

Results of a hollow-cylinder calculation are given in Fig. 7 for the upper half of SPR II, which has an outside radius of 4.039 in., an inside radius of 0.825 in., and a length of 4.1 in. The cylinder material is uranium − 10 wt.% molybdenum, and the temperature varies throughout the cylinder as the measured neutron flux. The temperature rise is calculated using Eq. 13 with a maximum of 489°C and a burst width of 38 μsec. This figure shows the dynamic axial expansion of a point at the average radius on both the top and bottom of the cylinder. Negative expansion is in the negative direction of the coordinate system, or downward. The radial expansions of the outside and glory hole surfaces at a point located at one-half the length are also shown; negative expansions are inward. These curves show that the expansion peaks in the axial direction correspond to expansion
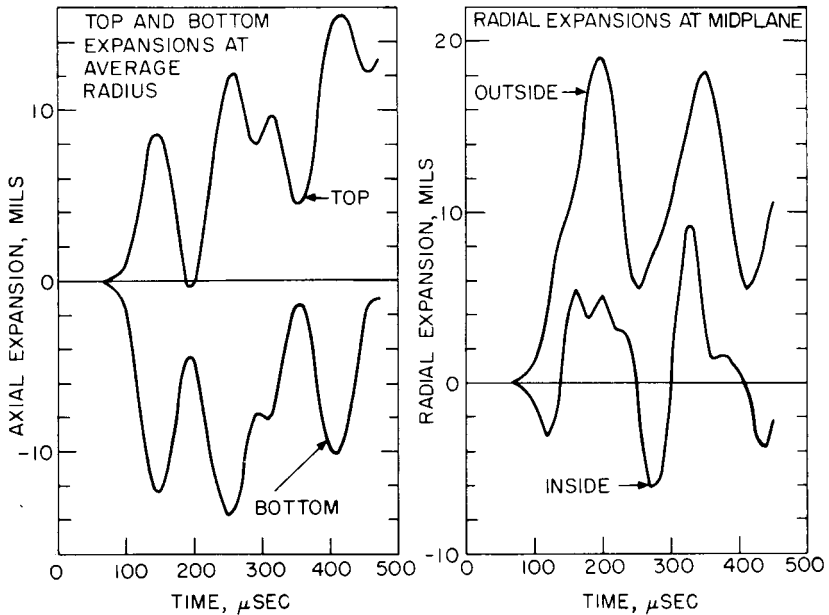
Fig. 7—Results of two-dimensional calculations for a hollow cylinder (upper half of SPR II).

valleys in the radial direction. Likewise, peaks in the radial direction correspond to valleys in the axial direction. The predominant vibrational period of 160 μsec for the radius and 110 μsec for the axis are shown, as well as higher vibrational periods along the glory hole.

Comparison Between One-Dimensional and Two-Dimensional Analyses

The numerical solution of two-dimensional equations is more complex and requires from 10 to 20 times more computer time than the solution of one-dimensional equations. However, this increased expense is justified because two-dimensional calculations produce more-accurate results. A comparison between the two different analyses for a solid rod and a hollow cylinder is given in Table 2. The one-dimensional rod calculations used a solution of Eq. 8, and the results of a two-dimensional calculation for the rod have already been shown in Fig. 6. The one-dimensional (1-D) results give twice the expansion, almost four times the stress, and about a one-third-smaller vibrational period than the two-dimensional (2-D) results. The hollow-cylinder comparisons are made for the conditions of a burst with a 560°C temperature rise and a width of 33 μsec, using the

Table 2

COMPARISON BETWEEN ONE- AND TWO-DIMENSIONAL CALCULATIONS

Geometry	Maximum expansion, mils		Maximum tensile, stress, psi		Oscillation period, μsec	
	1-D	2-D	1-D	2-D	1-D	2-D
Rod	110	50	310,000	80,000	170	230
Hollow cylinder						
Outside radius	38	27	100,000	77,000	130	170
Inside radius	24.5	12.5	320,000	140,000		

dimensions of SPR II. As was the case for the rod problem, the one-dimensional results show larger expansions and stresses and a smaller period than the two-dimensional calculations. Since the one-dimensional calculations inherently limit motion to only one direction, they should overestimate the stress magnitudes achieved in practice. Hence, the two-dimensional analysis should be used as a more accurate method of determining dynamic thermoelastic expansions and stresses. This will be further demonstrated in a later section of the paper by comparing calculations with experiment.

COMPARISON OF CALCULATIONAL TECHNIQUES
WITH EXPERIMENTAL MEASUREMENTS

None of the theoretical treatments described previously are really meaningful without confirmation from experimental data. Considerable investigation has been made into the mechanical behavior of fast burst reactors.[3,9-10] In general, these investigations have involved observing the displacement of fuel surfaces with transducers and measuring stresses induced in structural members during burst operation with strain gauges.

Efforts to compare the theoretical analyses of Burgreen and Austin with experimental data have not been extensive. However, some comparisons are available using Burgreen's analysis from published design stresses[11] and measurements conducted during a test to failure on the Army Pulsed Radiation Facility Reactor (APRFR).[1,10] The calculated and measured bolt stresses are shown in Fig. 8, and the average fuel-plate stress and the measured outer-surface hoop stress are shown in Fig. 9 as a function of reactor yield. The theoretical numbers are about 5000 psi higher than experimental for bolt stress and 15,000 psi higher for the fuel assembly. The measured stresses were not the maximum stresses that occurred across the fuel plate since these maximum stresses probably occurred at the inside radial
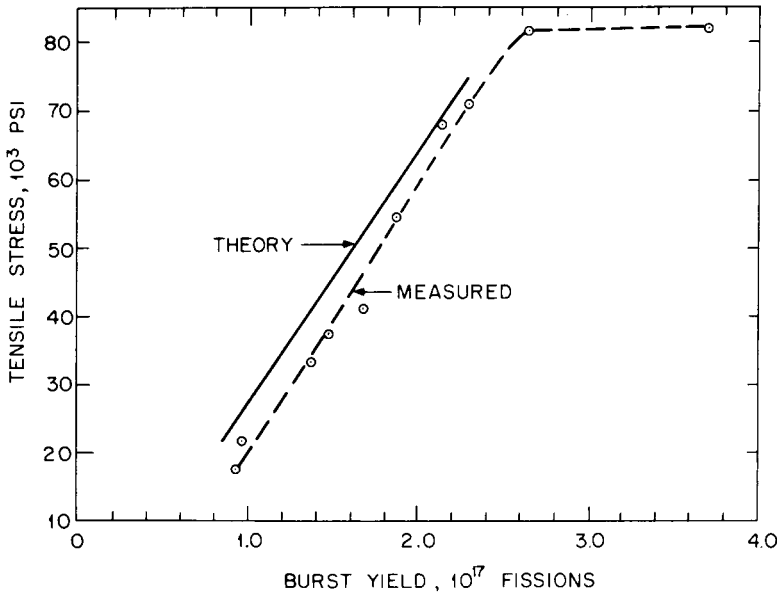
Fig. 8 — *Comparison between theoretical and measured bolt stress in the APRFR.*
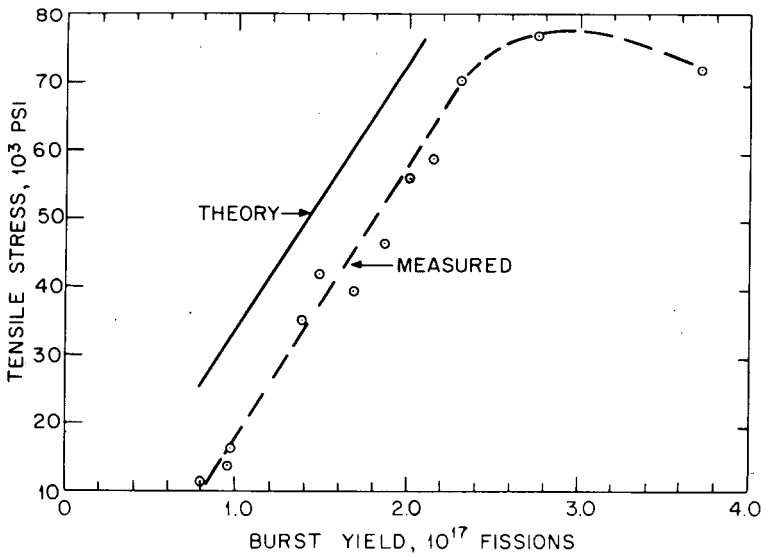
Fig. 9 — *Comparison between theoretical and measured hoop stress in the APRFR.*

surface where measurements could not be made. Therefore average stresses in the plate would be greater than those measured at the outer surface.

As in the comparison between the one- and two-dimensional analyses, the one-dimensional calculations tend to overestimate measured displacements. Figure 10 compares one-dimensional calculations and measurements for the outside surface and glory hole surface
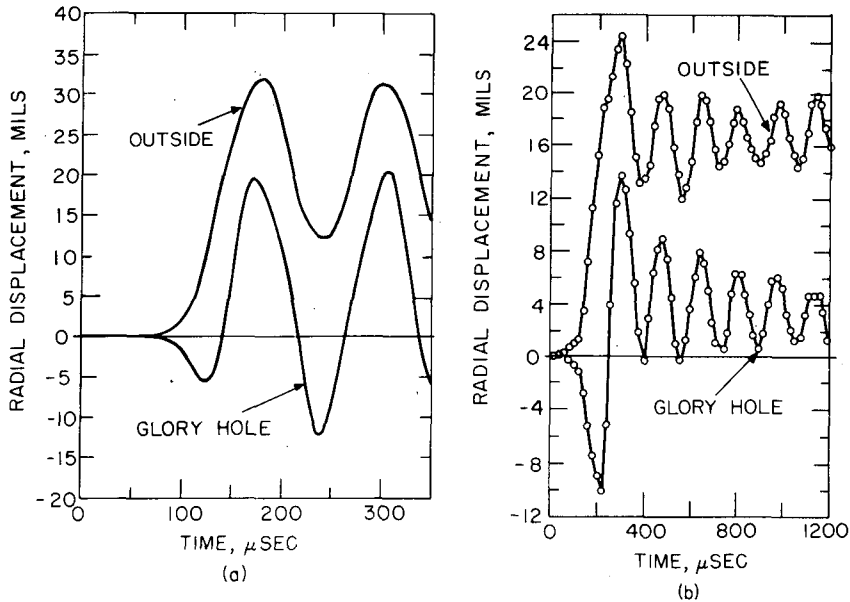
Fig. 10—Comparison between one-dimensional calculations and expansion measurements on SPR II. (a) Calculated displacements. (b) Measured displacements.

displacements of the central core plate of SPR II (0.825-in. inside radius; 4.039-in. outside radius) for a burst with a maximum temperature rise of 509°C and a width at one-half maximum of 38 μsec. The calculations used Eq. 13 for the temperature rise and produced a maximum outside expansion of 32.3 mils and a maximum glory hole expansion of 19.6 mils. The time between oscillation peaks of 130 μsec is the natural vibrational period of the plate. The experimental data for the plate show a maximum outside expansion of 24.5 mils and a maximum glory hole expansion of 13.8 mils; however, the experimental vibrational period is about 170 μsec. Thus, the calculations overestimate the peak outside expansion by about 31% and the peak inner expansion by about 42%; the vibrational period is underdetermined by 31%.

The magnitudes of the experimental oscillations in Fig. 10 de-
crease because of internal damping in the fuel material; this phe-
nomenon is not included in the one-dimensional theory. The qualitative
agreement between theory and experiment is quite good. If the tem-
perature-rise function described by Eq. 12 is used in the calculations
instead of Eq. 13 for the same heating time, the agreement between
theory and experiment at the outside surface is considerably im-
proved, but the experimental glory hole expansions exceed the calcu-
lations by about 25%. The comparison between theory and experiment
using Eqs. 12 and 13 for the temperature rise is shown in Fig. 11 for
maximum radial expansion vs. peak temperature rise in the fuel plate.
From Fig. 11 we see that even though Eq. 13 gives a more accurate
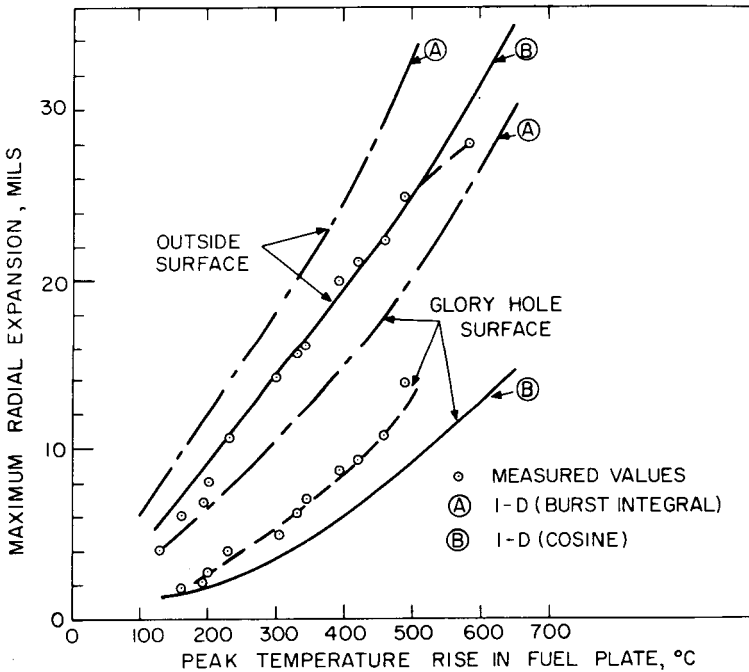
Fig. 11 — One-dimensional calculated and measured maximum radial expan-
sions of SPR II fuel plate.

description of the temperature rise during a burst, better agreement
between one-dimensional theory and experiment is achieved if Eq. 12
is used as the temperature-rise function. The agreement at the outside
radius is especially good. The presence of four control-rod holes
(0.938-in. in diameter) complicates the geometry and may account for
the larger measured glory hole expansions.

Some dynamic and static comparisons between experimentally de-termined displacements and two-dimensional calculations using Eqs. 14 and 15 are given in Figs. 12 and 13. The calculations were performed for the upper half of SPR II for a burst with a maximum temperature rise of 489°C and a width of 38 μsec, and the measurements were made on one of the central core plates. The calculated radial vibra-tional period of 170 μsec compares quite favorably with the measured period of 180 μsec. The outside surface expansions show fairly good agreement between theory and experiment with a difference of about
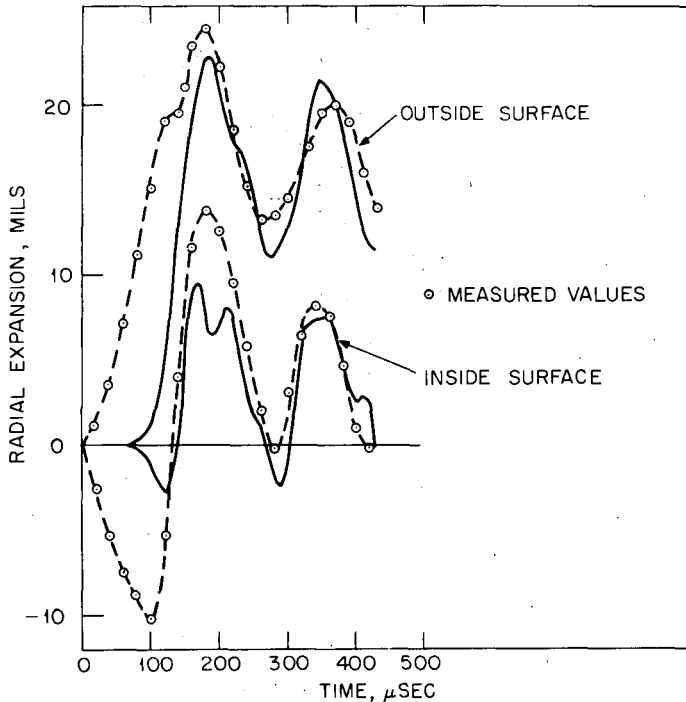
Fig. 12—Dynamic comparison between two-dimensional calculations and ex-periment for SPR II expansions.

1.5 mils at the peak expansions. The time scale for the measurements is normalized to the first expansion peak of the calculations. The initial disagreement between theory and experiment up to 120 μsec is probably due to the sensitivity of the transducers to the pulse radia-tion environment. Higher modes of oscillation are present in the calculations than are seen in the measurements owing to several factors. The transducers are unable to resolve the higher frequencies, and the data are obtained only for every 20 μsec, which would tend to

smooth out the higher modes. Also, the glory hole surface should behave more like a plate since there are gaps between adjacent fuel plates. A plate would not exhibit the higher vibrational modes. These calculations used the temperature-rise dependence of Eq. 13 and show surprisingly good agreement with measured displacements.

The maximum radial expansions are shown in Fig. 13 as a function of peak temperature rise in the fuel plate. The difference between experiment and the two-dimensional calculations is only 2 mils at the
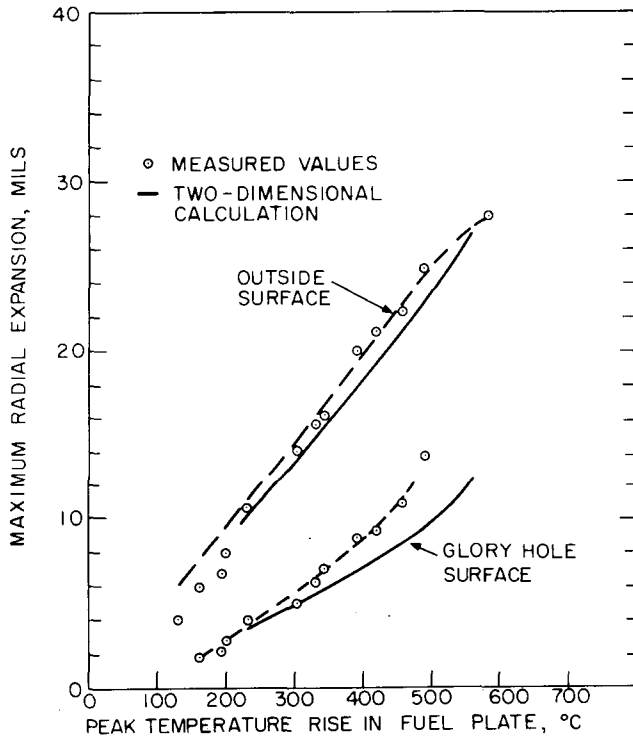
Fig. 13 — Two-dimensional calculated and measured maximum radial expansions of SPR II fuel plate.

outside surface. The discrepancy between experiment and theory at the glory hole gets larger as the temperature rise increases. However, the glory hole expansions are still calculated more accurately in Fig. 13 than with the one-dimensional analysis. The agreement between theory and experiment in Figs. 12 and 13 is excellent considering that the actual core geometry is considerably more complex than the right-circular cylinder used in the calculations.

CONCLUSION

The effect of temperature-dependent properties, such as modulus of elasticity and expansion coefficient, has been studied by including the temperature dependence of these quantities in the one-dimensional calculations. The displacements and vibrational periods calculated with temperature-varying properties showed poorer agreement with experiment than did the calculations with temperature-independent properties. Hence, all the calculations are performed using the material properties measured at room temperature. The true behavior of these properties under conditions of rapid heating and loading is unknown.

These thermoelastic analyses cannot predict when failure will occur in a fuel component. A conventional static failure criterion cannot be used because the fuel material is stronger under the dynamic loading conditions experienced in a fast burst reactor than under static loading conditions, as demonstrated by Hoge[13] for dynamic tensile testing of uranium−10 wt.% molybdenum samples. Failure stresses of about twice the static tensile stress were observed at strain rates of about 100 in./in./sec. Dynamic measurements conducted on the glory hole of SPR II have shown similar results. When the measured displacements are converted into stress, the maximum hoop stress can be determined as a function of burst yield. Stresses in the range from two to three times the static tensile strength at the temperature of the glory hole surface were observed without plate failure for strain rates of about 200 in./in./sec at temperatures of 500°C to 600°C. Thus, a failure criterion based on twice the static tensile strength appears reasonable in fast burst reactor design. Calculated stresses must exceed twice the ultimate tensile strength before the fuel component is considered to fail. However, data concerning the effect of rapid loading on tensile strength are available for only a limited number of fuel alloys. The ability of the environment around a fuel component to induce stress corrosion in the alloy can be a more serious limitation on the long-term performance of a fast burst reactor than simply the magnitude of the dynamic stresses.

This paper has discussed a variety of techniques for calculating dynamic displacements and stresses in a fast burst reactor. In general, the agreement between theory and experiment improves as the calculational procedure becomes more involved. The two-dimensional calculations provide the best agreement with measurements; however, the one-dimensional analyses have proven quite useful for parametric studies. With the proper temperature-rise function, the one-dimensional calculations can be made to fit measured maximum expansion values with reasonable accuracy as shown in Fig. 11.

ACKNOWLEDGMENT

REFERENCES

1. J. T. Mihalczo and J. A. Reuscher, Pulse Production Experiments with the Army Pulsed Radiation Facility Reactor, *Nucl. Sci. Eng.*, (to be published).
2. R. L. Long, Report of Reactor Excursion During Test of Modified Core, U. S. Army Test and Evaluation Command, White Sands Missile Range, N. Mex., July 1965.
3. J. A. Reuscher, Dynamic Mechanical Characteristics of the Sandia Pulsed Reactor II, *Trans. Amer. Nucl. Soc.*, 11: 220 (1968).
4. D. Burgreen, Thermoelastic Dynamics of Rods, Thin Shells, and Solid Spheres, *Nucl. Sci. Eng.*, 12: 203-217 (1962).
5. D. Burgreen, Thermoelastic Dynamics of a Bolted Pulse Reactor Assembly, Report UNC-AMR 65-560, United Nuclear Corp., June 30, 1965.
6. D. Burgreen, Thermoelastic Dynamics of a Pulse Reactor, *Nucl. Sci. Eng.*, 30: 317-327 (1967).
7. A. L. Austin, Thermally Induced Vibrations of Concentric Thin Spherical Shells, *Nucl. Sci. Eng.*, 20: 45-52 (1964).
8. T. F. Wimett, R. H. White, W. R. Stratton, and D. P. Wood, Godiva II — An Unmoderated Pulse-Irradiation Reactor, *Nucl. Sci. Eng.*, 8: 691-708 (1960).
9. J. M. Richter, Mechanical Shock Measurements on the White Sands Missile Range Fast Burst Reactor, Report USA TECOM Project 9-6-0067-00, Army Missile Test and Evaluation, White Sands Missile Range, N. Mex., October 1967.
10. J. A. Reuscher and J. M. Richter, Dynamic Mechanical Measurements on the Army Pulsed Radiation Facility Reactor, *Trans. Amer. Nucl. Soc.*, 10: 612 (1967).
11. R. W. Dickinson et al., Safety Analysis Report for Army Pulsed Radiation Facility Fast Pulse Reactor, USAEC Report BRL-R-1356, Aberdeen Proving Ground, February 1967.
12. R. L. Coats and P. D. O'Brien, Pulse Characteristics of the Sandia Pulsed Reactor II, *Trans. Amer. Nucl. Soc.*, 11: 219 (1968).
13. K. G. Hoge, Some Mechanical Properties of Uranium — 10 Wt.% Molybdenum Alloy Under Dynamic Tension Loads, USAEC Report UCRL-12357, Lawrence Radiation Laboratory, 1965.
14. W. R. Stratton, A Review of Criticality Accidents, in *Progress in Nuclear Energy, Technology, Engineering, and Safety,* Series IV, Vol. 3, Pergamon Press, Inc., New York, 1960.
15. J. A. Reuscher and M. R. Scott, Numerical Analysis of Two-Dimensional, Dynamic Thermal Stresses in a Hollow Cylinder, in The Effective Use of Computers in the Nuclear Industry, Symposium Proceedings, Knoxville, Tennessee, April 21—23, 1969, USAEC Report CONF-690401, pp. 542-560, 1969.

DISCUSSION

MILEY: I am curious about the spatial distribution of the temperature function. You used a uniform heating, which would seem to be somewhat of an approximation. Is the calculation sensitive to the spatial distribution as well as the time function?

REUSCHER: I did not mean to imply that I used a uniform temperature profile for any of the solutions in the paper; in fact, I forgot to mention that for the 2-D calculations in a hollow cylinder the spatial relation of the neutron flux in SPR II was used as the distribution of temperature with respect to space. If one assumes a uniform temperature profile across the SPR II plate just described and performs a one-dimensional calculation, the magnitude of the calculated displacements is roughly the same as that for a distributed temperature with the same average temperature rise. The stresses are different, however, because one has to subtract a temperature term from the strain terms that are determined from the displacement information. The result is that one calculates, in some cases, considerably different stress values. The effect of various temperature functions on the calculated values is discussed in the paper.

KURSTEDT: You said that the two-dimensional displacement solution gave you better agreement with experiment. Did the two-dimensional displacement formulation give you better accuracy in the neutronics solution?

REUSCHER: We have not really looked at the 2-D calculation coupled with the neutronics. I would expect it would give you much better results. We have coupled a point kinetics model with a one-dimensional calculation and been able, after adjusting certain parameters, to get a reasonable representation for the pulse although it overestimates the magnitude of the observed displacements. I would expect in taking the 2-D calculations and coupling them with a neutron kinetics problem that we would get reasonable and probably valid results.

KURSTEDT: It would seem to me, though, in calculating the power vs. time (or flux vs. time) that with the 2-D case you would just have that many more feedback coefficients to fit to experimental data, and point neutronics is sufficient for the fast burst reactor. With the 2-D displacement formulation, you would have two feedback coefficients resulting in a more difficult neutronics calculation. With a 1-D radial displacement formulation, the feedback is dependent only on radial displacement. The only problem in predicting the experimental results would be to determine the feedback coefficient. This would be quite sufficient for power calculations; but, of course, if a stress or displacement calculation is required, a two-dimensional analysis is quite necessary. The required information is the key to the necessary complexity of the displacement formulation.

REUSCHER: Hopefully, if you could describe the kinetics from a two-dimensional transport code, you would not have to use experimentally adjusted coefficients.

1-4 STATISTICS OF BURST OPERATION

GORDON E. HANSEN
University of California, Los Alamos Scientific Laboratory,
Los Alamos, New Mexico

SUMMARY

The probability distribution in burst yield or burst time following ramp or step reactivity insertion is determined by the probability, $P(n,t)$, of n neutrons at time t. Numerical programs[1-3] exist which give $P(n,t)$ in terms of initial neutron and precursor populations, source strength s, and system reproduction number $k(t)$. Analytic solutions by Bell[4] give $P(n,t)$ for a number of limiting cases. Three asymptotic forms of special interest to this paper apply to zero initial population, constant source, and $k(t \to \infty) > 1$; they are[4]

1. No delayed neutrons, $k(t)$ arbitrary, $\bar{n}(t)$ = mean neutron population at time t.

$$P(n,t)\, dn = \frac{(\eta n/\bar{n})^{\eta}}{(\eta - 1)!} \exp\left[-\eta n/\bar{n}\right] \frac{dn}{n}$$

where $\eta = 2sl/\bar{\nu}\Gamma_2$ and $\Gamma_2 = \overline{\nu(\nu - 1)}/\bar{\nu}^2$.

2. One precursor group, $k(t)$ constant with $(1 - \beta)$, $k = k_p > 1$, and $\eta n/\bar{n} < 1$.

$$P(n,t)\, dn = \frac{(\eta n/n)^{\eta}}{(\eta - 1)!} \exp\left[2\eta \alpha \beta \tau/(k - 1)\right] \frac{dn}{n}$$

where $\eta = 2sl(k-1)/\bar{\nu}\Gamma_2(k_p-1)$.

3. One precursor group, $k(t)$ constant with $k_p < 1$, and $\eta n/\bar{n} < 1$.

$$P(n,t)\, dn = \frac{(\eta n/n)^\eta}{(\eta-1)!} \exp\left[2\eta\alpha\tau\right]\frac{dn}{n}$$

where $\eta = 2s(1-k_p)/\bar{\nu}\Gamma_2$.

Quite generally, the condition $k(t \to \infty) > 1$ yields the asymptotic form $P(n,t)\, dn = f(n/\bar{n})dn/\bar{n}$ seen previously. This merely implies that sample populations eventually follow the kinetics equation $dn/n\, dt = d\bar{n}/\bar{n}\, dt = \alpha(t)$. The probability that the neutron population is n at t in dt is thus $P(n,t)n\alpha(t)\, dt$.

For Dragon-type bursts, i.e., bursts produced by specified reactivity transients $k(t)$, the probability distribution in, say, peak power is given directly by $P(n,t_f)\, dn$ where t_f is the time at which $k(t)$ drops past unity. For a self-quenching burst, the reactivity is a specified function of time only until the neutron population reaches a magnitude sufficient to produce feedback; by this time, however, the neutron population is already following the kinetics equation, and the future of $n(t)$ is determined completely by the initial condition $n(t_0) = n_0 \gg 1$. The probability distribution in burst yield $E(t_0)$ or burst time $t(t_0)$ is then given by the probability distribution in initial conditions, $P(n_0,t_0)\, n_0\alpha(t_0)\, dt_0$. For example, the ramp $k(t) = 1 + at$ applied to a system whose kinetics equation is

$$\frac{dn}{dt} = \left(at - b \int_{-\infty}^{t} n\,\frac{dt'}{l}\right)\frac{n}{l} + S$$

results in a burst yield $E(t_0) \simeq E(t_1)\left[1 + a(t_0^2 - t_1^2)/l \ln (2a^3l/\pi b^2 s^2)\right]^{\frac{1}{2}}$, where t_1 is the time at which the mean neutron population $\bar{n}(t)$ reaches the fiducial value n_0. With $n_0/n(t_0) = \exp\left[-a(t_0^2 - t_1^2)/2l\right]$, one then has $P(n_0,t_0)n_0\alpha(t_0)\, dt_0 = \left[\eta^\eta/(\eta-1)!\right]\exp\left[-\eta a(t^2 - t_0^2)/2l\right]\exp\left\{-\eta\exp\left[-a(t_0^2 - t_1^2)/2l\right]\right\}at_0\, dt_0/l$. For a source-strength parameter $\eta > 1$, the mean value of the burst yield approaches $E(t_1)$, and the mean square deviation is small. Enriched-uranium-metal systems can have η values of the order 10^{-6}, and here mean burst yields[5] may exceed $E(t_1)$ by a factor $\sim \eta^{-\frac{1}{2}}$.

REFERENCES

1. G. I. Bell, W. A. Anderson, and D. Galbraith, Probability Distribution of Neutrons and Precursors in Multiplying Medium, Part II, *Nucl. Sci. Eng.*, 16: 118-123 (1963).
2. H. Hurwitz, Jr., D. B. MacMillan, J. H. Smith, and M. L. Storm, Kinetics of Low Source Reactor Start-ups, Part I, *Nucl. Sci. Eng.*, 15: 166-186 (1963).
3. H. Hurwitz, Jr., D. B. MacMillan, J. H. Smith, and M. L. Storm, Kinetics of Low Source Reactor Start-ups, Part II, *Nucl. Sci. Eng.*, 15: 187-196 (1963).
4. G. I. Bell, Probability Distribution of Neutrons and Precursors in a Multiplying Assembly, *Ann. Phys. (N. Y.)*, 21: 243 (1963).
5. G. E. Hansen, Assembly of Fissionable Material in the Presence of a Weak Neutron Source, *Nucl. Sci. Eng.*, 8: 709-719 (1960).

Fast
Burst
Reactor
Design

Session 2

2-1 HISTORY AND DEVELOPMENT OF FAST BURST REACTORS 1944–1965

DAVID P. WOOD,* PAUL D. O'BRIEN,† and THOMAS F. WIMETT‡
*Albuquerque Operations Office, U. S. Atomic Energy Commission, Albuquerque,
New Mexico; †Sandia Corporation, Albuquerque, New Mexico; ‡University of
California, Los Alamos Scientific Laboratory, Los Alamos, New Mexico

ABSTRACT

A brief history of the development of fast burst reactors during the period
1944–1964 is given, including comments on a reactor built in the Soviet Union
and the eight fast burst reactors built and operated in the United States. Prac-
tical applications of fast burst reactors, their origin, physical characteristics,
modes of operation, and limitations are discussed.

This paper reviews the history and development of fast burst reactors
from 1944 to 1965. Practical applications of fast burst reactors, their
origin, physical characteristics including shutdown mechanisms, modes
of operation, and limitations are covered.

PRACTICAL APPLICATIONS

A fast burst reactor, the laboratory facility that most nearly
simulates the radiation environment of an atomic weapon explosion,
is invaluable to scientific personnel who desire to study the transient
effects of the interaction of radiation with matter. These reactors
have also been employed[1] for (1) basic studies of the fission process,
i.e., the measurement of delayed-neutron and gamma characteristics;
(2) radiation dosimetry; (3) calibration of radiation alarms for crit-
icality accidents; and (4) radiobiology.

ORIGIN OF FAST BURST REACTORS

The Dragon[2] reactor is the first known nonexplosive fissile system
or reactor whose reactivity exceeded (by intent) prompt critical.

This controlled supercritical condition was reached Jan. 8, 1945, at Los Alamos Scientific Laboratory (LASL); the fuel-temperature rise is quoted as 0.001°C, and the yield is estimated to have been about 2×10^{11} fissions.

The Dragon reactor was made prompt critical for about 0.01 sec when a slug of fissionable material was dropped through a vertical hole in the core, which consisted of variable amounts of UH_{10} reflected with beryllia or diluted with polyethylene. The Dragon operated only 25 days, during which 537 successful drops were made.

The concept of a reactor operating from prompt neutrons was further stimulated by the unplanned excursion[2,3] of a cylindrical, unreflected ^{235}U Jemima Assembly at the LASL critical-mass facility. The excursion produced approximately 1.5×10^{16} fissions. The system and the fissile material were not damaged, no one was irradiated, and the experimental area was not contaminated. The self-terminating property of this excursion stimulated modification of Godiva I for burst operations, and that assembly became the first facility for routinely generating large bursts of fission-spectrum neutrons in times less than 100 μsec.

The fast burst reactors developed during the two decades 1945–1965, often referred to as the first generation of fast burst reactors, logically fall into two groups, enriched-uranium and alloyed-uranium fast burst reactors. The characteristics of these two groups are described in the following sections.

ENRICHED-URANIUM FAST BURST REACTORS

Godiva I (Lady Godiva), Godiva II, KUKLA, SPR, and FRAN were constructed with enriched-uranium (93.5% ^{235}U) cores and control components.

Godiva I and II

Both Godiva assemblies (designed, built, and operated by person-nel of the LASL critical-mass facility) have been retired. These reac-tors and their operating equipment were housed in a remotely operated assembly building located about 1200 ft from the control room.

GODIVA I. The original Godiva[1,4] was built in 1951 for use as a bare critical assembly of simple geometry and in 1953 was modified to permit prompt critical burst operation. An unreflected assembly of ~53 kg of uranium, it was basically spherical, about 6.8 in. in diam-eter. Two horizontal parting planes permitted disassembly into three roughly equal sections for large shutdown effectiveness. The center section containing the irradiation port and control rods was fixed

in position by small tubular steel supports. The upper and lower sections, however, were retractable by means of pneumatic cylinders, and they provided the reactor with two independent scram mechanisms.

After a lengthy survey of characteristics, including behavior under super-prompt critical conditions, the principal function of Godiva I became the generation of short ($\sim$100 μsec) intense ($\sim$10^{16} neutrons) bursts for irradiation purposes. Measurement of the properties of delayed neutrons from various fissionable isotopes was probably the most important experimental use made of this assembly. After 6 years and over 1000 bursts, Godiva I was replaced by Godiva II.

GODIVA II. Godiva II[1,5] was the first metal reactor designed specifically for the routine production of fission bursts. Operated initially in June 1957, the assembly consisted essentially of the main section of annular rings, two control rods, a burst rod, and a safety block. The core geometry was a near-cylindrical version of Godiva I, and the fuel mass of the core was $\sim$57.7 kg of uranium.

For facilitating irradiation operations, the core was mounted on a small portable stand that housed all actuating machinery, control-element position sensors, and electrical interlocks. The three operating rods and the safety block entered the core from the bottom to provide the maximum available space around the core for sample irradiations. The safety block served two purposes: (1) it provided a large shutdown reactivity ($30) and (2) it served to partition the reactor along the radius in such a manner that shock waves originating at the center were prevented from reaching the surface of the stationary part, i.e., the natural period of mechanical vibration was thereby reduced. Reactivity adjustment was accomplished by two rods of about 1 kg each and one smaller 480-g rod. Near delayed critical reactivity was controlled by the small rod and one large rod, which permitted up to $2 reactivity correction to compensate for the tamping effect of nearby reflecting materials.

All exposed core surfaces except the safety block were nickel clad to control oxidation, and the three control rods were flashed with chromium over the nickel to ensure smooth operation in their close-fitting nickel-lined channels.

During the three years of Godiva II operation, about 2000 prompt bursts were produced without observable deterioration. The most extensive experimental program performed with this assembly was the study of prompt gammas from fission.

KUKLA

The KUKLA Prompt Critical Assembly,[1,6] designed and built by personnel of the Lawrence Radiation Laboratory (LRL), Livermore, Calif., in 1961, is an untamped spherical assembly fabricated from

approximately 60 kg of cast-uranium metal. It is mechanically supported from underneath to minimize the effects of neutron reflection from supports and associated equipment.

The cylindrical safety block, with a mass of ~7 kg, is the major scram component. Scram is accomplished by a pneumatic cylinder in 0.04 sec from the fully inserted position. Two control rods, each having a mass of 0.84 kg, are individually inserted during the adjustment to delayed critical. Neither rod is "fast scrammed" since the safety block and burst rod have sufficient reactivity worth to ensure shutdown.

The exposed uranium surfaces of KUKLA are nickel flashed with a nominal 0.5-mil coating to protect against surface oxidation and wear during operations and to limit contamination during handling. In addition to the nickel coating, the exterior surface of the sphere and the sides and bottom of the safety block have been plated with a 10- to 15-mil thickness of cadmium to reduce room-returned neutron effects.

After several years of successful operation at LRL, KUKLA operations were terminated. This reactor is presently used in Gulf General Atomic's APFA (Accelerator Pulsed Fast Assembly) accelerator-booster configuration. It has been modified so that prompt critical operation is no longer possible.

SPR

A second model of the Godiva II core, now identified as SPR,[1,7] was fabricated at LASL for operation in the Sandia Pulse Reactor Facility (SPRF) commencing in 1961. The cylindrical core is composed of 57.9 kg of uranium and is surrounded at a distance of ~1 cm by a perforated aluminum protective screen. The major departures from Godiva II design are: (1) an increase in the worth of control rods to a total of $3 in reactivity, (2) cadmium plating over nickel flashing, and (3) the modification of the safety-block drive mechanism. The purpose of the cadmium is to reduce neutron coupling with the variety of objects to be irradiated external to the reactor.

The reactor was mounted on a hydraulically operated elevator that lowered it into a concrete pit after operation. A 12-in.-thick lead radiation shield could slide over the pit to permit personnel entry into the building soon after a burst had been produced.

Probably the most unique features associated with this reactor were the various modes of operation developed to accommodate the diverse needs of experimenters. These modes will be discussed under Modes of Operation.

In May 1967, after 5600 operations, SPR was replaced by an advanced core design designated as SPR II. Presently, the SPR core

is being modified for use as a booster in the development of an accelerator-driven assembly.

FRAN

FRAN,[1,8] a fast burst reactor designed by LRL for operation at the Nevada Test Site (NTS) began operation in 1962. This reactor attempts to maximize the attainable burst yield in a pure uranium assembly and produces an estimated 5×10^{16} fissions/burst.

The major innovation is the mechanical arrangement for supporting the stationary fuel plates. In earlier designs, threshold damage produced by shock waves usually occurred in the bolts used to assemble the fuel rings. The uranium bolts generally used for this purpose yield first under shock produced by the power transient in the fuel plates. In the FRAN design clamping is accomplished externally by two $3/4$-in.-thick steel rings which overlap each end of the cylindrical stack of five annular fuel pieces. The plates are connected by six $3/4$-in. steel draw bolts located $\sim 1/2$ in. away from the fuel surface. In operation the steel support rings are capable of deflecting with a large effective spring constant when the fuel expands. Fuel-temperature rises approaching 350°C have been obtained on this assembly with limited permanent deformation in either the steel supports or fuel plates. Absence of greater deformation in the fuel is also attributed to less crystal-growth effect than experienced in earlier models, owing to finer uranium grain structures resulting from improved casting techniques.

To reserve the central core volume for a large annular sample irradiation void (4 in. deep, $1/2$ in. thick, and $3\frac{1}{8}$ in. OD), the designers mounted the bottom fuel disks ($\sim 1/5$ total mass) on a movable support to serve as the safety block. Control and burst rods necessarily enter the stationary section from above to avoid interference with safety-block motion. The safety block controls the largest rate of reactivity, i.e., about \$40/sec. The total mass is ~ 63 kg.

FRAN operations by LRL personnel at NTS were discontinued several years ago, and the reactor is presently being readied for operation at the National Reactor Testing Station, Idaho, in a program for developing improved nuclear instrumentation.

ALLOYED-URANIUM FAST BURST REACTORS

The second group of fast burst reactors is comprised of the Health Physics Research Reactor (HPRR), the White Sands Fast Burst Reactor (FBR), and the Super KUKLA, all of which have core and control-element components constructed of enriched uranium alloyed with 10 wt.% molybdenum.

This alloy was selected not only because it has excellent metal-
lurgical and chemical stability but also because under appropriate
heat treatment it develops higher tensile strength than that of uranium
by a factor of ~4 at room temperature.

Health Physics Research Reactor

The HPRR[9,10,11] was designed and constructed by Nuclear Develop-
ment Associates based on an Oak Ridge National Laboratory (ORNL)
conceptual design and with the support of critical experiments per-
formed by ORNL. It is the first fast burst reactor to depart from
an unalloyed-uranium-metal assembly.

This reactor was used initially in the BREN (Bare Reactor
Experiment Nevada) Operation at NTS from January to August 1962
and is presently housed in the DOSAR facility at ORNL.

Operation BREN was justified to support the Ichiban study under-
taken in 1956 to evaluate the radiation doses received by survivors
of the nuclear bombings of Hiroshima and Nagasaki, Japan, in 1945.
The HPRR was attached to a hoist platform on the 1500 ft tower at
NTS. The reactor was operated in the steady-state mode at a power
level of about 1 kw. During the second phase of the study, it was
pulsed, and the spectrum of the fission-produced gamma rays was
studied as a function of time after burst.

The core consists essentially of an annulus of uranium -10 wt.%
molybdenum enriched to 93.14% in ^{235}U, 8-in. OD, 2-in. ID, and 9 in.
high, surrounding a 2-in.-diameter stainless-steel central cylinder.
Attached to the steel cylinder is the 11.19-kg safety block, with an
outer diameter of ~3.5 in. and a height of 6.50 in. The basic uranium $-$
molybdenum assembly consists of a stack of annular disks held
together by nine uranium -10 wt.% molybdenum bolts which thread into
the bottom disk. The bolts are hollow to permit reactivity adjustment
with uranium $-$molybdenum plugs.

The disks are also penetrated by three holes to accommodate
the $\frac{5}{8}$-in.- and 1-in.-diameter control rods and the $\frac{3}{4}$-in.-diameter
burst rod. A $\frac{5}{16}$-in.-diameter hole serves as a sample irradiation
space.

The stationary section is suspended from above. The safety
block is a 3.5-in.-diameter fuel annulus threaded onto a steel center
plug, which in turn is threaded to a smaller diameter shaft extending
upward out of the core where it is magnetically coupled to an actuator
mechanism. For shutdown the safety block is driven out of a central
cavity at the bottom of the stationary section. The two control rods
and burst rod are actuated from above and enter the core from above.
All exposed uranium $-$molybdenum surfaces are nickel plated.

In preliminary operations of HPRR, burst yields in excess of 10^{17} fissions were readily obtained with a corresponding fuel-temperature rise of ~500°C; this may be considered a reasonable upper limit for routine operations because of the onset of uranium – molybdenum phase transformation at temperatures much beyond ~500°C.

The HPRR reactor generates tailless bursts of power pulses which are not followed by the ~1-Mw plateau typical of earlier Godiva assemblies. A shock-induced scram mechanism utilizes a phenomenon, first observed in Godiva I, whereby the safety block is ejected spontaneously as a result of the very rapid heating of the fuel. In the case of HPRR, the effective scram time is 225 μsec.

WSMR Fast Burst Reactor

The White Sands Missile Range (WSMR) Fast Burst Reactor (or Molly-G)[12] was designed and developed by Kaman Nuclear Corporation, with the exception of the core, which was designed by the WSMR engineering staff with consultation services supplied by LASL and Sandia Corporation. The core is similar to HPRR in its cylindrical shape and in the use of the uranium – 10 wt.% molybdenum alloy. Requirements for irradiation applications are satisfied by mounting the core on a small stand similar to that of SPR or Godiva II (thus its nickname "Molly-G" for molybdenum-alloy Godiva). The portable stand is normally fastened to a mechanical lift that lowers the assembly into a pit that may be covered by a shield (as in SPR) inside a large underground reactor building, or the assembly may be transported readily on a fork lift to an outdoor site for free-space experiments.

The core is 8 in. in diameter and $7\frac{5}{8}$ in. high with a 4-in.-diameter safety block surrounding a 1.25-in.-diameter stainless-steel core cylinder. Total weight of uranium – molybdenum is ~97 kg in this configuration. Reactivity is controlled by the usual two control rods and a burst rod (~$1.50 each); in addition, there is provision for manual adjustment of ~$1 by a mass adjustment or shim ring located at the top of the core. For example, a shim ring of iron adds about $1, whereas one of uranium – molybdenum adds about $3 in reactivity. The fuel rings are bolted together and to the support plate by $\frac{3}{4}$-in. bolts. Those bolts currently in use are made of a special high-strength nickel alloy, Inconel X, which exhibits a yield strength of ~180,000 psi.

During a preliminary series of bursts at LASL to establish limits for routine operation, the maximum burst-temperature increase observed on Molly-G was 480°C in the zone of peak power density. The resultant shock experienced by the assembly (Inconel) bolts exceeded the yield point, producing a net elongation of ~0.02 in. in each bolt. Similar observations were observed during the checkout of the HPRR.

In operation at WSMR, the core has produced ~2000 bursts of ~6 × 10^{16} fissions with peak fuel-temperature increases in the neighborhood of 250°C without observable damage. The shock-induced separation of the safety-block magnet produces an early scram similar to that described for HPRR operation.

Super KUKLA

Of the second group of uranium−molybdenum devices, Super KUKLA[13] has the largest and highest yield. The basic design was developed by LRL, and the assembly machine was constructed by the Baldwin-Lima-Hamilton Company with technical direction by LRL. The reactor, which went into operation in December 1964, is designed to serve as a prompt-irradiation source for a wide variety of samples, which may be exposed externally or in a large internal cavity.

The core structure is basically a cylindrical shell open at the top; it includes a cavity 18 in. in diameter and ~24 in. high. The wall thickness is 6 in. The height is variable and is nominally 37 in. at critical, with no reactivity perturbation in the cavity. The shell is composed of a stack of uranium−10 wt.% molybdenum alloy rings in which the uranium is enriched to 20%. Total fuel mass is ~5000 kg. The top of the cavity is reflected by a 6-in. tungsten disk attached to the sample container. Large critical-mass adjustments can be made by changing fuel disks at the bottom of the lower core half; minor adjustments are made by changing rod enrichment from 20% to 40%. For continuous control a gang of six shim rods operated individually or in combination enters the core from above and employs double-ballscrew actuators. A similar gang of six rods enters from below into the lower core half and is used as a burst rod by a double-action hydraulic cylinder. Reactor shutdown is accomplished by dropping the lower core half, which is also hydraulically actuated. Large telescoped cylindrical springs with extremely large spring constants are incorporated for vertical shock suppression in the fuel stacks.

The maximum temperature increase observed in preliminary operations is 140°C, which corresponds to a total yield of ~2 × 10^{18} fissions—by far the largest prompt burst yield obtained for repetitive systems. The design yield figure for this device is ~5 × 10^{18} fissions. Because of the relatively large pulse width (~700 μsec), no inertial shock effects have been experienced.

FAST NEUTRON BURST REACTOR (RUSSIAN)

The Fast Neutron Burst Reactor (IBR)[14], designed and built in Russia, is included in this paper for interest because of its unique

design and because it is the only known foreign-designed fast burst reactor that falls within the time frame under discussion.

The IBR, located at the Joint Institute for Nuclear Research at Dubna, U.S.S.R., achieved criticality in June 1960.

This burst reactor produces periodic pulses with an average power of about 6 kw for physical research, primarily for neutron time-of-flight experiments. The frequency of the bursts can be varied within the limits 8 to 80 bursts/sec; however, it can also be used for the production of large single bursts.

The bursts of power in the reactor are generated by a fast mechanical variation of its reactivity, during which periodic supercriticality of the reactor is attained. The half-width of the power burst is 36 μsec. During the remaining time the reactor is subcritical.

The singularity of the behavior of the IBR is that the value of the effective portion of delayed neutrons is very small. In normal operation of the reactor, it is $\sim 10^{-4}$, e.g., about a hundred times smaller than the corresponding value for the usual steady-state reactor with uranium fuel. This circumstance, of course, produces an especially high demand for precision of the regulating system.

The active zone of the IBR has a fixed part and two movable parts. The periodic change of reactivity of the system takes place as a result of the displacement of the movable parts, which consist of two bushings of ^{235}U mounted in two rotating members. The reactor becomes supercritical and the power bursts are developed only when the main and auxiliary bushings are simultaneously superposed with the fixed part of the active zone.

The stationary part of the active zone consists of plutonium rods in stainless-steel jackets. Each rod is fastened by a conical shank in the upper or lower lattice of the active zone. Single-ended fastening of the rods guarantees a negative temperature coefficient of reactivity.

The control system and reflectors provide the change of reactivity of the system during start-up operation, shutdown of the reactor, and control of the power level in all cycles of operation. For emergency shutdown two rods in the stationary part, suspended on electromagnets, are used.

A special apparatus, intended for the production of single power bursts (reactivity booster), is provided in the reactor.

MODES OF OPERATION

The two normal modes of operation for fast burst reactors are steady state and prompt burst. These are no unique features associated with the steady state; therefore only the burst mode is described.

Burst Mode

The procedure for the routine production of fission bursts for fast burst reactors, with the exceptions noted, is, first, establish the delayed critical configuration by a short low-level power run, next, retract the safety block for a period of several minutes to permit the delayed-neutron population to decay, and then reinsert the safety block. This step is followed by insertion of the burst rod, which rapidly boosts reactivity to the desired supercritical point. The resulting power excursion is quenched by thermal expansion of the fuel, and the residual plateau power level is terminated by automatic scramming of the reactor.

FRAN.   The sequence of burst operation for the FRAN reactor is modified as follows: the control rods are adjusted to place the reactor on a positive period corresponding to 30¢ above delayed critical; the safety block is removed for ~15 min to allow delayed-neutron precursors to decay; the burst rod worth 85¢ is inserted; and burst is initiated by insertion of the safety block.

SUPER KUKLA.   The burst-generation procedure followed in Super KUKLA operations differs in two aspects from the usual burst mode. First, the delayed critical operation is performed with the burst gang inserted; then the burst gang is withdrawn. The shim rods are adjusted so that insertion of the burst-rod gang leads to the desired reactivity; this adjustment is followed by insertion of the burst-rod gang. Second, the neutron source remains in place during the burst mode to reduce to a negligible level the probability of producing an oversized burst.

HPRR.   The burst sequence for the HPRR is as follows: after insertion of the safety block, the reactor is placed on a slightly positive period by proper adjustment of the regulating and mass adjustment rods (it has been determined by positive-period measurements that a period of ~95 sec gives the standard burst yield); the safety block is withdrawn to allow the delayed-neutron population to decay; and the burst is then initiated by inserting the safety block and firing the burst rod to its "in" position.

Other Modes

Two additional modes of operation, namely, square wave and tailless bursts, were developed for the SPR by P. D. O'Brien and his Sandia Corporation staff.

SQUARE WAVE.   This method of operation was developed to meet an experimental requirement for a higher gamma dose rate than

could be obtained with normal steady-state operation of SPR — or with any other available gamma source.

This method required operation of the SPR at a relatively high steady-state power for times on the order of tens of seconds. Ideally the power–time history of the reactor during these operations should approach a square wave.

The experimental requirement for fast rise time obviously implies short positive and stable reactor periods; a lower limit of 1 sec (e-folding period) was chosen as a goal to use only after considerable experience with the longer periods.

For operating at such short periods, the safety block was modified to permit its use as a control rod with a rate of reactivity control variable from 2.3¢ to 23¢/sec.

The normal sequence of operation to establish delayed critical was followed. The control rods were then withdrawn until the assembly was made 29¢ subcritical.

The normal burst sequence was followed, and, upon insertion of the burst rod, the reactor was supercritical by 78¢ and reactor power increased in a 1-sec period. The safety block was then withdrawn as the reactor approached the desired power level. This method gave better results than expected.

Neither SPR nor SPR II is now equipped for square-wave operation.

TAILLESS BURSTS.   In normal operation, burst reactors of the first series characteristically produce a prompt pulse in which the peak power is of the order of 10^4 Mw followed by a plateau level of the order of 0.5 Mw. The duration of the plateau depends upon the response time of the scram system; it is ~30 msec. Another characteristic of such reactors is the random variation in delay time, the interval between the attainment of maximum reactivity and the time of burst initiation. With no external neutron source, the mean delay time for Godiva II is ~3 sec and for SPR is ~80 msec. A technique of programmed burst initiation in SPR was developed to reduce the undesirable plateau and also to provide more precise and predictable timing of the power pulse. This technique introduces a short pulse of neutrons from a pulsed D–T generator at the instant maximum reactivity is attained. The plateau is shortened to a few milliseconds by preprogramming scram initiation, and the power pulse is predictable in time to an uncertainty of 1 to 2 μsec. The neutron source currently employed for this purpose, located about 8 ft from the reactor, generates 2×10^8 neutrons (14 Mev) in a 10-μsec pulse. This programming is unnecessary on later Godiva models whose designs incorporate the spontaneous shock-induced scram feature.

LIMITATIONS

Maximum burst yields in the enriched-uranium reactors generally are limited by fuel integrity during the severe shocks associated with the rapid temperature increases. Pure uranium metal, particularly as-cast uranium, is subject to surface roughening, anisotropic crystal growth, and creation of internal voids. Such effects were observed and were presumably caused by burst thermal cycling or irradiation, and they occurred for temperature rises (from ambient) of ~200°C — far below the melting point. Mechanical shock to structural members is also a limiting factor in most of the early burst machines, with the exception of FRAN as noted earlier.

Alloyed-uranium fast burst reactors maintain dimensional stability when subject to more extreme temperature cycles than can be tolerated with normal uranium metal. Extensive metallurgical tests on this type of burst reactor have indicated relatively small crystal growth and excellent phase stability during or following repeated large temperature cycles of ~500°C. However, this temperature cycle appears to be an operational limiting value based on LASL's tests on the WSMR Fast Burst Reactor described previously.

SUMMARY

This review of the history and development of fast burst reactors for a period of over two decades indicates that steady progress has occurred. Most of the developments are traceable to the national laboratories, but it is encouraging to see the wider use and development activities on fast burst reactors in other government and commercial organizations. Of the nine fast burst reactors discussed, seven are still in active use, which is good testimony to the important contributions they have made to a wide variety of scientific disciplines.

REFERENCES

1. T. F. Wimett, Fast Burst Reactors in the U.S.A., USAEC Report SM 62/53, Los Alamos Scientific Laboratory, 1965.
2. W. R. Stratton, A Review of Criticality Accidents, *Progress in Nuclear Energy*, Technology, Engineering, and Safety, Series IV, Vol. 3, Pergamon Press, Inc., New York, 1959.
3. E. C. Mallary, G. E. Hansen, G. A. Linenberger, and D. P. Wood, Neutron Burst from a Cylindrical Untamped Oy (Enriched U) Assembly, USAEC Report LA-1477, Los Alamos Scientific Laboratory, 1952.
4. R. E. Peterson and G. E. Newby, An Unreflected U-235 Critical Assembly, *Nucl. Sci. Eng.*, 8: 691 (1960).
5. T. F. Wimett, R. H. White, W. R. Stratton, and D. P. Wood, Godiva II — An Unmoderated Pulse-Irradiation Reactor, *Nucl. Sci. Eng.*, 8: 691 (1960).

6. E. R. Christie and B. W. Mar, The Kukla Prompt Critical Assembly, USAEC Report UCRL-6105, Lawrence Radiation Laboratory, 1960.
7. P. D. O'Brien, Hazards Evaluation of the Sandia Pulsed Reactor Facility (SPRF), USAEC Report SC-4357A(RR), Sandia Corp., 1961.
8. FRAN Prompt Burst Facility, Hazards Summary Report, USAEC Report COVA-711, Lawrence Radiation Laboratory, Mar. 21, 1962 (classified).
9. F. W. Sanders, F. F. Haywood, M. I. Lundin, L. W. Gilley, J. S. Cheka, and D. R. Ward, Operation Plan and Hazards Report-Operation BREN, USAEC Report CEX-62.02, Oak Ridge National Laboratory, April 1962, and Changes and Additions to Operation Plan and Hazards Report for Operation BREN, 1962.
10. J. T. Mihalczo, Superprompt-Critical Behavior of an Unmoderated, Un-reflected Uranium−Molybdenum-Alloy Reactor, *Nucl. Sci. Eng.*, 16: 291-298 (1963).
11. M. I. Lundin, Health Physics Research Reactor Hazards Summary, USAEC Report ORNL-3248, Oak Ridge National Laboratory, 1962.
12. Kay B. Carver, Preliminary Hazards Summary Report for the Molly-G Reactor, Report KN-63-685-11, Kaman Aircraft Corp., Nuclear Division, 1963.
13. W. S. Gilbert, F. A. Kloverstrom, and F. Rienecker, Jr., Safety Analysis Report for the Super Kukla Prompt Burst Reactor, USAEC Report UCRL-7695, Lawrence Radiation Laboratory, 1964.
14. G. E. Blokhin et al., A Fast Neutron Burst Reactor, *Atom. Energ.* (USSR), 10: 437-446 (1961), translated by H. J. Chick and T. F. Wimett, Los Alamos Scientific Laboratory.

2-2 GODIVA IV

THOMAS F. WIMETT, ROGER H. WHITE, and ROBERT G. WAGNER
University of California, Los Alamos Scientific Laboratory,
Los Alamos, New Mexico

ABSTRACT

Preliminary results obtained with a new fast burst assembly are presented. The fuel is U−1.5 wt.% Mo alloy. Assembly features include a new scheme for securing fuel components in the core.

INTRODUCTION

Performance of fast burst reactors has been limited in the past by physical damage due to mechanical shock rather than by more basic fuel limitations, such as high-temperature phase changes. For minimum burst duration, the fuel must be solid metal with the obvious restriction that cores cannot be cast on one piece because of criticality considerations. Accordingly, a typical core comprises six or more separate castings, with as many as nine bolts of fuel or high-strength alloy to secure them together. Burst-yield limitation in such assemblies usually is due to bolt elongation or thread loosening as a result of thermal expansion of the fuel.

The primary purpose of Godiva IV is to provide a flexible core and support assembly for use in a burst reactor design development program. Design emphasis has been focused on maximum power density and minimum burst duration. The use of the present system as an irradiation facility has received only minor consideration.

In the preliminary version of Godiva IV reported in this paper, special attention has been given to the severe mechanical shock problems. Core-component design and core geometry are being studied to minimize the transfer of shock energy to the supporting structure. The damage threshold for individual fuel pieces hopefully will be raised as a result of the investigation of various fuel alloys.

95

CORE DESIGN

The Godiva IV assembly and controls are shown in Fig. 1. The fuel, shown unshaded in Fig. 2, is a U−1.5 wt.% Mo alloy (the uranium is ~93.5% ^{235}U) with a general configuration similar to that of Godivas II and III. Fuel components are all aluminum-ion plated and have a total mass of ~66 kg. Three external C-shaped clamps, $\frac{3}{4}$ in. thick by
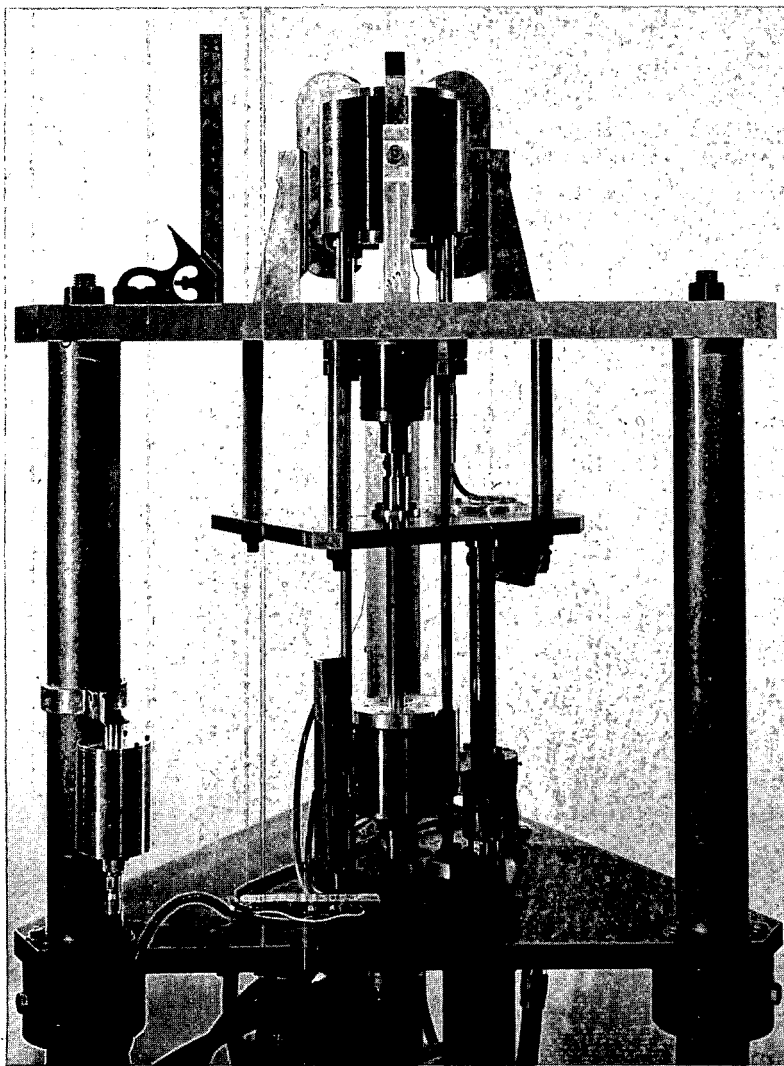
Fig. 1 — *First version of Godiva IV on three-legged support stand showing stationary ring assembly above the top shelf with safety block visible just below and the electromagnetic latching assembly above the bottom shelf.*
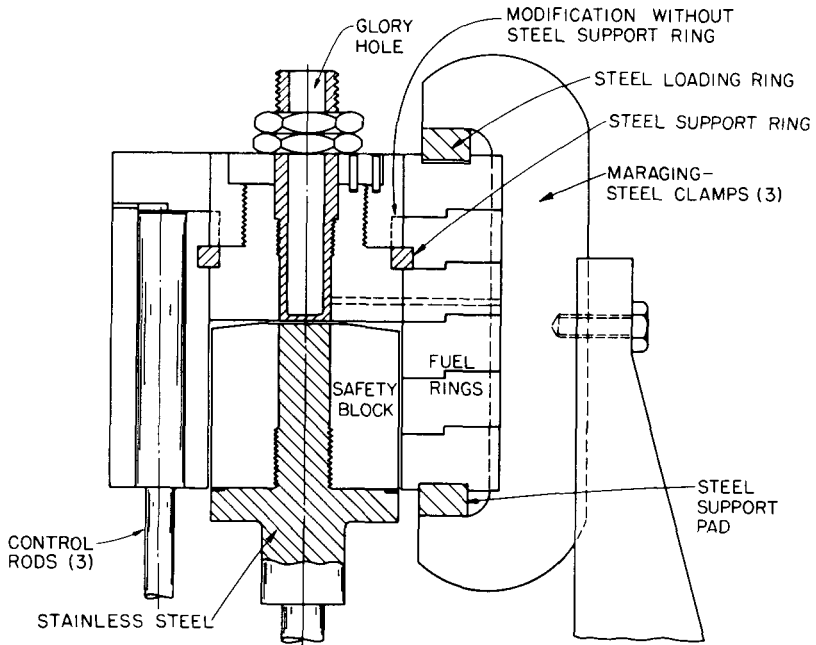
Fig. 2—Godiva IV core detail.

1$\frac{3}{4}$ in. wide, fabricated from high-strength maraging steel, fasten the stack of six stationary fuel rings.

The stationary assembly is bolted to vertical steel supports with the bolts threaded into the midpoint of each clamp. This center-of-shock mounting serves to minimize shocks imparted to the support stand. The central fuel pieces have been attached to the outer fuel cylinder by a split steel retaining ring, shown shaded in Fig. 2, and in a later modification by the second fuel ring with a reduced inside diameter as indicated by the dotted line.

Between the C-clamps and the fuel are steel pieces that distribute the load at the fuel surface and, more importantly, provide shock absorption at the top. The top piece is a solid loading ring that is relieved about 0.06 in. on the underside over about 2 in. circumferentially at each C-clamp position to act as a spring for vertical expansion. This ring is depressed ~0.005 in. in a special hydraulic press to permit installation of the C-clamps.

The burst assembly is supported on a three-legged structure visible in Fig. 1 which houses actuators for reactivity control elements that enter the core from below, as in earlier Godiva assemblies. The safety block is threaded onto a stainless steel support mandrel at the lower end

so that thermal expansion exerts a downward thrust on the support shaft, opening a magnetic coupling to provide shock-induced scramming.

BURST CHARACTERISTICS

Operating characteristics of Godiva IV are similar to those of Godiva II except for a slightly longer neutron lifetime (Rossi-alpha at delayed critical, α_R, $= 0.85 \times 10^6$ sec^{-1}). Peak burst temperature increases reached 525°C with burst widths of ~24 μsec. Associated surface fluences are ~10^{14} neutrons/cm^2, and peak fluxes are ~4×10^{18} neutrons/cm^2/sec.

Total burst yield for the most recent set of data is shown plotted against reciprocal reactor period in Fig. 3. Peak power and burst
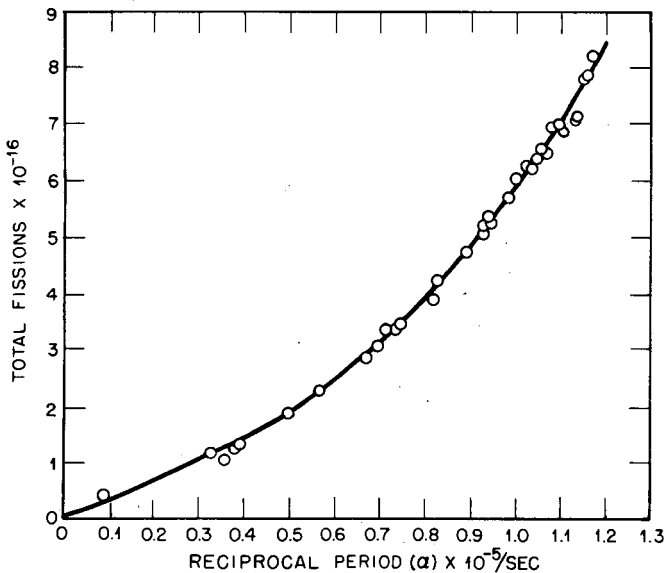
Fig. 3—*Burst fission yield vs. reciprocal reactor period. Yield = $C\alpha (1 + \alpha^2 \tau^2)$, where $\tau = 8.9$ μsec.*

duration measured at half-maximum power are shown in Fig. 4. Yield data were obtained from aluminum (n, α) detectors calibrated relative to fission activation of uranium foils placed in the core center. Where aluminum detectors were not used, burst temperature increase was used as an index of burst yield. Peak power was measured by response of a plastic scintillator photodiode detector. Power calibration was accomplished by using the approximate relation at some large yield, $Y = 4P_m \ \Delta t/3.52$, where P_m is peak burst power and Δt is burst duration as defined previously.
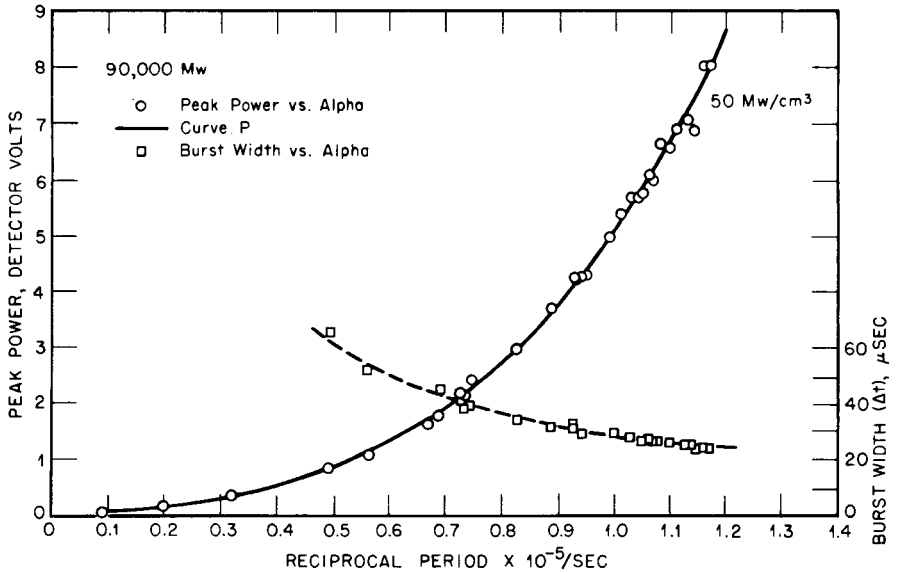
Fig. 4—*Peak burst power and burst duration vs. reciprocal reactor period. Power* = $\alpha^2(1 + \alpha^2\tau^2)/2b\alpha_R$, *where* $\tau = 8.9$ μsec.

The average inertial lag time, τ, for this assembly is 8.9 μsec, arrived at by adjusting this parameter in the first-order analytical expressions presented in Figs. 3 and 4 for best fit with the data.

FISSION DENSITY AND NEUTRON LEAKAGE FLUX

For Godiva IV a limited effort was made to measure fission densities and a total leakage flux independent of radiochemistry techniques. Some effort was also made to obtain relevant information regarding neutron spectra. Fission-density values were obtained from fission-activation measurements[2] with low-density ^{235}U foils irradiated at the top of the safety block and calibrated by means of back-to-back fission chamber.* (The fissile deposits for the fission chamber were previously intercompared with secondary-standard deposits used by Stein and Smith et al.[3,4] in a recent measurement of $\sigma_f(^{235}U)/\sigma_f(^{238}U)$ between 1 and 5 Mev.) Fission densities from the two bursts, good to perhaps 6%, exceed by 14% a radiochemistry value determined at the same position on the safety block.

---

*The chambers and the fissile deposits were kindly furnished by Munson Thorpe of the Los Alamos Scientific Laboratory.

A leakage flux per core fission for Godiva IV was obtained from fission-foil activation responses at two positions: 2 in. above the fuel surface on axis and near the core center. With computed fission distributions and a selected cross section of $\sigma_f(^{235}U) = 1.29 \pm 0.07$ barns, a value of $8.7 \pm 1 \times 10^{13}$ neutrons/cm^2 per 10^{17} fissions was derived[5] for the upper position. (Correction from the Lady Godiva center spectrum to Godiva IV is less than 1%.)

Specification of neutron spectra in and about a fast-neutron system like Godiva IV is an unsettled issue. Only one aspect of the spectra may be considered established, namely, the preservation of the ^{235}U-fission-spectrum shape above an energy of about 2 Mev. In Godiva IV, responses of the high-energy activation detectors, P(n,p), Al(n,p), ^{56}Fe(n,p), and Al(n, α), are almost indistinguishable from their well-established responses in the ^{235}U fission-neutron spectrum. This result is consistent with those from similar measurements in other Pajarito fast criticals[6] and is further confirmed by the well-known photoplate data of Rosen.[7] In Table 1 therefore the high-energy-group flux (E > 1.4 Mev) is a ^{235}U fission-spectrum component.

Spectrum measurements for Godiva IV are presented in Table 1 along with established results for the undiluted spherical assembly, Lady Godiva. The spectral indexes listed imply the accompanying three-group fluxes and chiefly indicate spectrum differences. Uncertainties, considered relative to Lady Godiva center spectrum, are a few percent. Measurement and computation are not in very good agreement; observed spectra are generally more energetic, with the old photoplate data an important exception. (Computations also disagree with observed neutron lifetimes in Godiva IV, the latter implying a less energetic spectrum.[13] See also J. T. Mihalczo, Session 1, Paper 1.)

The softening of Godiva IV spectra due to the internal and external steel is evident. At the center the fission-spectrum component above 1.4 Mev is down by 40% relative to a ^{235}U fission spectrum and down by 10% relative to Lady Godiva center spectrum. The axial leakage spectrum is even more affected: in contrast with Lady Godiva, the fission-spectrum component in the axial leakage for Godiva IV is actually smaller than in the center. The unusual pileup of neutrons between 0.6 and 1.4 Mev is based upon a $\bar{\sigma}_f(^{235}U)/\bar{\sigma}_f(Np)$ index acquired indirectly, and it will require verification.

PRELIMINARY RESULTS

Power densities attained on this assembly without damage to the clamps and supports are considerably higher than any attained previously. Peak power density occurs near the top of the safety block

Table 1

OBSERVED SPECTRAL INDEXES AND THREE-GROUP SPECTRA

| | Observed spectral indexes | | Energy groups, Mev | | | Av. energy, Mev |
	$\dfrac{\overline{\sigma}_f(^{235}U)}{\overline{\sigma}_f(^{238}U)}$	$\dfrac{\overline{\sigma}_f(^{235}U)}{\overline{\sigma}_f(Np)}$	$0-0.6$	$0.6-1.4$	$1.4-\infty$	
^{235}U fission spectrum[8] (nominal)			0.18	0.28	0.54	1.9_4
Lady Godiva*						
Central .spectrum						
Spectral indexes	$6.24 \pm 3.5\%$	$1.21 \pm 3.5\%$	0.31	0.28	0.41	$\sim1.5_8$
Computation, ENDF/B†			(0.33)	(0.30)	(0.37)	
Leakage spectrum						
Spectral indexes	$6.0 \pm 2\%$	$1.18 \pm 2\%$	0.29	0.28	0.43	$\sim1.6_3$
Differential measurements						
Photoplate[11]‡			(0.33)	0.29	0.38	$\sim1.5_0$
Time of flight[12]§			0.26	0.31	0.43	$\sim1.6_5$
Computation, ENDF/B†			(0.29)	(0.30)	(0.41)	
Godiva IV						
Central spectrum						
Spectral indexes	$6.91 \pm 2\%$	$1.27 \pm 2\%$	0.34	0.29	0.37	$\sim1.4_7$
Computation, Hansen—Roach†			(0.38)	(0.29)	(0.33)	
Axial leakage spectrum,						
Spectral indexes	$7.4 \pm 4\%$	$1.16 \pm 6\%$	0.28	0.37	0.35	$\sim1.4_7$

*Uranium—metal sphere (93.5% ^{235}U), critical radius $=8.7$ cm.

†Computation by the discrete ordinates method using ENDF/B[9] or Hansen—Roach[10] cross sections as indicated.

‡Extrapolation to below 0.2 Mev is based on Eq. 1 in Ref. 6.

§Reduction of zero-degree time-of-flight data for this table includes a computed correction to the full angular leakage flux.

about a centimeter into the fuel outside the steel support mandrel. The maximum peak power density observed to date is nearly 50 Mw/cm^3 as indicated at the upper right corner of Fig. 4. Significantly, no damage has been observed in the safety block for densities of this order. Failures observed were cracks in the second fuel ring from the top. This ring was fractured and replaced twice before the cause of failure was determined. It was found that the radial clearance provided between the top central fuel cylinder and the outer rings was insufficient, which resulted in an added constraint on the outer rings. Failure involved fractures that radiated outward from the control-rod clearance holes to the outside ring surface as a result of stress concentration.

The modified assembly incorporates increased clearance around the upper inside cylinder and a modified second fuel ring, as mentioned earlier. With these modifications it should be possible to increase burst yield and approach the damage threshold associated with dynamic stress within the fuel pieces. Calculations based on kinetic energy of fuel expansion predict this threshold to be yielding of the fuel clamps at $\sim 10^{17}$ fissions.

If dynamic-stress failure of the fuel should continue, an effort will be made to improve the yield strength of the metal, first by heat treatment, then by the substitution of a different fuel alloy. A joint metallurgical program is currently underway at Los Alamos Scientific Laboratory and Sandia Corporation to investigate uranium alloys for burst reactor applications.

ACKNOWLEDGMENTS

REFERENCES

1. T. F. Wimett, R. H. White, W. R. Stratton, and D. P. Wood, Godiva II — An Unmoderated Pulse-Irradiation Reactor, *Nucl. Sci. Eng.*, 8: 691-708 (1960).
2. J. A. Grundl, A Study of Fission-Neutron Spectra with High-Energy Activation Detectors. I. Detector Development, *Nucl. Sci. Eng.*, 30: 39-53 (1967). Also Spectral Index Measurements and the Extraction of Spectra, Internal Report N-2-8198, Los Alamos Scientific Laboratory, September 1968.
3. H. L. Smith and J. P. Balagna, A Method of Assay of ^{235}U, ^{238}U, and ^{237}Np Fission Foils, USAEC Report LA-DC-7625, Los Alamos Scientific Laboratory, 1966.

4. W. E. Stein, R. K. Smith, and J. A. Grundl, Relative Fission Cross Sections of ^{238}U, ^{237}Np, and ^{235}U, USAEC Report LA-DC-7617, Los Alamos Scientific Laboratory, 1966.

5. L. B. Engle, G. E. Hansen, and H. C. Paxton, Reactivity Contributions of Various Materials in Topsy, Godiva, and Jezebel, *Nucl. Sci. Eng.*, 8: 568 (1960).

6. J. A. Grundl and G. E. Hansen, Measurement of Average Cross-Section Ratios in Fundamental Fast-Neutron Spectra, in *Nuclear Data for Reactors*, Symposium Proceedings, Paris, 1966, Vol. 1, pp. 321-326, International Atomic Energy Agency, Vienna, 1967 (STI/PUB/140).

7. J. A. Grundl and A. A. Usner, Spectral Comparisons with High-Energy Activation Detectors, *Nucl. Sci. Eng.*, 8: 598-607 (1960).

8. J. A. Grundl, A Study of Fission-Neutron Spectra with High-Energy Activation Detectors. Part II. Fission Spectra, *Nucl. Sci. Eng.*, 31: 191-206 (1968).

9. R. J. LaBauve and M. E. Battat, Los Alamos Scientific Laboratory, personal communication, 1969.

10. G. E. Hansen and W. H. Roach, Six- and Sixteen-Group Cross Sections for Fast and Intermediate Critical Assemblies, USAEC Report LAMS-2543, Los Alamos Scientific Laboratory, 1961.

11. G. M. Frye, Jr., J. H. Gammel, and L. Rosen, Energy Spectrum of Neutrons from Thermal-Neutron Fission of ^{235}U and from an Untamped Multiplying Assembly of ^{235}U, USAEC Report LA-1670, Los Alamos Scientific Laboratory, 1954.

12. J. M. Neill, K. Crosbie, and J. L. Russell, Jr., Neutron Spectrum Measurements Across a Bare ^{235}U Metal Sphere, USAEC Report GA-9284, Gulf General Atomic Inc., 1969.

13. G. E. Hansen, Status of Computational and Experimental Correlations for Los Alamos Fast-Neutron Critical Assemblies, in *Physics of Fast and Intermediate Reactors*, Symposium Proceedings, Vienna, 1961, Vol. 1, International Atomic Energy Agency, Vienna, 1962 (STI/PUB/49).

DISCUSSION

YOCKEY: The Chairman would like to ask what is the total fluence in the glory hole, and what is your peak flux rate?

WIMETT: Peak surface flux rate is of the order of 2×10^{18} neutrons/cm^2/sec. The peak fluence is something over 10^{14} neutrons/cm^2. Glory hole values are about an order of magnitude higher.

O'BRIEN: How do you detect the presence of cracks operationally? Do they shut you down?

WIMETT: We just chose to stop running after cracks were observed. We lost on the order of 2¢ reactivity in this last damaging burst.

MUEHLHAUSE: Do you think there would be any virtue in preparing these assemblies with some initial thermal distribution, i.e., generate an opposite radial-stress distribution from the one that the excursion induces to avoid internal stress deformation during the pulse?

WIMETT: I am not an expert on stress analysis, but my guess would be that you would not gain much because whatever stress you get initially is going to be reflected into an opposite stress. In this case

your preloading and prestressing would add to the reflected wave, probably. There must be someone else here who is more expert on stress.

MUEHLHAUSE: I was thinking you might be able to turn around thermal gradients from one sign to the other to avoid certain internal stresses.

WIMETT: My guess is that it would be hopeless just because of the problem of these stress waves reflecting. You start out with a stress at the center, and it reflects as surface traction; so, I do not know in what way the preloading could counteract both those stresses.

STATHOPLOS: There are two types of stresses, of course; one is due to a thermal gradient, and that is a constant kind of thing. The other, the inertial stress, the one you are talking about, does reverse signs; so it would be very difficult to preload to take account of or to counteract the inertial stresses, because they are oscillating back and forth. Perhaps one could do something about the thermal stress, which is a constant.

WIMETT: Oh yes, I guess perhaps that is what the earlier question posed. It had to do with eliminating that stress due to temperature gradient. It might help. So far we really have not observed failure due to that effect, although we know we may eventually.

MUEHLHAUSE: May I make another comment on that? There has been a suggestion, maybe it has been by several people, that one can build radial slots into the fuel metal, which would largely alleviate the thermal stress. I do not know whether it would do much about inertial stress, but that one suggestion might work.

WIMETT: Yes. We have given that a lot of consideration. We had to stop ourselves twice, I think, from cutting slots. We looked at this the first time it cracked on the outside and considered putting in some stress relief by slotting on the outside of the rod holes. It does not particularly matter where the slots are as long as you reduce radial dimensions over which these temperature differences can give you trouble. But we talked ourselves out of it, and I am glad we did. But if we do reach that form of stress failure, slotting will be our first form of relief. This has been done at Sandia. I will not discuss it since it will covered in one of the later papers.

MUEHLHAUSE: Was the alloy you were working with alpha phase or gamma phase?

WIMETT: It is alpha phase at this point. The advice of our metallurgists was that they are capable of casting such fine-grained material that it does not particularly matter whether it is an alpha or gamma.

MUEHLHAUSE: There is no problem with thermal cycling?

WIMETT: Not that we know of. For example, FRAN was an alphaphase system, and it has produced plenty of bursts without growth due to the alpha phase.

2-3 SANDIA PULSED REACTOR II

R. M. JEFFERSON
Sandia Laboratory, Sandia Corporation, Albuquerque, New Mexico

ABSTRACT

On the basis of experience gained from the operation and evaluation of other fast burst reactors, the SPR II was designed to be capable of producing a fast-neutron fluence of 10^{15} in a 35-μsec pulse inside a 1.5-in.-diameter glory hole. This second-generation fast burst reactor uses 105 kg of 93% enriched uranium alloyed with 10 wt.% molybdenum as fuel, which, when fully assembled, forms a right-circular cylinder 810 in. in diameter by 8.2 in. in height.

During the extensive operating history of this reactor, a number of design innovations and operational techniques have been developed to allow higher levels of operation, increased reliability, and improved safety. These developments and operational experiences involving fuel failures are detailed.

INTRODUCTION

In May 1960 the first Sandia Pulsed Reactor was brought critical and subsequently used in radiation-effects testing for a series of more than 5600 operations over a period of seven years. Experience gained with that reactor, the Health Physics Research Reactor (HPRR), and other fast burst reactors indicated the possibility of substantial improvement in the pulse yield with modest changes in reactor design. This possibility, coupled with requirements for a fast burst reactor with a reasonably sized glory hole in which neutron fluences on the order of 1×10^{15} neutrons/cm^2 could be achieved in a single pulse, led to the design effort culminating in the Sandia Pulsed Reactor II (SPR II). Thus the SPR II answers a specific need and is based upon experience and development information from Oak Ridge, Los Alamos, White Sands, and Sandia reactors. Since the SPR II was brought critical in May 1967, it has performed more than 1000 operations for experimental programs.

Although the design objectives of SPR II have been met, operations at the design level caused severe cracking of one fuel plate of the original fuel assembly. Burst operation at substantially lower yields producing $300-350°C$ ΔT at the hottest part of the fuel assembly continued through approximately 850 operations, at which time the fuel assembly was replaced with one modified to reduce stresses. Operation at the design yield appears entirely satisfactory from the standpoint of fuel integrity, although a new problem of damage to the control-rod drives has delayed routine operation at design yield. The characteristics of SPR II at two typical operating points are outlined in Tables 1 and 2.

Table 1

SPR II PROMPT BURST CHARACTERISTICS

Yield, fission	1.0×10^{17}	1.6×10^{17}
Maximum fuel-temperature rise, °C	340	560
Initial period, μsec	16	12
Pulse width at half maximum, μsec	46	32
Prompt-neutron decay constant, sec^{-1}	0.68×10^6	0.68×10^6

Table 2

CHARACTERISTICS OF SPR II RADIATION OUTPUT

	Pulse size			
	340°C ΔT pulse		560°C ΔT pulse	
	Surface	Glory hole	Surface	Glory hole
Neutron fluence, neutrons/cm^2	2.0×10^{14}	6.0×10^{14}	3.2×10^{14}	1.0×10^{15}
Peak neutron flux, neutrons/cm^2/sec	4.4×10^{18}	1.4×10^{19}	1.0×10^{19}	3.1×10^{19}
Gamma dose, H_2O rads	3.1×10^4	1.4×10^5	4.8×10^4	2.3×10^5
Gamma dose rate, H_2O rads/sec	6.7×10^8	3.0×10^9	1.5×10^9	7.2×10^9

REACTOR DESCRIPTION

Fuel System

The SPR II consists of six rings or plates and four rods of 93% enriched-uranium metal alloyed with 10 wt.% molybdenum (arranged
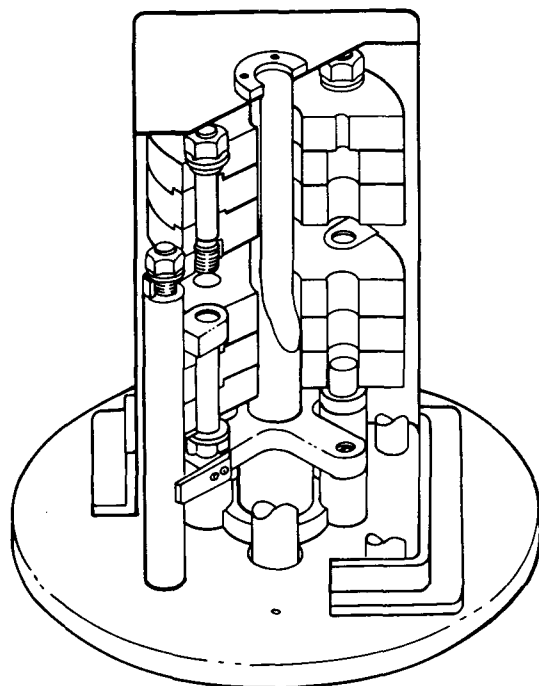
Fig. 1 — Cutaway of SPR II fuel system.

as shown in Fig. 1) which together weigh 105 kg. In its most compact arrangement, the fuel assembly is 8.078 in. in diameter and 8.206 in. high with a 1.625 in. diameter hole along the axis of the cylinder. The six plates, which account for approximately 100 kg of the fuel weight, are mounted in two distinct halves. The three upper plates are fastened together by four high-strength A-286 alloy steel bolts threaded into A-286 alloy steel fingers that protrude beyond the cylindrical surface of the upper fuel assembly to mounting posts. Thus the upper fuel assembly is held stationary above the primary mounting surface of the reactor stand. The remaining three fuel plates are fastened together by a second set of four A-286 alloy steel bolts threaded into special A-286 nuts and subsequently mounted on the four fingers of a spider fixed at the top of an axially located drive shaft. This lower core half, called the safety block, is axially aligned below the upper fuel assembly and is capable of being driven over a distance of 2 in. to make contact with the upper core half. This motion of the safety block provides a shutdown capability in excess of $10.

The fuel system is completed by three control rods and a burst rod, each of which weighs 1.2 kg and is 0.875 in. in diameter by 10.625 in. long. These rods fit into cavities in the fuel 0.938 in. in

diameter by about 7 in. deep (not all the way through the assembly). The additional length of these rods is for mechanical convenience and not for nuclear considerations. The overall arrangement described is shown schematically in Fig. 2.
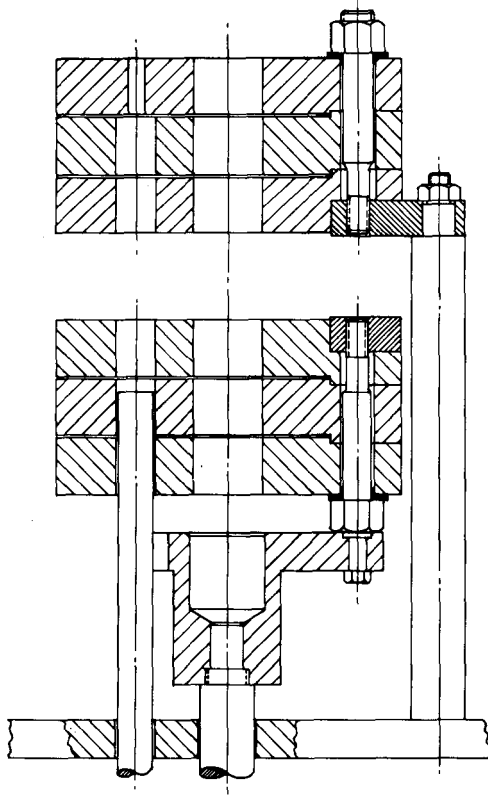
Fig. 2— Cross section of SPR II fuel system.

Several features of this core merit additional discussion. Investigations on earlier burst reactor designs revealed the existence of severe shock forces generated by the nearly adiabatic heating and subsequent expansion of the fuel material.[1] These shocks produce oscillations in the fuel assembly sufficiently severe to cause damage to the fuel rings (see J. A. Reuscher, Session 1, Paper 3). An acoustical impedance mismatch has been introduced between the plates to damp these oscillations in the axial direction and to reduce the stress in the bolts holding the fuel plates together. This is accomplished by a feature designed to also eliminate transverse stresses in the bolts. A lug and matching recess arrangement is around each of the four bolt holes in

each plate, as shown in Fig. 3. These four keying elements lock the fuel plates together to prevent lateral or rotational motion. Since the male lug is 20 mils longer than its mating female recess, a corresponding gap is introduced between plates. This gap mitigates the shocks produced within the fuel assembly and provides space for thermal expansion of the individual fuel plates. Since the components of the assembly have small contact areas only at the edges and since major portions of the heating and expansion take place near the center of the plate, this gap is very effective in reducing the stress introduced into the bolts.[2] Even so, tensile stresses in the bolts as high as 225,000 psi have been inferred from measurements.[3]
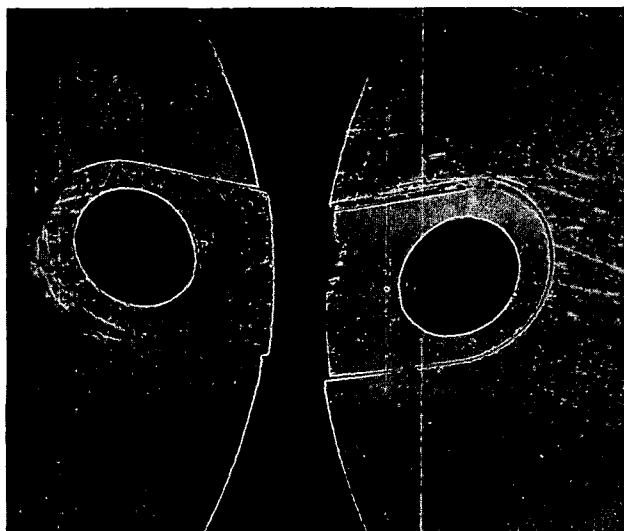
Fig. 3—SPR II fuel-plate interlocking arrangement.

Although the dynamic stresses in the fuel-assembly bolts appear to have been in excess of their static yield points, no failures in bolts have been experienced in SPR II. There have been several failures, however, in the fuel components.[4] During a series of progressively larger bursts undertaken with the intent of achieving the design operating level of the reactor, no difficulties were encountered other than the occasional need for bolt tightening, as experienced in the operation of earlier Godiva-type reactors, up to a burst level of 478°C ΔT.

A subsequent 509°C burst was accompanied by a loud report similar to that of a rifle shot, and two observers saw a shower of sparks on the closed-circuit television monitor (the shroud had been

removed). No particular significance was attributed to the sound since at that time no previous experience indicated that the sound was abnormal for a 500°C burst. The sparks were suspected to be the result of pyrophoric fuel particles being separated from the surfaces of the center (hottest) fuel rings during their mechanical oscillations. Since a brief visual examination revealed no conspicuous evidence of damage and since delayed-critical operations indicated no change in fuel configuration, operations at the 500°C ΔT level were continued (with very repeatable results). A subsequent attempt to increase the burst yield produced a ΔT of 606°C (somewhat higher than expected) during which another small display of sparks was observed. Inspection of the reactor then revealed a broken control rod that failed through a thread-relief area at its lower end (see P. D. O'Brien, Session 4, Paper 6). (In the current SPR II core this intrinsic failure has been eliminated by increasing the length of the control rod and changing from male to female threads.) Disassembly and inspection of the core following the control-rod failure revealed a crack in the C-1 ring (see Fig. 4) which extended outward from the glory hole through a radial
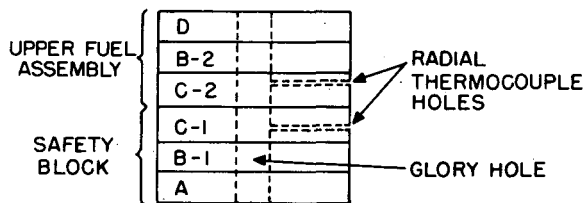
Fig. 4—SPR II fuel-plate designations.

thermocouple hole. Figure 5 shows the crack as it appeared at that time. The penetrating dye used to reveal the full extent of the crack greatly exaggerates its width.

After the broken control rod had been repaired and the other two control rods modified, SPR II was reassembled, and operations were resumed at reduced levels. During the 850 operations between that time and retirement of the damaged fuel assembly, other cracks appeared in the C-1 plate as well as in three of the remaining five plates. Figure 6 shows the condition of the C-1 plate at retirement. In spite of the ever-increasing number of failures, the reactor continued to perform satisfactorily at reduced yields.

These observed failures are considered to have two interrelated causes. The initial failure along the radial thermocouple hole was most likely a tensile failure perpetrated by this stress riser. Although other stress-related failures were observed, some fuel cracks are also believed to be associated with stress corrosion (e.g., the cracks
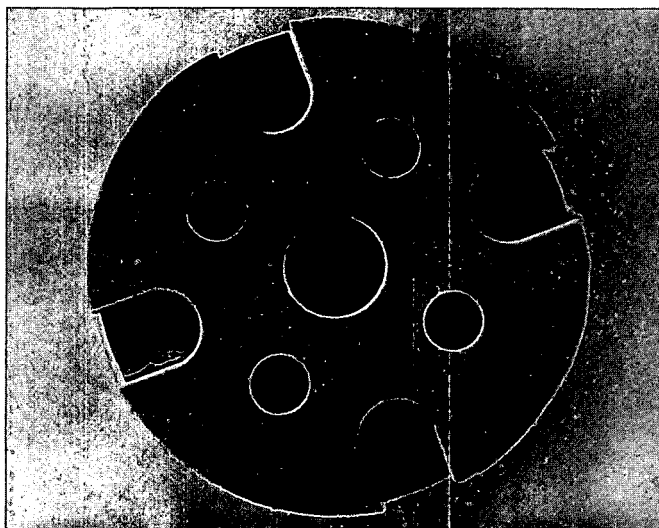
(a)
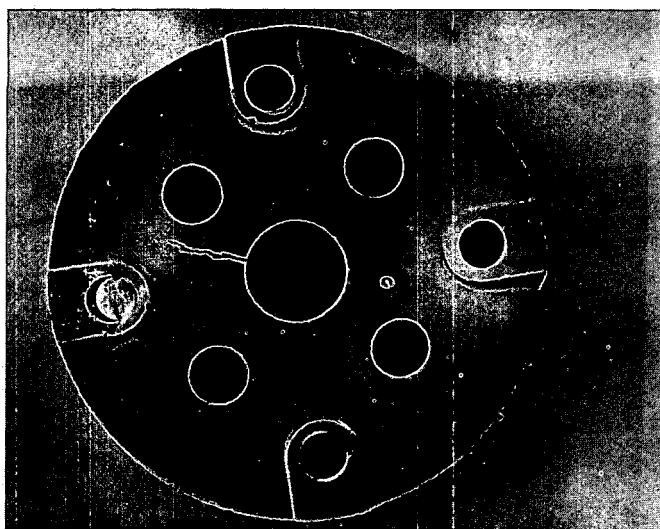
(b)

Fig. 5— The C-1 plate of the SPR II when crack first appeared. (a) Top; (b) bottom.
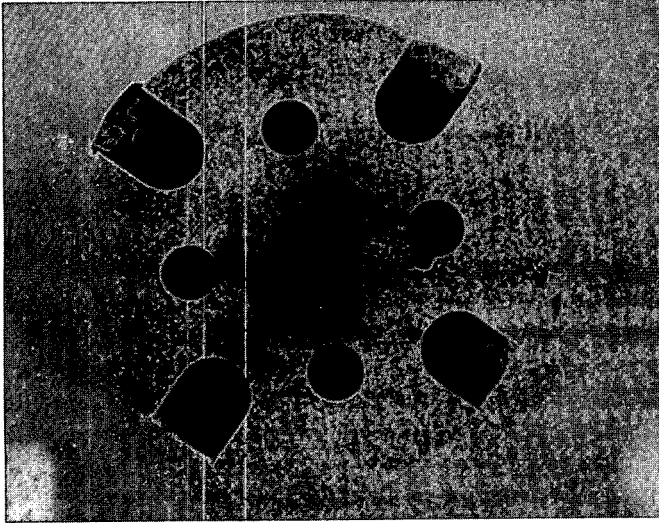
(a)
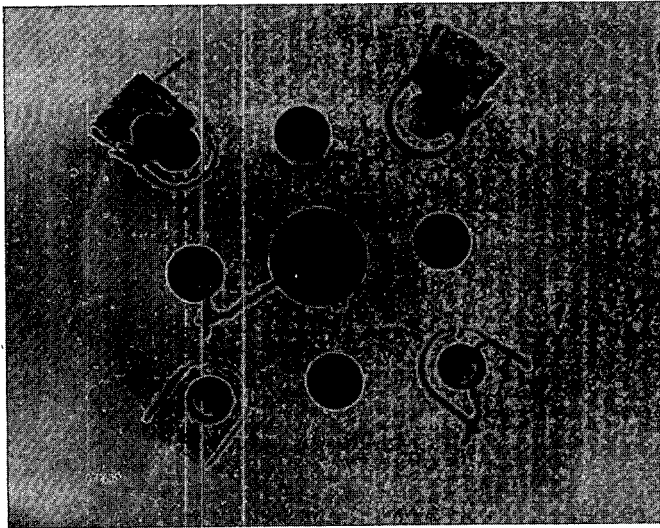
(b)

Fig. 6—The C-1 plate at retirement. (a) Top; (b) bottom.

near the bolt holes in the C-1 ring shown in Fig. 6). Elimination of the corrosion problem involved a change in the cooling system (discussed later in this paper), and an attempt to reduce stress problems necessitated a change in fuel-plate design. Since the initial failure had occurred along a radial thermocouple hole, which represented a stress riser, all thermocouple holes, both radial and axial, were eliminated
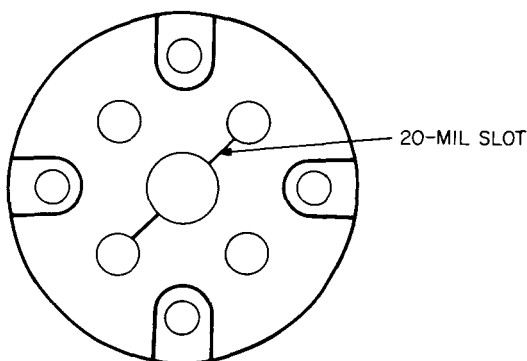
Fig. 7—Modified C plate.

from the C-1 and C-2 plates. Furthermore, since dynamic measurements on the C-2 ring indicated peak hoop stresses of twice the static yield strength of the fuel material (see J. A. Reuscher, Session 1, Paper 3), the C-1 and C-2 rings were modified by cutting two 20-mil-wide slots through the plate between the glory hole and control-rod holes as shown in Fig. 7. Experience with the modified core indicates these modifications were successful in reducing peak stresses in the fuel.

Drive Systems

The fuel system previously described is mounted on a mechanized stand that positions the fuel and controls its various motions. The upper fuel assembly is mounted on the primary mounting surface of the reactor stand by four posts. The safety block is axially aligned below the upper fuel assembly on a shaft driven by a two-speed d-c motor through a belt drive, worm-gear reducer, and Acme screw. Experience at Oak Ridge National Laboratory on the HPRR indicated the desirability of incorporating a magnetic coupling in the safety-block drive system to provide shock-induced scrams of the reactor.[5] Therefore on SPR II the safety-block drive shaft is made in two sections coupled by an electromagnet. With this arrangement any burst with a yield exceeding ~150°C ΔT (corresponding to an initial

period of less than 30 μsec) develops sufficiently strong shock forces to eject the safety block by breaking the magnetic coupling.[6] This arrangement offers the distinct advantage of a self-initiating scram, independent of the electronic scrams and considerably faster (safety-block movement occurs within 225 μsec). This very-high-speed mechanical response of the system effectively reduces the length of the delayed critical tail characteristic of most Godiva-type reactors. Although the shock forces generated by pulses below ~150°C ΔT are insufficient to break the magnetic coupling, a nearly symmetrical pulse can still be produced by using preprogrammed initiation and scram signals to drop the safety block a few milliseconds after the burst.

Also mounted on the primary mounting surface of the reactor stand are the three control-rod drives and the burst-rod drive. The control-rod drives consist of a d-c drive motor coupled to a drive pinion through electric and mechanical clutches. The drive pinion, riding on a rack fitted into the hardened control-rod shaft, can thus operate the control rod over its normal 6.75-in. travel. With an adjustment of the current on the electric clutch and an adjustment of the mechanical clutch, the drive system can function without slip under normal conditions and yet slip under the shock loads imposed during the pulse. This clutch slippage is intended to prevent damage to the gear and rack teeth during these high-load periods. The clutch is also used to drop the control rod under scram conditions. (The SPR II was the first fast burst reactor to utilize scramming control rods.) Because of the intentional slippage of the drive train, rod position is monitored through a separate pinion coupled directly to a ten-turn pot in a standard null-balance readout system. The inertia of this position pickup is low enough that the sudden accelerations produced by the induced shocks do not damage the rack or pinion. Control-rod alignment is maintained by a split linear ball bushing located between the drive pinion and the position-sensing pinion and by a Graphitar bushing about 9 in. away at the upper end of the rod-drive package. This upper bushing rides on the fuel portion of the rod throughout its travel, thus imposing the requirement for the 10.625-in.-long fuel rod for the 6.75-in. travel. Mounted on the lower end of the rod-drive package is an oil-filled dash pot to decelerate the rod at the end of its stroke.

When the new core was installed, it was placed on a separate stand to allow check-out concurrent with routine operation of the old core. This dictated, among other things, all new control-rod drives. In these new control-rod drives problems have appeared since the reduction of the fuel-assembly stress and corrosion difficulties. The experience at Sandia has been that any new fast burst core will require an initial period of break-in during which bolts and other screwed connections, such as the control-rod-to-shaft joint, must be tightened periodically, but, with the new SPR II core, the control-rod and burst-rod joints

demanded almost daily tightening if repeatable operation was to be maintained. Obviously something in the joint was failing. Disassembly and inspection revealed that a spacer used to adjust the rods in relation to their drives was being coined by the repeated shock loads imposed upon it.

Another problem detected at the same time and also attributable to the shock forces experienced by the control-rod drive system involved the screws used to attach the rack (used to drive the control rod) to the shaft. Several efforts to eliminate this difficulty have been tried without total success although a mechanical stop placed between the end of the rack and the end of the keyway into which the rack fits has been the most successful effort to date.
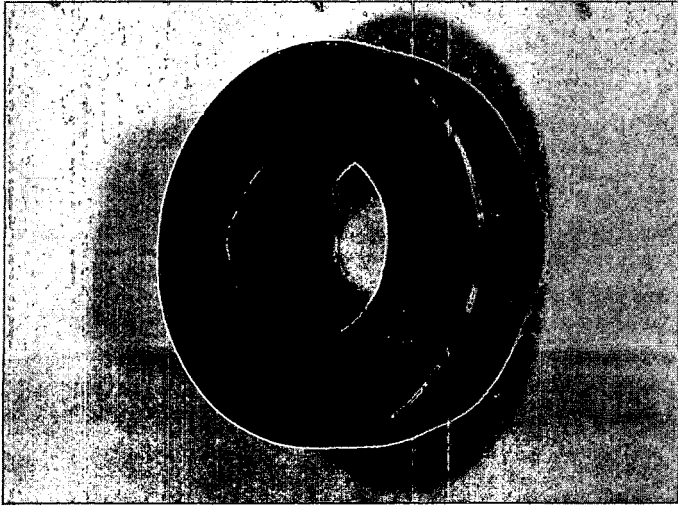
Fig. 8—Shock-induced damage to switch washer.

Perhaps the most dramatic illustration of the shock forces imposed upon the control-rod drive system is the failure of the switch washer shown in Fig. 8. This washer actuates the upper and lower limit switches. Since mechanical stops limited travel in both directions, the only loads imposed upon this washer are those produced by shock. These shock loads were sufficient to deform the washer and shear the $\frac{1}{8}$-in. pin.

Containment, Decoupling, and Cooling

The escape of fission products from the fuel assembly of SPR II is minimized by aluminum-ion plating of all fuel components. This ion plating also protects the fuel against corrosion during high-temperature

operation. Evaluation of the desirability of heat treating (diffusing) the plating indicated that the fission-product retention was greater on the untreated plates. Although this ion plating is the best protective coating presently available for this application, it is impossible to coat all the surfaces of such complex shapes. Therefore other means of containment are also used.

REACTOR SHROUD.   Completely covering the reactor, as shown in Fig. 1, is a thin aluminum shroud that serves several functions. By completely covering the fuel assembly and by means of a distribution system built into its structure, the shroud directs the flow of gas over the fuel system to achieve relatively efficient cooling. By virtue of this same complete enclosure, any fission products escaping from the fuel are contained by the shroud and carried off by the cooling system (which is passed through absolute and activated-charcoal filters).

Cemented to the shroud is a thin layer of Sylgard (a silicon base elastomer) loaded to 50 wt.% elemental ^{10}B. This material greatly diminishes the reactivity contribution of moderating materials external to the reactor. For example, a polyethylene slab 8 in. square by 2 in. thick contributed 56¢ of reactivity to the system when no decoupler was present but only 28¢ when the decoupling shroud was in place (see R. L. Coats and R. L. Long, Session 4, Paper 4). The effectiveness of this material during the pulse is illustrated in Fig. 9, which shows that the kinetic response of the system to the polyethylene slab is virtually eliminated by the decoupling shroud.[6] Figure 9 does not indicate that, while the polyethylene slab produced a pulse approximately 10 times as wide as normal when no decoupling shroud was employed, the same sample had no effect on pulse width when the shroud was in place. In contrast, nonmoderating materials near the reactor produce changes in reactor behavior which are unchanged by the shroud.

Irradiation of samples of the boron-loaded Sylgard in the Sandia Engineering Reactor prior to its use on SPR II indicated that neutron-induced embrittlement of the plastic material would limit the life of a decoupling shroud to about 300 bursts. Other suitable methods of fabricating decoupling materials proved impractical or excessively expensive; so Sylgard was used. Since the original shroud survived in excess of 800 operations, no further attempts will be made to find a better material.

COOLING SYSTEM.   The initial cooling scheme employed on SPR II consisted of blowing compressed air on the fuel assembly from a distribution manifold fitted inside the shroud. This air passed down around the fuel and was then exhausted from the shroud through a filter into the reactor room. A refrigerative dryer was used to reduce the moisture content and to cool air to make a more effective coolant. As a result of experience with the first core, the fuel-cracking problem
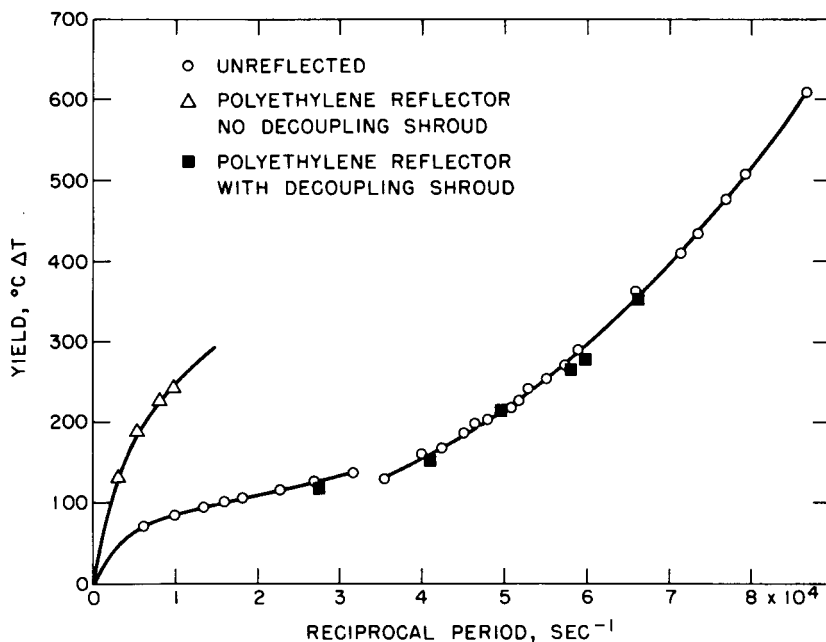
Fig. 9—Effectiveness of SPR II decoupling shroud.

appeared to be at least partially caused by stress corrosion, which can logically be associated with the presence of oxygen and moisture during the high-temperature high-stress intervals of operation.

Originally plans were to install an inert-gas cooling system,[7] so tests were performed using dry nitrogen gas obtained by boiling liquid nitrogen. As a result of these tests, a liquid-nitrogen storage tank and evaporator were installed and used on about the last 150 operations of the original core and on all operations of the new core. With the use of the existing distribution and exhaust system, the cooling rate of the reactor was improved by about 30%. When the cooling gas is first turned on, the evaporator and all lines are warm enough so the gas introduced to the shroud is ~15°C. As gas flow continues, the evaporator and lines cool. Therefore as the reactor temperature falls so does the gas temperature, an effect which maintains a large temperature differential and the higher cooling rate.

More important though, blanketing the fuel system with a dry inert gas seems to significantly reduce the stress-corrosion problem. Under these conditions the new core has been operated to pulse levels as high as 595°C ΔT without damage. Although the ultimate effectiveness of this cooling system has not yet been evaluated and although the mechanical design changes discussed previously undoubtedly have also

helped, no cracks have been observed in the new fuel system whereas the original core had developed cracks by this point in its history. Furthermore, the discoloration of the ion plating observed on the first core and attributed to high-temperature diffusion of the aluminum into the uranium has been retarded on the new core.

Reactor Controls

The control system for SPR II is generally quite standard; however, it does incorporate some features, first employed on its predecessor, which experience has proven quite effective in improving safety and utilization.

EXTERNAL INITIATION. The design and operation of the original SPR were very similar to Los Alamos Scientific Laboratory's Godiva II, and like that reactor it produced a burst with two distinct phases — the "prompt spike" and the "tail" that followed the spike and persisted until the reactor was scrammed, some 30 msec later. Even this short a tail was achieved only after concerted efforts to improve the response times of the relays, valves, and other mechanical portions of the system. Another aspect of the burst was that the time between complete insertion of the burst rod, i.e., attainment of maximum reactivity, and the occurrence of peak power in the spike varied statistically. Although the average time[8] from maximum reactivity to peak power for SPR was about 75 msec, delays as long as 1 sec were not at all uncommon. These variations made it impossible to synchronize experiments with the peak of the burst, and in some cases recording capability was exhausted before the burst took place.

Burst-peak timing was improved on SPR by utilizing an external pulsed deuterium—tritium neutron source to initiate the burst. The source, triggered when the reactor achieved its maximum reactivity condition, produced about 10^8 14-Mev neutrons in a 10-μsec pulse. Since the probability of burst initiation within the first microsecond of such a neutron pulse is virtually 1, the only variation in time from initiation signal to peak power resulted from source jitter (negligible) and the error in establishing initial reactivity, which determined the period on which the reactor power rose. This same system has been used on SPR II with the result that errors in predicting the time at which peak power will occur are consistently less than 20 μsec. Other fast burst reactors are also employing this technique.[9]

AUTOMATIC SEQUENCING. With the ability to predict the time of the burst peak came the ability to time the various functions of the reactor to eliminate the tail. In conjunction with the development of

external initiation, a 100-kc timer was installed to program the control sequence so that the scram coincided in time with the falling edge of the burst spike. The sequence used is burst-rod insertion, scram initiation, and source pulsing. Signals indicating the conpletion of each step must be received by the system before the next step can be initiated. This system has also been carried over and used on SPR II. The breakaway of the magnetic coupling in the safety block on SPR II would appear to obviate the need for such a programmed sequence but such is not the case. As mentioned previously, the shock forces generated in small-yield bursts are not sufficient to disengage the magnet; therefore without the programmed scram the burst would again have a tail. Also, the programmed scram disengages the control-rod drive clutches prior to the arrival of the shock forces, thus reducing the loads that larger bursts impose on that drive train.

A typical timing sequence used on SPR II (for a 300°C ΔT burst) would be to insert the burst rod 400 msec before an arbitrary zero time, wait 388 msec for insertion and damping of the burst rod, initiate the scram signal, and about 0.12 msec before zero initiate the source-pulse signal. These settings vary for different burst sizes and are determined experimentally.

INTERLOCK BYPASS SWITCHES. Early experience at Sandia with fast burst reactor control systems revealed the necessity for bypassing certain sequence or condition interlocks to check out the reactor or to operate under other than ordinary conditions. The universally employed technique of clip leads was initially used to bypass these interlocks. This procedure introduces at least two significant safety problems. Should the operator, who must leave the console and enter it from the back, pick the wrong terminals with his clip lead he could bypass safety functions or operate portions of the reactor unintentionally. Since the clip lead is hidden in the back of the console, its existence is sometimes unknown to other operators or even forgotten. Therefore on the SPR and SPR II reactors all approved interlock bypass functions are permanently wired into the console and brought out to a switch panel on the face of the console. These switches, mounted behind a locked panel, are accessible only to the reactor supervisor. The condition of each bypass is indicated by two panel lights mounted on the face of the locked panel. Under normal conditions when an interlock is functioning, the lower (green) light is on, and, when the bypass switch is operated, the lower light is extinguished and the upper (amber or red) light is turned on. Thus the condition of the interlocks is displayed in a way that should eliminate any uncertainty or error. Since all authorized interlock bypasses are wired in permanently, there should be no occasion for the use of clip leads with their inherent safety problems.

OPERATIONAL EXPERIENCE

As discussed previously, the decoupling shroud on SPR II is very effective in decoupling the reactor neutronically from experiments placed around the outside surface of the fuel. Although the glory hole is lined by a stainless steel thimble, no decoupling material is present. Therefore samples placed in the $1\frac{1}{2}$-in. glory hole are very strongly coupled to the reactor. An experiment to evaluate these effects was conducted by determining the reactivity contribution of various materials located over a range of positions within the glory hole thimble.[10]

This experiment revealed that materials having high scattering cross sections and low absorption cross sections (lead and aluminum) exhibit a negative-reactivity effect at the center of the core but a much greater positive-reactivity contribution near the core boundary. This behavior is interpreted to be the result of neutrons being scattered out of the core by the sample when in the center and back into the core when the sample is near the core boundary. Materials of high absorption cross section (e.g., ^{10}B), as expected, displayed a very strong negative-reactivity contribution near the center of the core. Again, because of scatter back into the core, a similar positive contribution, although much smaller, is present as the poison sample approaches the core boundary. In contrast to these materials, a sample of polyethylene with its high hydrogen content displayed a positive-reactivity contribution throughout its range of positions, reaching a maximum in the center of the core.

Figure 10 compares some of these results. The curve for hydrogen was obtained by subtracting the effect of carbon (graphite) from that measured for polyethylene on the assumption that the effects of carbon and hydrogen in polyethylene are independent.

Evaluation of the effect of sample size on its contribution revealed that the absolute value of the worth per gram-atom decreases as sample size increases. This reduction is primarily the result of flux flattening and flux depression by the sample.

All the above measurements were made in the delayed critical mode; a few prompt critical bursts were also made with polyethylene and ^{10}B samples in the glory hole. Comparison of these data with free-field data revealed that poisons in the glory hole tend to depress the worth of the burst rod without significant effect on the prompt-neutron decay constant. As theory and previous experiments predict,[11] the polyethylene sample in the glory hole reduces the prompt-neutron decay constant, thus producing longer initial periods and smaller bursts for similar control-rod adjustments. Although both poison and moderating materials in the glory hole tend to reduce the glory hole fluence, a significant positive contribution to fluence was obtained by placing 2-in.-long copper slugs (reflectors) at the top and bottom of the glory hole. Since these end reflectors reduce leakage, they also
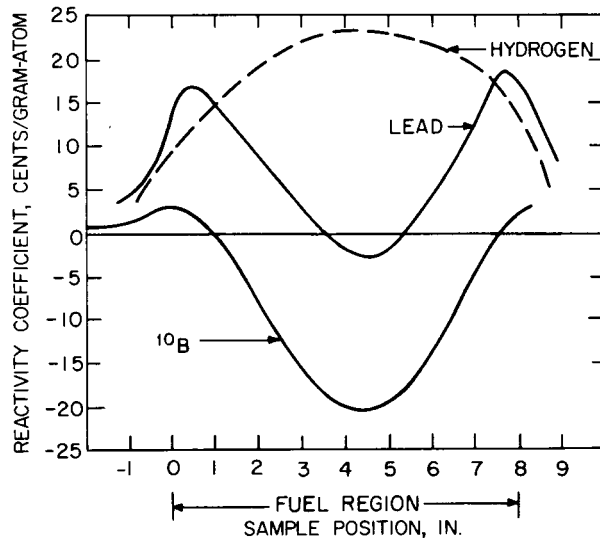
Fig. 10—Reactivity coefficient of selected materials as a function of position in SPR II glory hole.

modify fission-density distributions, which may, in turn, lead to fuel-temperature problems.

These data indicate some of the problems associated with the operation of a fast burst reactor with samples in a glory hole. Experience with SPR II also indicates the necessity for added caution in operating the reactor with samples in the glory hole although pulsing the reactor a few times at lower levels with the sample in place is sufficient to establish the necessary data points for a satisfactory extrapolation to larger yields.

CONCLUSIONS

The Sandia Pulsed Reactor II has now been in operation for over 1000 pulses and normally operates at an average rate of about 20 pulses per week. Difficulties have been encountered in large-yield bursts, but the problems involving fuel failures by stress corrosion and tensile failure appear to have been greatly reduced. The problems involving control-rod drives are being corrected, and nothing indicates that routine operation at design level will not be realized in the near future. This level of operation has been made possible through utilization of design techniques and materials developed by various organizations working on fast burst reactor technology. This reactor has proved quite satisfactory in that experimenters can expect repeatable performances at radiation levels of significant interest.

REFERENCES

1. J. A. Reuscher and J. M. Richter, Dynamic Mechanical Measurements on the Army Pulsed Reactor, *Trans. Amer. Nucl. Soc.*, 10: 612 (1967).
2. J. A. Reuscher, Thermal Stress Analysis for the Sandia Pulsed Reactor II, *Trans. Amer. Nucl. Soc.*, 10: 242 (1967).
3. J. A. Reuscher, Dynamic Mechanical Characteristics of the Sandia Pulsed Reactor II, *Trans. Amer. Nucl. Soc.*, 11: 220 (1968).
4. P. D. O'Brien, SPR II: Early Operational Experience, USAEC Report SC-DR-67-801, Sandia Corporation, 1967.
5. J. T. Mihalczo, J. J. Lynn, J. E. Watson, and R. W. Dickinson, Superprompt Critical Behavior of a Uranium – Molybdenum Assembly, *Trans. Amer. Nucl. Soc.*, 10: 611 (1967).
6. R. L. Coats and P. D. O'Brien, Pulse Characteristics of the Sandia Pulsed Reactor II, *Trans. Amer. Nucl. Soc.*, 11: 219 (1968).
7. R. L. Coats and P. D. O'Brien, SPR II Safety Analysis Report, USAEC Report SC-RR-66-2706, Sandia Corporation, 1967.
8. K. L. Haynes and P. D. O'Brien, Precisely Timed Initiation of a Fast Burst Reactor, *Trans. Amer. Nucl. Soc.*, 6: 284 (1963).
9. G. E. Elder, Design, Operation, and Utilization of the White Sands Missile Range Fast Burst Reactor, *Trans. Amer. Nucl. Soc.*, 8: 50 (1965).
10. R. L. Long, Reactivity Contributions in the Glory Hole of the Sandia Pulsed Reactor II, USAEC Report SC-CR-68-3571, Sandia Corporation, 1968; also *Nucl. Appl.*, 6(1): 8-15 (Jan. 1969).
11. R. L. Coats, Kinetic Behavior of a Reflected Fast Burst Reactor, *Trans. Amer. Nucl. Soc.*, 9: 468 (1966).

DISCUSSION

YOCKEY: Is your reactor shutdown factor reduced by the gaps between fuel plates?

JEFFERSON: I do not know that it is a great deal different from what it was in SPR I, and that is the only thing with which to compare it. There is, of course, some difference because we are using an alloyed fuel rather than pure uranium, but we do not have any way to measure any difference in negative temperature coefficient between this design and one without gaps because we have not built one without gaps. As Reuscher pointed out in his paper (see Session 1, Paper 3), the majority of the reactivity effect is caused by radial expansion, and these gaps do not change that.

KING: Did the slots you cut in the rings improve the situation so you had no further cracking?

JEFFERSON: We think so. We now have a significant number of pulses on the new core operated up to temperature excursions of 595°C, and so far we have not detected any cracks in the fuel. We are now beyond the point where we developed cracks previously.

MILEY: You mentioned that the cold-nitrogen cooling allowed you to increase the number of pulses per day, but you did not give a number.

JEFFERSON: We now produce 5 pulses in an 8-hr day.

MILEY: As an experimentalist who uses this type of reactor, I believe that it would be of interest to study possible methods of increasing the efficiency of cooling methods to obtain a larger number of pulses per day. This would, in my opinion, greatly increase the utility of the reactor.

JEFFERSON: As an operator who has to maintain these reactors, I am violently against that increase because of the activity buildup in the fuel.

MILEY: I understand that problem, but I am not convinced that we have reached an optimum number.

2-4 THE VIPER CORE

J. J. McENHILL
Atomic Weapons Research Establishment, Aldermaston, Berkshire, England

ABSTRACT

The VIPER reactor was first pulsed super critical in August 1967 at the Atomic Weapons Research Establishment, Aldermaston; since then 150 bursts have been produced. The pulse width is 400 μsec, and the peak yield is 3.5×10^{17} fissions.

In principle the reactor is similar to Godiva, but it has certain different features. The core consists of fuel rods of partly enriched uranium embedded in a matrix of copper and epoxy resin. The prompt negative coefficient of reactivity is largely due to the Doppler effect in ^{238}U, an effect which is enhanced by the moderating properties of the epoxy resin.

DESIGN PRINCIPLES

The fast burst reactor VIPER[1,2] is similar in principle to Godiva but has a few different features. The core is built of fuel rods, and therefore its composition can be changed. The Doppler effect in ^{238}U is used to provide a large part of the inherent temperature coefficient. The design yield is 3×10^{17} fissions, and the pulse width, for the core composition currently being used, is about 0.5 msec. A thick reflector is used to conserve fuel and to provide a space big enough for the irradiation of experiments 1 ft in size. The reflector also helps to decouple the core from its surroundings.

The design premise was that uranium-metal fuel would withstand repeated pulsing to 450°C. For a yield of 3×10^{17} fissions we would therefore require at least 200 kg of metal. With reasonable packing the ^{235}U-reflected critical mass is much less than 200 kg; so uranium of intermediate enrichment can be used. This factor is attractive because the Doppler effect in ^{238}U provides a significant inherent shutdown component compensating for the low temperature coefficient of

125

fuel in the form of rods. With 37.5%-enriched uranium and some hy-
drogenous material in the core to soften the neutron spectrum, the
Doppler temperature coefficient compensates adequately.

It was first pulsed super critical in August 1967, and since then
about 150 pulses have been run.

CORE CONSTRUCTION

The uranium fuel, 37.5% enriched-uranium alloyed with 1.25 wt.%
molybdenum, is in the form of cylindrical rods, each 11.4 in. long and
0.400 in. in diameter, clad in stainless steel. The cladding prevents
possible reaction of hot fuel with air and also provides a means of
holding each fuel rod at its midpoint so that the forces developed during
the pulse heating will balance and will not load the reactor structure.
The cladding is pinched to the fuel rod at a circumferential notch in the
center of the rod. Figure 1 shows the fuel-element design. Each ele-
ment is cast and machined to size and contains 155 g of ^{235}U in 418 g of
uranium.

The fuel rods are loaded into the core as a triangular lattice with a
pitch 0.51 in. (Fig. 2). The fixed central block, 8 in. by 15 in., contains
spaces for 478 elements, and each of the two side blocks contains
spaces for 133 elements. Each block is enclosed in a stainless steel
box. The side blocks are attached to hydraulic rams and can be slowly
raised into position to assemble the critical core or rapidly driven
down. There is a central hole into which the pulse rod is driven to start
the prompt-critical transient. A sectional view of the core is shown in
Fig. 3. The fuel elements are located by three low-expansion-steel
lattice plates that define the triangular matrix. The holes in the central
plate are displaced radially outward by 0.010 in. with respect to the
holes in the top and bottom plates to prevent simple inward bowing of
the fuel elements due to the radial transverse temperature gradient.
The elements rest on a base plate of steel and are held down by springs
bearing down on the core-box lid. The springs are strong enough to en-
sure that each element remains seated on the base plate after the pulse
is complete. The space between the fuel elements and the lattice plates
is filled with matrix plates of copper or aluminium-loaded epoxy resin.
Matrix plates are available in thicknesses of 0.375 in. or 0.187 in. and
in various shapes which fit together in layers that fill the core boxes as
in Fig. 2. The matrix area is divided in this way to allow for expansion
of the materials when the reactor is heated. The amount of hydrogen in
the core can be varied by varying the number of epoxy resin pieces
loaded into the core matrix. Generally the matrix material is the same
in any one horizontal layer, as shown in Fig. 3, which represents the
loading used for the current assembly, VIPER 1. The core is loaded to

SEALED HELIUM ATMOSPHERE

FUEL ROD
(MOLYBDENUM-
URANIUM ALLOY)

GROOVE SWAGED
IN CAN TO SUPPORT
FUEL ROD

STAINLESS STEEL CLADDING
0.4 IN. ID × 0.015 IN. THICK

SEALED HELIUM ATMOSPHERE
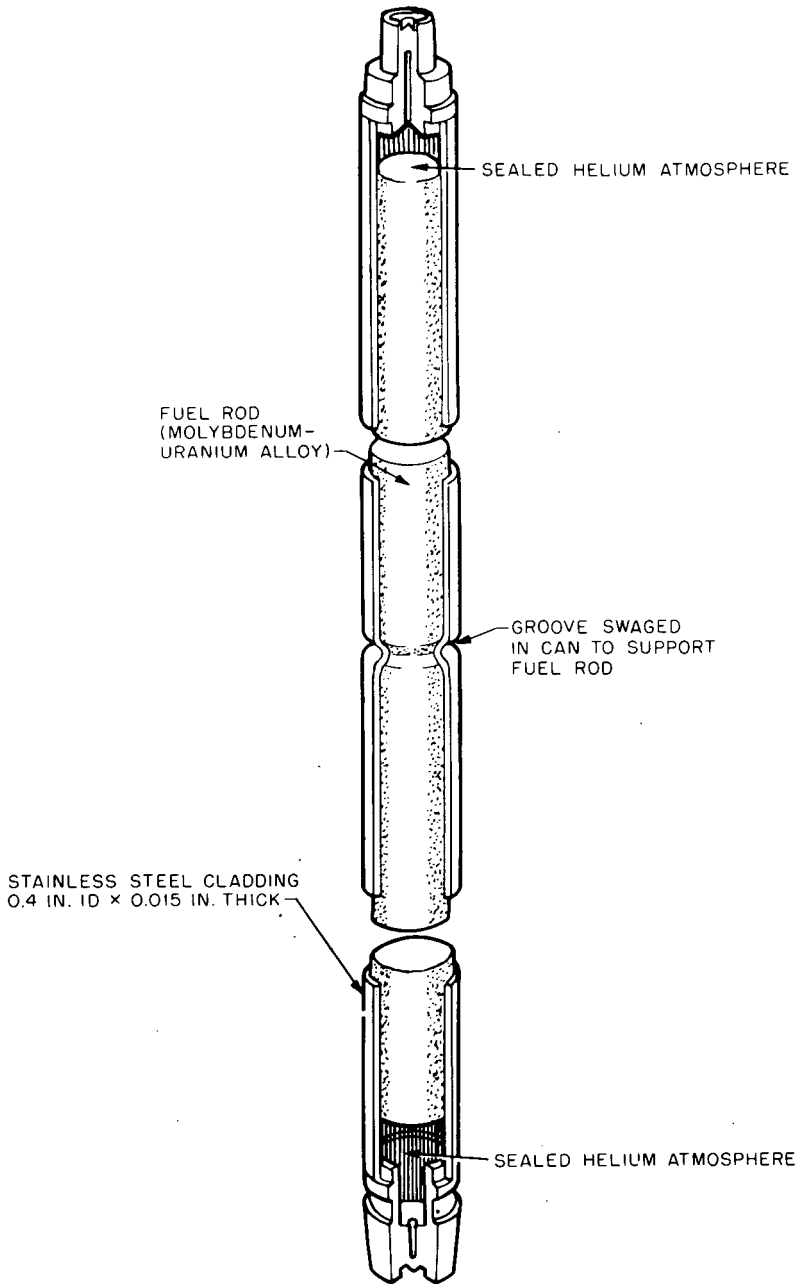
Fig. 1 — VIPER fuel rod.
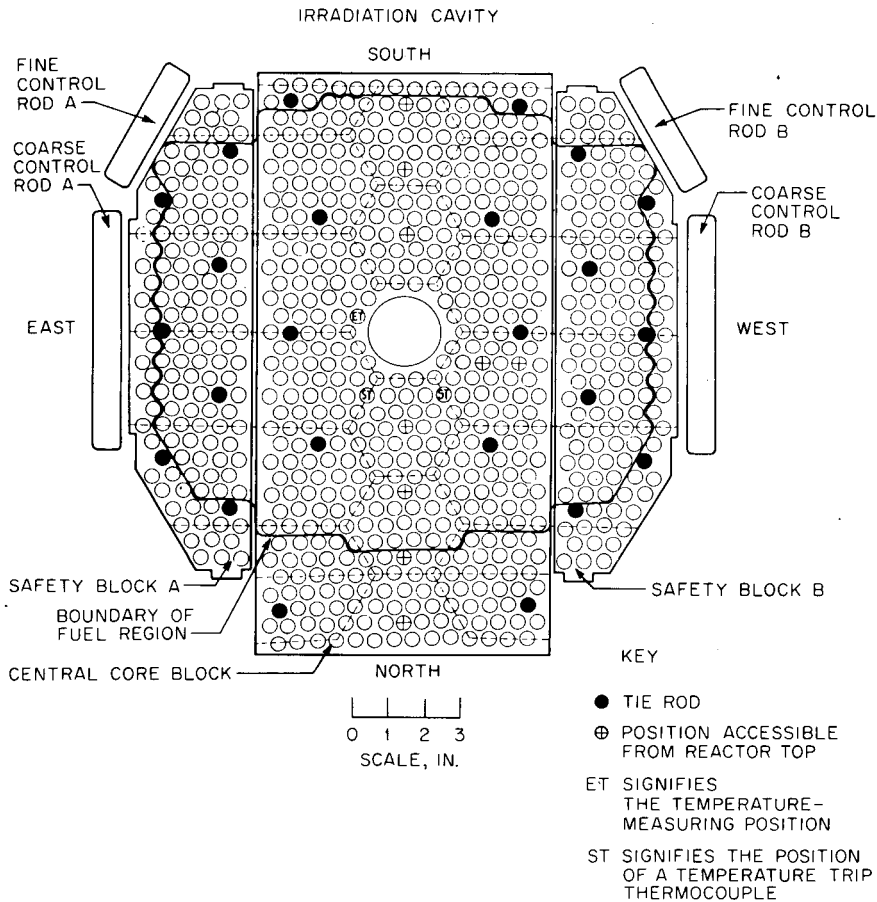
Fig. 2 — VIPER core plan.

critical, and any spare lattice positions are then filled with copper rods of approximately the same dimensions as the fuel elements. The outline of the core loading used for VIPER 1 is indicated by a black line in Fig. 2.

An isometric diagram of the reactor core is shown in Fig. 4.

The maximum volume fraction of uranium alloy in the core is 45%, and the minimum voidage amounts to 12.6%. The actual volume fractions in VIPER 1 are:

Fuel	Steel	Copper	Epoxy resin	Void
45.0	14.0	14.0	9.5	17.5
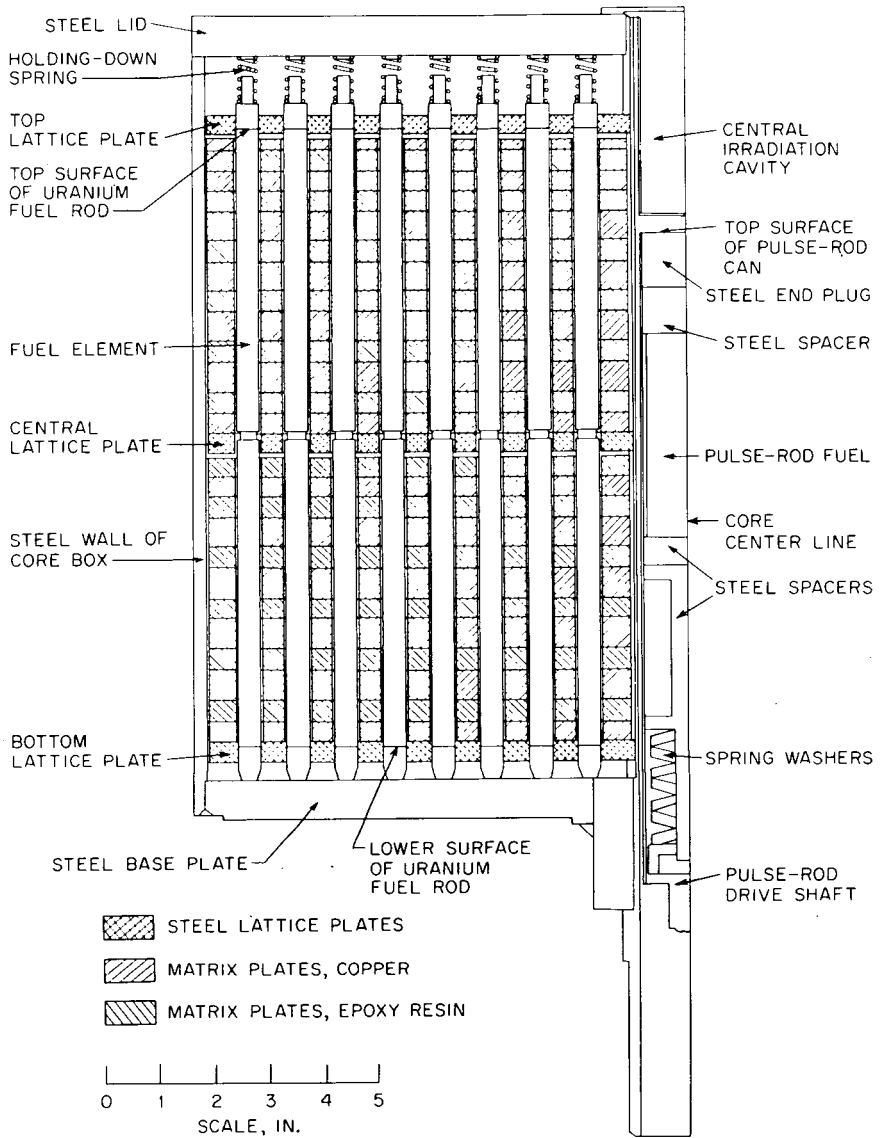
Fig. 3 — *Vertical section of the VIPER core from the center line to the north side.*

The atomic ratio H:^{235}U is 0.46, and the critical mass is 83 kg of ^{235}U.

Although in principle the core composition can be changed, e.g., a core with no moderator could be built to give a pulse width about 30%
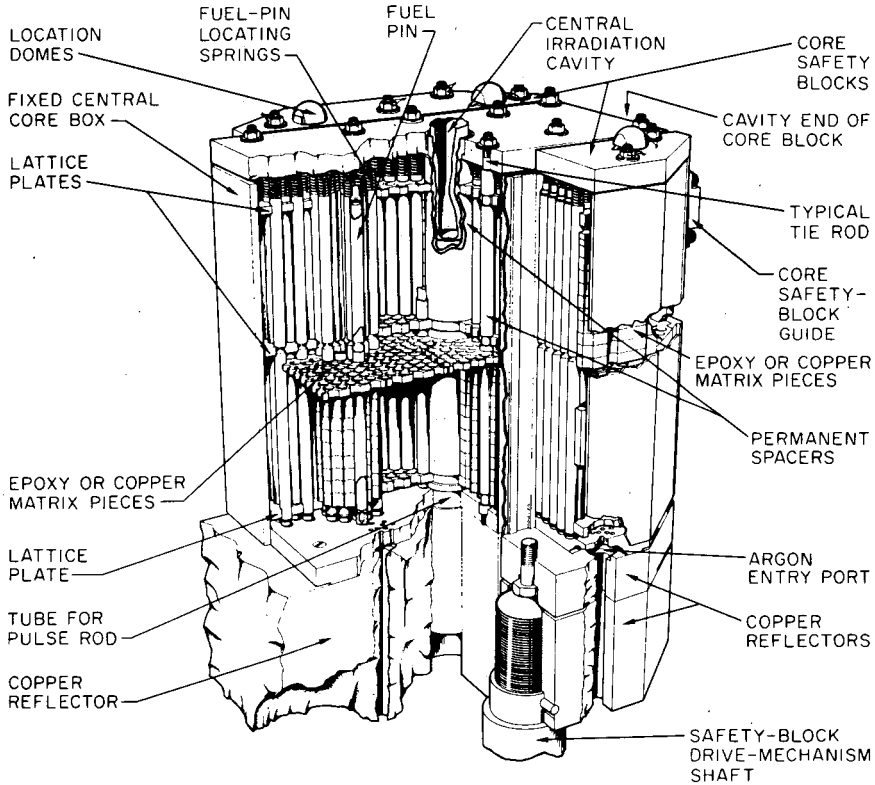
Fig. 4 — An isometric diagram of the VIPER core.

smaller than at present and a core with more moderator would give
about 50% larger pulse width, it has not yet been necessary to change
the core composition.

REACTOR LAYOUT

A plan of the reactor core and reflector is shown in Fig. 5, and a
vertical section drawing is shown in Fig. 6. The core is surrounded by
copper at least 8 in. thick on all sides, the top reflector being in the
form of a single slab that can be raised to give access to the top of the
core. Two fine and two coarse control rods filled with boron enriched
in ^{10}B are provided at the outer edge of the core for reactivity adjust-
ment. They are driven up or down by motors mounted on the reflector
lid. When fully down the boron-loaded region extends over the full core
height, and when fully raised the space is filled by brass followers.
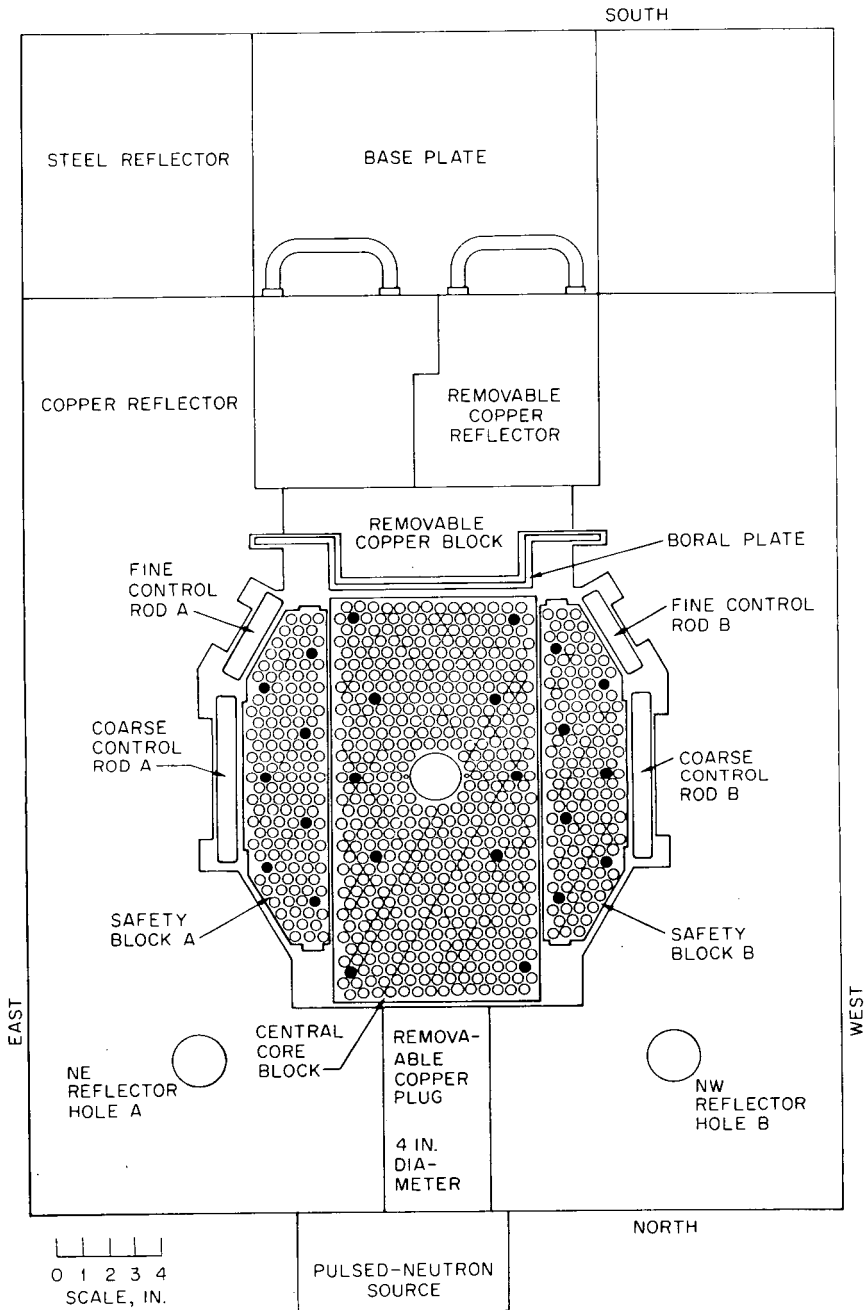
Fig. 5 — Plan of the core and reflector of VIPER.
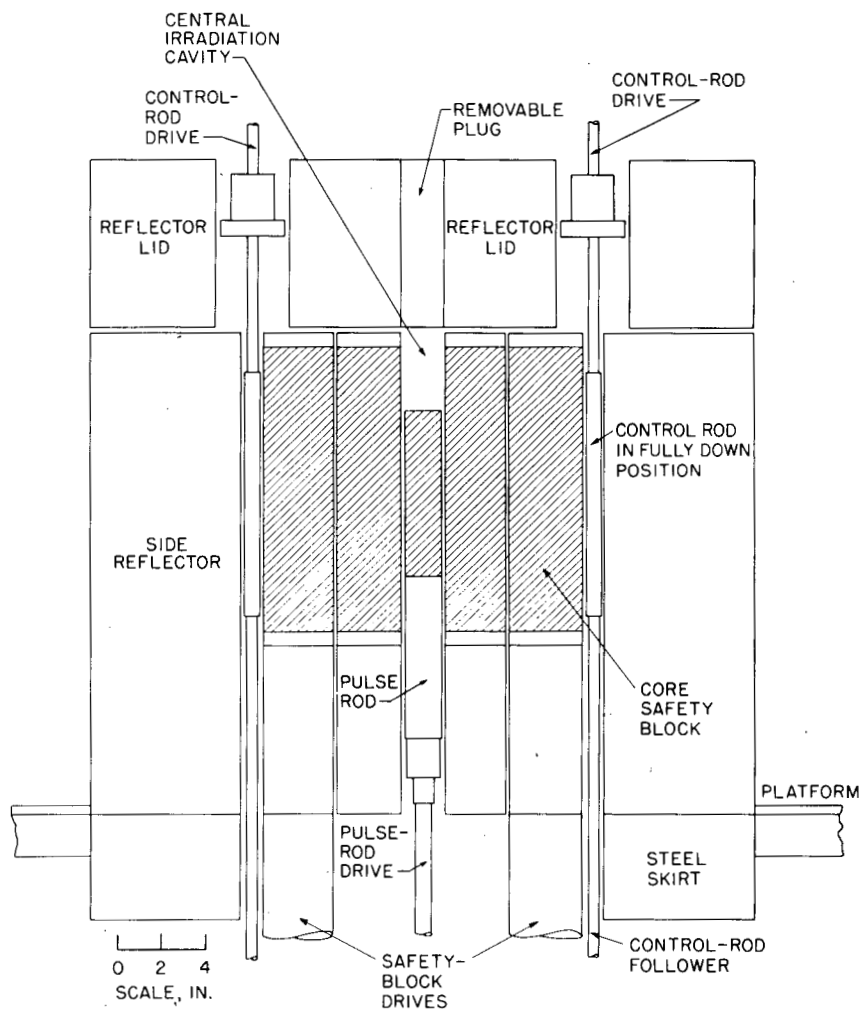
Fig. 6 — Vertical section of the core and reflector of VIPER.

Part of the side reflector is in the form of removable blocks, and the base plate is extended on that side so that a large irradiation cavity about 13 in. square and 11 in. long can be provided when necessary by rearranging the reflector blocks. A boral plate may be inserted to decouple the core from any slow neutrons produced in an irradiation experiment in the cavity. A space for smaller irradiation experiments is provided by the top portion of the central hole in which the pulse rod moves, access being provided by a removable plug in the top reflector. This central irradiation cavity is 1.75 in. in diameter and 3.5 in. long and is 3 in. from the core center at its nearest point. Two other experi-
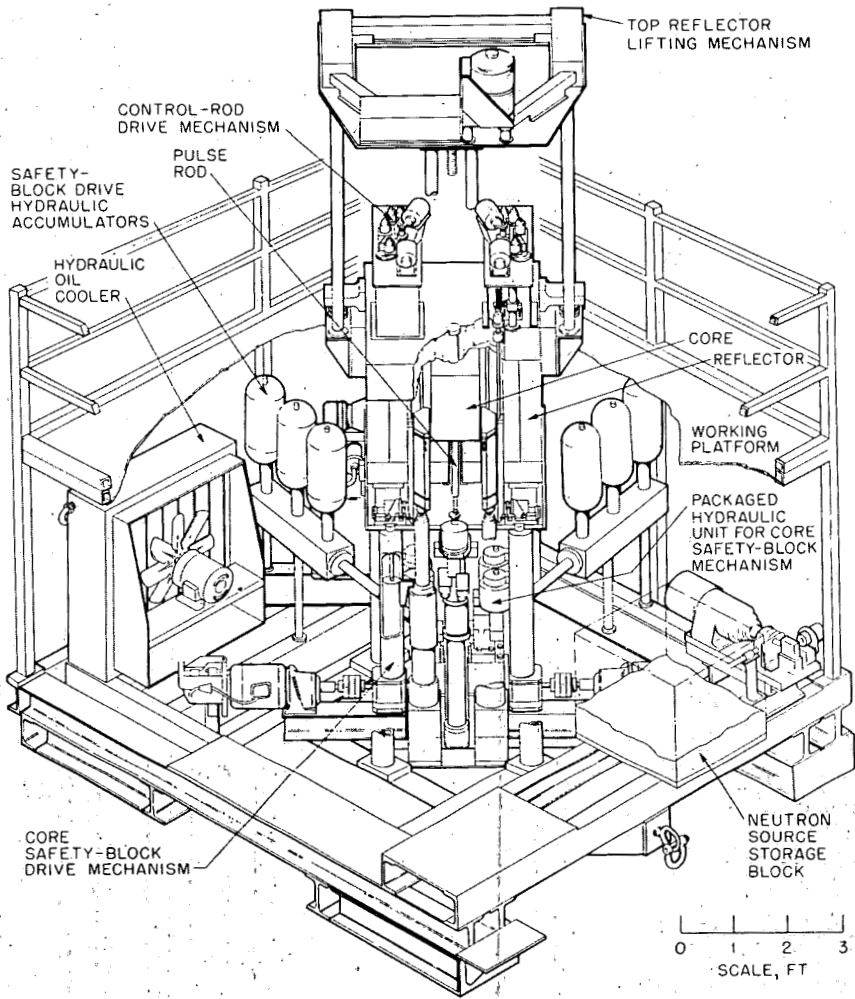
Fig. 7—General view of VIPER.

mental holes are provided in the corners of the reflector. On the north side of the reactor there is a 4-in. plug which can be removed to accommodate a pulsed-neutron source used for neutron-lifetime measurements and for time-of-flight spectrometry. The neutron beam for spectrum measurements passes through the region of removable blocks on the south side. The reflector region below the core is extended in a skirt to act as a radiation shield around the safety blocks when they are lowered.

A general view of the reactor is shown in Fig. 7. It has a base measuring 9 ft × 9 ft, is 13 ft high, and weighs 12 tons. The main feature

of the operating mechanisms is the hydraulic system for fast withdrawal of the safety blocks immediately after the reactor pulse. Energy for this purpose is stored in compressed nitrogen in a series of hydraulic accumulators, three for each safety block. Other ancillary items are a neutron source to provide an adequate neutron flux during start-up, a pneumatic drive system for the pulse rod, and a hoist for the reflector lid. There is also a pulsed-neutron source to initiate the reactor pulse when required. Provision is made to supply argon gas to the reactor core continuously so that the core components are always surrounded by an inert atmosphere when hot. The reactor has no forced-cooling system, and it requires about 6 hr to cool after a full-size pulse.

The reactor is mounted on a substantial frame that can be moved along rails when necessary into a position where a pulse of neutrons can be injected and where a beam can be extracted into a flight tube for time-of-flight spectrometry. It is housed in a large concrete-walled containment cell that also houses the low-power experimental fast reactor VERA.

CONTROL UNITS AND PULSE ROD

The reactor is controlled by movement of safety blocks or control rods. The safety blocks, which are portions of the fuel region of the core, are each worth at least 5% in reactivity. They are lowered to provide the necessary margin of safety when the reactor is being loaded with fuel or with irradiation samples, and they are subsequently raised as the first step in the approach to critical. Upward movement over the 12-in. stroke is complete in 3 min. The blocks are driven rapidly down with an acceleration of about 5 g to terminate the plateau heating following a prompt critical reactor pulse. Each block is supported on a 3-in.-diameter rod driven by a double-acting 4-in.-diameter hydraulic piston. The pressures on either side of this piston are adjusted so that the net upward force is sufficient to raise the block, its movement being accurately controlled by a lead screw and nut. When rapid shutdown is required, the trip signal opens vent valves in the lower cylinder, and the pressure in the upper cylinder then drives the block down, using stored energy from a hydraulic accumulator. The block begins to move 20 msec after the current supply to the vent valves is broken by the trip signal, and the time required to remove the first dollar of reactivity is 47 msec.

The control rods are brass boxes loaded with enriched boron. Each of two coarse rods contains about 440 g of ^{10}B and is worth about $1.2; each of two fine rods contains about 70 g of ^{10}B and is worth about $0.2. The control rods provide sufficient reactivity control to balance the effect of irradiation samples and to provide an alternative means of reac-

tor shutdown. They are also used to balance the reactor accurately at the critical condition.

The pulse rod, illustrated in Fig. 3, consists of a steel tube containing a 1.55-in.-diameter by 4.125-in.-long cylinder of uranium metal weighing 2.35 kg, which is of the same type and enrichment as used for the fuel elements. The reactivity worth ($1.27) is chosen so that a full-size pulse can be produced by driving the rod from its fully-out to its fully-in position starting with the reactor at delayed critical. A small margin of extra reactivity is incorporated to allow for variations in pulse-rod worth due to core rearrangements. For the rapid insertion required in pulsed operation, the rod is driven pneumatically, and it covers its full 14-in. stroke in 220 msec. This is sufficiently rapid to reduce the probability of preinitiation to an acceptable level provided there is no significant neutron emission from experimental components in the irradiation cavities. For checking reactivity balances the rod may be driven at slow speed through a nut and lead screw.

CORE MATERIALS

The fuel has to have the following qualities: (1) adequate strength to resist deformation under dynamic loading at high temperature, (2) minimum dimensional changes after thermal cycling, and (3) stability in the radiation environment. The suitability of uranium alloyed with 1.25 wt.% molybdenum was confirmed by tests of its strength and its resistance to thermal cycling.

During the reactor pulse the material in the fuel rods is compressed, and a compression wave travels to the end of the rod, where it is reflected as a tension. The maximum stress occurs at the rod center where the calculated average stress for a full-size pulse is 2 tons/sq. in. with a peak at the notch of 8 tons/sq. in. The center fuel temperature is about 100°C at the compression peak and about 320°C at the tension peak. The fuel strength was measured by plain bar tests of the fracture stress and the elongation at temperatures up to 600°C. Further tests of a similar type were made on bars notched in the same way as the actual fuel rods. These experiments showed that the 1.25 wt.% molybdenum alloy had adequate margins of strength and ductility for regular use in 400°C pulses and that damage by local yielding at the notch would not be expected in pulses up to 500°C.

The growth of the uranium alloy due to thermal cycling was measured by electrical heating in a vacuum and in argon. The samples were cycled between 60°C and 500°C once every 2 min.; heating took place in 2.5 sec; and the growth was measured after 500 and 1000 cycles. The tests were then repeated over the same temperature range with a salt-bath heating system. The results show that the thermal-cycling-growth

resistance of the 1.25 wt.% molybdenum alloy is satisfactory; the material is unlikely to extend by more than 0.1% as a result of 1000 cycles to 500°C.

The stability of the fuel after prolonged irradiation has not been tested. In 1000 full-size pulses the accumulated neutron dose is about 10^{18} neutrons/cm^2, and the mechanical properties of the fuel will be checked before this stage is reached. Other fuel effects considered were burn-up, which amounts to 0.0001% after 1000 pulses and is therefore not important, and chemical reaction between uranium and stainless steel, which should not be important since it proceeds very slowly at temperatures below 520°C.

The moderator has to have the following qualities: (1) it should contain an adequate proportion of hydrogen, (2) it should be capable of fabrication into the necessary shapes for the lattice, and (3) it should withstand heating to temperatures corresponding to a full-size pulse without damage, significant loss of hydrogen, or distortion. The material chosen for this purpose was an aluminium-filled epoxy resin with the following percentage composition by weight:

Aluminium	28.2
Carbon	50.8
Hydrogen	4.30
Oxygen	16.70

The material had a hydrogen content of 0.062 g/cm^3 and a density of 1.44 g/cm^3. Small blocks of it were tested by heating in an inert atmosphere for 10 hr at various temperatures. Above 200°C there was a small weight loss which increased slowly with temperature up to 300°C and fairly rapidly at higher temperatures. However, allowing for the total time spent at maximum temperature in each pulse, the total weight loss in 1000 pulses to 300°C would be about 1%, which is acceptable. The maximum moderator temperature in a full-size pulse is 267°C.

YIELD AND RADIATION DOSES IN THE FULL-SIZE PULSE

The maximum yield in a pulse in VIPER 1 is determined by the maximum temperature (275°C) to which the epoxy resin components can be heated without significant deterioration. Assuming a starting temperature of 25°C, the peak temperature at the core thermocouple corresponding to maximum yield is 237°C, the average fuel temperature rises to 332°C, and the peak fuel temperature is 456°C.

The measured maximum yield expressed in fissions is 3.63×10^{17}.

The integrated doses of neutron and gamma radiation at various positions in and around the reactor are shown in Table 1.

Table 1

RADIATION IN A FULL-SIZE VIPER PULSE

Location	Gamma radiation dose, r	Integrated neutron dose rate, neutrons/cm²/sec
Central irradiation cavity (bottom surface)	1.3×10^5	1×10^{15}
Core—reflector interface (on reactor midplane)	5×10^4	0.9×10^{15}
Large irradiation cavity (13 in. × 13 in. × 11 in. cavity with boron plate on core surface)		
Inner face	3.5×10^4	5×10^{14}
Center	1.1×10^4	
Outer face	8×10^3	
Outer surface of reflector (top surface, near reactor center line)	1.1×10^3	3×10^{13}

REFERENCES

1. J. W. Weale, H. Goodfellow, M. H. McTaggart, and E. G. Warnke, The Fast Pulsed Reactor VIPER. I. General Description. *J. Brit. Nucl. Ener. Soc.*, 7(4): 313-327 (October 1968).
2. M. H. McTaggart, H. Goodfellow, W. B. McCormick, and J. W. Weale, The Fast Pulsed Reactor VIPER. II. Reactor Physics Measurements and Analysis. *J. Brit. Nucl. Ener. Soc.*, 7(4): 328-342 (October 1968).

DISCUSSION

GLASGOW: Why did you choose copper for the reflector and for the space between the fuel elements? Was it for the neutronics or for the economics?

McENHILL: We wanted something to reflect the neutrons which was of reasonable cost. It was partly neutronics, partly economics. I think we probably misfired on the economic side as copper is now very expensive.

2-5 DESIGN OF THE ARMY PULSE RADIATION FACILITY REACTOR

H. P. YOCKEY,* M. I. LUNDIN,† and A. STATHOPLOS‡

*Ballistics Research Laboratory, Aberdeen Proving Ground, Maryland; †Oak Ridge National Laboratory, Oak Ridge, Tennessee; ‡Nuclear Technology Corp., White Plains, New York

ABSTRACT

The design objectives established for the Army Pulse Radiation Facility Reactor require a surface fluence of 1 to 3×10^{14} neutrons/cm^2 per burst, a burst width of $40 \pm 5\,\mu$sec, a peak flux at the core surface of 2 to 3×10^{18} neutrons/cm^2/sec, a total fission yield of 1 to 3×10^{17}, steady-state operation at 10 kw, and burst repetition in 2 hr. A parametric study of the Health Physics Research Reactor led to a core of larger diameter and smaller height-to-diameter ratio, making possible the inclusion of a glory hole 1.5 in. in diameter. Each core part is aluminum-ion plated to control corrosion. The core is kept in an atmosphere of dry nitrogen to control stress-corrosion cracking. All design specifications were met or exceeded.

The design objectives for the Army Pulse Radiation Facility Reactor (APRFR) required a surface fluence of 1 to 3×10^{14} neutrons/cm^2 per burst, a burst width of $40 \pm 5\,\mu$sec, a peak leakage flux at the surface of 2 to 3×10^{18} neutrons/cm^2/sec, total fissions 1 to 3×10^{17}, steady-state operation at 10 kw, and burst repetition in 2 hr. Since the Health Physics Research Reactor (HPRR) and its facility[1] most nearly met the Army requirements, the approach for the APRFR was to prepare a moderately improved and updated version of the HPRR. The design was modeled after the HPRR, and all design decisions pertaining to the HPRR were reexamined considering experiences at all burst reactor facilities.

A parametric study of the reactor physics of the HPRR-type reactor was conducted to investigate the effect of the following variables: (1) diameter of central stainless steel rod, (2) reduction of fuel enrichment, and (3) ratio of core height to diameter (H/D). The primary

139

factors evaluated were fission yield limited by stress, fluence, maximum temperature in the core, and burst full width at half maximum.

The flux flattening that results from a 2-in. stainless steel central rod allows the total fission yield to increase about 30%. The fluence at 1 m also increases by 30%. The maximum core temperature drops from 405°C to 327°C. The burst width increases from 30 to 39 μsec. The increase in burst width is within design objectives, and the larger fluence and yield and lower temperatures are desirable. The reactor configuration with a large central nonfuel region allows the incorporation of a centrally located glory hole of useful size. An increase in total yield can also be obtained by decreasing the enrichment from 93 to, say, 80%. This decrease in enrichment is a disadvantage with respect to a design that incorporates a nonfuel central rod because the maximum-to-average power ratio is reduced and because the maximum core temperature is reduced for a given yield.

Rather large variations of core height-to-diameter ratio are required for minor improvements in the fission yield at the expense of appreciable increases in the total critical mass. Large variations in the height-to-diameter ratio actually reduce the fluence or the flux near the surface of the reactor core where most of the experiments are located.[2] Little, if any, benefit and possibly some deleterious effects occur from appreciable deviation from a minimum-mass height-to-diameter ratio. The interaction of height-to-diameter ratio and central-void effects resulted in choosing a height-to-diameter ratio equal to 0.89 rather than to 1.13 as in the HPRR. This choice enlarged the central void and allowed the addition of an axially located glory hole large enough for samples or apparatus of significant size. For such samples the flux and fluence were increased by about a factor of 3 over that available at the surface, which obviously results in a considerable increase in the usefulness of the reactor.

The total fission yield in most fast burst reactors is limited by static and dynamic thermal stresses. Accordingly, the relative sizing and location of control rods, fuel-assembly bolts, fuel rings, and the safety block were investigated in detail. The limiting stresses were located, and the sizing of components was adjusted until approximately the same stress limitation appeared in each part. The fuel rings are held together by nine U−10 wt.% Mo bolts. The stress analysis showed that these bolts functioned primarily as very stiff energy-absorbing springs. Therefore the shank was undercut below the thread root diameter to increase the energy absorption capability.[3]

Uranium parts are usually plated to prevent sloughing of UO_2 and fission products. Unsuccessful attempts have been made to avoid stress-corrosion cracking by this means. Both nickel and aluminum-ion plating were tried.[4] Results indicated a clear superiority of aluminum-ion plating; therefore all parts in service are so treated.

Stress-corrosion cracking is a serious problem in applications of U−10 wt.% Mo. Hoenig and Sulsona[5] showed that both oxygen and water vapor must be removed from the ambient atmosphere. The core parts are shrouded to contain a dry nitrogen atmosphere. The static and dynamic stresses relax below threshold for stress-corrosion cracking in a few minutes. Cooling can then be accomplished by blowing dry air over the core.

All design objectives were met or exceeded. On the basis of early operational data, performance is as follows: maximum fission yield 2.1×10^{17}, surface fluence 2.8×10^{14} neutrons/cm^2, burst width 40 μsec, and peak leakage flux 6×10^{18} neutrons/cm^2/sec. In the glory hole the maximum fluence will be 9.4×10^{14} neutrons/cm^2 and maximum flux 2×10^{19} neutrons/cm^2/sec.

PARAMETRIC STUDY OF REACTOR PHYSICS

Reactor Structural Model

The reactor structural model used throughout the parametric study is illustrated schematically in Fig. 1. Basic features included: (1) a central stainless steel rod to which the safety block is attached at a position which is roughly at its axial midpoint, (2) a bolted reactor assembly consisting of annular cylindrical fuel disks, (3) flexible "finger" supports to allow essentially unrestrained core expansion in all directions, and (4) hollow bolts whose shank cross-sectional area is equal to the minimum thread root area to prevent stress concentration in the threads and to maximize energy-absorption capacity. The cold clearance gaps between the safety block and the rest of the reactor assembly (as shown in Fig. 1) were kept constant for purposes of this study. For physics calculations the core was assumed to consist of 95 vol.% U−10 wt.% Mo, 1.5 vol.% stainless steel (in addition to the central stainless steel region), and 3.5 vol.% void.

For each core configuration a series of calculations was performed to establish (1) static physics characteristics, including critical mass, power distributions, prompt-neutron lifetime, and radial and axial temperature coefficients of reactivity; and (2) reactor transient power behavior in the prompt critical regime, e.g., burst yield and width vs. initial reactivity insertion. The calculation method used to obtain information in these areas is described briefly in the following section.

Calculation Methods

Critical mass, power distributions, and radial and axial temperature coefficients were obtained using a two-dimensional transport theory code, DDF, on a CDC-1604 computer. The code employs the
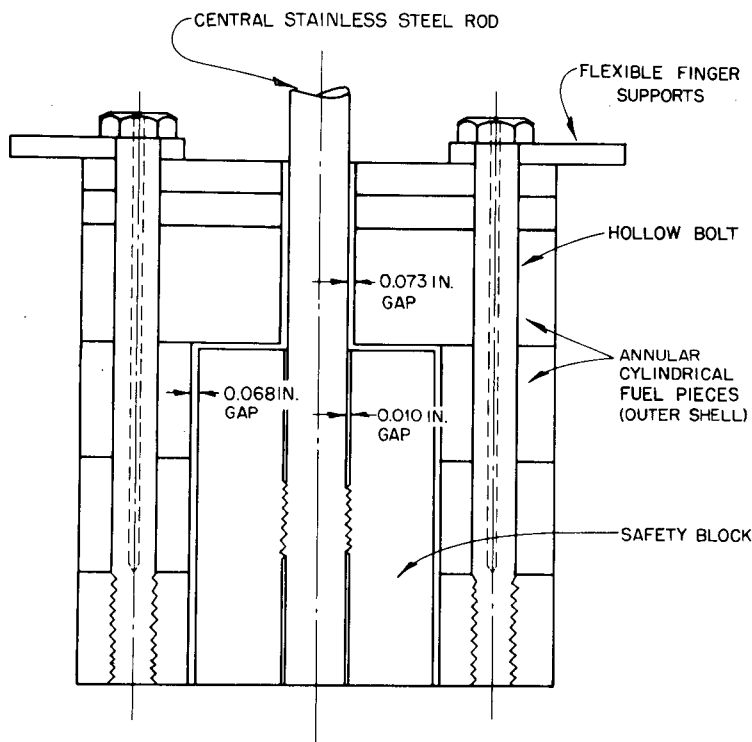
Fig. 1 — Reactor model for parametric study.

S_n method of solving the Boltzmann transport equation. All calculations used the S_4 approximation and a convergence criterion, ϵ, of 10^{-3}. The bulk of the parametric study was done using a 1-group cross-section set obtained from 6-group Hansen−Roach cross sections. The machine calculations were supplemented by experimental data and simple 1-group diffusion theory calculations where possible.

Temperature coefficients of reactivity were calculated by subjecting the assembly to a 1000°C uniform temperature increase and allowing unrestrained expansion of all fuel pieces. The expansion coefficient used for U−10 wt.% Mo was $12.6 \times 10^{-6}/°C$.

The prompt-neutron lifetime for each reactor core was estimated from published calculations and measurements for a variety of fast burst reactors.

The equation used to describe the prompt critical power behavior of the reactors was

$$\overset{..}{F}(t) = \alpha_\rho \, \rho(t) \, \overset{.}{F}(t)$$

where $F(t)$ = total fissions (or energy) at time t

$\rho(t)$ = reactivity above prompt critical as a function of time t

$\alpha_p = \beta_D / \ell$ prompt-neutron decay constant at delayed critical

β_D = delayed-neutron fraction

ℓ = prompt-neutron lifetime

The reactivity above prompt critical was described by

$$\rho(t) = \rho_0 - Ay_r(t) - By_a(t)$$

where $\rho(t)$ = prompt reactivity ($\$$) as a function of time t

ρ_0 = initial reactivity addition ($\$$) above prompt critical

$y_r(t)$ = radial displacement (cm) of fuel as a function of time t

$y_a(t)$ = axial displacement (cm) of fuel as a function of time t

A = radial-expansion reactivity coefficient ($\$$/cm)

B = axial-expansion reactivity coefficient ($\$$/cm)

The power behavior of the reactor was determined through the following sequence of operations:

1. Select an initial reactivity insertion ρ_0.

2. Assume a total fission yield and reactor power–time history.

3. Compute core-boundary displacements, $y_r(t)$ and $y_a(t)$, on the basis of 2.

4. Compute reactor power–time history on basis of displacements calculated in 3.

5. Compare assumed power–time history, 2, with computed power–time history, 4. If burst yield and width agree to within 10%, stop the problem; otherwise iterate using computed power–time history in step 2.

Results

The results of calculations for nine basic reactor-core configurations covering three central stainless steel rod diameters (0, 1, and 2 in.) and three core diameters for each steel rod diameter are presented in Table 1. The prompt-neutron decay constant for each configuration was estimated from published measurements and calculations for a variety of fast burst reactors. As a result of calculations by Mihalczo,[2] the decay constant was assumed independent of the core height-to-diameter ratio for the range of values covered here. The prompt decay constant varies approximately linearly with central stainless steel rod diameter from a value of 8.4×10^5 sec^{-1} with no stainless steel to about 6.4×10^5 sec^{-1} for a 2-in.-diameter steel rod. The prompt critical power behavior for each of the nine core configurations in Table 1 was calculated for three values of initial

Table 1

STATIC PHYSICS RESULTS

	Reactor number								
	1	2	3	4	5	6	7	8	9
Central stainless steel rod diameter, in.		0			1			2	
Core diameter, in.	6.5	7.52	9.06	7.0	8.0	10.0	7.4	8.0	11.0
Core height, in.	13	7.52	5.55	12.1	7.7	5.4	14.65	9.8	5.5
Core height-to-diameter ratio	2	1	0.61	1.73	0.96	0.54	1.98	1.23	0.5
Critical mass, kg U−10 wt.% Mo	115	89.5	94	121.3	101.3	111.6	155.2	122.7	134.3
Total temperature coefficient, ¢/°C	−0.3	−0.3	−0.3	−0.29	−0.3	−0.29	−0.3	−0.31	−0.3
Axial temperature coefficient, ¢/°C	−0.13	−0.11	−0.08	−0.11	−0.09	−0.05	−0.12	−0.11	−0.06
Radial temperature coefficient, ¢/°C	−0.17	−0.19	−0.22	−0.18	−0.21	−0.24	−0.18	−0.20	−0.24
Safety-block power fraction	0.2	0.2	0.21	0.23	0.23	0.22	0.2	0.2	0.22
Outer-shell power fraction	0.8	0.8	0.79	0.77	0.77	0.78	0.8	0.8	0.78

prompt reactivity insertion. Results of burst yield and burst width vs. initial reactivity insertion were then tabulated. These results are illustrated in Figs. 2 and 3, which show burst width vs. stainless steel rod diameter and burst width vs. core height-to-diameter ratio, respectively, for burst yields of 1×10^{17} and 2×10^{17} fissions.

STUDY OF STATIC AND DYNAMIC STRESS

Calculation Methods

In all the reactor cases considered, maximum stresses were calculated for the safety block, outer shell, and bolts. These maximum stresses for each burst were compared with the allowable design stress to determine the maximum burst obtainable for each reactor configuration. The allowable design stress was defined as 90% of the ultimate tensile strength corresponding to the highest temperature in the component. The ultimate tensile strength of U−10 wt.% Mo as a function of temperature is shown in Fig. 4 for both cast and wrought material. The allowable design stress in all cases has been based on the use of cast material (lower curve). Tensile data for U−10 wt.% Mo subsequently obtained from samples obtained during fabrication indicated that the ultimate tensile strengths were 20 to 30% higher than those used in this paper. This increased allowable strength means that actual maximum allowable burst yields should be larger than calculated.
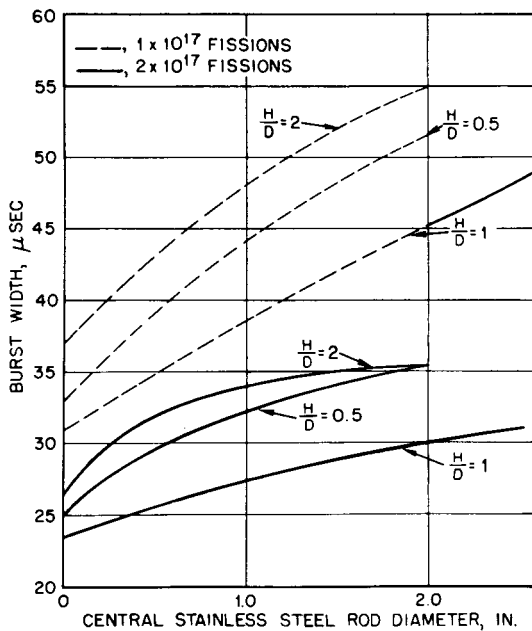
Fig. 2 — *Burst width vs. central stainless steel rod diameter.*
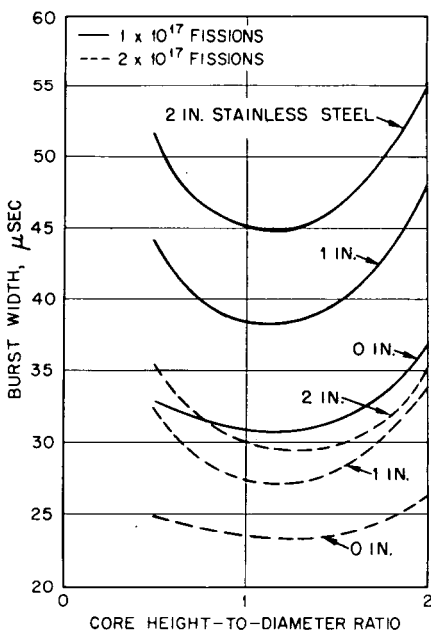
Fig. 3 — *Burst width vs. core height-to-diameter ratio for bursts of 1 and 2 ×*
10^{17} fissions.
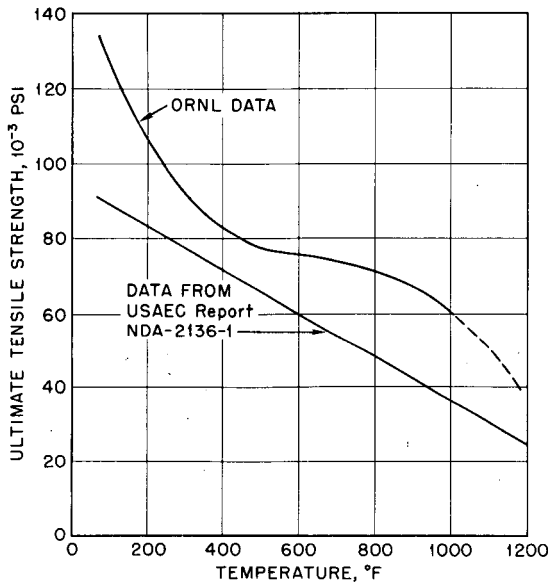
Fig. 4—*Ultimate tensile strength of cast U–10 wt.% Mo vs. temperature.*

The bolt stresses were obtained using the following expression,[3] which is valid for bolts in cases where $T_p/T_n > 1$:

$$\sigma_{max} = E\alpha T_0 \left(1 + \frac{A_2}{A_1}\right)^{1/2} \frac{T_n}{2T_p}$$

If $T_p/T_n < 1$, then

$$\sigma_{max} = \frac{EV_0}{C} \left(1 + \frac{A_2}{A_1}\right)^{1/2}$$

where E = Young's modulus
     α = thermal expansion coefficient
     T_0 = average temperature rise in outer shell
     A_2 = outer-shell cross-sectional area (minimum)
     A_1 = bolt cross-sectional area (minimum)
     T_n = fundamental period of vibration of bolt
     T_p = pulse (heating) period
     V_0 = mean velocity of outer-shell pieces
     C = speed of sound in U–10 wt.% Mo

These expressions were plotted as $\sigma_{max}/E\alpha T_0$ vs. A_1/A_2 for various values of T_p/T_n. These curves were then used in obtaining bolt stresses.

The stress in the outer cylindrical shell of the reactor core consists of inertial stress and transient thermal stress. The inertial stress was computed by methods developed by Burgreen.[3] Since the maximum temperature in the outer shell occurs at the inner edge, the inner edge is also the point of minimum allowable design stress. The inertial and thermal stresses were algebraically added at the inner edge and compared with the allowable stress at that point. In almost all cases the allowable stress at the inner edge was the stress that limited fission yield in the reactor.

The stress in the safety block also consists of inertial and transient thermal stress. The thermal stress, however, is small since the temperature gradients in the safety block are generally small. The inertial stress was computed by using a bar model for the safety block and the appropriate stress-reduction factors.[3]

Results

Using the results of burst width and yield as described previously, stresses in the bolts, safety block, and outer shell of each reactor configuration were calculated as functions of burst yield. Initially, calculations were made for each core, assuming a standard safety-block size and a fixed ratio of outer-shell to bolt cross-sectional area. The standard safety block was defined as having a diameter equal to half the core diameter and a fuel mass equal to 14.5% of the total core mass. The shell-to-bolt cross-sectional area, A_2/A_1, was fixed at a value of 11.

Stresses in the bolts, safety block, and outer shell of each core were determined as functions of burst yield. The yield at which each component reached its stress limit was identified. In almost all cases the limiting stress was reached first in the outer shell of the core assembly. For the tall cylinders (core height-to-diameter ratio = 2), however, the bolts had also approached their limiting-stress values at about the same fission yield at which the outer-shell stress had become limiting.

The limiting fission yield and corresponding burst width for each reactor configuration are listed in Table 2. The maximum core temperature, the fission yield per unit core mass, and the maximum neutron fluence 1 m from the reactor center are tabulated.

A second set of calculations was performed for reactors 4 to 9 to determine the effect of safety-block size. In these reactors the safety-block diameter was maximized while a minimum outer-shell thickness of 1.5 in. was maintained to ensure accommodation of the bolts necessary for shell clamping. The shell-to-bolt cross-sectional area ratio was maintained at 11, the same value used for the small safety-block study. The limiting stress in each of these reactors was again at the

Table 2

MAXIMUM PERFORMANCE OF BASIC CORE CONFIGURATIONS

Reactor No.	Height-to-diameter ratio	Critical mass, kg U−10 wt.% Mo	Stress-limited yield, fissions	Max. core temperature rise at limited yield, °F	Pulse width at limited yield, μsec	Yield/mass, fissions/kg	Neutron fluence 1 m from reactor center, neutrons/cm^2
1	2.0	115	1.25×10^{17}	720	32	10.8×10^{14}	1.38×10^{12}
2	1.0	89.5	1.03×10^{17}	750	30	11.5×10^{14}	1.14×10^{12}
3	0.61	94	1.03×10^{17}	735	32	10.9×10^{14}	1.14×10^{12}
4	1.73	122	1.35×10^{17}	650	36	11.1×10^{14}	1.50×10^{12}
5	0.96	101	1.17×10^{17}	670	35	11.6×10^{14}	1.21×10^{12}
6	0.54	112	1.25×10^{17}	660	38	11.2×10^{14}	1.39×10^{12}
7	1.98	155	$1.7 \ \times 10^{17}$	610	39	11.0×10^{14}	1.89×10^{12}
8	1.22	123	1.36×10^{17}	620	39	11.1×10^{14}	1.54×10^{12}
9	0.5	134	1.36×10^{17}	570	43	10.1×10^{14}	1.51×10^{12}

inner edge of the outer core shell; however, as the core height-to-diameter ratio approached 2, the bolt stress became limiting. The larger safety blocks allowed higher maximum yields from these cores ranging from an increase of 6% at a height-to-diameter ratio of 1.73 to 25% at a height-to-diameter ratio of 0.5.
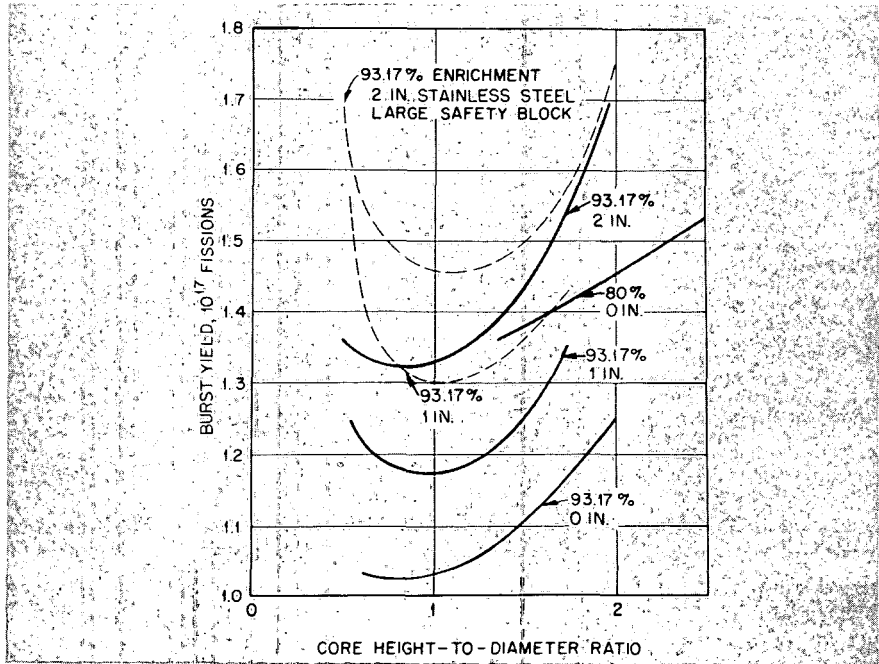
Fig. 5—*Limiting burst yield vs. core height-to-diameter ratio.*

Stress calculations were also performed for two 80%-enriched cores, designated reactors 10 and 11, with no central stainless steel rod. Results were obtained for core height-to-diameter ratios of 2.5 and 1.38. At the 2.5 ratio, the bolts reached a limiting stress at a yield of 1.53×10^{17} fissions. At the 1.38 ratio, the outer shell was limiting at a yield of 1.37×10^{17} fissions. For low-enrichment cores, as for the previous full-enrichment cores, the bolt stress appears to be limiting at core height-to-diameter ratios in excess of about 2.0, and maximum yield per unit core mass appears to decrease at ratios exceeding 2.0.

Since maximum fission yield, maximum neutron fluence, maximum reactor temperature, and burst width are important performance criteria, they have been summarized vs. core height-to-diameter ratio for the standard and large safety-block designs, in Figs. 5 to 7.

Fig. 6—Maximum core temperature vs. core height-to-diameter ratio.

Fig. 7—Burst width vs. core height-to-diameter ratio for limiting fission yield.

METALLURGICAL PROBLEMS

In general, metals are seldom used in the pure form, especially for load-bearing or stressed parts. It is natural, then, to look for an alloy of uranium with superior mechanical properties. Pure uranium has two drawbacks that lend further emphasis to a search for a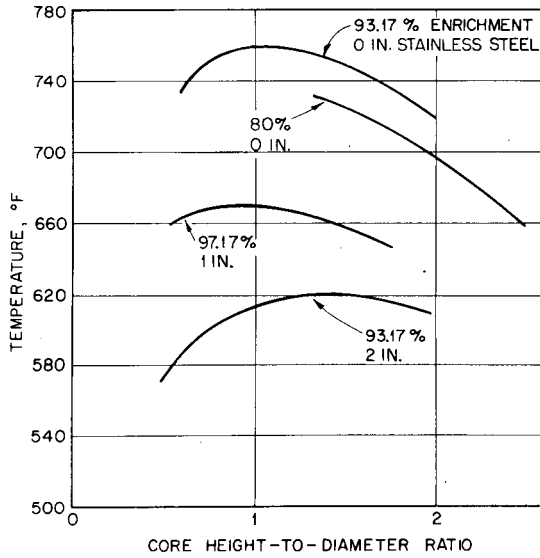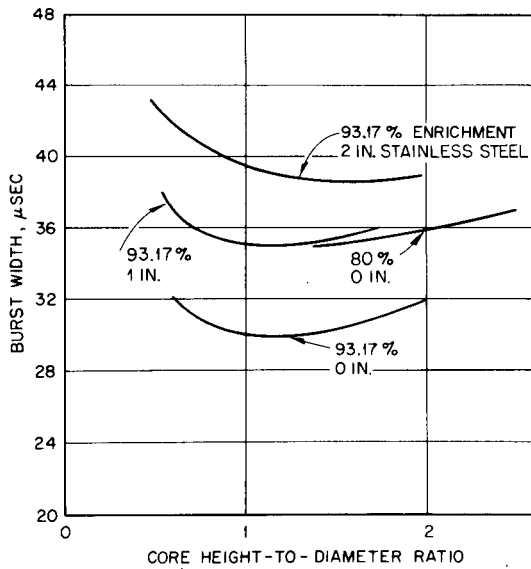 suitable alloy, namely, a dimensional instability under thermal cycling and pyrophoricity. Study[6] of the available literature at the time design decisions were being made on the HPRR indicated that the use of U−10 wt.% Mo increased the yield strength available to the designer from 43,000 psi for pure uranium to the 90,000- to 140,000-psi range. The alloy was demonstrated[7] to be sufficiently dimensionally stable under thermal cycling. Tests showed that U−10 wt.% Mo is not pyrophoric, and it is regarded as an improvement over pure uranium even considering its susceptibility to stress-corrosion cracking and its notch sensitivity.

Pure uranium exists in three crystalline forms — alpha, beta, and gamma. The alpha phase is stable below 662°C and exhibits an orthorhombic crystalline structure. The beta form is stable from 662 to 770°C; this phase is complex tetragonal. The gamma phase is body-centered cubic and is stable above 770°C to the melting point at 1130°C. The addition of alloying elements, specifically molybdenum, stabilizes the gamma phase. The time−temperature transformation curve shows that in alloys with about 10 wt.% molybdenum the gamma phase may be quenched to room temperature. The gamma phase is dimensionally stable under thermal cycling, in marked contrast to the well-known ratcheting found in pure uranium. This stability is usually attributed to its body-centered cubic structure, which provides a high degree of isotropy. The gamma phase is also stable under radiation damage although the burnup in fast burst reactor service is not large enough to require this property.

When design decisions were being made for the APRFR, some experience in the use of U−10 wt.% Mo in burst reactors had already been obtained with the HPRR, the White Sands Missile Range Reactor (WSMR), the Super KUKLA,[8] and at Sandia Corporation. In general, the material was satisfactory. Plating and stress-corrosion cracking were the principal problems. The maximum burst size that can be obtained with the fast burst reactor appeared to be limited by mechanical properties; subsequent tests have proven that this is the case. Alloys of uranium stronger than U−10 wt.% Mo had also been developed. Information on these alloys which must be evaluated for use in a fast burst reactor, such as high-temperature strength, fatigue strength, and dimensional stability in thermal cycling, was not available, however. These alloys are in the alpha phase. The alpha phase

is of higher density than the gamma phase, and the difference is sufficiently large to affect materially the neutronic calculations. Therefore U–10 wt.% Mo was chosen; the use of other alloys is not regarded to be within the scope of the present engineering design program but is the subject of another investigation.

The core components were machined from induction-melted vacuum castings heat treated to retain the gamma phase. Carbon is the impurity that is most important and most difficult to control. General concurrence is that carbon affects both the yield strength and ductility and should be kept as low in concentration as possible, in any event below 200 ppm.[8–10]

Tensile specimens for determining tensile and ductility properties were prepared. The tensile and ductility properties were measured in room air and in argon. The results shown in Fig. 8 indicate that the argon atmosphere afforded an important protection, and the ductility was preserved at high temperature. Young's modulus for specimens tested in argon varied from 11.5×10^6 at $75°F$ to 10.2×10^6 at $1000°F$.
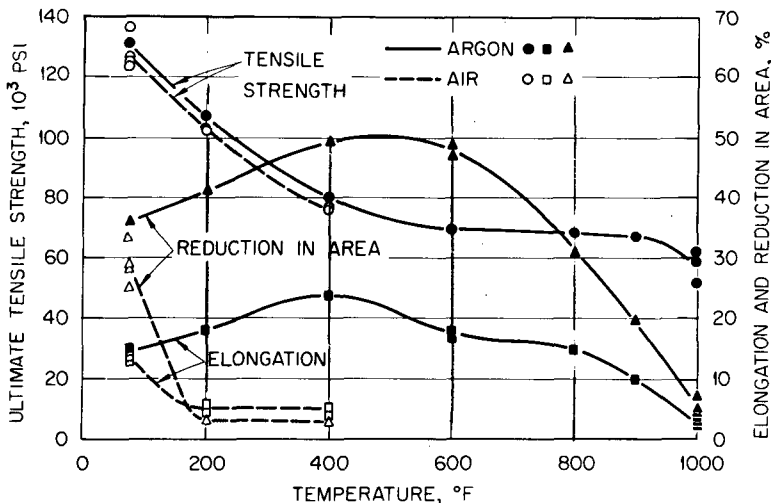
Fig. 8—Tensile ductility properties of U–10 wt.% Mo alloy.

An improvement in the plating was clearly desirable since nickel plating on uranium has been found to peel, flake, and blister. It was decided to compare nickel-plated parts with aluminum-ion-plated parts during criticality testing. The results with the two methods would then be evaluated. The aluminum plating stood up very well in the tests; this method was adopted for the final APRFR core.

The dynamic thermal stresses generated in a fast burst reactor are large and at high frequency (governed by natural modes of vibra-

tion). Thus the strain rates are very high, i.e., of the order of 500 in./ in./sec. Uranium – 10 wt.% molybdenum is one of a number of metals which show an increase in yield strength at high strain rate.[8] This effect is substantial and may amount to a doubling of yield strength at very high strain rates. Conservative design practice does not allow this effect to be relied upon although it is worth noting, nevertheless.

Numerous metals including brasses, steel, aluminum, and titanium alloys under stress in corrosive environments will crack and fail if stress exceeds a certain value that depends on specific conditions. The phenomenon is not well understood, is highly variable, and no doubt is due to various causes in different materials under different conditions. Each case must be investigated individually, and a means of protection must be found to suit each application.

Uranium – 10 wt.% molybdenum is susceptible to stress-corrosion cracking in room air. Two approaches have been taken: (1) find a satisfactory plating to prevent access of the element responsible and (2) eliminate the corrosive compounds in air, i.e., oxygen and water, or utilize a noble gas. Failure of coatings, as far as stress-corrosion cracking is concerned, is universally reported.[10] (Nevertheless, a plating is needed to prevent sloughing and spread of radioactive contamination.) Until a coating that is effective against stress-corrosion cracking is developed, the second alternative must be used.

As previously mentioned the ductility of U–10 wt.% Mo was greatly increased at high temperature in an atmosphere of argon. The use of this gas would solve the problem; however, a more economical gas is desired. Since dry air in large quantities is economical, that medium is a good candidate. Hoenig and Sulsona[5] made a rather extensive investigation of stress-corrosion cracking in various atmospheres, using the field-emission microscope to detect cracks and to study the surface condition of samples. Studying the effect of a number of ambient gases, they found that under dry nitrogen no surface cracks appeared after 1000 cycles up to a stress of 36,000 psi. This finding is in agreement with Peterson and Vandervoort,[10] who discovered that vacuum dry nitrogen and dry CO_2 protect against stress-corrosion cracking at the same value of stress. On the other hand dry air was not satisfactory, indicating that both water and oxygen must be removed from the ambient atmosphere.

The cooling time for the APRFR at large bursts is about 90 min. Dry nitrogen is expensive as a coolant for this entire period. Fortunately transient and dynamic thermal stresses are relaxed below the critical level in a few minutes. It is only necessary therefore to provide dry nitrogen as a blanket prior to and for a few minutes after the burst. The cooling may then begin with the use of dry air blown about the core. This is the means of combating stress-corrosion cracking currently in use.

DESIGN DECISIONS

The generation of a practical design involves using idealized parameter studies and material surveys in the context of problems of fabrication and operation. The flux flattening achieved by a 2-in. stainless steel central rod indicated that a glory hole to achieve access to the high-flux region of the core could be provided. The diameter of this glory hole was arbitrarily set at 1.5 in. When not in use for experiments, a plug is provided to fill 50% of the cavity. The glory hole must be surrounded by a protective liner, and clearance must be provided for installation of the tube and for scramming the safety block. When all fabrication and installation tolerances are considered, the inside diameter is $2\frac{3}{16}$ in. for the central stainless steel safety-block holder, as shown in Fig. 9.

With regard to the core height-to-diameter ratio, the studies discussed previously indicated that a ratio somewhat less than 1, namely 0.89, would be the best choice. This decision established the diameter of the core at 8.90 in. The diameter of the HPRR fuel rings is 8.00 in.

A design of the safety block which differed from that of Fig. 1 was studied. This design is shown in Fig. 9 in its final form. The full height of the safety block shown controls 15% more reactivity than the 3/4-length block shown in Fig. 1. Since it is positioned at or near its maximum effectiveness, the sensitivity of the safety block to positioning reproducibility is much less critical. The motion required to reduce the reactivity by $1, however, is much larger. The contribution to the total fission yield that occurs in the tail of the burst as the safety block is removed must be evaluated therefore for different heights of the safety block. This study showed that for a burst yield of 5×10^{16} the full-height safety block permits a contribution from 11 to 20% of the total yield in the tail of the burst. The 3/4-length block permits a contribution of from 6 to 11%. However, in the fission-yield value of interest for this reactor, that is, 1 to 2×10^{17} fissions, this tail contribution drops considerably and is not expected to exceed 3% at a fission yield of 2×10^{17}.

The calculations were based on an acceleration of 2 g without consideration of the added acceleration due to the inertial shock. Since the inertial shock is especially strong in high-yield pulses, the contribution of the tail is expected to be even smaller than 3%. The full-height safety block was incorporated in the design; this represents one of the major departures from the HPRR.

The bolt design shown in Fig. 9 was changed from that of Fig. 1 for a number of reasons. Service and fabrication in the HPRR had shown that it is not feasible to plate the inside of the hollow bolt. The
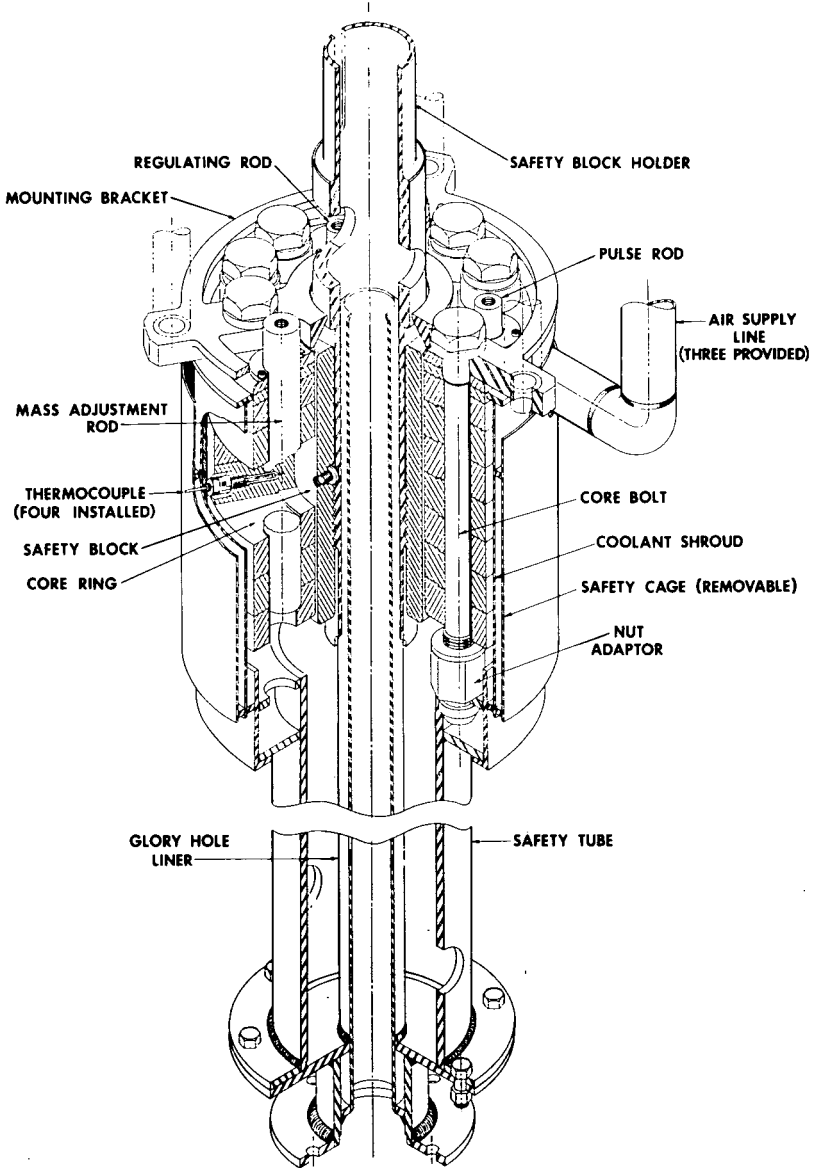
Fig. 9 — Core assembly of the APRFR with glory hole liner.

difficulty of drilling a true hole contributed to the cost. The reduced-shank design was therefore adopted. The bolts were threaded into the bottom plate of the core which was used in the tests to damage.[2] The distortion of this plate and galling of the core bolts jammed four of the bolts. It was necessary to break them to disassemble the core. The design was changed to secure the bolts individually with nuts, as shown in Fig. 9.

A coolant shroud, (Fig. 9), encloses the core to direct the flow of air. Attached to the coolant shroud is a safety cage which is required to maintain a minimum distance of 0.5 in. to the core surface. The function of the safety tube is to prevent the inadvertent lowering of the core too near the floor, which could prevent the removal of the safety block, and the floor would add a large amount of reactivity. The reactivity worths of the reactor components measured both at APRFR and the Oak Ridge Critical Experiment Facility (CEF) are shown in Table 3.

Table 3

REACTIVITY WORTH OF REACTOR COMPONENTS

Component	Total worth, ¢	CEF measurement,[4] ¢
Regulating rod	75.5	72
Mass adjustment rod	172.4	168
Burst rod with 2.125-in. adaptor	127.7	*
Glory hole liner	24.5	No data available
4 TC inserts	5.0	*
Cooling shroud and safety cage	154	148
Displacement gauge mounting plate	Not present	49
Nitrogen can	2.0	*

*These are new components, and hence no CEF data are available.

After the configuration of Fig. 9 was adopted, the detailed sizing of parts was accomplished by calculating the localized stress at critical points in the core bolts, fuel disks, and safety block, as well as in the mounting-bracket-ring core-support rod, regulating-rod-shaft mounting-bracket fingers, and safety-block holder as a function of burst yield. The stainless steel parts were designed with a substantial margin of strength to withstand the shock of bursts large enough to damage the core. The core-component sizes were adjusted so that the limiting stress was reached at approximately the same total fission yield. The largest and safest routine burst yield was thus established at 1.5×10^{17} fissions. Burst tests[11] performed at CEF established that no distortions occurred at a burst yield of 2.1×10^{17}. The difference in these

figures reflects the conservatism of the detailed design calculations and the lack of well-established criteria for failure in fast burst reactor service.

METALLURGICAL SPECIFICATIONS

The metallurgical specifications for the APRFR reflected an attempt to use the best possible practice in fabrication of this core. Changes from the HPRR specifications represent a reduction in permissible impurities content. Carbon content was reduced from 500 ppm to 250 ppm. An iron plus chromium plus nickel limit of 200 ppm was added, as was a separate hydrogen limit of 3 ppm. The specified minimum mechanical properties and the required ductility were increased.

All the U−10 wt.% Mo-alloy parts were cast in a vacuum-type induction heater. High-purity molybdenum powder was blended with uranium stock in a graphite crucible that had been plasma coated with zirconium oxide to reduce carbon pickup. Each charge was heated to 1400°C and held for 30 min to obtain complete molybdenum solution. The charge was then cooled to 1320°C, poured into a graphite mold, flame-coated with zirconium oxide, and furnace cooled. Each part was then heat-treated at 900°C for 24 hr and again furnace cooled. The parts were then rough machined, sampled, and inspected. Bolts and rods were made from multiple-part melts.

All analyses were well below specifications for impurities in the fuel-ring castings. For rods and bolts, where the surface-area-to-volume ratios are high, some analyses were slightly in excess of target. None was high enough to warrant rejection of a part. All parts were inspected by sampling the top and bottom of each pour and testing for 40 elements by spectrographic means. Gas, wet chemistry, and metallographic analyses were also made. All samples were free of microsegregation, and all samples had essentially 100% retained gamma phase.

After rough machining, each piece was inspected visually, X-rayed, and X-rayed again after final machining to the level of 2 to 2T. Flaws were machined away as required.

Each part was aluminum-ion vapor plated and then heat-treated. Heat treatment consisted of heating the part to 600°C for 1 hr under vacuum. Complete coverage with the aluminum converted to various uranium−aluminum intermetallics was indicated by X-ray diffraction.

One representative casting was cut into tensile specimens. The results of these tests, when taking past experience into consideration, indicated that no further tensile testing was required.

CONCLUSION

Reexamination and reevaluation of the design decisions pertaining to the HPRR and the application of new information and techniques learned at WSMR, Sandia Corporation, and at the Super KUKLA facility resulted in a substantially improved core for the APRFR. The criticality tests at CEF included a series of burst tests which were deliberately extended in fission yield until the core pieces sustained permanent damage.[2] This was done to establish experimentally the maximum routine operating yield and to verify the design calculations. A number of the detailed design changes described were made as a result of these tests. The calculated performance characteristics are given in Table 4.

Table 4

APRFR PERFORMANCE ESTIMATE

	Burst size, fissions		
	1.5×10^{17}	2.1×10^{17}	3.7×10^{17}
Fluence, neutrons/cm^2			
Core surface	2.0×10^{14}	2.8×10^{14}	4.9×10^{14}
Glory hole	6.7×10^{14}	9.3×10^{14}	1.6×10^{15}
Flux rate, neutrons/cm^2/sec			
Core surface	4.3×10^{18}	6.0×10^{18}	1.1×10^{19}
Glory hole	1.4×10^{19}	2.0×10^{19}	3.7×10^{19}
Dose, tissue rads			
Core surface	7.6×10^{5}	1.1×10^{6}	1.9×10^{6}
Glory hole	2.5×10^{6}	3.6×10^{6}	6.3×10^{6}
Dose rate, rads/sec			
Core surface	1.6×10^{10}	2.3×10^{10}	4.2×10^{10}
Glory hole	5.3×10^{10}	7.7×10^{10}	1.4×10^{11}

REFERENCES

1. John T. Mihalczo, Superprompt Critical Behavior of an Unmoderated, Unreflected Uranium−Molybdenum Alloy Reactor, *Nucl. Sci. Eng.*, 16: 291-298(1963).
2. J. T. Mihalczo, Increased Yields from Fast Burst Reactors. I. Effects of Increased Mass on Uranium and Uranium−Molybdenum Critical Cylinders, USAEC Report ORNL-TM-1125, Oak Ridge National Laboratory, April 1965. J. T. Mihalczo, J. J. Lynn, J. E. Watson, and R. W. Dickinson, Superprompt Critical Behavior of a Uranium−Molybdenum Assembly, *Trans. Amer. Nucl. Soc.*, 10(2): 611(1967). J. T. Mihalczo, Static and Dynamic Measurements with the APRF Reactor, USAEC Report TM-2330, Oak Ridge National Laboratory, 1969.
3. D. Burgreen, Thermoelastic Dynamics of Rods, Thin Shells, and Solid Spheres, *Nucl. Sci. Eng.*, 12: 2(1962).
4. D. M. Mattox and R. D. Bland, Aluminum Ion Plating of Uranium Reactor Parts for Corrosion Protection, *J. Nucl. Mater.*, 21: 349-352(1967).

5. S. A. Hoenig and H. Sulsona, A Field Emission Microscopic Investigation of the Effects of Ambient Atmosphere on the Stress-Corrosion Cracking of Uranium–Molybdenum Alloys, U. S. Army Terminal Ballistics Laboratory, Aberdeen Proving Ground, Aberdeen, Maryland, Mar. 9, 1968.
6. G. Breidenbach et al., Preliminary Design of the ORNL Fast Burst Reactor, USAEC Report NDA-2136-1, Nuclear Development Corp. of America, July 1960.
7. B. Minushkin, Thermal Cycling Tests on Uranium–10 wt.% Molybdenum for the ORNL Fast Burst Reactor, USAEC Report NDA-Memo-2136-2, Nuclear Development Corp. of America, July 1960.
8. F. Rienecker and W. H. Moran, Uranium–Molybdenum Alloy for Use in a Prompt Burst Reactor, *J. Basic Eng.*, 87(4): 865, (December 1965).
9. K. G. Hoge, Some Mechanical Properties of Uranium–10 wt.% Molybdenum Alloy Under Dynamic Tension Loads, USAEC Report UCRL-12357(Rev. 1), Lawrence Radiation Laboratory, 1965.
10. C. A. W. Peterson and R. R. Vandervoort, Stress Cracking in the Uranium–10 wt.% Molybdenum Alloy, USAEC Report UCRL-7767, Lawrence Radiation Laboratory, 1964.
11. J. A. Reuscher and J. M. Richter, Dynamic Mechanical Measurements on the Army Pulsed Reactor, *Trans. Amer. Nucl. Soc.*, 10(2): 612(1967).

DISCUSSION

ENNIS: What periods are we talking about here? How fast were you inserting reactivity? I understand what your neutron flux was.

STATHOPLOS: The reactivity is introduced stepwise by a rapid insertion of the burst rod. The burst width corresponding to the 1.5×10^{17} fissions burst was, I believe, about 40 μsec.

2-6 EXPERIENCE WITH
FAST BURST REACTOR MATERIALS

M. S. FARKAS
Battelle Memorial Institute, Columbus Laboratories, Columbus, Ohio

ABSTRACT

The properties of alpha-phase and gamma-phase uranium alloys are compared with respect to fast burst reactor design and operation. Particular emphasis is given to problems associated with the use of the U−10 wt.% Mo fuel. Possible future directions in alloy development are examined.

INTRODUCTION AND BACKGROUND

This paper discusses uranium-base fuels for fast burst reactors that operate at pulse widths of the order of tens of microseconds, such as the Sandia Pulsed Reactor II and the Godiva IV. Because dilution of uranium with alloying elements tends to broaden the pulse width, the fuel alloys of concern will be arbitrarily limited to dilutions of less than 10 wt.%.

When examining uranium alloys within the limits stated, it is logical to divide them into two groups — alpha-phase alloys and metastable gamma-phase alloys. These alloys may be classified broadly with respect to properties of importance to burst reactor design. However, we must consider two important facts: first, fast burst reactor fuels are generally machined from castings, and, second, mechanical properties of heat-treatable alloys will depend on the thermal history imposed by the operation of the reactor. Table 1 gives a general comparison between the properties of alpha-phase uranium alloys and gamma-phase uranium alloys containing 10 wt.% or less in additions. The properties of unalloyed uranium are included for comparison. The information in Table 1 is self-explanatory; however, the important properties from the standpoint of fast burst reactor design

161

are Young's modulus E, yield strength Y, heat capacity C, and the thermal expansion coefficient α. By analysis it can be shown that in a simple case reactor power may be maximized by maximizing the expression

$$\frac{YC}{\alpha E}$$

Use of the above expression would be an oversimplification of the task of fast burst reactor design, which is indeed more complex. The above expression is based strictly on a thermal analysis that does not account for any inertial effects. Better criteria must be established for figure-of-merit ratings to compare potential burst reactor fuels. However, using the above expression and the heat capacities, thermal expansion coefficients and the best room-temperature mechanical properties given in Table 1 yield a factor of about 1 for alpha-phase alloys and a factor of 5.5 for gamma-phase alloys.

URANIUM–10 WT. % MOLYBDENUM

The choice of U–10 wt.% Mo as a burst reactor fuel was natural since it is the only gamma-phase alloy that had been developed for steady-state reactor use and indeed the most stable gamma-phase alloy available at 10 wt.% dilution or less. Compared to unalloyed uranium this alloy has higher strength and lower modulus.

Now let us examine the considerations which should be made when U–10 wt.% Mo is used as a fast burst reactor fuel.

Maintenance of the Gamma Phase

The time–temperature–transformation (TTT) diagram[1] for U–10 wt.% Mo is present in Fig. 1. This diagram shows that time at high temperatures below about 590°C contributes to the transformation to alpha uranium plus delta uranium–molybdenum. Time at about 500°C is particularly critical because the transformation can begin in only 8 hr. From Fig. 1 the effect of lower molybdenum content on TTT behavior can be seen by examining the curve for U–8 wt.% Mo. The maximum transformation rate occurs at 500°C and begins in only about 0.8 hr.

The current fast burst reactors cool fast enough to prevent transformation. However, if a reactor is used for a large number of bursts below 590°C, then the time at temperature during cooling will contribute to destabilization of the gamma phase and possibly will initiate transformation. The cumulative effects of this type of operation can be erased by pulsing to gamma-phase temperatures.

Table 1

COMPARISON OF THE CAST PROPERTIES OF UNALLOYED URANIUM, ALPHA-PHASE URANIUM ALLOYS, AND
GAMMA-PHASE URANIUM ALLOYS CONTAINING 10 WT.% OR LESS OF ALLOYING ADDITIONS

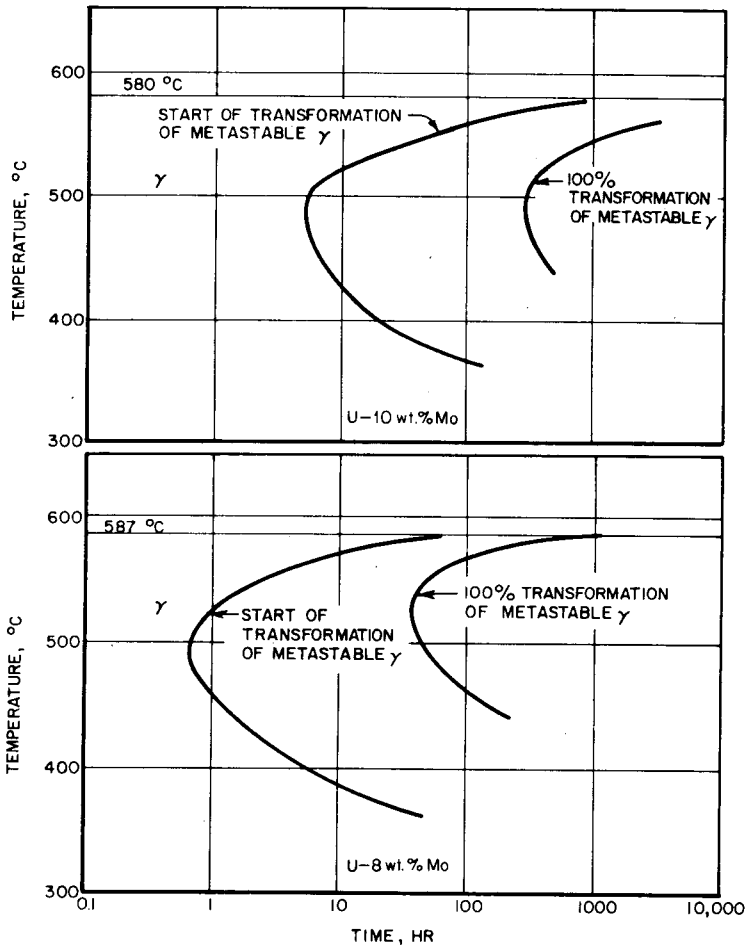| Properties	Unalloyed uranium	Alpha-phase uranium alloys	Gamma-phase uranium alloys
Phases present	Alpha-uranium	Alpha-uranium plus small amounts of second phase	Gamma-phase uranium
Oxidation resistance	Poor	Poor, but better than un-alloyed uranium	Better than alpha-phase alloys but protection still needed for high-temperature applications
Thermal-cycling growth	Yes	Some growth, but minimal in certain alloys	None
Thermal considerations	Operations limited by alpha−beta trans-formations at 660°C	Operation probably limited by alpha−beta trans-formation about 660°C	Gamma-phase is metastable and must be maintained to assure retention of gamma-phase properties
Stress corrosion	None known	None known	Susceptible to stress-corrosion cracking under certain condi-tions
Room temperature, as-cast mechanical properties			
Yield strength, 10^3 psi	22−35	50−70	90−120 (as-cast and gamma treated)
Tensile strength, 10^3 psi	60−85	60−100	90−130 (as-cast and gamma treated)
Young's modulus, 10^6 psi	22−24	22−24	10−13 (as-cast and gamma treated)
Elongation, %	5−10	2−20	10−16 (as-cast and gamma treated)
Thermal properties, 25−600°C			
Thermal expansion coefficient, °C^{-1}	20	≈20	≈13.5
Heat content, cal/g/°C	6.58	≈6.6	≈8.0

Fig. 1 — *Time—temperature-transformation diagram for the U—10 wt.% Mo alloys quenched to temperature from 900°C.* [From P. E. Repas, R. H. Goodenow, and R. F. Hehemann, Trans. Amer. Soc. Metals, *57: 151-152 (1964)*.]

The consequences of small amounts of transformation of the U—10 wt.% Mo alloy in a burst reactor are not well understood, but significant property changes and thermal-cycling distortion could be expected if a large amount of transformation occurs.

Fuel Homogeneity

Manufacture of U—10 wt.% Mo alloy castings is not without its difficulties. A problem area is that of both macrosegregation and microsegregation. Macroinhomogeneity of induction castings, which are well stirred in the molten state, is not an important problem. How-

ever, small differences in molybdenum content occur; and, when these are combined with microsegregation they can be serious, especially in large castings. Microsegregation occurs as a result of the difference in the liquidus and solidus temperatures; the first liquid to freeze is molybdenum rich, and the last liquid to cool is uranium rich. There-fore a gradient of molybdenum content exists across the dendrites that grow from the melt. This gradient may not be evident on microscopic examination. Generally, a homogenization treatment for 24 hr at 900°C is used. The diffusion rate of molybdenum in uranium is low, and, if coarse dendrites are present, a completely homogeneous structure may not be obtained. The consequence of remaining microsegregation, especially in a region of low molybdenum content, is a less-stable gamma phase. That is, low molybdenum content in a cored structure could lead to transformation in shorter times than are expected.

Stress Corrosion

Evidence thus far suggests that U−10 wt.% Mo and other gamma-phase uranium alloys are, in general, susceptible to stress corrosion. The combined actions of stress and a corrosive atmosphere cause failure at a stress below the actual yield strength of the alloy. Stress corrosion is believed to have been the cause of some rather dramatic failures in U−10 wt.% Mo alloy.

One of the first-known failures occurred in the late 1950's at Battelle Memorial Institute. A rod of gamma-phase U−10 wt.% Mo was cold swaged. Upon examination the next day, the rod was shattered, as shown in Fig. 2. Other such experiences were noted elsewhere. Cracking was observed during and after fabrication of U−10 wt.% Mo bolts for the KUKLA fast burst reactor. In another case, U−10 wt.% Mo bolts were removed from the Army Pulse Radiation Facility Reac-tor (APRFR) after testing beyond design limits. Since the core was slightly distorted, removal of the bolts was difficult. After removal the bolts cracked severely. It is now apparent that the residual stress in combination with atmospheric corrosion was the probable cause of failure.

Studies performed recently have illustrated the role of residual stress in stress-corrosion cracking and have also pointed to the harmful effects of oxygen, hydrogen, and water vapor.[2] Table 2 lists the contributing factors and possible remedies to the stress-corrosion problem. The affect of stress corrosion in a "normal environ-ment" on the tensile strength[3] of U−10 wt.% Mo and U−8 wt.% Mo−0.5 wt.% Ti is presented in Fig. 3. These tests were performed with dead-weight loads and show time dependency. Under the conditions of the test, U−10 wt.% Mo withstood 37,500 psi for long periods of time, and U−8 wt.% Mo−0.5 wt.% Ti withstood 62,000 psi. These strength
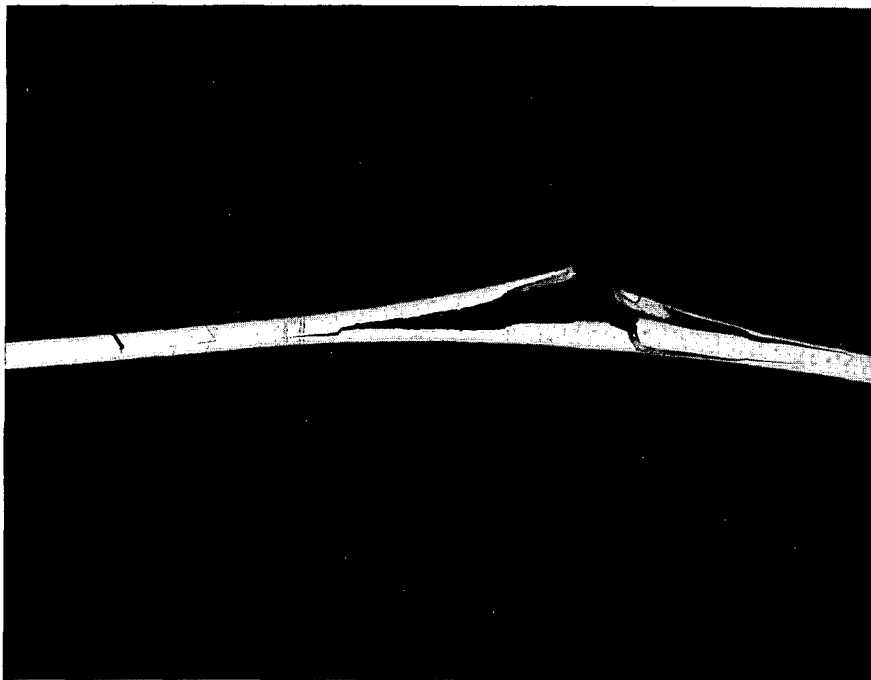
Fig. 2—Typical appearance of a swaged gamma-phase U—10 wt.% Mo alloy that cracked after swaging.

Table 2

CONTRIBUTING FACTORS AND REMEDIES FOR STRESS
CORROSION IN URANIUM—10 WT.% MOLYBDENUM ALLOYS

Contributing factors	Remedies
Residual stress from quenching treatment, cold working, machining, or possibly from previous loading	Low-temperature heat treatment
Oxygen	Use of dry nitrogen, CO_2, or inert gas
Water vapor	
Hydrogen	Protective plating

values, however, could vary with relative humidity, amount of residual stress, and other factors.

What does this mean in regard to the use of U—10 wt.% Mo in fast burst reactors? Referring to Fig. 3, for the short periods of time for which the reactor fuel is under stress, stress corrosion is

apparently inoperative. The effect of repetitive-burst operation and stress corrosion on bare U – 10 wt.% Mo remains to be determined.

URANIUM-1.5 WT. % MOLYBDENUM

The Godiva IV reactor has been constructed using U – 1.5 wt.% Mo as a fuel material. This alloy was chosen instead of uranium because it represented an improvement with regard to strength characteristics
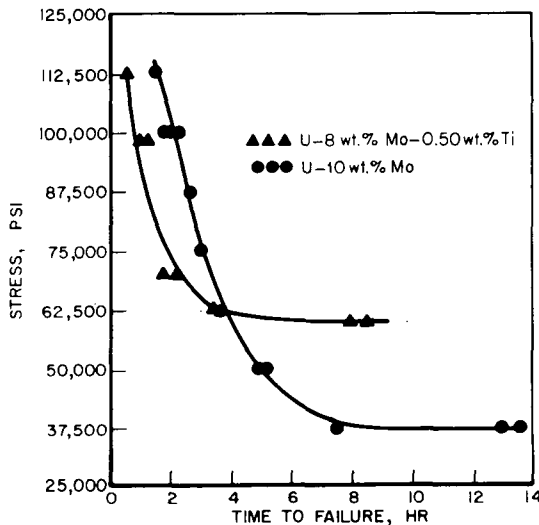

Fig. 3 — *Delayed-failure characteristics of two gamma-phase uranium alloys. Note that stress corrosion lowers the ultimate strength of the alloy evolved.*[3]

of unalloyed uranium and because its properties are relatively un-affected by heat treatment. The gamma-phase alloys were not con-sidered for this application because of stress-corrosion problems. In this reactor the fuel was not plated originally; aluminum ion-plating was added after oxidation became a serious problem. (Con-sidering the results discussed in the previous section it may be fortunate that U – 10 wt.% Mo was not used.) The choice of the U – 1.5 wt.% Mo alloy was the result of an alloy development program performed at Los Alamos. This alloy has exceptionally good ductility for an alpha-phase alloy and has a tensile strength of approximately 100,000 psi. In addition, this alloy's mechanical properties do not change appreciably with heat treatment, thus assuring uniform be-havior during burst reactor operation.[4]

FUTURE DIRECTIONS FOR FAST BURST FUELS

Fuel Improvement

Improvements in current fuels can be viewed as needed limited changes. With U−10 wt.% Mo, the most needed improvement is elimination of its stress-corrosion susceptibility, which may be accomplished simply by operation with a completely clad fuel or in an atmosphere of dry nitrogen. Another possibility for improvement is to study the effect of small additions of alloying elements on the stress corrosion of this alloy. The addition of small amounts, 1 wt.% or less of platinum or another noble metal which is a gamma stabilizer appears promising.

With U−1.5 wt.% Mo there are currently no major problems though oxidation, and thermal-cycling stability might be limiting. For oxidation resistance aluminum-ion plating or some other coating could be utilized (see preceding section). For thermal cycling stability the most that can be accomplished is the achievement of a random large-grain structure.

Alpha-Phase Alloys

As noted in Table 1, of the alpha-phase alloys that are known to be cast we can expect a modulus of 22 to 24×10^6 psi. This property does not change significantly with alloy content as long as we are in the realm of alpha-phase alloys. The best tensile strengths now available with reasonable ductility are of the order of 100,000 psi. Some more work should be performed with possible alloying additions to attempt improvement of tensile strength, and the data should be obtained at high strain rates.

Gamma-Phase Alloys

When looking for gamma-phase alloys for possible use in place of U−10 wt.% Mo, we must remember that molybdenum is the most potent gamma-phase stabilizer that has been investigated. Therefore, when approaching the problem of developing an alloy which might be substituted for U−10 wt.% Mo, we must consider the question of whether or not less gamma-phase stability can be tolerated in burst reactor operation. For instance, in Fig. 1 the TTT diagram is presented for U−8 wt.% Mo. Can this alloy be used in a current burst reactor without transforming? Or possibly, can it be used even though it transforms? Similar questions arise when known metastable gamma-phase alloys are considered.

If gamma-phase stability equivalent to or better than that of U− 10 wt.% Mo is desired, at least one possibility is open. From the current

information on the uranium–rhenium system, U–8 to 10 wt.% Re alloys appear to hold promise.[5] The mechanical properties and the TTT curve for these alloys are not known.

The modulus of elasticity of gamma-phase alloys is 9 to 13×10^6 psi, and the best tensile strengths are of the order of 130 10^3 psi. Alloys having higher tensile strengths might possibly be developed.

Beta-Phase Alloys

The beta-phase region in most uranium-alloy systems is quite limited in extent, and therefore only limited possibilities exist for developing a metastable beta-phase alloy for burst reactor use. Beta-phase alloys would be expected to have higher strengths than alpha-uranium alloys, but the modulus of elasticity is unknown. An alloy of U–0.3 wt.% Cr–0.3 wt.% Mo retains beta uranium when quenched; however, the phase is metastable and transforms at room temperature. There do appear to be some possible alloy compositions that would result in retained beta on slow cooling. On the basis of the solubility of various elements in beta uranium, these additions appear to be the best beta stabilizers: rhodium, platinum, iridium, and rhenium. Their solubility in the beta phase is 4, 3, 5, >2, and 2 wt.%, respectively.

ACKNOWLEDGMENT

REFERENCES

1. P. E. Repas, R. H. Goodenow, and R. F. Hehemann, Transformation Characteristics of U–Mo and U–Mo–Ti Alloys, *Trans. Amer. Soc. Metals,* 57: 150-154 (1964).
2. S. A. Hoenig and H. Sulsona, A Field Emission Microscopic Investigation of the Effects of Ambient Atmosphere on the Stress-Corrosion Cracking of Uranium–Molybdenum Alloys, U. S. Army Terminal Ballistics Laboratory, Ballistics Research Laboratory, Aberdeen Proving Ground, Aberdeen, Maryland, Mar. 9, 1968.
3. C. A. W. Peterson, A Stress-Cracking Study of a Gamma-Extruded U–8 wt.% Mo–0.5 wt.% Ti Alloy, USAEC Report UCRL-14132, Lawrence Radiation Laboratory, 1965.
4. J. Taub, Los Alamos Scientific Laboratory, private communication, 1968.
5. R. J. Jackson, D. E. Williams, and W. L. Larsen, The Uranium–Rhenium Alloy System, *J. Less-Common Metals,* 5: 443-461 (1963).

DISCUSSION

YOCKEY: The Army has developed uranium alloys that have strengths over 200,000 psi. Do you have any comment on the use of those alloys?

BAUER: They are principally for armor or projectile applications. You could try them, but they are low-ductility materials with high strength. They are not single-phase alloys. Strength is obtained by the presence of a finely dispersed second phase. I had not really thought about them for this application, but they are around 90% uranium, too, containing about 8 wt.% molybdenum with other alloy additions. The major problem in their application would probably be in loss of strength with time at elevated temperature owing to coarsening of the dispersion.

Actually there is less of the alloy material than there is in U−10 wt.% Mo in some of these. One family of these alloys contains 1% of molybdenum, niobium, and zirconium and 0.5% titanium. In a burst reactor very little time is spent at high temperature.

RUSSELL: Although this is not my field, the curve you showed of the fatigue strength decreasing in a matter of hours from dead-weight loading was one of the most astounding things I have seen. Is this a common thing with uranium alloys, or something that only happens with peanut butter, or what?

BAUER: It is common to gamma-phase alloys, both this type alloy, uranium−niobium-base alloys, and the retained gamma-phase in general.

RUSSELL: Do normal construction materials show this particular type of behavior?

BAUER: I think not as a general rule. The effect may be so pronounced because the gamma phase is metastable.

STATHOPLOS: You mentioned that you thought there would be a potential problem with alpha alloys if one went to higher temperatures. Is this because the grain size grows?

BAUER: Grains grow, yes, and particularly with higher temperatures of operation you cannot eliminate distortion of alpha-phase alloys. You are still dealing with the alpha-uranium phase, and the alpha-uranium phase is anisotropic. You cannot get completely away from the thermal-cycling growth problem.

Repetitively
Pulsed
Reactors

Session 3

3-1 THE OPERATIONAL EXPERIENCE AND DEVELOPMENT OF PERIODICALLY PULSED REACTORS AT DUBNA

V. D. ANAN'EV, D. I. BLOKHINTSEV, B. N. BUNIN, I. M. FRANK, L. K. KULKIN, I. M. MATORA, V. M. NAZAROV, V. T. RUDENKO, E. P. SHABALIN, F. L. SHAPIRO, and Yu. S. YASVITSKII

Presented by D. I. Blokhintsev
Joint Institute for Nuclear Research, Dubna, USSR

ABSTRACT

A number of design improvements made on the IBR on the basis of operational experience are described. Some peculiarities of the reactor under operating conditions of infrequent pulses are given along with a short description and the main parameters of the high-power periodically pulsed reactor IBR-2 with an LIU-30 as an injector. Some major experimental works on nuclear physics and solid-state physics performed using the IBR are discussed.

The periodically pulsed fast reactor IBR was constructed in 1958−1959 and put into operation in July 1960. Since that time it has been operated for 25,000 hr and has produced 65,000 kw-hr of power. A detailed description of the theory of the IBR and its design are given in Refs. 1 to 4 (see Figs. 1 to 3).

Continuous operation of the IBR made it possible to collect sufficient material to permit positive conclusions to be made regarding the reactor's reliability, stability in operation, and fitness for performing a wide range of physical investigations. During operation some units and, as a result, the entire reactor were considerably improved to provide better reliability and to obtain better physical characteristics for installation.[5−8]

Successful operation of the IBR stimulated the construction of the IBR 30, an improved and more powerful version of the IBR and a forerunner of the next generation of repetitively pulsed reactors, IBR-2. This 4-Mw liquid-metal-cooled reactor is being designed by the Joint
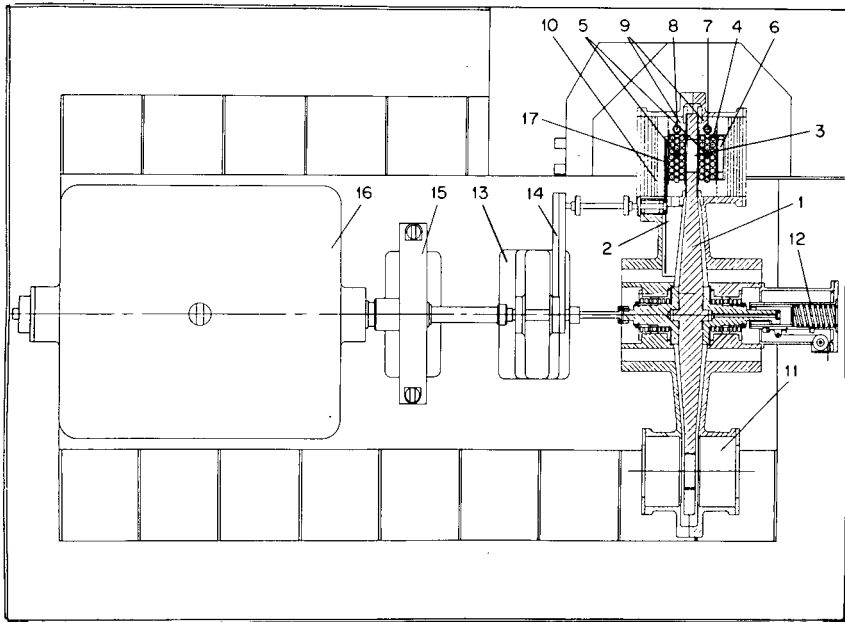
Fig. 1—Schematic drawing of the IBR.

(1) Rotating disk
(2) Subsidiary disk
(3) Main bushing
(4) Plutonium rods
(5) Scram rods
(6) Coarse control
(7) Automatic regulator rod
(8) Manual control rod
(9) Side reflector
(10) End reflector
(11) Shielding glass
(12) Mechanism for adjustment of main bushing in shielding
(13) Accelerator
(14) Reducing gear of the auxiliary bushing
(15) Brake
(16) Electrical drive
(17) Auxiliary bushing
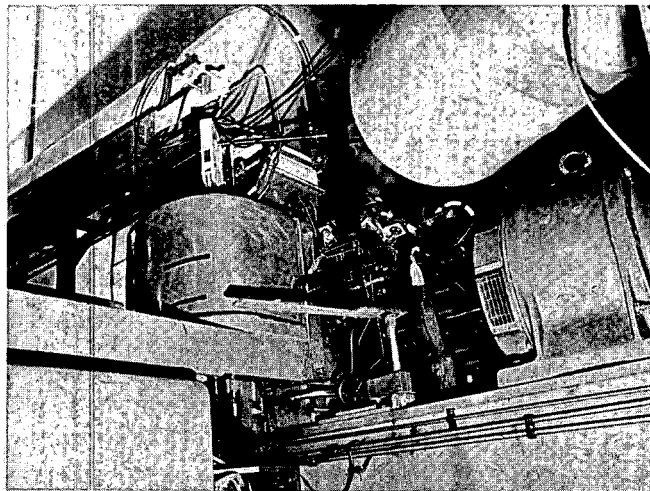
Fig. 2—General view of the IBR reactor.
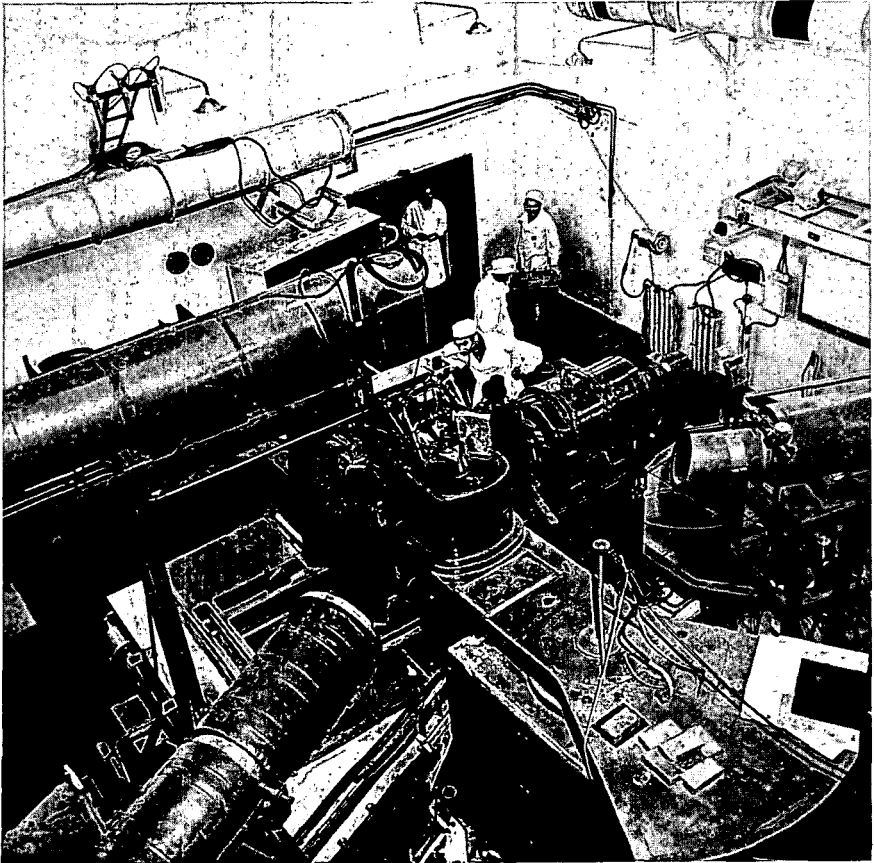
Fig. 3—General view of the reactor hall.

Institute for Nuclear Research (JINR) together with other design organizations of the USSR.

OPERATIONAL EXPERIENCE OF AND IMPROVEMENTS TO THE IBR REACTOR

A periodically pulsed reactor must have a device to provide periodic pulsation of reactivity. This device consists of two disks with uranium inserts, a d-c engine, and a system of rotation transfer from the engine to the disks. During the entire period of reactor operation, the following failures were revealed:

1. Damage of one of the journal bearings of the main disk, which caused the shaft to skew; however, the fuel elements remained safe. At present higher quality bearings are used in the reactor, and an extra

safety set of bearings has been installed to restrict the skewness of the roller if the working set should be broken.

2. Destruction of the bearing and transfer parts of the auxiliary disk owing to radiation polymerization of a viscous lubricant. Therefore the viscous lubricant was replaced by a flowing one.

3. Wear of the teeth of the coupling that connects the shaft of the reductor and the main disk, caused by torsional vibrations in the system. A coupling with rubber spacers to damp vibrations was placed between the rolls.

4. Much attention was paid to the steel coating of the main uranium insert, which tended to swell shortly after start-up.

This swelling caused concern since the gap between the reactor core and the disk surface was only 1.7 mm. For controlling the shape of the coating, capacity detectors were put inside to detect the shape of the coating during the rotation of the disk. By the summer of 1963 the swelling was 0.6 mm above the disk surface. For safety during operation, the speed of disk rotation was decreased from 5000 to 3000 rpm, and the gap between the disk and the reactor core was extended.

At the end of 1963, the disk with the uranium insert was replaced by another one with a coating 0.6 mm thick instead of 0.4 mm thick. Examination of the used uranium insert showed no changes in its shape. Analysis of the conditions of insert operation and some experiments on models indicated that the swelling of the coating is conditioned by temperature tensions in the coating and is aggravated by centrifugal forces. We hope that the changes made in the design of the coating on the basis of these data will make it possible to essentially increase the permissible heat load on the inserts of the IBR-30.

The auxiliary movable insert that varies the pulse repetition rate determines the magnitude of secondary pulses of power (satellites), which occur during the passage of the main insert through the reactor core if the auxiliary insert is outside the core. Physical research on the reactor showed that the presence of satellites sometimes complicates the handling of experimental data. To decrease the amplitude of secondary pulses, the former auxiliary insert was replaced by a new, heavier one with an efficiency of about 1%. Many inconveniences resulted from the necessity to change reductors and to provide manual synchronization of the main and auxiliary disks when pulse repetition rate is varied. Added in 1965 was an electrical–mechanical system that allowed a remote shift of the reductor to another drive without interrupting the synchronization of the rotation of the main and auxiliary disks.

In 1964 the cooling system of the reactor was reconstructed. In particular, the flow of air for fuel rods was increased up to 170 m^3/hr, and forced-air cooling was provided for the safety rods. These im-

provements made it possible to raise the average power of the reactor up to 3 kw and then up to 6 kw. The temperature of the fuel-rod canning was 180°C at 6 kw. The temperatures of the coating of the uranium insert and of the disk near the insert were measured by thermosensitive colors. According to these measurements, the temperature of the uranium in the center of the insert was estimated to be 190 to 260°C.

Initially the kinematics of the reactor permitted its operation at power pulse repetition rates of 5, 10, 25, and 50 sec^{-1} (at a disk-rotation speed of 3000 rpm). However, a number of improvements to the mechanical parts made operation of the reactor possible under other conditions of reactivity pulsation. For some physics experiments it is desirable to increase the amplitude of power pulses, i.e., to decrease the pulse repetition rate at an unchanged power. This concerns, first, experiments with very slow neutrons (a long time of flight from the source to the detector) and, second, those cases in which the background intensity is proportional to the time of analyzer operation (i.e., the background is of nonreactor origin). In these latter cases a decrease in the repetition rate makes it possible to get a better relation of the effect to the background.

In 1966 the IBR was operated in the mode when packets of pulses were formed with the frequency of $\frac{1}{8}$ cycles/sec; the cycle of pulses inside the packet was equal to $\frac{1}{50}$ sec and was determined by the frequency of rotation of the main moving core. The nature of pulse variation in time is shown in Fig. 4.

Operation with infrequent pulses of a constant amplitude was carried out in the summer of 1968. The repetition rate was equal to 1
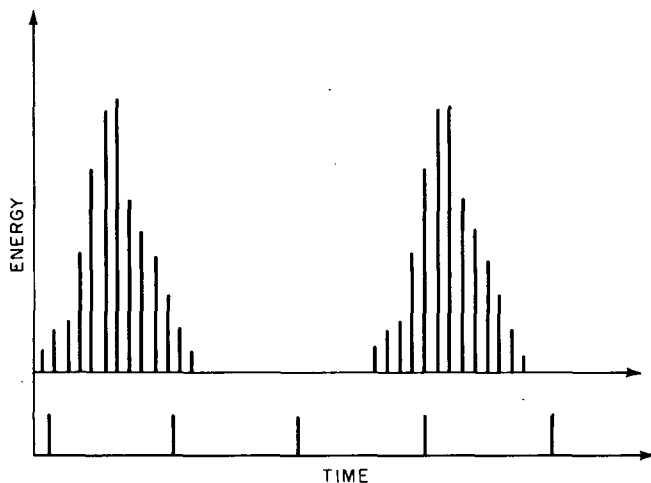

Fig. 4—Scheme of reactor pulse power in the IBR operating condition of alternative amplitude pulses.

pulse/5 sec. The energy of one power pulse was 10^{15} fissions, which cor-
responds to an average heating of the reactor fuel elements of about
$10°C$. The peak power at the pulse was 700 Mw. Quite unexpectedly in
these conditions of operation, the pulse width of fast-neutron pulses
considerably decreased. At a pulse repetition rate of $\frac{1}{5}$ sec and an
average power of 6 kw, the measured value of the pulse half-width was
56 μsec and in the conditions of infrequent pulses, 36 μsec (Fig. 5). The
neutron detector used in measurements of pulse shape was a thorium
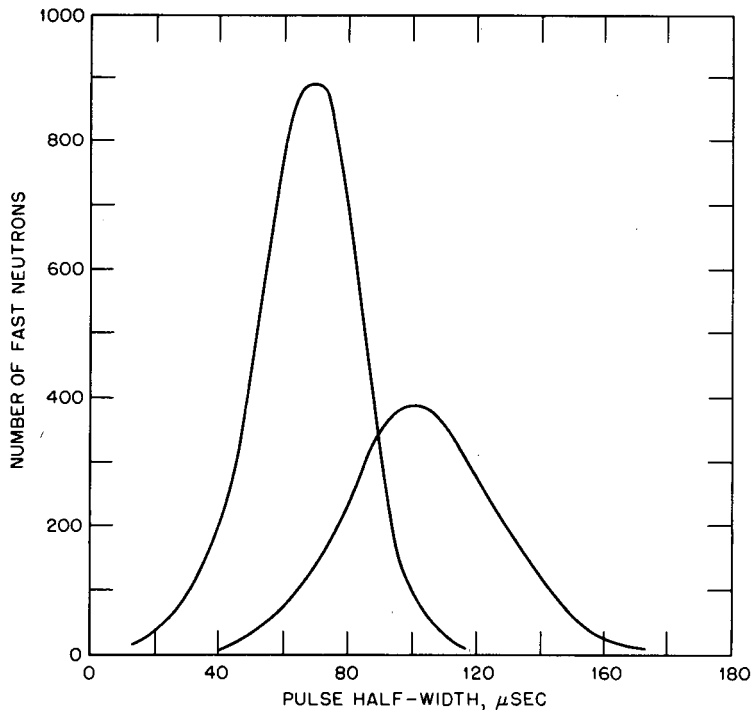
Fig. 5—Shape of the IBR reactor power pulses at the repetition rate 5/sec and
0.2/sec.

fission chamber placed 6 m from the reactor core, pulses from which
were sent through an electronic amplifying unit to the time analyzer
with an intermediate memory with dead time of 1 μsec. The observed
reduction of the pulse width and the shift in the position of the maximum
of the pulse indicate the presence of a powerful negative effect of
reactivity during the pulse, the value of which is estimated as 10^{-3} ab-
solute units of reactivity.

   Tension gauges detected nonstationary processes in the steel
cladding of the fuel rod during and after the pulse. The tension gauges
were glued to the surface of the fuel-element cladding at two points in

the reactor median plane, one at the most distant point from the center (No. 1) and the other at an angle of 90° with respect to it (No. 2), the rod being a distance of 4.3 cm from the reactor center. The lower end of the fuel element was fixed; the upper end was loose. The frequency of longitudinal vibrations of the cladding (the negative value of the ordinate in Figs. 6 to 9 corresponds to the extension of the cladding) was about 8000 cycles/sec at the maximum amplitude of 3×10^{-3} mm, which is in a rather good agreement with the values calculated using the methods of Randles.[9] The observed delay of the maximum of
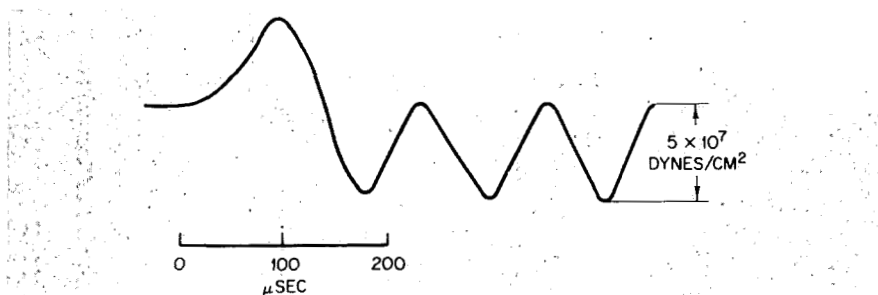
Fig. 6—*Vibrations of steel fuel-rod cladding in conditions of infrequent pulses (detector No. 1).*
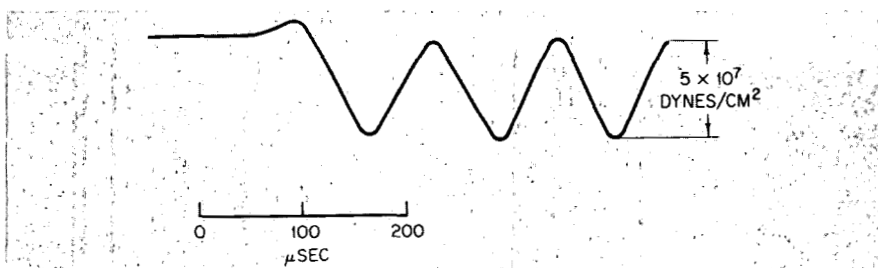
Fig. 7—*Vibrations of steel fuel-rod cladding in conditions of infrequent pulses (detector No. 2).*

cladding extension with regard to power pulse corresponds to that theoretically predicted. On the basis of the measurements, we can rather definitely conclude that the thermal expansion of plutonium does not result in the above-mentioned dynamic effect of reactivity. The contraction of the cladding (the positive ordinate in Figs. 6 to 9) at the moment of pulse, detected by gauge No. 1, seems to be due to fuel-rod skewness caused by the unevenness of heat release in the rod cross section. The fuel-rod skewness may be a reason for the negative jump of reactivity. However, an insufficient amount of experimental data makes it difficult to describe unambiguously the real picture of fuel-rod
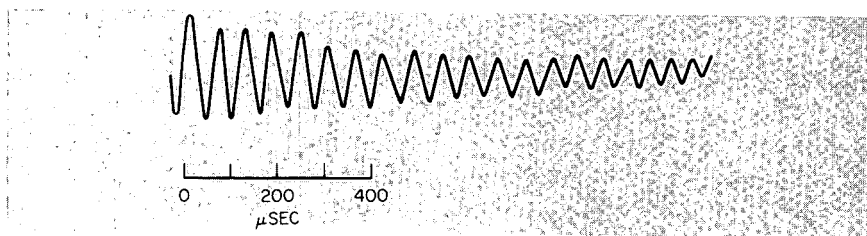
Fig. 8—Damping of longitudinal vibrations of the fuel-rod cladding.
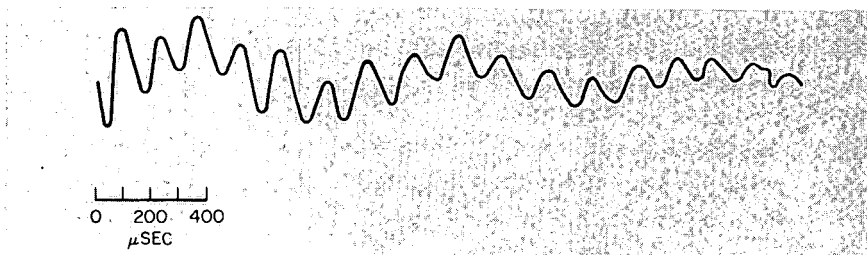
Fig. 9—Damping of transverse vibrations of the fuel-rod cladding.

dynamics and of reactor kinetics at the moment of thermal shock. Since the effects discovered experimentally influence the physical characteristics of pulsed reactors, e.g., their safety, stability in operation, and the ability of the fuel rods to hold up under operation, some additional investigations will be carried out on the IBR-30 reactor.

The first attempt to multiply by 100 to 200 times the short neutron burst generated by an electron pulse from the microtron in the center of the reactor core was made[8] at the beginning of 1965. Since that time the IBR has been operated alternatively in the booster and reactor mode. The periods when the microtron was not operated in conjunction with the IBR were used for its intensive study and improvement. The IBR microtron system has been operated about 3000 hr for experiments. The parameters of this system[10-12] are given in Table 1.

The maximum power of the system in the booster mode of operation was achieved not only by increasing the electron current but also by increasing the diameter of the uranium target from 10 to 15 mm, (three times the diameter of the beam), which resulted in the yield of neutrons from the target reaching its maximum value of 1.5×10^{-2} neutron/electron at an electron energy of 30 Mev. The continuous operation of the IBR in conjunction with the microtron showed that an increase in the accelerated electron current above 100 ma in a pulse could hardly be expected.

Therefore it was decided to disassemble the microtron and to use the LIU-40 to inject electrons into the IBR-30. The linear accelerator will be installed vertically above the reactor. The parameters of the accelerator and booster with LIU-40 are given in Table 1. Much attention was paid to the target of the linear accelerator on which the efficiency of the conversion of electrons into neutrons is dependent.

Table 1

THE CHARACTERISTICS OF INJECTORS AND BOOSTERS OF
THE LABORATORY OF NEUTRON PHYSICS

Parameter	IBR microtron	IBR-30 with LIU-40
Energy of electrons injected into target, Mev	24 to 30	44
Electron current onto target during a pulse, ma	60 to 80	180
Duration of electron pulse, μsec	1.7 to 1.9	1.8
Pulse-repetition rate, sec^{-1}	50	100
Booster mean power at a half-width of 3 μsec, kw	1 to 1.2	20 to 30
Duration of continuous operation, hr	100 to 200	

Some thermal−physical calculations and experiments carried out with the electron flux of the microtron made it possible to choose an optimal design of target for operation in the IBR-30 core. High-melting-point alloys of plutonium will be used as target material. The target will be cooled by gaseous low-pressure helium. The maximum temperature of the target cladding is expected to be about 800°C. The characteristics of the beam in the LIU-40 make it possible to use the IBR-30 in the booster mode of operation at almost maximum power. The principles of design in the IBR-30 remain the same in the IBR. However, for operation at a mean power of 20 to 30 kw and for easier operation of the reactor under difficult radioactive conditions, some changes were made in some of the reactor parts. An increase in heat removal from the reactor core is achieved by a decrease of the fuel-rod diameter and an increase of air flow up to 300 m^3/hr. The power produced in the moving part of the core will be equally distributed between two ^{235}U inserts. The kinematic scheme of the reactor will enable operation at practically any pulse repetition rate, i.e., from 100 sec^{-1} to single pulses with the energy of 10^{16} fissions. A normal alternate operation of the two uranium inserts is possible only if their efficiencies differ by no more than 10^{-5} reactivity units. Other-

wise an unequal amount of power is produced in the inserts. The fabrication of inserts with the required precision is practically impossible. Therefore some measures are foreseen to balance the inserts physically. Considering the unfortunate solution of fastening the reactor core on the IBR disk jacket, a possibility of changing the pulsation device of the reactor without dismantling the reactor core is foreseen.

The main characteristics of the IBR-30 are listed in Table 2. Start-up of the reactor is planned for 1969.

Table 2

CHARACTERISTICS OF THE IBR-30 REACTOR

Mean thermal power, kw	30
Power during a pulse at a frequency of 5 sec^{-1}, Mw	150
Fissions/pulse	Up to 10^{16}
Half-width of power pulse at a frequency of 5/sec, μsec	50
Neutron generation time, sec	10^{-8}
Volume of the reactor core, liters	2
Fast-neutron flux in the core, averaged over time, neutrons/ cm^2/sec	10^{13}
Fast-neutron flux in the core at a maximum pulse, neutrons/ cm^2/sec	5.10^{16}
Leakage of thermal neutrons from the moderator surface, averaged over time, neutrons/cm^2/sec	6.10^{10}
Half-width of thermal-neutron pulse, μsec	90

The physics investigations carried out on the IBR and the IBR microtron system are related to the following four areas:

1. The study of the neutron as an elementary particle; estimation of neutron polarizability in the electrical field of the nucleus;[13] a new method of measuring the neutron−electron interaction;[14] the first observation[15] of ultracold neutrons (velocity, 5 m/sec). The use of ultracold neutrons will permit a substantial increase in the accuracy of the measurements of the time of neutron decay and neutron electrical dipole moment.

2. Nuclear physics, especially studies of neutron resonances: the development of a method to polarize neutrons with an energy of 1 to 10^4 ev;[16] the use of polarized neutrons and polarized nuclear targets in solving the important problem of the spin dependence of neutron− deuteron scattering[17] and the determination of the spins of holmium neutron resonances;[18] the study of the alpha decay of excited nuclear states occurring in the form of neutron resonances;[19,20] and the study

of characteristics of the neutron resonances of a large number of nuclei, including fissioning ones.[21]

3. Some problems that are of importance to nuclear power engineering: the measurement of neutron spectra generated in the propagation of fission neutrons in matter;[22] the capture and fission cross sections and their ratio for the most important fissioning nuclei in a wide energy range;[23] and the study of the Doppler effect in uranium in the region of intermediate neutron energy.

4. Physics of condensed matter: the development of the time-of-flight method for the study of neutron diffraction by the magnetic substances in intense magnetic fields (such fields can be generated only in the form of infrequent pulses, and diffraction measurements are practically impossible on stationary reactors in this case); and the study of the critical states of liquids, the atomic dynamics of liquids and crystals, and impurities in crystals using the method of quasielastic and inelastic scattering of neutrons.[25-28]

A considerable amount of information obtained in the fields mentioned are either quite new or essentially more accurate compared to those known before. To a considerable extent the possibility of carrying out these investigations is conditioned by the advantages of the IBR as a neutron source for neutron spectrometry.

THE IBR-2

The IBR-2 is a device that can have a wide range of applications in nuclear investigations, in the study of condensed matter by neutron-physics methods as well as applied works connected, for instance, with the study of pulsed radiation effects.

The device is comprised of a repetitively pulsed fast liquid-metal-cooled reactor, a high-current linear induction electron accelerator LIU-30, and experimental facilities (Fig. 10). Two modes of operation are possible: (1) an electron beam is sent from the accelerator to the target placed in the core of the subcritical pulsed reactor, i.e., a booster mode of operation, and (2) the reactor is used without the injector in a condition of pulsed operation.

The Reactor

The IBR-2 reactor is a fast reactor with a highly enriched core made of PuO_2, which is the same as that of the stationary BR-5 reactor and which has been tested in operation.[29,30] Pulsation of reactor power is achieved by modulation of reactivity by moving a part of the reflector with regard to the reactor core.

The reactor core, 40 cm high, is an irregular hexagon in the horizontal plane and consists of fuel assemblies of the type used in the
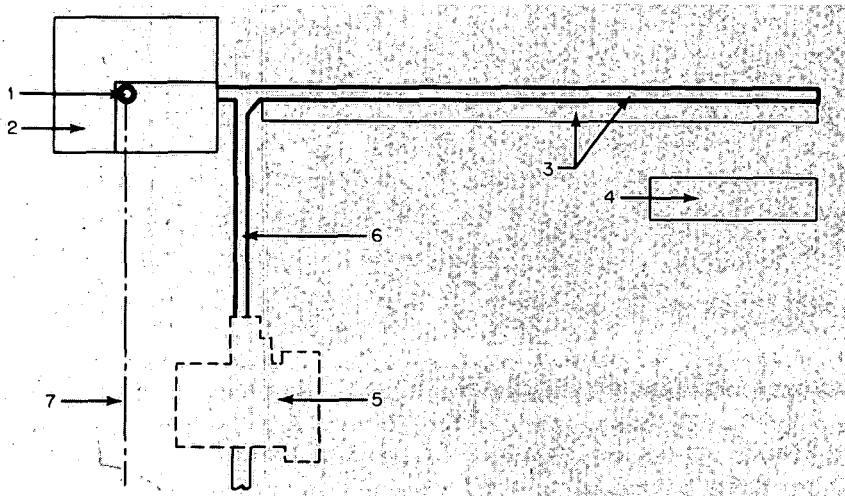
Fig. 10—A layout of the IBR-2.

(1) Reactor
(2) Reactor building with experimental hall
(3) Accelerator building
(4) Center building for measuring
(5) The operating building of the IBR
(6) A 100-m neutron guide of the IBR
(7) A 1000-m neutron guide of the IBR-2

BR-5 reactor with the spacing of 27 mm. The fuel assemblies are forced into the lower supporting steel plate. There are seven fuel rods in each of the assemblies; some 71 fuel assemblies are placed in the reactor core. The fuel rods are fixed at both ends and coiled by a wire 0.5 mm in diameter for separation. The overload of fuel assemblies is achieved while keeping the reactor vessel airtight. The used-up fuel assemblies are cooled by sodium above the core before removal. Seven central cells of the core are occupied by a channel, the lower part of which is used to locate the electron accelerator target and the upper part is used to expose samples. The target is situated at the half-height of the core. Initially the target material will be tungsten cooled by sodium circulating in an isolated loop.

The reactor core is in a double-walled steel vessel. The gap between the walls is used for sodium leakage control and hot-air supply to heat the reactor. The sides of the hexahedron are surrounded by air-cooled tungsten elements 80 mm thick which serve as control rods. The main and auxiliary coaxial moving reflectors are adjacent to the largest side of the hexahedron. The rotors of the moving reflectors have three trapezoidal bulges, one of which is a proper reflector and the other two are for equilibrium. The rotor is 120 cm in radius and 6.5 cm thick (Figs. 11 and 12). It is rotated at 3000 rpm by an a-c engine. The auxiliary reflector is rotated by the same engine through
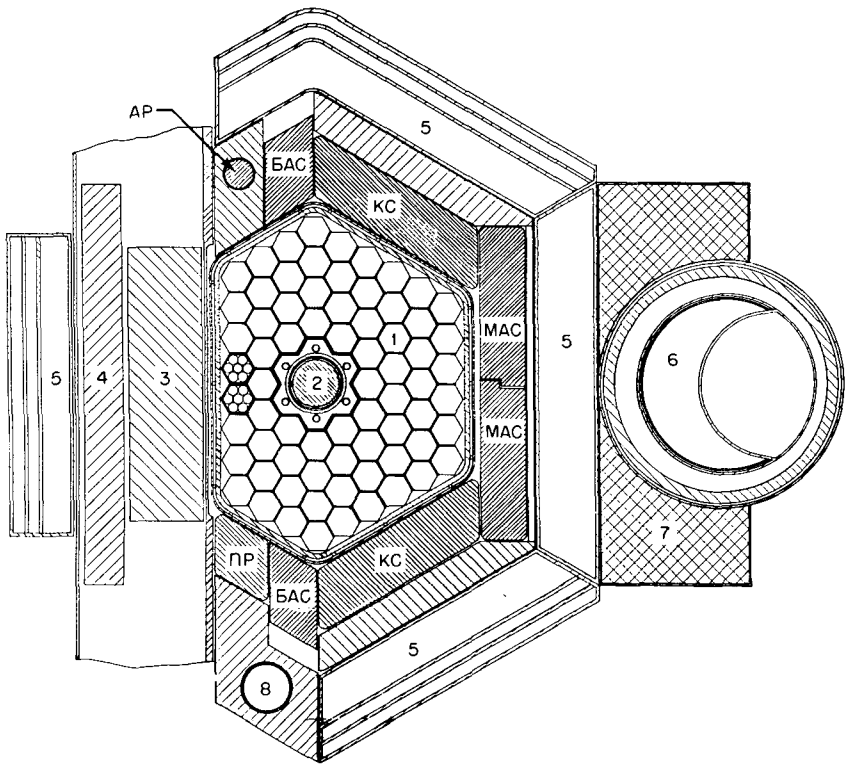
Fig. 11 — The plan of the reactor core.

(1) *Fuel assembly*
(2) *Accelerator target*
(3) *Main moving reflector*
(4) *Auxiliary moving reflector*
(5) *Sectioned light-water moderators*
(6) *Cold moderator*
(7) *Reflector of the cold moderator*

(8) *Exposure channel in reflector;*
    БАC, fast safety rods; MAC, slow
    safety rods; KC, compensating
    control rods; ПР, medium-effi-
    ciency control rods; AP, automatic
    control rod

a transmission, and its speed may be changed. The reactor can be operated at four possible pulse repetition rates, namely, 50, 25, 10, and 5 pulses/sec. The highest repetition rate occurs when the auxiliary reflector is stopped. The pulsation device is contained in a thin-wall airtight jacket filled with helium. The control rods KC-1 and KC-2 are intended for compensation of burnup of ^{239}Pu and temperature reactivity effect; the medium-efficiency rod is used for smooth variation of reactivity during the start-up of the reactor.

The automatic control rod (AP) is moved by a stepping engine of low inertia. The safety of the reactor is provided by four safety plugs worth 3.2%; two of them are operated by a hydraulic machine. The fast safety plugs (the worth of БAC is 0.4%) operate between power pulses
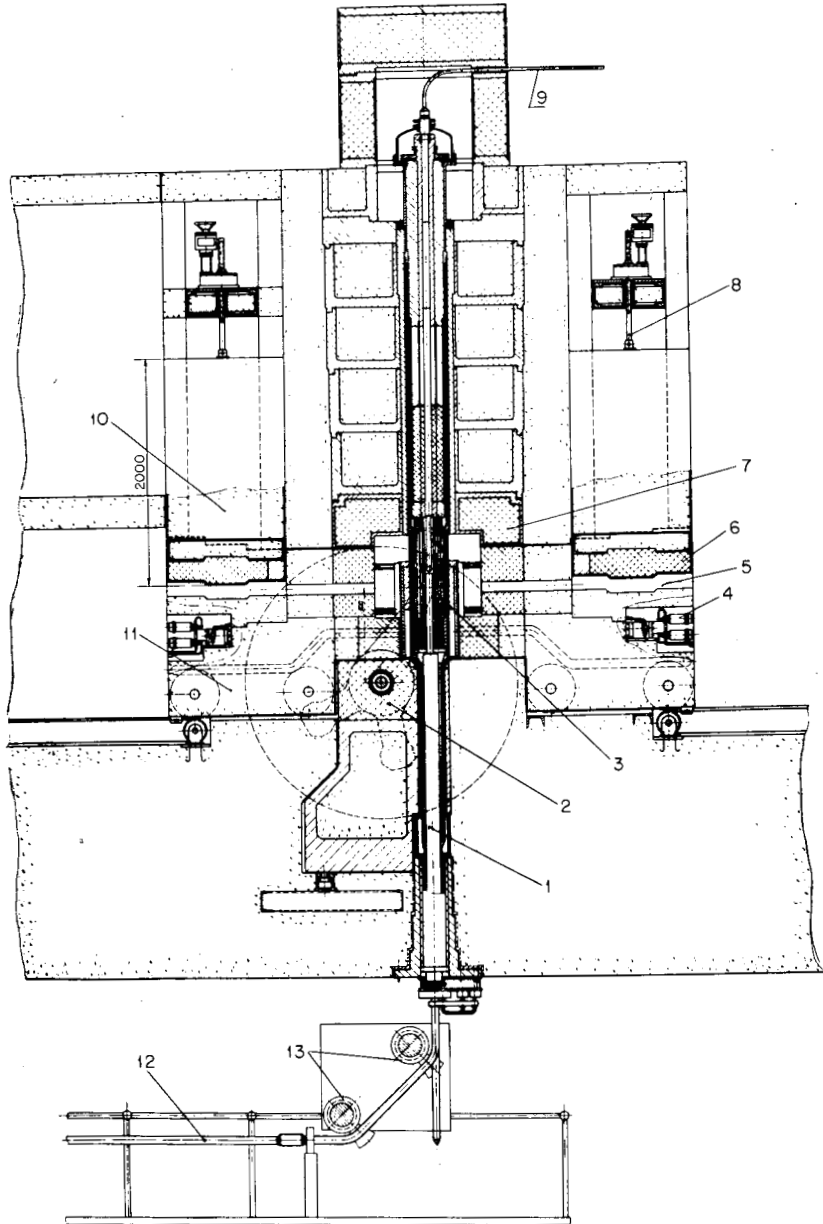
Fig. 12— Vertical cutaway view of the IBR-2.

(1) Accelerator target channel
(2) Moving reflector rotor
(3) Reactor core
(4) Hydraulic drive of fast safety rods
(5) Neutron-beam channel
(6) Shutter of beam channel
(7) Thermal and radiation shield
(8) Shutter drive
(9) Central exposure channel
(10) Inner concrete biological shield
(11) Movable shield with reflectors and moderators

during the period of 0.02 sec. The ejection of the slow safety plugs is performed by gravity when the supporting magnets are switched off.

The cooling system of the IBR-2 core is, in principle, similar to that of the BR-5 stationary reactor, which proved to be reliable during continuous operation. The cooling system has three double loops. The coolant in the first and second loop is liquid sodium, and air is in the third one. The loops are doubled for safety. Circulation of sodium in the primary and secondary loops will be achieved with the aid of electromagnetic pumps. The input and output sodium temperatures are 300°C and 400°C, respectively. The flow rate of the coolant at a mean power of 4 Mw is supposed to be 120 tons/hr. The cooling-system design foresees the opportunity of natural circulation of sodium in case the pumps fail to operate. Table 3 gives the main characteristics of the reactor. The data of this table are calculated using the Monte Carlo method code[31] and are confirmed by the results of the mock-up of the reactor.

Table 3

CHARACTERISTICS OF THE IBR-2 REACTOR

Mean thermal power, Mw	4
Power during a pulse:	
At a frequency of 5/sec, Mw	7700
At a frequency of 50/sec, Mw	700
Power released between pulses, Mw	0.22
Power released in satellites at a frequency of 5/sec, Mw	0.026
Burst energy at a frequency of 5/sec, fissions	2.5×10^{16}
Global leakage from the reactor, neutrons/sec	1.75×10^{17}
Half-width of power pulse at a frequency of 5/sec, μsec	90
Neutron generation time, sec	4.2×10^{-8}
Core volume, liters	17.9
Reactor operating run at design power until 5% burnup, days	1000

Experimental Setup

The reactor is situated in the center of a biological shield, formed by two coaxial rings (Fig. 13). The space between the rings is occupied by experimental facilities. The space serves also as a place for assembly and disassembly of stationary reflectors, light-water moderators, tube conveyers, etc., which are installed on shielding trolleys. Three-fourths of the outer concrete shield ring is surrounded by an experimental hall of 2600 m^2 in area. The linac electron guide and deflecting magnets, which turn electrons at 90° (Fig. 12), are situated in
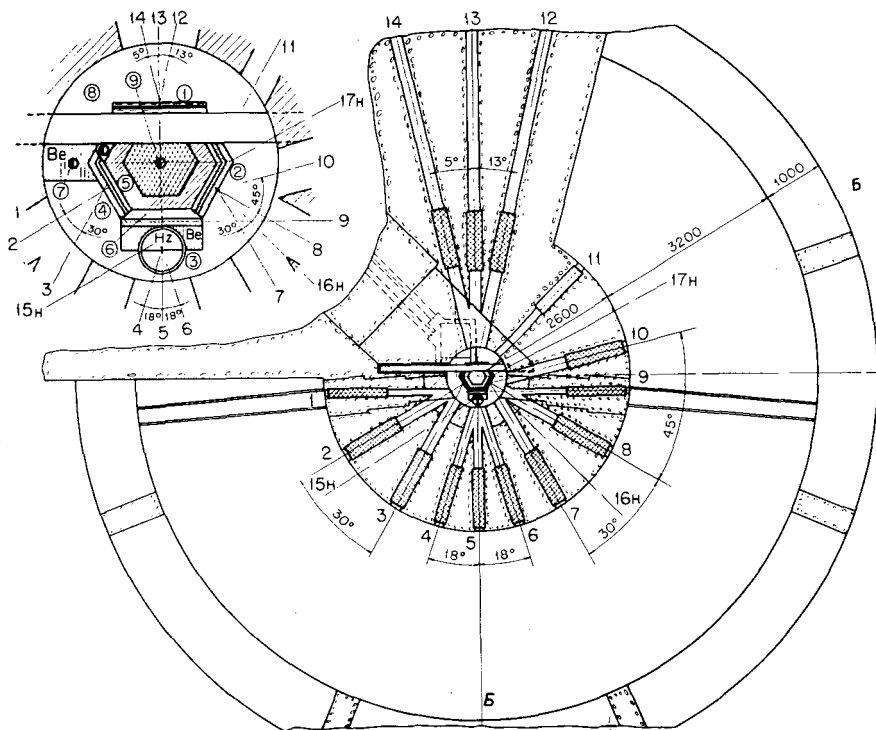
Fig. 13 — Shielding and horizontal neutron-beam holes of the IBR-2.

(1) Intermediate neutron moderator
(2) Thermal-neutron moderator
(3) Cold-neutron source
(4) Thermal-neutron moderator
(5) Stationary reflector
(6) Light-water moderator

(7) Exposure thermal-neutron channel
(8) Exposure fast-neutron channel in reflector
(9) Exposure fast-neutron channel in the middle of the core (the figures are in circles)

the hall beneath the reactor. Moderators can be placed either in the vicinity of the reactor reflectors or in the shield and moved by a special device at $40°$ with regard to the horizontal plane. Figure 13 gives the arrangement of the horizontal neutron-beam holes and moderators around the reactor core. Moderators 1, 2, and 4 are light-water ones consisting of isolated sections, which permits their thickness to be varied to 35, 45, and 55 mm to obtain a maximum neutron-beam intensity in the energy interval required. The design of moderator loops permits a homogeneous and independent poisoning of the moderator or any of its sections.

Moderator 1, situated close to the moving reflector, can be used mainly as a source of intermediate neutrons. The moderator is traversed by three horizontal channels 200 mm in diameter, one of

which is 1000 m and two of which are 500 m in length. Moderators 2 and 4 will be sources of thermal and epithermal neutrons. Neutrons fly from these moderators through six horizontal guides 200 m in diameter and two inclined guides 150 mm in diameter. Channels 1 and 9 represent a straight-through tangential channel, which can be used, for instance, for experiments with "neutron gas" (the study of the parameters of nn-scattering). Both these channels are installed on shield trolleys, which permits their orientation to moderators 4 and 2, if required. To generate cold neutrons ($\lambda > 4\text{Å}$) a liquid-hydrogen moderator with a volume of 1000 cm^3 is located behind light-water moderator 6. Gaseous helium with an input temperature of 11.5°K is used for its cooling. The maximum temperature of hydrogen in the chamber is 25-24°K, and 4 atm of pressure is kept in the moderator chamber to prevent hydrogen from boiling. The effective temperature of neutrons leaving the moderator is expected to be 50°K. The cold moderator is traversed by horizontal channels 4, 5, and 6, each 150 mm in diameter. The possibility of installing a hot moderator to increase the yield of epithermal neutrons is being considered. Beryllium oxide is supposed to be used as a material for the hot moderator, in which case, it should be heated to 1800 to 2000°C by reactor radiation. The installation of three tube conveyers is foreseen. Table 4 presents the neutron-flux intensities that are expected.

Injector for the IBR-2 Reactor

An electron accelerator has been chosen as the injector since its construction is simpler and its operation is more reliable compared with accelerators of heavy particles.

The principles of operation and design of the LIU are very simple.[32, 34] This accelerator consists of a row of pulsed transformers (toroidal inductors), for which the electron beam accelerated along the inductor axis is a secondary winding. The cost of the LIU is decreasing while the efficiency is increasing, with reduction of the diameter of the inductors.[33] Therefore the outer diameter of the LIU permalloy core of the inductors was chosen to be 260 mm. The average power of the electron beam is expected to be 15% of the total power supply of the accelerator.

Table 5 gives the parameters of the LIU. The LIU-30 units have the following characteristics. The electron gun is meant for a pulse voltage of from 300 to 500 kv, the emission current from the cathode being 300 amp. The inductors, in each of which the energy increase is 23 to 25 kev, will be manufactured from a 50% iron−nickel permalloy. The inductors are cooled by distilled water. The pulse-reversing magnetism is generated by pulsed line-type modulators. Some artificial nonuniform long lines with an impedance varying from one cell to another according to a certain law are used as energy accumulators.

Table 4

PARAMETERS OF NEUTRON BEAMS ON THE IBR-2
REACTOR

Thermal-neutron flux, neutrons/cm^2/sec	
From the surface of moderator 6, averaged over time	5.8×10^{12}
From the surface of moderators 2 and 4, averaged over time	3.5×10^{12}
In exposure channel 7, averaged over time	8×10^{13}
From the surface of moderator 6 at a maximum pulse at a frequency of 5/sec	10^{16}
In the straight-through tangential channel at a maximum pulse	9×10^{16}
Half-width of thermal neutrons, μsec	
In moderators 2, 4, and 6	120
In exposure channel and in cold moderator	200
Neutron flux in energy interval 0.46 ev to 1 ev from the surface of moderator 1, neutrons/cm^2/sec	0.4×10^{12}
Flux of neutrons with $\lambda = 5$ Å from the surface of the cold moderator at a neutron maximum pulse, neutrons/Å/cm^2/sec	4.2×10^{14}
Flux of fast neutrons with an energy of 0.4 kev to 10 Mev in the central exposure channel averaged over time, neutrons/cm^2/sec	3×10^{14}

Table 5

PARAMETERS OF THE LIU-30

Energy of electrons, Mev	30
Current during a pulse, amp	250
Electron pulse duration, μsec	0.5
Repetition rate, sec^{-1}	50
Outer diameter of the inductor, mm	260
Accelerator length, m	160
Power supply of the installation, averaged over time, Mw(e)	1.35
Electron-beam power, averaged over time, Mw	0.2
Number of neutrons per pulse from a thick unmultiplying uranium target, neutrons	1.2×10^{13}

Power thyratrons serve as ion commutators. One modulator feeds several inductors simultaneously. The energy storage line is charged by a d-c source through a choke coil, which provides the so-called "resonance condition of operation." In this case the voltage on the line exceeds the voltage in the current source.

Since the accelerator is long, delivery of accelerating pulses onto the inductor is compatible with the passage of electrons through the inductors. The focusing and correction of beam-axis deflections from the inductor axis are performed by special-current coils and short solenoids placed between inductor sections. Separate focusing and correcting elements have independent power supplies. Because of the large length of the accelerator, the magnetic field of the earth will deflect electron trajectories with regard to the accelerator axis between inductor sections. This effect is compensated by the special current coils.

The accelerated electron beam will be controlled by gauges that measure the total electron current, its space distribution, and the position of the beam with regard to the accelerator axis.

The average power of the IBR-2 plus the LIU-30 booster vs. the half-width of pulse is given in Fig. 14.
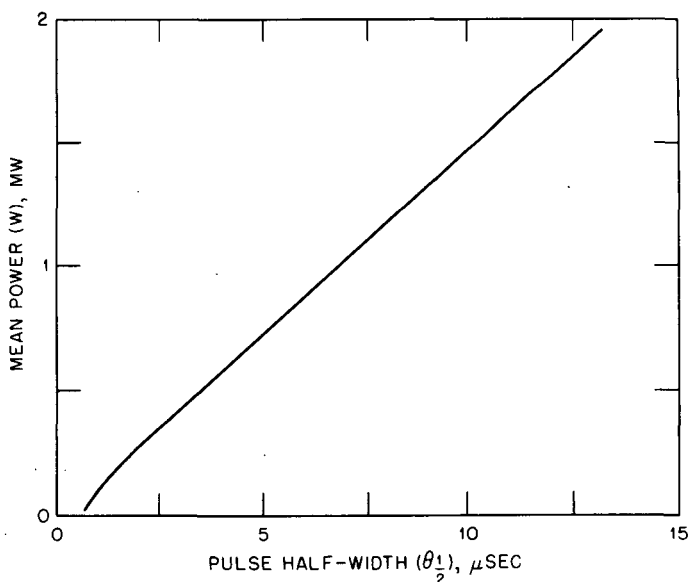

Fig. 14—The mean IBR-2 reactor power vs. the half-width of the pulse for booster operation; the pulse half-width $\theta_{1/2}$ and the power W are expressed in microseconds and megawatts, respectively.

REFERENCES

1. I. I. Bondarenko and Yu. Ya. Stavisskii, Pulsed Zone of Operation of a Pulsed Reactor, *At. Energ. (USSR)*, 7(5): 417 (1959).
2. G. E. Blokhin et al., Fast Neutron Pulsed Reactor, *At. Energ. (USSR)*, 10(5): 437 (1961).
3. G. E. Blokhin et al., Fast Neutron Pulsed Reactor, in *Physics of Fast and Intermediate Reactors*, pp. 399-417, Symposium Proceedings, Vienna, 1961, International Atomic Energy Agency, Vienna, 1962 (STI/PUB/49).
4. I. M. Frank, Pulsed Reactor of the Laboratory of Neutron Physics at the Joint Institute for Nuclear Research. Report of the Ninth Session of the Scientific Council of the Joint Institute for Nuclear Research on the Works Performed by the Laboratory of Neutron Physics, November 1960, Preprint of the JINR, 1961.
5. V. D. Denisov, Zh. A. Kozlov, Lü Ming, V. M. Nazarov, G. N. Pogodaev, E. N. Shabalin, and Yu. S. Yazvitskii, Certain Results of Investigation of IBR, Preprint of the JINR R-1257, 1963, presented at the International Conference on Reactor Physics and Technology, Prague, April 1963.
6. Lü Ming, E. P. Shabalin, and Yu. S. Yazvitskii, Experimental Studies of Pulsed Reactor Fluctuations, *At. Energ. (USSR)*, 16: 1 (1964).
7. B. N. Bunin, I. M. Matora, S. K. Nikolaev, L. B. Pikel'ner, I. M. Frank, E. P. Shabalin, F. L. Shapiro, and Yu. S. Yazvitskii, Operating Experience with the IBR Reactor, Its Use for Neutron Investigations and Its Characteristics on Neutron Injection from a Microtron, in *Proceedings of the Third International Conference on Peaceful Uses of Atomic Energy, Geneva, 1964*, Vol. 7, p. 473, United Nations, New York, 1965.
8. V. D. Anan'ev, I. M. Matora, G. N. Pogodaev, V. T. Rudenko, E. P. Shabalin, F. L. Shapiro, and I. M. Frank, Pulsed LNF JINR Reactor and the Perspectives of Pulsed Reactor Uses in Neutron Spectroscopy, Preprint JINR 2372, 1965.
9. J. Randles and R. Jaarsma, Some Problems of Stress Wave Production Encountered in the Study of Pulsed Fast Reactor Dynamics, EURATOM Report EUR 3654e, 1967.
10. V. D. Anan'ev, P. S. Antsupov, S. P. Kapitsa, I. M. Matora, V. N. Melekhin, L. A. Merkulov, and R. V. Khar'yuzov, The 30 MeV Microtron Injector for IBR, *At. Energ. (USSR)*, 20(2): 106 (1966).
11. V. D. Anan'ev, P. S. Antsupov, I. M. Matora, L. A. Merkulov, and R. V. Khar'yuzov, Microtron of the Neutron Physics Laboratory at the JINR, Preprint JINR 9-3283, 1967.
12. L. B. Pikel'ner and V. T. Rudenko, IBR Pulsed Reactor with Injector, in Research Applications of Nuclear Pulsed Systems, Panel Proceedings, Dubna, July 1966, pp. 203-211, International Atomic Energy Agency, Vienna, 1967 (STI/PUB/144).
13. Yu. A. Aleksandrov, G. S. Samosvat, Zh. Sereeter, and Tsoi Gen Sor, Scattering of Kilovolt Neutrons by Lead and Electrical Polarization of Neutrons, *JETP Letters (USSR)*, 4(5): 196 (1966).
14. Yu. A. Aleksandrov, A. M. Balagurov, E. Malishevski, T. A. Machekhina, L. N. Sedlakova, and Ya. Kholas, Preprint of JINR R3-4121, 1968.
15. V. I. Lushchikov, Yu. N. Pokotilovskii, A. V. Strelkov, and F. L. Shapiro, Preprint JINR R3-4127, 1968.
16. P. Draghicescu, V. I. Lushchikov, V. G. Nikolenko, Yu. V. Taran, and F. L. Shapiro, *Phys. Lett.*, 12: 334 (1964).
17. V. P. Alfimenkov, V. I. Lushchikov, V. G. Nikolenko, Yu. V. Taran, and F. L. Shapiro, *Phys. Lett., B*, 24(3): 151 (1967).
18. V. P. Alfimenkov, V. I. Lushchikov, V. G. Nikolenko, Yu. V. Taran, and F. L. Shapiro, Determination of Neutron Resonance Spins of ^{165}Ho Nuclei

by Means of Polarized Penetration Through Polarized Target in the Energy Range from 0 to 55 ev, *Yadern. Fiz.*, 3(1): 56 (1966).

19. I. Kvitek and Yu. P. Popov, *Phys Lett.*, 22(2): 186 (1966).

20. Yu. Popov and M. Stempinskii, Spectra of α Particles During Decay of ^{148}Sm Excited States with Spins 3^- and 4^-, *JETP Letters (USSR)*, 7(4): 126 (1968).

21. Yu. V. Ryabov, Wang Yung Chang, E. Dermendzhiev, and Chang Po Shu, Parameters of ^{239}Plutonium Levels, Preprint JINR R-2713, 1966.

22. I. I. Bondarenko, V. G. Liforov, V. N. Morozov, M. N. Nikolaev, V. A. Parfenov, and V. A. Semenov, Measurements of Neutron Spectra in Nickel, Iron, and Stainless Steel, *At. Energ. (USSR)*, 18(6): 593 (1965).

23. Yu. V. Ryabov, So Ton Sik, N. Chikov, and N. Yaneva, Measurements of the Relation of Radiative Capture Cross Sections and Fission of ^{235}U and ^{239}Pu in the Neutron Resonance Energy Region, *At. Energ. (USSR)*, 24(4): 351 (1968).

24. I. Sosnovska, E. Sosnovski, S. V. Kiselev, A. N. Kshnyakina, and R. P. Ozerov, Neutronographic Studies of Nuclear and Magnetic Structure of BiFeO$_3$ by Means of Time-of-Flight Method, Preprint JINR-2653, 1966.

25. V. V. Golikov, I. Zhukovskaya, F. L. Shapiro, A. Shkatula, and E. Yanik, Scattering of Cold Neutrons in Water and Certain Organic Materials, Preprint JINR-R-1903, 1964.

26. V. V. Nitts, I. Sosnovska, and E. Sosnovski, Studies of Neutron-Phonon Interactions in the Fast Pulsed IBR Reactor, Preprint JINR R-1847, 1964.

27. I. Natkaniec, K. Parlinski, J. A. Janik, A. Bajorek, M. Sudnik-Hrynkiewicz, Local Vibrations of Impurity Atoms in Copper and Lead, Preprint of JINR E I4-3825, Dubna, 1968.

28. L. A. Bulavin, A. V. Voronel', Yu. M. Ostanevich, A. P. Simkina, and A. V. Strelkov, Coefficient of Self-Diffusion of Ethane Near the Critical Liquid-Vapor Point, Preprint JINR R14-3824, 1968, presented at the Symposium on Inelastic Scattering of Neutrons, Copenhagen, May 20−24, 1968.

29. O. D. Kazachkovskii et al., *At. Energ. (USSR)*, 24: 136 (1968).

30. A. I. Leipunskii et al., *At. Energ. (USSR)*, 5: 345 (1964).

31. V. I. Kochkin and E. P. Shabalin, The Monte-Carlo Method Use in Calculation of Pulse Reactor with a Movable Reflector, Preprint JINR-11-4098, 1968.

32. N. S. Christofilos, R. E. Hester, W. A. S. Lamb, D. D. Reagun, W. A. Sherwood, and R. E. Wright, *Proceedings of the International Conference on High-Energy Accelerators, Dubna, 1963*, p. 1073, Atomizdat, 1964.

33. I. M. Matora, On the Theory of Linear Induction Accelerator, Preprint JINR R9-3184, Dubna, 1967.

34. A. I. Anatskii et al., *At. Energ. (USSR)*, 21: 439 (1966).

DISCUSSION

LARRIMORE: Could you tell us about the schedule for the IBR-2.

BLOKHINTSEV: Up to this date I have no formal decision from the Scientific Committee of our Institute, but I hope I shall have a positive decision soon. It would take several years to complete this installation.

McENHILL: I would like to know how you produce the very cold neutrons traveling with the velocity of 1 to 2 m/sec. Also, what current of neutrons at that velocity do you achieve with this system?

BLOKHINTSEV: We produce ultra-cold neutrons using the total reflection of these neutrons from a copper tube. The number of these neutrons is 1 neutron/100 sec. These experiments were performed under less than optimum conditions.

McENHILL: In the reflecting tube for reflecting these cold neutrons, do you use a specialized tube, say of nickel, for reflecting the very cold neutrons down?

BLOKHINTSEV: Copper.

MIHALCZO: Is 4 Mw the best power to construct such a system, or is 10 or 20 Mw better? Have you done optimization studies on the power?

BLOKHINTSEV: You mean why did we choose 4 Mw? I do not like to make big jumps; it is better to proceed step by step.

LARRIMORE: Have you decided on a fuel for IBR-2? Is it going to be plutonium oxide?

BLOKHINTSEV: Yes, we chose the fuel elements very similar to the elements of the BR-5 reactor at Obninsk. We have had good experience with them.

LARRIMORE: When you are using the IBR-1 in both the pulsed reactor and accelerator pulsed reactor mode, are you using it roughly half and half, or mostly in one of these ways or the other, or does it depend on the experimental program?

BLOKHINTSEV: This depends on the experimental program. In general, we used IBR-1 half and half in both modes of the operation.

MILEY: As I understand it, the IBR-30 uses a moderator block to produce thermal neutrons, i.e., a thermal-neutron pulse. Could you describe the moderator block?

BLOKHINTSEV: We usually used water as the moderator-block. For ultracold neutrons we used polyethylene.

MILEY: Polyethylene? What size is it?

BLOKHINTSEV: The size was about 1 mm thick.

BECKURTS: I have a question concerning the data of IBR-2. If I understood you correctly, you will have a burst half-width of 90 μsec. This sounds very large compared to what people have been striving for. Is that because you find it very difficult to get a shorter one, or is it because your experimental people are not interested in shorter burst widths.

BLOKHINTSEV: Of course it is better to have a shorter duration of pulse than 90 μsec, but it is not so important for us because we have two modes of operation, namely, pulse reactor mode and electron accelerator injection.

BECKURTS: I see. This quoted figure referred to the pulsed reactor operation?

BLOKHINTSEV: Yes.

BECKURTS: I see. But then would you have peak powers comparable to those figures given in the table that you have just shown?

BLOKHINTSEV: Those figures were for pulsed reactor operation. Data with the injector are given in the paper.

LARRIMORE: For the IBR-30 where are you going to put the electron accelerator? As I remember, in the pictures of the IBR layout the microtron was in a little room directly above the IBR.

BLOKHINTSEV: We use the same room for the new linear accelerator which previously housed the microtron. It is, as you indicate, located above the pulsed reactor.

3-2 BROOKHAVEN PULSED FAST RESEARCH REACTOR

J. M. HENDRIE, K. C. HOFFMAN, H. J. C. KOUTS, R. J. PARSICK, J. P. PHELPS, G. A. PRICE, M. REICH, H. TAKAHASHI, and H. H. WINDSOR
Brookhaven National Laboratory, Upton, New York

ABSTRACT

The repetitively pulsed fast reactor is of interest as a high-intensity source for neutron-beam experiments. The design characteristics of a conceptual pulsed reactor operative at an average power of 30 Mw are discussed. The peak power during a pulse is about 4700 Mw, and the pulse width at half-maximum power is 90 μsec. The reactivity is varied by reflector sections on high-speed rotors carried past a bare face of the core. A two-rotor system is preferred to provide for variation of the repetition rate between 20 and 60 pulses/sec.

The performance of the system described is limited by the ability of the fuel to withstand the cyclic thermal and inertial stresses caused by power pulsing. The high-cycle-fatigue strength of a cermet fuel with a molybdenum matrix was determined in the unirradiated condition, and these data were used as the basis for the core design. Developments and tests on this fuel and on other potential pulsed reactor fuels, such as U−Nb−Zr ternary alloys and a U−Th dispersion, are outlined. A series of critical experiments and beam-source optimization studies performed in support of the design effort is described.

INTRODUCTION

The repetitively pulsed fast reactor is under study at Brookhaven National Laboratory as a high-intensity neutron-beam source for research. Two alternate concepts are being investigated: a pulsed reactor in which the reactivity is modulated by mechanical means and an accelerator pulsed reactor in which neutrons are injected into the system from the target of an electron accelerator coincidentally with mechanical modulation of the reactivity. Preliminary studies of these concepts[1] indicated that the performance of the pulsed reactor, in

terms of burst magnitude and pulse width, is limited by the ability of the fuel to withstand the cyclic thermal and inertial stresses produced by power pulsing and by the rate of reactivity variation of the reactivity pulsation device. The performance of the accelerator pulsed reactor, however, is limited primarily by the output of the electron accelerator that is used to generate the injected neutrons; the fuel stresses and the reactivity pulsation device requirements are not so severe as in the pulsed reactor.

The studies that have been performed have concentrated on the reference design of a pulsed reactor in which performance is limited by the repetitive stresses developed in the fuel and on supporting fuel-development work, critical experiments, and beam-source studies. Discussions of these four major areas of work comprise the main sections of this paper.

The goal of the reference design for the pulsed reactor is to develop a realistic maximum performance system that will provide the basis for evaluating the experimental utility of the concept. The current state of the reference design is described in detail in the next section. When this design has been evaluated, the system will be optimized to improve its performance, if possible.

In the absence of experience with fuels operating at high power levels in a repetitively pulsed reactor, it is essential to select a fuel for the reference design which is amenable to theoretical calculation of its response to power pulsing and is sufficiently developed so that its mechanical properties are known and can be used as the basis for the design. A PuO_2–Mo cermet was selected as the current reference fuel because it best satisfies the above requirements and it promises to have a high burnup potential. Tests performed on the cermet fuel and on other candidate fuels are described under Fuel Test and Development.

Studies of the accelerator pulsed reactor have not progressed as far as those of the pulsed reactor. The accelerator pulsed concept requires a fuel with a higher fissile-material loading because its core tends to be more compact. Test work is planned on such a fuel, U–10 wt.% Mo. On the basis of currently available data, the design parameters outlined in the preliminary studies[1] of the accelerator system still appear feasible.

A fast reactor critical assembly, the Critical Experiment Pulsed Fast Reactor, designated CEPFR-1, was designed, constructed, and operated to provide design data for the pulsed reactor reference design and to provide a means of testing the reliability of the predictions of reactor performance. The CEPFR-1 facility and the results obtained thus far with the facility are described under the section Critical Experiments.

Beam-source experiments have been performed to study the characteristics of hydrogenous moderating blocks in pulsed reactors. The purpose of this work is to provide a basis for the design of the moderating blocks to produce the maximum yield of thermal neutrons with a pulse width commensurate with the burst width of the reactor. The results of these experiments are described under Beam-Source Studies.

PULSED REACTOR REFERENCE DESIGN

Design Description

The current version of the reference pulsed reactor core is 60 liters in volume, is cooled with sodium, and is fueled with a 60 vol.% PuO_2-Mo cermet. The reactor operates at an average power of 30 Mw, and the design repetition rate is 60 pulses/sec. At this repetition rate, the fuel will be exposed to about 10^9 power pulses in 200 full-power days of operation. The fuel burnup after 200 days will be about 2 at.%. Since there are many inertial-stress cycles in the fuel during each power pulse, the expected cyclic-stress exposure is at least 10^{10} cycles, which is well into the high cycle fatigue range. The performance of the reactor is limited by the high cycle fatigue properties of the cermet fuel, and the current reference design core is based upon the results of fatigue tests of unirradiated specimens of the cermet fuel, with UO_2 substituted for PuO_2.

Reactivity is varied by means of two rotors carrying sections of reflector past a bare face of the core. The reflector-block material is a titanium alloy, Ti -5 wt.% Al -5 wt.% Zn -5 wt.% Zr, and the rotor hub may be either of the same material or of a higher strength material, such as maraging steel. Even if similar materials are used for the reflector block and hub, a mechanical joint between the two is required to facilitate periodic replacement of the block. The favored rotor arrangement is one in which the core does not fall in the plane of rotation of the rotor. Such an arrangement dictates a horizontal shaft for each rotor, with shafts offset horizontally from the core region. A sketch of the core region and the pulsation devices is shown in Fig. 1. The reflector pulse block that provides most of the reactivity variation is carried on a high-speed rotor of 36-in. radius spinning at 3600 rpm. The tip speed is 1130 ft/sec, which represents a conservative design for these materials. The high-speed rotor determines the pulse characteristic, and the speed of the second rotor can be varied to control the repetition rate such that a pulse is produced only when the pulse blocks of both rotors pass the core simultaneously. The two-rotor reactivity pulsation system allows variation

of the repetition rate between 20 and 60 pulses/sec; but, to stay within the fuel cyclic-stress limitations, the average reactor power must be reduced as the repetition rate is lowered to hold the burst magnitude at an approximately constant level.
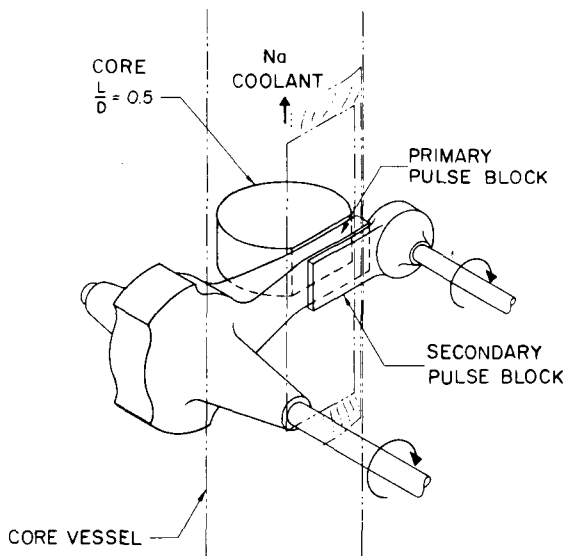
Fig. 1 — Pulsed reactor core and pulse-block arrangement, with horizontal shafts.

   The rotor housing is partially evacuated to reduce the aerodynamic drag. The energy generated in the rotor tip as a result of gamma and neutron heating is radiated to the rotor housing, which is cooled by nitrogen gas. Preliminary calculations indicate that the steady-state reflector-block temperature will be about 800°F.
   The core has an equivalent height-to-diameter ratio of about 0.5. The short core is advantageous in this geometry in that the reflector pulse block and the coolant both pass the core in the short direction. Thus the reactivity curve is sharpened at the peak, and the bulk-coolant temperature rise is minimized. A disadvantage may be a reduction in the thermal flux in the beam-source moderating regions around the periphery of the core. As an alternate, a core with a height-to-diameter ratio close to 1 and with a different rotor arrangement (Fig. 2) is being considered. However, this paper will be limited to the flattened core of Fig. 1.
   The characteristics of the current reference design pulsed reactor have been estimated, and they are given in Table 1.

The reactor-shield zone and primary-system layout are shown in plan view in Fig. 3 and in elevation in Fig. 4. The sodium-cooled core is contained in a core vessel with the beam-source moderator blocks and radial reflector outside the core vessel in a nitrogen-
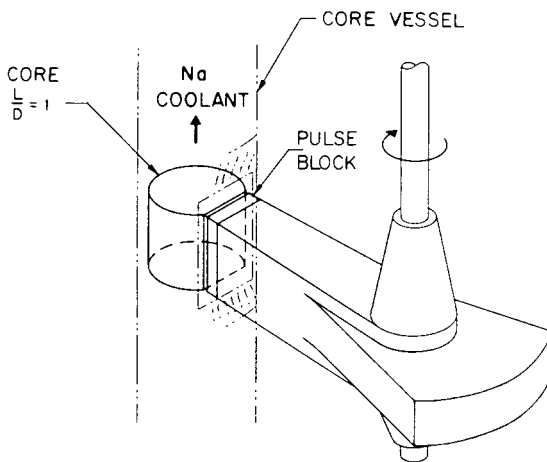
Fig. 2—*Alternate pulsed reactor core and pulse-block arrangement, with vertical shaft.*

cooled zone. The core vessel extends to an overhead pot containing the primary-coolant circulating pumps and heat exchangers. The primary-system components are either flanged or plugged into the system, and the connections are located within the sodium pot. This concept facilitates access to and replacement of primary-system components. Provision is also made for periodic replacement of the core vessel since it will be subjected to irradiation damage owing to its proximity to the core. The location of the intermediate heat exchanger above core level provides for natural-circulation cooling of the core in the event the circulation pumps are inoperative.

Fuel handling will be performed in a cell located above the core vessel. Access to the control rods, moderator blocks, and reflector sections, and facilities for replacement of the core vessel are provided in this cell. A separate cell on the same level is provided over the pot for the maintenance and replacement of primary-system components.

The pulsation device will be maintained in a cell on the same level as the experimental area. A shield plug is set close to the rotor housings with sealing strips around the periphery to form a minimum-volume cavity for the core region and pulsation device. This cavity,

Table I

SUMMARY OF PULSED REACTOR REFERENCE-DESIGN CONDITIONS

General Characteristics

Fuel material	60 vol.% PuO_2 − Mo cermet
Coolant	Na
Core volume, liters	60
Design repetition rate, sec^{-1}	60
Range of variability of repetition rate, sec^{-1}	20 to 60
Average power, Mw	30
Peak power, Mw	4700
Pulse width at half-power, sec	90×10^{-6}
Prompt reactivity between pulses, $	−15
Prompt-neutron lifetime, sec	5×10^{-8}
Parabolic reactivity coefficient α, m^{-2}	2

Thermal and Hydraulic Characteristics

Coolant flow, gal/min	6200
Core inlet temperature, °F	400
Bulk coolant Δt, °F	121
Average core power density, Mw/liter	0.5
Peak core power density, Mw/liter	1.05
Maximum temperature rise in fuel during pulse, °F	22.5
Maximum fuel center line temperature, °F	650

Mechanical Characteristics

Fuel element, outside diameter, in.	0.155
Cladding thickness, in.	0.015
Pin spacing, pitch-to-diameter ratio	1.10
Primary rotor diameter, in.	70
Primary rotor speed, rpm	3600
Primary rotor tip speed, ft/sec	1100
Secondary rotor diameter, in.	40
Secondary rotor speed, rpm	1200 to 3600

lined with energy-absorbing material to absorb the blast energy associated with an accident, provides leak containment. A seal is provided where the core vessel penetrates the floor of the core-region cavity so that, in the event of a vessel rupture above that point, the cavity would not drain but would flood to keep the core covered with coolant. This seal must be decoupled when the core vessel is replaced. All the piping below the level of the core cavity has secondary leak containment, including the flanged joint at the lower end of the core vessel, which must be disconnected to permit removal of the core vessel. Access to this joint is provided in a cell located beneath the reactor cavity.

Fig. 3 — *Plan view of pulsed reactor.*

Labels in figure:

CORE VESSEL

HEAT-EXCHANGER BUNDLES

SECONDARY ROTOR

SECONDARY-SODIUM PIPING

PRIMARY-SODIUM PIPING

N₂ REFLECTOR COOLING

ROTOR DRIVES

DUMP TANK

BEAM PORTS

CONTROL RODS

BIOLOGICAL SHIELD

THERMAL SHIELD

MODERATING REGION

REFLECTOR
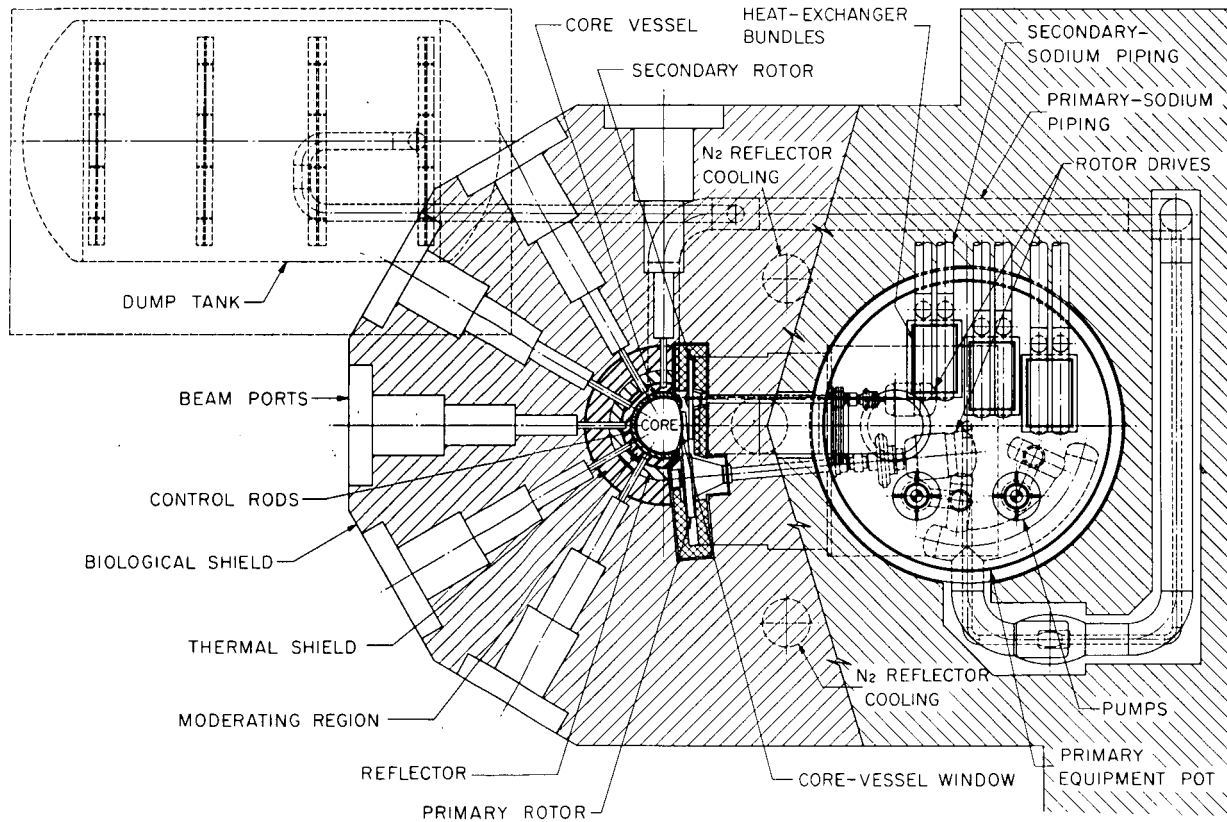
PRIMARY ROTOR

N₂ REFLECTOR COOLING

CORE-VESSEL WINDOW

PUMPS
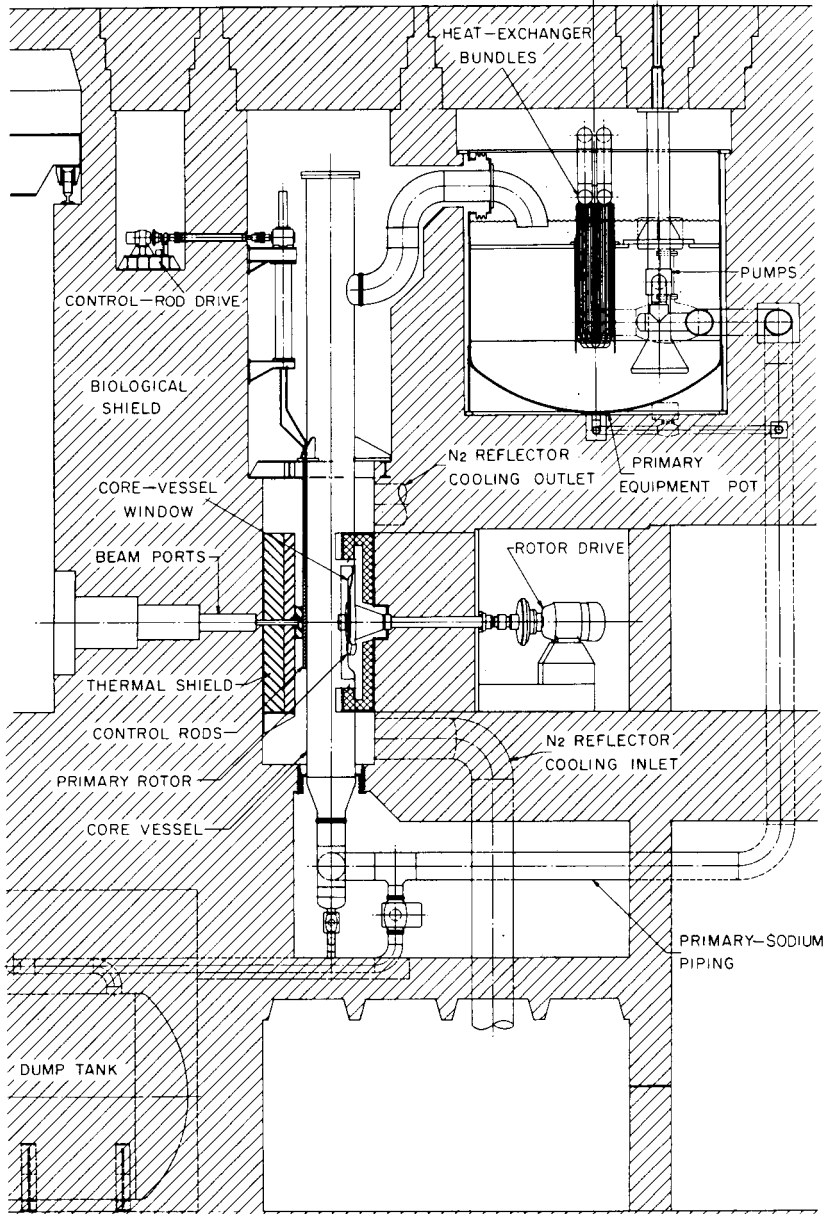
PRIMARY EQUIPMENT POT

CORE

Fig. 4—Elevation of pulsed reactor.

Electrical trace heating will be provided on all piping, and nitrogen-gas heating will be used in the core region and primary-system pot.

Thermal Analysis

The thermal characteristics of the reference core have been analyzed using a three-dimensional heat-transfer code, LION, that was obtained from the Knolls Atomic Power Laboratory and adapted for use on the CDC-6600 computer at Brookhaven. A specimen of the thermal analysis performed for a local power density of 1.9 Mw/liter is shown in Figs. 5 and 6. For this specimen case the pulse was assumed to have a half-width of 60 μsec, and the repetition rate was 22 pulses/sec. The fuel element in this case was a 0.125-in.-diameter pin of cermet fuel with a 0.015-in.-thick cladding of molybdenum metallurgically bonded to it. Figure 5 is a graph of the temperature of each nodal point at the axial peak of the core hot pin. Nodes 51 through 57 cover the fuel from center line to surface; nodes 58, 59, and 60 are in the cladding; node 106 is on the cladding surface; and node 117 is in the coolant stream. In this case, the fuel temperature increased at a rate of about $2 \times 10^6 °F/sec$ for about 70 μsec after the start of the pulse, although the cladding remained unaffected for this period. The rapid chilling of the outer portion of the cermet, node 57, as a result of heat
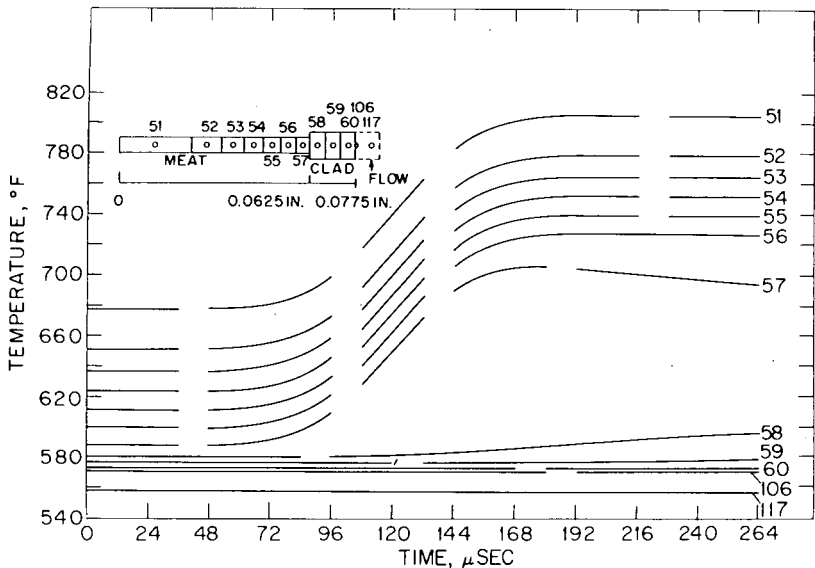
Fig. 5 — Temperature history of nodes at the axial peak of the hot pin during and following a power pulse.

loss to the high-thermal-conductivity cladding, is illustrated by the decrease in temperature indicated after about 180 μsec. This chilling caused a steep temperature gradient at the fuel–cladding interface and led to a significant alternating thermal stress applied on top of the average thermal stress that existed due to the steady-state temperature gradient in the pin. Figure 6 shows the actual temperature profile in the pin as a function of time and indicates the steep temperature gradient in the vicinity of the fuel–cladding interface after 216 μsec. The maximum gradient actually occurs at 192 μsec; the stresses were calculated at that time. After 45 msec all temperatures have returned to their initial values, indicating that equilibrium pulsing conditions have been obtained.

Fig. 6 — Transient temperature profile at axial peak of hot pin.

Stress Analysis

Pulsed operation leads to two sources of cyclic stress. The first is a cyclic thermal stress resulting from the chilling of the fuel surface after a power pulse. This chilling occurs before the fuel center line temperature has been reduced and thus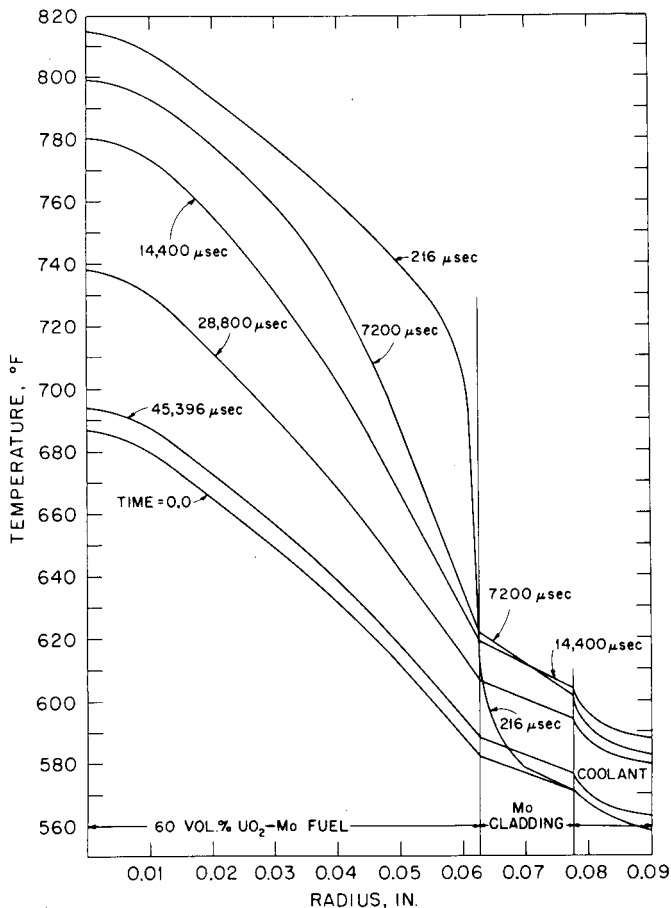 increases the temperature gradient from center line to surface. The result is an alternating thermal stress applied in addition to the mean thermal stress due to the steady-state gradient associated with the average reactor power. There is one stress cycle of this type per power pulse.

The second cyclic-stress component is the inertial stress that results from the extremely rapid heating rate during a pulse and from the inability of the fuel to physically expand in equilibrium with the temperature. This stress induces longitudinal and radial vibrations of the fuel pin and produces many stress cycles per individual power pulse. The rate of amplitude decay, hence the number of stress cycles per power pulse, depends on the internal and external damping.

For an analysis of the cyclic thermal stress, the transient temperature data are used as input to the code TEAR. This code provides an analytical solution to generalized plane thermal-stress problems involving layered materials. Figure 7 shows the radial (σ_r), circumferential (σ_θ), and axial (σ_z) stresses corresponding to the tem-
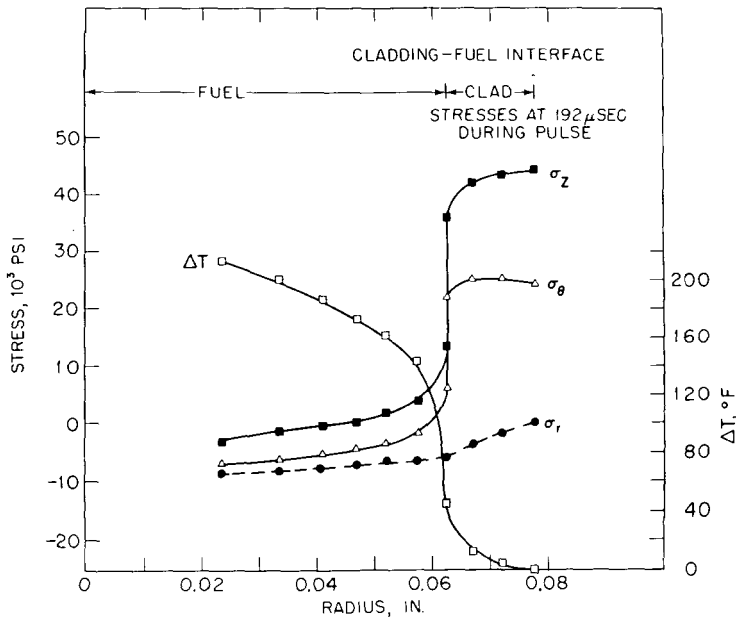

Fig. 7 — Thermal stresses in fuel pin at time of peak thermal gradient.

perature pattern at the time of the peak temperature gradient at the
fuel – cladding interface for the specimen thermal case shown in Figs. 5
and 6. The cladding is in tension in the circumferential and longitudinal
directions, and it maintains a compressive thermal stress in most of
the fuel. The stress in the fuel near the interface, however, is tensile.

It is apparent from the specimen case results that the use of a
cladding with a lower thermal conductivity, such as Inconel, might
offer some advantage in reducing the chilling effect at the fuel surface.
The same advantage could be obtained by using an insulating barrier,
but the axial restraint of the fuel by the cladding would be poor. Analy-
sis of a PuO_2–Mo cermet fuel clad with Inconel indicates that the
fuel-surface tensile stresses are reduced by a factor of about 2. Most
of this reduction is due to the decreased surface-chilling effect, with
the balance due to a better match of the Young's modulus–thermal
expansion coefficient product of the fuel and cladding.

The determination of the inertial stresses in a clad fuel element
is more difficult. The one-dimensional case of thin unclad rods sub-
jected to a ramp temperature input has been solved by Burgreen.[2]
A series of computer codes are under development at Brookhaven to
handle the more general stress problem in a pulsed reactor and to
analyze both the thermal and inertial stresses simultaneously. These
shock codes use a finite-difference method for solving equations of
motion of an elastic body subjected to rapid heating. Features of these
codes that have not been included in previous work in this field are:

1. Extension to three-dimensional problems.
2. Inclusion of the inertial term.
3. The capability of analyzing layered (clad) materials.
4. The capability of handling arbitrary temperature input functions.

The first code of the series, for homogeneous axisymmetric
bodies, has been checked out satisfactorily against Burgreen's one-
dimensional model for inertial stresses and displacements in a long
thin unclad rod. The results also compare satisfactorily with the
Pochhammer solution for longitudinal vibrations in an infinite cylinder.[3]
Another trial run was made for the stresses in a rapidly heated thick
cylinder with a length-to-diameter ratio of 1.4. There is no analytical
solution to this problem; however, the same problem was solved using
an adaptation of a code developed by the Sandia Corporation, and there
was excellent agreement between the two methods of solution. Thus
the agreement obtained in these restricted cases between the Brook-
haven code and other methods of solution indicates that the code is
working satisfactorily. The other codes in the series applicable to
layered axisymmetric bodies and finally to heterogeneous nonsym-
metric bodies are now being completed.

Accurate values for the inertial stress will not be available until the layered-body shock code is operating. For the present we must depend upon simple approximations. A one-dimensional model indicates that the inertial stress will fall between $\frac{1}{4}$ Eα ΔT and $\frac{3}{2}$ Eα ΔT, depending upon the length of the fuel element, where E is the modulus of elasticity, α is the coefficient of expansion, and ΔT is the temperature increase in the fuel during a pulse.

If the alternating inertial stress is assumed to equal $\pm$Eα ΔT, the following conditions are obtained for the specimen case of Figs. 5 and 6:

Mean thermal stress, psi:	5500
Alternating thermal stress, psi:	$\pm$2800
Alternating inertial stress, psi:	$\pm$6400

The frequency of the alternating inertial stress is in the range of 10 to 20 kc/sec, corresponding to the longitudinal resonant frequency of the fuel pin. The inertial stress is superimposed on a thermal stress that varies in the specimen case from 2700 psi just prior to a pulse to 8300 psi shortly after a pulse, and then decreases again to 2700 psi. The alternating inertial stress decays in amplitude after a pulse at a rate (as yet undetermined) governed by the damping characteristics of the fuel assembly. The specimen case thus gives an alternating stress of $\pm$6400 psi with a peak mean stress of 8300 psi.

It should be noted that the current reference design core operates at much milder conditions than those of the specimen case. The current reference design core, with a peak power density of 1.05 Mw/liter and a repetition rate of 60 pulses/sec, has the following stress conditions at the axial peak of the hot fuel pin:

Mean thermal stress, psi:	3050
Alternating thermal stress, psi:	$\pm$580
Alternating inertial stress, psi:	$\pm$1310

The high-frequency alternating stress here is $\pm$1310 psi with a peak mean stress of 3630 psi. These conditions were chosen to be within the current allowable stresses for the cermet fuel of $\pm$1500 psi alternating, 4500 psi mean for a 10^{10} cycle life.

In several areas of the stress analysis, these assumptions, which require further study, were made:

1. The number of inertial-stress cycles that the fuel will be exposed to per pulse is unknown since the damping has not been determined. The current design assumption is that the decaying inertial-stress wave train will be equivalent to 10 full-amplitude inertial-stress cycles per power pulse, applied at the peak thermal stress. This design assumption is subject to revision as a result of detailed analyses

to be done with the layered-body shock code modified to include damping effects.

    2. The effects of irradiation and burnup on the ultimate strength and fatigue properties are unknown. A program is planned to provide these data.

    3. In this analysis the pulse energy has been assumed to be generated uniformly in the cermet, whereas, in fact, it is generated in the oxide particles alone. Analyses are to be performed of the micro-stresses induced by the rapid heating of 150-μ cermet particles within metal matrices. Ultimately, reliance must be placed on proof tests where a fuel pin can be subjected to fission heating to produce this effect and to evaluate its influence on fuel failure.

    4. The reference fuel is a PuO_2—Mo cermet; the material that has been tested thus far is a UO_2—Mo cermet. The effect of the substitution of plutonium for uranium in the cermet is not expected to be serious but must be considered.

Physics Analysis

    Survey calculations were performed of the critical volume and neutron lifetime of some candidates for pulsed reactor fuel materials. The results are tabulated in Table 2. The calculations were

Table 2

SURVEY CALCULATIONS FOR REFERENCE DESIGN

Fuel	Critical volume, liters	Neutron lifetime, nsec
40 vol.% PuO_2—Mo cermet	94	61
60 vol.% PuO_2—Mo cermet	38	41
60 vol.% ^{235}U—Mo cermet	135	70
$^{235}UO_2$ ceramic	37	
30 vol.% ^{235}U—Th dispersion	175	83
50 vol.% ^{235}U—Th dispersion	50	56

    Note: 1. Coolant volume fraction, 26% (sodium).
           2. Cladding and structure volume fraction, 30%.
           3. Core lined with 2 cm of $B_4^{10}C$ between core and reflector.
           4. Core reflected with 28 cm of stainless steel (75%) and
              sodium (25%).

done for cores lined with a 2-cm-thick absorbing layer made up of $B_4^{10}C$ and tantalum. The effect of this liner, in general, is to reduce the neutron lifetime by a factor of 2 and to increase the core volume by a factor of 1.5, in comparison with an unlined core with the same composition. The survey calculations of critical volume were done in

cylindrical geometries (height-to-diameter ratio = 1) by the S_4 method. The volumes were checked, and the lifetimes were calculated in spherical geometry with AIM-6; the agreement between the critical volumes calculated by the two techniques was excellent. In both cases the Hansen and Roach group constants were used.

After the 60 vol.% PuO_2–Mo cermet was selected for the reference design and the reference core geometry and compositions were established, detailed calculations of the critical volume, neutron lifetime, and parabolic reactivity coefficient α were performed with the Monte Carlo code 05R ALFA. The geometry and materials of the various core regions used in those calculations are indicated in Fig. 8. The
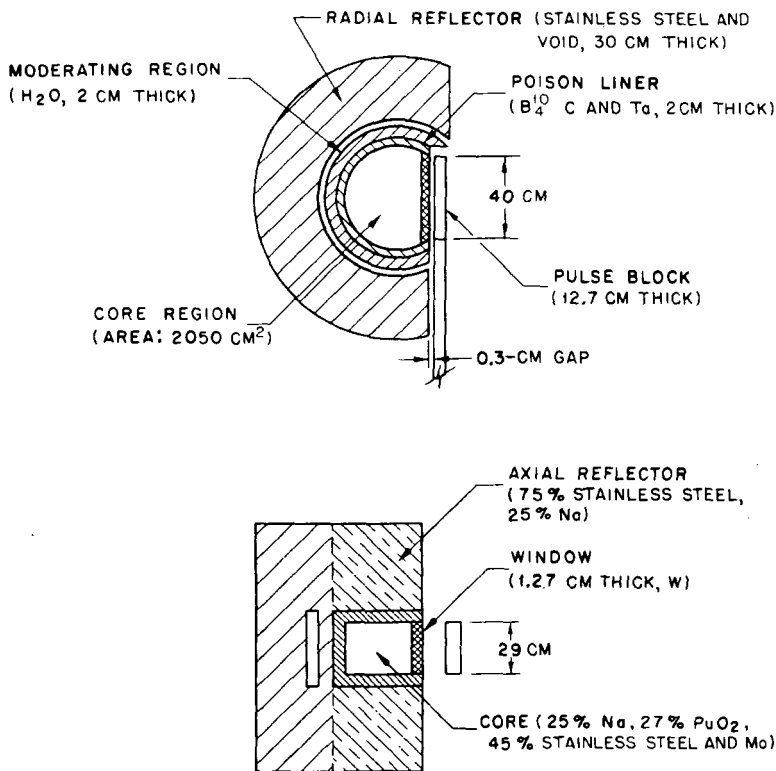

Fig. 8 — Core geometry and composition for reference-design physics analysis.

accuracy of this code was tested by applying the code to calculations of the CEPFR-1 core parameters, and the agreement between calculated values and experimentally determined values of all parameters, with the exception of the neutron lifetime, was very good. In the neu-

tron lifetime large discrepancies existed between calculated and mea-
sured values for cores with no poison liners. However, for cores with
a poison liner on all surfaces except the pulse block face, the agree-
ment was good. Therefore the calculational techniques applied to the
reference core, which is lined with poison material, are concluded
to be valid.

The reactivity change associated with a moving reflector block was
calculated for rectangular cores similar to the CEPFR-1B critical
assembly. The calculations were done using the S_N method ($N = 4$, 6,
8, and 8T) in x—y geometry for cores with various arrangements of
poison liners and cavities. The S_{8T} uses a new weighting function that
was constructed to accurately describe the anisotropic flux with a
small number of angular segments. The values for Δk corresponding
to movement of the reflector block from a position centered on the
bare core face to a position displaced by 1.27 cm from the center are
summarized in Fig. 9 for various arrangements of poison liners. From
this analysis it was concluded that an absorbing liner on a portion of
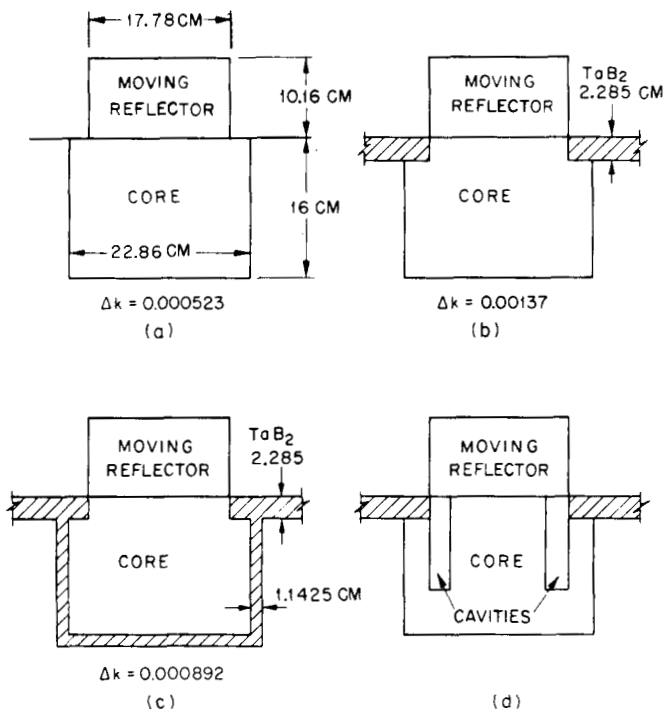

Fig. 9—Promising methods of increasing the Δk corresponding to small move-
ments of the pulse block. The values of Δk are those calculated for a 1.27-cm
displacement of the pulse block from the indicated position.

the bare core face increases the reactivity change associated with movement of the reflector block. The effect of the absorbing liner between the core and the stationary reflector on the Δk is small, although poison material in this location is quite effective in reducing the neutron lifetime. Cores with cavities, as shown in Fig. 9, were also studied; however, the convergence of the calculated reactivities was not satisfactory, and no conclusions could be reached concerning the effectiveness of core cavities in enhancing the reactivity change.

FUEL TEST AND DEVELOPMENT

Selection of Candidate Fuel Materials

Battelle Memorial Institute (BMI) made a detailed survey of fuel materials for application to the pulsed reactor and the accelerator pulsed reactor. All available data on alloy, cermet, and dispersion fuels that met the initial screening criteria were compiled.[4] The initial screening criteria required that the fuel must:

1. Contain a minimum of 3.5 g/cm^3 of fissile material.
2. Be capable of about 2 at.% burnup.
3. Contain minimum amounts of elements with low atomic numbers to provide for a minimum neutron lifetime.
4. Be capable of being clad for operation in liquid-sodium coolant.
5. Be suitable for operation at surface temperatures between 200°C and 400°C and at power densities of 2 to 4 Mw/liter.

The fuels that satisfied these criteria are listed in Table 3. The fuels that were selected for the pulsed reactor and the accelerator pulsed reactor are indicated in the appropriate column of the table. The selection of fuels for the two concepts is based on the results of preliminary studies which indicated that the fuel with a high fissile content was needed for the accelerator-injected concept and more dilute fuels could reasonably be used for the pulsed reactor. In some cases the core volume using a dilute ^{235}U-bearing fuel is quite large, and the material is of more interest if it contains the isotope ^{233}U. These cases are indicated by the asterisk.

A three-phase fuel test and development program was envisaged to determine the capability of the candidate fuels. The outline of the program is:

Phase I: Development of fabrication techniques and determination of mechanical properties, including fatigue behavior, of the materials in the unirradiated condition.

Phase II: Steady-state irradiation of materials and postirradiation testing to determine the effect of irradiation.

Table 3

SUMMARY OF FUEL SURVEY

Fuel	Uranium or plutonium loading, g/cm^3	Application		Comments
		Pulsed reactor	Accelerator pulsed reactor	
Alloys				
U−40 wt.% Al	3.5			Too dilute
U−10 wt.% Mo	15		X	
U−10 wt.% Nb	15			Inferior to U−10 wt.% Mo
U−40 wt.% Zr	6	X*		
U−20 wt.% Nb−27 wt.% Zr	5.7	X*		
Ceramics				
UO$_2$	9.2	X		
UC		X		
PuO$_2$	9.6		X	
PuC			X	
Cermets and dispersions				
60 vol.% PuO$_2$−Mo	5.8	X		
60 vol.% UO$_2$−Mo	5.5	X*		
60 vol.% Pu or UO$_2$−stainless steel				Stainless steel matrix inferior to Mo
Liquid				
PuO$_2$ (or UO$_2$)−Na paste		X		
Pu−Fe−Ce		X		

* Of interest primarily with [233]U isotope.

Phase III: Proof tests that simulate, as closely as possible, operation in a high-performance pulsed reactor. No single test can produce all the effects of reactor operation; so a series of tests will be required, each of which will simulate one or more of the critical aspects of pulsed reactor exposure.

The materials indicated in Table 3 cover a wide range with regard to their states of development. Also, the properties determined for some of these materials in the unirradiated condition will be meaningless. The ceramic and liquid fuels are examples. The U−Zr alloy falls into this category because it is not a gamma-phase stable material and because the effect of irradiation on the properties of this material is expected to be significant. The U−10 wt.% Mo alloy also fits into this category; however, in the interest of obtaining some data on which to base a reference design of the accelerator pulsed reactor, Phase I testing of this alloy is planned.

Development work has been done on a UO_2–Mo cermet, the U–Nb–Zr ternary alloy, and the U–Th dispersion. Of these, the cermet material is in the most advanced state of development, and specimens of this material have been subjected to high-cycle-fatigue tests. The results of the work thus far are described in the following sections for each of these three fuel systems. Because the high cycle fatigue properties of the UO_2–Mo cermet have been determined to a sufficient degree to provide a basis for reactor design and because the effect of irradiation is not expected to be as severe in the cermet as in the other fuels, the cermet was selected for the pulsed reactor reference design.

Development of U–Nb–Zr Ternary Alloys

Interest in this ternary-alloy system is based on constitution work done by Russian investigators[5] which shows that there is a stable gamma–uranium-phase field extending from the niobium corner to uranium contents as high as 58 wt.%. Existence of the stable gamma phase promises good resistance to the effects of irradiation and cyclic stressing for this alloy. No data were available for these alloys, and no fabrication experience was reported.

Several specific alloys of the ternary system were fabricated by BMI. Polished sections of the first castings indicated the presence of center line "pipe" that was very fine and could not be detected in radiographs or in unpolished sections of the castings. Subsequent castings were performed using an Al_2O_3 collar in the top section of the mold in an attempt to slow down the rate of heat loss from the melt and thus provide for better feeding of molten metal into the solidifying region.

A casting of U–31 wt.% Nb–12 wt.% Zr was heated in vacuum for 4 hr at 1000°C and for 2 days at 1250°C. Metallographic examination indicated that homogenization was obtained and that the alloy was indeed single phase. However, a large grain size was exhibited, and a less severe homogenization treatment was attempted. Homogenization at 1250°C for 12 hr in vacuum proved to be adequate to obtain a homogeneous fine-grained single-phase material. Fabrication of this material by hot rolling at 1000°C and at 1250°C resulted in cracking. Similar unsuccessful results were obtained for castings with the composition U–62 wt.% Nb–7 wt.% Zr. In addition, contrary to predictions based on the available phase diagram, a small amount of a second phase was distributed uniformly throughout the grain boundaries of this alloy. The second-phase contamination may have been the result of a deviation from the desired composition, an impurity phase, or a phase stabilized by minor impurities.

A third ternary composition, U–20 wt.% Nb–27 wt.% Zr, was
selected in an attempt to produce a fabricable material and to gain the
advantage of a wrought structure not obtainable in the other two U–
Nb–Zr alloys. Two castings of this alloy were prepared by arc melt-
ing and were cast into graphite molds. The resulting structure was
single phase and homogeneous after 12 hr at 1250°C in vacuum. How-
ever, large grain sizes were obtained. Before improving the grain
size, fabrication by hot rolling at 1315°C was attempted. Both castings
were successfully rolled to a diameter slightly over 0.25 in. The alloy
oxidized heavily, and, if the temperature of the specimen was allowed
to drop much below 1315°C, it became very difficult to work. Seven
additional arc castings were made in tapered molds and were homog-
enized for 4 hr at 1250°C. For fabricating the castings, right-circular
cylinders were first machined from the castings. Two cylinders were
coated with MgO by exposure to burning magnesium ribbon and were
placed in molybdenum cans. The canned specimens were hot rolled
at 1315°C. Two passes were made through the rolling mill, and di-
ameter reductions of 12.3 and 15.2% were achieved.

Tensile tests were performed on specimens of the three ternary
compositions that were studied, and the results of these tests are
presented in Table 4.

Table 4

TENSILE PROPERTIES OF U–Nb–Zr TERNARY ALLOYS AT 800°F

Alloy	Modulus, 10^6 psi	Ultimate strength, psi	0.2% offset yield strength, psi	Area reduction, %
U–27 wt.% Zr–20 wt.% Nb	12.5	91,200	75,700	32.5
U–31 wt.% Nb–12 wt.% Zr*	12.0	36,000		0
U–62 wt.% Nb–7 wt.% Zr*	17.0	36,000		0

*As-cast.

Development of U–Th Dispersions

Uranium–thorium dispersions are of interest because of the higher
fissile-atom concentrations that are obtainable in comparison with a
cermet containing the same volumetric fraction of UO_2. The uranium
is present in the dispersion in the alpha phase. However, if it is con-
tained in small microspheres by a continuous thorium matrix, the ir-
radiation behavior may be satisfactory. Development of this material
was pursued at BMI to develop fabrication techniques and to determine
the limit on uranium content.

The first attempts to produce a Th–30 vol.% U dispersion were
made at 1000°C, as appeared to be necessary from the literature on

powdered thorium. Subsequent attempts at temperatures as low as 800°C resulted in essentially fully dense specimens. The effects of sintering pressure and temperature were investigated for a Th–40 vol.% U dispersion. The pressure ranged from 5000 to 17,000 psi, and the temperature ranged from 750 to 1000°C. For temperatures above 750°C the microspheres showed excessive deformation. At 750°C the highest pressures produced negligible deformation. The density of the specimen was influenced more by pressure than by temperature; so densities greater than 90% of theoretical could be achieved even at 750°C by using pressures of 15,000 to 17,000 psi. An attempt was made to fabricate tensile specimens by blending and cold pressing the 40 vol.% dispersion into pellets $\frac{1}{2}$ in. in diameter by $\frac{1}{2}$ in. long. Eight pellets were loaded into each of five tantalum tubes, which were then evacuated and sealed by electron-beam welding. The five specimens were hot isostatically pressed at 750°C and 17,500 psi for 3 hr. All these specimens broke during machining along one of the bond lines between specimens.

Development and Test of Cermet Fuels

Two matrix materials were considered for cermet fuels; stainless steel and molybdenum. The stainless steel matrix was of interest because it was the more highly developed of the two. However, the low thermal conductivity and high coefficient of expansion of the stainless steel cermet were disadvantages in comparison with the molybdenum cermet. On the basis of these properties, the molybdenum cermet was selected over the stainless steel cermet. It has been assumed that the nature of the ceramic material used in the cermet, i.e., UO_2, UC, PuO_2, or PuC, has little effect on the mechanical properties of unirradiated specimens.

General Electric Co., Nuclear Materials and Propulsion Operation (GE-NMPO), fabricated UO_2–Mo cermet specimens of 40, 60, and 80 vol.% UO_2 and measured the tensile strength, thermal expansion, thermal conductivity, and sonic velocity of specimens of these materials. The results of this work are described in Ref. 6, and the mechanical test data are summarized in Table 5. The specimens were machined from cylindrical slugs of depleted UO_2 dispersed in a molybdenum matrix and in some cases were clad with pure molybdenum. The ceramic particle sizes used in the various specimens were 40, 150, and 400 μ.

Additional specimens were fabricated for fatigue testing. Fatigue tests were performed on the 60 vol.% UO_2–Mo cermet with a 150-μ ceramic particle size at two frequencies, 186 and 14,000 cycles/sec. The low-frequency tests were conducted by BMI using a machine owned by Brookhaven National Laboratory. The inert-gas system used

Table 5

TENSILE-TEST RESULTS FOR Mo$-$UO$_2$ CERMET SPECIMENS IN HELIUM

Specimen No.	Fuel loading, vol.%	Fuel particle size, μ	Room-temperature static modulus, 10^{-6} psi	Test temperature, °F	Static modulus at temperature, 10^{-6} psi	Yield stress,* 10^{-3} psi		Ultimate stress,† 10^{-3} psi	Elongation,† %
						0.02%	0.2%		
C-1-a1	80	150	14.2	800		3.6		4.6	0.1
C-1-a2	80	150		800		4.4		4.6	0.3
C-1-a3	80	150		800	9.8	3.9		4.4	0.2
A-1-a4	60	150	12.1	1500		6.6		7.2	1.1
A-1-a5	60	150		1500				6.9	0.6
A-1-a6	60	150		1500	19.7			12.9	0.1
A-1-a1	60	150	17.4	800	14.17	8.3		10.3	0.6
A-1-a2	60	150		800	10.6			12.6	0.3‡
A-1-a3	60	150	6.5	800		5.3	7.8	7.9	0.6
A-2-a1	60	40	20.5	800				13.5	0.3
A-2-a2	60	40		800				10.2	0.4
A-2-a3	60	40		800				13.7	0.2
A-1-a7-G§	60	150	14.3	800				10.5	0.2
A-1-a8-G§	60	150		800	10.4			10.4	0.1
A-1-a9-G§	60	150		800	11.5			11.5	0.4

A-1-b1¶	60	150	15.4	800		8.5	11.5	13.3	1.1
A-1-b2¶	60	150		800				16.6	1.1
A-1-b3¶	60	150		800	20.2	8.9	11.1	13.6	1.7
A-1-c1**,††	60	150		800		9.2		11.2	0.5
A-1-c2**	60	150	18.2	800	7.5	8.2		10.9	0.5
B-1-a1	40	150	15.4	800		8.1	11.5	15.1	2.9
B-1-a2	40	150		800		12.6	15.0	17.1	2.4
B-1-a3	40	150		800	10.4	9.2	11.6	14.3	1.2
A-3-b1	40	400	14.0	800		7.9	10.6	12.4	1.9
A-3-b2	40	400		800		9.5	11.5	14.9	3.0
A-3-b3	40	400		800		8.8	11.2	13.7	1.2
D-1	0		48.5	800		7.1	10.1	37.8	52§
D-2	0			800		7.3	9.8	37.7	53§
D-3	0			800		7.7	9.9	36.8	51§

*0.005 min^{-1} strain rate.

†1.0-in. gauge length × 0.25-in. diameter.

‡Based on overall length of specimen.

§G = General Electric molybdenum; all other specimens are Sylvania molybdenum.

¶Vapor coated with 0.005-in. molybdenum.

**Clad with molybdenum by autoclaving and machined to 0.003-in. thickness.

††Cladding removed from half of gauge length in machining (because of nonconcentricity).

for the elevated-temperature tests did not provide adequate gas purity, and severe oxidation of the specimens occurred during the tests. As a result, further tests at the low frequency were performed at room temperature. The high-frequency tests were conducted with ultrasonic equipment at Hydronautics, Inc. This testing was performed in a high-purity inert-gas environment at 750°F. All fatigue testing of the cermet was done at a mean stress of 4500 psi. Strain gauges were attached to all specimens to monitor test conditions. Before the start of each fatigue test, the modulus of the material was measured. This measured value was used to calculate the cyclic stress from the cyclic strain that was monitored on the specimen during the test. The test results are plotted in Fig. 10. The predicted fatigue curves are
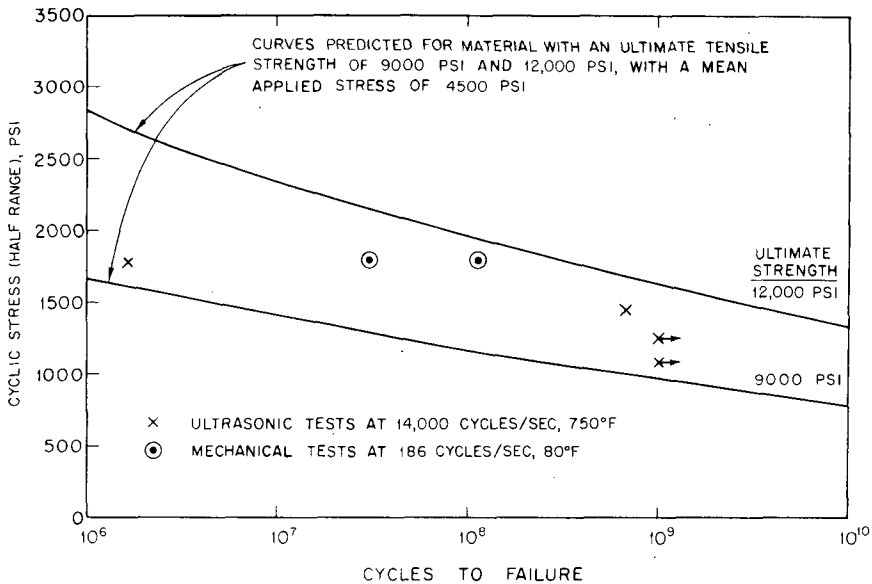

Fig. 10—High cycle fatigue life of 60 vol.% UO_2–Mo cermet. All specimens were tested with a mean applied stress of 4500 psi.

also plotted in Fig. 10 for two assumed values of the ultimate tensile strength that bracketed the range of tensile strengths measured by GE-NMPO for this material. The Goodman criteria were used for the predicted curves, and all the data are consistent with the predicted behavior. This agreement provides the basis for the cermet fuel fatigue properties used in the reference design of the pulsed reactor.

CRITICAL EXPERIMENTS

General Description

A fast reactor critical assembly designated CEPFR-1 was constructed in support of the pulsed reactor reference design work. This assembly, consisting of a core of uranium, stainless steel, and aluminum, reflected by stainless steel, was used for measurements to test the reliability of theoretical predictions of the reactor parameters. Experiments to provide basic data were done on assemblies that were geometrically simple.

The basic component of the assembly was a split-bed machine that allowed separation of the core into two nominally equal sections. The table surfaces of the machine were two polished granite slabs 3 by 6 by 1 ft, giving a working surface of 6 by 6 ft when the halves were together. The core and reflector were constructed of elements whose dimensions were 1.5 by 1.5 in. in cross section and 39 in. in length. Core elements were made of 1.5-in.-square, 0.035-in. wall, stainless steel tubing with 12 in. of solid stainless steel in the bottom end, a $14\frac{3}{4}$-in. fuel section, and $12\frac{1}{4}$ in. of stainless steel in the upper section. The fuel section contained uranium, aluminum, and stainless

Table 6

COMPOSITION OF CEPFR-1A CORE

Element	Core atomic density, 10^{-24} atoms/cm^2	Reflector atomic density, 10^{-24} atoms/cm^2
^{235}U	0.01160	
^{238}U	0.0008406	
Iron	0.02337	0.05967
Aluminum	0.008555	
Chromium	0.006452	0.01693
Nickel	0.002843	0.007502
Copper	0.0001544	0.0001117
Manganese	0.0005231	0.001293
Magnesium	0.00005043	
Carbon	0.0000916	0.0002365

Note: Core volume = 20.825 liters, and excess reactivity = 92¢.

steel pins to achieve the desired core-region atom densities. The fuel was in the form of 0.170-in.-diameter pins. The fuel material was highly (93.2%) enriched-uranium metal, with a thin (about 0.0001 in.) fluorocarbon coating. The composition of the assembly CEPFR-1A, which is typical of the assemblies reported here, is shown in Table 6.

Standard reflector elements were 1.5-in.-square by 39-in.-long stainless steel bars. Some cans, identical to those used for loading core elements, were loaded with boron carbide with a filler bar of stainless steel 0.5 in. thick. The cans were always loaded into the assembly so that the steel bar was next to the core. Other cans were loaded with boron carbide and a 0.25-in.-thick strip of tantalum metal. These cans were loaded into the assembly so that the tantalum bar was next to the core.

The four control-rod blades were loaded with an appropriate number of fuel, stainless steel, and aluminum pins to maintain the overall core volume fractions. The rod motion was horizontal and normal to the direction of the table motion; the length of the fuel loading along the direction of travel corresponded to the width of any given core.

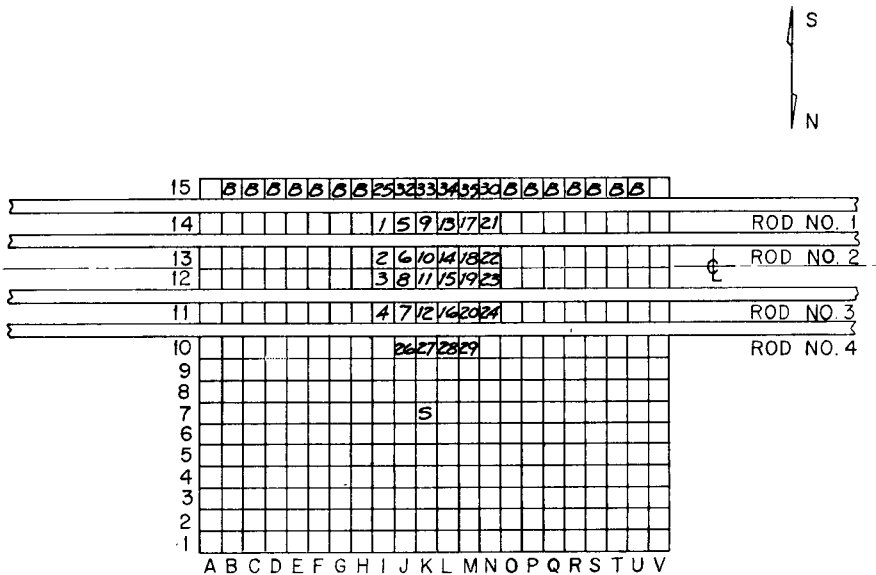Figure 11 shows a typical plan of an assembly, in this case CEPFR-1C.

Fig. 11 — Plan view of a typical CEPFR-1C assembly. Each cell unit = 1.5 by 1.5 in. Control-rod width (including sheath) = 0.875 in. Numbered cells contain fuel. S = Source location. B = B₄C-loaded elements. □ = Reflector elements.

Some of the more important measurements performed in the CEPFR-1 series are outlined below. The measurements made on a given assembly are summarized in later sections.

1. Safety Measurements. On each assembly a number of experiments were carried out to determine the operating characteristics and

to measure quantitative values of parameters affecting safety. Included in these were control-rod worths, rate of reactivity addition by various modes, worths of hydrogenous reflector in and about the assembly, the effect of increasing the steel-reflector thickness, some cursory power measurements, and health physics radiation surveys.

2. Fixed-Reflector Worth Effects. In addition to the investigation of the worth of hydrogenous material in and about the core, measurements were made of the effective worth of small blocks of various materials placed in the reflector near the core. These were made to get an idea of the comparative magnitude of metal and hydrogenous material reflectivity. In addition, the worth of a stainless steel reflector bar was measured as a function of location near the core boundary.

3. Moving-Reflector Worth Effects. The reactivity worths of reflector blocks near an open core face were measured as a function of the position, block geometry, and block material. The size of the open core face varied, and in some cases a barrier of boron carbide or boron carbide and tantalum was placed between the reflector block and the reflector steel extending beyond the open core face. The effect of such barriers on the parabolic coefficient of the reactivity curve was studied. In addition, the effect on the parabolic coefficient, α, of core cavities or core reentrant holes was studied for a number of assemblies. (The coefficient α is defined from the parabolic form of the reactivity vs. position curve in the vicinity of the maximum: $\rho(x) = \rho_{max} - \alpha x^2$.)

4. Neutron-Lifetime Measurements. The neutron lifetimes for selected assemblies and conditions were measured by the Rossi-alpha technique. For most measurements a fission chamber was located at or near the core—reflector interface. A number of different kinds of fission chambers, as well as He^3 detectors, were used in an effort to improve the measurement of neutron lifetime. Measurements using a specific fission detector located in a region as similar as possible from core to core were used as a standard.

CEPFR-1A Experiments

CEPFR-1A was an assembly reflected by about 12 in. of steel on all sides. The nominal core size was 9 by 9.5 by 14.77 in.

The worth of small blocks of various materials in the reflector next to the core was measured. A reflector element was removed, and a drive device was made so that a small block of material could be placed at the core midplane and then removed by remote control. The blocks used in this experiment were all $1\frac{3}{8}$ by $1\frac{3}{8}$ by $3\frac{1}{2}$ in. After achieving criticality and a suitable power, the sample was drawn upward until it was completely out of the reflector, the reactivity seen

on the analog meter being plotted against the sample position through-
out. Typical curves are shown in Fig. 12. It should be noted that
hydrogenous materials caused a maximum in the reactivity curve.
"In" to "out" reactivity worths of various materials are:

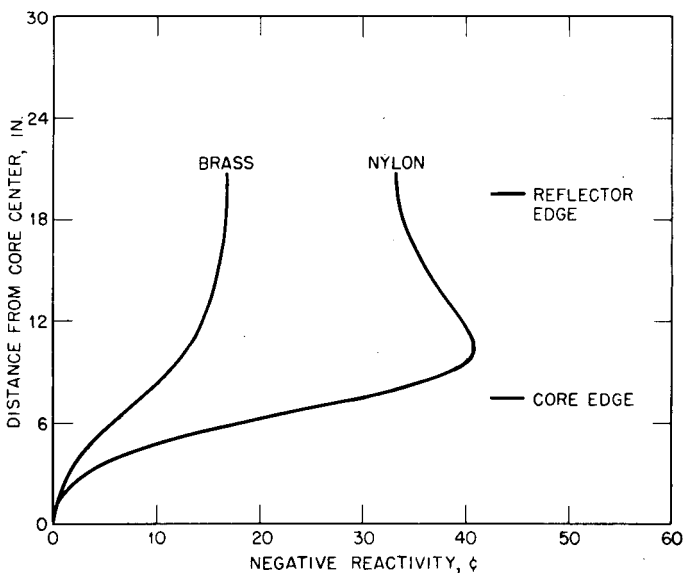| Sample material	Worth, ¢
Cadmium	−7.8
Palladium	−12.0
Aluminum	−12.8
Brass	−17.0
Copper	−18.4
Carbon (graphite)	−20.9
Nylon	−33.5
Lucite	−37.0

Fig. 12 — *Worth of small blocks in the CEPFR-1A reflector.*

The worth of an entire steel reflector element at several different
positions was determined by measuring the change in reactivity when
the element was removed. These worths averaged around 50¢ for re-
flector elements next to the core.

The neutron lifetime for CEPFR-1A was measured with a standard
fission-counter detector located in the steel reflector near the re-
flector—core boundary. Several measurements were taken, and the
weighted mean of these measurements gave a lifetime of 200 nsec,
calculated with the assumption that β_{eff} was 0.007.

CEPFR-1B Experiments

The CEPFR-1B assembly had one core face exposed, and the core volume was increased to compensate for the lost reflector worth.

The measurements made on the CEPFR-1B cores consisted of a survey of the effect of various reflector blocks placed in front of the open core face. Block materials and geometries were changed, and for each case a study of block position vs. reactivity was made, as well as a measurement of neutron lifetime when the block was exactly in front of the open core face.

The reactivity was determined as a function of reflector-block position by moving the particular block away from its maximum reactivity position when the assembly was just critical. In nearly all cases the block was moved in a plane parallel to the plane of the open core face; in one case it was moved perpendicularly away from the open core face. The assembly reactivity was obtained from an analog computer programmed to solve the kinetic equations using an input signal from an ion chamber at the assembly.

Results of the measurements are summarized in Table 7.

Table 7

MEASUREMENTS ON CEPFR-1B

Block material	Block* size	Excess k,† $	Block worth, $	α, ¢/cm^2	l, (nsec)
Stainless steel	A	1.75	5.75	1.91	137
Stainless steel	B	0.30	4.20	1.35	135
Polymethyl methacrylate	A	2.85	7.10	3.15	159
Beryllium	A	5.70	10.40	3.36	191
Nickel	A	2.35	6.50	1.91	134
Nickel	B	0.75	5.00	1.50	132
Stainless steel	C	<0.10	1.70	0.57	130
None		0.25			136
Carbon steel	A	<0.05	4.45	1.20	135

*A = 14.8 by 9 by 4 in.
 B = 14.8 by 9 by 2 in.
 C = 14.8 by 3 by 4 in.
 †With the block in its most reactive position and k effective = 1 for the core specified, i.e., at the start of the sliding-block measurement.

CEPFR-1C Experiments

Figure 11 shows a plan of a typical CEPFR-1C assembly. The experiments on CEPFR-1C involved reflector-block measurements for various sizes and materials of blocks which covered a variable-width open core face. The total reactivity worths of the different blocks varied by a number of dollars. In addition, the width of the open core

face was changed by replacing outer-row fuel and reflector elements with poison elements.

Some conclusions regarding the CEPFR-1C experiments may be summarized as follows:

1. For the steel reflector block, and with poison elements used to define the core window, the use of B_4C alone in the amounts tested in the CEPFR-1C assemblies appears to do little for α. There is some improvement of α with the addition of tantalum to the B_4C. Poison barriers appear to be effective in increasing the value of α for steel reflector blocks when sufficient poison is inserted.

2. With the beryllium reflector block, the use of B_4C + Ta poison to define the window substantially enhances α. This is probably a result of the slowing-down properties of beryllium, which give the barrier a higher effective absorption.

3. Of all the reflector materials tested, the beryllium block is superior in terms of α and in terms of total reactivity swing. The lifetime is affected adversely, increasing from about 140 nsec with steel reflectors to about 190 nsec with beryllium reflectors.

4. Tungsten is a good window material when used in combination with a steel reflector block. The α with a tungsten window was measured to be greater than the α with no window (air) although the difference was not large.

5. There appears to be little advantage obtained in either the α values or total reactivity effect by reducing the reflector-block width or the open-face width.

CEPFR-1D Experiments

The CEPFR-1D cores were built to investigate the effect of core cavities (reentrant holes) on the reflector-block reactivity and on α. The cores were widened from a standard 9 in. in earlier assemblies to 12 in. to achieve the core cavities. This change required different control-rod loadings since the rods move in the direction which defines core width and must be loaded to that width for clean geometry. Rods 1 and 2, which ran in the region in which there were cavities, were loaded with voids in an appropriate location to align with the cavities. The core elements remained unchanged, except that the cavities were made by insertion of fuel elements in which the fuel region was not loaded. Thus the cavities included the 0.035-in. walls of the cans.

Some conclusions regarding the CEPFR-1D experiments may be summarized as follows:

1. The average values of α were in all cases reduced by the presence of the cavities, and the total block worths were less for the same size of sliding block.

2. The cavities caused the reactivity vs. position curves to depart from a parabolic shape by about 30% in the direction of sharpening the peak of the curve.

3. Windows of either lead or tungsten were found to have little effect on α over that which was observed for a similar size air gap. The overall reactivity swing was reduced by about 10% by either a $\frac{1}{2}$-in. window of lead or tungsten over that measured for a similar air gap. Another effect of the presence of a window or gap was the diminishing of the nonparabolic behavior of the sliding-block reactivity curve discussed in (2). With no gaps or windows, the nonparabolic effect was about 30%; with gaps or windows $\frac{1}{2}$ in. thick, the nonparabolic effect was reduced to the order of 6% for the window and 18% for the air gap; with 1-in.-thick gaps or windows, the effect was no longer appreciable.

4. Shortening the cavities 1.5 in. (from 7.5 in.) by the addition of one fuel element in each increased α, the total reactivity swing, and the nonparabolic effect by 10, 6, and 4%, respectively.

5. Increasing the amount of tantalum to three times its normal amount in two elements adjacent to each side of the 9-in. core opening had no appreciable effect on α or the total block worth, contrary to the observations on CEPFR-1C. This apparent contradiction may be due to the difference in core configuration (the CEPFR-1C had a solid core whereas the CEPFR-1D had two cavities in the core) or to having *exceeded the optimum tantalum loading in the above elements.*

BEAM-SOURCE STUDIES

Experiments are in progress to study the characteristics of hydrogenous moderating blocks in pulsed reactors. The purpose of these studies is to provide a basis for the design of moderating blocks that will give the maximum yield of thermal neutrons with a pulse width commensurate with the natural pulse width of the reactor.

Preliminary steady-state, pulse-shape, and spectrum measurements have been made to study the characteristics of various thicknesses and geometries of polymethyl methacrylate (Lucite) and polyethylene at room temperature and liquid-nitrogen temperature in both the pulsed and steady-state modes. A detailed analysis has been done at room temperature on 24- by 24-in. stacks of various thicknesses. The data were used to synthesize the relative merit of various thicknesses of Lucite and polyethylene as moderating blocks for a fast pulsed reactor.

Steady-State Measurements

These measurements were conducted using neutrons from a ^{235}U fission plate. The spectrum is assumed to be comparable to the leakage spectrum from a fast reactor, although probably somewhat harder. The study has concentrated on hydrogenous moderators since hydrogen is the only element that can moderate the fast neutrons in the time required.

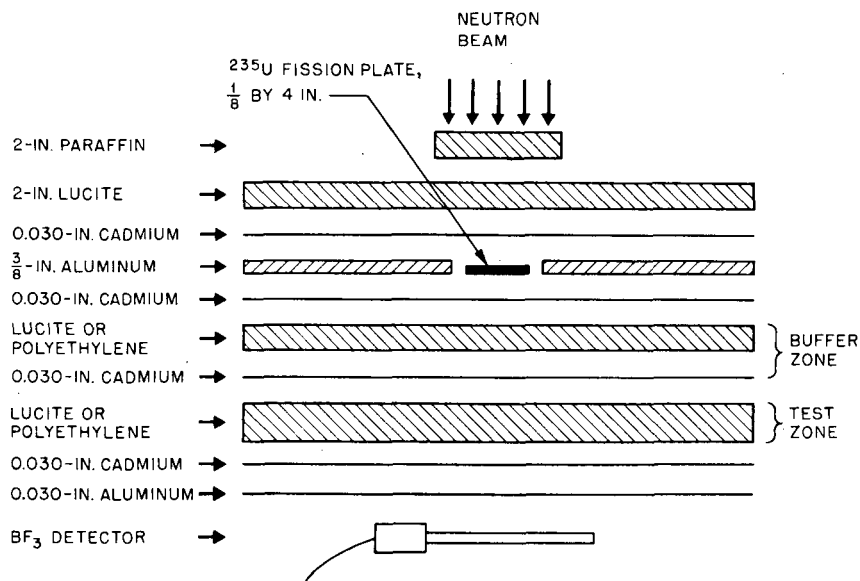The experimental arrangement is shown in Fig. 13. The Brookhaven Medical Research Reactor was operated at 100 watts nuclear

Fig. 13 — Beam-source test assembly.

power for all runs. The beam from the patient-facility beam port was thermalized by 2 in. of paraffin and 2 in. of Lucite before it impinged on the ^{235}U fission plate. The test assembly immediately behind the fission plate moderated the fission neutrons. The resultant neutrons were counted by a BF_3 detector, which is very nearly a $1/v$ detector, since the absorption probability for 2200 m/sec neutrons is only 0.04. Count rates were taken under four conditions for each assembly, i.e., with and without fission plate and with and without the cadmium plate immediately in front of the BF_3 detector. From these four count rates, it was possible to eliminate those neutrons originating in the reactor neutron beam and also to differentiate between thermal neutrons (sub-

cadmium) and epicadmium neutrons that had originated as fast neutrons in the fission plate.

In most cases the moderating blocks were 24 in. square with variable thickness. However, one rectangular prism, 3 by 3 by 24 in. was studied for comparison. Unless otherwise noted, the moderating blocks were 24 in. square.

The neutron-yield results for Lucite are shown in Fig. 14 and for both materials in Table 8. A buffer zone or region between the fission
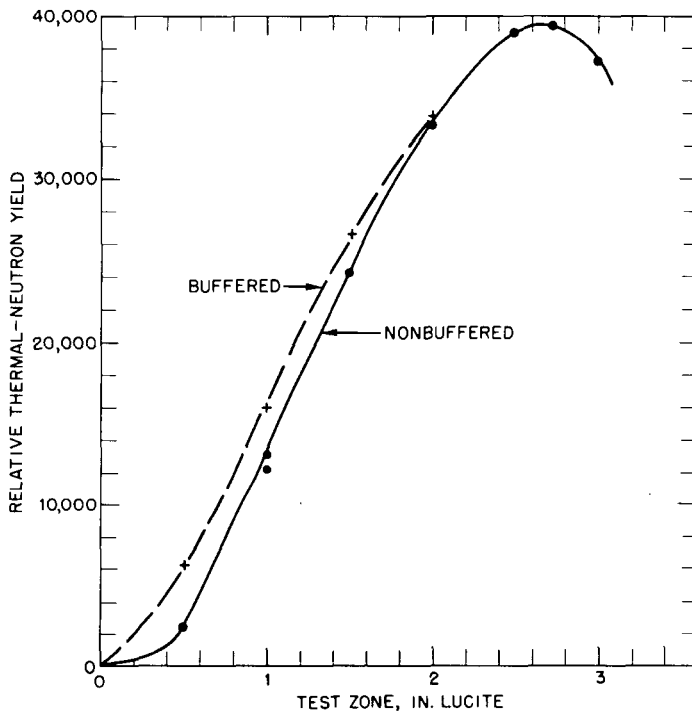

Fig. 14—Steady-state thermal-neutron yield for Lucite with a subcadmium steady-state fission source.

plate and the test zone composed of either Lucite or polyethylene and separated from the test region by 0.028 in. of cadmium was effective in increasing the thermal-neutron yield, presumably without affecting the neutron-pulse shape. The improvement in yield was observed to occur predominately in the small assemblies. No improvement is seen for the intermediate assemblies; in the larger assemblies the thermal-neutron yield decreases when a buffer zone is inserted.

Both Lucite and polyethylene were used to investigate differences that might result from molecular-binding effects and from hydrogen-

Table 8

SUMMARY OF BEAM-SOURCE EXPERIMENTS

Temperature, °K	Stack description	τ, μsec	$1/\beta$, m/sec	$\varphi\,(10^4)$, 10^{-7}	$\varphi\,(10^4)$, 10^{-7}	$\dfrac{\varphi\,(1/\beta)}{\varphi\,(10^4)}$	X	Steady state Thermal flux relative to peak Lucite thermal (φ_S^∞)	Steady state Epicadmium relative to peak Lucite thermal
300	1-in. Lucite 24 by 24 in.	34	2900	1.08	0.28	3.85	0.875	0.334	0.07
77	1-in. Lucite 24 by 24 in.	~90	1750	1.30	0.29	4.48	0.805		
300	2-in. Lucite 24 by 24 in.	75	2900	6.6	0.85	7.75	1.045	0.843	0.07
300	2-in. Lucite 24 by 24 in.	75	2900	3.3	0.38	8.66	0.987	0.843	0.07
77	2-in. Lucite 24 by 24 in.	~165	1750	0.65	0.1	6.5	0.958		
77	2-in. Lucite 24 by 24 in.	~120	1800	1.9	0.3	6.35	1.00		
300	3-in. Lucite 24 by 24 in.	130.5	2900	4.4	0.36	12.20	1.13	0.95	0.0405
77	3-in. Lucite 24 by 24 in.	~182	1700	2.0	0.2	10.0	0.904		
300	4-in. Lucite 24 by 24 in.	172	3000	4.6	0.25	18.4	0.848		
300	1-in. polyethylene 24 by 24 in.	39 (43)	3100	2.1	0.36	5.83	0.857	0.59	0.0785
300	2-in. polyethylene 24 by 24 in.	89	2900	4.4	0.32	13.75	1.065	1.08	0.0607
300	3-in. polyethylene 24 by 24 in.	136	3000	4.2	0.27	15.5	1.131	0.835	0.033
300	1-in. Lucite cadmium + 1-in. Lucite buffer	35	3000	1.65	0.34	4.85	0.835	0.405	0.07
300	1½-in. Lucite cadmium + ½-in. Lucite buffer	51	2950	3.1	0.38	8.15	0.759	0.67	0.07
300	3- by 3- by 24-in. Lucite†	80	2700	0.6	0.075	8	0.755	0.347*	0.0325

*Run normalized to give relative yield without the bottom aluminum buffer.
†With $3\frac{1}{4}$-in. aluminum side reflector $+\,3\frac{1}{4}$-in.-thick aluminum buffer separated by cadmium.

atom densities. When the thermal-neutron yields from Lucite and polyethylene are compared on an equal hydrogen-atom basis, little difference exists except for the amount of hydrogen present in thicknesses greater than about 1.5 in. of either moderator. At greater thicknesses the Lucite moderating block gives a slightly lower yield than does polyethylene. This difference may be due to geometric effects since Lucite has a lower hydrogen-atom density and hence the BF_3 detector is slightly farther away from the source.

Pulsed Experiments

The pulsed experiments were carried out using a Kaman model 810 source to supply 14-Mev neutron pulses having a width of 3 μsec at the rate of 10 pulses/sec to the stacks. The source was located below the stacks, and the neutron detector was located above the stacks. The cold stacks were contained in an aluminum box covered on the bottom and sides with cadmium and insulated from its surroundings on all sides by 3 in. of expanded polystyrene. Liquid nitrogen was poured into the aluminum box, in intimate contact with the moderator, to reduce the temperature of the box to approximately 77°K.

Pulse-shape and spectrum measurements were carried out for both room-temperature and cold stacks. The pulse shapes emitted from the surface of the room-temperature moderator blocks were determined by following the neutron intensity leaking from the top 24- by 24-in. face with a $B^{10}F_3$ counter as a function of time, after initiating the 3-μsec pulse of neutrons at the bottom 24- by 24-in. face. The time behavior of the neutron leakage was followed with a TMC 256-channel analyzer using the time-of-flight logic unit. In most cases the channel width of the analyzer was set at 4 μsec. The pulse-shape measurements were carried out with the $B^{10}F_3$ counter both directly on the moderator surface and with it separated from the surface by 0.028 in. of cadmium so that both the thermal and epithermal behavior could be determined.

Similar measurements were carried out for the cold studies except that the detector was separated from the stack by the expanded polystyrene insulation. For interpreting these runs, measurements were performed of pulse shape for various thicknesses of insulation between the stack and the detector.

The spectra of the neutrons leaking from the room temperature and cold stacks were determined by carrying out time-of-flight measurements with the $B^{10}F_3$ detector mounted from 1 to 3 m above the upper surface of the stack and the time analyzer set to a 32-μsec channel width.

The data taken in both the pulse-shape and spectra measurements were corrected for background, dead time, and counter sensitivity.

The data were analyzed assuming the neutron-velocity spectrum could be described by the sum of a Maxwellian and a v^{-x} tail

$$\varphi(v) \ dv = A(\beta v)^2 \ e^{-(\beta v)^2} \ dv + B \left(\frac{v}{v_0}\right)^{-x} \ dv \qquad (1)$$

The spectra are characterized in Table 8 by the parameters $\varphi(1/\beta)$, $\varphi(10^4)$, $\varphi(1/\beta)/\varphi(10^4)$, and x. The peak flux in the Maxwellian component of the neutron spectra is $\varphi(1/\beta)$, and the flux at 10^4 cm/sec is $\varphi(10^4)$. The latter is an arbitrary velocity in the epithermal region where the velocity spectrum is nearly $1/v$ in character. The ratio $\varphi(1/\beta)/\varphi(10^4)$ is the ratio of neutron fluxes at 10^4 cm/sec (epithermal) and at $1/\beta$ cm/sec (thermal). In all cases x was found to be nearly unity, which would be expected if the energy spectrum were $1/E$ in the epithermal region.

Synthesis of Test Data

The measured decay constants and yields of low-energy neutrons from the various room-temperature source blocks that have been studied were used to synthesize the relative performance of these sources at a pulsed reactor. Synthesis was carried out assuming that the pulsed reactor had a 50-μsec pulse width and that a useful figure of merit could be written

$$\frac{\varphi_{max}}{W^2}$$

where φ_{max} is the peak thermal flux intensity and W is the full width of the thermal-neutron pulse at half-maximum.

The value of φ_{max} was calculated for various thicknesses of Lucite and polyethylene using Kley's[7] formulation

$$\varphi_{max} = \varphi_S^\infty (1 - e^{-50/\tau}) \ \text{neutrons/cm}^2/\text{sec} \qquad (2)$$

where φ_S^∞ (relative steady-state flux from the thermalization block) and τ (block decay constant in μsec) were experimentally determined.

The thermal pulse width at half-maximum (W) emerging from the thermalization block for a 50-μsec reactor pulse was calculated also assuming Kley's formulation

$$W = 50 + \tau \ ln \ (1 + e^{-50/\tau}) \ \mu\text{sec} \qquad (3)$$

The figures of merit as a function of thickness of Lucite and polyethylene blocks were determined; the Lucite results are shown in

Fig. 15. The figure of merit peaks at a 1.2-in. thickness of Lucite and
a 0.8-in. thickness of polyethylene, and at the peak the polyethylene
figure of merit is about 50% greater than for the Lucite. The poly-
ethylene has about 50% greater hydrogen density than Lucite, which
illustrates the importance of using a moderator block with as high a
hydrogen density as possible. It is also interesting to note that the 3-
by 3- by 24-in. Lucite prism has a figure of merit of less than 40%
that observed with a 24- by 24-in. Lucite block having the same pulse
width (~2 in. thick).
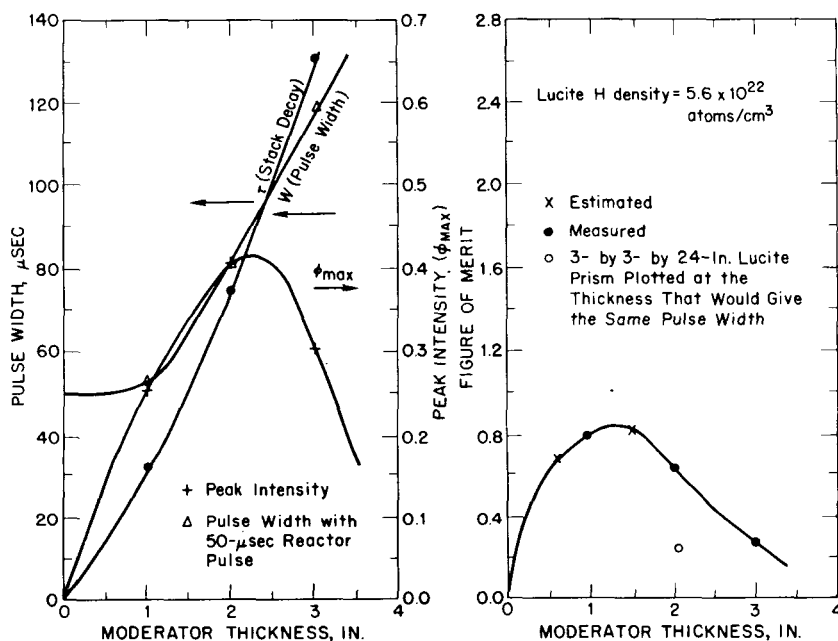
Fig. 15—*Pulse shape and figure of merit in Lucite moderator block, 20°C.
Lucite H has a density of 5.6×10^{22} atoms/cm^3.*

ACKNOWLEDGMENTS

REFERENCES

1. K. C. Hoffman, R. Parsick, M. Reich, and M. Levine, Engineering Problems
   in Pulsed Neutron Sources, USAEC Report BNL-10454, Brookhaven National
   Laboratory, 1966.

2. David Burgreen, Thermoelastic Dynamics of Rods, Thin Shells, and Solid Spheres, *Nucl. Sci. Eng.*, 12: 203–17 (1962).
3. L. Pochhammer, Über Fortpflanzungsgeschwindigkeiten kleiner Schwingungen in einem unbegrenzten isotropen Kreiszylinder, *J. f. reine u angew. Math Bd.*, 81: 324–336 (1876).
4. M. S. Farkas, Mechanical and Physical Properties of Fuels and Cladding Materials with Potential for Use in Brookhaven's Pulsed Fast Reactor, USAEC Report BMI-X-455 (Part I), Battelle Memorial Institute, 1967.
5. The Structure of Alloys of Certain Systems Containing Uranium and Thorium, USAEC Report AEC-tr-5834, 1961.
6. J. F. Collins and P. N. Flagella, Fabrication and Measurement of Properties of Mo−UO$_2$ Cermets, USAEC Report GEMP-545, General Electric Co., 1967.
7. W. Kley, Neutron Physics Experiments with the SORA Reactor, in *Research Applications of Nuclear Pulsed Systems*, Dubna, 1966, Panel Proceedings, International Atomic Energy Agency, Vienna, 1967 (STI/PUB/144).

DISCUSSION

McTAGGART: I would like to ask a question about your lifetime measurements on the critical mock-ups. What material was the reflector without a poison liner?

HOFFMAN: Stainless steel.

McTAGGART: In our experience not with steel but nickel and copper, the calculations of flux in these reflectors and the contribution which the neutron population makes to the neutron lifetime is quite often wrongly calculated because of inadequate data. The presence of a boron liner between the core and the reflector eliminates these low-energy neutrons from the reflector, and this may be why you get better agreement between the lifetime calculations for this poison-liner system.

HOFFMAN: Yes, that is quite probable.

BLOKHINTSEV: You made a statement that you had some experience with fluid-metal fuel elements. What do you think about the possibility of using fuel elements of this type?

HOFFMAN: We have thought about it a little bit. The experience at Brookhaven has been on liquid-bismuth systems which are quite dilute, and to get a high uranium content you have to go to a slurry. The most obvious liquid fuel seems to be molten plutonium, and that indeed is a possibility in the future.

BLOKHINTSEV: Is it in the far or near future?

HOFFMAN: We have not reached that decision yet.

LARRIMORE: Would someone from Los Alamos like to say something about molten plutonium? No? Okay.

CLACK: Your summary says that the reactor is to be used for high-intensity beam applications or beam research. Would you care to comment on probable research applications?

HOFFMAN: I wouldn't care to comment, but there may be some-one in the audience who would. No volunteers? We feel that it can be applied to the general class of research being performed at the high-flux reactors on solid-state physics studies. I couldn't get any more specific than that.

HENDRIE: In the presence of an assortment of eminent experts, perhaps Karl Beckurts could help us out since he is at least tempo-rarily on the staff at Brookhaven, and I do not propose to talk about experiments while experts are around.

BECKURTS: I think it might be worthwhile to cover that in the session tomorrow.

3-3 SHORT MODERATOR PULSES
AND BOOSTER SYSTEMS

R. G. FLUHARTY
Los Alamos Scientific Laboratory, University of California,
Los Alamos, New Mexico

ABSTRACT

A simple description of booster and accelerator-pulsed reactor properties is given in terms of point reactor kinetics. A concept of an accelerator pulsed reactor of ∼3 Mw average power and 5-μsec pulse widths at pulse rates up to 200 pulses/sec is presented. The major features are ^{239}Pu fuel and a partially voided core concept which yields shorter neutron lifetimes and flexible moderator and flight-path configurations by eliminating beam tubes. Methods for obtaining short moderator pulses are illustrated with methods for estimating beam intensities.

Booster reactors are defined as reactor systems in which neutron multiplication is obtained utilizing an external accelerator source. Generally, the reactivity is held constant, but many recent proposals provide for cyclic variation of the reactivity. As such, cyclic or periodic boosters or accelerator pulsed reactors require a source and operate below prompt critical during pulse-source multiplication; but, they have an average reactivity below delayed critical. The following discussion consists of three parts.

The first part is a very simple review of booster and accelerator pulsed reactor systems for those who are unfamiliar with them. No new results are included. I am indebted to Gary Russell[1] for the calculations and figures used in this section.

The second section describes a pulsed reactor concept that has many ideas based upon accelerator target technology. Most of the work was performed at Idaho Nuclear Corporation for the AEC.[1] Brief comments on modification and further developments at Los Alamos Scientific Laboratory (LASL) are also included.

The third section introduces an approach for estimating beam intensities. It should also provide guidance for experimental moderator optimization.

GENERAL BOOSTER CONSIDERATIONS

The general properties of repetitively cycled systems have been discussed by Larrimore[2] in more detail than can be covered here. A major conclusion is that the realizable pulse gain is limited by the delayed-neutron sources. This limitation can be seen from the following expression for the ratio of the power generated due to delayed neutrons to the total power:

$$\frac{P_d}{P_{av.}} = \frac{\beta}{\Delta k_p} \tag{1}$$

where P_d is the power from delayed-neutron sources, $P_{av.}$ is the total average power, and $\Delta \bar{k}_p$ is the average value of the prompt reactivity. This result follows immediately from subtracting the prompt gain, $1/\Delta \bar{k}_p = 1/(1 - \bar{k} + \beta)$, from the total gain, $1/(1 - \bar{k})$ ($\bar{k}$ is the average neutron multiplication), and dividing by the total gain. Likewise, the ratio of the power from the delayed neutrons to the power in the pulse can be expressed

$$\frac{P_d}{P_p} = \frac{\beta^*}{1 - k} \tag{2}$$

where P_p is the pulse power and β^* is the conventional effective delayed-neutron fraction. Note that β above is equal to $k\beta^*$. The limitation is a special case of the general statement that any steady-state reactor must actually be subcritical in the presence of neutron sources. Criticality is defined in the usual sense of equilibrium from fission regeneration.

Equations 1 and 2 are especially convenient because reactivities in dollars yield the power fractions directly. If, for example, the reactor is operating at an average reactivity of $4 below delayed critical, then Eq. 2 yields the fraction $\frac{1}{4}$ or 25% delayed power between pulses to pulse power. The $4 is equivalent to ~$5 prompt reactivity.

Note that Eqs. 1 and 2 are completely independent of the method of pulsing or reactor configurations. The only reactor dependence is through the nuclear-fission isotope used because of the different delayed-neutron fractions. The effects of the different delayed-neutron fractions are illustrated in Fig. 1, which shows the total and prompt gains as a function of neutron multiplication k for a nonreactivity-
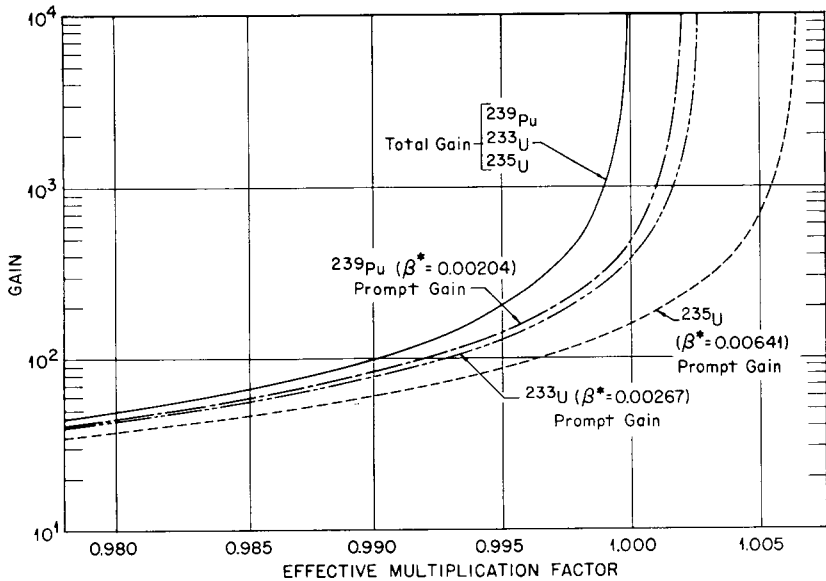
Fig. 1 — Comparison of the actual prompt-neutron gains for ^{233}U, ^{235}U, and ^{239}Pu with the total gains for a reactor operating with varying effective multiplication factors.

modulated booster. Because the prompt-neutron gain is $1/\Delta k_p$, the gain must be less than $1/\beta$ to avoid going delayed critical. This places rough absolute limits on gains less than 400 to 500 for ^{239}Pu and ^{233}U and 140 for ^{235}U. For the 25% background-to-pulse-power case above, these limits are reduced from 80 to 100 for ^{239}Pu and 28 for ^{233}U. These lower limits are more realistic because the 25% average power between pulses is much nearer the maximum acceptable limit.

This 25% maximum acceptable limit is a point frequently misunderstood; the argument is that, since the ratio of pulse-height peak to rate between pulses is very high, an excellent signal-to-noise ratio still exists. This point is illustrated in Fig. 2, which shows pulse heights and backgrounds for different fission isotopes. Actually this signal-to-noise argument is good, provided the events to be observed occur during the pulse. However, for neutron time-of-flight experiments, the source-pulse neutrons occur at the detector, spread out in time over the period between pulses. As a first approximation the neutrons at the detector are equally distributed over the period; so the signal-to-noise ratio is 4:1. In addition to the time-of-flight usage, for any experiment in which delayed events are being observed, appropriate signal-to-noise considerations must be made which are similar in character to those mentioned for time-of-flight experiments. In Fig. 2 about 65% of the power is generated between pulses for ^{235}U.
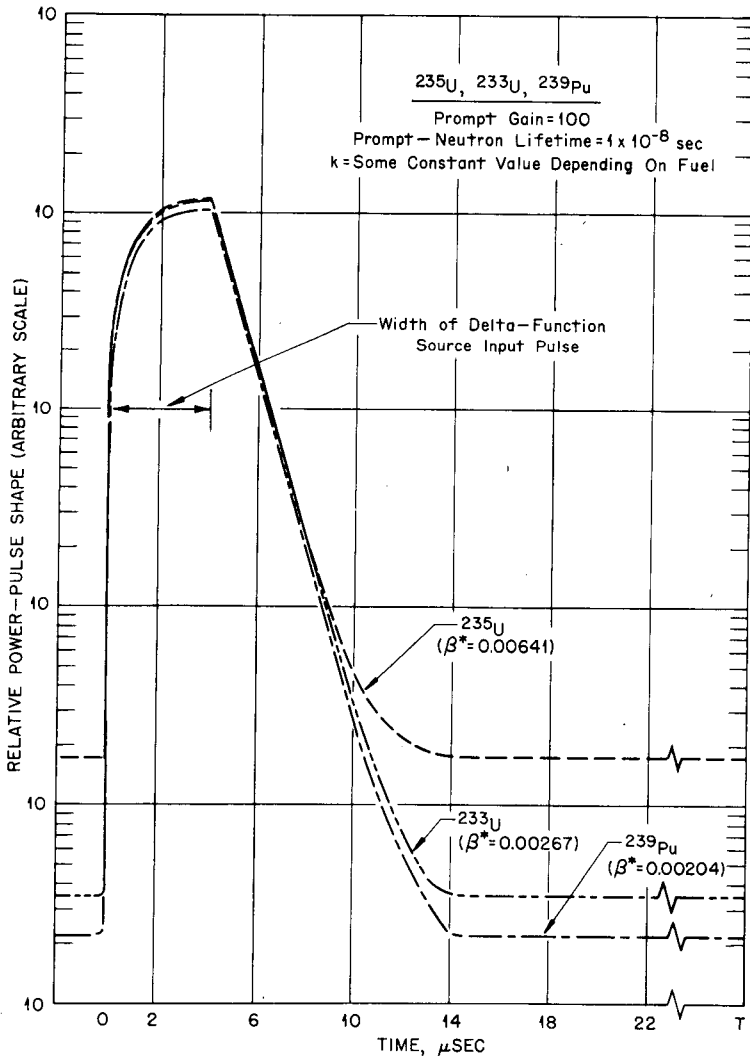
Fig. 2—Details of the relative power-pulse shapes for ^{233}U, ^{235}U, and ^{239}Pu for the same gain and neutron lifetimes. Note that the peak amplitude of ^{235}U is highest because the pulse is added to a higher background, and the peak-to-background ratio is far superior for ^{239}Pu.

Operating charged-particle accelerator neutron sources in combination with boosters without reactivity modulation could not exceed a few hundred kilowatts for the limits discussed; methods for removing these limits have been proposed. One proposal[3] suggests that β can be reduced by removing the delayed-neutron precursors, but the idea has not been developed. The most useful approach would be to
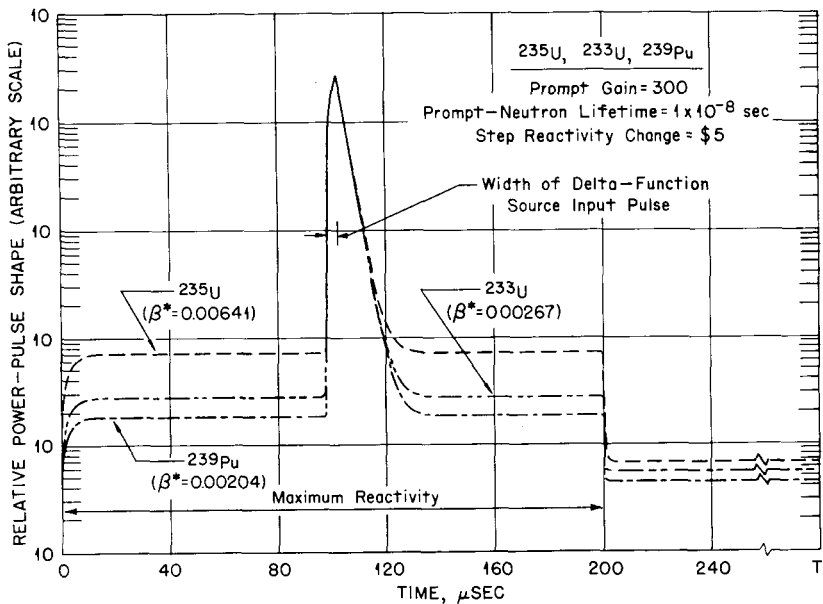
Fig. 3—Plot of the power-pulse shape as a function of time over one period for the same gain and neutron lifetime for ^{233}U, ^{235}U, and ^{239}Pu. The relative effects of the different delayed-neutron fractions are illustrated for a step reactivity insertion for 200 μsec.

chemically remove the delayed-neutron precursors from recirculating homogeneous reactors, but homogeneous reactors have proven so difficult as static systems that flowing systems have not yet been attempted. Most proposals (including the following) for source-driven systems include the use of cyclic reactivity insertion, which allows the system to approach delayed critical or to exceed delayed critical for a small fraction of the period. For the rest of the period, the reactivity returns to well below delayed critical, providing an average multiplication that is well below delayed critical. The source is introduced when the prompt reactivity is low, yielding a high source gain ($\epsilon = 1/\Delta k_p$); the background is determined, however, by the average $1/\Delta \bar{k}$, which is less than $1/\beta$. An idealized representation of this operation is shown in Fig. 3.

For such a source-driven system, the prompt reactor period is the product of the neutron gain times the prompt-neutron lifetime, which is given by

$$\tau_p \equiv 1/\alpha = Gl = l/\Delta k_p \qquad (3)$$

where α is the prompt decay constant, G is the gain, and l is the average neutron lifetime in the reactor. For many applications the value

of τ_p is specified; and, because the reactor lifetime is fixed, the gain is fixed. Or, in a positive sense, the reactor designer can increase gains for specified τ_p by minimizing the neutron lifetime. For example, the requirement of a pulse width of 10^{-7} sec restricts the gain to 5 for a lifetime of 2×10^{-8} sec and to 10 for 1×10^{-8} sec. In contrast, specifying a pulse of 3×10^{-6} sec would allow gains of 150 and 300, respectively, for the corresponding neutron lifetimes. Note that reactivity modulation would be required for the high gains at 3 μsec if the additional specification of 25% background-to-pulse power is required, but for the lower gains the background-to-pulse power is 1 and 2%, respectively, with reactivity modulation. In fact, for the lower gain cases, modulation would be of very little value because practical modulation amplitudes are small compared to the 0.2 and 0.1 values of prompt reactivity for the gains of 5 and 10. A very good swing or amplitude for modulation is a swing of 0.03 in Δk_p.

Note that the conclusions on total gains are completely independent of the time width or pulse shape of the source pulse, but the additional effect of a finite time width for the source pulse is to lower the allowable reactor period because of the increased pulse width introduced. The effect of the reactor neutron lifetime on pulse shape and width for fixed gain and source pulse width is shown in Fig. 4. From the
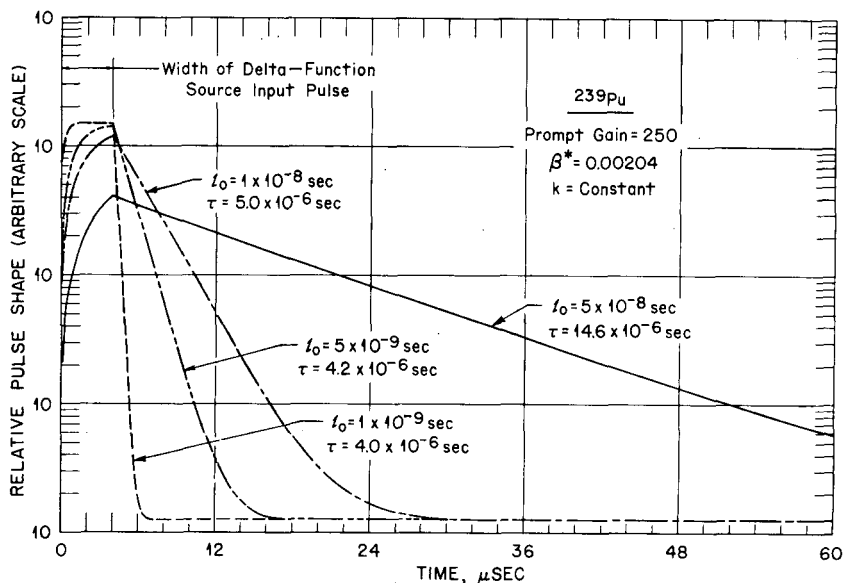

Fig. 4—*Effect of variation in the prompt-neutron lifetime on the reactor pulse shape. The areas under each pulse are the same because the gains are the same; the instantaneous or rate gains at the peaks are noticeably depressed for longer neutron lifetimes.*

figure we see that the above statement is oversimplified, and the restriction on gain should indeed be greater if a need to retain the input pulse shape exists. Also, the restriction on gain is weakened by the source pulse width if the overall pulse width is not limiting. Note that the same gain is assumed for all lifetimes for this figure.

Assuming a pulsed reactor operating near critical, the neutron leakage is very nearly given by the ratio

$$\frac{\text{Leakage}}{\text{Total neutrons produced}} = \frac{\eta - 1}{\eta} \tag{4}$$

where η is the effective number of neutrons produced per neutron absorbed. A comparison that illustrates the relative advantage of ^{239}Pu as a fuel is given in Table 1 for typical reactor systems. Note that although the leakage neutron yield is maximum for ^{239}Pu, the pulse width is also largest because of the larger prompt gain allowed by the lower delayed fraction. The corresponding leakage neutron rates for ^{235}U and ^{233}U could be attained for ^{239}Pu at lower average power and with a lower pulse width.

Table 1

COMPARISON OF FUELS FOR REACTORS OPERATING AT THE
SAME AVERAGE TOTAL POWER*

Parameter	^{235}U $\beta^* = 0.00641$ $\nu = 2.46$ $\eta = 2.13$	^{233}U $\beta^* = 0.00267$ $\nu = 2.51$ $\eta = 2.33$	^{239}Pu $\beta^* = 0.00204$ $\nu = 2.93$ $\eta = 2.69$
Prompt gain	422	584	685
Prompt leakage gain†	222	333	430
Total gain	937	943	1061
Av. total power, Mw	9	9	9
Peak power/av. background power	634	1016	1011
Prompt energy in pulse, %	45	62	65
Av. prompt leakage rate,† neutrons/sec	1.69×10^{17}	2.53×10^{17}	3.27×10^{17}
Effective pulse width, μsec	6.5	8.0	9.0

*($S_s = 9.5 \times 10^{17}$ neutrons/sec, $l_0 = 1 \times 10^{-8}$ sec, $T_s = 4$ μsec, $t_k = 750$ μsec, repetition rate = 200 pulses/sec, reactivity swing = 5.0.)
†Maximum possible.

REPETITIVELY PULSED REACTOR CONCEPT

A preliminary reactor concept[1] with many attractive features consists of a small plutonium booster reactor producing 3 to 10 Mw of average power in conjunction with a charged-particle neutron source. The combination of a reactor (booster) and a charged-particle neutron

source provides a facility of great flexibility as a reactor-technology tool because of the wide range of pulse frequencies, power-pulse heights, and pulse widths that can be produced. Pulse frequencies variable from 0 to 200 pulses/sec and widths variable between 10^{-7} and 10^{-5} sec are representative with corresponding peak power-pulse heights (3000 Mw) within the limits imposed by average power and shutdown shock conditions. In the neutron-spectrometer mode of operation, the reactor is operated as a subcritical neutron pulse amplifier, amplifying short neutron-driving pulses from the charged-particle source. In this operational mode, high neutron gains and corresponding high reactor pulse power are obtained by rotating reactivity controls. The average reactivity of the reactor is maintained well below delayed critical, but the cyclic reactivity variation permits short-time operation between delayed and prompt critical for large amplification of the source pulse.

Schematic representations of the preliminary concept are shown in Figs. 5 to 7. Figure 5 is a cutaway view of the reactor and moderator system. The 8- by 8-in. cylindrical reactor core consists of fuel and liquid-sodium coolant. A central tube through the core provides access for the electron or other charged-particle beam and a plutonium target. The target cooling is contained in the particle-beam tube, allowing independent maintenance of the target. The upper half of the central tube also provides access to test samples from the reactor top. Irradiation space is also available in the elliptical containment vessel. The moderators for neutron spectroscopy sources are cooled to 80°K with liquid nitrogen. Liquid-helium cooling to obtain lower temperatures could easily be incorporated if studies indicate sufficient merit, but liquid-nitrogen temperatures are adequate for large performance gains. Two 1-m-radius rotating reactivity controls, which are in phase, are shown as they approach the reactor to provide the cyclic reactivity control. Studies are being made including fuel as a part of the rotating reactivity control. The reactor pulse frequency can be varied by operating the two rotating reactivity controls at different frequencies. This approach is desirable because the pulse characteristics are relatively unaltered compared to a single rotor control when repetition rates are varied. A horizontal section of the Facility Repetitively Pulsed Reactor (RPTF) reactor concept and moderator is shown in Fig. 6. The drawing shows the rotating reactivity controls in the position for maximum reactivity. Only a few of the fuel pins of a total array throughout the core are shown to allow clear presentation of the rotor position. The relative positions of the reflector, ^{10}B decoupling shield, and moderator are also shown. Figure 7 shows the relative vertical positions of the charged-particle target, reactor core, moderators, sample holder, and rotating fuel. It also
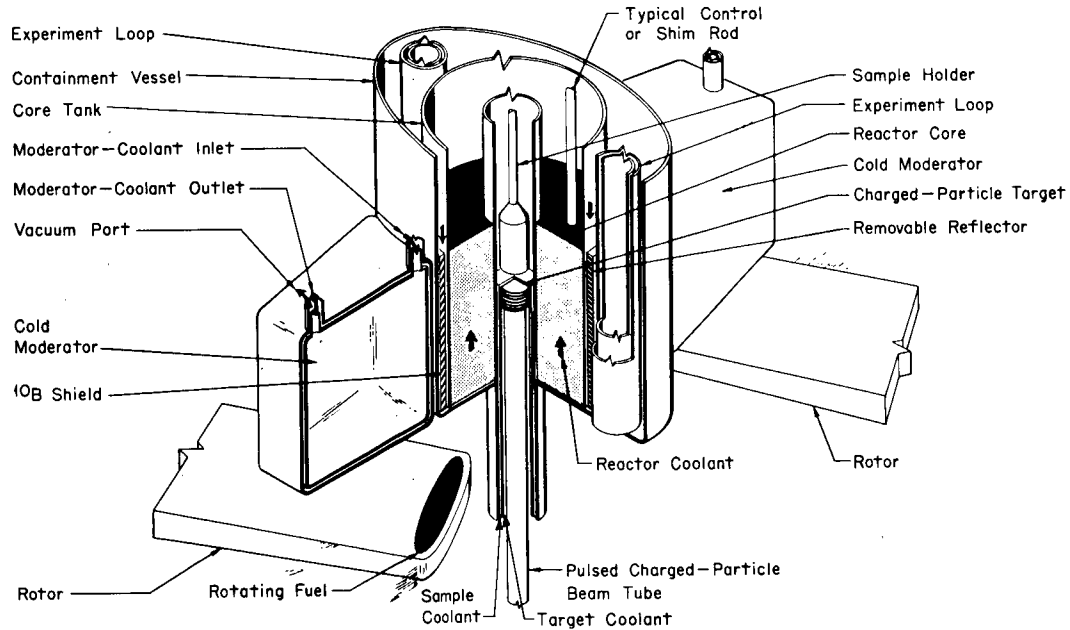
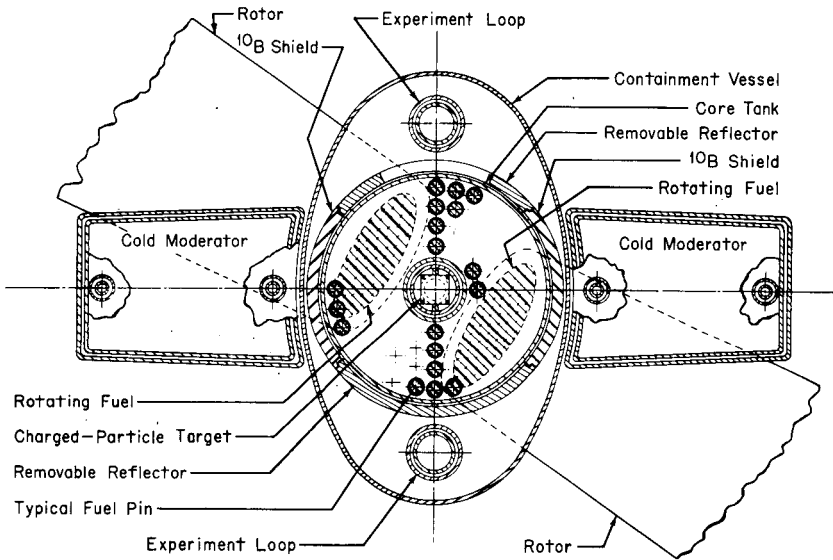Fig. 5—*Cutaway view of a concept of the RPTF reactor and moderator system.*

Experiment Loop

Containment Vessel

Core Tank

Moderator—Coolant Inlet

Moderator—Coolant Outlet

Vacuum Port

Cold Moderator

^{10}B Shield

Rotor

Rotating Fuel

Sample Coolant

Target Coolant

Pulsed Charged—Particle Beam Tube

Reactor Coolant

Typical Control or Shim Rod

Sample Holder

Experiment Loop

Reactor Core

Cold Moderator

Charged—Particle Target

Removable Reflector

Rotor

Fig. 6—*Horizontal section through the center of the RPTF reactor core and moderator.*
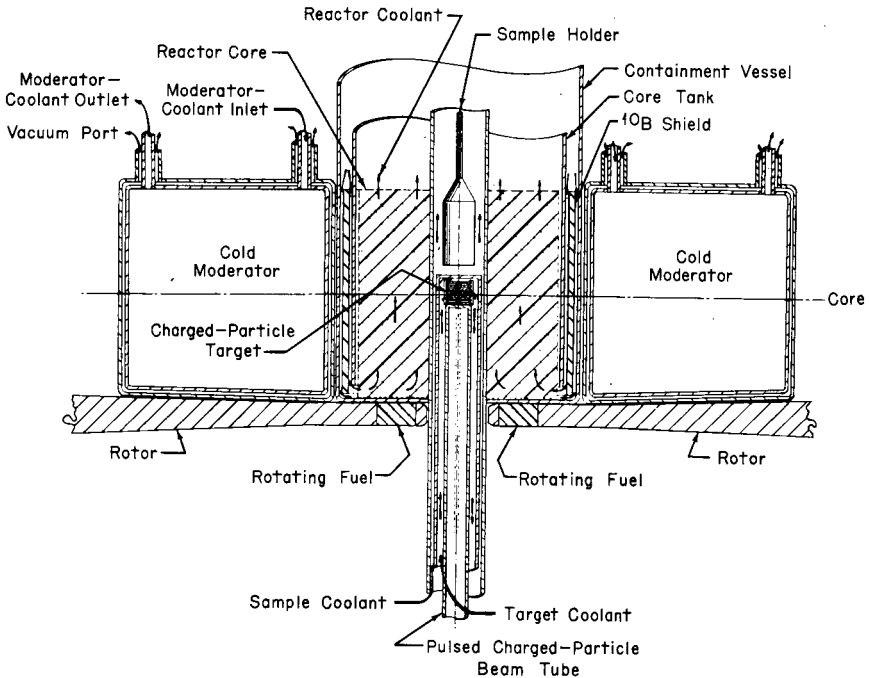
Fig. 7—*Vertical section through the center line of the RPTF reactor core and moderator.*

gives the direction of flow for the reactor, moderator, sample, and target coolants.

In Fig. 8 beam-tube configurations and a larger view of the rotational system are shown. Multiple beam access to a common moderator surface is obtained by voiding space around the reactor. The voided
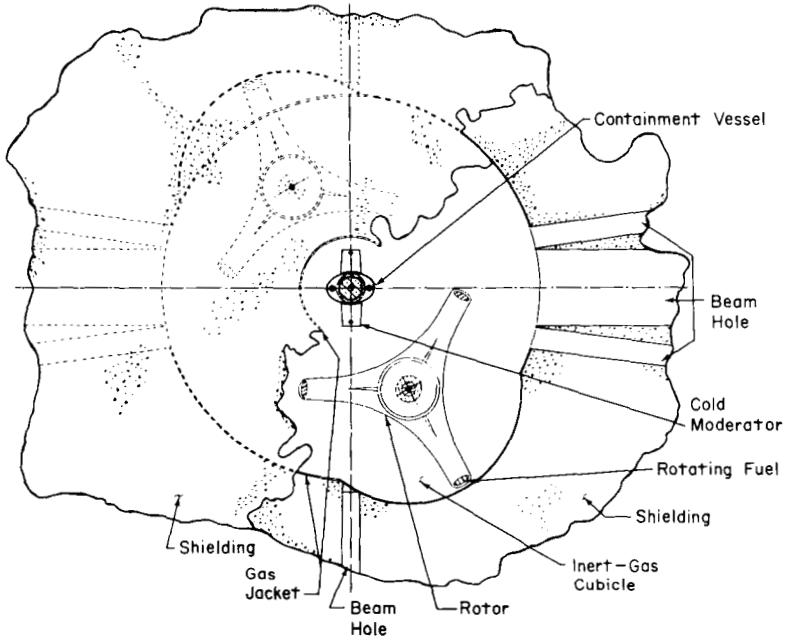

Fig. 8—*Horizontal view showing typical beam-tube configurations and relative positions of the rotating fuel with respect to the RPTF reactor core.*

space also provides great flexibility in the test utilization of the reactor, and it could even allow a complete change of the reactor system. Safety advantages are also inherent in the voided concept. The voided region is cooled by gaseous helium. The helium system will provide an additional radioactivity containment.

A schematic diagram of the neutron source and reactor building of the RPTF is shown in Fig. 9, and another aspect of facility flexibility is shown. This aspect, represented by a separate charged-particle target cell, illustrates that the charged-particle source and the reactor can be operated independently. The reactor design allows for operation as a pulsed reactor in a super-prompt critical mode in contrast to the booster or neutron-amplifier mode. At the same time, the electron beam can be utilized to study heat- and energy-transfer problems separately. The normal target power density from such an
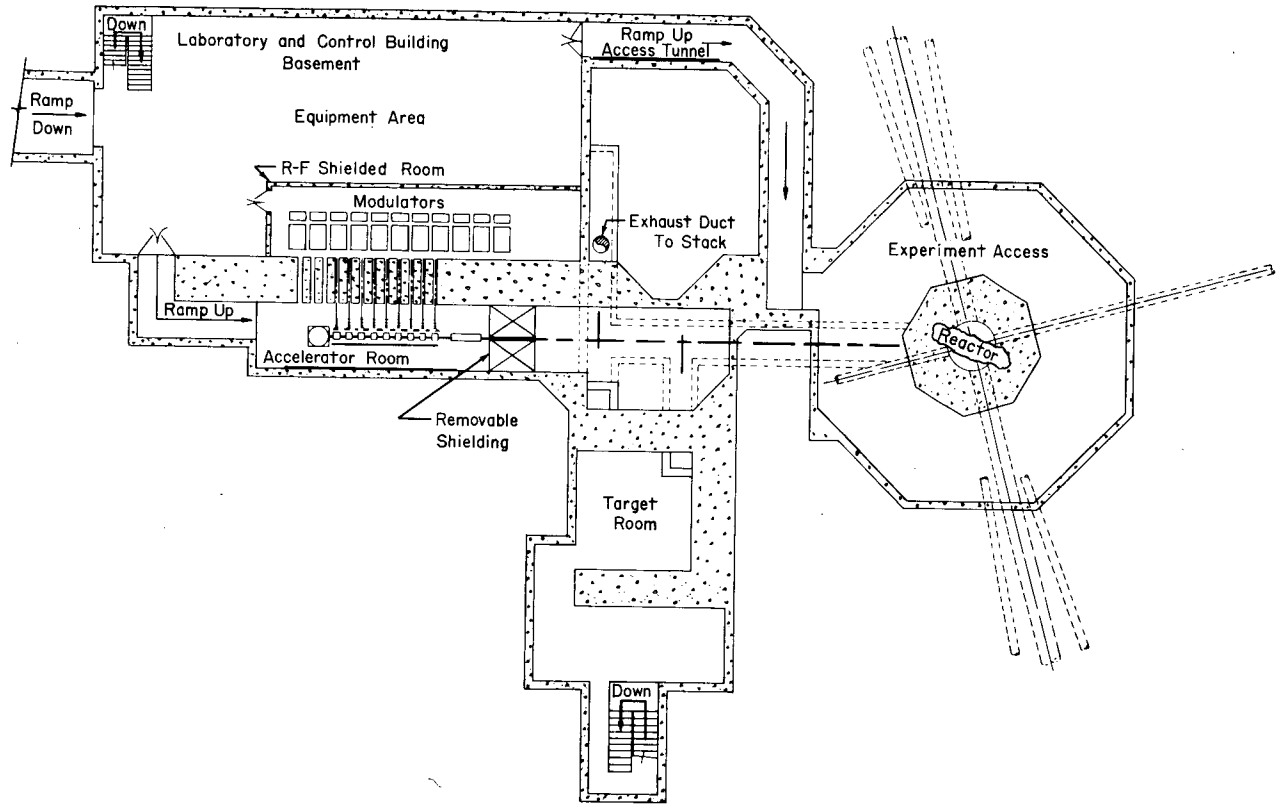
Fig. 9— *Plan view of the charged-particle neutron source and reactor building.*

electron beam is at least 10 times that of the reactor itself, and this power density can be increased (~25 to 30 Mw/liter) by focusing the beam to a smaller size.

The accelerator needed to supply the neutron source is considered to be a reasonable extrapolation from linacs now in operation. The original Idaho Nuclear Corporation proposal visualized a 100-Mev 1.25-amp peak current with 4-μsec pulses, and pulse rates of 200 pulses/sec. This proposal provides 100 kw on the target, which is about a factor of 2 increase over the highest powers available from known operating linacs. Recent study has centered around specifications of 8-amp peak current, 60 Mev, 3-μsec pulses, and 100 pulses/sec. These specifications would supply 144 kw on target, and they could be obtained by a conservative extrapolation of the 80-amp peak current PHERMEX linac. The enhanced target power provides a greater margin of safety against errors in the estimated neutron yields or in lowering the design gain and hence the pulse width.

Basing costs of such accelerators upon the scale-up in average power results in a 5 to 10 million dollar range. It is most likely that the 800 cycles/sec megaHertz (L band) machines would perform best at higher voltages and lower currents, but equivalent performance is promised in the same price range. A recent proposal by Knapp[4] using side-coupled cavities promises to provide the source strength for considerably less than 5 million dollars. Because of the efficient conversion from radio frequency to electron energy, significantly lower operational cost would also result. Studies of the maximum current limits for such systems are required to confirm this potential.

A major purpose for the void around the reactor is to minimize the neutron lifetime. An example of the merit of this approach is given in Table 2 from LASL calculations.[5] The realization of the full bare configuration cannot be expected because the entrance and exit coolant, moderators, and reflector safety controls will compromise these numbers. Also, calculation methods to determine the dependence of the void on size are only now being developed. Experimental critical

Table 2

NEUTRON LIFETIMES FOR CYLINDRICAL MODEL

	12 g Pu/cm^3		16 g Pu/cm^3	
	Reflected	Unreflected	Reflected	Unreflected
Neutron lifetime for infinite cylinder, sec	7.8×10^{-8}	0.90×10^{-8}	6.7×10^{-8}	0.66×10^{-8}
Neutron lifetime for core height-to-diameter ratio = 1	3.1×10^{-8}	0.93×10^{-8}	2.4×10^{-8}	0.67×10^{-8}

studies will be required before accurate evaluations can be made of these factors. It does not seem unreasonable to expect neutron lifetimes of less than 2×10^{-8} sec for partially voided configurations.

The voided-core concept provides the following possible additional advantages:

1. Maximum neutron leakage per fission (1.5 to 1.9 neutrons/fission) available from the core. These leakage neutrons can be utilized for experiments but are also potentially available for breeding.

2. Enhanced effectiveness of mechanical reactivity insertion because of the high leakage sensitivity.

3. Increased negative temperature coefficients due to stronger leakage dependence upon thermal expansion.

4. Internal expansion chamber capability for safety containment.

5. Flexibility for changing experiments near the reactor core, i.e., a single target moderator can be viewed by a number of neutron beams without conflicting beam pipes near the core.

6. Simplified cooling requirements for the reactor shield.

Many of these points must be classed as predictions because they have not been demonstrated by experiment or calculation, but they do offer interesting points for exploration.

The advantage of high η for high neutron leakage for source reactors has already been discussed, and emphasis upon the breeding aspect is a digression from the research aspect since the research reactor is not intended for use as a breeder. However, the idea leads parenthetically to some interesting considerations about voids for breeding reactors. Generally, the effect of a reflector consisting of ^{238}U or ^{232}Th for conversion is to degrade the fast-fission-spectrum neutrons into a lower energy region that is unattractive for ^{239}Pu because of enhanced capture and lower fission at the lower energy. The void decouples the bare system from the degraded spectrum, preserving the high potential breeding ratio of the bare system. This idea needs computational verification and parametric study, and optimization remains relatively unexplored.

ESTIMATES OF TIME-OF-FLIGHT BEAM INTENSITIES

If we assume a uniform moderator without internal sources or regeneration, the vector transport equation for the flux at $\vec{v}$, $\vec{r}$, $\vec{t}$ can be expressed by the operational equation

$$\frac{\alpha \phi}{\alpha t} = A\phi \tag{5}$$

where $A \equiv B + K$, B is the sum of leakage, downscattering, and absorption terms, and K is an integral of a scattering kernel operating on the

flux integrated over all other vector space involving the sample volume and vector space. According to Williams,[6] the solution can be expressed

$$\phi(v,t) = M(v)e^{-\lambda_0 t} + \sum_i A_i(v)e^{-\lambda_i t} + \int_{v\epsilon_{min}}^{\infty} e^{-\lambda t} A(\lambda v) \, d\lambda \qquad (6)$$

where $M(v)$ is an equilibrium Maxwellian-like distribution, the second term represents higher energy eigenfunctions (which can be shown to represent near-equilibrium before the final distribution is obtained), and the third term is a continuum distribution. The equilibrium and near-equilibrium eigenfunction solutions are interpreted to contain upscattering as well as downscattering, whereas the transient continuum solution only contains downscattering. Thus, for a system at zero degrees, the continuum distribution alone would remain because the neutrons would continue to moderate indefinitely without absorption. The qualitative agreement with this interpretation is illustrated in Fig. 10, where the time distribution at a fixed energy or velocity has been measured[7] for leakage neutrons from a polyethylene sample at room temperature and for the same sample at $\sim 80°$ K.

An experimental measurement of the time-dependent spectrum of polyethylene is represented in Fig. 11. The narrow ridge leading down to the Maxwellian is seen in the foreground. The evolution of the transient to the stable Maxwellian is not readily evident, but Fig. 10 is based upon an actual constant energy—time measurement, and indeed the energy distribution can be interpreted as a Maxwellian, with the consideration that it is a diffusion-hardened leakage spectrum. A rough schematic of the process represented is shown in Fig. 12, the view is from the top as in an equipotential plot. The heavy black lines represent twice the dispersion and the maximum value of the distribution function. Equiflux contours are very schematically represented. The peak and the width progress together in the continuum transient, diverging linearly until upscattering starts as equilibrium is approached. The two representations of the distribution become orthogonal as equilibrium is attained. Note the continuation of the continuum transient for zero temperature.

The major discussion in the following pages will be about the transient continuum or slowing-down portion of the solution. The fact that the properties of the solutions of the transport equation are not a closed subject is only noted, and the discussion will be restricted to simple cases, alleviating the necessity of more rigorous development in this active field. Some reference to the theory will be made as it applies to the experimental approach being outlined. The experimental approach could, in turn, be of direct interest in testing the theories, but the basic objective will be to optimize the coupling between pulsed reactors and experiments. In this sense, the approach is that of an engineering development program or an applied measurement technique.
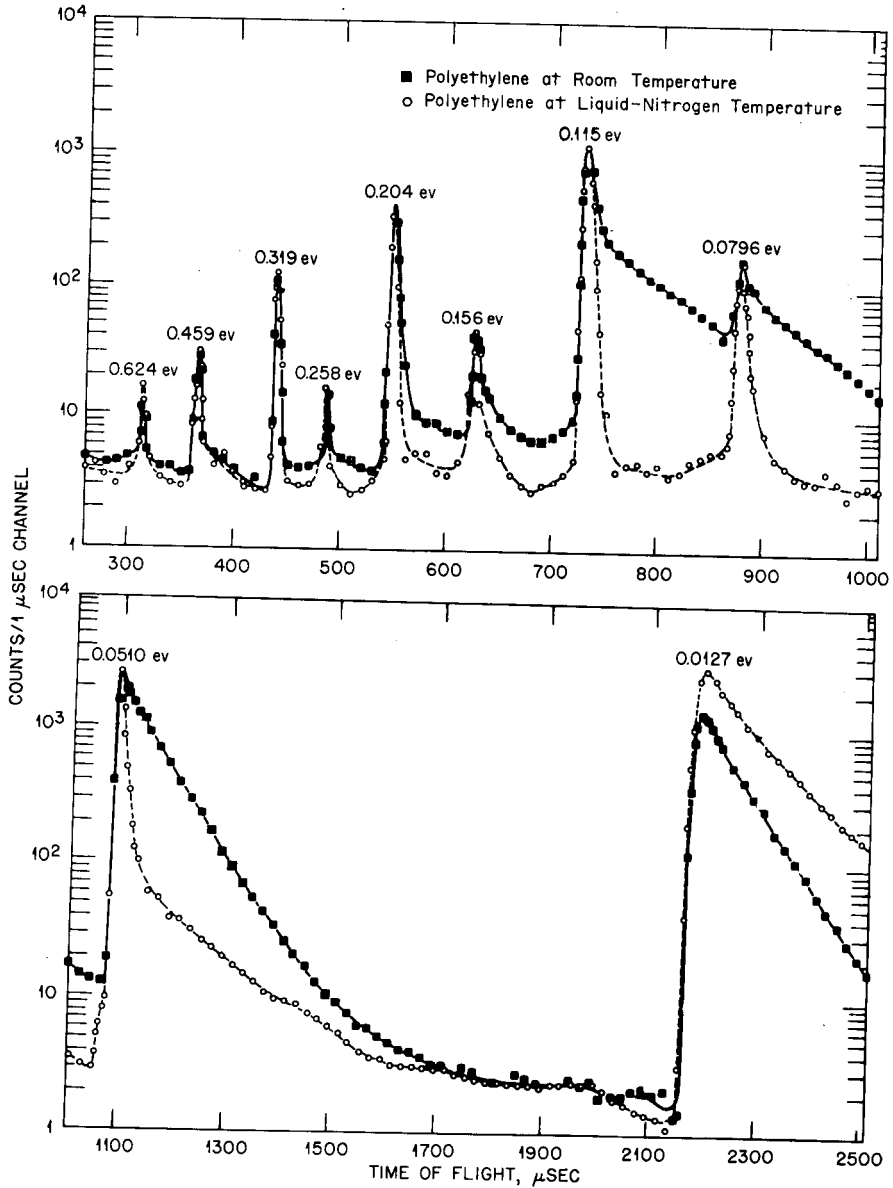
Fig. 10— The delta-function time-dependent neutron leakage at various energies from 4- by 4- by 3-in. polyethylene at room temperature and at 80°K.
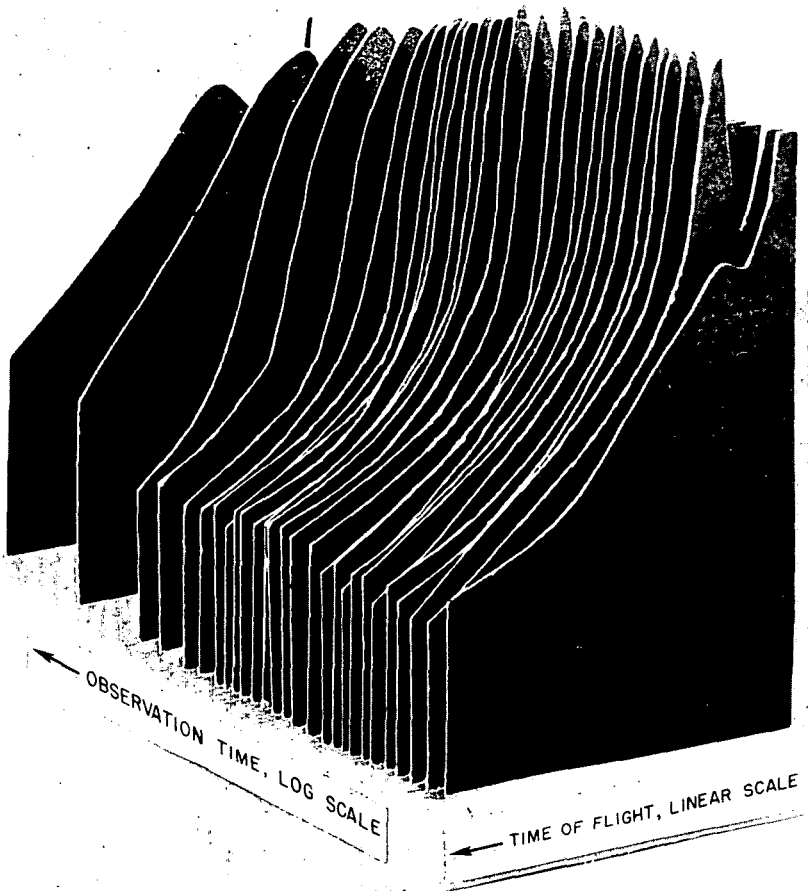
Fig. 11—Experimental neutron spectra plotted as a function of time after the introduction of a delta-function source.

Assuming an infinite medium at zero degrees, an analytical solution of the time-dependent slowing-down neutron density for a monotonic hydrogen gas is given by

$$N(E,t) \ dE \ dt = \frac{1}{2} \ (\Sigma vt)^2 \ e^{-\Sigma vt} \ \frac{dE}{E} \ dt \qquad (7)$$

where Σ is inverse mean free path and has been assumed constant for all energy, v is the average velocity, t is the time, and E is the neutron energy. The major approximation neglects the variation of cross sections with energy. Experimental data given in Fig. 13 show that the
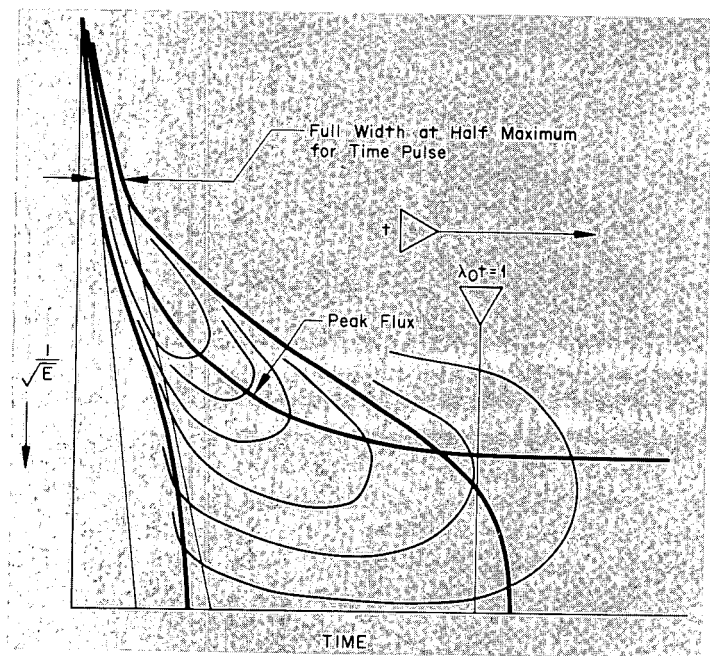
Fig. 12—Equiflux plot of the neutron time—energy distribution after introduction of a delta-function source. The straight outside lines indicate the dispersion of width of the time pulse; the center is the peak of the distribution. The final energy distribution is a diffusion-cooled Maxwellian decaying away with a single exponential.

experimental data are accurately described by the functional shape without specifying amplitude and cross-section values. The maximum, average value, second moment, and dispersion are given in the expressions below:

$$t_{max} = \frac{2}{\Sigma v}$$

$$\bar{t} = \frac{3}{\Sigma v}$$

$$\bar{t}^2 = \frac{12}{\Sigma v}$$

$$\Delta t = \sqrt{\bar{t}^2 - \bar{t}^2} = \frac{\sqrt{3}}{\Sigma v} \tag{8}$$

Assuming that $\Sigma = 1.4$ cm^{-1}, a rule-of-thumb value for the reciprocal product $1/\Sigma v$ for the hydrogenous medium is

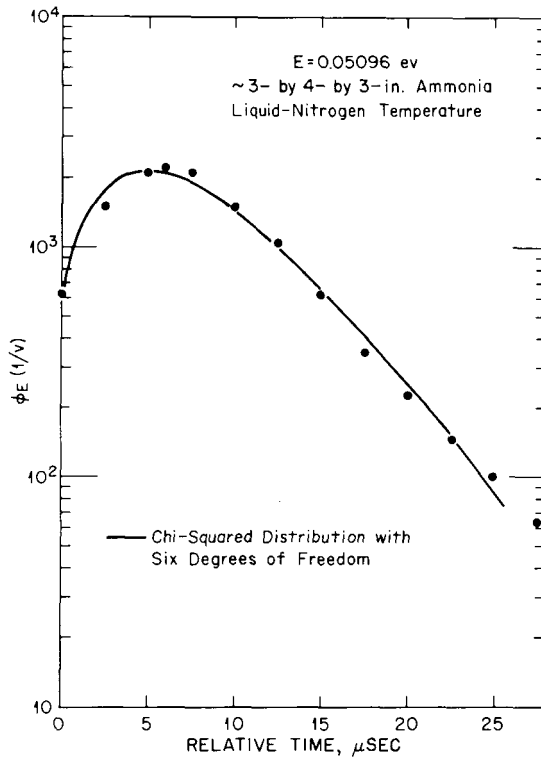$$t_v = \frac{1}{\Sigma v} = 1/2\sqrt{E} \ \mu sec \tag{9}$$

Fig. 13—A fit to the time distribution of 0.05-ev leakage neutrons from solid ammonia at 77°K using a chi-squared distribution of six degrees of freedom. Note that this has an equivalent functional form as Eq. 7.

where E is in electron volts. The above equations provide the basis for estimating epithermal-neutron pulse widths where it is assumed that τ_p, the full width at half maximum, is given by $\tau_p = 2 \times 0.7 \, \Delta t = 1.4 \, \Delta t$. For the idealized case of $\Sigma = 1.4 \, cm^{-1}$, the value of τ_p is given by

$$\tau_p = \frac{1.2}{\sqrt{E}} \, \mu sec \tag{10}$$

where E is in electron volts. This equation yields a value of 5.2 μsec at 0.05 ev; the experimentally observed values are 9 μsec for solid ammonia, 15 μsec for polyethylene, and 17 μsec for water. The difference is assumed to be the lower product of the inelastic-scattering cross sections and mean logarithmic energy loss compared to the free-atom case. Subsequent calculations assume a 10-μsec pulse width at 0.05 ev.

A more general and quite accurate formula describing the time distribution for any medium was developed by Koppel[8] using the

Greuling–Goertzel approximation. This approximation can be considered as a higher order age equation approach, and the appropriate expression obtained is

$$\phi(v,t) = \frac{1}{\Gamma(2/\gamma)} \, e^{-y} \, y^{(2/\gamma)-1} \tag{11}$$

where Γ = the gamma function

$$y = \frac{\xi}{\gamma} \Sigma_s \, vt$$

and

$$\gamma = \frac{1 - \alpha - \alpha\epsilon - \dfrac{1}{2\alpha\epsilon^2}}{1 - \alpha - \alpha\epsilon}$$

where ξ is the usual average logarithmic energy decrement, α is the maximum energy loss per collision, and $\epsilon = ln \, 1/\alpha$. For estimates for heavy moderators, the following Russian[9] slowing-down spectrometer values are recommended:

$$\bar{t} = \frac{M}{\Sigma v}$$

$$\overline{\Delta t} = \sqrt{\frac{2M}{3}}/\Sigma v \tag{12}$$

where M is the mass of the moderator.

These time functions are schematically represented in Fig. 14, and their magnitudes can be estimated from the formula given. A time-of-flight experiment at a distance R can be represented by a linear time transformation of the time distribution by a time given by $t_{of} = R/v$. The classical time-of-flight specification is that t_{of} be much greater than $2 \, \overline{\Delta t} = \tau_p$, which avoids the problems posed by the non-separability of velocity and time in Eqs. 7 and 10. If this specification is not satisfied, the problem needs to be treated using partial differentials. More generally, the implied uniform sources and infinite media, which are required to provide the given solutions, are not realistic; energy separability must be examined. Even where such separability can be made, the complicated source distribution and delta-function time source imply complex eigenfunctions or exponentials that are necessary to describe the wave-front character of the continuum transient. However, the simple point of the time delay
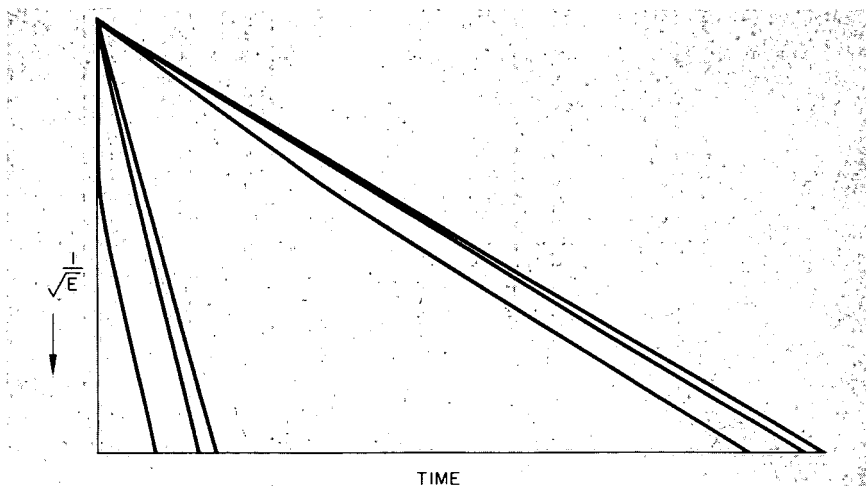
Fig. 14 — Graph of the time—width distribution (near the initial time) showing the effects of an energy-dependent source including inelastic scattering. The latter effect is overemphasized. The second time distribution is that seen at the end of a time-of-flight path.

and the dispersion in this delay will be general and must be accounted for in time-of-flight experiments. It is usually treated as a source-thickness correction, but greater refinements are expected to show that this correction is inadequate. This question will be left open here.

The basically complicated calculation of the space, energy, and time distribution of the flux within the medium will be avoided by discussing the problem from an empirical, experimental point of view. The immediate discussion will be restricted to the three observables: the source strength q, the leakage currents, and the equilibrium thermal leakage. The source strength is assumed to be the first interaction neutrons in the moderator from an external source. This distribution would be best determined by a Monte Carlo calculation, but rough estimates are not difficult. The total source q is desired. The leakage flux is experimentally observed to have an energy dependence de-, scribed by the modified 1/E expression

$$\phi(E) \, dE = \frac{K_l \, dE}{E^n} \tag{13}$$

Typically, experiments have been performed to optimize ϕ as a function of thickness of the moderator. These optima are energy dependent,[10] but the values of n usually fall between 0.85 and 0.95, the lower value being obtained for higher energy optimization. In the infinite medium, the flux becomes $K_l \, dE/E$, and the exponent lower than 1 is a

measure of the competition between moderation and leakage. Within the infinite medium the integral of the flux gives something like $17K_l$ for a unit density hydrogenous moderator, whereas the integral over Eq. 13 gives, for example, $34K_l$. Because the number 17 represents the case for all source neutrons reaching thermal, a fractional relation can be established:

$$\frac{1}{17} = \frac{1}{34} + \frac{1}{N_{thermal}}$$ (14)

where $N_{thermal}$ is the normalization constant integral over energy for the internal neutron flux (all-volume sum) with leakage. For the case chosen, $N_{thermal}$ is also 34, or half the neutrons reach thermal and half leak out. For an optimum moderator for resonance neutrons, the case of one-half leakage and one-half reaching thermal is observed to be a reasonable approximation. Thermal measurements also provide reasonable confirmation of this result.

A prescription or recipe for estimating beam fluxes (neutrons/cm^2/sec) is given by

$$\phi = \frac{E^{(1-n)} SF_1 F_2 F_3 K \, dE}{E} \Omega$$ (15)

where S = total source strength
    F_1 = fraction of the source impinging on the moderator
    F_2 = fraction of neutrons staying in the moderator
    F_3 = fraction of the leakage observed by the experiment, suggested to be estimated by taking the fractional buckling for the surface viewed
    K = normalization constant for the leakage spectrum
    Ω = solid angle subtended by 1 cm^2 at the detector or beam sample position, and this is $\frac{1}{4} \pi R^2$ if R is large compared to the surface dimensions of the moderator being viewed

The optimization problem for a particular experiment is in itself complicated, and, for a large variety of beams, many optimization studies will be required before the best solution is found. Usually the beam fluxes will be $(10^{-5} - 10^{-4} \, SdE \, \Omega/E)/E$.

Calculations can be made to determine equivalent-source fluxes, and these will be found to be disappointing because the moderator optimization has been made to maximize ϕ_{peak}/τ^2, where ϕ_{peak} is the peak of pulse and τ the time width. A maximum moderator pulse flux equivalent of 10^{16} neutrons/cm^2/sec for thermal neutrons is about the best that can be obtained. This flux is postulated from a total neutron leakage of 1.7×10^{17} neutrons/sec from the reactor, and it assumes the

equivalent flux to be determined from the source leakage being one-half the equivalent flux and allowing a factor of 4 for peak-to-average flux from a rectangular slab. However, this approach should only be used to emphasize the basic difference in optimization of beam leakage at short time vs. optimizing the moderator flux.

The merits of the short pulse-leakage optimization can only be realized by comparing experimental intensities because source comparisons in the terms of flux alone leave out many area, geometric, and collimation factors. For example, a conventional steady-state reactor flux of 10^{17} neutrons/cm^2 and 10-cm-diameter beam ports would produce fewer neutrons per square centimeter at the end of the flight path than the 10^{16} neutrons/cm^2 pulsed source above if it is necessary to use a chopper to obtain the 10-μsec pulse. The major difference is the chopper collimation limit on the source area that can be used. In contrast, the total area (~ 400 cm^2) would be potentially available if energy resolution is the only restriction (the need for angular definition of the beam could certainly modify this comparison).

As presented, the proposal places great emphasis upon tangent beams, which are generally desirable because of the inherent advantage to shielding and background problems. This advantage results since the direct reactor radiation is once scattered in leaving the reactor, and it is degraded in energy and much easier to suppress experimentally. Cases occur in which the neutron intensities favor side view of the moderator perpendicular to the general source direction. Macklin and Harvey[11] have shown that the halo target adopted for the ORELA produces higher beam intensities than a moderator placed between the target and experiment. The Idaho studies[6] also indicate enhanced source intensities when viewing perpendicular to the source for special moderator cases. Further study of this question will be required, and the important point is to raise the question of the side-view alternative.

The above discussion emphasizes the desirability of retaining maximum flexibility in allowing moderator − source modification in the reactor design. In addition to the desire to allow optimization for different experimental needs, separate and frequent maintenance on cold moderators should be allowed for until enough experience has been obtained to demonstrate the lack of such need or how to design around the need. Aside from the practical engineering considerations, maximum source intensities (as discussed previously) will probably negate the perpendicular-moderator scheme because maximum total intensities are obtained by use of the largest F_1 and the total area possible. The subject is by no means closed, and the need for flexibility to allow for moderator modifications is enhanced thereby.

The previous discussion has been almost exclusively directed toward neutron beams, but important experiments must be carried out

near the reactor. One case that should be mentioned is that of neutron reactors where it is important to optimize the flux. Here advantage can be taken of the time-dependent moderation of the neutrons as the Russians[9] have done in their slowing-down spectrometer by using a lead moderator. Here the neutron hold-up in time, because of low energy loss per collision, yields markedly enhanced resonance fluxes and time separation giving $\sim 30\%$ fractional energy resolution. High peak 1/E pulse fluxes can be expected. The optimum reactor pulse width will vary rapidly with energy. For 5-μsec reactor pulses the optimum flux starts at 50 to 100 ev and remains for lower energies. The upper limit can be extended by lowering the reactor pulse widths if the same peak power is retained.

ACKNOWLEDGMENT

REFERENCES

1. R. G. Fluharty, F. B. Simpson, G. J. Russell, and R. H. Morris, A Proposal for a Repetitively Pulsed Test Facility, USAEC Report IN-1149, Idaho Nuclear Corp., 1967.
2. J. A. Larrimore, Physics of Periodically Pulsed Reactors and Boosters; Steady-State Conditions, Power Pulse Characteristics, Kinetics, *Nucl. Sci. Eng.*, 29: 87 (1967).
3. R. G. Fluharty, in *Neutron Time-of-Flight Methods*, p. 383, Symposium Proceedings, European Atomic Energy Community, Brussels, 1961.
4. E. A. Knapp, Los Alamos Scientific Laboratory, private communication, 1969.
5. B. M. Carmichael, Los Alamos Scientific Laboratory, private communication, 1969.
6. M. M. R. Williams, *The Slowing Down and Thermalization of Neutrons*, John Wiley & Sons, Inc., New York, 1966.
7. R. G. Fluharty, F. B. Simpson, G. J. Russell, and J. H. Menzel, Moderator Studies for a Repetitively Pulsed Test Facility, *Nucl. Sci. Eng.*, 35: 45-69 (1969).
8. J. Koppel, Time-Dependent Neutron Spectra, *Nucl. Sci. Eng.*, 8: 157-163 (1960).
9. A. A. Bergman, A. I. Isacoff, I. D. Murin, F. L. Shapiro, I. V. Shtranikh, and M. V. Cazarnovsky, A Neutron Spectrometer Based on Measuring the Slowing-Down Time of Neutrons, in *Proceedings of the International Conference on the Peaceful Uses of Atomic Energy, Geneva, 1955*, Vol. 4, p. 135, United Nations, New York, 1956.
10. A. Michaudon, The Production of Moderated Neutron Beams from Pulsed Acceleration, *Reactor Sci. Tech.*, 17: 165 (1963).
11. R. L. Macklin and J. A. Harvey, Oak Ridge National Laboratory, private communication, 1966.

DISCUSSION

HENDRIE: There was an elevation of the core and of the rotors either with or without fuel running just below the core. Have you looked at the reactivity swing as a function of the separation of the rotor surface from the lower core surface?

FLUHARTY: No, we have not. Geometrically, the rotor is large enough; so it looks as if we could stand separations of the order of inches without serious loss in the reactivity because of the relative size of the paddle. In other words, the paddles are large compared to inches.

HENDRIE: I expect this might be true for a fueled slug on the rotor. I wonder if it is true for a reflector block. The SORA people found a very strong reactivity-swing dependence on that separation.

FLUHARTY: They were more worried about rates than we are. We have proposed to operate this as a pulsed reactor, but, if we do, we are going to have to look at questions like this more closely. For a booster or accelerator pulsed reactor these problems are not nearly as severe.

HENDRIE: We would like to use something like that on our version, but we find such a strong reactivity dependence that it just gets out of hand.

BLOKHINTSEV: What power do you intend to develop in your booster installation?

FLUHARTY: We are in the neighborhood of your proposal with an average power of 3 Mw. This figure looks very conservative, and it seems reasonable to go on up to 6 Mw. The volumes we are talking about are in the range of 6 to 10 liters.   '

BLOKHINTSEV: What about a realization of your idea?

FLUHARTY: You mean where do we stand in terms of actually getting on with the job? We are still very much in the proposal stage; as you can see, what we are talking about here is a concept. The engineering ideas have been looked at, and they seem to be conservative—less than 10° rise in the fuel per pulse. We are comparing with steady-state systems, and it is not a big extrapolation on that basis. But we are just proposing at this point.

3-4 OAK RIDGE UNION CARBIDE Y-12 REPETITIVELY PULSED EXPERIMENT

J. T. MIHALCZO
Union Carbide Corporation, Nuclear Division, Y-12 Plant,
Oak Ridge, Tennessee

Editors' Note: This paper was unavailable for publication.

3-5 SORA

J. A. LARRIMORE, R. HAAS, K. GIEGERICH, V. RAIEVSKI, and W. KLEY
EURATOM, Ispra, Italy

ABSTRACT

The pulsed reactor SORA, designed at the Common Research Center of EURATOM at Ispra as a source for neutron-physics experiments, is described. The design of the reactor facility and its operational characteristics are reviewed, and operational control and safety and reactor safeguard considerations are discussed.

INTRODUCTION

The SORA reactor is a pulsed fast reactor designed at the Common Research Center of EURATOM at Ispra to serve as a neutron source for beam research in neutron and condensed-state physics using the time-of-flight measurement technique.* Construction has been proposed at Ispra as a replacement for the existing 5-Mw heavy-water research reactor and as an important step in the development of pulsed reactors as intense neutron sources.

Detailed design studies on SORA started in 1963. From July 1964 to January 1966, the design and specifications for the entire reactor plant were prepared under a contract between EURATOM and the consortium BELGONUCLEAIRE/SIEMENS–SCHUCKERTWERKE. A critical-experiment program for SORA was carried out under a EURATOM–U. S. Atomic Energy Commission agreement at Oak Ridge National Laboratory from the fall of 1965 to the fall of 1966. Numerous theoretical and experimental studies in reactor physics and design,

---

*The term "pulsed reactor" is used to describe a reactor that is periodically, or repetitively, pulsed by reactivity insertions.

experimental facilities, safety, dynamics, and control have been carried out at Ispra.

The SORA reactor design and experimental use have been described at previous stages in its development, notably at Karlsruhe in 1965[1] and at Santa Fe in 1966.[2] In this paper we review the design of the reactor facility and its operational characteristics, and we discuss operational control and safety features and reactor safeguard considerations.

DESCRIPTION OF THE REACTOR FACILITY

The layout of the SORA reactor facility has been established on the basis of experimental, operational, and safety requirements. Experimental requirements, similar to those for steady-state reactors used for neutron-beam experiments, are: a variety of types of neutron sources, good access to the neutron sources, good shielding to reduce experimental background, adequate space for experimental setups, plus a few special requirements, e.g., the possibility of extending beams beyond the reactor building.

The layout follows the lines of other research reactors. The experimental and operational areas are separated as much as possible, allocating almost the entire area above the main floor to the experimenters and almost the entire basement area to the operators. For this reason and for safety reasons, we have located practically all the core cooling-loop components in the basement. Handling of the core, the vessel internals, and the pulsation device is done above the main floor.

Safety considerations have played a major role in establishing the plant design and operating conditions. In addition to many normal operational provisions, ultimate safety is assured by a two-barrier containment: the reactor block shield as containment for explosive effects and the steel reactor building as containment for any fission-product activity released.

Figure 1 is a cutaway view of the reactor showing the general arrangement. In this section some details about the various parts of the reactor will be given.

The Core

The key to optimized performance of a fast pulsed reactor (or accelerator pulsed reactor) is small core volume, giving low prompt-neutron generation time, high worth of external reflectors, and a high ratio of leakage neutrons to fission neutrons. Attaining a small core volume means minimizing coolant and structural volume fractions. By
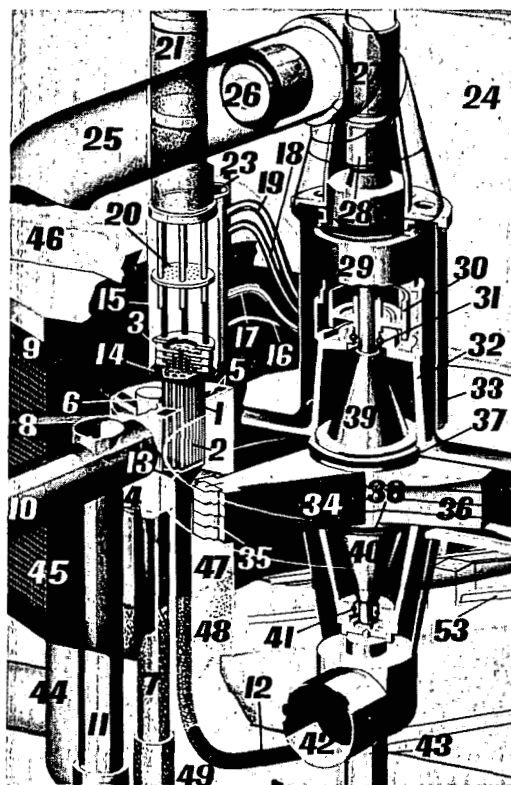
Fig. 1 — *Cutaway view of SORA.*

(1) Fuel element
(2) Core window
(3) Subassembly support plates
(4) Reflector
(5) Control rods
(6) Moderator
(7) Moderator loading tube
(8) Horizontal beam tube
(9) Slanted beam tube
(10) Large beam tube
(11) Irradiation tube
(12) Coolant inlet pipe
(13) Lower plenum
(14) Vessel support rim
(15) Upper plenum
(16) Auxiliary-loop outlet
(17) Main-loop outlet
(18) Overflow line
(19) Cover-gas line
(20) Core hold-down structure
(21) Vessel shield plug
(23) Vessel instrumentation extension
(24) Pulsation cell
(25) Cooling-gas inlet pipe
(26) Cooling fan

(27) Connector for electrical connec-
     tions
(28) Rotor-positioning drive
(29) Main drive motor
(30) Barrel for position indication
(31) Main rotor bearing
(32) Helium-tight rotor housing
(33) Housing for cooling-gas flow
(34) Main rotor arm
(35) Beryllium reflector block
(36) Balancing arm
(37) Upper emergency bearing
(39) Upper shaft butt
(40) Lower shaft butt
(41) Lower bearing
(42) Cooling-gas outlet
(43) Connector for helium and lubri-
     cation
(44) Graphite-shield coolant inlet
(45) Graphite shield
(47) Lower reflector
(48) Shield block
(49) Shield block
(53) Pulsation-device rails

using an array of fuel elements with rather large diameter (15 mm) rods in close-packed hexagonal geometry, we attain in SORA a fuel volume fraction of 0.79 and a total core volume of less than 6 liters. The core cross-sectional area is about the same as that of a water-reactor subassembly. However, for easing nuclear-safety problems during fuel loading, unloading, and storage, the core is divided into three concentric subassemblies, and the inner subassembly, a central seven-rod cluster, is loaded last. This division into subassemblies also eased the cooling requirements (for which we use gas) during fuel handling. It did, however, raise a question about clearances necessary in the core for loading and unloading the subassemblies without damaging the fuel elements. Tests recently completed on a core mock-up indicate that small clearances are required, which should not cause other problems.

The close packing of the fuel elements causes circumferential variations in the heat removal from the fuel element which, in turn, cause circumferential temperature variations in the cladding (see Core Heat-Removal Characteristics). These temperature differences cause axial thermal stresses considerably larger than other types of cladding stresses expected and create the possibility of thermal-stress fatigue due to start-up—shutdown cycles. This factor has led us to consider alternate cladding materials for SORA, materials having higher yield strength or better conductivity than stainless steel. With the use of an Inconel, a power level of 1 Mw in SORA will be possible without difficulty.

Regarding the choice of a uranium alloy for SORA, the advantages of the fuel used in the Experimental Breeder Reactor No. 2 (EBR-2), U-5 wt.% Fs, over U-9 wt.% Mo becomes increasingly evident: 9% higher uranium density, 20% higher thermal conductivity, and the rapidly deepening understanding of swelling behavior under irradiation. It seems completely reasonable[3] to expect 0.8 at.% burnup with less than 5 vol.% swelling at central temperatures up to 550°C. This corresponds to an irradiation life of about 1.5 years for the highest rated fuel and 2.5 years for average rated fuel, at 1 Mw mean power.

Pulsation Device

The design of the pulsation device was developed with the criterion that the overall mechanical reliability had to be as high as possible considering that certain parts are subject to wear and to radiation damage. The resulting basic features are:

1. Vertical axis of the device.

2. Symmetric rotor design relative to rotor vertical midplane.

3. Compact, transportable, and exchangeable unit that does not require adjustment after installation in the reactor block.

4. Provisions for maintenance and inspection outside the reactor block to guarantee that the pulsation device maintains the characteristics of a new device during operation periods.

The materials were chosen on the basis of performance characteristics and neutron activation.

The use of beryllium as a moving reflector has several significant advantages: high reactivity worth as a reflector, low weight, and low activation. Beryllium also has good strength and reasonable ductility in the operating-temperature range of 100 to 200°C. At these temperatures fast-neutron irradiation results in an increase in strength and a loss of ductility owing to helium production [mostly from $(n,2n)$ reactions], which will limit the lifetime of the beryllium in SORA to a few years. For this reason, annual or biannual replacement of the pulsation-device rotor is foreseen during the first years of operation, and we expect that eventually only replacement of the beryllium pieces will be necessary. For reasons of safety as well as fabrication, the total beryllium reflector is divided into four blocks, 6 cm high, 11 cm wide, and about 7 cm thick.

The beryllium pieces are attached at the end of the long arm of a three-armed propeller, the two balancing arms being shorter to reduce their reactivity effect when they pass near the core. The rotor and conical hollow-shaft butts are made of the well-known Ti−6 wt.% Al− 4 wt.% V alloy that provides a high strength-to-weight ratio and low activation under irradiation. The rotor is made up of four identical layers 6 cm high, to each of which is keyed one beryllium block. The connections are made by three high-strength-steel keys, each of which takes a centrifugal force of 2.5 tons during operation at 3000 rpm. These keys are prestressed by four titanium wedges so that elongation will not occur at rotor speeds up to 4000 rpm.

The mechanical safety factors, considered as the ratio of maximum stress to yield or ultimate strength, at operating conditions are high in comparison with those used in the design of other rotating equipment. The minimum safety factors against yield stress are 3.3 in the beryllium, 3.8 in the steel keys, 3 in the fixation region of the titanium rotor, and 8 in the rest of the titanium rotor, which is designed for uniform stress. The separation of the beryllium and rotor into four separate pieces and the use of the three-key connections give additional high reliability against a sudden breakage of a large segment of the beryllium or its fixation.

The rotor operates in a narrow leak-tight housing filled with helium gas to reduce friction power. The use of helium also limits the Mach number to 0.3. The aluminum-alloy housing is designed to have a high rigidity. Part of this rigidity is supplied by external fins provided to assist the transfer of the friction heat from helium through the

housing to a special nitrogen cooling circuit. This circuit passes 9000 m^3/hr of nitrogen (S.T.P.) between the housing and an outer aluminum casing to remove approximately 30 kw of heat. The thin flat window in the housing, next to the core, presents no fabrication problem. This window, a square plate of forged aluminum with 2-mm minimum thickness, is welded into the housing ring with controlled prestress to increase its stability.

The rotor shaft butts are supported by oil-lubricated bearings, the upper one supporting the rotor weight and the lower one serving only for radial guidance. In addition, emergency graphite bearings above and below the rotor, with 0.25-mm normal radial clearance, assure support of the rotor during stoppage in case of a serious failure of a bearing.

The upper rotor shaft butt is connected through a tooth coupling to the motor shaft; a torque limiter is positioned between so that, in case the motor shaft should seize, the rotor may spin to rest without interference. The motor is a two-pole asynchronous motor with a squirrel-cage rotor fed by a special power transformer that provides the desired velocity control of better than ±0.5%. An electromagnetic brake, a geared pickup barrel for position signals, and a slow-speed positioning drive with electromagnetic clutch are also provided.

Reflector and Controls

The reflector that surrounds the core on five of its six sides has been designed to:

1. Provide a second containment for the active NaK circuit in the core region.

2. Efficiently reflect fast and intermediate neutrons back to the core.

3. House the seven control and safety rods and the two moderator cryostats.

4. Prevent the return of thermal and epithermal neutrons from the scatterers and thermal shield to the core.

5. Permit an efficient conversion of fast neutrons to slow neutrons in the moderators.

The second vessel containment system is provided by a steel layer that closes off the reflector from the vessel and other surroundings. An inner region of the reflector is made of a good fast reflecting material, a W−Ni alloy, which also has the advantage of good epithermal-neutron absorption. The high conductivity of this material aids the transfer of heat deposited by gamma rays to nitrogen coolant flowing in channels located at the front and rear. Surrounding and supporting the inner reflector region is a stainless steel structure that also guides the control rods and moderators.

Separation between the thermal-neutron sources and the core is provided by an absorber layer located between the W−Ni alloy and the stainless steel parts of the reflector and around the front of the two moderator cryostats. The absorption capability is specified as equivalent to 0.25 g/cm^2 of ^{10}B for neutron energies up to 10 ev.

Seven reflector control rods perform the required safety, regulation, and reactivity compensation functions. The safety and reactivity compensation rods are located as close as possible to the core to obtain maximum reactivity worth. Smaller reactivity worth is required for the automatic control rods, one fast-acting rotary and one slow-acting, and they are located farther from the core.

Experimental Facilities

The two principal neutron sources are located in cryostats placed in the 14-cm-diameter vertical holes in the reflector, close to the core. Each cryostat feeds four horizontal 10-cm-diameter beam tubes, two centered at 6 cm above core midplane and two centered at 6 cm below core midplane. This arrangement will allow the moderator geometry and composition to be optimized differently for the upper and lower set of beam tubes. For example, in the cold source, which is planned for the central cryostat, one part may include a beryllium filter and the other may not.

The preliminary layout of the cold source has an inner half-cylinder of ice (volume about 1.5 liters) and outer half-cylinder of beryllium. The cooling of the estimated 800 watts is performed by a liquid-nitrogen or gaseous-helium loop. For the thermal source, a volume of about 1 liter and a heat generation of about 500 watts is estimated.

Additional experimental facilities include four slanted beam tubes viewing the upper layers of the two cryostats, two horizontal beam tubes for fast neutrons oriented toward the core window, and a large-diameter (30 cm) special-purpose beam tube intersected by a vertical irradiation tube.

Flanged penetrations through the reactor building are provided for each horizontal beam tube, and an area of up to 100 m is available outside the building for experimental purposes. In the direction of one of the fast-neutron beam tubes, a distance of 1000 m is available.

Reactor Block and Shields

The reactor block shield surrounding the core and the so-called "pulsation cell" where the pulsation device is located is made of heavy concrete with steel reinforcement except for the inner 40 cm surrounding the pulsation cell, which is made of special borated concrete. This layer and the aluminum covering of the pulsation cell reduce the

activation level inside the reactor block. A movable lead shield located in the cell is provided to shield core radiation when the pulsation cell is opened with the fuel in place. A graphite thermal shield is located between the reflector and the concrete shield in the beam-tube area to reduce the heat generation level in the concrete. This graphite layer is covered with boral to absorb the thermal neutrons produced, and it is cooled on its surfaces by nitrogen-gas flow. The heat generation is estimated to be 10 kw, almost all of which is due to neutron capture in the boral.

Cooling Circuits

The core heat is transferred through primary and secondary NaK circuits and rejected to the atmosphere in air-cooled heat exchangers. A 50-kw auxiliary NaK system is provided for shutdown cooling. Cooling of the friction heat of the pulsation device and the heat generated in the reflector, controls, and shields, as well as the room containing the NaK loops, is by nitrogen circuits that transfer the heat through freon secondary systems to water-cooled terminal heat exchangers.

Handling of Activated Parts

The fuel subassemblies are transferred from the core to a hot cell in the basement and vice versa in a special transfer machine that is handled by the building crane. Inert-gas cooling is used during transfer operations. A second simpler machine is used for handling other reactor-vessel internals (shield block, instrumentation insert). The pulsation device is moved within the pulsation cell from outside with special manipulators at the back of the cell and is handled by the building crane through a top hatch in the block shield. A special warm workshop for maintenance and testing is being planned adjacent to the reactor building. Control rods and moderator cryostats are handled in a room below the reactor block from which access is provided to the hot-cell area.

Nuclear Control and Safety Instrumentation

Nine neutron-detection channels are provided: two start-up channels, two mean power (log) channels, three safety channels, and two movable-control channels. The detectors view the thermal-neutron pulse in the graphite, which has a peak-to-average value of about 15 and a width of about 1 msec. Timing signals are obtained from the pulsation device. Conventional detection chains have been adopted for the nuclear instrumentation although it is planned to incorporate specialized detection chains into the control and safety system at a later date.

OPERATIONAL CHARACTERISTICS

The reactor physics, pulse characteristics, and core heat-removal characteristics are discussed in this section. A summary is given in Table 1.

Reactor Physics and Pulse Characteristics

The reactor physics calculations for SORA concern pulse characteristics, core steady-state design, and moderator design. Develop-

Table 1

PRINCIPAL REACTOR OPERATIONAL CHARACTERISTICS

Reactor Physics Characteristics	
Prompt-neutron generation time, nsec	20
Delayed-neutron fraction	0.0064
Reactivity worth of moving reflector, $\Delta k/k$	0.038
Parabolic reactivity pulse constant (α), $\Delta k/k$ cm^2	5×10^{-4}
Isothermal temperature coefficient, $\Delta k/k/°C$	-1.4×10^{-5}
Total worth of control rods, $\Delta k/k$	0.030
Maximum prompt reactivity at pulsed criticality, $\Delta k/k$	80×10^{-5}
Time-averaged neutron flux in core, neutrons/cm^2/sec	
Total averaged over core	8.7×10^{13}
Above 0.9 Mev averaged over core	4.0×10^{13}
Core volume, liters	6
Core uranium loading, kg	61

Pulse Characteristics	^{235}U (600 kw)	Plutonium (1 Mw)
Pulse frequency, sec^{-1}	50	50
Moving-reflector peripheral velocity, m/sec	283	283
Maximum pulse power, Mw	160	320
Power pulse half-width, μsec	56	54
Ratio of peak to background power	1600	6100
Peak thermal flux in reference central moderator, neutrons/cm^2/sec	1.5×10^{15}	3.6×10^{15}
Thermal-flux half-width in reference central moderator, μsec	75	75

Core Heat-Removal Characteristics (600 kw)	
Average core power density, kw/liter	100
Peak-to-average power ratio	1.6
Average fuel-element linear power, watts/cm	230
Coolant inlet temperature, °C	200
Coolant average velocity, m/sec	6
Average coolant-temperature rise, °C	54
Average heat-transfer coefficient, watts/cm^2/°C	1.5
Maximum fuel temperature, °C	435
Maximum cladding peripheral temperature difference, °C	86
Pressure drop in reactor vessel, kg/cm^2	1.7

ment of new methods was required in all three areas. The latter two areas have been experimentally complemented by a comprehensive critical-experiment program and by moderator experiments.

Both analytical[4,5] and numerical[6] methods for calculating pulse characteristics have been developed. In the analytical work, the original theory of Bondarenko and Stavisskii[7] has been generalized and extended to pulsed boosters. The numerical method is a three-energy-group two-space-region kinetics model using input data obtained from stationary S_N flux and adjoint calculations.

The theoretical methods used for calculating the steady-state physics characteristics have been previously described.[2,8] Both the specially developed Monte Carlo[9] code TIMOC and the S_N codes are used.

Physics design parameters for SORA are now calculated by the following codes:

1. TIMOC: core reactivity, moving-reflector worth and differential reactivity effects (except α), generation time.

2. S_N codes: core reactivity, core power distribution, control-rod worths, core reactivity coefficients, neutron kinetics input data for AIREK-PUL, reactor and moderator flux distributions.

3. AIREK-PUL: core and moderator pulse characteristics in a three-group two-space point model.

No satisfactory method is available for calculating α.

The SORA critical experiment program[10] was performed at the Critical Experiments Facility of Oak Ridge National Laboratory with EURATOM participation from September 1965 to September 1966. These experiments were performed on a rather exact geometrical mock-up of the SORA design. The core was mocked up by highly enriched ^{235}U rods located in vertical holes in an iron matrix. Measurements were made of moving-reflector reactivity worths and pulse shapes for beryllium and iron blocks with widths between 11 and 26 cm and for various window configurations. (The window denotes the structures between the core and moving reflector.) The experimental program also included many measurements of control-rod and simulated-moderator worths and of various reactivity effects.

Larger than expected discrepancies in core reactivity were found in detailed cross-check calculations between the critical experiment and the design by TIMOC and 2DXY codes. These discrepancies have stimulated a cross-section evaluation program based on the ENDF-B cross-section tape. Reactivity calculations as a function of the number of fuel elements in the core for the current reference design are plotted in Fig. 2, which shows a difference of about 4% in k_{eff} and an associated uncertainty in core loading of plus or minus four elements.
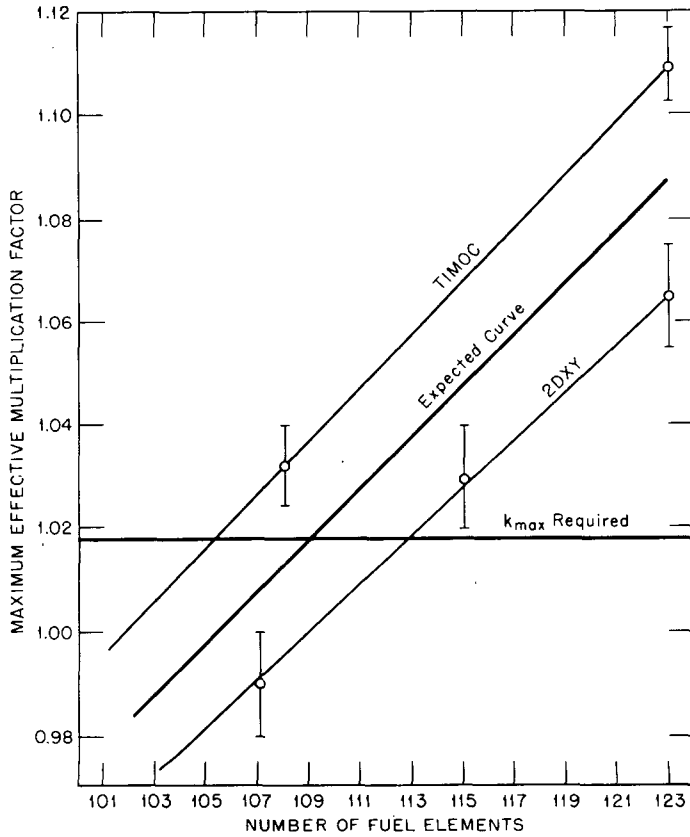
Fig. 2—Maximum effective multiplication factors as a function of the number of fuel elements in the core.

The dependence of the reactivity worth and α value of beryllium moving reflectors on the window thickness, as determined in the critical experiment, is shown in Fig. 3. Lines of constant worth in dollars ($\$1 = 0.0064$) and α in ¢/cm^2 are shown. The present reference design has an 11-cm beryllium reflector and a 10-mm window, giving $5.9 worth and a 7.8 ¢/cm^2 α value. Increase in the beryllium width would improve both worth and α and is therefore under consideration.

The theoretical calculations and experimental measurements for the neutron sources have been discussed previously.[2] In the first series of experiments[11] the relative neutron yields of various moderator configurations at room and liquid-nitrogen temperature were measured. These measurements were extended to determine the time behavior of neutron pulses at single energies.[12] Considerations on the
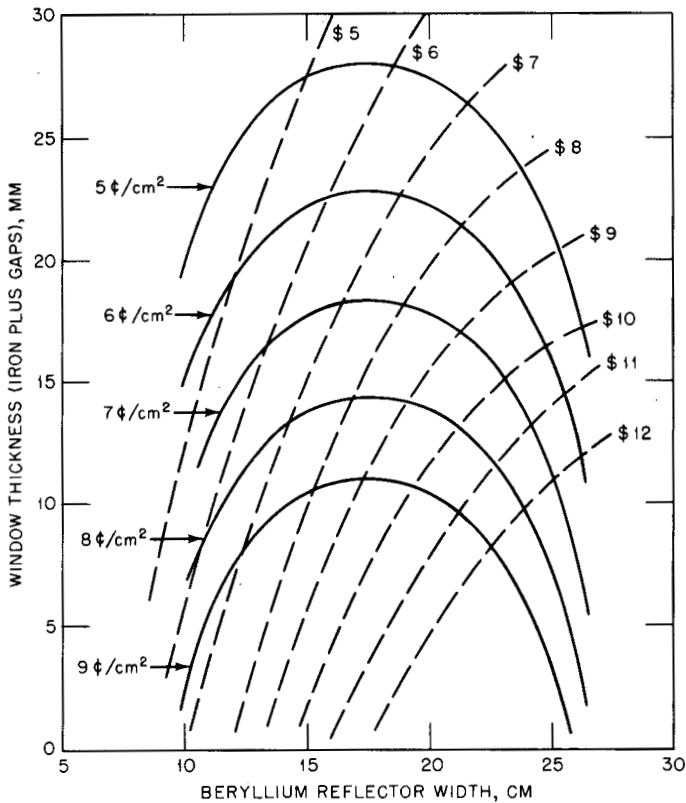
Fig. 3—Beryllium reflector reactivity worths and α values from the SORA critical experiment.

design and optimization of experimental setups at pulsed reactors have developed continuously. [13-16]

Core Heat-Removal Characteristics

In rod bundles with small spacings and liquid-metal cooling, heat transfer to the coolant is closely coupled with heat transfer inside the fuel element. A solution to this problem has recently been completed, and a computer program has been put into operation at Ispra.[17] Heat conduction is calculated in the fuel, bond (or gap), and cladding, including the possibility of anisotropic fuel conductivity (e.g., due to radial cracks). Conduction is considered in the coolant using velocity distributions (as a function of pitch-to-diameter ratio) which were experimentally determined. Neglect of eddy conduction makes the results conservative for Peclet numbers above several hundred, but this effect

is of small importance in SORA or similar systems. The results show a large reduction in average heat-transfer coefficient, in comparison with annular geometry, and illustrate the importance of good fuel, bond, and cladding conductivities in improving peripheral conduction and in thereby reducing circumferential temperature differences in the cladding.

Results are shown in Table 1 for NaK coolant (200°C inlet temperature, 6 m/sec velocity), stainless steel cladding (0.3 mm), sodium bond (0.2 mm), and U−5 wt.% Fs fuel. Parameter calculations have been performed to evaluate the effect of material conductivities and dimensions on maximum fuel temperature and maximum cladding peripheral temperature difference.

OPERATIONAL CONTROL AND SAFETY

Control and Safety Systems

The reactivity of the reactor is controlled by seven rods serving the following functions (P = pulsed operation; S = stationary operation):

ROD	FUNCTION
Safety rods (2)	Fast scram
Fast control rod	P: fast automatic control
Slow control rod	P: automatic compensation of fast control rod
Regulation rod	Start-up; S: automatic control
Adjustment rod	P: reactivity compensation from delayed to prompt criticality
Compensation block	Long-term reactivity compensation

Mock-up testing of pneumatically actuated drives for the fast safety rods have been carried out on two systems, one using fast-opening valves and the other using a pneumatic−mechanical latch system. The first, on which testing is more advanced, has demonstrated initial rod movement of 5 cm within 42 msec after a scram signal. This performance is within the specification that the reactor be shut down within two pulses after a high-pulse scram signal.

The automatic control function in pulsed operation is divided among two rods for greater safety: a rotary rod with 10 pcm* worth and a maximum speed of 1 rps and a vertically operated rod with about 40 pcm worth and a maximum insertion speed of 1.4 pcm/sec. The

---

*The abbreviation pcm is a very convenient unit of absolute reactivity: 1 pcm = $10^{-5} \Delta k = 10^{-3}\% \Delta k \cong .00001$ change in reactivity.

slow rod centers the fast rod in its range. The fast rod is driven by a
d-c motor, with low time constant and high rotor inertia, directly
connected to the control-rod shaft.

The safety system is divided into two interconnected parts, the
nuclear-safety system and the pulsation-device safety system. This
division results from the requirements to operate the pulsation device
with the reactor shutdown and to operate the reactor in both pulsed and
stationary modes. The nuclear-safety system initiates two safety
actions: fast scram by rapid removal of the two safety rods, backed up
by removal of other rods, and slow scram by extraction at normal
speed of the safety and other rods. The pulsation-device system ini-
tiates two principal safety actions: fast stoppage of the rotor (in about
5 min) and normal stoppage of the rotor. These two safety systems are
interlocked to provide the necessary shutdown action for reactor and
pulsation device, depending on the type of malfunction signal.

Operational Characteristics

Requirements for reactivity control during reactor operation arise
from long-term reactivity effects, relatively prompt-acting effects, and
scram and shutdown considerations. Operational reactivity inventory
diagrams in Fig. 4 show the maximum reactivity condition and the
pulsed and stationary operating conditions at the beginning of fuel life.
The excess reactivity requirement of 1830 pcm (0.0183 Δk) above de-
layed critical includes allowances for the difference between delayed
and pulsed criticality, fuel burnup and swelling, changes in moderators,
fuel-loading reactivity step, and reserve.

The similarity of pulsed and stationary reactor kinetics has been
previously discussed.[5,7] The usual inhour equation can be used for
mean power periods if a fictitious delayed-neutron fraction is intro-
duced. This has the value 31 pcm for SORA. The percentage variation
in the peak pulse power caused by small variations in the peak prompt
reactivity is about 4% per pcm.

During start-up in the pulsed mode, the dependence of the pulsed
reactor multiplication factor[4,5] K on the peak reactivity is important.
This relation is shown for SORA in Fig. 5. Also shown in Fig. 5 is the
subcritical source multiplication m, defined for a pulsed reactor as
$K/\beta(1 - K)$. In routine start-up after establishing the core-cooling con-
ditions, the pulsation device is started, bringing the source multiplica-
tion to about 20. The two safety rods, the compensation block, and the
adjustment rods are inserted in sequence. The reactor is then about
600 pcm subcritical, with source multiplication about 30 and K = 0.16.
The regulation rod is then introduced continuously up to about 50 pcm
below pulsed subcriticality. At this point the actual critical approach
begins, and the reactivity insertion rate is progressively reduced from
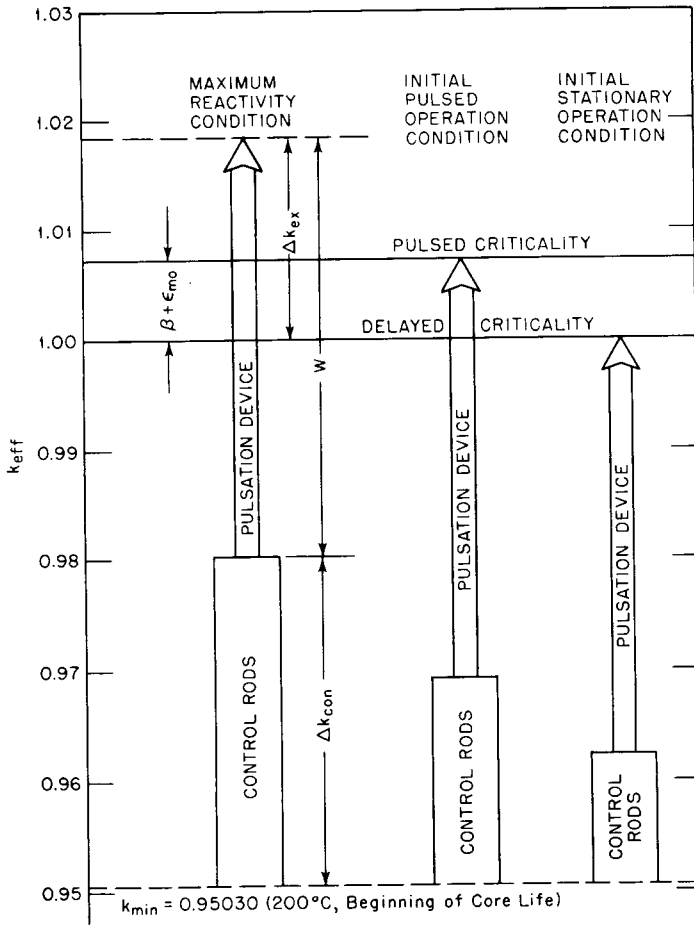
Fig. 4 — Reactivity inventory diagrams.

3 pcm/sec to 0.3 pcm/sec. An interlocked semiautomatic procedure for constant period is presently being considered.

Associated Studies

Two studies connected with evaluation of operational control and safety are worthy of note. The first is a reactor simulation and control study aimed at providing the information concerning the transient behavior of the reactor needed for the design, for operation, and for safety analyses. Initially a mean value (i.e., period-averaged) kinetics model was studied using both a digital program and transfer-function analysis. The model included two-temperature thermal feedback and a
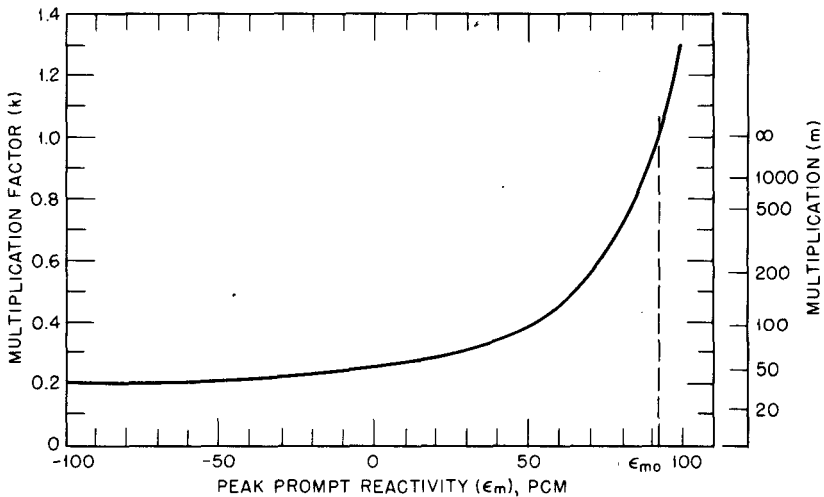
Fig. 5 — Multiplication factor K and multiplication m vs. peak prompt reactivity.

fast control loop, which was optimized using transfer-function techniques. Problems studied included reactor start-up and system response (with and without control) to reactivity, coolant inlet temperature, and coolant velocity step and ramp changes.

More recently, a discrete-time simulation was begun using a discrete-neutron kinetics model for pulsed reactors[18] in which the time behavior of the delayed-neutron precursor concentrations is considered explicitly only just before and just after each power pulse. The power pulse is represented by a delta function, and a general integration of the precursor equations between pulses is used. A multiprecursor-group treatment has been included in a digital simulation code, including thermal and control feedbacks. A one-precursor-group treatment will be incorporated in a digital-analog pulsed reactor simulator. At the present time, reoptimization of the fast control loop is underway.

The second study concerns the effects of pulsing on the SORA fuel element. First results reported[19] showed the distribution of the available vibration energy between the fuel and the cladding and the maximum stresses to be expected from single pulses. Limits for fuel-element damage due to pulsing effects were shown to be far above operating conditions. More-recent work has focused on the damping of the vibrations between two pulses. The dominant damping effect will be contact between fuel and cladding at the bottom of the element. Experimental measurements have shown that internal friction in the fuel and viscous effects at the surface will not be important.
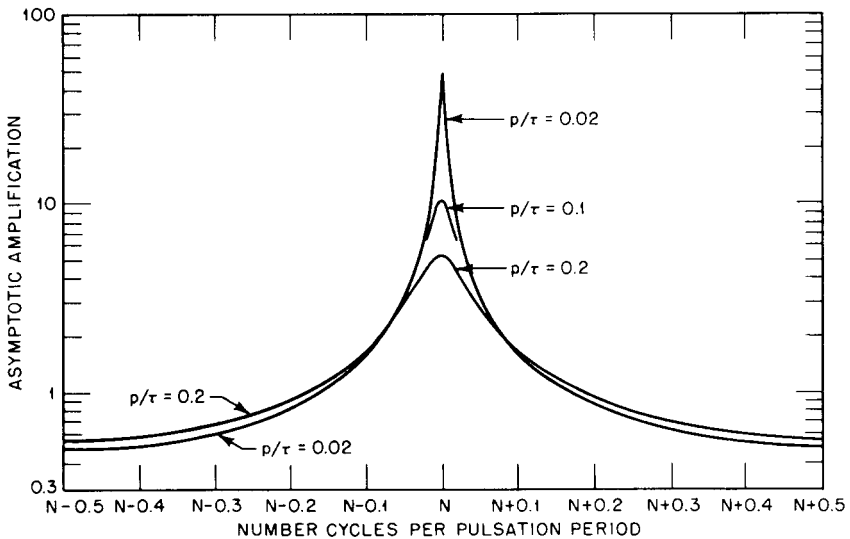
Fig. 6 — *Asymptotic amplification, A, as a function of the number of cycles per pulsation period, fp, for various values of the damping, p/τ. (τ is damping time constant and p is the pulse period.)*

A theoretical study of the buildup of vibration amplitude due to repeated pulsing has given significant results.[20] When the fundamental vibration frequency of the fuel slug is not an exact multiple of the reactor period, destructive interference occurs. Curves of asymptotic amplifications, i.e., amplitudes relative to single-pulse amplitudes, vs. the number of fuel vibration cycles per pulsation period are shown in Fig. 6 for three values of damping. The peak amplification, which occurs when $fp = N$ is an integer, is $1/[1-\exp(-p/\tau)]$ where p is the pulse period, τ is the damping time constant, and fp is the number of fuel vibration cycles per pulsation period. For 65% of the frequency range, however, the maximum amplitude is less than the single-pulse amplitude, quite independent of the magnitude of damping. Calculations of the transient buildup in pulse amplitude show that this buildup takes several seconds. In SORA the effective damping caused by contact of the bottom of the fuel with the cladding is expected to be so large that no appreciable amplitude buildup occurs.

REACTOR SAFEGUARDS ANALYSIS AND STUDIES

Considerable effort has been devoted to assessing the operational and ultimate safety of SORA. Recently a thorough study of conceivable malfunctions was completed which confirmed the large margins of safety provided by inherent and design features of the reactor.

The most severe accident conditions are connected with reactivity incidents. Three types have been identified: accidents due to breakage of the pulsation device, reactivity insertions with the pulsation device running normally, and a core melting—reassembly accident caused by complete failure of the primary cooling system. The maximum credible accident is attributed to a particular specific failure of the pulsation device — the sudden breakage of the reflector-block fixation region in a titanium rotor layer.

Several new codes have been developed for analyzing the reactivity accidents. The DOPPELAS program[21-23] computes the temperature rise in the fuel during an excursion due to a step reactivity input between two pulses, with allowance for a prompt Doppler feedback (positive in SORA) and an inertially delayed negative axial thermal-expansion feedback. DOPPELAS has been used to establish fuel-element damage thresholds for ramp reactivity insertions with the pulsation device running normally. These thresholds are given in Table 2 for

Table 2

THRESHOLD REACTIVITY RAMP RATES FOR FUEL-ELEMENT DAMAGE
OR MELTING, $/SEC

Pulse after start of ramp	6-mw power level		600-kw power level	
	Fuel-element damage	Fuel melting	Fuel-element damage	Fuel melting
1	25	27	7.2	8.9
2	12.5	13	3.6	4.5

source power and full power. The lowest is $3.6/sec, which would cause fuel-element damage on the second pulse after start of the reactivity insertion. The safety system will shut down the reactor by the third pulse. The largest accidental reactivity ramp rate identified in the analysis of malfunctions was $0.01/sec, which would not cause system damage even if the safety system was inoperative.

For the evaluation of severe transients, including those resulting from assumed fractures of the pulsation-device rotor, the SOREX-1 code has been developed.[23,24] This code includes models to evaluate the reactivity input caused by breakage of the rotor: kinetic behavior of the broken fragment, compression of the core by the broken fragment, and axial expulsion of the coolant during the compression pulse. The nuclear excursion is evaluated using the modified Bethe—Tait method for an equivalent sphere with rigid outer boundary. The fuel equation of state used in SOREX-1 has been evaluated using the corresponding-states correlation; the results of a Van der Waals model were used as independent corroboration.

In accordance with the philosophy of the preliminary safeguards evaluation, conservative assumptions have been made at each stage of the calculational models previously mentioned. The largest credible energy release has been conservatively estimated to be 430 Mw-sec total energy, of which 325 Mw-sec is available for mechanical destruction. The initiating event for this accident is the instantaneous fracture of the fixation region of one pulsation-device rotor layer at an angle of 10.8° before it reaches the center-window position. Although these energy releases are the basis for the containment evaluation and specification, further development of the excursion analyses to represent both the actual design and the physical models more realistically is expected to result in a large reduction in the maximum credible accident.

The reenforced-concrete reactor block contains the explosive effects of any destructive reactor accident. The initial feasibility was shown using an equivalent static-pressure method for spherical geometry which allows for both shock and blast pressures. A combined theoretical−experimental program was started in 1967 to treat in more detail the actual geometry and special parts. The experimental program, using conventional explosives in scaled models, is aimed at providing data on shock and internal-missile effects in real geometry, blast pressure buildup and decay, behavior of reenforced concrete under explosive loadings, and shock-wave destruction in the beam-tube channels. From the first test series significant results are now being obtained for model laws and for gas-exhaust and heat-sink effects on blast-pressure decay. This program has already considerably deepened our understanding, and we expect it to provide us with the information necessary for assuring adequate and realistic excursion containment.

CONCLUSIONS

The additional design and development work for the SORA reactor since the SINS meeting in September 1966 has further confirmed the conclusions in our paper presented at that meeting.

SORA does not pose particularly difficult operational or safety problems. Experimental and theoretical physics studies have confirmed the suitability of reflector pulsing used in SORA and have shown that SORA will be an excellent thermal- and cold-neutron source for time-of-flight experiments. Control and safety studies indicate that normal operational control can be readily performed and that malfunctions will not cause damage to the reactor or danger to operating or experimental personnel. Studies also demonstrate that the containment system provided will assure that the maximum credible

accident does not cause a significant hazard to the surrounding population.

DISCUSSION

V. R. NARGUNDKAR (letter to G. R. Keepin after the conference): Our department has planned to build a pulsed fast reactor. I am giving some of its features here. The pulsed fast reactor will be fueled with PuO_2, and a molybdenum − iron reflector will be used. The average power will be about 30 kw, and forced-air cooling will be used. The reactor will be reflector pulsed, with a 50-μsec pulse width and a repetition rate of 50 pulses/sec.

I have been associated with this project for a year or so. We have finalized the design of the critical facility, and we expect to reach criticality in early 1970 and to continue critical experiments for 2 years. The pulsed fast reactor is expected to be ready around 1973.

REFERENCES

1. V. Raievski et al., The Pulsed Fast Reactor as a Source for Pulsed Neutron Experiments, in *Pulsed Neutron Research*, Symposium Proceedings, Karlsruhe, 1965, Vol. 2, p. 553, International Atomic Energy Agency, Vienna, 1965 (STI/PUB/104).
2. J. A. Larrimore, R. Haas, K. Giegerich, V. Raievski, and W. Kley, The SORA Reactor: Design Status Report, in *Intense Neutron Sources*, Seminar Proceedings, Santa Fe, 1966, USAEC Report CONF-660925, 1967.
3. Argonne National Laboratory, Reactor Development Program, Progress Report January 1968, USAEC Report ANL-7419, p. 56, Argonne National Laboratory, 1968.
4. G. Blaesser, R. Misenta, and V. Raievski, The Kinetic Theory of a Fast Reactor Periodically Pulsed by Reactivity Variations, EURATOM Report EUR-493, 1964.
5. J. A. Larrimore, Physics of Periodically Pulsed Reactors and Boosters: Steady State Conditions, Power Pulse Characteristics and Kinetics, *Nucl. Sci. Eng.*, 29(1): 87 (1967).
6. T. Asaoka and R. Misenta, Kinetic Theory and Calculations in a Few-Energy-Group Two-Space-Point Model for a Fast Reactor Periodically Pulsed by Reactivity Variations, EURATOM Report EUR-2273, 1965.
7. I. I. Bondarenko and Yu. Ya. Stavisskii, Pulsed Operation of a Fast Reactor, *At. Energ. (USSR)*, 7: 417 (1959); translation in *J. Nucl. Energy, Parts A and B*, 14: 55 (1961).
8. H. Rief, H. Kschwendt, and R. Jaarsma, Reactivity Calculations for a Periodically Pulsed Fast Reactor by the TIMOC Code, paper presented at the International Conference on Research Reactor Utilization and Reactor Mathematics, Mexico City, 1967.
9. H. Rief and H. Kschwendt, Reactor Analysis by Monte Carlo, *Nucl. Sci. Eng.*, 30: 395 (1967).
10. G. Kistner and J. T. Mihalczo, Critical Experiments for the Repetitively Pulsed Reactor SORA, USAEC Report ORNL-4263, Oak Ridge National Laboratory, 1968.

11. B. Arcipiani, G. Fraysse, S. Menardi, and G. Riccobono, A Study by Measurements of Neutron Spectra of a Thermal and Cold Neutron Source To Be Used in a Fast Pulsed Reactor, *Energ. Nucl. (Milan)*, 14(3): 151 (1967).

12. G. Riccobono, G. Fraysse, and S. Menardi, A New Evaluation of the Performance of a Thermal and Cold Neutron Source To Be Used in a Fast Pulsed Reactor, *Energ. Nucl. (Milan)*, 15(11): 717 (1968).

13. R. Haas and H. B. Moeller, A Study on the Performance of Neutron Beam Experiments at the Pulsed Fast Reactor SORA, EURATOM Report EUR-490, 1963.

14. W. Kley, The Use of Pulsed Reactors in the Field of Neutron and Solid-State Physics, EURATOM Report EUR-2538.e, 1965.

15. W. Kley, The Use of the SORA Reactor for Neutron Physics Experiments, in IAEA Panel on *Research Applications of Nuclear Pulsed Systems*, Panel Proceedings, Dubna, 1966, International Atomic Energy Agency, Vienna, 1967 (STI/PUB/144).

16. W. Kley, The Use of the SORA Reactor for Neutron Physics Experiments, paper presented at the International Conference on Research Reactor Utilization and Reactor Mathematics, Mexico City, 1967, USAEC Report CONF-670501-17.

17. R. Nijsing and W. Eifler, Analysis of Liquid Metal Heat Transfer in Assemblies of Closely Spaced Fuel Rods, *Nucl. Eng. Design*, in press.

18. G. Blaesser and J. A. Larrimore, Discrete Kinetics for Pulsed Reactors, *Nucl. Sci. Eng.*, in press.

19. J. Randles and R. Jaarsma, Some Problems of Stress Wave Production Encountered in the Study of Pulsed Fast Reactor Dynamics, EURATOM Report EUR-3654, 1967.

20. J. Randles, Amplification of Vibrations Due to the Repetition of Thermal Shocks in a Pulsed Fast Reactor, EURATOM Report EUR-4060, 1968.

21. J. Randles, Feedback Due to Elastic Waves and Doppler Coefficient During the Excursions of a Pulsed Fast Reactor, *J. Nucl. Energy, Parts A and B*, 20: 1 (1966).

22. J. Randles, Accident and Self-Regulation Studies of Pulsed Fast Reactors, *J. Nucl. Energy, Parts A and B*, 20: 713 (1966).

23. J. Randles, Analysis of Accidents in Pulsed Fast Reactors: Computer Programs DOPPELAS and SOREX-1, EURATOM Report EUR-3915, 1968.

24. J. Randles, Theoretical Analysis of Hypothetical Destructive Accidents in a Pulsed Fast Reactor, in *Fast Reactor Physics*, Symposium Proceedings, Karlsruhe, 1967, International Atomic Energy Agency, Vienna, 1968 (STI/PUB/165).

Fast Burst Reactor
Operating
Experience

Session 4

4-1 SURVEY OF FAST BURST REACTOR OPERATING PROCEDURES

ROBERT L. LONG
University of New Mexico, Albuquerque, New Mexico

ABSTRACT

The operating procedures of six of the eight operating fast burst reactor facilities are reviewed. Significant variations both in philosophy and in details of operation are discussed. Some recommendations are made for standardization of operations requirements.

INTRODUCTION

From my experience working at several burst reactors and after carefully reviewing the written procedures for a number of facilities, I have noticed significant variations in the philosophy and details of operations at various facilities. This paper attempts to identify the common practices, as well as the variations. Operations manuals from six of the eight operating fast burst reactor facilities were reviewed with particular attention to (1) staffing requirements, (2) review and approval of experiments, (3) radiological safety control of personnel, (4) reactor check-out and start-up procedures, (5) burst-sequence procedures, (6) maintenance, and (7) emergency procedures.

WRITTEN PROCEDURES AND RECORDS

Table 1 summarizes the information obtained concerning the length of written operating procedures, the amount of detail found in the procedures, and the formal records kept (as identified in the written procedures). As shown in the table, the written procedures vary in length from about 35 to 130 pages. The Super KUKLA and Godiva IV

Table 1

SURVEY OF WRITTEN PROCEDURES

Facility	Length	Amount of detail	Records kept

APRFR
Aberdeen
Proving
Grounds,
Md.
	Operating,
	96 pp.;
	28 figs.*
		Very detailed. Speci-
		fies switches by
		name and tells
		which lights come
		on at a specified
		time, etc.
			1. Operations log
			2. Operations checklists
			  a. Preoperational
			  b. Daily instrument
			  c. Pulse data sheet
			  d. End-of-day
			  e. Steady-state data
			    sheet
			  f. Outdoors operations
			  g. Core assembly
			  h. Weekly and monthly
			3. Instrument calibration
			  card file
			4. Instrumentation and
			  equipment modification
			  repair card file

FBRF
White
Sands
Missile
Range,
N. Mex.
	Operating,
	78 pp.
	Emergency,
	21 pp.
		Quite detailed.
		Specifies which
		switches, which
		lights; etc.
			1. Operations log
			  a. Daily
			  b. Burst operation
			  c. Power operation
			  d. Transport procedure
			  e. Monthly
			2. Burst reactor log of
			  operations
			3. Experimental plan file
			4. Maintenance card file

FRAN
National
Reactor
Testing
Station,
Idaho
	Operating,
	130 pp.
		Step-by-step in-
		struction through
		sequence. Gen-
		erally does not
		refer to specific
		switches, lights,
		etc.
			1. Console log
			2. Bypass log
			3. Experiment log
			4. Burst diagnostics book,
			  FRAN burst form
			5. FRAN prestart-up
			  instrument checklist
			6. Maintenance records

HPRR
Oak
Ridge
National
Labora-
tory,
Tenn.
	Operating,†
	167 pp.
	Emergency,
	10 pp.
		Very detailed.
		The APRFR
		patterned after
		HPRR.
			1. Operations log
			  a. HPRR check-out
			    sheets
			  b. Steady-state log
			  c. Burst log sheets
			2. General operations log
			3. Trouble log
			4. Experiment log
			5. Maintenance card file
			6. Reactor controls change
			  memorandums
			7. HPRR change memo-
			  randums

Table 1 (Continued)

Facility	Length	Amount of detail	Records kept

SPR II
Sandia
Labora-
tory,
N. Mex.
	Operating,‡
	62 pp.
	Emergency,
	10 pp.
		Brief step-by-step
		instructions. Does
		not refer to specific
		lights, switches,
		etc.
			1. Operations log
			   a. Daily checklist
			   b. Monthly checklist
			2. Burst operations log
			3. Experimental request
			   file

VIPER
Atomic
Weapons
Research
Estab-
lishment,
United
Kingdom
	Operating,
	35 pp.
	Emergency,
	3 pp.
		Step-by-step instruc-
		tions through se-
		quences. Generally
		does not refer to
		specific switches,
		indicators, etc.
			1. Detailed operating log
			2. Physicists' log
			3. Trip sequence record
			   book
			4. Operating certificate
			   file
			5. Pulse summary log
			6. Critical approach file
			7. Core lattice records
			8. Fissile materials
			   storage log
			9. Fault record book
			10. Reactor fault report
			11. Reactor maintenance
			   sheet file
			12. Reactor drawings and
			   circuit diagrams
			13. Reactor modification
			   file

*Included for general reference.
†Includes description of the reactor of the facility, and of the maintenance procedures.
‡Includes 35 pp. of descriptive material.

facilities do not have formally prepared operations manuals; therefore they do not appear in Table 1.

Some of the operating procedures incorporate large amounts of descriptive material, and the Health Physics Research Reactor (HPRR) manual includes maintenance procedures. The Fast Burst Reactor Facility (FBRF) has two separate maintenance manuals, one for electrical and mechanical maintenance and the other for instrumentation maintenance. Some manuals also include emergency procedures; other facilities have separate emergency procedures. The most-detailed emergency procedures seem to be those for the FBRF.

The types of records and available checklists also vary greatly, with VIPER having requirements for the largest number of records. The degree of formality about record keeping seems to depend very much on the safety review authority for a particular reactor facility. Those facilities with a large number of required formal records seem to adapt very quickly to a routine, which makes the record keeping acceptable, if a bit annoying at times.

In evaluating the written procedures with regard to length and amount of detail, it is difficult to favor any specific format; however, details about "which switch to push" and "which lights should light" may mask the more important aspect of following correct and deliberate operating sequences. The minute details of operating the console itself are really learned only through actual operation of the controls. A few of the manuals are so lengthy that the essential steps in the operating sequence are difficult to locate and identify. After having participated in writing the manuals for two of the facilities listed in Table 1, I prefer the step-by-step instructions (e.g., as in the SPR II and VIPER manuals) which are not broken and chopped up by hardware details.

The use of formal checklists to assure the following of a correct sequence seems to be especially favored at the reactors operated by the military at the Army Pulse Radiation Facility Reactor (APRFR) and FBRF. Such checklists are useful, but the operation underway is more important than the completion of the checklist. That is, when following the checklist could lead to an unusual or undesirable situation, the operation must be halted and any change in sequence must be reviewed by appropriate operations personnel before modifications are made and the sequence continued.

PROCEDURES CONTENT

Staffing Requirements

Four levels of staff competence and responsibility exist at most reactor facilities. The titles at each level vary somewhat, with Reactor Operator being the only title common to all facilities. The levels are listed in Table 2 with an appropriate title* and a brief summary of the responsibilities at each level. Since these levels are common to most facilities, this organizational arrangement is apparently satisfactory. The number of staff at the reactor supervisor and operator levels depends on the reactor work load and on the degree to which the reactor staff is assigned other responsibilities.

All the facilities have a specified training program for their staff with certification at the end of the training program being based on a written and oral examination administered by the Facility Supervisor, usually with the assistance of an examining committee. Satisfactory completion of the training program and qualification for the staff position is then certified by the Facility Supervisor. Most of the facilities require that the Operations Supervisor hold a college degree in engineering or the physical sciences, or the equivalent. Many of the

---

*These titles will be used in the discussions throughout the rest of this paper.

Table 2

STAFF LEVELS

Title	Number at each level	Responsibilities
Facility Supervisor	1	Senior technical management level. Responsible for overall supervision of reactor facility. May also have responsibility for other reactors or radiation facilities. Appoints and certifies training and qualification of reactor staff. Provides for review of operations and establishes policy.
Operations Supervisor	1	Senior technical supervisory level. Responsible for review and approval of all reactor operations and experiments. Supervises and approves modifications on design and procedures within limits laid down by management and safety review committee. Supervises programs for studying and measuring reactor characteristics.
Reactor Supervisor	2 or more	Technical supervisory level. Responsible for day-to-day supervision of reactor operations. Present at the reactor facility for all operations. Monitors and directs all operations of the reactor. Assists Operations Supervisor in planning and review of experiments.
Reactor Operator	2 or more	Technical operations level. Responsible for manipulation and control of the reactor under supervision of Reactor Supervisor. Performs inspection and maintenance of equipment.

Reactor Supervisors also hold college degrees, but it is not uncommon to find experienced technicians working very satisfactorily at this level.

Most of the facilities have a formal requirement for staff members to participate in some minimum number of operations over a specified time period to maintain certification. This requirement seems especially important considering the experimental nature of these facilities and the relative ease with which significant changes in operating characteristics may occur.

Most of the facilities have two committees with responsibilities for planning and review of operations. These committees are usually (1) an operations committee and (2) a safety review committee.

The operations committee is usually made up of the Operations and Reactor Supervisors plus a health physics representative and perhaps one other experimentalist, e.g., a frequent user of the facility within the organization. This committee reviews experimental requests and monitors the day-to-day operation of the facility.

The safety review committee, composed of persons other than the operations staff and sometimes with representatives from other reactor facilities, reviews and approves operating limits, unusual experiments, major modifications to either procedures or facility and reactor design, and the overall administration of the reactor safety program. From my experience the chairman of this committee should be someone who is not in either the local technical or administrative chain of supervision. Since the committee sometimes imposes restrictions on the operation of the facility, a chairman with line responsibility may find a conflict between his requirement to provide an unbiased review of safety questions and his desire to see a particular experiment or modification accomplished.

Another interesting aspect of the facility staffing is the variation in the number of staff members required to be present for reactor operations. Although most facilities require that at least two persons be present in the control room for the reactor to be operated in the steady state, one facility requires three persons at all times, and another requires only one "responsible observer" (not a certified Reactor Operator) to monitor steady-state operations with servo control. For burst operations all but one facility require the presence in or near the control room of a minimum of three persons: a Reactor Supervisor, a Reactor Operator, and an Operator-in-Training or health physics monitor. Especially for reactors that are burst frequently or operated at relatively high (1-kw) steady-state power levels, the presence of a health physics monitor as part of the operations staff can prevent chronic radiation exposure over the specified safe limits.

Review and Approval of Experiments

Procedures for review and approval of experiments at all facilities are based on the concept of the Operations or Facility Supervisor approving those experiments falling within specified limits set by the safety review committee and higher authority review organizations (e.g., the U. S. Atomic Energy Commission). Experiments not within these limits are submitted to the safety review committee for review and approval. There are, however, great variations in the details of obtaining approval for experiments and in the amount of authority delegated to either the Operations or Facility Supervisors.

The facility with the simplest review procedure requires only that an experimental plan be submitted to the Operations Supervisor for his review and approval. He reviews the experiment from the standpoint of its effect on the safety of reactor operations and approves or disapproves it. At this facility only experiments of a very unusual nature, those involving the use of high explosives or exceeding a

reactivity worth of $1.50, must be referred to the safety review committee.

The facility with the most complicated review procedure requires that an experimental plan be prepared for each series of experiments. This plan must include a thorough description of the experiment and indicate any limits on operation, any potential hazards, and any special procedures required. The plan is then submitted to an operations committee for review and approval. (The Operations Supervisor acts as chairman of this committee.) With the approval of the operations committee, the plan is then submitted to the Facility Supervisor for his approval. He, in turn, submits it to the safety review committee for their approval. This committee then submits the experimental plan to the top level of technical management for final approval. Once an experimental plan has received final approval, the Operations Supervisor may then approve minor changes before or during the actual conduct of the experiment series.

Three of the remaining four facilities have an operations committee that assists the Operations Supervisor in the review and approval of experiments. In the last facility each experimental plan must be reviewed and approved by both the Operations and Facility Supervisors. As indicated at the beginning of this section, experiments of an unusual nature (e.g., explosives or large reactivity worths) are referred to the safety review committee.

At one facility a university consultant periodically reviews the experimental program and operational data. The Facility Supervisor indicates that these reviews have been quite helpful in providing insight into potential procedural and design difficulties.

The use of an operations committee in the review procedure permits a variety of viewpoints to be applied to each experimental plan and removes the requirement that the Operations Supervisor be familiar with all the potential problem areas in any given experiment. Keeping the responsibility for approval of experiments at the operations level encourages the operations staff to be fully alert and to avoid falling into the attitude of "The Safety Review Committee said it's all right, so let her rip!" Ultimate safety of any experiment always lies with the individuals actually carrying out the operations.

Radiological Safety Control of Personnel

There are two primary methods of controlling the access of personnel to the reactor area during operations. The first method is that applied at the HPRR and APRFR (these reactors are essentially unshielded) where a muster badge system is used. Anyone entering the fenced-in limited-access area is issued a numbered badge by a security guard. Persons holding these badges are then located by

visual or voice contact to ensure that all persons in the reactor area are in the remotely located or shielded control building during the reactor burst.

The other method is generally applied at the facilities with heavily shielded reactor cells. The cell is cleared of personnel by the operations staff just prior to operation, and access to the cell is prevented usually by a physical lock (but at some facilities by electrical interlock systems that prevent power from being applied to the door drives). Both methods appear to work quite satisfactorily.

Reactor Check-Out and Start-Up

As expected, all the facilities follow a prescribed procedural checklist for reactor check-out and start-up. The purposes of the pre-operational checks are to ensure (1) safety of personnel during reactor operation, (2) satisfactory performance of the reactor control and safety systems, and (3) proper arrangement of experimental equipment with respect to the reactor. At VIPER the Operations Supervisor and Reactor Supervisor must agree on the settings of trip levels and on the reactivity corrections for the desired burst yield. These data are then recorded in the reactor logbook prior to start up.

Prior to start-up on FRAN, the Operations and Reactor Supervisors independently calculate the limit on one of the FRAN control-rod insertions. The movement of the control rod is then physically limited by inserting an aluminum plug into the control-rod hole in the reactor core. The limit on the control-rod insertion is that the total available excess reactivity with all rods inserted must not exceed the amount required to produce a burst yield of 5×10^{16} fissions. After the delayed critical configuration is established, the total available excess reactivity is determined experimentally; if it exceeds the limit, the operation is terminated, and the aluminum plug is changed.

The start-up or approach to a delayed critical steady-state operating level is just about the same at any of the facilities. All facilities permit the burst rod to be inserted (and latched in most cases) prior to safety-block insertion if the reactor is to be operated at a high power level and if an appreciable temperature rise is anticipated. On VIPER the burst rod has a slow electromechanical drive and can be used as a control rod when desired.

All the procedures require close observation of the start-up (count-rate) instrumentation channels when inserting the safety block and termination of the operation (by scramming) if it appears the reactor will be critical with only the safety block fully seated. In addition to this precaution, on VIPER the safety block must be stopped after each 2 in. of insertion (full insertion is 8 in.), and the count rates must be measured with a scaler and compared to data from the pre-

vious operation. These data are quite reliable in indicating the relative change in reactivity of the system, primarily because the reactor has a much larger neutron start-up source (10 to 15 curies of polonium – beryllium) than usually used on reactors in the United States.

Burst Sequence

CORRECTION FOR DESIRED BURST YIELD.   Interesting and per- haps significant variations appear in the sequences leading up to a burst at each of the six facilities. On all the reactors the usual ap- proach to critical sequence is followed with insertion of the safety block and subsequent insertion of the control rods to achieve a low-power steady-state operating condition.

On the HPRR the Reactor Supervisor then specifies the control-rod adjustment required to give the desired amount of prompt reactivity when the burst rod is inserted at a later time in the sequence. On the APRFR the Reactor Operator and the Reactor Supervisor independently determine the required reactivity correction and control-rod move- ment. When they have agreed, the control-rod correction is made by the Reactor Operator and verified by the Reactor Supervisor.

Next, on both the APRFR and HPRR, the period resulting from the rod movement (may be positive or negative) is measured by plotting the count rate as a function of time from two scaler-timers receiving signals from fission-counter detectors. The measured period must correspond to the desired reactivity correction (allowed devia- tion not specified), or the control-rod adjustment must be changed and the period remeasured. The safety block is then withdrawn to permit the neutron level to decay to essentially the spontaneous fission source level (wait period).

On the FBRF and SPR II the Reactor Operator determines that the reactor is delayed critical by observing the output of a linear micromicroammeter on a chart recorder. The definition of delayed critical is that no detectable power level change occurs during a 2-min observation interval. The Reactor Supervisor verifies the de- layed critical condition and specifies the required control-rod correc- tion. The correct movement of the control rod by the Reactor Operator is then observed and confirmed by the Reactor Supervisor, and the safety block is removed to begin the wait period.

On FRAN after delayed critical is established, the safety block is cycled out and in twice to assure proper seating, and delayed criti- cal is again established. Since the burst rod has a reactivity worth of approximately 90¢, the control-rod correction always involves an addition of reactivity such that the worth of the burst rod plus the worth of the control-rod reactivity addition equals the desired prompt reactivity addition. The control rod is then inserted the desired

amount, and the safety block is again removed. After about 3 min the safety block is reinserted, and the stable reactor period (corresponding to the control-rod reactivity addition) is measured. The operations must be terminated if the measured and predicted reactivity differ by more than 1¢. If the reactivity addition is correct, the safety block is removed to begin the wait period.

On VIPER the Reactor Supervisor and Reactor Operator make independent calculations of the required control-rod correction which are recorded in separate logbooks. They then compare their calculations, resolve any differences, and both verify the delayed critical control-rod positions by a 2-min observation of steady-state power level. The control-rod correction is made, the new position recorded, and the reactivity adjustment again calculated. After movement of the control rod, the pulse rod is adjusted (it has both a slow and fast drive) to reestablish delayed critical. The change in reactivity is determined from the pulse-rod calibration curve and must agree with the change calculated from the control-rod movement. The pulse rod is then driven to its withdrawn position, and the safety block is removed to begin the wait period.

A comparison of the procedures for the correction for desired burst yield shows that sequences at two of the reactor sites do not provide any check on the control-rod reactivity correction other than verifying the corrected position on the rod-position indicators. Three of the sequences require that stable reactor period measurements be made to verify the correct control-rod reactivity adjustment; one sequence uses a slow drive capability and calibration curve of the burst rod to verify the control-rod reactivity adjustment. Only two of the six sequences require two independent calculations of the actual reactivity correction required, and only one of these insists on actually keeping separate logs to try to ensure that the calculations are really independent.

The discussion of this particular sequence may appear lengthy, but it seems to be the most crucial in the entire burst operation. The significant differences in the care with which this sequence is accomplished are probably the result of pressures by safety review committees. Another possible factor is the difference in experience of the staffs at the facilities. At least an independent check on the calculation of the reactivity correction would seem desirable; to ensure such a check being carried out for each burst, it should probably be formalized in some way.

CORRECTION FOR TEMPERATURE CHANGE DURING WAIT PERIOD.
The reactor core can change temperature during the wait period. If the core cools, reactivity will be added ($\sim$0.3 /°C for most of these reactors) to the prompt reactivity addition at the end of the

wait period. Three of the reactors prevent (by electrical interlocks) any movement of the control rods during the wait period, but the reactor procedures require that, if the change is greater than a specified amount (varying from 1 to 5°C), the sequence must be halted and restarted with the reestablishment of delayed critical. Two of the reactors have interlocks so that reactivity can only be withdrawn during the wait period, and a correction for cooling is made just prior to reinserting the safety block.

One reactor permits either an addition or withdrawal of reactivity during the wait period to compensate for temperature changes. Since an inadvertent movement of a control rod and the subsequent addition of reactivity during the wait period could go undetected because of the low neutron population and high degree of subcriticality, this degree of flexibility is perhaps unwarranted.

PROMPT-BURST PRODUCTION. At the end of the wait period and after the temperature check, the prompt burst is produced by reinsertion of the safety block, followed by insertion of the burst rod. The one exception is FRAN, where the burst rod is inserted first, followed by the safety block. The burst is subsequently initiated either by spontaneous fission source neutrons or by an external deuterium –tritium pulsed source, if precise timing of the burst is desired. All the procedures require that a careful record of the reactor performance be entered in the log and that the predicted and actual performances be compared. Satisfactory performance of the reactor safety circuits must also be verified.

Maintenance and Emergency Procedures

Detailed analyses of the maintenance and emergency procedures are outside the scope of this paper. In both cases the procedures are very specialized for each reactor system and for each facility. The length and detail of both maintenance and emergency procedures are probably greatest at the two U. S. Army reactor facilities, APRFR and FBRF.

CONCLUSIONS

In this review of fast burst reactor operating procedures, many similarities in both sequence and philosophy of operation are evident. There are, however, some significant variations. The length of the written procedures varies greatly; and, for very long and greatly detailed operations manuals, the essential steps in the operating sequences are somewhat difficult to follow and identify. The use of checklists for important sequences is desirable, but in using them

the operations staff must continue to evaluate the situation and halt the operation if following the checklist could lead to an unsafe condition.

The staffing of the facilities is fairly similar, but the number of persons required for reactor operations does vary. The makeup of the safety review committee is also different. It seems important that the chairman of this committee be a person who is not in either the local technical or administrative chain of supervision.

Procedures for the review of experimental plans vary significantly, and an operations committee with review and approval authority is important because the committee (1) brings different points of view to the review of the experimental plans and (2) encourages alertness and a sense of responsibility for safety among the operations staff.

The reactor check-out and start-up procedures are similar, but significant variations exist in the determination of the correction for burst yield. A procedure is desirable for providing an independent check on the calculation of the reactivity correction, with some means for ensuring that this correction has actually been made.

In the remainder of the burst sequence, procedures are quite similar, but the inadvertent insertion of reactivity during the wait period should be carefully guarded against both through administrative control and interlocks, where possible.

Although not specifically discussed in this paper, carefully written and meaningful operating limits are essential in the safe day-to-day operation of any reactor. For further discussion of these operating limits see R. L. Seale, Session 7, Paper 1, and A. De La Paz, Session 7, Paper 3.

DISCUSSION

GOSSMAN: Would you indicate the approximate worth of the burst rods at the different reactor facilities? Do they all run about $1, maybe a little less, or a little more?

LONG: Two out of the six facilities use burst rods that are worth less than $1; so they always add reactivity and always measure a positive period. The other four that I reviewed have a burst rod which is worth more than a dollar—usually $1.10, or as high as $1.15 for VIPER where the neutron lifetime is longer and more reactivity is needed.

GOSSMAN: On FRAN we have a control system in which the final insertion is with a safety block. The burst rod itself is not used for initiating the burst. Is this the case in any other facilities that you investigated?

LONG: No, it is not, and I do mention that in my paper. All the rest insert the safety block followed by the burst rod.

BANFIELD: In your table showing the supervisory personnel where do you find the lines normally drawn between people with scientific degrees and without?

LONG: That is in the paper, too. The facility supervisors without exception are required to have at least a bachelor's degree. The operation supervisors at most facilities must have an engineering or physics degree or equivalent. However, it is not unusual to find technicians functioning as operations supervisors and doing a very fine job.

McENHILL: I would like to make a point here. It could possibly depend on the type of reactor and on the utilization program. The history and experience of operating steady-state research reactors show that there has been a continual degradation in the level of academic qualifications considered essential for supervisors. Whereas we once felt professional engineers were essential, we now give technicians considerable responsibility in running steady-state research reactors. On the other hand, with a system in which the experimental program is continually changing, it becomes very difficult to decide just what the reactor is because it is a compound of the initial concept plus the experiment. In such a fluid situation where experiments are varying from day to day, I guess you need high-quality professional and well-experienced supervision.

4-2 OPERATIONAL EXPERIENCES
WITH FAST BURST REACTORS

L. B. HOLLAND
Oak Ridge National Laboratory, Oak Ridge, Tennessee

ABSTRACT

Operational experience with the few fast burst reactors that are utilized as sources of radiation for experimental purposes as opposed to those that are used to study the kinetics of the reactor itself is presented. The reactors discussed include the HPRR, the SPR II, Super KUKLA, VIPER, and the WSMR reactor. In addition to some statistics on the performance of the reactors, this paper touches on the integrity of the fuel elements, the mechanical support structure, the reactor instrumentation, and problems encountered with experiments, maintenance, and operation.

This paper is limited to the operational problems with second-generation fast burst reactors to minimize any overlap of information with other papers in these proceedings. Information about first-generation fast burst reactors was summarized in 1965 by Wimett,[1] and fast burst reactor history to date was reviewed by D. P. Wood (see Session 2, Paper 1). The second generation of fast burst reactors, which are primarily used as sources of steady-state or pulsed radiation for experimental purposes, includes the Health Physics Research Reactor (HPRR), the Sandia Pulsed Reactor (SPR II), the Super KUKLA, the VIPER, and the White Sands Missile Range Fast Burst Reactor (WSMR). Some comments are made concerning the Army Pulse Radiation Facility Reactor (APRFR). Information concerning these reactors was supplied by Paul O'Brien of Sandia, Fred Kloverstrum and L. R. Peterson of Lawrence Radiation Laboratory, John Weale of Aldermaston, Robert Long of the University of New Mexico, and Armando De La Paz of the White Sands Missile Range.

FUEL CLADDING

As discussed in other papers at this symposium, the fuel for bare-metal cores is usually clad to prevent corrosion and to contain fission products. Both aluminum-ion plating and nickel electroplating are in current use and are considered a partial answer to the problems.

Aluminum-ion plating on the SPR II cracked circumferentially on the outer surface of one fuel piece even before cracks appeared in the fuel plates. Since the crack was in a position that could not be attributed to stress or temperature effects, it was postulated that the crack was due to corrosion at the site of a defect or possibly to water vapor diffusing through the plating.

The nickel plating on the fuel rings and chrome flash over nickel on the HPRR control rods are in good condition after several years, but the reactor has had relatively few bursts. In 1964 cladding on some of the threaded uranium – molybdenum bolts stripped off, causing a bolt to jam in the bottom fuel ring. The failure was attributed to improper cleaning of the metal before plating. The bolts with defective cladding and the bottom fuel ring were stripped, cleaned, and replated with nickel, and the bolts were flash coated with gold. This plating also remains in good condition to date.

The nickel cladding on the 40%-enriched-uranium control rods of the Super KUKLA reactor is crinkled slightly owing to the 500°C temperature that the rods attain in a maximum burst. The crinkling is not considered to be a problem.

Both aluminum-ion plating and nickel electroplating were used on the APRFR fuel that was used in the test to failure reported by Mihalczo.[2] The aluminum-ion plating held up better in these tests.

FUEL INTEGRITY

The highly enriched-uranium – molybdenum fuel rings have failed under various operating conditions on different reactors. Mihalczo[2] reported that during tests at Oak Ridge National Laboratory (ORNL) one high-level burst of 3.7×10^{17} fissions, after very few other lower yield bursts, created longitudinal cracks through radial thermocouple holes in the APRFR core. Jefferson (see Session 2, Paper 3) reported that a few months after increasing the burst yield of the SPR II to produce maximum temperatures above 500°C, longitudinal cracks through radial thermocouple holes and breakout of pieces of fuel near bolt holes were noted. Prior to this increase in burst yield, about 400 bursts had been completed on SPR II with no visible damage. In the HPRR, cracks are slowly propagating longitudinally from radial thermocouple holes in the inner surface of the fuel disks in a manner

similar to that in the SPR II. For the HPRR core the maximum temperature has been limited to 315°C, and the integrated exposure is equivalent to 410 pulses of 1×10^{17} fissions. The fuel pins of the VIPER reactor were radiographed after about 150 bursts, and there were no signs of damage or dimensional change.

CONTAMINATION

If there is a defect in the fuel cladding or a failure in the fuel structure of an operating reactor, a concomitant contamination problem usually exists. For bare-metal fast burst reactors, contamination is sometimes noted without these failures. Before any fuel defects were noted at the HPRR, some contamination was found and attributed to fuel particles that were not removed after holes were drilled through the safety block for roll pins. This contamination essentially disappeared after the through holes were thoroughly cleaned. Airborne contamination has not been detected inside the reactor building; if it were to occur, the building exhaust is adequately filtered. Similar contamination was found at the WSMR after cladding peeled from one safety block. No evidence of contamination was noted during operation with a second safety block.

Contamination from the SPR II became a very real problem when cracks appeared in the fuel. The problem was attacked in two steps. First, the cooling air that was exhausted from the reactor shroud was passed through a 1-cfm absolute filter followed by two Mine Safety Appliance air line filters (in parallel) which contained activated charcoal. The charcoal filters were ordered without iodine preloading to eliminate any problem from the iodine in the filter. The filters minimized but did not eliminate the contamination. The second step was to install a three-stage filter of fiberglass, paper absolute filters, and activated charcoal in the building exhaust system which exhausts 5000 cfm from the building with a differential pressure of $5\frac{1}{2}$ in. of water. These filters practically eliminated contamination problems in other than the reactor area.

RADIATION EXPOSURE

Even if a contamination problem does not exist with some fast burst reactors, the fuel in all of them is so radioactive after high-yield bursts that the exposures received in performing maintenance on the reactors are very high. Because of this factor, other personnel are used where possible to make some of the experimental changes, especially when the experiments do not follow the developed procedures. At all facilities an effort has been made to minimize the personnel

exposures during the setup and retrieval of experiments. For example, the reactor is moved into position after the experiment is set up, and the reactor is moved away before any equipment is retrieved. Also, procedures and equipment have been developed for remote removal of in-core samples. The exposure records at Sandia Corporation, where about 10 persons each received a total exposure of 1.5 r or more in the first quarter of 1968, and at the HPRR, where rarely does one individual receive an exposure of 1 r in a quarter, show that exposure rates follow the operating history of the reactor. This will continue to be the case unless methods are developed to further minimize reactor maintenance and to further expedite the setup and retrieval of experiments.

MAINTENANCE

Much of the maintenance required on fast burst reactors is mechanical in nature, which is not surprising considering the shock forces involved in a burst. The difficulties range from elongation of bolts that hold the core together to deformation and even to breakage of components.

During early testing of the WSMR, shock effects bent the core-support plate. A heavier plate is now in use, but the plate still must be replaced periodically.

Various materials have been used for fast burst reactor core bolts with slightly different results. As was the case for other Godiva-type reactors, elongation of the core bolts was experienced during early operation of the SPR II. The bolts, which are made of special high-strength stainless steel (A-286), loosened during the first few bursts after reassembly but finally assumed a set. Even the loosening that followed reassembly of the core diminished with continued operation and is no longer a problem. The core bolts for the WSMR are made of Inconel, and bolts installed in September 1968 have elongated 3 to 4 mils. At one time uranium—molybdenum alloy was used for the three core bolts on the WSMR, but the bolts were overstressed at high yields. The nine core bolts for the HPRR are made of uranium—molybdenum alloy. The design called for overstressing the bolts slightly at installation, loosening them, and repeating the process several times. The original bolts are still in use with no measurable elongation due to burst operation.

Although core bolts loosen during burst operation, there is no guarantee that they will be free when it is necessary to disassemble the core. Stainless steel is notoriously bad in this respect, and it lived up to its reputation on the SPR II. Galling ceased to be a problem when the stainless steel bolts were treated with Lub-Loc 1000, a high-

temperature graphite coating supplied by Electrofilm Inc. of Holly-wood, Calif. There has been no tendency for the HPRR uranium—molybdenum bolts to bind since they were replated as mentioned previously. The uranium—molybdenum bolts for the APRFR also were difficult to remove after the critical experiments at ORNL, but this was after the above-design-level burst mentioned previously. For facilitat-ing removal in case of binding, the APRFR was changed so that the bolts thread into nuts instead of the lower fuel plates.

On some reactors all devices fastened on the superstructure with screws or bolts loosen after repeated burst operation. Lock washers extend the length of service, but the bolts eventually still work loose. On the WSMR and on the SPR II, microswitches used for the control-rod limit indication have been broken. On the SPR II the microswitches used for limit switches are located on the lower portion of the reactor support structure, where the radiation level is relatively low. On the HPRR the loosening of bolts holding switches, etc., in place has not been a problem, undoubtedly because of the lower burst levels and lower burst frequency, but perhaps because of the type of switches used and the method of mounting. On the HPRR these switches do not receive any direct impact from the rods.

Reliable monitoring of the position of movable fuel or control ele-ments is of utmost importance. Since the safety block is the largest piece of movable fuel and since in most cases it is moved between burst preparation and the burst itself, it is crucial that the safety block be repositioned accurately. In addition to position indicators on the safety-block drive, switches are used to indicate that the safety block itself is driven against a fixed stop or against fixed core elements. These switches are a common source of trouble, and maintenance on them is a very real cause of radiation exposure. Much thought and ef-fort has been expanded to develop safety-block inserted switches that will perform satisfactorily and when necessary will be easy to main-tain. There still is a market for a better "mousetrap," or in this case, a better seated switch for fast burst reactors.

Failure of rod-position indicators occurs infrequently, and usually the failure is quite evident. On one occasion, however, one of the six linear potentiometers that indicate shim-rod position for the Super KUKLA reactor malfunctioned in such a way that the operators did not know where the rod was physically. The discrepancy was confirmed through discrepancies in delayed critical settings between the burst rods and the shim rods. The potentiometer was replaced, and the calibration start-up procedures were redone, but with a loss of several operating days.

Radiation damage to scintillation detectors or glass darkening of photomultiplier tubes placed near burst reactor cores is quite com-

mon. Methods of circumventing the problems vary. These devices are part of the fast-scram system for the Super KUKLA reactor and are located approximately 4 in. from the fuel. An independent detector is placed at the same location to monitor the neutron level in each burst. When the sensitivity of the fast-scram detectors begins to decrease appreciably, they are replaced. At Sandia the scintillator used with a photodiode for burst shape and period measurements deteriorated much faster on the SPR II than the scintillators did on the SPR. At first the scintillators were to be replaced at 6-month intervals to combat the problem, but, they were moved further from the core, and the deterioration is not so acute. At VIPER glass components in the scintillation detectors have been removed where possible to combat the loss in the transmission due to glass darkening.

BURST YIELD ACCURACY

A most interesting and important aspect of the operation of fast burst reactors is the accuracy the operators achieve in obtaining the target yield. For the most part the accuracy is quite good; however, problems with some machines do continue, and isolated difficulties persist with others.

Preinitiations, or bursts that start before the desired reactivity is completely inserted, cause the yield to be low. They are to be expected with some probability, but on the VIPER reactor they have occurred with a higher probability than expected. Development work was undertaken to minimize preinitiations by increasing the insertion speed of both the burst rod and the safety block. The results to date are not too successful, but work is continuing.

The ability to produce yields accurately is extremely good for the higher yields on most reactors. With the SPR II, for example, bursts with maximum temperature rises in the range of 500°C are made within 1 to 2% of the predicted rise. For lower yields the difficulty of predicting increases, but predictions are still accurate within 10 to 15°C for bursts with temperature rises in the range of 100°C. Inability to make accurate low-yield bursts is a problem in other reactors.

At Super KUKLA the shape of the inhour curve varies because of differences in the neutronic characteristics of samples placed in the irradiation cavity. With samples that lengthen the effective prompt-neutron lifetime of the assembly, bursts of low yields were terminated by the scram action of the fast safety system rather than the thermal expansion of the core. Since such bursts were not closely reproducible, a key-switched scram delay circuit was added to delay the scram action by 17 msec. The added delay allows the burst to be terminated by

thermal expansion of the core, which markedly improves the ability to reproduce low-yield bursts.

Low-yield bursts at the HPRR, approximately 1×10^{16} fissions, also are terminated by scram action of the safety system rather than by thermal expansion of the core. Since there has been little demand for very low yield bursts, this early scram is no real problem. But the accuracy of achieving a target yield even for high-level bursts has always been a problem at the HPRR. A considerable improvement was realized during early operation after it was noted that insertion of the burst rod caused the safety block to oscillate. A system was developed to critically damp the stopping of the burst rod upon insertion. This improvement eliminated oscillations of the safety block before the burst occurred and minimized, but did not eliminate, scatter in the burst yield. Further improvements were made in the safety-block suspension system, but scatter of 10 to 15% in burst yield is still common, and it is no better at high yields.

With the Super KUKLA reactor, the operators have difficulty in determining the actual exponential period for bursts near prompt critical, i.e., in the range of periods from 5 to 200 msec, owing to a 50-msec peak-to-peak sinusoidal oscillation which is superimposed upon the exponential rise in neutron population. The oscillations are attributed to reactivity changes produced by mechanical vibrations of the burst rods after they strike their insert stops. For an accurate determination of the exponential period, the outputs of several detectors must sometimes be normalized and plotted over three or four decades on a semilog graph to separate the sinusoidal component from the basic exponential.

UNEXPECTED REACTIVITY CHANGES

Of all difficulties, the unexpected change in reactivity stands apart from all the rest. Some reactivity changes, owing to the action of the operators and fortunate timing, did not result in either the loss of the experiment or damage to the core. Such changes are not covered as incidents or accidents in these proceedings (see P. D. O'Brien, Session 4, Paper 6). The failure of the shim-rod position indicator on the Super KUKLA reactor, which was mentioned earlier, could have resulted in a reactivity uncertainty of 5¢ or for the intended burst yield of 1.5×10^{18} fissions an error of 7×10^{17} fissions. A more dramatic change in reactivity occurred between two consecutive bursts with the SPR II.

Late in the operating day, the delayed critical calibrations of the SPR II indicated a 23¢ increase in reactivity. Operations were sus-

pended, and the radioactivity was allowed to decay overnight before the reactor was examined. The operators discovered puddles of water on the fuel. The water had been sprayed on the core because of failure of the drier in the reactor cooling-air system. The air line was dried out, and the reactor was operated at a temperature of $200°C$ to evaporate all the water from the fuel; as expected, the 23¢ in added reactivity evaporated with the water.

OUTDOOR OPERATION

Because of the increased burst yield of SPR II compared with SPR, operation of the SPR II at full yield at the outdoor burst site was impossible, and therefore no provisions were made for outdoor operation. For experiments that must be located at large distances from the core, a 12-in.-diameter beam port, which is pointed in the direction of the outdoor burst site, was made through the wall of the reactor building. Normally, this port is plugged with a stepped concrete-filled cylinder that is removed only for those experiments for which the beam port was designed. The beam port has been used very little, and, when it is, radiation scattering into nearby buildings is an additional problem. The WSMR and the HPRR were also designed for outdoor operation. The HPRR, however, is not operated outdoors because its building has little or no effect on the reactor operation and because there is sufficient room for the necessary separation between the reactor and the experiments inside the building.

EXPERIMENTS

Some experiments are interesting because of the worries they create for the operators. One such experiment was the deliberate detonation of a small amount of the explosive RDX as soon as possible after a burst with the SPR II. The explosive was contained in a heavy steel can guaranteed to contain the explosive energy of twice the charge used in the experiment. There were no spare samples, and one of the requirements of the test was that the explosive not be detonated unless the burst yield exceeded some specified minimum. To eliminate the chance of predetonation of the explosive and the resultant shift in reactivity before the burst actually took place, the explosive was fired manually from the control console as soon as an observer had ascertained from the period meter that the burst was sufficiently large to satisfy the requirements of the experiment. Also, an interlock prevented firing the RDX until the scram action had started. The experiment was entirely satisfactory and almost anticlimatic after all the concern for safety.

CONCLUSIONS

Most of what has been presented in this paper is a collection of isolated incidents or observations so that little can be said in summation. Operating experiences, however, continue to demonstrate that these machines require constant attention to ensure not only that every part of the reactor system performs as designed but that everything that affects its operation performs correctly, including the operators and any experimental equipment. Also, improvements in reactor performance, which include increasing the number of pulses per day, must be accompanied by improvements in design to minimize personnel exposures during reactor maintenance and experiment preparation.

ACKNOWLEDGMENTS

REFERENCES

1. T. F. Wimett, Fast Burst Reactors in the United States of America, in *Pulsed Neutron Research*, Symposium Proceedings, Karlsruhe, 1965, Vol. 2, p. 529, International Atomic Energy Agency, Vienna, 1965 (STI/PUB/104).
2. J. T. Mihalczo, J. J. Lynn, J. E. Watson, and R. W. Dickinson, Superprompt Critical Behavior of a Uranium–Molybdenum Assembly, *Trans. Amer. Nucl. Soc.*, 10(2): 611 (November 1967).

DISCUSSION

GOSSMANN: You indicated a fairly high degree of reproducibility in burst operations with respect to temperature rises. What would be the degree of reproducibility due to positioning accuracies on the control rods, safety block, etc.? Do you have any information on that? Are we talking about a tenth of a cent reproducibility or hundredths of cents, or what?

HOLLAND: We have looked at all these various things, like repositioning of the safety block, dropping it off and putting it back, moving control rods, possible temperature variations through the whole core, heating one side of the core and seeing what the effects were. These were all very small numbers as far as the error in the burst yield was concerned for the Health Physics Research Reactor. None of these things could give us the change that would produce the spread in our burst yield.

GOSSMANN: I was interested in whether there was more or less an established or an accepted limit of the degree of reproducibility

of delayed criticals, not considering changes induced by, say, burst generation?

HOLLAND: Not to my knowledge. I think everyone has his own ideas about how accurately you can get to delayed critical or how accurately you measure the period if you put in a positive or negative period to get a particular yield.

O'BRIEN: I would like to comment on the last question. I think we consider it acceptable if we can reproduce our delayed critical reactivity within a couple of tenths of a cent. Ordinarily it is better than that, but we consider two tenths of a cent acceptable.

HOLLAND: If you are asking for a number, we use three tenths and feel that that is acceptable because we always get better than that.

4-3 FAST BURST REACTOR EXPERIMENT IRRADIATION EXPERIENCE

A. DE LA PAZ
Department of the Army, White Sands Missile Range, New Mexico

ABSTRACT

Extensive experience accumulated during irradiation of experiments in fast burst reactor facilities has demonstrated that the effect of the experiment being irradiated on the reactor characteristics is the primary operational safety consideration. The general nature of these effects and the associated procedures to be applied are presented for various categories of fast burst reactor experiments.

Experience with experiments irradiated in fast burst reactor facilities is extensive and varied. The versatility of fast burst reactors has led to their use in a wide range of experiments, including the irradiation of materials, circuits, and electronic components, as well as dosimetry, radiobiological, and ecological experiments. Fast burst reactors are especially accommodating since they can be operated in either the burst or steady-state mode, depending on the experimental requirements.

The nature of the experimental programs conducted at fast burst reactor facilities depends upon the objectives of the facility. Some reactors are operated primarily in the burst mode for the irradiation of experiments to study transient effects; others are operated in either the burst or steady-state modes in accordance with the requirements of different experimenters. Table 1 lists the fast burst reactor facilities that have been built and operated in the United States.

Experience in the irradiation of experiments at fast burst reactors has centered on the importance of the effect of the experiment being irradiated on the burst characteristics of the reactor. This experience has shown that the effects must be properly accounted for to fully ensure the safety of all reactor operations. Where this experience does not exist, e.g., during the initial start-up of a reactor, it is essential that burst operations be conducted with a variety of materials, such as

313

Table 1
FAST BURST REACTORS[1]

Reactor	Type of fuel	Nominal fissions per burst	Location	Start-up date
Godiva I	Oralloy	$\leq 10^{16}$	Los Alamos Scientific Laboratory, N. Mex.	1951
Godiva II	Oralloy	2×10^{16}	Los Alamos Scientific Laboratory, N. Mex.	1957
Nuclear Effects Reactor (Super KUKLA)	Oralloy	2×10^{16}	Lawrence Radiation Laboratory, Livermore, Calif.	1959
Sandia Pulse Reactor (SPR)	Oralloy	2×10^{16}	Sandia Corporation, Albuquerque, N. Mex.	1960
Nuclear Effects Reactor (FRAN)	Oralloy	5.6×10^{16}	National Reactor Testing Station, Idaho	1962
Health Physics Research Reactor (HPRR)	U−10 wt.% Mo	1.8×10^{17}	Oak Ridge National Laboratory, Oak Ridge, Tennessee	1962
WSMR Fast Burst Reactor (FBR)	U−10 wt.% Mo	1.0×10^{17}	White Sands Missile Range, N. Mex.	1964
Sandia Pulsed Reactor (SPR II)	U−10 wt.% Mo	$\sim 2.2 \times 10^{17}$	Sandia Corporation Albuquerque, N. Mex.	1967
Los Alamos Pulsed Reactor	U−1.5 wt.% Mo	$\sim 2.2 \times 10^{17}$	Los Alamos Scientific Laboratory, N. Mex.	1967
Army Pulse Radiation Facility Reactor (APRFR)	U−10 wt.% Mo	$\sim 2.2 \times 10^{17}$	Aberdeen Proving Grounds, Md.	1968

those which would be involved in typical experiments. These operations not only provide valuable information on the reactor but also add to the operational capabilities of the reactor staff. The initial work in this area was carried out at Los Alamos Scientific Laboratory. A program was conducted at the White Sands Missile Range Fast Burst Reactor (FBR) to evaluate the reflectivity effects of materials on the nuclear characteristics of the reactor.[2] Although this program was conducted during the early operation of the reactor, the results are still of considerable use and applicability to the FBR. Further expansion and development of these studies is currently underway.

Placing an experiment in close proximity to a fast burst reactor results in reflection of neutrons into the fuel region during reactor operation. This reflection of neutrons increases the overall reactivity of the reactor. The magnitude of this reactivity increase can be evaluated from the change in control-rod positions at delayed criticality with the experiment as compared to the same condition without the experiment. The difference in control-rod positions, evaluated in terms of the equivalent reactivity worth, represents the worth of the experiment.

Further, the reflectivity effect of the experiment leads to a change in the flux distribution in the reactor fuel. If the experiment is located adjacent to one of the control rods or burst rods, the reactivity worth

of the specific rod will be increased as a result of the flux change associated with the neutron reflection. This effect is of vital importance in the case of the burst rod since changes in its reactivity worth are not directly observed or subject to evaluation until the reactor burst takes place. This effect is normally accounted for by withdrawal (in the usual case) of control-rod reactivity at the time of delayed criticality to ensure that only the desired amount of prompt reactivity is added to the reactor at the time of insertion of the burst rod.

A decoupling shield with a neutron-absorbing material on its outer surface may be used to partially overcome the effects of the experiment being irradiated. Neutrons reflected from the experiment are thermalized and then absorbed so that their effect is diminished. Unless this procedure is followed, under some circumstances the reactor and the experiment may be so interrelated that they become a coupled system. The use of a decoupling shield is therefore a vital part of reactor operations involving the irradiation of experiments.

Because of their effect on the reactor burst characteristics, experiments being irradiated must be arranged so that no change in experiment location or mass characteristics takes place during the operation of the reactor. This is especially important during the wait period since the reactor operator has no direct way of knowing or evaluating the effect of a change in the experimental arrangement if one were to occur. If changes occur and are unaccounted for, a reactor burst of an unanticipated yield will take place. Movement of the experiment must be forbidden during reactor operations unless it is properly understood and evaluated prior to the start of the operation.

The accumulated experience in the irradiation of experiments in fast burst reactor facilities is presented in terms of general categories of experiments. The effect of the experiments on the operation of the reactor is then summarized.

MATERIALS AND ELECTRONIC SYSTEMS STUDIES

Fast burst reactors currently in operation, with the exception of the Health Physics Research Reactor (HPRR),[3] conduct extensive burst operations for materials and electronic systems transient-effects studies. Experiments in this category normally are of such a size and mass that the reactor characteristics are not affected significantly. These experiments usually involve the irradiation of a few samples or components, e.g., circuit boards, at a time; therefore, large masses of reflecting-type materials are not associated with these experiments. Transistor experiments are routinely irradiated on a repetitive basis with no significant effect on the operational characteristics of the reactor.

Occasionally experiments involving the irradiation of materials or electronic systems are conducted with many items mounted together for irradiation in one burst operation which result in a heavy overall experiment. Another example of a large experimental arrangement is the irradiation of a material or a system at a desired neutron-to-gamma ratio, thus requiring the use of shielding. The overall result is an experimental arrangement having such a large mass that the associated reflectivity effects significantly influence the nuclear characteristics of the reactor. Experiments in this category have been performed on a routine basis without any compromise to the safety of the reactor at the SPR II and its predecessor,[4] the SPR, as well as the FBR.[5]

Irradiation of an experiment may involve its movement during reactor operation. As noted previously, experiments of this type should be irradiated only after a detailed review has been conducted prior to the operation. The movement of the mass of the experimental arrangement may not be directly obvious. For example,[6] an experiment conducted at the FBR involved using a battery as the power supply. The experimenter had planned to add the battery electrolyte prior to the burst, but this action was not explicitly stated in the test plan and therefore was not known by the reactor operating group. When the experiment was irradiated, the experimenter remotely actuated the electrolyte injection setup, and the electrolyte was added to the battery prior to the burst. When the burst took place the yield was significantly lower than anticipated because the battery electrolyte had moved in a direction that resulted in a reactivity reduction. Fortunately the electrolyte moved away from the reactor. If it had moved toward the reactor, the resulting burst would have been hazardous, possibly resulting in a major accident. Because of this incident the operating procedures for the FBR were modified to require that any experiment proposed for irradiation that involves a fluid or movement of the experiment must be reviewed and approved by the reactor safeguards committee prior to its performance.

It should be noted that review of a proposed experimental plan prior to its performance does not relieve the reactor operating staff of the need to evaluate the effect of the experimental arrangement on the reactor prior to and during the operation of the reactor before the burst takes place. This preevaluation is absolutely necessary since it is not possible for any experimenter (from a practical standpoint) to present the proposed experimental plan in such detail to permit an exact evaluation. Even if an exact evaluation were possible, the reactor operating staff and its associated review body cannot predict the possible effect of all experimental arrangements on the reactor, especially when the proposed experiment differs from those previously performed.

An example of the difficulty of predicting the exact effects of an experimental arrangement on reactor operations is shown by an experi-

ment proposed for irradiation at the FBR. This experiment involved the irradiation of materials having explosive characteristics. These experiments were enclosed in aluminum containers supported on an aluminum structure located near the reactor.[7] The proposed experimental plan was reviewed by the appropriate review bodies and approved for performance. When it was mounted in the reactor area and the operation was begun, the reactivity worth of the experiment was found to exceed the administratively established value of $1.5 reactivity, the point at which the reactor safeguards committee must be informed before the operation can progress any further.[8] Although the reactivity worth of the experimental arrangement was suspected to be close to this value, the actual worth was considerably higher. After consultation with the reactor safeguards committee, the mass adjustment ring was changed (it is mounted on top of the reactor fuel-ring assembly) to account for approximately 65¢ of the reactivity contributed by the experiment, thus permitting the irradiation to be conducted.[9] Reactor burst operations were then conducted in accordance with both the requirements of the experiment and the operational safety of the reactor.[10]

The irradiation of experiments involving materials or electronic components may significantly affect the nuclear characteristics of the reactor prior to either the time of delayed criticality or the point at which the reactor burst takes place. If the structural mass of the experimental arrangement is large enough, its reactivity contribution may also be large enough to result in a reactor burst or in a rapid power level increase when the safety block is inserted into the fuel region. For example, during operation of a Godiva-type reactor for irradiation of an experiment,[11] a very rapid increase in power (terminated by a scram) took place when the safety block was inserted into the fuel region. Another example occurred at the FBR when the reactor experiment involved a considerable amount of polyethylene located near the reactor. When the safety block was inserted, the count rate of the start-up neutron instrumentation was observed to be significantly higher than in the usual case, and the reactor went on a long (approximately 25 sec) period. No further effect was noted, and after observing the power level increase at a stable period, the reactor was shut down and the experimental arrangement modified to make its effect less pronounced.[12] These examples show that the effect of experiments may exceed the reactivity control available in the control rods, possibly resulting in a rapid power level increase or possibly a burst when the safety block is inserted into the fuel region.

EXPERIMENTS INVOLVING EXPLOSIVE MATERIALS

Experimental programs at fast burst reactors have included the irradiation of experiments involving explosive materials. The irradia-

tion of these materials may, for example, involve the transient studies of propellant material subjected to a reactor burst. The principal effect that must be considered in the irradiation of these experiments is the possible ignition of the explosive reaction. For avoiding this situation most of these experiments are conducted with the explosive material placed in containment vessels designed to withstand the energy release associated with the explosive reaction. The review of the safety of the proposed experiments in this category includes the verification that the containment vessels will withstand the applicable explosive energy release.

Once the explosive material to be irradiated is contained, the next consideration involves the mass and location of the experimental arrangement. Because of the use of containment vessels and their associated structure, the mass of the overall experimental arrangement may be high enough to significantly affect the operational characteristics of the reactor. Containment vessels normally employed in these experiments are usually made of aluminum since only small quantities of the explosive material are irradiated at any one time. A steel containment vessel may be employed in other cases, e.g., in the irradiation of an explosive bolt.

The irradiation of experiments having explosive materials at fast burst reactors has been safely performed with no situation noted in which the presence of the explosive material compromised the safety of the reactor systems. For ensuring that this effort is conducted and properly coordinated with considerations associated with reactor safety, written procedures may be desirable which specify the requirements to be met before an experiment involving explosive material may be irradiated. The requirements that should be covered include: (1) the control to be exercised over the explosive material prior to, during, and after irradiation; (2) a general identification of the personnel authorized to handle the material; (3) the storage location of the material prior to irradiation; and (4) the designation of areas where the experiment is to be dismantled following irradiation. Experience at the FBR has indicated that the availability and use of written procedures covering these requirements ensure the proper understanding of all concerned and make for a more effective overall operation. In addition to these requirements the FBR procedures[13] include the requirement that this category of experiments must also be reviewed and approved by the reactor safeguards committee prior to performance.

RADIOBIOLOGICAL EXPERIMENTS

Fast burst reactors have been used in a variety of radiobiological experiments. These experiments have involved the irradiation of sheep, goats, rats, monkeys, and baboons; the experiments have been performed primarily at the HPRR, SPR, SPR II, and FBR.

Experiments involving the irradiation of animals in burst operation of the reactor have been so extensively conducted that the procedures involved form a basic part of the experimental irradiation procedures of a fast burst reactor facility. The principal consideration, as in the other types of experiments, is the location and movement of the experiment. Since the animal may move, it is essential that he be properly secured and restrained so that no movement which could affect the reactor is allowed to take place. Review of the proposed experiment must ensure that such is the case prior to performance of the irradiation.

In actual practice complete securing of the animal may not be possible or desirable. In some of these cases the animal is placed sufficiently far from the reactor that its movement will have no significant effect, e.g., experiments involving the irradiation of rhesus monkeys conducted at the FBR require that the monkey have some degree of freedom of his arms. Under these circumstances the monkey is placed facing away from the reactor and is located within a boxed enclosure. To further ensure that there is no effect on the operation of the reactor, the distance from the reactor to the monkey is normally maintained at approximately 18 in. It should be noted, however, that experiments involving the irradiation of monkeys have been safely performed with the monkey placed closer to the reactor (approximately 10 in. from the core center line). Under these circumstances small variations in delayed critical control-rod positions in the reactor have been observed for equivalent conditions. The differences have been attributed to movement of the monkey.[14]

The effect of increasing the size of the animal being irradiated can best be seen by considering further the experience at the FBR. Following the experiments with the rhesus monkeys, baboons were used in the same general program, which required that more effective and positive steps be taken to restrain the animal during the reactor burst operation. A collapsible cage was used which compressed to restrain the animal and remotely released following the burst to provide the desired freedom of movement at the end of the operation. Further protection was provided by placing the baboons further away than the monkeys (approximately 3 ft from the reactor). The reactor burst operations conducted during this time were normal, and no effect of movement was observed.

EXPERIMENT IRRADIATION INVOLVING STEADY-STATE OPERATION

The experimental irradiation requirements at fast burst reactors may require extensive irradiation in the steady-state mode of operation of the reactor. The operational program of the HPRR, for example, primarily involves the steady-state operation of the reactor.[15] As a further example, the operational program of the FBR has involved an increasing amount of steady-state operations.[16]

The effect of the experiment being irradiated on the nuclear characteristics of the reactor is much less significant and potentially less hazardous in the steady-state mode of operation compared with the burst mode. Dynamic movement of the burst rod is not involved in the steady-state mode. Either the burst rod is inserted and clamped in the fuel region or else it is left out of the operational sequence and not moved. The only significant effect on the reactor is the reflection of neutrons which can be evaluated from the control-rod positions at delayed criticality, as is done in the burst mode.

Experience in the steady-state irradiation of experiments at the FBR indicates that extensive operation of the reactor in this mode, where the usual operation is conducted at 5 kw for 1 hr or less, results in considerably higher radiation levels in the reactor area which may seriously limit any major maintenance effort on the reactor systems. In addition, during the steady-state operation of the reactor, the indication of particulate air activity in the reactor operations area increases considerably above the level normally encountered in the burst mode. This increase occurs primarily because normal operations of the FBR are conducted with no exhaust of air from the reactor cell area. An absolute filter system has been installed in the cell exhaust, and action is currently underway to provide the installation of a system to continuously monitor the activity of the cell exhaust air. When this installation is complete a proposal that the normal mode of conducting all reactor operations be with the cell-exhaust system turned on will be suggested. This should provide for a much lower buildup in levels of radioactivity in the reactor operations area during steady-state irradiation of experiments.

Experience with this overall category of experiments has indicated that the requirements applied to the review of experiments proposed for irradiation in the burst mode are more than adequate for those proposed for performance in the steady-state mode. As noted previously, attention should be given to the scheduling of steady-state operation during periods of operation which are not immediately followed by maintenance on the reactor systems.

CONCLUSIONS

The accumulated experience in the operation of fast burst reactors has involved the irradiation of numerous experiments having various characteristics. This experience has demonstrated that reactors of this type can be safely used in the irradiation of experiments covering a wide range of reactor operational requirements. The primary factor involved in the irradiation of experiments is the effect of the experiment on the nuclear characteristics of the reactor, particularly in the

burst mode of operation. Experience has shown that the magnitude of these effects must be evaluated and accounted for to ensure that proper control is exercised over the operation of the reactor. The requirements covering the performance of this evaluation are a necessary part of the administrative procedures that must be available at all fast burst reactor facilities.

REFERENCES

1. A. De La Paz, Safety Evaluation of Fast Burst Reactors, *Nucl. Safety,* 10(5): 372-377 (October 1969).
2. R. L. Long, Effects of Reflectors on the Burst Characteristics of an Enriched U−Mo Fast Burst Reactor, technical memorandum, White Sands Missile Range, August 1965.
3. L. P. Holland, Oak Ridge National Laboratory, personal communication, 1969.
4. P. D. O'Brien, Sandia Corporation, personal communication, 1969.
5. A. De La Paz, Experimenters at the FBR, internal memorandum, Nuclear Effects Directorate, White Sands Missile Range, 1968.
6. Reactor Operating Logbook for the WSMR Fast Burst Reactor, 1964.
7. Proposed Test Plan for WSMR Fast Burst Reactor, July 1968.
8. Operating Procedures for the WSMR Fast Burst Reactor, Technical Manual. Part II. (Rev., May 1966).
9. Reactor Operating Logbook for the WSMR Fast Burst Reactor, 1968.
10. Reactor Operating Logbook for the WSMR Fast Burst Reactor, 1968.
11. P. D. O'Brien, Sandia Corporation, and T. Wimett, personal communication, Los Alamos Scientific Laboratory, 1969.
12. Reactor Operating Logbook for the WSMR Fast Burst Reactor, 1968.
13. Standard Operating Procedures No. 8, Irradiation of Experiments Involving Explosive Materials, Nuclear Effects Directorate, December 1968.
14. Reactor Operating Logbook for the WSMR Fast Burst Reactor, 1965 and 1966.
15. L. B. Holland, Oak Ridge National Laboratory, personal communication, 1969.
16. Listing of FBR Experimenters, internal memorandum, Nuclear Effects Directorate, White Sands Missile Range, 1968.

DISCUSSION

PETERSON: At Super KUKLA we have large reactivity samples on the order of several dollars (plus or minus), and we also have to determine the effect of changes in prompt-neutron lifetime for a given sample. I wondered if you have encountered this problem of determining changes in neutron lifetime at your facility.

DE LA PAZ: Most of our experiments are of fairly constant characteristics; we do not get involved with that type of experimental program to any extent.

GLASGOW: Have you done any quantitative work on reflector effects here ?

DE LA PAZ: The initial work was done, as I said, by Bob Long while he was at White Sands. We are preparing to update this work.

Quite frankly we only recently got in a position where we could carry out a program of this type by setting aside a given amount of reactor time.

McENHILL: The next paper describes some idealistic experiments on the effect of shielding materials on the reactor characteristics. I think that as the history of fast burst operation progresses, there may be some point in having some type of data center where one can obtain the sort of data that would be useful for operators using particular facilities with particular types of assemblies as a sort of rough-and-ready guide to get them into the right direction as far as reactivity is concerned.

4-4 REFLECTOR AND DECOUPLING EXPERIMENTS WITH FAST BURST REACTORS

RICHARD L. COATS* and ROBERT L. LONG†
*Sandia Laboratory, Sandia Corporation, Albuquerque, New Mexico
†University of New Mexico, Albuquerque, New Mexico

ABSTRACT

Results are reported of systematic studies of various reflector effects on burst characteristics conducted at the White Sands Missile Range Fast Burst Reactor Facility and at the Sandia Pulsed Reactor Facility. A calculation model is described, and the calculated results are compared with experimental findings.

INTRODUCTION

The White Sands Missile Range Fast Burst Reactor Facility (FBRF) and the Sandia Pulsed Reactors (SPR and SPR II) are Godiva-type reactors operated in the super-prompt critical mode to produce high-intensity short-duration radiation pulses.[1-4] (See also R. M. Jefferson, Session 2, Paper 3.) External reflectors have long been known to affect the prompt-burst characteristics of this type of reactor.[1] The initial prompt period, peak fission rate, burst width, and total fission yield for a given reactivity insertion are quite different from the values for the unreflected reactor system. A difference in the characteristics of outdoor (free-field) and indoor operation of Godiva I and Godiva II was also noted and attributed to the return of wall-reflected neutrons to the fuel assembly during indoor operation.

Systematic studies[5,6] of various reflector effects have been conducted at the White Sands Missile Range (WSMR) and at Sandia. The FBRF studies were primarily experimental, and most of the reflectors used were in the form of rectangular blocks 20 by 20 by 2.54 cm or 1.0 cm thick. Materials studied were aluminum, steel, wood, Lucite, paraffin, water, and boral. In the experimental studies at Sandia, the reflectors

used were polyethylene and steel right-circular cylindrical shells of various thicknesses located at radial distances of 7.6 to 25.4 cm from the fuel surface of the SPR.

A calculation model developed at Sandia, similar to that of Cohn's reflected kinetics model,[7] permits a multienergy representation of the reflected neutrons, including the transit and residence times involved. Multiple reflection is neglected. A monoenergetic description of the neutrons in the fuel is employed, with the energy of the reflected neutrons entering the core accounted for by effectiveness values. Monte Carlo techniques determine the various abundance factors and time constants associated with the reflected-neutron groups.

REFLECTED FAST BURST REACTOR KINETICS MODEL

The formulation of the reflected kinetic model presented here is restricted to small reflectors (worth a few dollars in reactivity) and is based on the following assumptions:

1. The following single-energy space-independent kinetics equations are applicable to the unreflected reactor:

$$\frac{dn(t)}{dt} = \frac{k(1 - \gamma\beta)^{-1}}{l} n(t) + \sum_i \gamma_i \lambda_i C_i(t) + S(t)$$

$$\frac{dC_i(t)}{dt} = \frac{k\beta_i n(t)}{l} - \lambda_i C_i(t)$$

where $n(t)$ = fuel neutron population at time t
$\quad C_i(t)$ = population of the ith delayed-neutron-group precursor at time t
$\quad\quad \lambda_i$ = decay constant of ith delayed-neutron group
$\quad\quad k(t)$ = neutron multiplication factor for system at time t
$\quad\quad\quad l$ = prompt-neutron lifetime for unreflected system
$\quad\quad\quad \beta_i$ = ith delayed-group fraction of total neutrons from fission
$\quad\quad\quad \gamma_i$ = effectiveness of ith delayed-neutron group in producing fission
$\quad\quad \gamma\beta = \sum_i \gamma_i \beta_i$
$\quad\quad S(t)$ = rate of source-neutron production from extraneous sources, such as spontaneous fission, (α,n) reactions, etc.

2. No significant spatial or spectral shift in the neutron distribution in the fuel occurs when a reflector is placed near the reactor.

3. These equations can be extended to the case of a reflected reactor by adding time-dependent source terms which account for the return to the core of the reflected neutrons and their effectiveness in causing fission.

The validity of the first assumption has been substantiated many times for small reactors with no appreciable return of leakage neutrons to the reactor. The second assumption has been verified for small reflectors by the results of flux measurements.[8] The validity of the third assumption is demonstrated by the accuracy with which the reflected kinetic model predicts the observed reflector effects.

The system to be analyzed consists of a small fuel system and a single reflector separated from the fuel by a distance x. The following formulation parallels that of Cohn[7] but is generally more applicable, being particularly suited to the description of a reflected fast burst reactor.

A neutron which escapes from the fuel with energy E′, enters the reflector, and returns to the fuel at energy E has associated with it its lifetime in the reactor before leakage, $\tau_1(E')$; the transit time from the reactor to the reflector, $\tau_2(E')$; the residence time in the reflector, $\tau_3(E',E)$; the transit time from the reflector to the reactor, $\tau_4(E)$; and the lifetime in the reactor before being absorbed or escaping from the reactor again, $\tau_5(E)$. It is assumed for all cases studied that the effect of multiple reflection can be ignored. Furthermore, it is assumed that the E′ and E dependence of the various time constants can be separated and that a fixed value of τ_2 can be assigned to all reflected neutrons from a given reflector regardless of their energy. This restriction has no significant effect on the results of the model for moderating reflectors since τ_2 is very small compared with $\tau_4(E)$ for all important reflected-neutron energies. In the following formulation τ_1 and τ_5 are included in the fractional and effectiveness definitions, and they are assumed to have little effect on the average lifetime of the fuel neutrons.

The reflected-neutron energy distribution is divided into M distinct energy groups. For convenience the neutron population within the reflector is thought of in terms of the sum over all energy groups of the number of neutrons that ultimately escape from the reflector within any energy group and return to the reactor.

The pseudo neutron population C′ in the reflector can be described for each of the reflector leakage-neutron energy groups by

$$\frac{dC_j'(t)}{dt} = \beta_j' k \frac{n(t - \tau_2)}{l} - \frac{C_j'(t)}{\tau_{3_j}}$$

where $C_j'(t)$ = population at time t of source energy neutrons in the reflector which ultimately reenter the core as reflected neutrons of the jth energy group

$n(t - \tau_2)$ = fuel neutron population at time $t - \tau_2$

β_j' = fraction of fission neutrons that escape the fuel and, after reflection, return to the fuel as reflected neutrons of the jth energy group

τ_2 = time required for a typical fuel leakage neutron to travel from the fuel to the reflector

τ_{3_j} = the mean residence time in the reflector of a reflected neutron of the jth energy group

γ'_j = effectiveness of jth reflected-neutron group in producing fission

Extension of the neutron-balance equation for the fuel region to include the reflected neutrons is accomplished by the addition of source terms representing the reflected-neutron contribution in the following form:

$$S(t) = \sum_j \gamma'_j \frac{C'_j(t - \tau_{4_j})}{\tau_{3_j}}$$

where τ_{4_j} is the time for a reflected neutron of the jth energy group to travel from the reflector to the fuel and all other terms are as previously defined. The ordinary point reactor kinetics equations cannot simultaneously satisfy the critical (k = 1) and steady-state conditions unless the external source term is zero. In most cases the source term is independent of the reactor; but, in the case of the reflected reactor considered here, the rate at which neutrons are added to the core under steady-state conditions is given by

$$\sum_j \beta'_j \frac{n}{l}$$

If the term $\gamma\beta$ appearing in the neutron-balance equation of the point reactor kinetics equations is replaced by $\gamma^*\beta^*$ and if it is required that the resulting neutron balance satisfy the critical steady-state conditions, the following relation is found to be necessary:

$$\gamma^*\beta^* = \sum_i \gamma_i \beta_i + \sum_j \gamma'_j \beta'_j$$

Replacing $\gamma\beta$ with $\gamma^*\beta^*$ preserves the usual meaning of k and allows the equations to satisfy simultaneously the critical (k = 1) and steady-state conditions.

The reflected kinetics equations can now be formulated; they are

$$\frac{dn(t)}{dt} = \frac{k(1 - \gamma^*\beta^*) - 1}{l} n(t) + \sum_i \gamma_i \lambda_i C_i(t) + \sum_j \gamma'_j \frac{C'_j(t - \tau_{4_j})}{\tau_{3_j}} \quad (1)$$

$$\frac{dC_i(t)}{dt} = \frac{k\beta_i n(t)}{l} - \lambda_i C_i(t) \qquad \text{where } i = 1, N \qquad (2)$$

$$\frac{dC_j'(t)}{dt} = \beta_j' \frac{k}{l} n(t - \tau_2) - \frac{C_j'(t)}{\tau_{3j}} \qquad \text{where } j = 1, M \qquad (3)$$

Except for the lag-time dependence on τ_{4j} and τ_2, the terms accounting for the reflected neutrons have the characteristics of additional delayed-neutron groups. This form is convenient because many solutions applicable to a bare reactor may be carried over to the reflected model. Furthermore, the new terms that are introduced in the unreflected-reactor model can be calculated using experimentally determined quantities.

The solution of this set of linear differential equations is of interest for the special case in which the neutron level is increasing with a constant period T. The solutions for C_i and C_j' become

$$C_i(t) = \frac{k\beta_i n(t)}{l[(1/T) + \lambda_i]} \qquad i = 1, N \qquad (4)$$

$$C_j'(t) = \frac{k\beta_j' n e^{-(\tau_2/T)}}{l[(1/T) + (1/\tau_{3j})]} \qquad j = 1, M \qquad (5)$$

Substitution into Eq. 1 yields, in dollar notation,

$$\rho(\$) = \frac{l^*}{\gamma\beta T} + \sum_i \frac{f_i}{1 + \lambda_i T} + \sum_j f_j' \frac{(\tau_{3j}/T) + 1 - e^{-[(\tau_2 + \tau_{4j})/T]}}{(\tau_{3j}/T) + 1} \qquad (6)$$

where $\rho(\$) = \rho/\gamma\beta$
$\qquad \rho = (k - 1)/k$
$\qquad l^* = l/k$
$\qquad \gamma\beta = \sum_i \gamma_i \beta_i$
$\qquad f_i = \gamma_i \beta_i / \gamma\beta$
$\qquad f_j' = \gamma_j' \beta_j' / \gamma\beta$

Equation 6 is the relation between the reactivity and the stable reactor period for the reflected reactor; it differs from the familiar inhour relation for a bare core only in the last terms. Note that all the previous definitions of the bare reactor parameters are preserved.

REACTIVITY EFFECTS OF REFLECTORS

Typical Irradiation Experimental Arrangements

A typical irradiation experimental arrangement may completely surround the reactor and may contain a great variety of objects placed at distances ranging from a few centimeters to several meters from the surfaces of the core and safety shield. Table 1 contains a brief de-

Table 1

REACTIVITY WORTHS OF TYPICAL EXPERIMENTAL ARRANGEMENTS
AT THE FBRF[9]

Description	Reactivity worth, $
Missile guidance package ~35 cm in diameter at 6 cm from safety shield.	0.20
Four Lucite boxes (10 by 10 by 5 cm) containing silicon oil and printed circuit boards arranged symmetrically around the core at 1 cm from safety shield; assorted detectors at 2.5 cm from safety shield.	1.02
Two metal boxes containing semiconductors and electronic components, one boron ball, and sulfur pellets, at surface of safety shield.	0.22
Two transistorized circuit boards, one boron ball, and a dry-charge battery (25 by 20 by 5 cm) arranged symmetrically around the core at 2.5 cm from safety shield.	1.09
About 50 transistors mounted on styrofoam board having a radius of 12.7 cm. Components at about 1 cm from safety shield and surrounding 180° of reactor.	0.32
One small transmitter and tower structure, one small power supply, one modulator and commutator, one battery pack, one sensor mount (thermistor and photodiode); all components at 0.5 cm from safety shield and surrounding 180° of reactor.	0.85

scription and the reactivity contribution of a number of the experimental arrangements exposed to the FBRF. Determination of the reactivity contribution of an experiment is based on control-rod-worth calibration curves and the measured change in delayed critical control-rod positions.

Burst Effect of Reflectors

The first systematic studies of the effects of reflectors on burst-operation characteristics were performed at the FBRF. Most of the reflectors studied were in the form of rectangular plates 20 by 20 by 2.54 or 1.9 cm. Two large rectangular boxes were also used, one of Lucite and the other of boral. Table 2 contains a description of each reflector arrangement, its reactivity contribution, and an abbreviated description by which the reflector will be referred to throughout the rest of this paper.

The reactivity worths of a single plate of each material were also determined. These worths were usually a few percent higher than the average value obtained for a single plate from the measurement of the

Table 2

REACTIVITY WORTHS OF FBRF REFLECTORS

Abbreviated description	Description	Reactivity worth, $
Boral box	Inside dimensions 30.5 by 30.5 by 47.5 cm, bottom open, top covered, box material 0.635 cm thick, contains 0.366 g/cm^2 of B$_4$C, 5 cm from fuel to near surfaces of box.	0.92
Aluminum plates	Four each, 20.3 by 20.3 by 1.9 cm, at 5.7 cm from fuel to near surfaces of plate.	1.15
Stainless steel plates	Four each, 20.3 by 20.3 by 2.54 cm, at 5 cm from fuel to near surfaces of plate.	2.38
Plywood plates	Four each, 20.3 by 20.3 by 2.54 cm, at 5 cm from fuel to near surfaces of plate.	0.71
Lucite plates	Four each, 20 by 20 by 1.9 cm, at 5.5 cm from fuel to near surfaces of plate.	1.48
Lucite box	Inside dimensions 41.3 by 41.3 by 61 cm high, ends open, wall thickness 1.9 cm, at 10.5 cm from fuel to near surfaces of box.	1.74
Paraffin plates	Four each, 20 by 20 by 1.9 cm, at 5 cm from fuel to near surfaces of plate.	2.25
Water plates	Four each, held in polyethylene bags placed in wire baskets having dimensions 20.3 by 20.3 by 2.5 cm, at 8.5 cm from fuel to near surfaces of plates.	0.95
Water plates plus boral box	Identical to above descriptions, boral box placed between water and reactor fuel.	1.83

worth of all four plates simultaneously. The reactivity worth of the four water plates was also determined for a spacing of 4.5 cm from the fuel to the near surfaces of the plates. At this spacing the reactor went super-delayed critical upon seating of the safety block. From the control-rod-worth calibration and the measured positive period of the power excursion, the reactivity worth of the plates was determined to be $2.60.

The reflector geometry used in the experiments on SPR was chosen to simplify the mathematical treatment and to facilitate a parametric investigation of the reflector time constants τ_3 and τ_4. The

reflectors were 6-in.-high cylinders with various inside diameters and thicknesses. The transit time τ_4 was investigated by varying the transit distance while holding constant the thickness of the reflector and hence the reflector-neutron energy spectrum. The residence time τ_3 was inferred by extrapolating the results to zero transit time. Since polyethylene is a good moderator, it was chosen as the primary material to be studied. The effects of steel reflectors were also studied to compare the effects of moderating and nonmoderating reflectors.

An aluminum stand was constructed to support the reflectors in a manner to ensure that the aluminum was at the greatest possible distance from the fuel assembly. This reflector stand was located by and supported on the reactor support structure so that the position of the reflector with respect to the fuel assembly could be reproduced accurately. Table 3 contains a description of the reflectors used in the SPR experiments.

Table 3

REACTIVITY WORTHS OF SPR REFLECTORS

Material	Thickness, in.	Inner diameter, in.	Reflector worth, ¢	Apparent change* in burst-rod worth, ¢
Polyethylene	1	$17\frac{1}{2}$	64.1	0.50 ± 0.3
	2	$17\frac{1}{2}$	85.7	0.70 ± 0.3
	1	$14\frac{1}{8}$	121.3	1.15 ± 0.3
	1	$12\frac{1}{2}$	185.2	$1.5\ \ \pm 0.3$
	1	$22\frac{3}{4}$	30.2	0.25 ± 0.3
	1	$26\frac{1}{4}$	18.9	0.20 ± 0.3
Steel	$\frac{3}{4}$	18	46.31	$1.1\ \ \pm 0.3$
	$\frac{3}{4}$	16	66.51	1.65 ± 0.3
	$\frac{3}{4}$	14	99.9	$2.5\ \ \pm 0.3$

*Discussed in a later section.

For both the SPR and FBRF, reflectors or experimental equipment placed near the reactor generally contribute less than $2 of reactivity to the system. The perturbation of the spatial neutron-flux distribution within the fuel is not expected to be large, and therefore it is not expected to seriously affect the control-rod calibrations. The radial neutron-flux distribution of the SPR assembly was mapped under bare and reflected conditions. The reflectors induced a change in the neutron flux at any point in the fuel of no greater than 2%. The SPR neutron flux in the region between the fuel and the reflector was mapped using sulfur dosimetry. A steel reflector worth $1 in reactivity perturbed the neutron flux in this region by about 10%. A polyethylene reflector worth $1.21 in reactivity induced a somewhat smaller perturbation.

Differential and integral control-rod-worth calibrations were obtained for the SPR and the FBRF assemblies for the unreflected condition and for each of the reflector conditions studied. As expected, little difference was noted between the bare and the reflected calibration curves. An increase in the total integral worth of the control rods was noted; but, even for the highest worth reflector, the change was only 5%. The effects on burst-rod worth, though also small, are significant; they are discussed in a later section.

EFFECTS OF REFLECTORS ON THE KINETIC RESPONSE OF A FAST BURST REACTOR

The effect of a reflector on the kinetics of a burst reactor depends on the reflector parameters. The bare reactor parameters are fixed quantities for a given fuel assembly, but the reflector parameters can vary widely since they depend on the reflector material and the geometrical configuration of both the fuel assembly and the reflector. For example, a moderating reflector has a much softer leakage spectrum than a nonmoderating reflector, and the weighted average transit time τ_4 is therefore longer for the moderating material.

In the absence of any reflected-neutron contributions, the relation between the stable reactor period and the initial reactivity is given by the inhour equation

$$\rho(\$) = \frac{l^*}{\gamma\beta T} + \sum \frac{f_i}{1 + \lambda_i T} \tag{7}$$

For super-prompt critical conditions, T is very small, and the relation reduces to

$$\rho_p(\$) = \frac{l^*}{\gamma\beta} \alpha \tag{8}$$

where $\alpha = 1/T$ and $\rho_p(\$) = \rho(\$) - 1$. Equation 8 is the expression commonly used in the experimental determination of both the prompt-neutron decay constant and the point on an arbitrary reactivity scale which corresponds to prompt criticality. When the experimentally determined initial reciprocal period is plotted as a function of initial reactivity about some arbitrary reference reactivity, a straight line should result, according to Eq. 8. The slope of this line should be inversely proportional to the prompt-neutron lifetime, and the intercept of the line with the reactivity axis should define the prompt critical point $(\rho = \beta)$. With the prompt critical point defined, the reactivity

worth of the burst rod can be determined. This technique is referred to
as the slope – intercept method.

For both reactors the value of the unreflected burst-rod reactivity
worth was determined by both critical measurements and the slope –
intercept method discussed in the preceding paragraph. A difference of
approximately 3¢ in the values of the unreflected burst-rod worth ob-
tained by the two methods is attributed to the influence of room-
reflected neutrons and to uncertainties regarding the correct value to
use for the effective delayed-neutron fraction. Further investigation is
necessary before absolute values of the burst-rod worth can be
determined.

For large reactivity additions such that the system is near prompt
critical, the reactor period is quite small, and the reflector terms in
Eq. 6 become significant. In the reactivity region near prompt critical,
reactor periods are quite small compared with the mean lifetime of the
shortest-lived delayed-neutron-precursor group and yet are large com-
pared with the reflector time constants τ_2, τ_3, and τ_4 for both the poly-
ethylene and steel reflectors discussed in this paper. If the room-
reflected neutrons are ignored, Eq. 6 can be expressed

$$\rho_p(\$) \cong \frac{l_r^*}{\gamma \beta T} \qquad (9)$$

where

$$\rho_p(\$) = \rho(\$) - 1$$

and

$$l_r^* = l^* + \gamma \beta \sum_j f_j' (\tau_{3j} + \tau_2 + \tau_{4j})$$

Thus if this effect were described in terms of bare point reactor
kinetic equations, one would conclude that there had been an apparent
change in the prompt-neutron decay constant $(l/\gamma\beta)$ produced by the
addition of a reflector. The magnitude of the change is primarily a
function of the total worth of the reflector, the hardness of the reflec-
tor leakage spectrum, the effectiveness of the reflected neutrons in
causing fission, and the spacing between the reflector and the fuel.

For reactivity additions large enough to produce reactor periods of
the order of 15 μsec, the time constants τ_{3j} and τ_{4j} of the lower energy
groups are no longer small compared with the reactor period. An ob-
servable departure from the linear relation between reciprocal period
and prompt reactivity $\rho_p(\$)$ will result if the energy spectrum of the
reflected neutrons is quite soft. This effect is not observed in the case

of nonmoderating materials since β_j for the lower energy reflected-neutron groups is negligibly small. For very large separation distances between reflector and the reactor (as in the case of room-reflected neutrons), at least one low-energy reflected group can exist with a time constant that is large compared with the reactor period in the prompt critical region. Let this group be the kth reactor group.

Equation 6 can now be expressed

$$\rho_p(\$) \cong f'_k - \frac{l^*}{\gamma \beta T} + \sum_{j \neq k} \frac{(\tau_{3_j}/T) + 1 - \exp[-(\tau_2 + \tau_{4_j})/T)]}{(\tau_{3_j}/T) + 1} f'_j \qquad (10)$$

If the time constants associated with the remaining reflector groups are small compared with T, Eq. 10 can be written

$$\rho_p(\$) \cong f'_k - \frac{l^*r}{\gamma \beta T} \qquad (11)$$

A bare reactor description would then imply that there has been a change not only in the prompt-neutron lifetime but also in the value of β. This would influence the value of the burst-rod worth so determined.

When a reflector is placed near the fuel, care must be used when applying the slope–intercept method to determine the prompt critical point. Without data in the region of prompt criticality, the value of the burst-rod worth estimated by such a technique would be smaller than the actual value. This is especially true when a significant number of room-reflected neutrons are present since the time constants could be relatively large and could easily satisfy the conditions of Eq. 9. The room-reflected neutrons then could be responsible for the discrepancy between the values of the burst-rod worth determined by the different methods because the value obtained by the slope–intercept method is invariably smaller.

Such an effect was noted when the FBRF burst-rod worth was compared for indoor and outdoor operation. Assuming the value of β to be invariant, the value of the burst-rod reactivity worth apparently decreased by 1.0¢ when moving the system indoors. One infers from this decrease that the room-reflected neutrons had a reflected fraction f_k of 1.0¢ which satisfied the conditions of Eq. 9.

FBRF and SPR Experimental Data

Figure 1 shows the reciprocal period vs. the prompt reactivity data obtained for the different reflector conditions at the FBRF. The slope–intercept method was used to determine the prompt-neutron decay constants and burst-rod worth for the various FBRF reflector conditions. Table 4 presents the results of this analysis. On the FBRF
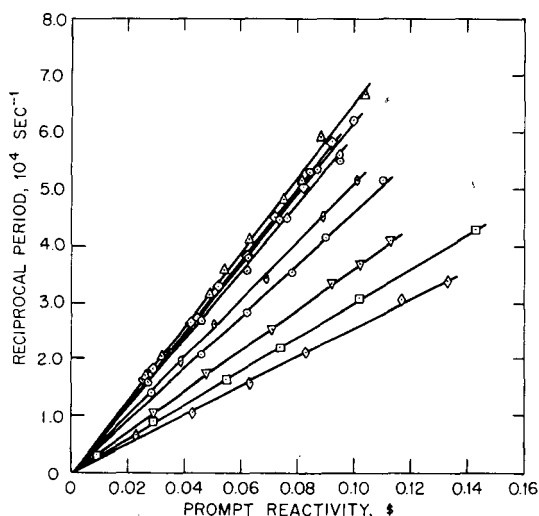
Fig. 1—Reciprocal period as a function of prompt reactivity for various reflector configurations for FBRF.

Table 4

PROMPT-NEUTRON DECAY CONSTANT AND
BURST-ROD WORTHS FOR FBRF

Reflector	Symbol*	Burst-rod worth,† $	Prompt-neutron decay constant 10^6 sec^{-1}	Burst width,‡ μsec
Boral box		0.110	0.67	48
Aluminum plates	△	0.120	0.65	50
Stainless steel plates	○	0.149	0.62	53
Plywood plates	◇	0.105	0.59	57
Lucite plates	○	0.119	0.46	62
Lucite box	□	0.094	0.30	91
Paraffin plates	◊	0.127	0.26	98
Water plates	▽	0.092	0.36	77
Water plates plus boral box	⊙	0.133	0.51	60
No reflectors	◇	0.085	0.65	49

*Symbols identify data in Fig. 1.
†Reactivity above prompt critical.
‡Width at half maximum power for burst yield of 5×10^{16} fissions.

a correlation appears to exist between the burst-rod worth and the reactivity added by the reflector; this correlation is discussed later in this paper. Other data for the FBRF, e.g., yield vs. reactivity, indicate the same characteristics as the SPR data which will now be presented.

Figures 2, 3, and 4 are the results of reciprocal period vs. prompt reactivity measurements for SPR, and the figures indicate a linear relation for the free-field and nonmoderating reflected conditions, as is expected. This linear relation was also observed for low prompt reactivity for the polyethylene reflectors used in SPR experiments.
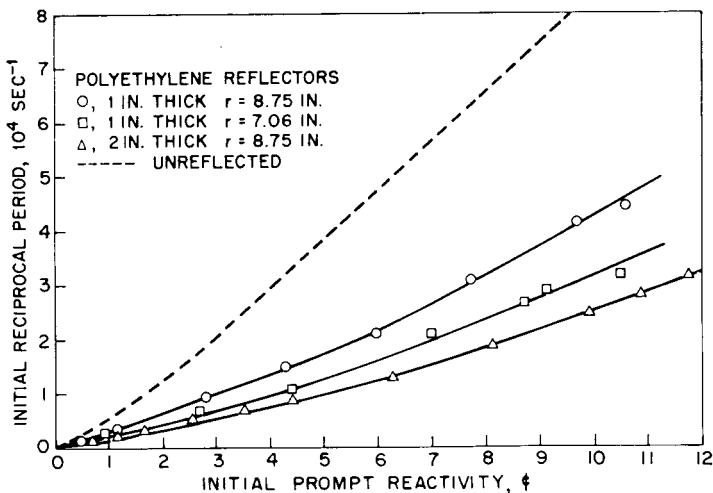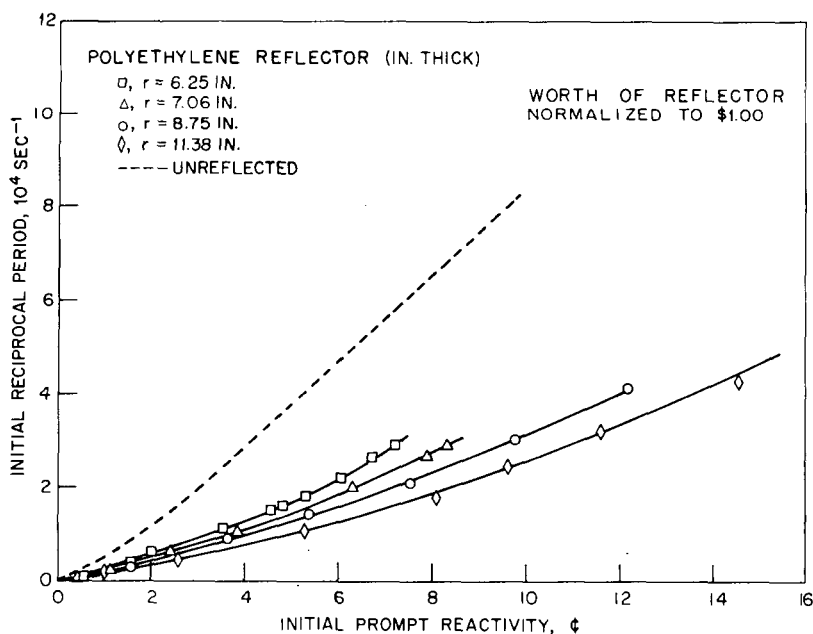

Fig. 2—*Reciprocal period as a function of prompt reactivity for various polyethylene reflectors for SPR where r = distance from reactor center line to inner surface of reflector.*
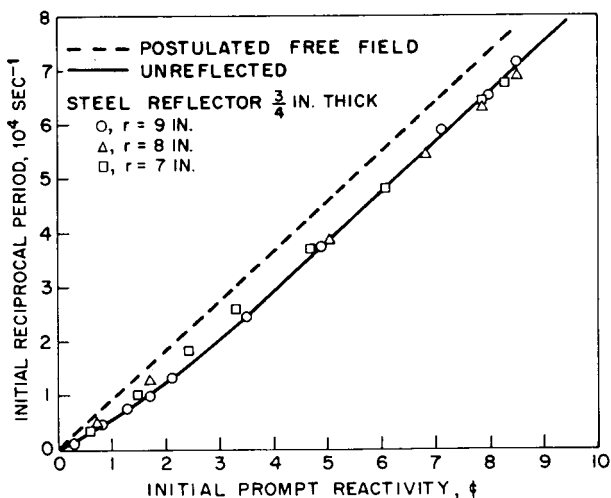
Fig. 3—*Reciprocal period as a function of prompt reactivity for various steel reflectors of uniform thickness for SPR where r = distance from reactor center line to inner surface of reflector.*
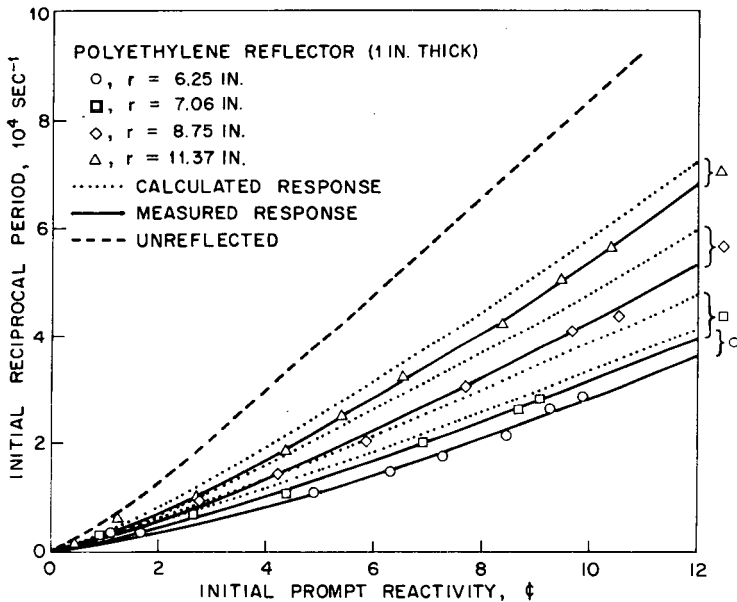
Fig. 4 — *Reciprocal period as a function of prompt reactivity for various poly-ethylene reflectors of uniform thickness for SPR where r = distance from the reflector center line to inner surface of the reflector.*

Comparison of Calculations and Experiments for SPR

For relating the predictions of Eq. 6 to experimental results, the reflector parameters, τ_2, τ_3, τ_4, etc., were calculated for a few of the SPR reflector arrangements using a Monte Carlo computer code developed for that purpose. Computer time was considerably reduced by using a discrete spatial and angular representation of the neutron distribution. The computer calculation employed 87 neutron energy groups, and it was tested by calculating various SPR bare kinetics parameters and comparing the results with known values.

Using either the experimentally determined Godiva I neutron-leakage spectrum or one which was calculated for the SPR assembly by Monte Carlo techniques, τ_2 was determined to be negligible for all distances involved in this study. Monte Carlo techniques were also used to determine the inner-surface reflector leakage spectrum for various thicknesses of polyethylene reflectors and to determine the residence time of neutrons $\tau_3(E)$ in the reflectors as a function of the energy of the neutrons escaping from the reflector. The results are given in Figs. 5 and 6. The lines represent an estimated best fit to the computed data. The results of a DDK calculation performed by Wimett[4] for the reflected-neutron energy spectrum from the inner surface of a
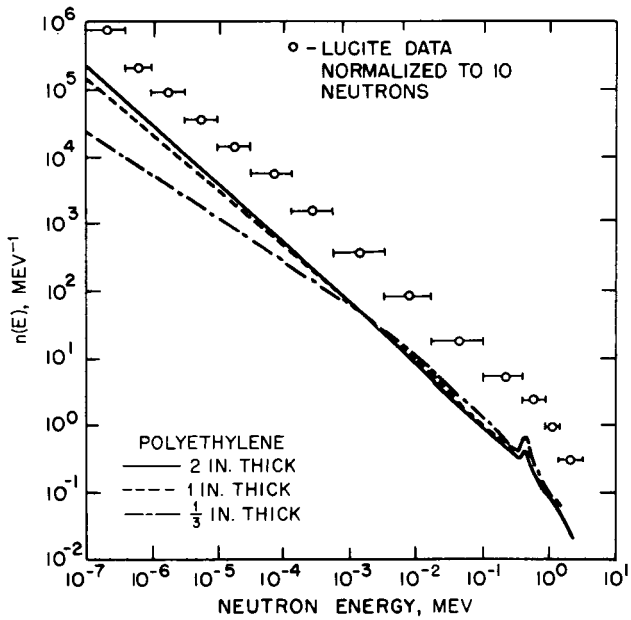
Fig. 5—*Reflected-neutron spectrum from inner surface of various polyethylene reflectors.*
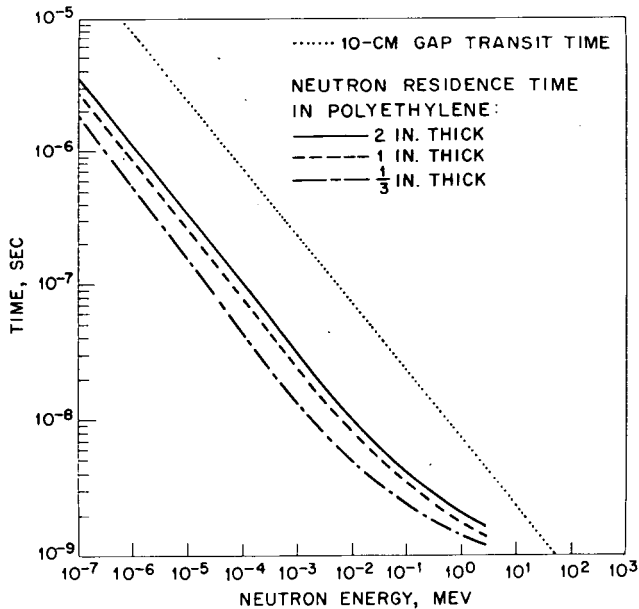
Fig. 6—*Monte Carlo calculated neutron residence time in polyethylene.*

1-in.-thick Lucite reflector is also shown in Fig. 5. Wimett's computed data were normalized to 10 neutrons for convenient display, and the Monte Carlo computed polyethylene data are normalized to 1 neutron. The transit time $\tau_4(E)$ is inversely proportional to the velocity of the neutrons escaping from the reflector, and for convenience it is given in Fig. 6 in terms of the time required to travel a distance of 10 cm. Multiple reflection was neglected in the determination of $\tau_4(E)$ and $\tau_3(E)$.

Using the calculated reflector leakage spectrum and effectiveness estimates based on further Monte Carlo calculations, the reflected-group effective fractions $\gamma'_j \beta'_j$ were determined. The effect of the SPR cadmium shroud was included in the effectiveness estimate. The relation

$$W = \sum_j \gamma'_j \beta'_j$$

was used to normalize the computed data to the measured worth W of the reflector. This relation is obtained by hypothetically removing the reflector from a system described by Eqs. 1, 2, and 3 and determining the reactivity that must be added to reestablish steady-state conditions.

Equation 6 was plotted in Fig. 4 using the reflector parameters calculated by Monte Carlo techniques for one SPR reflector configuration. The essential features of the experimental and calculated curves are the same. The difference between the curves may be attributed to uncertainty in the estimate of reflected-neutron effectiveness and the inability to determine accurately the actual value of the burst-rod worth in the presence of room-reflected neutrons. The departure from linearity is evident in both the calculated and experimental results.

For a given material of a given thickness, the effective reflected fraction $\gamma'_j \beta_j$ is directly proportional to the measured worth of the reflector. Let a_j be the constant of proportionality and define $\Delta(T)$ for a given reflector as

$$\Delta(T) = \frac{1}{\sum_j \gamma'_j a_j} \sum_j \gamma'_j a_j \frac{(\tau_{3_j}/T) + 1 - \exp\left[-(\tau_2 + \tau_{4_j})/T\right]}{(\tau_{3_j}/T) + 1}$$

The value $\Delta(T)$ is the additional prompt reactivity per unit reactivity worth of a reflector required to produce a given reactor period. Neglecting delayed neutrons, Eq. 6 reads

$$\Delta_R(T) = \frac{\rho(\$) - \left[(l^*/\gamma\beta T) + \Delta_{RR}(T)W_{RR}\right]}{W(\$)} \tag{12}$$

where $\Delta_R(T)$ pertains to a given experimental reflector of reactivity worth $W(\$)$ and $\Delta_{RR}(T)$ pertains to room-reflected neutrons of worth $W_{RR}(\$)$.

In the absence of an experimental reflector, $\Delta_{RR}(T)W_{RR}$ can be determined experimentally using the relation

$$\Delta_{RR}(T)W_{RR} = \rho(\$) - \frac{l^*}{\gamma\beta T}$$

The left-hand side of Eq. 12, consisting entirely of experimentally obtainable or known quantities, serves as a basis for studying the reflector effect.

Inspection of Eq. 12 shows that if the transit time τ_4 is important Δ should increase monotonically as the distance between the fuel and the reflector is increased. The SPR experimental results confirm this effect, and one concludes that τ_4 is a significant quantity. The reactivity worth of the reflectors was normalized to $1.0, and the resulting values of Δ were used in Eq. 12 to give $\rho(\$)$ as a function of $1/T$. The results, given in Fig. 7, clearly indicate that, as the distance to the reflector increases, the reflector effect becomes more pronounced.

Fig. 7—*Reciprocal period as a function of prompt reactivity for various polyethylene reflectors of uniform thickness on SPR where r = distance from reactor center line to inner surface of reflector.*

The total fission yield is given in Figs. 8, 9, and 10 as a function of initial reciprocal reactor period. A considerable increase in burst yield for a given initial reciprocal period results from the addition of a moderating reflector. All SPR yield data can be related to fissions by the conversion factor

$$F(\text{fissions}) = 1.82 \times 10^{14} \, (\Delta\theta)$$

where θ is in degrees centigrade.
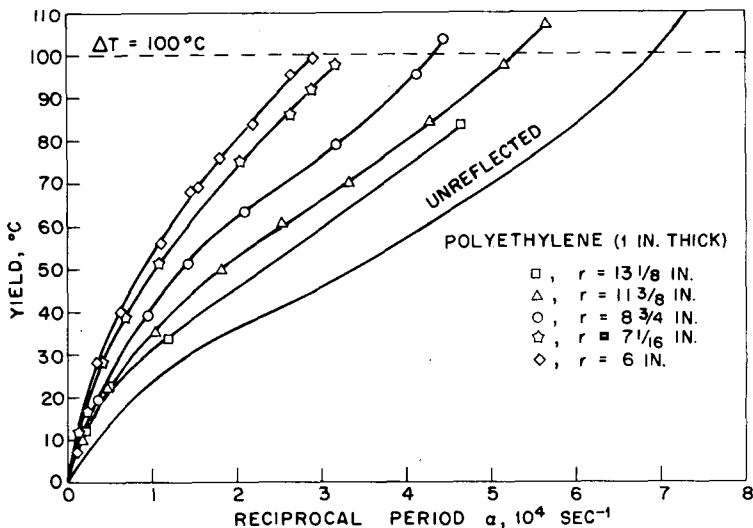
Fig. 8 — *Energy release per burst as a function of reciprocal period for various polyethylene reflectors where* r = *distance from reactor center line to inner surface of the reflector.*

An expression derived by Wimett[4], using a bare reactor description, implies that the yield for a given initial period is directly proportional to the neutron lifetime. The reflector effect can be treated as a change in neutron lifetime for most of the reflectors; one therefore expects an increase in yield to result from the addition of a reflector.

Very little effect was observed in the case of the nonmoderating materials since the effective change in the neutron lifetime was quite small.

The relation between burst width at half maximum and initial period was also investigated; it was found to be essentially independent of prompt-neutron lifetime in the range investigated, as would be predicted on the basis of the model developed by Wimett.
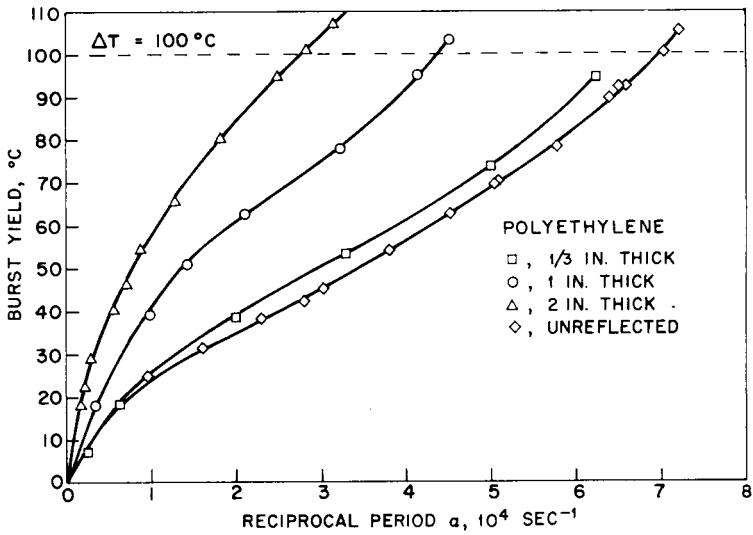
Fig. 9—Energy release per burst as a function of reciprocal period for various polyethylene reflectors. The distance from the reactor center line to the inner surface of the reflector is $8^3/_4$ in.
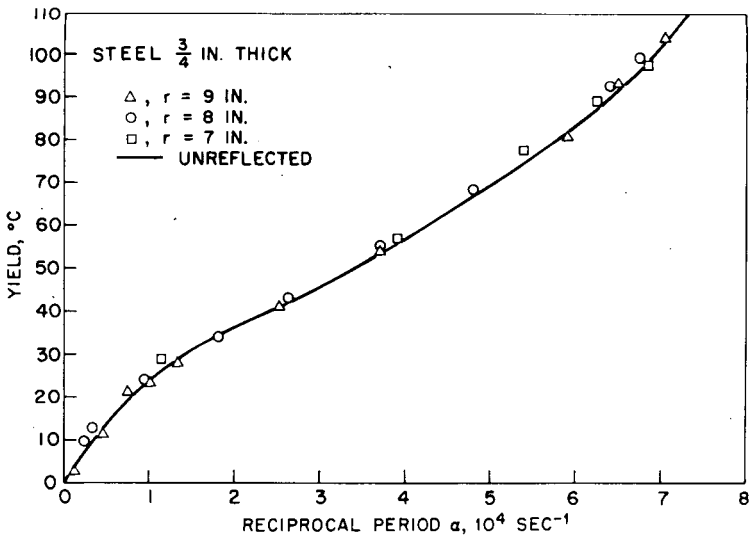
Fig. 10—Energy release per burst as a function of reciprocal period for various steel reflectors for SPR where r = distance from the reactor center line to inner surface of reflector.

The burst width at half maximum is given in Fig. 11 as a function of burst yield. The figure emphatically illustrates the broadening of the burst for a given yield when a moderating material is located near the fuel. The peak fission rates obtained during the bursts are given in Fig. 12 as a function of burst yield. The peak fission rate for a given initial reactor period was observed to increase upon the addition of a reflector, as would be expected on the basis of the Wimett model. Thus for a given reactor period, higher dose rates and greater total yield are possible for a reflected system.
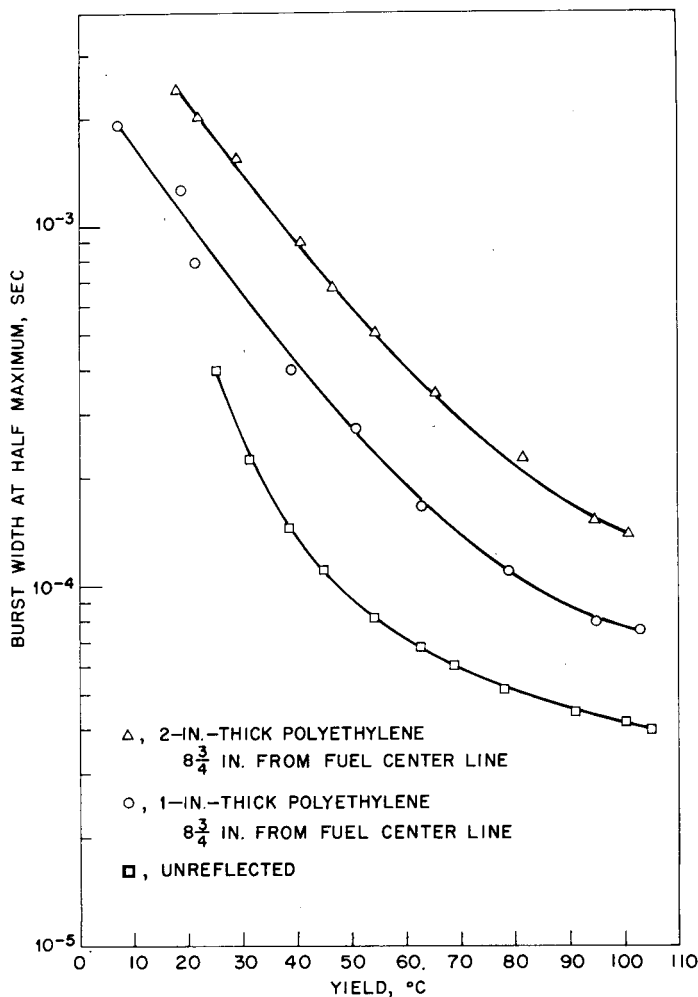
Fig. 11 — *Burst width at half maximum fission rate as a function of burst yield for various polyethylene reflectors for SPR.*
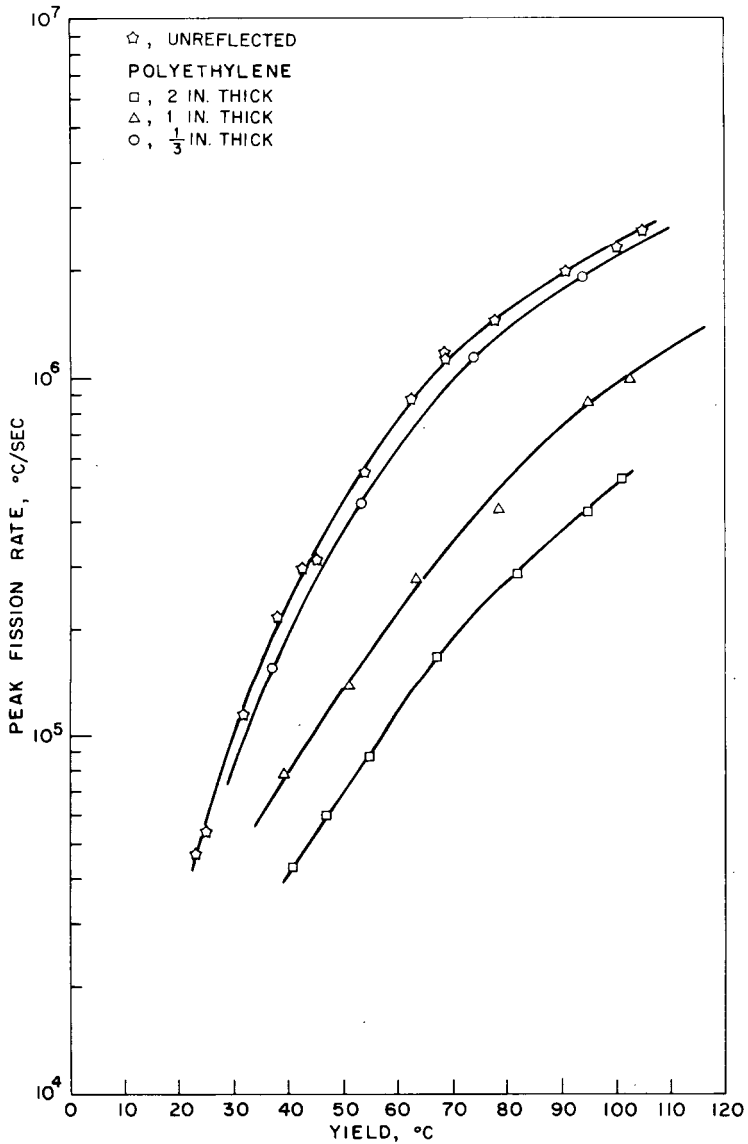
Fig. 12—*Peak fission rate as a function of burst yield for various polyethylene reflectors for SPR.*

EFFECTS ON BURST-ROD WORTH AND DECOUPLING

Burst-Rod Worth vs. Reactivity Added

The change in burst-rod worth as a result of placing an experiment close to the core is potentially hazardous. Therefore it is important to try to correlate this change in worth to some easily measured parameter, such as the reactivity added by the experiment. Figure 13 shows the increase in burst-rod worth plotted as a function of reflector reactivity worth for each reflector condition on the FBRF. The measured
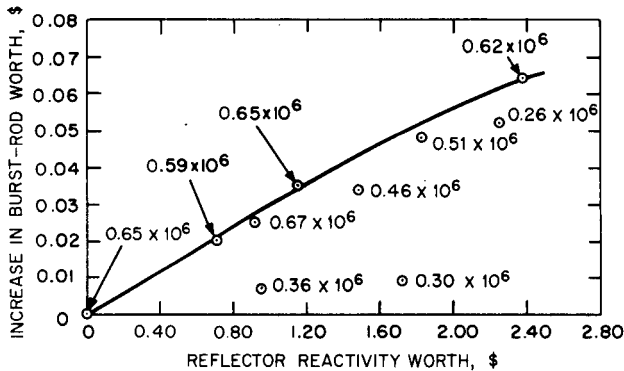
Fig. 13—*Increase in FBRF burst-rod worth as a function of reflector reactivity worth.*

value of the prompt-neutron decay constant is shown for each data point. A smooth curve can be drawn through the data points for which this constant has not changed very much from the unreflected value. With the exception of the paraffin data point (0.26×10^6 sec^{-1}), a family of curves might be generated for each value of decay constant. The generation of such a family of curves may be difficult experimentally since both the reactivity worth and the decay constant change as moderating reflectors are moved toward or away from the reactor.

Figure 13 has been used at the FBRF to predict reasonably well the effect on burst-rod worth of several large experimental test setups. However, it should be emphasized that the change in burst-rod worth is a smooth function of reactivity added only for symmetrical reflector conditions.

For the SPR data the slope−intercept method was modified to produce results consistent with Eq. 6 and was used to determine the change in the burst-rod reactivity worth attributable to a reflector. This determination established a reactivity reference for measurements above prompt critical. In both reactors, nonmoderating materi-

als were found to induce the greatest increase in the burst-rod worth. The results for SPR are given in Table 3, and the results for FBRF are given in Table 4. An uncertainty of approximately ±0.3¢ results from the difficulty in adequately accounting for the room-reflected neutrons.

Burst-Rod Worth vs. Reflector Position

A limited number of bursts was obtained for asymmetrical reflector conditions on the FBRF. Four bursts were obtained with a single 20.3- by 20.3- by 2.54-cm steel plate located at angular positions with respect to the burst rod of 30°, 60°, 120°, and 150°. The plate was placed at a distance of 5.0 cm from the fuel assembly. The reactivity worth of the reflector plate at each of the four positions was $0.65 ± 0.04. The variation in worth was probably caused by slight radial positioning errors.

The control-rod withdrawal correction for each of the four bursts was identical, and changes in burst size were attributed to the change in burst-rod worth resulting from the flux-distribution shift caused by the reflector plate. The actual reactivity inserted by the burst rod was calculated from the data obtained for α vs. ρ ($) and yield vs. α for the unreflected reactor. The assumption[9] was made that the prompt-neutron decay constant did not change.

Figures 14 and 15 show the results from four bursts with the steel plate and from two bursts with the large Lucite panel. (The Lucite panel, 61 by 61 by 2.54 cm, was located 11.5 cm from the fuel assembly and had a reactivity worth of $0.42 ± 0.02.) The lines through the data points are drawn from equations having the form $y = a_0 + a_1 \cos \theta$.

In addition to the data presented in Figs. 14 and 15, it would be of interest to study such things as (1) the effect of changing the reactivity
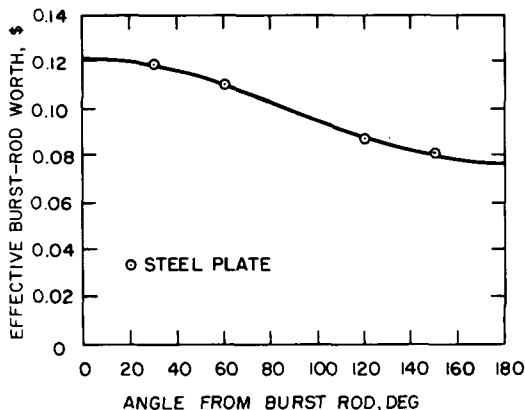
Fig. 14 — FBRF burst-rod worth for various reflector locations.
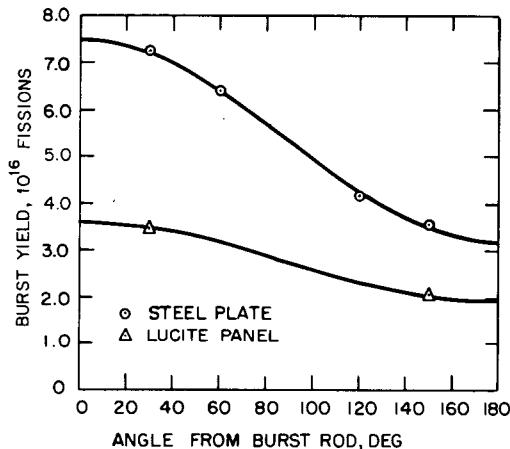
Fig. 15—Effect of reflector location on FBRF fission yield.

worth of the reflector, (2) the effect of changing the size and geometry of the reflector, and (3) the effect of moderating reflectors. Figures 14 and 15 have been used also to predict reasonably well the effect on FBRF burst-rod worth of some experimental test setups.

Decoupling

The coupling between a moderating reflector and the reactor has the undesirable features of making calculations of the burst characteristics for a given reactivity addition more complicated and of causing a broader pulse for a given fission yield. Although a model has been developed which adequately predicts the behavior of a reflected fast burst reactor, safer operation results when the calculational requirements are minimized.

As noted in the previous sections, moderating materials induce the greatest change in the burst characteristics of a fast burst reactor owing to the larger number of low-energy neutrons that are returned to the fuel from a moderating reflector. The transit time τ_4 and the residence time τ_3 associated with the low-energy groups (<1 ev) are quite large, and they greatly affect the dynamic response of the reactor system. However, by the proper use of absorbing materials, the return of the low-energy neutrons to the reactor can be prevented without affecting the transmission of Godiva spectrum neutrons.[10]

Cadmium has been used routinely as a decoupling shroud for several fast burst reactors, and it has been successful in diminishing the effect of moderating reflectors. A cadmium shroud was in place for all the experiments reported earlier in this paper for both the FBRF and

the SPR. The results of the experiments clearly indicate that cadmium may diminish the effect of moderating reflectors but certainly does not eliminate the effect.

An analysis by T. F. Wimett and G. E. Hansen of the Los Alamos Scientific Laboratory indicated that neutrons having energies above the cadmium cutoff were primarily responsible for the effect and that boron would be a much more effective decoupling material.

Boron was investigated as a decoupling material on both the FBRF and SPR using 0.25-in.-thick plates of boral, a metallic mixture of B_4C and aluminum. The 0.168-in.-thick core of the boral plates consists of 44.7 wt.% B_4C. The remaining material is aluminum. The water plates discussed previously resulted in an apparent change in the FBRF prompt-neutron decay constant of from 0.65×10^6/sec (unreflected condition) to 0.36×10^6/sec. When boral plates were placed between the water plates and the reactor, a prompt-neutron decay constant of 0.51×10^6/sec resulted, indicating that the effect of the water plates was diminished by the boral decoupler.

For the evaluation of boron as a decoupling material for the SPR II (see R. M. Jefferson, Session 2, Paper 3), the effectiveness of cadmium and boron was investigated experimentally using the SPR. Cadmium was found to diminish greatly the effect of the moderating reflector used whereas two $\frac{1}{4}$-in. boral plates virtually eliminated the effect. The results of the SPR experiments are shown in Figs. 16 to 19. The results are in good agreement with those predicted using fractions
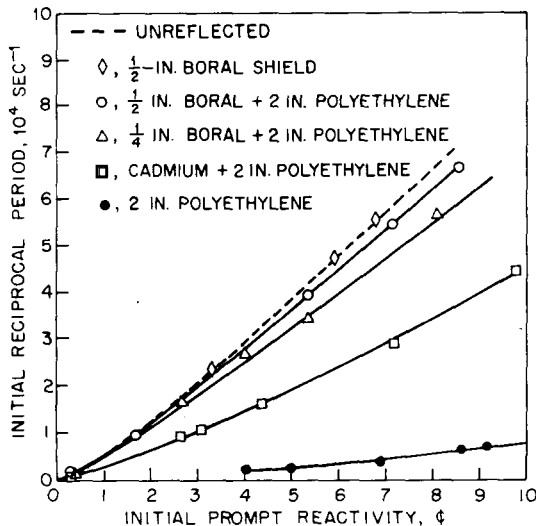
Fig. 16 — SPR initial reciprocal reactor period as a function of prompt reactivity.

348
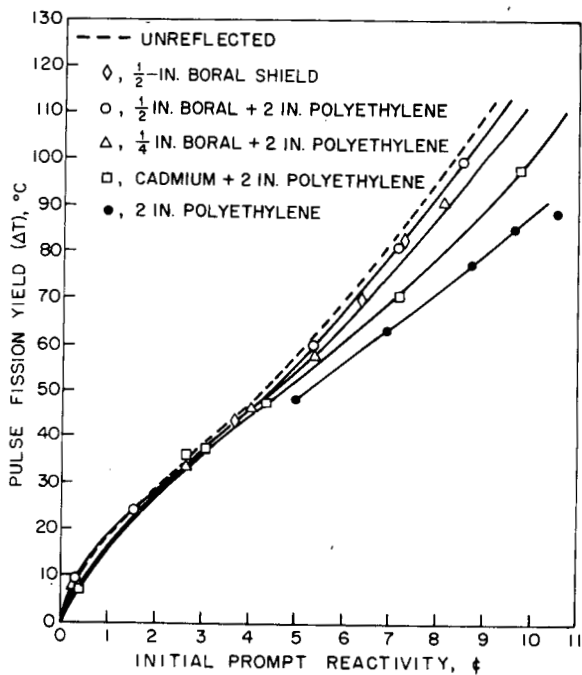
Fig. 17—*Effect of polyethylene reflector on SPR fission yield for various degrees of decoupling.*
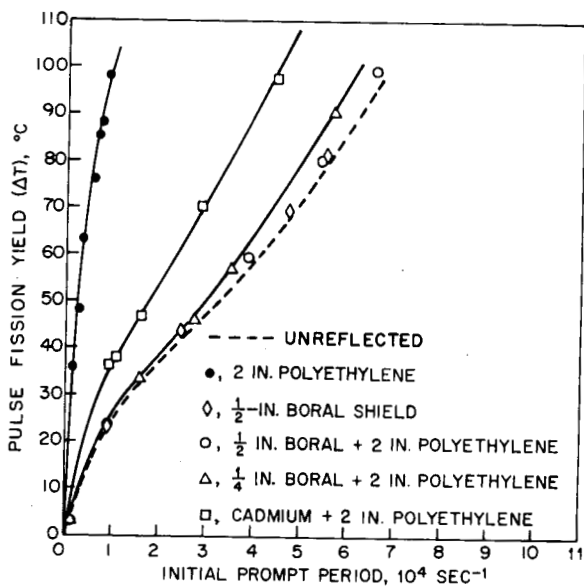
Fig. 18—*Effect of polyethylene reflector on SPR fission yield for various degrees of decoupling.*
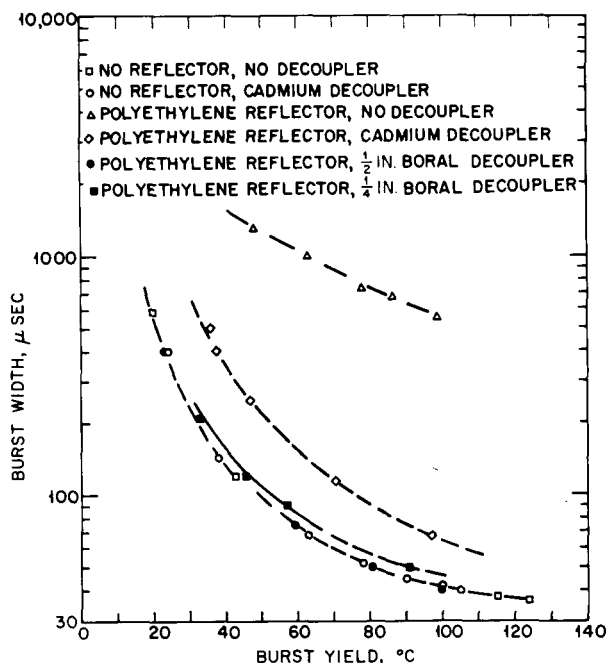
Fig. 19—Effect of polyethylene reflector on SPR pulse width for various degrees of decoupling.

Table 5

REACTIVITY CONTRIBUTION OF
2-IN.-THICK POLYETHYLENE SLAB

Decoupler	Polyethylene worth, ¢
No decoupler	62
0.01 in. cadmium	50
0.03 in. cadmium	45
0.06 in. cadmium	43
0.25 in. boral	35
0.50 in. boral	29

and time constants calculated by Monte Carlo techniques. A 2-in.-thick, 6- by 6-in. polyethylene slab placed 1 in. from SPR was used for both the experimental and theoretical investigations.

A boron-loaded decoupling shroud has the further favorable effects of diminishing the reactivity contribution of a moderating reflector. This result is clearly evident in Table 5 where the reactivity contribution of the 2-in.-thick polyethylene slab is given for various SPR decouplers.

ACKNOWLEDGMENT

REFERENCES

1. R. L. Long, Operating Characteristics of the WSMR Fast Burst Reactor in *Neutron Dynamics and Control*, pp. 386-397, Tucson, Ariz., April 5-7, 1965, D. L. Hetrick and L. E. Weaver (Coordinators), AEC Symposium Series, No. 7 (CONF-650413), 1966.
2. P. D. O'Brien, The Sandia Pulsed Reactor Facility (SPRF), USAEC Report SC-4737(M), Sandia Corporation, October 1962.
3. R. E. Peterson and G. A. Newby, An Unreflected ^{235}U Critical Assembly, *Nucl. Sci. Engr.*, 1: 112-125 (1956).
4. T. F. Wimett, R. H. White, W. R. Stratton, and D. P. Wood, Godiva II— Unmoderated Pulse-Irradiation Reactor, *Nucl. Sci. Engr.*, 8: 691-708 (1960).
5. R. L. Long, Effects of Reflectors on the Burst Characteristics of the WSMR Fast Burst Reactor, *Trans. Amer. Nucl. Soc.*, 8(2): 451 (1965).
6. R. L. Coats, Kinetic Behavior of a Reflected Fast Burst Reactor, *Trans. Amer. Nucl. Soc.*, 9(2): 468 (1968).
7. C. E. Cohn, Reflected-Reactor Kinetics, *Nucl. Sci. Eng.*, 13: 12 (1962).
8. R. L. Coats, Neutron Kinetics of a Reflected Fast Burst Reactor, USAEC Report SC-RR-67-802, Sandia Corporation, 1967.
9. R. L. Long, Effects of Reflectors on the Burst Characteristics of an En-riched Uranium—10 wt.% Molybdenum Alloy Fast Burst Reactor, Missile Science Division, White Sands Missile Range, Internal Memorandum No. 26, 1965.
10. R. L. Coats, Neutronic Decoupling of Fast Burst Reactors, *Trans. Amer. Nucl. Soc.*, 10(1): 243 (1968).

DISCUSSION

BRUNSON: In one figure you show the effect of the moderator without a decoupler and then a value for the moderator with various de-couplers — 136 mils of cadmium and a couple of boral thicknesses. Have you ever measured the reactivity worth of the decoupler without the moderator?

COATS: Yes, in every case.

BRUNSON: What was the magnitude of the effect?

COATS: The reactivity worth of the various decoupling materials was important in the design of the SPR II decoupling shroud. A de-coupling shroud consisting of boral plates was constructed for SPR II. This shroud proved to be excessive in reactivity worth and was re-placed by one using a ^{10}B-loaded silicon resin as the decoupling material.

The cadmium decouplers used in the SPR experiments described in the paper had a reactivity worth of about 15 to 20¢ for the position at which they were located during the experiment. The boral plates located at the same position had a reactivity worth of approximately 50¢.

FOELL: If one wanted to irradiate medium or lightweight materials in the glory hole, he would of course worry about this same reactivity effect that you have described here. Do you have the feeling that the decoupler material would be equally effective in the glory hole?

COATS: The physical dimensions of the SPR II irradiation cavity limit the material specimen to be placed in the cavity to small sizes. Although the reactivity effect for a given mass of moderating material is greater in the irradiation cavity than outside the system, the degree of moderation possible for a given reactivity worth is less. Thus decoupling with a low-energy-neutron absorber would not be as effective for experiments placed in the SPR II glory hole.

LARRIMORE: You know that repetitively pulsed reactors have four components, one of which is an absorber layer, so we are involved with the same problem you described. We have developed a three-group kinetics model which was published several years ago (EURATOM Report EUR-2273). How many groups do you use, how do you get your constants, and what are the energies?

COATS: Eighty-six neutron-energy groups were used in the analyses, i.e., determination of the reflected-group constants in the SPR experiments. The K. Parker (Aldermaston) cross sections were incorporated in the Monte Carlo calculations. Several energy groups were added to extend into the lower energy regions. The resultant total happened to be 86.

LARRIMORE: We have the feeling that you only have to worry about those neutrons which are around the order of microseconds because that is how wide your burst is; so, we think you could group all your neutrons which live for times up to, say, a microsecond, into one group and group those which have lifetimes of a microsecond or more into a second group. These turn out to be very low-energy neutrons in the electron volt range.

COATS: Well, again I cannot defend the large number of groups except to say that I did not want to go into any great detail in trying to choose groups over a broader range. I wanted to partition the energy scale as much as I could, and I did have a large number of cross-section groups.

PETERSON: On the question of the moderating materials in the glory hole, we do have some experience with this at Super KUKLA. We do get significant decoupling using cadmium or gadolinium. One pitfall to this, however, is that you can get a very good neutron sink and not even be able to go critical if you have the right geometries.

COATS: That is true, but you also have a much larger glory hole, and so you can see a greater moderation for a given reactivity worth.

4-5 PREOPERATIONAL TEST EXPERIENCE WITH THE ARMY PULSE RADIATION FACILITY REACTOR

A. H. KAZI, H. G. DUBYOSKI, and R. W. DICKINSON
U. S. Army Ballistic Research Laboratories, Aberdeen Research and
Development Center, Aberdeen Proving Ground, Maryland

ABSTRACT

This paper summarizes data obtained in preoperational tests of the Army Pulse Radiation Facility Reactor. During these tests a pulse with a yield of 6.09×10^{17} fissions was obtained, which is three times larger than the anticipated maximum operational yield. The center third of the safety block was melted. The centrally located fuel rings were distorted, and cracks have appeared between the holes and the inner diameter. The bolts were stretched and slightly bent but not broken. The pulse rod, regulating rod, and mass adjustment rod were slightly bent. Most of the $U-10$ wt.% Mo fuel parts no longer meet the original specifications and must be replaced for pulse operation. There was little or no damage to rod drive, supports, etc, no overexposure to radiation of the operations personnel, and no detectable external or airborne radioactive hazards. A number of changes in design, instrumentation, and procedure are being made to place the reactor into full operation at levels of approximately 2×10^7 fissions/pulse and 10 kw steady state.

This paper describes a preliminary analysis of preoperational tests performed on the Army Pulse Radiation Facility Reactor (APRFR) at the Ballistic Research Laboratories, Aberdeen Proving Ground, Maryland. These tests started with core assembly on July 17, 1968, and ended with pulse 68-30, which produced a yield of 6.09×10^{17} fissions. The yield of this pulse was considerably larger than expected, and as a result the reactor core was damaged. There was no other damage to other parts of the reactor, no detectable external or airborne radiation hazards, and no overexposure of personnel to greater than normal occupational radiation levels.

The primary cause of this inadvertent high yield appears at present to be that the reactivity of the pulse rod passed through a maximum before reaching its seated position. An initiation occurred near this

position so that a larger value of reactivity was effective rather than the expected and measured value at the seated position.

Under the section on reactor assembly and prepulse tests, pre-pulse calibration data are summarized and the assembly tested at APRFR is compared with the assembly tested at the Critical Experiment Facility (CEF) at Oak Ridge National Laboratory (ORNL). In this paper the initial pulse operation, including the maximum yield pulse and the postulated cause for the maximum pulse, are discussed, and a summary of reactor damage is given. The steps required to confirm the postulated cause of the maximum pulse and the steps required for resumption of APRFR operation are discussed under Conclusions. These steps are (1) replacement of damaged core parts; (2) performance of pulse-rod, regulating-rod, and mass-adjustment-rod calibrations at steady-state conditions to obtain data required to determine if the postulated cause can account quantitatively for all features of the excursion; and (3) changes in design, instrumentation, and operating procedures to permit operation of the APRFR with requisite safety at full-performance levels.

REACTOR ASSEMBLY AND PREPULSE TESTS

Initial Configuration

Reactor assembly for the preoperational tests was begun at APRF (Army Pulse Radiation Facility) in July 1968 following receipt of requisite safety approvals. Personnel involved included APRF staff and two specialists from ORNL.

Fuel rings were selected according to size and mass to achieve a critical core configuration with the thermocouple-instrumented fuel ring as close as possible to the center of the total core height. This is desirable since these thermocouples are used to monitor core temperatures which are maximum near the center of the core. Nine fuel bolts were each matched with an Inconel nut and lubricated with Molykote 505 to help assure free movement. The pulse rod, mass adjustment rod, regulating rod, and safety block were assembled. A number of nonfuel components are involved in the reactor assembly. These are listed in Table 1. The assembly is shown schematically in Fig. 1. Table 2 lists the approach-to-critical steps. The reactor first went critical at 1442 on July 24, 1968.

Following configuration E' on July 24, 1968, core F was assembled with a measured core height of 20.09 cm. This configuration provided adequate control range on the regulating rod and mass adjustment rod and was the basic core used in all experiments during this part of the APRFR preoperational tests. Detailed information on core F fuel components is given in Table 3.

Table 1

NONFUEL COMPONENTS USED FOR
APRFR CORE ASSEMBLY

Item	Number required
Core-support ring	1
Safety tube	1
Glory hole liner	1
Cooling shroud	1
Safety cage	1
Control-rod liners	3
Safety-block air deflector	1
Core bolt spacers, 19 mm ($^3/_4$ in.)	15
Core bolt spacers, 6.35 mm ($^1/_4$ in.)	9
Core bolt nuts	6
Safety-tube locking adaptors	3
Thermocouple inserts	4
Safety-block set screw	1
Regulating-rod adaptor	1
Mass-adjustment-rod adaptor	1
Pulse-rod adaptor	1
Several small pins and set screws	

Table 2

APPROACH-TO-CRITICAL CONFIGURATIONS OF APRFR

Core designation	Fuel alloy mass, kg	Core height, cm	Date	Time assembled
A	81.013	12.578	July 17	1500
B	100.797	15.771	July 19	1100
C	112.633	17.574	July 22	1500
D	118.410	18.463	July 23	1300
E	123.105	19.508	July 24	1000
E′	(Same as E plus safety shield and cooling shroud)			

Prepulse Calibrations

A number of differential regulating-rod and mass-adjustment-rod calibrations were performed. The maximum differential worth of the regulating rod was 5.22 ¢/cm (13.27 ¢/in.) and of the mass adjustment rod was 12.0 ¢/cm (30.5 ¢/in.). The pulse-rod worth was determined from delayed-critical measurements with pulse rod in and out. The reactivity worth of various components is summarized in Table 4. Differences between the APRFR and CEF data as listed in Table 4 are to be expected because of the slightly different core configuration at CEF, as discussed in the following:
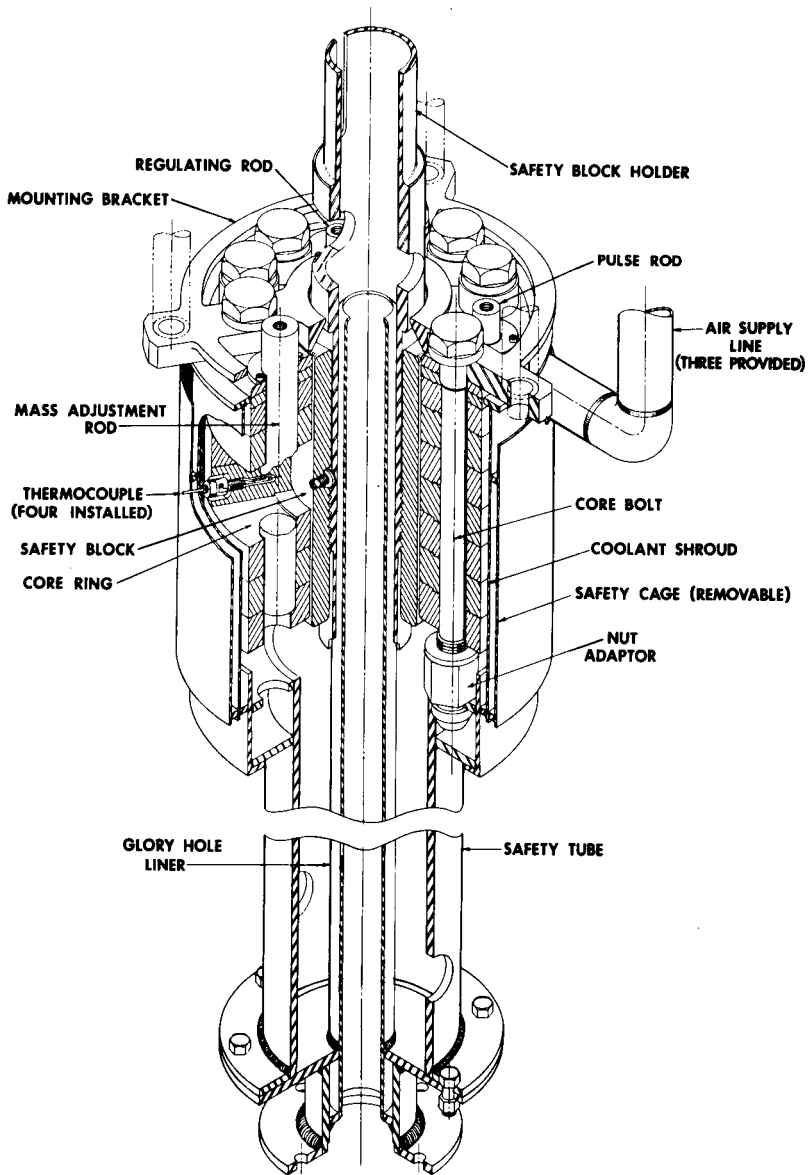
Fig. 1 — APRFR core assembly (shown with glory hole liner).

Table 3

APRFR CORE F FUEL COMPONENTS

Components and serial numbers	Weight, kg	Height, cm	Total weight, kg
Fuel rings (9):			
7882-20-0115	5.760	1.272 (top of core)	
7881-99-0009	2.288	0.526	
7882-40-0109	8.637	1.933	
7881-21-0001	11.954	2.667	
7881-19-0003	10.416	2.229	
7882-18-0070	14.516	3.404	
7882-38-0062	8.465	1.895	
7881-17-0004	14.561	3.254	
7881-16-0007	12.272	2.753	
Subtotal	88.869	20.033	88.869
Bolts (9):			
7882-17-0064	1.845		
7882-17-0065	1.841		
7882-17-0067	1.849		
7882-17-0069	1.845		
7882-17-0072	1.845		
7882-17-0073	1.849		
7882-17-0074	1.850		
7882-17-0075	1.842		
7882-17-0076	1.844		
Subtotal	16.610		16.610
Rods:			
Pulse rod			
7882-17-0061	1.467		
Mass adjustment rod			
7881-26-0051	1.964		
Regulating rod			
7881-27-0052	0.753		
Safety block			
7882-22-0085	15.730		
Subtotal	19.914		19.914
		Subtotal	125.393
		Minus pulse rod	1.467
		TOTAL WEIGHT	123.926

Table 4

REACTIVITY WORTH OF REACTOR COMPONENTS

Component	Total worth, ¢	CEF measurement,[1] ¢
Regulating rod	75.5	72
Mass adjustment rod	172.4	168
Pulse rod	127.7	*
Glory hole liner	24.5	No data available
Safety tube†	22.5	55
Thermocouple inserts (4)	5.0	*
Cooling shroud and safety cage	154	148
Displacement-gauge mounting plate	Not present	49
Nitrogen can	2.0	*

*These are new components, and hence no CEF data are available.
†The safety tube was mounted farther away from the core because of the core nuts; hence, its worth was less at APRFR than at CEF.

Differences Between APRFR and CEF Assemblies

The various differences between the assemblies tested at CEF and APRFR can be divided into three broad categories.

DIFFERENCES IN AUXILIARY COMPONENTS. The basic purpose of the tests[1,2] at CEF was to determine the pulse capabilities of the assembly and to check out the controls and instrumentation. Thus the CEF tests were more in the nature of a physics experiment and calibration, plus check-out of instrumentation. The maximum pulse yield obtained at CEF was 3.7×10^{17} fissions, and the data indicated the reactor could be operated with a maximum yield of about 2.1×10^{17} fissions/pulse.

At APRFR the aim of the preoperational tests was to obtain an operational reactor in such a configuration that would be a useful facility for its mission, namely, the safe routine performance of high-yield pulses for radiation effects and other user-oriented experiments. The standard CEF pulse assembly was bare except for experimental equipment nearby; the standard APRFR assembly included cooling shroud, safety cage, safety tube, and glory hole liner as shown in Fig. 1.

At CEF core-displacement gauges and a mounting plate were used during pulse operation. These gauges were used to obtain core-displacement data by Sandia and White Sands Missile Range personnel.[3] At APRF these components were not used.

CHANGES IN REACTOR DESIGN RESULTING FROM CEF EXPERIENCE. One of the purposes of the CEF tests was to identify possible design improvements. A number of changes were thus made at ORNL. These are:

Core Bolting.   In the CEF assembly the nine core bolts bolted into the bottom fuel plate. In the APRFR assembly the nine core bolts went through all fuel plates and were secured by Inconel nuts as shown in Fig. 1. This change was made as a result of core-disassembly difficulty following the tests at CEF.

Safety Block.   In the CEF assembly the safety block started essentially at the top of the core. The safety block installed at APRFR had been shortened; it started 0.889 cm below the top of the core. This change was made to provide faster reactor shutdown upon withdrawal of the safety block. By moving the safety block down into the core, initial safety-block withdrawal results in a greater rate of reduction in reactivity than when it starts at the core surface.

Thermocouples.   In the APRFR assembly the thermocouple holes and inserts in the center fuel plate were made larger but did not penetrate through the fuel to the central hole in the core, as they did in the CEF assembly, and the thermocouple inserts were strengthened. This change was made to eliminate the stress concentration at the thermocouples in place during design-yield pulse operation. During the tests at CEF, the fuel disks cracked at those locations, and the thermocouple inserts would tend to bounce out of the core during higher yield pulse operation.

Pulse Rod.   At CEF four different pulse rods were used at different times:

Pulse rod No.	Outside diameter, cm	Length, cm	Enrichment, %	Dynamic worth, ¢
1	1.920	32.21	93.2	
2	1.920	25.40	93.2	97.5
3	2.007	30.48	97.8	
4	2.007	25.40	97.8	110.5

The high-enrichment rods were used to increase rod worth to produce the desired pulse yields. In general, pulse-rod worths at CEF were found to be lower than required for operation at design yield. For the APRFR core the pulse-rod diameter was therefore increased, but enrichment was kept at 93.2%. The pulse rod used at APRFR was 25.40 cm long, and it had an outside diameter of 2.10 cm. The uranium was 93.15% enriched in ^{235}U.

Core Plating.   At CEF some fuel pieces were nickel plated and others aluminum-ion plated. All fuel pieces supplied to APRFR were aluminum-ion plated at ORNL because of the superior experience with aluminum-ion-plated fuel obtained at both CEF[4] and Sandia[5].

DIFFERENCES IN OVERALL REACTOR ENVIRONMENT.   The APRFR was operated in a reactor building of light-metal construction and at a

distance of 242.6 cm above the floor so that neutron room return was minimized. At CEF the experiments were carried out in a room completely shielded by thick concrete walls; but the core was removed from the walls, so the room-return effect was thought to be small. At both APRF and CEF, instrumentation was present above the core, which is thought to be the dominating room-return component.

Core Atmosphere and Cooling. At CEF the assembly was in air at room temperature, and cooling following a pulse was provided by a fan. At APRF cooling was provided by forced air flow; for higher yield pulses the core was kept in a dry-nitrogen atmosphere during a pulse to control stress-corrosion cracking, as indicated by research sponsored by the Ballistics Research Laboratories (BRL) at the University of Arizona.[6] A dry-nitrogen atmosphere is also used at the Sandia Pulsed Reactor on the basis of similar considerations.[7]

PULSE OPERATION

Initial Pulse Operation

Pulse operation was begun on Aug. 12, 1968. Personnel present included APRF staff as well as ORNL specialists. The characteristics of the reactor configuration used in this initial pulse operation are summarized in Table 5. Pulses 68-1 through 68-7 were of low yield

Table 5

CHARACTERISTICS OF REACTOR CONFIGURATION USED
DURING INITIAL PULSE OPERATION

Configuration designation	F
Core height, cm	20.09
Safety-block height, cm	20.47
Pulse-rod length, cm	25.40
Pulse-rod diameter, cm	2.10
Pulse-rod enrichment, %	93.15
Pulse-rod mass, kg	1.467
Total fuel mass on assembly (including all rods), kg	125.393
Height of core center above floor, cm	242.6
Auxiliary components installed: Cooling shroud, safety cage, safety tube, glory hole liner, and nitrogen can	

and were used to check out the instrumentation. Pulse 68-7 was the first for which a core-temperature rise was observed. Eight more pulses were obtained in this series, culminating in pulse 68-17 with a yield of 12.6×10^{16} fissions. Another pulse, 68-18, had been scheduled but was not performed. From the data obtained from these pulses, it

was determined that large negative reactivity adjustments of the order of -15¢ had to be made prior to each pulse to obtain the desired pulse yield.

It is desirable to attain the design yield by making a small reactivity adjustment. It was therefore determined that the pulse rod was too large and that its worth had to be reduced. This reduction in worth was accomplished by increasing the adaptor to reduce the length of the pulse rod in the core when fully seated. The pulse rod was a necessary assembly item; its length was to be determined during these tests. Based on pulse rod in vs. out measurements at delayed critical, the new pulse-rod worth was determined to be 110.3¢. This method of reducing pulse-rod worth is in error for pulse operation with the rod drive situated above the core since the rod will go through a reactivity maximum before reaching its fully seated position. Both configurations assembled for these tests were in error in this regard. The pulse rod went through a small reactivity maximum in the first configuration (core F) and through a larger maximum with the longer adaptor. With this new pulse-rod configuration, a new series of pulses was obtained. Pulse 68-19 was scheduled but not performed owing to delays with instrumentation calibrations. Pulses 68-20 through 68-22 were sub-prompt critical, whereas pulses 68-23 through 68-29 ranged in yield from 1.79×10^{16} fissions to 12.26×10^{16} fissions. The delayed critical prompt-neutron decay constant was about 0.60 μsec^{-1} compared with 0.55 μsec^{-1} at CEF. This pulse history failed to reveal that the pulse rod was going through a reactivity maximum before reaching its fully seated position. Pulse 68-29 was fired on Sept. 5, 1968. Its yield of 12.26×10^{16} fissions was satisfactorily close to the expected 13.3×10^{16} fissions. An assembly in which the pulse rod goes through a reactivity maximum before being fully seated can operate for some time without incident and apparently in a reproducible manner. Eventually a pulse will be initiated when the pulse rod has a reactivity worth that is higher than its value in the seated position, and a larger than expected yield will be obtained.

This situation apparently held for all pulses up to 68-30. The probability that the pulse would be initiated just as the pulse rod passed through its reactivity maximum depends upon a number of factors, including background source level, reactivity insertion rate, and total reactivity being added. In general, the probability that initiation will occur increases as reactivity rates and reactivity increase; therefore, as the APRFR assembly was being taken to its target yield of 2.1×10^{17} fissions, this probability increased sharply. The quantitative relations involved in this problem are currently being determined more closely in connection with a delayed-critical experiment at APRF.

Occurrence of Maximum Yield Pulse

Plans were made on the morning of Sept. 6, 1968, to fire pulse 68-30. A physical inspection of the reactor was made that morning; nothing unusual was noted. A new nitrogen bottle, which feeds the pneumatic supply for the neutron start-up source and pulse rod, was connected. It is also used to provide a nitrogen atmosphere immediately preceding and following a pulse. A heavy rain the evening before had caused some puddles on the reactor building floor but not close to the reactor.

The prepulse calibrations and preparations were being made under the direction of the ORNL reactor specialist and the APRFR reactor supervisor. As usual a delayed critical configuration was established as part of the pulse sequence, and no significant changes were observed since the previous pulse 68-29. A number of other APRFR personnel were in the control room, data-acquisition room, and the technical office of the control building.

According to the established procedures, the reactivity insertion step over the previous one should be about 0.5¢. The insertion was 8.05¢, which was 0.64¢ above the 7.41¢ of pulse 68-29. This increase was acceptable. From the extrapolation of previous pulse data, this increase should have produced a yield of 1.68×10^{17} fissions. The pulse occurred at 1058, and the following events were noted:

1. The pulse instrumentation went off scale: Thermocouple recorder on 1200°F scale, photodiode readout on oscilloscopes and tape.

2. A scaler used to measure the wait time between time zero on preburst timer and pulse signal from photodiode read 0.07415 sec. This is evidence that the pulse was initiated before being fully seated. The time required for the pulse rod to seat is about 0.09 sec.

3. The reactor assembly appeared intact as seen on the TV screens and had shaken only slightly following the pulse. However, a persistent glow was observed near where fuel pieces could be seen, namely, at the thermocouple holes and around the safety-tube holes near the scrammed safety block.

4. The safety block scrammed, and all other rods withdrew normally.

5. All scram circuits functioned.

6. Radiation levels were normal for a high-yield pulse.

7. The pulse rod "in" light did not activate. The safety-block magnet light did not go out even though the safety-block drive had gone down as it should have.

The core had been placed in a nitrogen atmosphere prior to the pulse. This was kept on trickle until 1114, when it was turned off to prevent the possible spread of contamination. The reactor cooling sys-

tem was also left off to prevent the possible spread of contamination. The 1200°F thermocouple recorder came back on scale 23 min. after the pulse. The in-core thermocouple was apparently not significantly damaged. Radiation levels and the state of the reactor indicated that there was no danger of release of radioactivity and that the reactor was shutdown. First entry into the reactor building was made at 1234 by two members of the reactor operations staff and the health physicist. No water was near the core. The floor beneath the reactor had been covered with white absorbent paper. A sulfur pellet, exposed to determine yield, was retrieved at 1252. The core assembly machine was placed below the safety tube and core to prevent the core from falling to the ground in the event the core bolts were broken. (They were not.) The facility was secured at 1555.

Subsequent inspection showed no loosened or missing components on the reactor structure. The dry-nitrogen-gas supply was investigated; it showed no evidence of having been able to supply moisture.

Preliminary analysis showed that the yield was about 6×10^{17} fissions and that the initial period was about 10 μsec. The melting point of the fuel (1150°C) had been exceeded; thus the safety limit of the APRF technical specifications of 1000°C had been exceeded. The required notifications were made that afternoon by the facility supervisor.

Characteristics of Maximum Yield Pulse

The yield of pulse 68-30 was 6.09×10^{17} fissions as determined from a sulfur pellet. The initial period as taken from a scope trace was 9.1 μsec, giving an alpha of 11×10^4 sec^{-1}. The core reached the alloy melting point of 1150°C. Extrapolation from pulse width at half maximum vs. period data indicated a width of 26.5 μsec. The reactivity required to produce 6.09×10^{17} fissions was extrapolated from the existing yield vs. reactivity data to be about 18¢.

The results of inspection of the pulse rod after pulse 68-30 are shown in Fig. 2. If we assumed that the center of the black portion of the pulse rod was in the center of the core during the pulse, then the 25.40-cm-long rod was 1.70 cm above the top of the 20.09-cm-high core and ended 3.61 cm below the core at the time pulse 68-30 initiated.

The insertion time of the pulse rod was 90 msec. The pulse timer indicated that the pulse initiated 74.15 msec following insertion. The rod was therefore 15.85 msec from seating. The rod was 4.52 cm above its seated position, which is 8.18 cm below the bottom of the core. Therefore the bottom of the rod was 8.18 minus 4.52, or 3.66 cm, below the core, and the top was 1.65 cm above the top of the core. This is consistent with the data deduced in the previous paragraph.
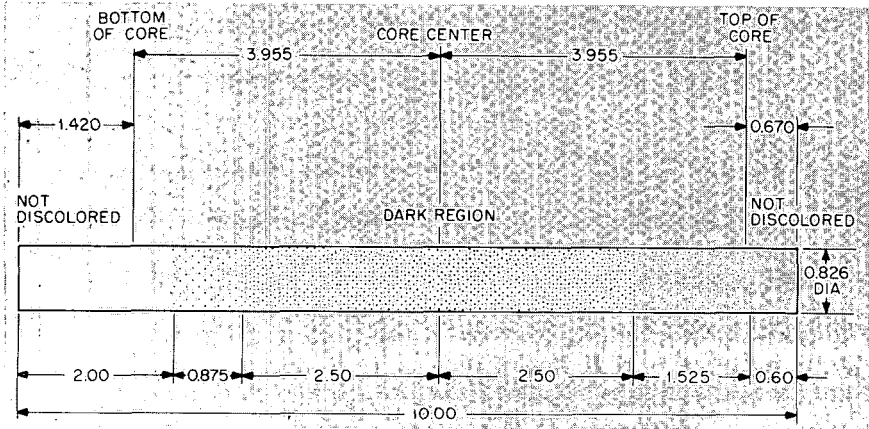
Fig. 2—Sketch of pulse-rod discoloration following pulse 68-30.

Table 6

REMOTE-AREA MONITOR READINGS FOLLOWING PULSE 68-30

Monitor	Dose rate 2 min. after pulse	Dose rate 10 min. after pulse	Dose rate 20 min. after pulse
Air-intake structure	750 mr/hr	80 mr/hr	18 mr/hr
Entrance to control building	70 mr/hr	10 mr/hr	1 mr/hr
Vestibule	None detectable		
Entrance to shielded access tunnel	0.4 mr/hr		
Control room	None detectable		
Instrument trailer room	None detectable		
Entrance to reactor building	None detectable		
Reactor building, near stairs	>100 r/hr	50 r/hr	25 r/hr
Outdoor test site	Not operating		
Reactor handling device	150 r/hr	50 r/hr	Fluctuating

Radiation levels were normal for a pulse of this yield, which is three times the projected maximum operational yield. The following data were obtained by the BRL health physics staff. Table 6 gives the dose rate measured by the 10 APRF remote-area monitors at various times after pulse 68-30. The measured dose rates and the way in which the dose rates decreased with time were normal for a pulse yielding 6×10^{17} fissions.

The APRF is bounded by a warning fence located at a radius of 1500 yd from the reactor. The total dose at this boundary due to pulse 68-30 was calculated to be 0.75 mrem; this is approximately three

times greater than the dose expected from a normal pulse yielding 2×10^{17} fissions. The total of 0.75 mrem is the sum of the neutron and gamma dose delivered during the pulse (0.25 mrem) and a gamma dose (approximately 0.5 mrem) delivered after the pulse, due to the residual activity of the reactor core. The Aberdeen Proving Ground boundary nearest the location of the reactor is 0.9 miles to the northwest. The total dose at this point due to pulse 68-30 is calculated to be 0.67 mrem.

In the APRF control building a particulate air monitor draws a continuous sample from the return duct of the control building's fresh-air supply through a fixed particulate filter. This monitor showed no increase in air activity in the control building due to pulse 68-30.

In the APRF reactor building radioactive particulate matter is formed by neutron activation in the reactor building during operations. Continuous sampling of reactor-building air is accomplished via a hose that runs from the reactor building to a particulate air monitor located in the trailer tunnel of the control building. Immediately following pulse 68-30, this monitor indicated a rapid increase in air activity in the reactor room. The rate at which the activity increased and the level it reached were normal for a pulse yielding 6×10^{17} fissions. Approximately 50 min after pulse 68-30, a 24-min sample was cut from the filter of the particulate air monitor. Analysis of this sample indicated an air concentration of 1.4×10^{-7} μc/cm^3 for beta$-$gamma activity and 5.9×10^{-13} μc/cm^3 for alpha activity. A plot was made of activity vs. time which indicated that the beta$-$gamma activity was decaying with a 36-min half-life and the alpha activity with a 35-min half-life. Further analysis of this air sample indicated that long-lived alpha emitters were not present.

The stack monitor draws a continuous sample from the stack discharge through a particulate filter and charcoal$-$iodine trap. Analysis of the filter and charcoal indicated the presence of ^{131}I. Analysis of the charcoal indicated an average ^{131}I concentration of 7.8×10^{-10} μc/cm^3 in the 5-hr postpulse stack discharge, resulting in a release of 200 μc of ^{131}I to the environment.

No increase in air activity was measured at three continuous air monitors located 1.25, 5.9, and 12.2 miles from the APRF. Exposure of all personnel was kept within normal occupational levels. In summary, these preoperational tests of the APRFR, including the maximum yield pulse, have not significantly contributed to the ambient radioactivity levels in the APRF environment.

Effects of the pulse on the physical condition of the core and reactor components are summarized under Summary of Damage to Reactor.

ANALYSIS OF CAUSE OF MAXIMUM YIELD PULSE

Probable Cause of Maximum Yield Pulse

Analyses made to date indicate that the extra reactivity required to produce 6.09×10^{17} fissions was present because of the position of the pulse rod. The maximum reactivity worth of the pulse rod is obtained when this rod is positioned approximately symmetrically in the core. The reactor must be designed and operated such that the pulse rod does not go through a reactivity maximum as a function of time. This criterion was not met in either of the two reactor configurations assembled for these tests.

A postulated qualitative set of differential pulse-rod-worth curves is shown in Fig. 3. Lines A and B are the dynamic worths of the pulse
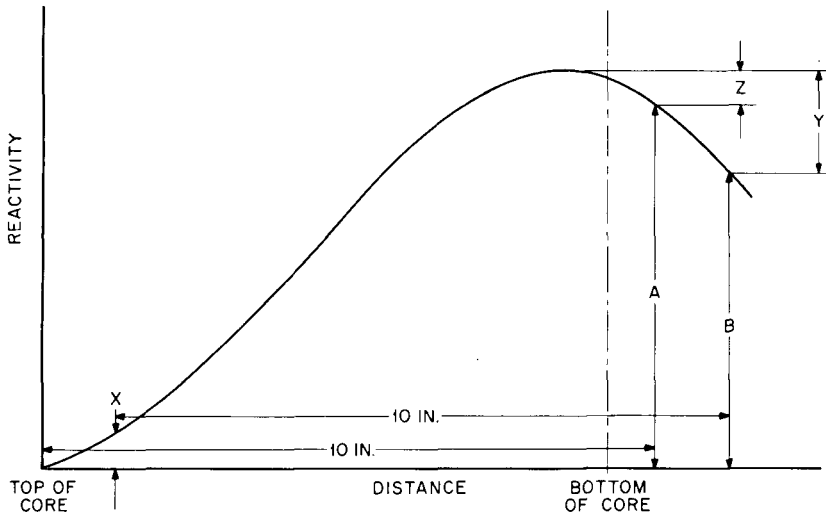
Fig. 3 — Postulated differential pulse-rod reactivity curves. (Not to scale.)

rod when fully seated for the two reactor configurations. For the first pulse-rod position the rod went through a maximum of z¢. A differential pulse-rod calibration is required for the exact geometry to determine z. An estimate for z is about 2¢ on the basis of CEF data. In this configuration a pulse would have been initiated before the pulse rod fully seated sooner or later, and an extra 2¢ at 2×10^{17} fissions would have resulted in ~3.5×10^{17} fissions. Moving the pulse rod down below the top of the core changed the position of the pulse-rod fuel relative to that of the core and reduced the pulse-rod worth by the amount x (2.88-cm steel vs. U−10 wt.% Mo). This caused the pulse rod to go

through a larger maximum of magnitude y before being seated. These effects may well account for the extra reactivity required to produce the increase to 6.09×10^{17} fissions from the planned 1.68×10^{17} fissions for pulse 68-30, namely, ~10¢. The above model seems to explain the observed events; however, further measurements and analysis, including a critical experiment, are required to establish more firmly the exact quantitative relations involved in pulse 68-30.

Other Postulated Sources of Unplanned Reactivity Additions

A number of other possible causes for the maximum pulse were analyzed and rejected as not having been able to provide the necessary excess reactivity. The possible causes examined include
1. Dislocation of auxiliary component.
2. Dropping of mass adjustment rod or regulating rod during wait period.
3. Presence of foreign object.
4. Erroneous safety-block seating.
5. Water from nitrogen supply.
6. Error in prepulse control-rod settings.

SUMMARY OF DAMAGE TO REACTOR

The fuel pieces assembled for the reactor configuration existing for pulse 68-30 are listed in Table 3. Following pulse 68-30 the core was partially disassembled and inspected. Further inspection and detailed metallurgical examination of selected pieces are planned. Visual inspection to date has revealed no signs of further cracks or crack propagation owing to stress corrosion or other causes. The damage is summarized in the following paragraphs.

Fuel Rings

The condition of the fuel rings is summarized in Table 7. The three top and bottom rings showed only small damage. The four rings fused together at the inside diameter could probably be separated without much difficulty, but this has not been attempted since these rings are being used in a critical experiment.

Bolts

All bolts showed only very slight dimensional changes and no visible cracks; they came out easily following pulse 68-30 in contrast with the experience at CEF where considerable difficulty was experienced in removing bolts which had bound together in the bottom ring. The condition of the bolts is summarized in Table 8. The present

Table 7

CONDITION OF FUEL RINGS FOLLOWING PULSE 68-30

Fuel-ring serial number	Height, cm	Weight,* kg	Condition
7882-20-0115	1.272†	5.760	No visible cracks, slightly warped; bottom inside diameter slightly charred.
7881-99-0009	0.526	2.288	No visible cracks, charred inside diameter.
7882-40-0109	1.933	8.637	No visible cracks, charred inside diameter.
7881-21-0001	2.667	11.954	Spalling around inside diameter.
7881-19-0003	2.329	10.416	Cracks visible between each bolt
7882-18-0070	3.404	14.516	and rod hole to the inside diam-
7882-38-0062	1.895	8.465	eter of top three plates; no vis-
7881-17-0004	3.254	14.561	ible cracks on outside; inside of plates charred and fused together.
7881-16-0007	2.753	12.272	No visible cracks, slightly warped; top inside diameter slightly charred.
Total	20.033	88.869	

*Prepulse data.
†Top of core.

Table 8

CONDITION OF FUEL BOLTS FOLLOWING PULSE 68-30

Bolt serial number	Weight,* kg	Necked,† mm	Elongation,† mm
7882-17-0064	1.845	0.2	3.0
7882-17-0065	1.841	0.3	3.7
7882-17-0067	1.849	0.4	3.1
7882-17-0069	1.845	0.2	3.3
7882-17-0072	1.845	0.3	3.0
7882-17-0073	1.849	0.4	3.5
7882-17-0074	1.850	0.5	3.7
7882-17-0075	1.842	0.6	3.1
7882-17-0076	1.844	0.2	3.8
Total	16.610		

*Prepulse measurement.
†Average measurement as compared with drawings.

experience shows the advantage of the present nut-and-bolt design compared with the earlier assembly of screwing the bolts into the bottom ring.

Control Elements

The safety block melted at the hot spot, and it showed gross material deformation. The regulating rod and the mass adjustment rod showed bows of 0.6 and 0.2 mm, respectively; the pulse rod bowed 2.1 mm.

Auxiliary Components

The control-rod liners, the safety-block hanger, and thermocouple inserts will be replaced. It is expected that the safety tube will be modified. It is planned to replace the core-support ring and three core-support rods even though these show no visible damage (these are inexpensive items). All rod drives appear to be undamaged.

CONCLUSIONS

The high-yield pulse of Sept. 6, 1968, having a yield three times larger than authorized, did not result in any detectable external or airborne radiation hazards, nor did it cause any overexposures of any personnel. Damage was essentially limited to fuel pieces, and damage to the reactor in general is small.

The efficient and timely implementation of the facility emergency procedures proved that the procedures were well organized and effective and the operations and health physics personnel well trained. The APRF staff quickly evaluated the situation and did not overreact. No emergency equipment or off-site personnel were called to the scene since none were required. A number of actions are presently in progress to make the APRFR fully operational.

Measurements at Delayed Critical To Establish Reactivity in Core at Time of Pulse 68-30

For confirming the hypothesis that the pulse-rod positioning caused the maximum pulse and for determining more accurately the reactivity in the core for pulse 68-30, a number of calibrations at delayed critical are required.

Differential-rod-worth curves will be obtained on all rods—pulse rod, regulating rod, and mass adjustment rod. The regulating-rod and mass-adjustment rod curves will be used as base-line measurements to compare with existing curves. The pulse-rod curves, using several

adaptors, will be used to determine the reactivity maxima. Core F has been reassembled to check physical compatibility of all parts, and this critical experiment can be performed with the present damaged core, provided another safety block is used. The safety block used during the experiments at CEF is available for this purpose. The reactor will, of course, not be pulsed during these measurements at and near delayed critical.

Repair of Core

As discussed in the preceding section, all used fuel pieces will be shipped to ORNL for inspection, remachining, or replacement as required.

Inspection of Reactor System

A complete inspection of the mechanical and electronic reactor system is being made. Studies are under way to investigate position reproducibility of all moving parts and their reactivity effects. Additions and modifications to instrumentation, including reactivity and core-temperature measurement channels, are being considered.

Design and Operation Modifications

The reactor design and operation are being modified so that pulse-rod motion as well as all other rod motions will always result in monotonically increasing reactivity as a function of time. Changes are being considered which would facilitate pulse-rod differential calibrations and improve reproducibility of other components, such as the safety block. The environmental control of the core and its instrumentation is being examined; different auxiliary components, such as cooling shroud, safety cage, safety tube, and nitrogen, will be integrated into one system.

Technical Report

A technical report will be issued following completion of all data analysis including completion of the critical experiment discussed previously.

In summary, operation of the APRFR to date has shown the basic soundness of the overall core design and mechanical systems. The reactor behaved considerably better than might be expected at a performance level well above current routine limits. On the other hand, a number of modifications in design, instrumentation, and operating procedures are clearly necessary. These will be described in detail once they are finalized and implemented.

ACKNOWLEDGMENTS

REFERENCES

1. J. T. Mihalczo, Static and Dynamic Measurements with the Army Pulse Radiation Facility Reactor, USAEC Report ORNL-TM-2330, Oak Ridge National Laboratory, June 1969.
2. J. T. Mihalczo, J. J. Lynn, J. E. Watson, R. W. Dickinson, Super-prompt Critical Behavior of a Uranium—Molybdenum Assembly, *Trans. Amer. Nucl. Soc.*, 10: 611 (November 1967).
3. J. A. Reuscher and J. M. Richter, Dynamic Mechanical Measurements on the Army Pulse Reactor, *Trans. Amer. Nucl. Soc., 10:* 612 (November 1967).
4. M. I. Lundin, A. P. Litman, and W. J. Leonard, Design and Metallurgical Aspects of the Army Pulse Radiation Facility Reactor, *Trans. Amer. Nucl. Soc.*, 10: 609 (November 1967).
5. P. D. O'Brien, SPR II: Early Operational Experience, USAEC Report SC-DR-67-801, Sandia Corporation, October 1967.
6. S. A. Hoenig and H. Sulsona, A Field Emission Microscope Investigation of the Effects of Ambient Atmosphere on the Stress-Corrosion Cracking of Uranium—Molybdenum Alloys, U. S. Army Technical Ballistics Laboratory, Ballistics Research Laboratory, Aberdeen Proving Ground, Aberdeen, Maryland (Mar. 9, 1968).
7. R. L. Coats and P. D. O'Brien, Pulse Characteristics of Sandia Pulsed Reactor II, *Trans. Amer. Nucl. Soc.*, 11: 219 (June 1968).

DISCUSSION

WILSON: Did you not make any calculations of the worth of the burst rod as a function of position prior to the operation of the reactor?

KAZI: Measurements were made of total-in and total-out reactivity worth at delayed critical.

ZITEK: You indicated that the previous bursts gave 12.3×10^{16} vs. 13.3×10^{16} fissions predicted according to a curve. What was that curve?

KAZI: The curve, for example, of the temperature vs. reactivity, where the temperature is proportional to yield or something like sulfur yield. The main curve we were using was yield vs. reactivity insertion. The previous history did not give any clue that we were going through a reactivity maximum simply because all the pulses initiated a couple of hundred milliseconds after the pulse rod was fully inserted. So this is really a case where the past history to that point gave no indication that we were running through this maximum; the only way that can be picked up is through previous calibrations.

4-6 FAST BURST REACTOR
OPERATIONAL INCIDENTS

PAUL D. O'BRIEN
Sandia Laboratories, Sandia Corporation, Albuquerque, New Mexico

ABSTRACT

This paper discusses the causes of 10 typical fast burst reactor incidents, the consequences of the incidents, and the actions taken to prevent recurrences. These 10 incidents by no means cover the spectrum of possible accident mechanisms; however, they do illustrate the overriding importance of administrative control in providing for safe operation under the almost unbelievably wide range of experimental conditions to which fast burst reactors are adaptable.

INTRODUCTION

During the last 15 years, the 11 fast burst reactors built and operated in the United States have produced nearly 15,000 super-prompt critical bursts. Not all these bursts have proceeded exactly as expected; the exceptions are the incidents, defined for the purpose of this paper as unplanned gross departures from normal operational behavior.

Incidents have played an important role in the evolution of fast burst reactors; in fact, an accidental prompt criticality (involving a remote-assembly machine called Jemima) was instrumental in the decision to modify Lady Godiva to become the first routinely operated fast burst reactor in the world. A number of significant improvements in design and in operating procedures have been the direct products of incidents. Probably the most notable example is the shock-induced scram, which first occurred as an operational anomaly during the start-up of the Health Physics Research Reactor (HPRR): by definition, the first such scram constituted an incident. (To give proper credit to M. I. Lundin and his associates at Oak Ridge National Laboratory, it should be noted that the concept of the shock-induced scram was

considered and then discarded as technologically premature early in the design of the HPRR.) Other developments arising from incidents have been less spectacularly serendipitous, but they have nevertheless contributed substantially to the convenience, the reliability, and, above all, the safety of fast burst reactor operation.

It is impossible, and not very important, to determine how many fast burst reactor incidents have occurred. The number is clearly very small considering that reactivity perturbations of only a few cents can produce either a disruptive power excursion or a zero-yield fizzle. Out of 15,000 bursts only two incidents occurred in which the fuel assembly was damaged beyond repair, and in four others less severe damage was sustained. The number of incidents in which the energy yield was below the threshold of damage is several times larger, the factor depending on how one quantifies "gross departure from normal" in the definition of incident. Some of the low-yield incidents occurred under circumstances in which only luck determined whether reactivity was unintentionally increased or decreased; others have been more or less fortuitous instances of preinitiation limiting the yield of potential high-reactivity excursions. Nevertheless, the small number of incidents and the even smaller number of truly disruptive accidents stand as testimony to the inherent safety of Godiva-type burst reactors. It is important to note that there has never been an injury or an overexposure of personnel to radiation in any fast burst reactor incident.

This paper discusses 10 typical incidents from the standpoint of the causes, the consequences, and the actions taken to prevent recurrences. Admittedly, some of the causes and corrections seem embarrassingly elementary; others are quite subtle. The justification for this discussion is simply that the incidents occurred, some more than once even at the same facility. All could have been prevented by paying more careful attention to design and procedures—or perhaps by applying information gained in earlier incidents, had that information been made available in the literature.

PROCEDURAL INCIDENTS

The incidents fall naturally into three categories: those resulting from design deficiencies, those associated with irradiation experiments, and those involving procedural errors. Obviously, procedural errors played a role in virtually all the incidents; but, these errors were the direct and primary cause of only two incidents considered here and, for that matter, of only two of those incidents about which information is available.

1. One such procedural incident involved an assembly whose total excess reactivity, with the safety block and all control rods fully inserted and with the burst rod withdrawn, was only about 40¢ (with respect to delayed critical). With conventional operating procedures, therefore, the minimum period possible during the initial approach to delayed criticality was of the order of 10 sec. This was considered inconvenient from an operational point of view, and it became the custom to "goose" the reactor, as the procedure was called, by inserting the burst rod with the control rods partially inserted. Much shorter reactor periods could be attained by this means, and the core neutron population could be built up rapidly. At this point in the sequence, of course, the burst rod was withdrawn, and the control rods were inserted to their delayed-critical positions; thereafter, the normal burst sequence was followed.

In this incident the operator, who was alone in the control room, inserted the control rods too far before firing the burst rod. An abnormally large burst resulted, and the core and core-support structure were slightly damaged.

The nonstandard operational sequence, even though it had been followed successfully many times previously, was the immediate cause of this incident. Other contributing factors were the solo operation of the reactor and the marginal excess reactivity available. (Parenthetically, it is worth noting that, at least on cylindrical reactors, this last deficiency can be overcome without machining new fuel components simply by clamping a small nonfuel ring around the fuel assembly. A brass ring about 1 in. high and $\frac{3}{16}$ in. thick was worth 50¢ when clamped around the base of Godiva II.)

2. The second procedural incident occurred at a different facility during the reactivity calibration of the safety block. With appropriate interlocks bypassed, the safety block was withdrawn stepwise, and the control rods were inserted at each step to reestablish delayed criticality. Control-rod calibration curves were then used to determine the worth of each increment of safety-block movement. A carefully planned, written test procedure was being followed under the direction of the facility supervisor; a reactor supervisor, an operator, and a health physicist were also present in the control room.

A point in the calibration procedure was reached at which the reactor was near critical with the burst rod and all control rods fully inserted; the neutron level was so low, however, that erratic instrument response made it uncertain whether or not the reactor was actually critical. Departing from the written procedure, the facility supervisor decided to return the reactor to an earlier configuration in which the reactor could be made supercritical. After building up

the core neutron population, he intended to return the reactor imme-
diately to the last doubtful configuration, expecting that he could posi-
tively determine if the reactor were critical. For this procedure it was
necessary to scram the reactor. The scrams were reset as soon as
the safety-block slow-drive mechanism reached its fully retracted
position, but at that time the control rods had moved only 0.7 in.
(worth a total, for both rods, of about 20¢) from their fully inserted
positions. The burst rod remained clamped in its most reactive
position. Among the interlocks that had been bypassed was one re-
quiring the control and burst rods to be withdrawn before the safety
block could be inserted. Starting at that condition, then, the facility
supervisor (with the passive concurrence of the other members of
the operating crew) ordered the pneumatic safety-block insertion
mechanism to be actuated. The reactor assembled rapidly toward
a configuration that potentially could have reached a reactivity of
40¢ above prompt critical, but preinitiation at about 15¢ limited the
fission yield to approximately 1.5×10^{17}. Damage was limited to newly
installed experimental fuel components; eventual damage of these
components was not at all unexpected—only the timing and the con-
ditions under which it occurred!

Again, the departure from established operating procedures was
the direct cause of the incident. Although the seriousness of the facility
supervisor's error in judgment cannot be minimized, a significant
contributing factor was the failure of the two operating crew members
to provide a human interlock against such errors. This incident is
similar to the first in the sense that, effectively, there was only one
operator. Obviously, little is gained by requiring operational crews
of more than one person unless each person carries out his duties
with a full awareness of his responsibilities.

These two incidents illustrate the overriding importance of care-
fully considered and rigidly enforced administrative controls in pro-
viding for the safe operation of a fast burst reactor. Proper control-
system design and elaborate written procedures can be effective in
reducing the number of opportunities for operational errors, but,
sooner or later at every facility, situations arise in which the control
system or the written procedures must be modified. In these situa-
tions the mechanism must have been established, administratively,
for assuring that these modifications are carried out safely. An
example of an effective administrative control, instituted at several
facilities following incident No. 2, is a regulation prohibiting an
experimenter from serving as a member of the reactor operations
crew during his experiment. Thus in incident No. 2, the individual
responsible for the calibration of the safety block would have had no
operational responsibility during the calibration; he would have been
able to devote his entire attention to the experiment itself. Although

he may have proposed the same departure from the written procedure, his proposal would have had to be evaluated by a second equally well-qualified individual—a reactor supervisor whose entire attention would have been directed toward the operational aspects of the calibration.

DESIGN-RELATED INCIDENTS

Although design improvements have been suggested by failures that occurred during a number of fast burst reactor incidents, design deficiencies have been causative factors in only a few improvements, three of which are discussed below. Sometimes the role of an inadequately designed component in causing an incident is obvious, and correction of the deficiency is straightforward. More often this is not true, and even the identification of the accident mechanism is a matter of speculation. In such cases of design deficiency, the parts that failed can be redesigned readily, but one is left wondering whether or not he has corrected the real cause of the incident. It is at least comforting to observe that there have been no repetitions of design-related incidents.

3. Following an abnormally large burst of one of the Super Godivas, investigations showed that a screw coupling between a control rod and its actuating mechanism had failed and that the rod was merely resting on its drive screw. The rod was therefore free to move in response to the forces imposed by the rather violent insertion of the burst rod. Only an extra $\frac{1}{2}$¢ of reactivity over the amount intended was required to explain the large burst, and, after other possibilities had been discarded, it was hypothesized that the control rod had broken during the previous burst. Then the unrestrained control rod had moved to a more reactive position (only 0.015 in. of motion was required) when the burst rod was inserted during the operation.

In retrospect, the coupling between the control rod and its drive mechanism was poorly designed: the failure occurred at the root of a male thread cut in the fuel material. All the rods were modified by cutting much larger female threads in the rods and securing them to their drive mechanisms by means of male-threaded steel adaptors. The resulting coupling was stronger because of the larger screw thread size, but perhaps equally as important was the fact that the smaller diameter component was now steel and therefore not subject to stress-corrosion cracking. The rods were removed from service after about 1000 bursts, and at that time no evidence of incipient screw joint failure had appeared.

4. An early incident involving a first-generation Godiva occurred while the reactor was being operated outdoors. Because of the very large variations in ambient temperature which occurred during the day, detection of small reactivity perturbations was difficult even though there was little change in experiment configuration from burst to burst. Although the energy yield in this incident was 1.4 times normal, a detailed inspection revealed no damage. (Years later, just prior to its retirement, the reactor was intentionally and repeatedly operated at twice-normal burst yields without damage.) The only clue to the cause of the incident was a small defect in the cadmium plating on the safety block.

The hypothesis was that a piece of cadmium had fallen into the safety-block drive mechanism in such a manner that it prevented full insertion during the delayed-critical calibration, but it had moved during the preburst waiting period so that the second insertion, just prior to the burst, was to a slightly more ($\sim 1 \text{¢}$) reactive position.

Obviously, the cause of this incident was never positively identified. The cadmium plating was entirely removed from the vicinity of the safety block, leaving only a thin nickel coating for protection against oxidation. Later the nickel was replaced by aluminum when the ion-plating process was developed at Sandia. Whether or not the incident in question was actually caused by a plating failure, there has never been a recurrence.

5. The only incident that can be attributed unambiguously to a design deficiency was the one caused by an actuator moving the burst rod through a position of maximum reactivity. Therefore, while the burst-rod worth as measured between its two end positions was as specified, the maximum worth was several cents higher. This fact went unrecognized through nearly 30 bursts and even through a design modification that exaggerated the condition. Data show that during every burst preceding this incident the burst rod had actually seated before initiation took place. Burst yields were therefore close to the predicted values, and there was no other indication that the reactor was not behaving normally. In this incident initiation occurred when the burst rod was near its position of maximum worth, and the reactivity was some 10¢ higher than intended. The reactor, of course, was extensively damaged.

When the incident was reviewed, its cause became obvious, and the design of the burst-rod actuator was readily modified to eliminate the reactivity peaking. That the peaking occurred at all and that it remained undetected through many operations illustrate the importance of unambiguous communication and definition of responsibility among the individuals and organizations concerned with the design and operation of a device as easily perturbed as a fast burst reactor.

A disquieting aspect of design-related incidents is that even in obvious cases like incident No. 5, reconstruction of an incident involves a certain amount of conjecture. One is then left wondering if he has corrected all the design deficiencies—or even the right one.

INCIDENTS ASSOCIATED WITH IRRADIATION EXPERIMENTS

If incidents caused by design deficiencies are disquieting, those associated with the irradiation of materials placed near a fast burst reactor are truly frightening. Because of the almost limitless variety of irradiation experiments and because of the insidious ways in which the materials in these experiments can affect the neutronics of a reactor, it is not surprising that most incidents occur during routine irradiation experiments. Interestingly enough, no really bizarre experiment, for instance, one involving the detonation of explosives near a reactor immediately after a burst, has ever resulted in an incident. Those experiments are readily recognized as potentially dangerous and are invariably planned with such care that the actual operation is almost anticlimactic.

Although one can hypothesize other experiment-related causes, every such incident to date has involved the movement of experimental equipment, either accidentally, during a burst sequence, or deliberately, between operations. The five incidents discussed below are typical, but they only suggest the wide range of possibilities for anomalous interactions between experiments and fast burst reactors.

6. In an experiment that might, by today's standards, be considered questionable from the standpoint of safety, a large moderating experiment was being irradiated near an early Godiva-type reactor. At the same time a second experiment was being irradiated in the burst-rod cavity. The burst rod had been removed, and the safety block was used to initiate the power transients. The total reactivity worth of the control rods was less than $1; this made it impossible to establish delayed critical with the safety block inserted and later, during the preburst waiting period, to add the $1+ of reactivity necessary to produce the desired burst yield. A procedure was developed in which the first step was insertion of the control rods to an experimentally determined position at which approximately 30 ¢ of reactivity remained available for later addition. Safety-block insertion then increased the reactivity to a level about 80 ¢ above delayed critical; the exact reactivity was determined by measuring the stable reactor period. Then, while the safety block was withdrawn to permit the decay of delayed-neutron precursors, an appropriate control-rod correction was made so that when the safety block was inserted the second time the level of reactivity required for the burst

was achieved. Although somewhat involved, this procedure was quite satisfactory until the large external experiment was modified. In the modification both the configuration of the moderator and its distance from the reactor were changed—not obviously but, as it happened, significantly. When operation was resumed, the control rods were driven to their previously determined initial positions. Insertion of the safety block for the period calibration initiated an excursion with a 12-times-normal yield, and the reactor was badly damaged.

The cause of this incident was not an unsafe operating procedure; it was the failure of the operations crew to appreciate the ease with which a small change in an experiment can produce a significant reactivity perturbation.

7. An incident embarrassingly similar to No. 6 occurred much later at a different facility and involved an improved but nevertheless first-generation Godiva. For a special experimental requirement, a technique had been developed by which relatively broad (~1 msec) pulses were produced by wrapping a $\frac{1}{2}$-in.-thick sheet of polyethylene around the safety screen surrounding the fuel assembly. (The effect of the polyethylene was, of course, to add reactivity and to increase the effective neutron lifetime.) The first phase of the experiment had been completed successfully several months earlier, and, in preparation for the second phase, the polyethylene had once again been installed on the reactor safety screen. In the interval between the two phases of the experiment, the diameter of the safety screen had been reduced from 9.5 to 8.0 in. to increase the radiation dose delivered to samples located at the point of closest experimental approach, i.e., at the screen. This modification was completely overlooked in the plan for resuming the broad-pulse experiment, and the reactivity worth of the polyethylene was some $2 more than expected. During the first approach to delayed criticality, with the control and burst rods withdrawn, the reactor scrammed during slow mechanical (as opposed to pneumatic) insertion of the safety block. Not until some seconds later did the reactor supervisor realize what had happened: the reactor had actually exceeded prompt criticality. The burst yield was very low (it produced no fuel-temperature rise), and there was no damage to the reactor.

Again, because the operations crew failed to consider the effect of a shift in the position of a piece of experimental apparatus, an incident occurred during an operation where safety had been demonstrated many times previously. Only the relatively slow rate of reactivity addition (~25¢/sec) limited the energy release in the excursion. A contributing factor was the slow response of the scram instrumentation because of the shielding effect of the polyethylene.

8. Among the first experiments irradiated in the vertical glory hole of a Super Godiva was one consisting of a prototype fission couple surrounded by several grams of ^{10}B. To assure that its position could be accurately reproduced from burst to burst, the experiment was mounted on a special support stand, the location of which was determined by dowel pins that mated with accurately located sockets on the reactor itself. For reducing the radiation exposure of the experimenter, the stand was designed so that it was automatically picked up by the reactor as the reactor was raised from its underground storage pit and was replaced on the floor as the reactor was lowered. This incident was really a series of some 40 bursts during which yield reproducibility was very poor: more than a quarter of the bursts had yields over 10% above or below the intended yield. The largest burst was only 20% higher than intended, so the reactor was not damaged.

Eventually investigators discovered that even with its elaborate design the support stand was not actually reproducing its position each time the reactor was raised. Therefore because of the very large effect of the ^{10}B on the flux distribution in the reactor core, the worth of the burst rod was slightly different for each position of the experiment, and a shift of only $\frac{1}{2}$ ¢ in burst-rod worth was sufficient to change the burst yield by 10%.

The gamma dose rate 1 m from the core was typically many tens of rads per hour between bursts, so manual adjustment of the support stand was impractical. A convenient and entirely satisfactory solution to the problem was the installation of a pilot light, readily visible on the closed-circuit television monitor, which is actuated by three microswitches in series, one microswitch at the bottom of each leg of the support stand. When the pilot light is on, the operator is assured that the experiment stand is properly positioned. The problem of poor reproducibility was eliminated, and the system is now in use for virtually all glory hole experiments.

9. One of the earliest radiation-effects research programs involving the use of a fast burst reactor was one in which it was desirable to move the experiment away from the reactor as soon as possible after a burst. The reactor itself was stationary, so the experiment was mounted on an electrically driven vehicle controlled by the experimenter from the reactor control room. In his anxiety to move the experiment at the earliest possible time, the experimenter adopted the habit of actuating his experiment vehicle on "zero" of the verbal countdown given by the reactor supervisor to the operator. At the time of this incident, external burst initiation had not yet been introduced, and time delays of several seconds between burst-rod inser-

tion and burst initiation were not uncommon. It was inevitable then that an occasion arose in which the experiment had started to move away from the reactor before the burst was initiated; the result was a zero-yield incident. If the drive motor reversing switch had been in its opposite position or if the experiment had rocked back on its stand before beginning its motion away from the reactor, a most serious accident might have resulted.

The experiment was continued after the experimenter had been made aware of the possible consequences of his action. When the identical incident occurred a second time, however, an interlock was installed to prevent the experiment drive motor from being actuated until after a reactor scram had occurred. It has become customary in newer facilities to require that power to all mobile experiments be supplied through an interlocked receptacle provided near the reactor.

10. Another zero-yield incident, this one involving a missile electrical system being irradiated very near the core of a Super Godiva, illustrates the importance of unambiguous communication between the experimenter and the reactor operations staff. In this instance the experimental plan stated that the electrical system, which included a wet-cell battery, would remain passive until 3 sec before the burst; at that time the circuit would be energized by activating the battery. The plan was approved, and equipment was set up in preparation for the first burst, which proceeded normally through the entire burst sequence except that there was no fuel-temperature rise and virtually no yield. Even a careful reexamination of the details of the experiment failed to produce an explanation for the incident, so it was decided to repeat the delayed-critical calibration to determine if there had been a change in the reactivity worth of the experiment (which had remained undisturbed since the incident). It was found that the worth had decreased some 13¢ so that the initial reactivity in the power transient was 5¢ below prompt critical rather than 8¢ above. Interrogation of the experimenter revealed that activating the battery entailed moving the electrolyte from an internal reservoir to the reaction chamber. Fortunately, the motion of the electrolyte was away from the reactor core; otherwise an excursion, potentially with an initial reactivity 21¢ above prompt critical, would have occurred.

The striking feature of these five experiment-related incidents is that none of them was caused by a flagrant lapse on the part of any individual involved. In every case an operating procedure that had been demonstrated to be safe in similar, but obviously not identical, experiments was being followed. By sheer good fortune only one of the incidents resulted in damage to the reactor; but all the incidents

were potentially damaging, and they were all equally serious from the standpoint that nothing except unusual foresight would have prevented them. A decoupling shroud would undoubtedly have reduced the magnitude of the power excursion in incident No. 6, but no mechanical device — no elaborate interlock system, no electronic motion detector, no computerized reactivity meter — would have prevented any of them.

CONCLUSION

These 10 incidents illustrate the fundamental difference between conventional reactors and fast burst reactors: engineered safety devices are at least as important as administrative controls in providing for the safe operation of conventional reactors, but administrative control is of overriding importance in the operation of fast burst reactors.

The incidents reported here are typical, but by no means do they cover the spectrum of possible accident mechanisms. Mistakes that have caused incidents in the past can certainly be avoided in the future; reporting some of those mistakes is a secondary purpose for this paper. The primary purpose is to stimulate the thinking of those persons responsible for the design and operation of fast burst reactors, with the hope that through more effective administrative controls the number of new accident mechanisms "discovered" can be reduced in the future.

BIBLIOGRAPHY

Kazi, A. H., H. G. Dubyoski, and R. W. Dickinson, Preoperational Test Experience with the Army Pulse Radiation Facility Reactor, Session 4, Paper 5, these proceedings.

Long, R. L., Report of Reactor Excursion During Test of Modified Core, FBRF Operations Report No. 2, White Sands Missile Range, 1965.

O'Brien, P. D., SPR II: Early Operating Experience, USAEC Report SC-DR-67-801, Sandia Corporation, 1967.

Paxton, H. C., and Glen A. Graves, Critical Masses of Oralloy Assemblies, *Nucleonics*, 15(6): 90 (1957).

Stratton, W. R., *Progress in Nuclear Energy*, Part IV, No. 3, pp. 171-172, 1960.

United States Atomic Energy Commission, Operational Accidents and Radiation Exposure Experience Within the United States Atomic Energy Commission (1943–1964), Superintendent of Documents, U. S. Government Printing Office, Washington, D. C., 1965.

DISCUSSION

SEALE: I have an observation to make. In the incidents that you mentioned and in most of the incidents that we have heard about in the past, the effect of preinitiation has been traditionally to limit yield

rather than to enhance yield. I think that the rather interesting aspect of the Aberdeen problem was that this was a case where preinitiation actually occurred at such a time as to enhance the yield. I guess the lesson there is that it does not hurt to do our physics.

O'BRIEN: Probably the most dramatic example of the "discovery" of a new design-associated accident mechanism that I know about is the Aberdeen incident.

BANFIELD: You touched on the idea that all these incidents can be directly or indirectly related to procedure somewhere along the line. My observation is that the operator or supervisor who is charged with the error in judgement or procedure is always very exposed to the criticisms, but he is also in a position to gain from the experience; not so for the person who makes the design or technical error.

McTAGGART: Preinitiation is a problem on VIPER. It can and quite often does give an increased pulse size. It emphasized in our operating procedures that the setting of the timer sequence which controls the length of the plateau tail has to be chosen so that if the pulse preinitiates the extra heating will not exceed the limits set for the reactor.

O'BRIEN: I objected some time ago, and I forgot that I objected, to describing the event at Aberdeen as a preinitiation. In my thinking that was not really a preinitiation. All the bursts that had preceded it were something other than normal bursts. This one actually did occur when it should have.

The
Future Generation
of
Fast Burst Reactors

Session 5

5-1 A HIGH-YIELD MOLTEN-SALT BURST REACTOR

A. M. PERRY
Oak Ridge National Laboratory, Oak Ridge, Tennessee

ABSTRACT

A pulsed molten-salt reactor appears capable of producing neutron fluences of 10^{16} neutrons/cm^2 in neutron-irradiation specimens in single bursts with widths of less than 1 msec. A reactor design is presented which achieves these goals, using as fuel the eutectic salt $LiF-UF_4$ (73-27 mole %). Neutronic, mechanical, and hydraulic analyses of the reactor are discussed.

For investigating certain types of neutron-induced radiation damage, very short intense bursts of fast neutrons must be produced. The time-integrated flux of neutrons (fluence) that can be produced in a single pulse of a fission reactor is limited, in part, by the volumetric heat capacity of the reactor fuel. The fused fluoride salts, such as those used in the Molten Salt Reactor Experiment (MSRE)[1] at the Oak Ridge National Laboratory(ORNL), have a very large capacity to absorb energy without a phase change. The salt $LiF-UF_4$ (73-27 mole %), for example, has an integrated heat capacity of about 4 Mw-sec/liter between the melting point of 490°C and the boiling point, which is above 1500°C at a pressure of 1 atm. Investigation of the possible use of a molten-salt reactor for generating single bursts of very high yield therefore seemed worthwhile, and three years ago, in early 1966, we made a brief study at ORNL to determine the feasibility and probable performance of such a reactor.

In this paper I shall outline some general conclusions of a preliminary survey of performance characteristics and describe two different versions of a molten-salt burst reactor. The first version, which I shall refer to as the hard-core reactor, appears to have extremely attractive performance, but it also has certain intrinsic difficulties which may or may not be insurmountable. The second version, which I

shall refer to as the soft-core reactor, circumvents these difficulties at the expense of a somewhat greater burst width but should otherwise perform as well as the first.

Our basic concept for the reactor consists of an annular molten-salt core surrounding a central experimental thimble or test cavity. The core, in turn, is surrounded by a thick shell serving as both reflector and container. The core contains no moderator other than the fuel salt itself, both to keep the neutron spectrum as fast as possible and to achieve the highest possible fission density around the test cavity. For rapid assembly of a configuration that must be well above prompt critical, we visualize injecting a slug of fuel into the core atop a piston of molten lead (with which the salt does not mix) and then into a surrounding catch basin where the heat generated in the burst is removed by a spray of lead droplets. Before describing such details further, however, I will indicate some of the general performance characteristics to be expected.

PRELIMINARY PARAMETER SURVEY

In evaluating the performance of a molten-salt burst reactor, we were concerned with the neutron fluence in the test cavity and with the duration of a single burst. Actually the energy fluence

$$F = \int_0^t dt \int_0^\infty \phi(E,t) \, E \, dE$$

rather than the particle fluence is considered a better indication of the amount of radiation damage produced per burst; the energy fluence was adopted as a figure of merit in comparing possible reactor configurations. This fluence can be calculated with ordinary static neutronics codes, provided the fission-density distribution during the transient is essentially the same as the steady-state mode; this was shown to be the case. The results of spherically symmetric one-dimensional multigroup diffusion calculations are shown in Fig. 1. The model for the calculations was a 12-in. spherical cavity enclosed by a 1-cm-thick nickel shell, followed by the salt annulus, a 5-cm nickel shell, and a 25-cm graphite reflector. In one case (122-cm core diameter), it was shown that a single 15-cm nickel shell produced the same results as the combined nickel−graphite layers. It may be seen from Fig. 1 that, although the total neutron flux in the test cavity and the burst yield continue to increase with increasing core size, very little is gained in energy flux or in the neutron flux above 100 kev for cores above 75 to 100 cm in diameter (core volumes of 200 and 500 liters, respectively). The reactors are all fast, with median fission energies on the order of 100 kev, and the required uranium enrichments range from 20 to 40%. (The mole
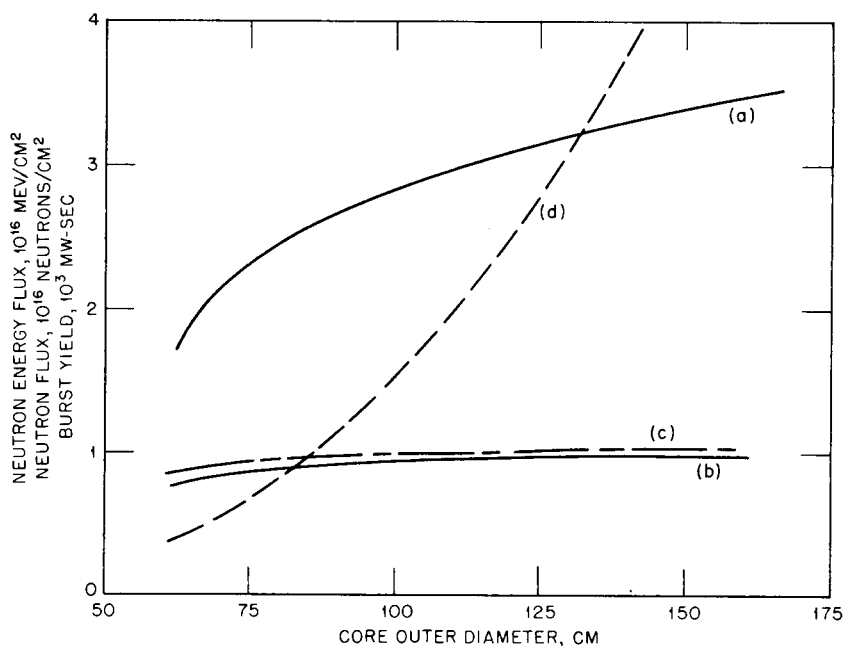
Fig. 1—Integrated neutron flux and burst yield vs. core size. Curve (a), total flux; curve (b), flux above 0.1 Mev; curve (c), neutron energy flux; curve (d), burst yield.

fraction of UF_4 in the salt is fixed at 27%.) These results indicate that an energy fluence of about 10^{16} Mev/cm^2 on target could be achieved with a molten-salt burst reactor having a maximum temperature rise of 1000°C (maximum energy density of 3.93 Mw-sec/liter), which encouraged us to carry the investigation further.

HARD-CORE BURST REACTOR

Two-dimensional six-group diffusion calculations were performed to provide a somewhat better representation of a practical core configuration, including entrance and exit passages for the salt. The computational model for a 200-liter core is shown in Fig. 2. A typical test specimen in the experiment thimble was represented by a somewhat arbitrary mixture of aluminum (28 vol.%), copper (10 vol.%), polyurethane foam (37 vol.%), and voids (25 vol.%). The uranium enrichment was adjusted to achieve prompt criticality at a temperature of 875°C, which is the average temperature expected at the peak-power point during a burst. Neutron cross sections and the salt volume were then adjusted to 500°C, the preburst salt temperature, and a second cal-
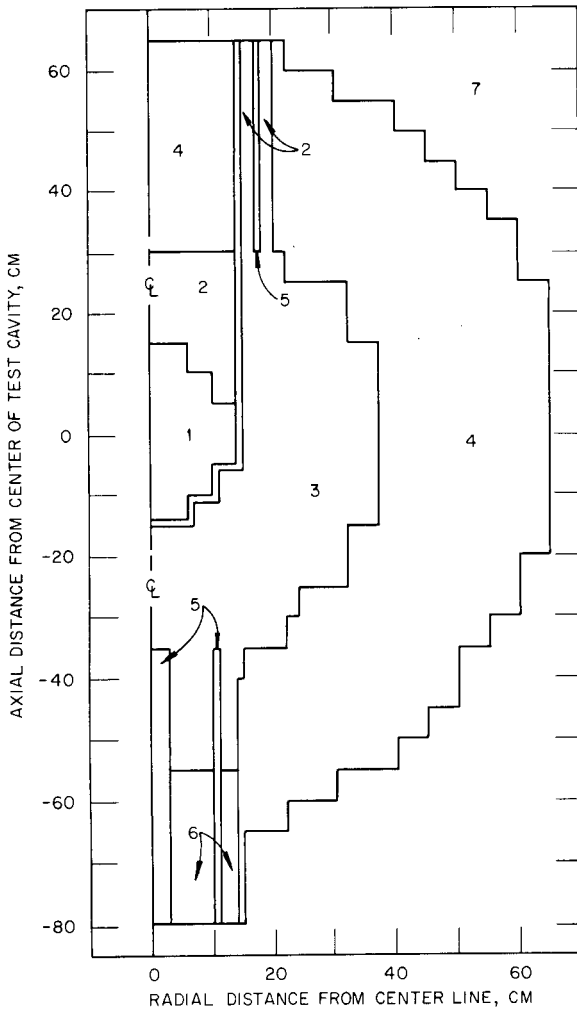
Fig. 2—*Model for two-dimensional calculations for 200-liter core.*

  1, Test specimen　　　*5, Poisoned Hastelloy vanes*
  2, Void　　　　　　　*6, Molten lead*
  3, Fuel salt　　　　　*7, Black boundary region*
  4, Hastelloy N

culation was performed to determine the required initial reactivity. Uniform addition of a 1/v poison to achieve $k = (1 - \beta)^{-1}$ then enabled us to calculate the prompt-neutron generation time and to verify that the transient and steady-state modes do not differ appreciably in shape. The initial asymptotic reactor period and the burst width (full width at half-maximum amplitude) were calculated from the expressions T =

Table 1

CHARACTERISTICS OF MOLTEN-SALT BURST REACTORS

	200-liter hard core	400-liter soft core
Core height, cm	65	80
Core outer diameter, cm	75	90
Figure of merit,* Mev/cm^2	0.6×10^{16}	0.7×10^{16}
Total neutron fluence, neutrons/cm^2	1.4×10^{16}	1.8×10^{16}
Neutron fluence (E > 100 kev), neutrons/cm^2	0.5×10^{16}	0.6×10^{16}
Prompt-neutron generation time, μsec	0.36	1.5
Required initial k_{eff}	1.044	1.016
Uranium enrichment, % ^{235}U	40	23
Initial asymptotic period, μsec	10	180
Burst width, μsec	35	700
Burst yield, Mw-sec (fissions)	490 (1.5×10^{19})	1200 (4×10^{19})

*Average neutron energy fluence in test specimen.

$l/(\rho - \beta)$ and $\tau = 3.5$ T, respectively. A summary of reactor character-
istics is shown in Table 1.

The very large initial excess reactivity required for the burst is,
of course, the result of a substantial negative temperature coefficient
of reactivity, which is itself the consequence of the large thermal ex-
pansion coefficient of the salt. The reason for calling this a hard-core
reactor will become apparent shortly.

WEAK- AND STRONG-SOURCE MODES OF ASSEMBLY

We believe that this kind of performance — an energy fluence of
nearly 10^{16} Mev/cm^2 and a burst width of 35 μsec — would be very
useful indeed. Unfortunately, a serious obstacle to achieving such a
narrow burst exists in the form of a rather strong inherent neutron
source in the molten-salt fuel arising primarily from (α, n) reactions
in fluorine. In the reactor just described, the source strength is greater
than 10^6 neutrons/sec, and it is easily shown that this is far too strong a
source to permit a leisurely insertion of reactivity well above prompt
critical.

We are concerned here with the probability that a persistent fis-
sion chain will not be established during the time t_0 required for the
reactivity insertion above prompt critical. Following much the same
line of argument as that outlined by Hansen,[2] we can easily show that
this probability, $P(t_0)$, is related to the source strength S, the reac-
tivity ρ, and the insertion time t_0 by the expression

$$-\ln P(t_0) = 0.5 \, St_0(\rho - \beta)$$

for a linear ramp insertion of reactivity. If we require that $P(t_0) \geq 0.9$, so that there is less than a 10% chance of preinitiation, then the above expression, on rearranging, becomes $S \leq 0.2/t_0(\rho - \beta)$ for a linear ramp. (Similarly, we can show that $S \leq 0.15/t_0(\rho - \beta)$ for a parabolic insertion, which is concave downward.) For example, if $t_0(\rho - \beta) = 10^{-3}$ (e.g., $\rho - \beta = 0.03$, $t_0 = 0.03$ sec), then $S \leq 200$ neutrons/sec would be acceptable without any restrictions on neutron generation time. However, there appears to be no chance of achieving so low a neutron-source strength in a molten-salt fuel.

We are led, therefore, to consider what combinations of reactivity, insertion time, and prompt-neutron generation time will result in acceptable burst characteristics if a persistent fission chain reaction is
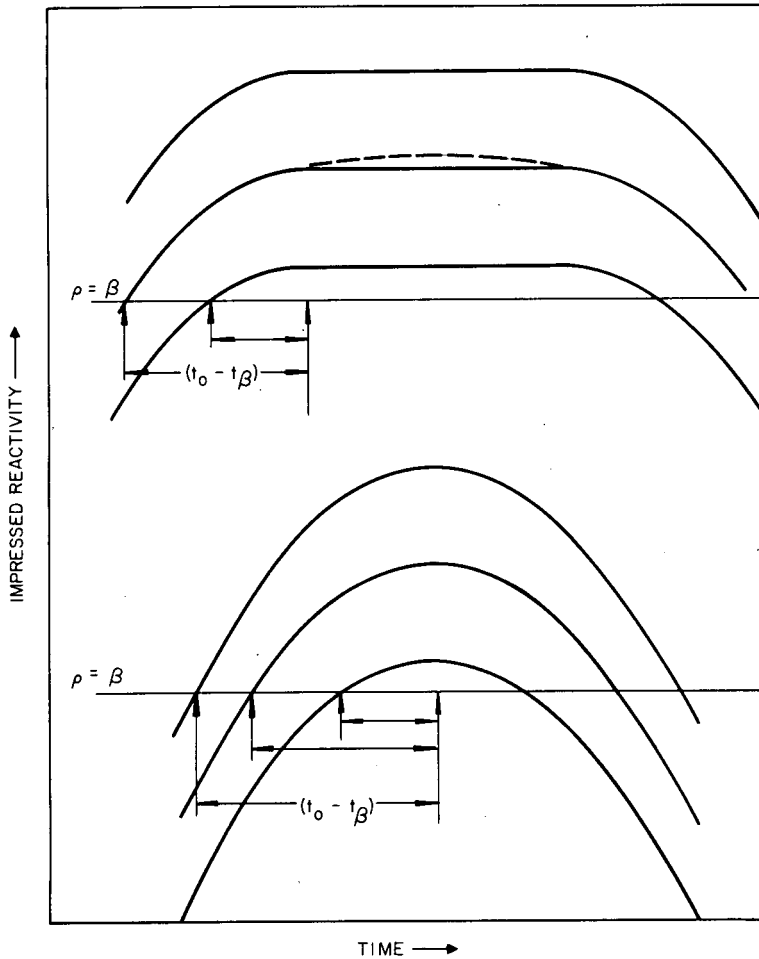
Fig. 3 — *Illustrative reactivity profiles.*

established at the outset, that is, if the ordinary reactor kinetics equations apply throughout the period of reactivity insertion. We have calculated the course of reactor transients for various combinations of these parameters, all intended to produce the same total burst yield (e.g., 1000 Mw-sec). Truncated linear ramp insertions, truncated parabolic insertions (concave downward), and continued parabolic insertions were included (see Fig. 3). The results are shown in Fig. 4 in
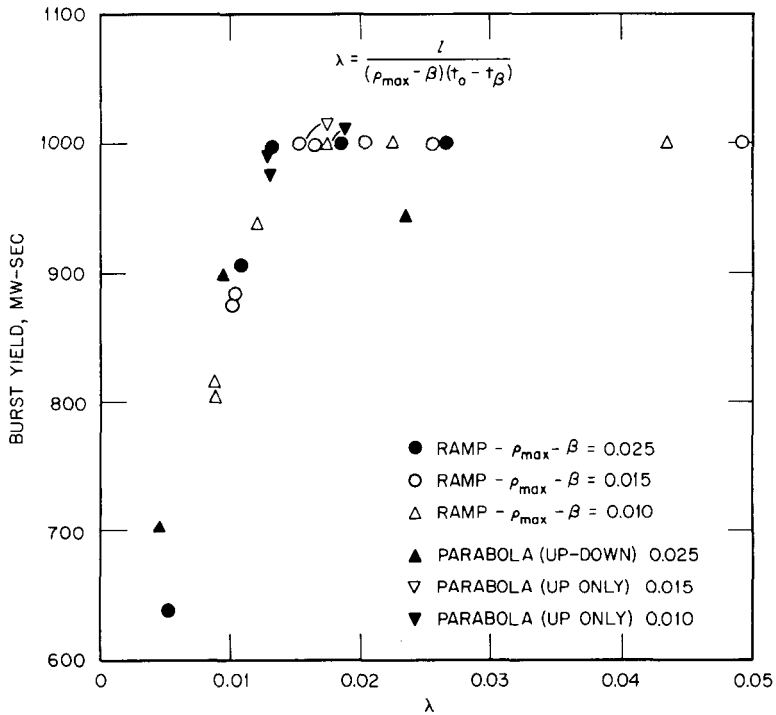
Fig. 4 — *Burst yield vs. parameter* λ.

which the burst yield is plotted as a function of the dimensionless parameter

$$\lambda = \frac{l}{(\rho_{max} - \beta)(t_0 - t_\beta)}$$

i.e., the expected initial asymptotic period divided by the reactivity insertion time above prompt critical. Figure 4 clearly suggests that for the truncated insertions the criterion $\lambda \geq 0.015$ should be satisfied; for continued parabolic insertions, the inequality should be replaced by an (approximate) equality.

Applying this criterion to the 200-liter hard core, we find that the reactivity insertion of 0.037 above prompt critical would have to be completed in less than 1 msec to achieve a full undistorted burst with the characteristics shown in Table 1. Unfortunately, we have not as yet identified a suitable method of accomplishing this—by fuel movement, by poison removal, or by altering the reflector configuration—that is consistent with preserving the reactor for subsequent reassembly. We have therefore reluctantly considered ways to slow down the response of the reactor.

SOFT-CORE BURST REACTOR

This result we have achieved in two ways: by increasing the neutron generation time and by decreasing the effective temperature coefficient of reactivity, thereby decreasing the excess reactivity that must be inserted to achieve the desired burst yield.

Increasing the prompt-neutron generation time by about a factor of 4 was accomplished by using a graphite reflector supported radially by a Hastelloy N wall and separated from the fuel salt by a niobium membrane. The graphite introduces some low-energy neutrons near the outer boundary of the core but has little effect on the neutron spectrum in the test cavity. In addition to increasing the prompt-neutron generation time, the graphite reflector, by reducing the peak-to-average-power density ratio, actually permits a small increase in the neutron energy fluence on target, so long as the peak power density remains at the inner boundary of the core. To show the effect of the graphite reflector, we made some spherically symmetric multigroup neutron-diffusion calculations for cores of 200, 400, and 600 liters, both with and without a test specimen in the cavity; results of these calculations are shown in Fig. 5. The discontinuities in the curves occur where the point of peak power moves from the inner to the outer core radius. This effect is illustrated in Fig. 6 for the 400-liter core with the test specimen present. In Fig. 7 we record the uranium enrichment required for each case; in Fig. 8 we show the influence of the graphite reflector on the prompt-neutron generation time. For the 400-liter core, with 14 cm of graphite, the generation time is 1.5 μsec. In Fig. 9 we see the neutron energy spectrum in the test specimen.

To reduce the temperature coefficient of reactivity, we wish to offset part of the thermal expansion coefficient of the salt. This may be done by incorporating gas bubbles in the salt, making it in effect much more compressible, or soft, so that rapid expansion of the liquid is accommodated temporarily by collapse of the gas bubbles rather than by gross expansion of the mixture. A mechanism for accomplishing this reproducibly is the array of small inverted cups shown in Fig. 10. As
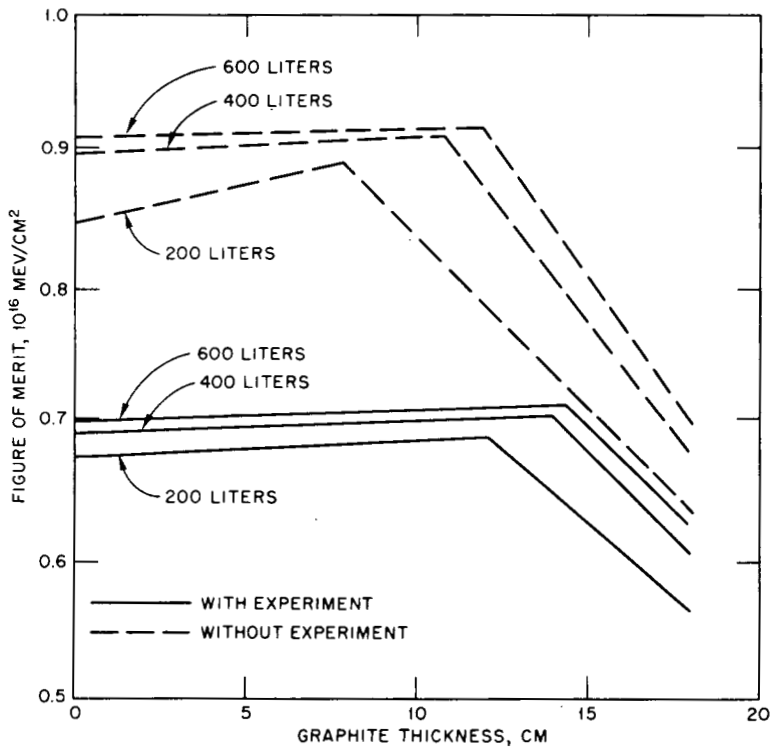
Fig. 5—Figure of merit vs. reflector thickness.
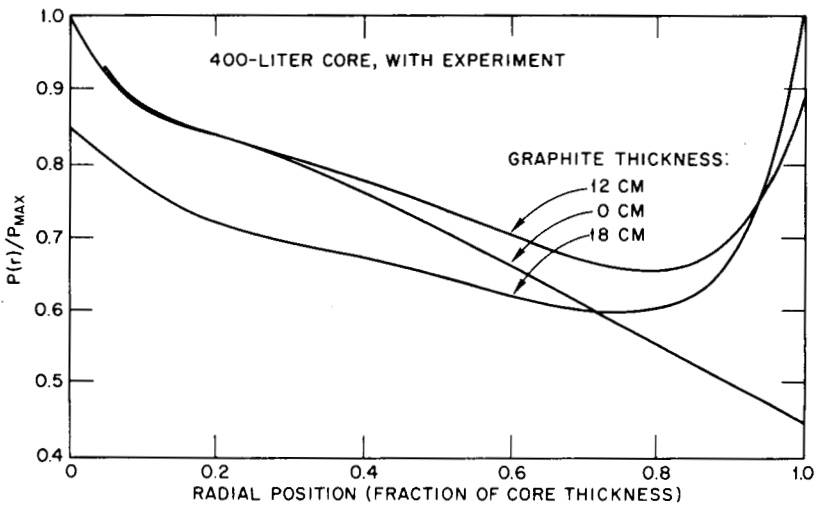
Fig. 6—Power-density distribution.
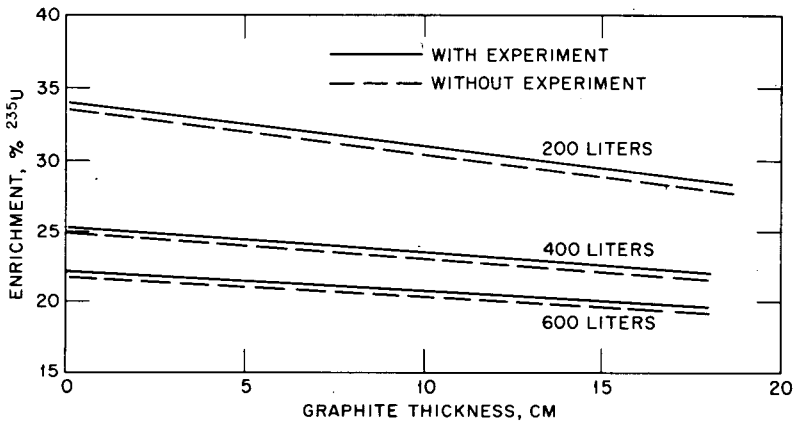
Fig. 7—*Fuel enrichment vs. reflector thickness.*
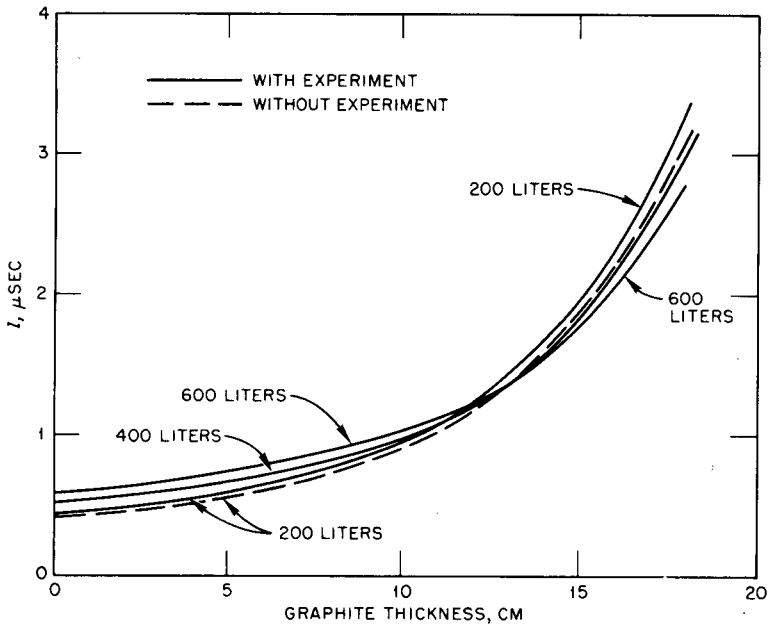
Fig. 8—*Prompt-neutron generation time vs. reflector thickness.*

the fuel salt surges into the core, some of the cover gas is trapped in the cups, providing an effective salt compressibility that depends on the total volume of gas contained within the cups and on the pressure of the cover gas prior to the burst.

This soft-core approach to reducing the required initial reactivity will result, of course, in a highly nonlinear reactivity feedback and will
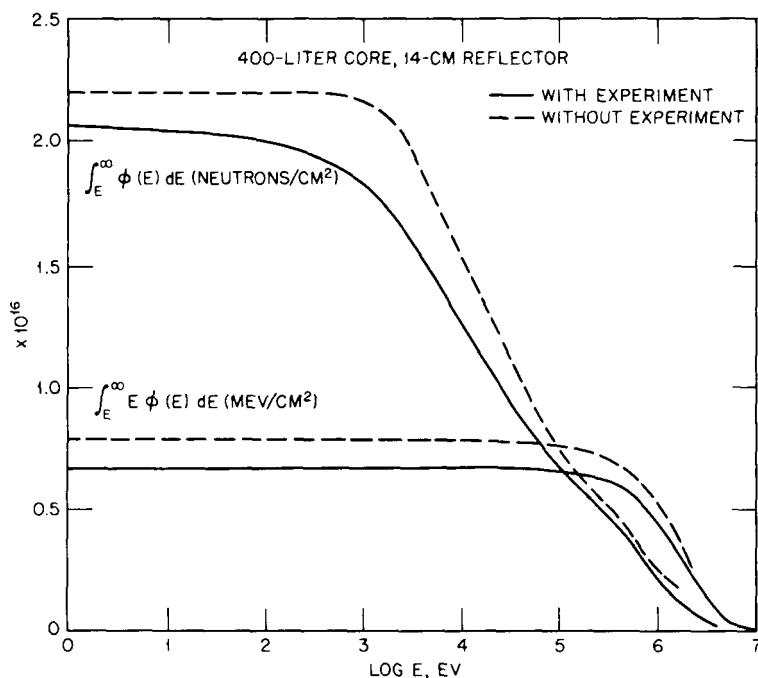
Fig. 9—Integral neutron energy spectrum in test specimen.

produce an unsymmetrical burst in which the final shutdown reactivity is much greater in magnitude than the initial excess reactivity. Also, the dependence of burst characteristics on initial conditions will be very difficult to calculate accurately in detail, and we cannot claim to have done so. We believe, however, that there will be enough flexibility in initial conditions to permit a systematic empirical determination of the conditions necessary to produce a desired burst, which can always be approached safely beginning with very low yields.

To estimate the excess reactivity required to satisfy the strong-source criterion, we assumed that the reactivity insertion profile is parabolic in shape, as shown in Fig. 3, and we calculated that approximately 30 msec would be required for the reactivity to rise 0.045 above delayed critical. Assuming that the same shape prevails if we reduce the maximum reactivity, we can find a unique relation between the excess reactivity and prompt-neutron generation time that satisfies the strong-source criterion. We find that a maximum reactivity of 0.008 above prompt critical is required for the calculated generation time of 1.5 μsec. This corresponds to an initial asymptotic period of 200 μsec and a burst width well under 1 msec.

A summary of burst characteristics for the 400-liter soft-core reactor is shown in Table 1.

EXPANSION CUP BRACES

EXPANSION CUPS ~1 CU. IN./CUP

B

B

GRAPHITE REFLECTOR

CONTAINER REFLECTOR

SECTION A-A

EXPERIMENTAL THIMBLE

TURNING VANES

EXPANSION CUPS

A

A

POISON VANES

ELEVATION SECTION B-B

COLUMBIUM LINER
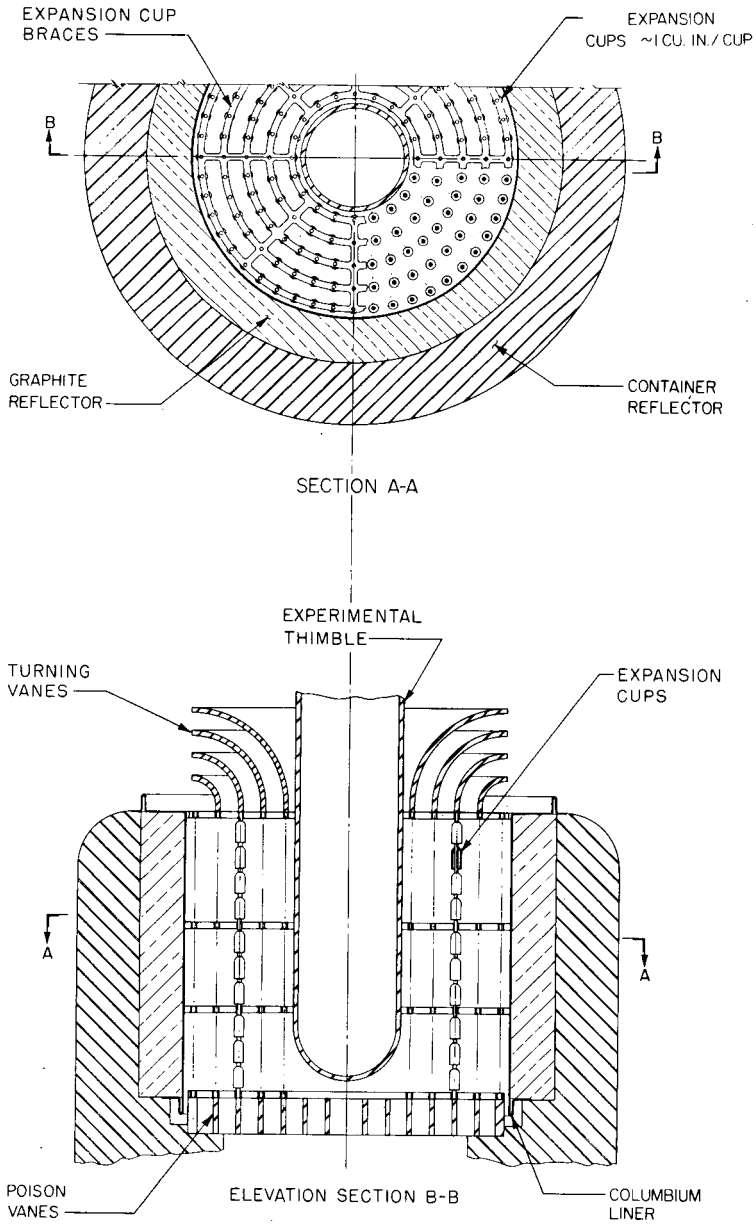
Fig. 10—Molten-salt burst reactor; soft-core sectional views of core region.

MECHANICAL AND HYDRAULIC ANALYSIS

Thus far I have discussed mainly the neutronics aspects of a molten-salt burst reactor. We have also attempted to identify the key engineering problems and to solve them. A vertical section of a representative soft-core configuration is shown in Fig. 11. Fuel is injected into the core by pressurizing the gas space over the lead in the reservoir. A pressure difference of approximately 70 psig is required to achieve a salt velocity of 15 ft/sec when the core is full. This pressure supplies the initial acceleration of the fuel salt and the lead column on which it rests; but, by the time the core is full, the pressure is mainly overcoming static and hydraulic head losses. The salt continues through the core, spilling over the top into the catch basin that surrounds the reflector. The entire transit time of the salt through the core is about $\frac{1}{2}$ sec.
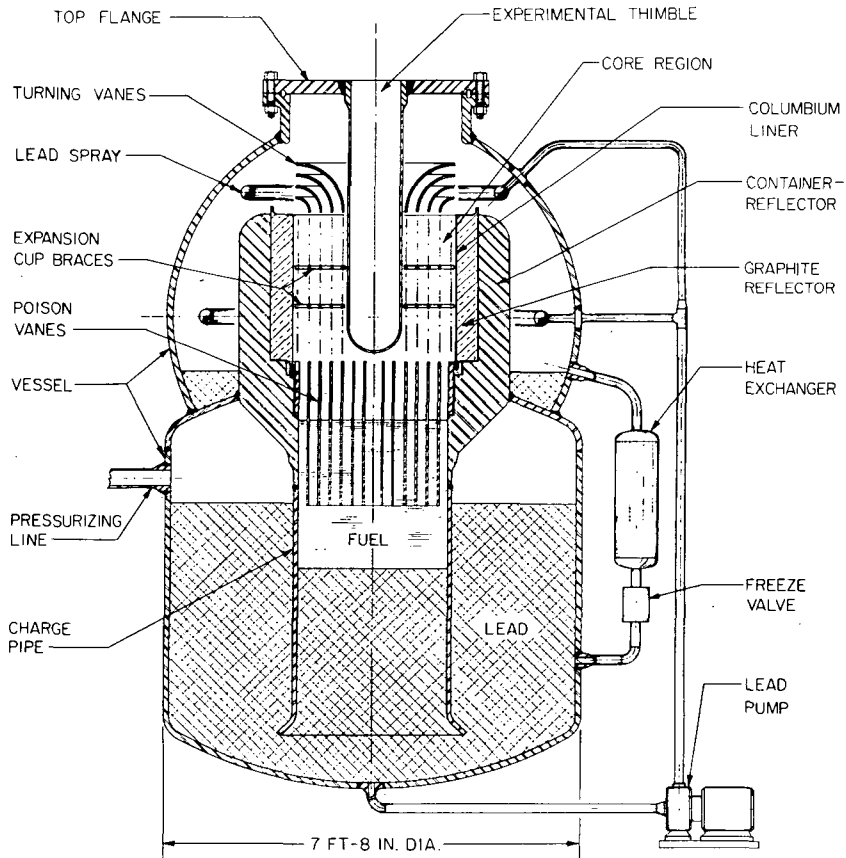
Fig. 11 — Molten-salt burst reactor concept.

Cool lead from the reservoir is discharged through the spray rings into the hot salt, cooling it very quickly to about 700°C.

Salt and lead are then cooled back to the initial temperature by circulating lead through the salt and through the air-cooled heat exchanger for approximately 10 min. By raising the lead level in the catch basin, we can slowly spill the cooled salt back through the core and into the charge pipe. The lead is drained by gravity back into the reservoir, returning the reactor to its preburst configuration.

The reactor system must of course be maintained at a temperature of 500°C prior to a burst. For this purpose the entire system shown in Fig. 11, except the heat exchanger, is enclosed in an insulated electrical furnace. Undoubtedly it will be necessary to insulate and cool the test specimens inside the thimble.

The transient pressure rise in the core during the burst is difficult to calculate accurately, though simplifying assumptions make it possible to estimate an upper bound. We believe the pressure in the hard-core configuration might rise to from 2000 to 3000 atm. In the soft-core configuration, the pressure necessary to drive the salt into the cups is estimated to be 100 atm, though the actual peak pressure during the burst could be appreciably higher than this, depending in part on the gas volume in the cups.

In calculating shapes and magnitudes of the bursts, we assumed that compressibility effects could be neglected, that is, that there is no significant lag in salt expansion as its temperature rises. This assumption may not be valid in fact and is almost certainly not valid for the hard core. If subsequent analysis should show such effects to be important, the effect will be to reduce the reactivity required to achieve a given burst yield and to increase the burst width.

For calculating stress levels in the core walls, alternating loads with negligible steady-state components were assumed. For the hard core the Hastelloy N container would have to be nearly 1 ft thick and the experimental thimble up to 3 in. thick — much more than was assumed in the neutronics calculations. This requirement, too, could prove to be a serious flaw in this otherwise very interesting configuration. For the soft core the membrane lining the reflector would have to be about $\frac{1}{2}$ in., if self-supporting, and less if supported by the reflector and Hastelloy N wall.

The reflector−container region was examined for thermal stresses resulting from gamma-ray heating during the burst. With 7% of the burst energy deposited in this region, the peak temperature rise is 175°C, the average rise is about 30°C, and the steepest radial temperature gradient is about 35°C/cm near the inner surface. These moderate conditions are not expected to cause significant thermal stresses.

Problems with materials compatibility do not appear to be serious in this reactor, and ample experience is available in the handling of molten salt and lead. We believe the lower temperature portions of the lead system can be made of Croloy. The parts that see high-temperature salt and lead may require a protective lining of niobium. The cup assembly should probably be made entirely of niobium. The high-pressure regions should probably be Hastelloy N with a niobium liner.

CONCLUSIONS

Although additional design and some component development work would evidently be required before one could build such a device, we believe that a molten-salt burst reactor could be built that would yield fluences in the test specimens of nearly 10^6 Mev/cm^2 in a single burst. The presence of a large intrinsic neutron source prevents assembly in the usual weak-source mode and may prevent achievement of the very narrow bursts that otherwise appear attainable. We have outlined the design of a reactor configuration that will permit assembly in the presence of a strong source, with a burst width less than 1 msec; further design innovations may possibly result in a worthwhile reduction in this parameter. Further details may be found in Ref. 3.

ACKNOWLEDGMENTS

REFERENCES

1. E. S. Bettis and W. B. McDonald, Molten-Salt Reactor Experiment, *Nucleonics, 22:* 67-70 (January 1964).
2. G. E. Hansen, Assembly of Fissionable Material in the Presence of a Weak Source, *Nucl. Sci. Eng., 8:* 709-721 (1960).
3. E. S. Bettis and A. M. Perry, A Feasibility Study of a Pulsed Molten-Salt Reactor, USAEC Report ORNL-TM-2487, Oak Ridge National Laboratory, in preparation.

DISCUSSION

THAMER: If a fused chloride fuel were used could not (1) the aver-age neutron energy be still higher and (2) the (α,n) source be less?

PERRY: There also are (α,n) reactions on chlorine, and you could reduce the source strength some but not enough. You would still have an intrinsic source of something in excess of 10^4 neutrons/sec with chlo-ride salts. It would be less than with fluoride salts but still too much for a weak-source mode of assembly.

THAMER: Presumably the flux would be somewhat harder, or could be so, with an appropriate chloride mixture. Although chlorine might give some (α,n) source, the source should be much less than that of fluorine, and the use of chlorides should decrease the problem of source strength.

PERRY: I think that simply changing from the fluoride to the chlo-ride salts would not alter the situation as I have described it because even a reduction of two orders of magnitude in the source strength would still not relieve us from having to assemble with the reactor es-sentially awake and responding at all times during the reactivity in-sertion.

THAMER: As in point (1) I was also thinking in terms of chlorine isotopes not having the high inelastic-scattering cross sections of fluo-rine.

PERRY: We have not examined this closely, and it is possible that one could get a somewhat harder spectrum with chloride salts.

CLACK: Could you get the necessary rate of reactivity insertion by firing a slug of solid fuel through a through tube?

PERRY: Moving a solid and getting the reactivity insertions in the time that would be required with a strong source would require accel-erations on the order of 10^4 g; I am not prepared to say this is not practical, but to me it does not look very practical.

5-2 THE SANDIA BOOSTER ASSEMBLY (EDNA PROGRAM)

R. L. COATS
Sandia Laboratories, Sandia Corporation,
Albuquerque, New Mexico

ABSTRACT

A description is given of the Electron Driven Nuclear Assembly (EDNA) concept being studied at Sandia Laboratory. The EDNA concept employs a 25-Mev 200,000-amp electron generator and a compact multiplying assembly. The design objective of the program is to provide a neutron fluence of approximately 1×10^{15} neutrons/cm^2 per pulse. The pulse width at half-maximum intensity is restricted to 1 μsec.

In the last few years significant advances have been made in the technology of high-voltage flash X-ray generators. Although primarily concerned with X-ray production, the generators are capable of producing useful quantities of neutrons for experiments through photonuclear reactions in appropriate materials. A high-voltage flash X-ray device, when coupled with a small fissile multiplying medium, can, in fact, compete with a fast burst reactor, such as the Sandia Pulsed Reactor II (SPR II), in producing usable neutron fluence. Such a coupled system offers both the advantage of much higher dose rates than those obtainable with fast burst reactors and the advantage of greater nuclear safety since the assembly is operated at subprompt critical.

The principle of operation of a high-voltage-generator – multiplying-medium combination (shown schematically in Fig. 1) is as follows: the high-energy electron beam produced by the generator is impinged on a high-Z target located, ideally, near the center of the multiplying assembly. A portion of the bremsstrahlung radiation produced in the target undergoes (γ,n) and (γ,f) reactions in the fuel material of the multiplier. The neutrons so produced are increased in number by subprompt critical multiplication in the assembly.
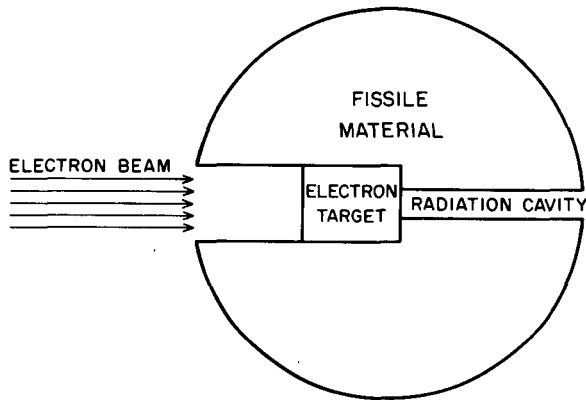
Fig. 1 — Booster concept.

This principle of operation has been demonstrated on the Gulf General Atomic, Inc., Accelerator Pulsed Fast Assembly (APFA)[1] and with the Harwell Neutron Booster[2] in England. In both systems a Linac is employed to generate the electron beam, and the neutron yield is therefore limited by the low electron currents typical of Linacs. The time-dependent behavior of a source-driven nuclear assembly has been described by Russell et al.,[3] along with a discussion of the nuclear parameters that govern the performance characteristics of such an assembly. Some measured and calculated information[4] concerning neutron production per electron incident on various materials is available in the literature.

There is need in radiation-effects research for more-intense radiation sources than are currently available. In answer to this need, Sandia Corporation is presently pursuing the development of the Electron Driven Nuclear Assembly (EDNA). The design objective of the EDNA program is to produce a usable neutron fluence of 10^{15} neutrons/cm^2 in a single pulse with a width at half-maximum intensity of 1 μsec. As presently conceived, EDNA would consist of a 25-Mv 200,000-amp generator and a Godiva-like multiplying fuel assembly.

A 25-Mv 200,000-amp generator requires an extrapolation of the technology developed in the design of the 12-Mv Hermes II device presently in use at Sandia. The performance characteristics of this new device cannot be accurately predicted but can be scaled from the existing generator performance. The practical considerations associated with the large energy content of the electron beam and the time-dependent fission densities required will necessitate sacrifices in the nuclear performance to maintain the mechanical integrity of the system.

Inroads into the major design problems have been made. The ability to drift a high-current electron beam is presently being investigated.

Preliminary results are promising but inconclusive. Studies have indicated that composite targets can be designed to absorb most of the electron-beam energy in nonfissile target materials at a minimal sacrifice in neutron production. The order of fuel component segmentation necessary has been identified by stress analysis of systems of interest, and concepts compatible with these findings are being explored.

Uranium-235 is being used as the principal fissile material in the present design studies, but ^{233}U is being considered in the event that the design objectives cannot be achieved using ^{235}U.

The EDNA program now in the feasibility phase at Sandia Laboratories is an attempt to provide a radiation source for experimenters which is capable not only of duplicating the pulse characteristics of existing fast burst reactors but also of generating dose rates far in excess of those produced by fast burst reactors. The overall design of such a facility as the one described previously can be broken into four separate, but not independent, design areas. These are: (1) the design of the high-voltage high-current generator; (2) the development of high-current beam-handling techniques; (3) the design and development of electron-beam targets compatible with the energy delivered in the electron pulse; and. (4) the design and development of a fuel assembly capable of withstanding the mechanical effects of the time-dependent fission densities required while maintaining a level of nuclear performance sufficiently high to ensure that design objectives will be met. These design areas represent a considerable extrapolation of existing technology. The remainder of this paper is devoted to a discussion of the important facets of each of the major design areas.

HIGH-VOLTAGE GENERATOR

As now envisioned, the EDNA high-voltage generator will be quite similar in concept to the 12-Mev Hermes II generator which has been under development at Sandia Laboratories for the past 3 years. Although the EDNA generator must be capable of operating at approximately twice the voltage to which Hermes II has been tested, the Hermes II performance characteristics provide a useful base from which to extrapolate performance characteristics to the EDNA generator.

The basic components of a flash X-ray system, such as Hermes II, are a Marx generator, a Blumlein transmission line, and an electron-beam-forming vacuum tube.[5] A Marx generator consists, simply, of a bank of capacitors which serves as the primary energy storage of the flash X-ray system. The operation of the Marx generator consists of charging the capacitors in parallel to the operating voltage and then

switching the capacitors in series to give a voltage multiplication of
n, where n is the number of capacitors. The Marx generator charges
the Blumlein transmission line in approximately 1 μsec. A Blumlein
transmission line consists of two transmission lines, which are
charged in parallel and, like the Marx generator capacitors, are
discharged in series in approximately 70 nsec. The Blumlein pro-
vides a rapid-discharge intermediate-energy storage between the
Marx generator and the X-ray vacuum tube.

The Hermes II Marx generator, consisting of 186 1-μf 100-kv
capacitors, has a maximum energy storage capability of 1 mega-
joule but is presently being charged to 0.5 megajoule. Upon the dis-
charge of the Marx generator capacitors in series, the stored energy
is transferred to the 30-ft-long Blumlein. This energy, in turn, is
rapidly transferred to the electron-beam-forming vacuum tube. A
high-voltage short-duration electron beam is formed, and it is impinged
on the high-Z anode, producing bremsstrahlung radiation.

The Hermes II generator shown in Fig. 2 is enclosed in a cylindri-
cal tank 20 ft in diameter and 80 ft long which is filled with 150,000 gal
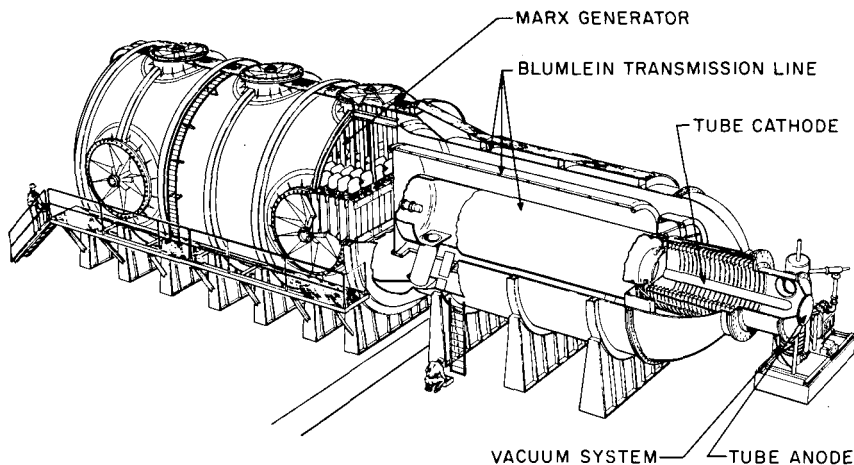
Fig. 2—Hermes II.

of high-quality mineral oil to provide electrical insulation. The gen-
erator has been tested up to a maximum tube voltage of 12 Mv and a
corresponding tube current of 200,000 amp. For such an operation, an
X-ray dose of approximately 6000 rad to water is produced 1 m from
the target; the effective duration of the radiation pulse is approximately
70 nsec. Hermes II will be operated with a nominal maximum tube
voltage of 10 Mv, a tube current of 160,000 amp, and an X-ray dose
at 1 m of 3000 rad. The machine is presently being operated con-

servatively to avoid voltage breakdown levels in the Blumlein support
structure, tube shorting on the vacuum side of the beam-forming-tube
insulators, and dendriting in the insulators of the vacuum tube. With
moderate design changes, Hermes II could be extended to 14-Mv op-
eration with a tube current of approximately 230,000 amp and with
improved pulse shape characteristics.

The time constants associated with both Blumlein oil switching
and the electron-tube inductance influence the time behavior of the
voltage developed across the X-ray tube and result in an efficiency
loss in transferring energy to the electron beam. A typical nor-
malized Hermes II voltage pulse shape is shown in Fig. 3 and com-
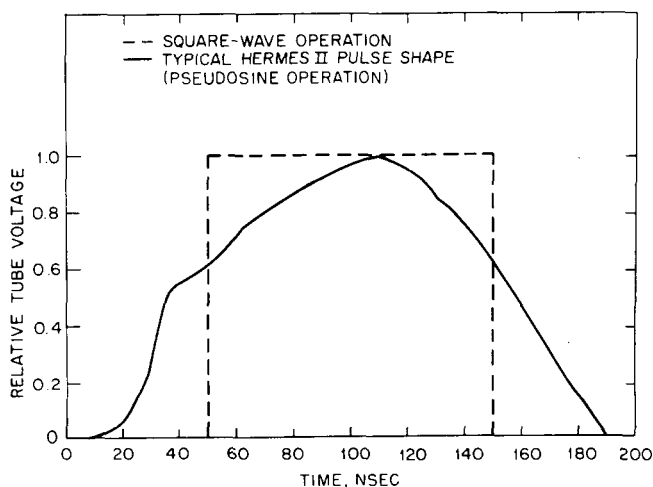
Fig. 3—High-voltage generator tube voltage as a function of time.

pared with an optimum pulse which would result from the elimination of
all undesirable delay times. The typical pulse shape and the optimum
pulse shape will hereafter be referred to as that which results from
pseudosine operation and square-wave operation, respectively. Owing
to the nature of the time-dependent voltage pulse, many of the beam
electrons produced in normal operation have an energy far less than
that required for significant neutron or X-ray production, and the
effective radiation pulse duration is significantly smaller than the
actual beam duration.

The basic design parameters of a 25-Mv 200-kamp generator can
be extrapolated from the research results leading to the development of
Hermes II. However, this extrapolation indicates that a large and
somewhat expensive installation will be required. The Marx genera-
tor for the EDNA machine will probably require an energy storage

capability of approximately 1 megajoule, which should not present serious difficulties. The Blumlein and oil volume requirements will scale with energy according to the Hermes II parameters.

The limitations placed on Hermes II by the voltage breakdown, tube shorting, and dendriting problems necessitate an investigation of these areas before the Hermes II design concept can be extended to a 25-Mv 200-kamp machine for booster application. Further research will also be required in the areas of multichannel oil switching in the Blumlein and of electron-tube cathode inductance to optimize the voltage pulse characteristics. Studies in each of the problem areas are now underway. Much experimental support can be given to the studies since Hermes II is now available for use in investigating these areas.

ELECTRON-BEAM TRANSPORT

The delivery of the electrons to the multiplying assembly represents a major problem area, primarily because of a lack of knowledge concerning drift phenomena for high-current high-energy electron beams. Little information is available concerning high-current electron transport, and virtually no information is available covering the 25-Mv 200-kamp region of interest.

The ability to drift the 3.5-Mev 45,000-amp Hermes I electron beam over a distance of several feet and around extreme bends in a drift chamber has been demonstrated at Sandia. (Hermes I is a scaled-down version of Hermes II.) The beam energy loss upon bending the Hermes I beam has not been determined. Equal success has been attained at other facilities[5] with beams of lower energy (~0.5 Mev) but with currents in excess of 100,000 amp. The ability to drift lower energy beams with relative ease, and even to divide the beam into two or more distinct beams, has been demonstrated. Experiments to date indicate, however, that a continued degradation, both in total beam energy and in the maximum energy per electron, occurs as the beam is drifted.

The nature of the electron beam must be well understood before the target design can be optimized. A loss in beam energy, particularly if this loss occurs in the higher energy component of the electron beam, can result in a severe loss in neutron production. The transverse component of electron motion in the beam influences the distribution of energy deposition in the target and the angular distribution of the resulting bremsstrahlung radiation. If the ease of beam handling demonstrated with lower energy beams can be demonstrated for the range of interest for the EDNA machine, many new beam—target concepts can be explored.

The Hermes II beam has been successfully extracted from the vacuum tube, and experiments are presently underway to determine the parameters associated with electron beams in the 7- to 10-Mev 100- to 200-kamp range. Once the characteristics of these beams are understood, an extrapolation to the 25-Mev 200-kamp level may be possible.

TARGET DESIGN

The object of the target design is to provide a target which (1) is efficient in neutron production, (2) is of a size and geometry useful for booster application, and (3) will prevent damage to the fuel assembly by the electron beam. The design depends strongly on the characteristics of the electron beam delivered by the high-voltage generator. Optimally the 25-Mev 200,000-amp electron beam of the EDNA generator would be monoenergetic and of constant current for the duration of the pulse. This type of pulse would correspond to square-wave operation and would result in the greatest efficiency in converting the energy store of the system into neutrons. The time constants associated with switching and those associated with the inductances of the high-voltage system prevent the achievement of pure square-wave operation, and the voltage shape is more likely to be like that of Hermes II shown in Fig. 3. The ^{238}U target-neutron production per megajoule of incident-electron-beam energy as a function of the maximum energy per electron of the pulse is shown in Fig. 4 for the two modes of operation. M. H. McGregor's[4] calculated data was used to determine the total neutron production in the target. Figure 5 indicates time-dependent target-neutron production.

There is reasonably good agreement between MacGregor's calculated data and some recent measurements made by D. E. Groce of Gulf General Atomic.[4] Groce's data indicate that an increase in neutron production of 20 to 30% can be achieved using ^{235}U, ^{233}U, or ^{239}Pu as the electron target material instead of ^{238}U. The use of fissile materials as principal targets in the EDNA scheme, however, would result in higher target energy densities than in ^{238}U owing to the increased heating from (n,f) reactions.

The efficient amplification of the neutrons produced in the target requires that the neutrons be produced in a region of high neutron effectiveness. In a bare homogeneous system, the highest neutron effectiveness is at the center of the assembly. The dimensions of the beam-entry cavity also influence the critical size of the assembly, which, in turn, determines the prompt-neutron lifetime and, consequently, the maximum prompt multiplication that can be achieved for a given pulse width. A large beam-entry cavity would ultimately result in lower
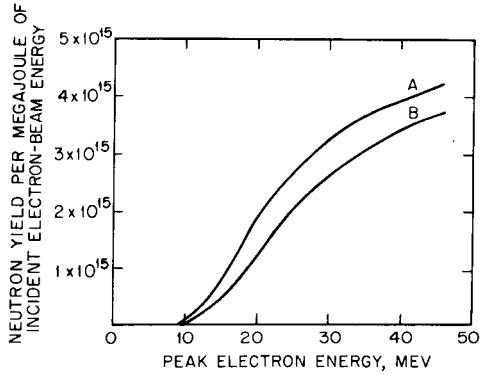
Fig. 4 — Neutron yield from thick ^{238}U target as function of peak electron energy. Curve A, Square-wave operation. Curve B, Pseudosine operation.
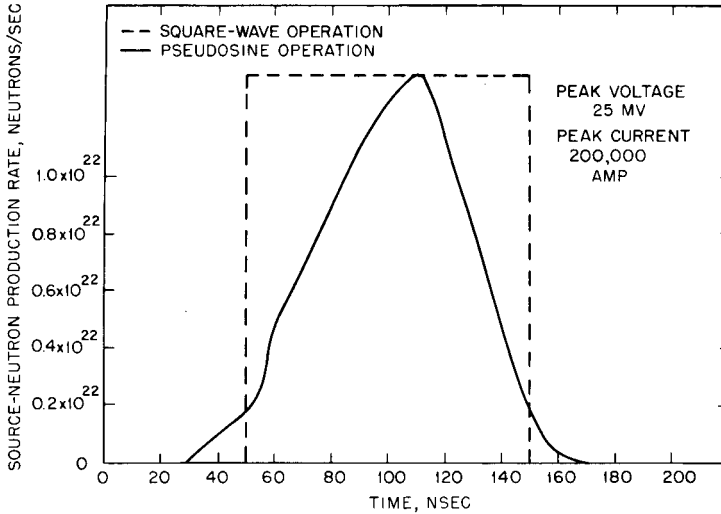
Fig. 5 — Time-dependent neutron production from ^{238}U target.

yield performance for a given system. Therefore, from the standpoint of neutron effectiveness and prompt multiplication, the diameter of the electron beam and the target dimensions must be kept small compared with the dimensions of the fuel assembly.

Materials problems will, however, dictate a lower limit on the beam diameter owing to the large amount of energy delivered in the electron pulse. For illustrating the conflict between the physics viewpoint and the materials viewpoint, consider a 3-in.-diameter, 200,000-amp, 25-Mv electron beam. For simplicity of discussion the beam pulse is assumed to be a square wave and to be of 100-nsec duration.

Such a beam diameter is very large from a physics point of view but results in an energy fluence of 11 kilojoules/cm^2 of beam area. If the beam were impinged directly on a uranium target, an energy deposition of approximately 150 cal/g would result near the surface of the uranium owing to electron ionization-collision losses alone, far in excess of the energy density required to melt the uranium.

Composite targets can be constructed which will absorb most of the beam energy in materials other than uranium or plutonium at a small sacrifice in neutron production. Consider a target consisting of a layer of some high-Z material, such as tungsten, a layer of some low-Z material, such as graphite, and a layer of uranium or plutonium, as illustrated in Fig. 6. The electron-beam incident on the tungsten
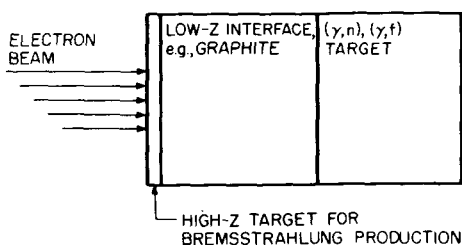
Fig. 6 — Composite target.

will produce bremsstrahlung radiation which is transmitted with little energy loss through the graphite to the uranium, thereby producing neutrons. The production of bremsstrahlung radiation, effective in producing neutrons, is a maximum for a tungsten thickness less than the maximum electron range; the purpose of the graphite is to prevent the electrons emerging from the tungsten from penetrating to the uranium. The thickness of the tungsten and graphite layers can be chosen to maximize neutron production with the restriction that no electrons penetrate to the uranium. If it is assumed that all the bremsstrahlung radiation produced in the tungsten by a 200-kamp, 25-Mev, 100-nsec square-wave pulse remains in a 3-in.-diameter beam, approximately 30 cal/g will be deposited at the front surface of the uranium as a result of bremsstrahlung heating. Even with the additional heating due to (γ,n), (γ,f), and (n,f) reactions, the temperature in natural or depleted uranium would remain below the melting point. The use of ^{235}U, ^{233}U, or ^{239}Pu would result in much higher temperatures because of the increased (n,f) contribution.

The use of composite targets, such as the one described in the preceding paragraph, would result in significantly lower energy depositions in the uranium or plutonium components of the target, but excessively high energy depositions would occur in the tungsten layer

of the target. Furthermore, the inertial stresses developed in all layers of the target by such rapid heating increase both the difficulty of maintaining the integrity of the target and of preventing damage to the fuel assembly. Segmentation of the target materials into small component pieces will result in a lowering of the dynamic stresses, but it is doubtful that target integrity can be maintained. In the likely event that one-shot target packages are selected for the EDNA program, the problem of containing heavy-metal vapors and fission products from the target and of preventing damage to the fuel assembly will remain a major concern.

The composite target given as an example is but one of many concepts to be explored. Other geometrical configurations (e.g., a target that is slanted with respect to the direction of the beam) offer not only the possibility of reducing the dynamic stresses that result but also of significantly lowering the energy deposition per unit mass of the target materials. Many materials, particularly the carbides, open the possibility of still further reduction in the temperatures of the target materials.

The development of the EDNA target package requires efforts in both theoretical and experimental programs. Existing computational models for electron transport and subsequent target heating are being improved. The techniques used for stress analysis in Sandia's fast burst reactor program are to be used for stress analysis of the target concepts. The results of these models form the basis for an experimental program using the existing Sandia flash X-ray devices and facilities outside Sandia Laboratories. The experimental program consists of an evaluation of various target concepts and materials from the standpoint of both neutron production and target integrity.

As part of the experimental program, Sandia recently conducted a series of experiments using the APFA facility. The purpose of these experiments was to determine the relative neutron production of various composite targets. The Linac provided a 200- to 400-mamp pulse of 17-Mev electrons. The beam was directed into a $3/4$-in.-diameter beam-entry cavity and impinged on a target package near the center of the multiplying assembly. For the experiment 17-Mev operation of the Linac was chosen because, at the time, it was thought that 17-Mv operation might be obtainable with Hermes II.

Figures 7 and 8 give the neutron production for target configurations similar to the composite target discussed previously in this section (Fig. 6). The results have been normalized to the production achieved by impinging the beam directly onto 235U. One inch of graphite was placed between the high-Z electron target and the uranium to ensure that no electrons capable of producing neutrons penetrated to the uranium. The results indicate that the composite targets studied were at least 20% less efficient in neutron production than a 235U (93%
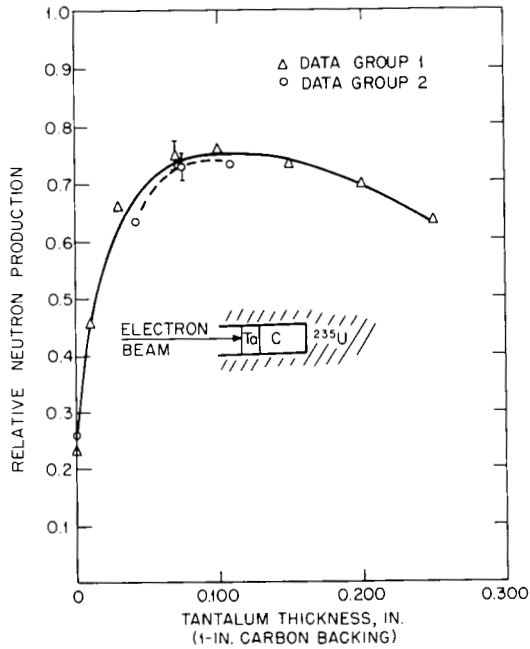
Fig. 7—Neutron production from composite target as function of the thickness of the high-Z layer. Values are normalized to production without tantalum or carbon.
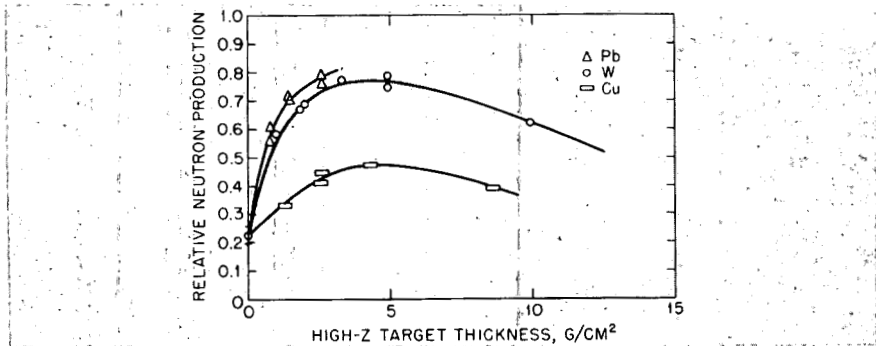
Fig. 8—Neutron production from composite target as function of tantalum thickness.

enriched) target. Similar results have been obtained using a mercury interface.[2]

Although it is reasonable to extrapolate the results obtained with 17-Mev electrons to the 25-Mev region of interest, future confirming experiments are planned.

FUEL ASSEMBLY DESIGN

General Considerations

The specific objective in the fuel-assembly design area is to pro-
duce a fuel system which (1) is compatible with the target design and
with the beam-transport requirements, (2) will withstand the rapid
temperature rise and dynamic stresses associated with the fission
density and rate required to meet the overall fluence requirements,
and (3) will (within the limitations imposed by the first two condi-
tions) produce in a small but usable irradiation cavity a total neutron
fluence of 10^{15} neutrons/cm^2 in a single pulse whose width at half-
maximum intensity is 1 μsec.

The total neutron yield of the fission pulse resulting from the sub-
prompt critical multiplication of an accelerator-pulsed source of
neutrons can be given to a good approximation by

$$Y_N = \gamma_s \, k \, M_p \int_0^{t_s} S(t) \, dt \tag{1}$$

where k = neutron reproduction number for finite geometry
M_p = prompt multiplication factor $[-1/k(1-\beta)-1]$
   γ_s = effectiveness of the source neutron in producing fissions
       relative to a normal mode distribution of neutrons produced
       by neutron-induced fission within the assembly
S(t) = time-dependent accelerator-induced neutron production rate
   β = effective fraction of all fission-produced neutrons that re-
       sulted from the decay of fission fragments
   t_s = duration of the accelerator-induced neutron pulse

Equation 1 is obtained using the one-energy-group space-independent
kinetic equations. The effect of delayed neutrons and reactivity feedback
have been ignored. The time-dependent behavior of the multiplied
neutron pulse depends on the time history of the accelerator-induced
neutron source; but, for source-duration times much less than that of
the multiplied pulse, the multiplied pulse width at half-maximum in-
tensity (hereafter referred to as half-width) can be approximated by

$$P.W. = \frac{t_s}{2} + M_p \, l \ln 2 \tag{2}$$

where l = prompt-neutron generation time and P.W. = pulse width.
Equation 2 is developed for a square-wave-source time behavior using
the one-energy-group space-independent kinetic equations. Again the
effects of the delayed neutrons and reactivity feedback are ignored.
The relation serves as a good approximation for other source-pulse
shapes, providing $t_s \ll$ pulse width.

Combining Eqs. 1 and 2 results in an approximate but useful relation between parameters pertinent in the design of the EDNA fuel assembly:

$$Y_N = \frac{\gamma_s k [P.W. - (t_s/2)]}{l \ln 2} \int_0^{t_s} S(t) \, dt \qquad (3)$$

The maximum neutron fluence that can be made available in the experiment cavity depends not only on the total neutron yield but also upon the geometrical configuration and the nuclear properties of the fuel assembly. For purposes of discussion, consider a bare homogeneous fast assembly, such as Lady Godiva[6] or Jezebel.[7] For a given time-integrated neutron-flux profile and a given neutron yield, the maximum neutron fluence available is inversely proportional to the product $\nu_f M_f \sigma_f$, where ν_f is the average number of prompt neutrons produced per fission, M_f is the mass of fissile material, and σ_f is the microscopic fission cross section of the fissile material. For a given neutron yield, the maximum neutron fluence available in the massive Super KUKLA[9] is less than that which would result from a similar but more compact system of higher enrichment.

Both the total neutron yield (for a given pulse half-width), by virtue of the prompt-neutron generation time of the assembly, and the maximum neutron fluence (for a given total neutron yield) are influenced by the size of the system. From a physics standpoint, the most desirable system for boosting is the smallest system. Three principal fissile materials, namely, ^{233}U, ^{235}U, and ^{239}Pu, are generally considered for booster applications. A few of the parameters governing the performance of three such bare homogeneous spherical systems are given in Table 1.

Table 1[6-8]

PARAMETERS FOR BARE HOMOGENEOUS SPHERICAL SYSTEMS

System	Critical mass, kg	Critical radius, cm	Prompt-neutron lifetime, nsec	$\dfrac{\overline{\nu \sigma_f}}{\overline{\nu_{25} \sigma_{f25}}}$	$\dfrac{\overline{\nu \sigma_f}}{\sigma_{f25}}$	
~93% ^{235}U	~53	8.72	~6	1.0	2.59*	1.0
^{239}Pu	~16	6.3	~3	1.68	3.07†	1.42*
^{233}U	~16	6.0	~3	1.70	2.72*	1.63*

*Godiva spectrum.
†Jezebel spectrum.

The ^{239}Pu and ^{233}U systems are far superior to a ^{235}U system with respect to the nuclear considerations alone, but, for a given neutron fluence, the ^{239}Pu and ^{233}U systems would experience much higher temperature rises. Furthermore, the alpha decay rate of ^{239}Pu and ^{233}U

constitute a potential health hazard that must be considered in the design of a working facility. The radiological health hazard associated with ^{233}U is further complicated by the activity buildup due to the presence of ^{232}U. Uranium-233, containing less than 1 ppm ^{232}U, is available, however. In view of the health problems associated with ^{239}Pu or ^{233}U and because of the greater amount of available information on ^{235}U systems, ^{235}U has been chosen as the principal fissile material for the initial design studies.

For examining the net effect of the design considerations in the following sections on the ultimate performance of a high-yield booster system, consider the performance characteristics of a solid 93%-enriched uranium system optimized for neutron fluence without regard to material limitations. Such a model serves as a reference for studying effects of various design considerations.

A ^{235}U assembly optimized for neutron fluence output, but ignoring material limitations, would be a solid sphere with negligibly small beam-entry and irradiation cavities. The performance characteristics of such an assembly driven by the EDNA generator are compared with existing APFA data in Table 2. The neutron-source production is

Table 2

PERFORMANCE CHARACTERISTICS FOR APFA AND EDNA GENERATORS

	APFA[10]	EDNA	EDNA
Peak electron energy, Mev	45	25	25
Voltage pulse shape	Square wave	Pseudosine	Square wave
Voltage pulse duration	4.5 μsec	100 nsec*	100 nsec
Peak electron current, amp	0.7	200,000	200,000
Electron-beam energy	142 joule	430 kilojoule	500 kilojoule
Neutron-source production	6×10^{11}	8.7×10^{14}	1.35×10^{15}
Source-neutron effectiveness	1.8	1.8	1.8
Neutron multiplication	1000	230	230
Fission pulse width, μsec	8	1	1
Fission yield, fissions	4.2×10^{14}	1.4×10^{17}	2.2×10^{17}
Peak neutron fluence, neutrons/cm^2	3.8×10^{12}	1.3×10^{15}	2×10^{15}

*Effective radiation pulse duration.

estimated for a ^{238}U target using MacGregor's calculated data, and a relative source-neutron effectiveness of 1.8 was chosen for all systems presented. Reactivity feedback was ignored, and the beam-entry and irradiation cavities were taken to be negligibly small. A prompt-neutron lifetime of 6×10^{-9} sec was used for the EDNA system.

It is important to emphasize that the performance characteristics stated for the EDNA concept in Table 2 are highly idealized and are not representative of a real system.

Thermomechanical Considerations

For providing a neutron fluence of 10^{15} neutrons/cm^2 in a single pulse, time-integrated fission densities comparable to those of high-yield fast burst reactors are required. For illustrating the severity of the stress problem associated with the EDNA design, an existing high-yield fast burst system, namely, SPR II, will be considered.

The Sandia Pulsed Reactor II is a Super Godiva fueled with 93%-enriched uranium alloyed with 10 wt.% molybdenum (see R. M. Jefferson, Session 2, Paper 3). Each of the six 1.3-in.-thick plates is an annulus with a $1\frac{1}{2}$-in. inner diameter and an 8.0-in. outer diameter. When fully assembled the 104-kg core forms a right-circular cylinder 8.0 in. in diameter and 8.2 in. high. An axial glory hole 1.5 in. in diameter defines an internal irradiation cavity in which a neutron fluence of 10^{15} neutrons/cm^2 may be produced in a single maximum-yield pulse.

The SPR II is operated in the superprompt critical mode; it delivers a neutron fluence of 10^{15} neutrons/cm^2 at the center of the glory hole in a 32-μsec half-width pulse. The fission yield for such a pulse is approximately 1.7×10^{17}, which produces a peak fuel temperature rise of 560°C. Without providing some form of stress relief, dynamic tensile stresses in excess of 160,000 psi are produced at the surface of the glory hole. Although this is far in excess of the static-yield strength at the corresponding temperature, the dynamic-yield strength is obviously not exceeded. A one-dimensional stress analysis indicates that a peak dynamic tensile stress in excess of 600,000 psi would result if SPR II were subjected to the same fission yield in a 1-μsec half-width pulse.

The EDNA fuel assembly will be subjected to comparable temperature rises but at rates approximately 30 times those for SPR II. The stress condition constitutes the major limitation in the fuel-assembly design. Subdivision of the fuel assembly into small components and the choice of proper fuel materials can result in considerably more favorable stress conditions but at a significant loss in nuclear performance. It is not sufficient merely to select a high-strength material; the material must be selected on the basis of a combination of such properties as the expansion coefficient, density, heat capacity, Poisson's ratio, modulus of elasticity, and the yield strength that will result in the most favorable stress conditions with minimum loss in nuclear performance. Complete information is available on only a few of the alloys of interest. The acquisition of additional data on other alloys is the basis of a fuel study now in progress.

Some knowledge of the behavior of U−10 wt.% Mo has been gained through the calculational and experimental studies of SPR II, and U−10 wt.% Mo has been used in the preliminary stress analysis of

the EDNA fuel assembly (see J. A. Reuscher, Session 1, Paper 3). To date two basic fuel component geometries have been investigated: small spheres and 10-in.-long rods of small diameters. Uniform heating was assumed for the spheres and for the radial dimension in the cylinders. An axial heating profile like that of the SPR II fuel was assumed for the cylinder. The calculations were performed using pulse profiles like those expected for the booster, if reactivity feedback is ignored (curve 1 in Fig. 9), and like that predicted by Fuch's model for super-prompt operation (curve 2 in Fig. 9). The components were assumed to be unconstrained by external materials. Some of the results are given in Figs. 10 and 11.
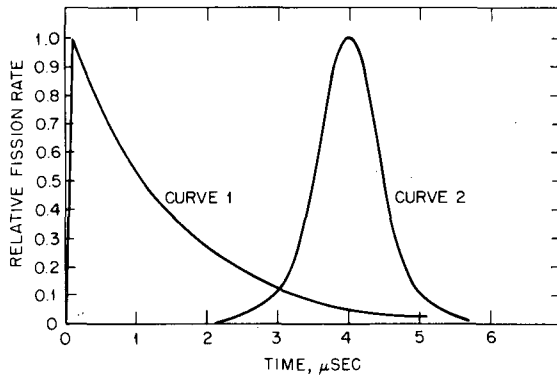
Fig. 9—*Fission rate as function of time. Curve 1, Expected booster pulse shape, (no reactivity feedback). Curve 2, Gaussian pulse shape.*
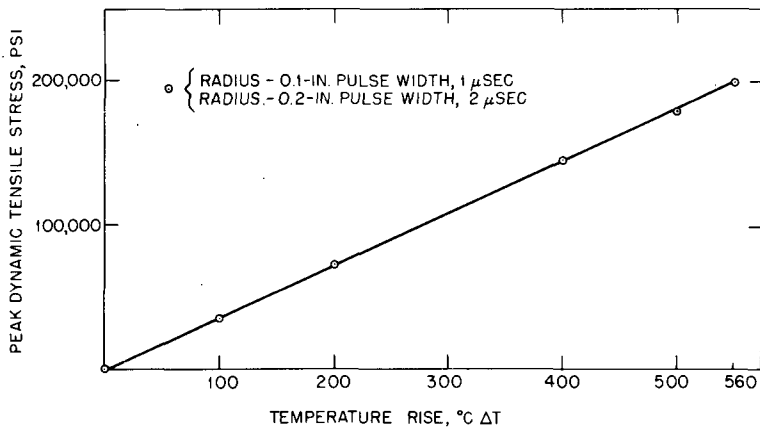
Fig. 10—*Peak dynamic tensile stress as function of temperature rise. Gaussian pulse shape, uniformly heated spheres of U—10 wt. % Mo.*
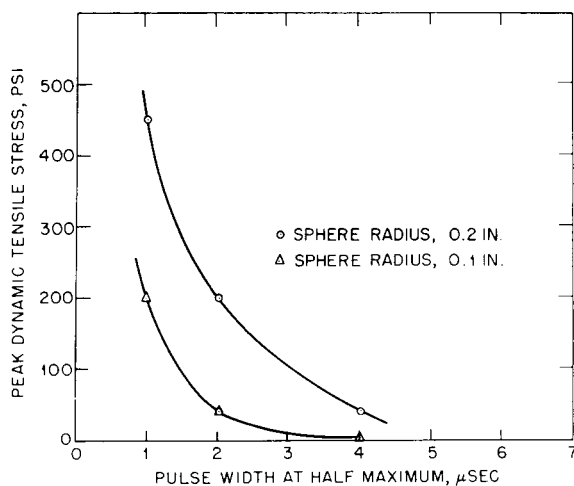
Fig. 11 — Peak dynamic tensile stress as function of pulse half-width. Gaussian pulse shape, $\Delta t = 560°C$; uniformly heated sphere of U−10 wt. % Mo.

The strong dependence of the peak dynamic tensile stress on the fuel component dimensions, the temperature rise, and the pulse duration is clearly evident. The results of other calculations indicate a significant dependence on the exact pulse profile. The peak dynamic stress for the expected booster profile was approximately 30% less than that for the Gaussian profile. On the basis of these preliminary results, spheres of diameter no greater than 0.25 in. and cylindrical rods with diameters less than 0.20 in. appear to be acceptable. As yet, no calculations have been performed for thin fuel plates. The results for other geometries suggest that very thin fuel plates (thickness ~0.100 in.) might be acceptable.

The segmentation required has a detrimental effect on most other phases of the design. The increased surface area imposed by segmentation increases the likelihood of corrosion and resultant alpha and fission-fragment contamination problems which could be severe if ^{233}U or ^{239}Pu are used. The use of a very thin protective coating and an inert-gas cooling system, such as that used for SPR II, appears mandatory. The increased surface area will, however, permit much more rapid cool down than is achievable with present fast burst reactors. The assembly of many small components will require a structural design unlike that of preceding fast burst systems; various concepts are now being studied.

The addition of diluents, such as molybdenum (to give better dynamic response), voids (produced by segmentation to reduce the stress levels), and cladding (to reduce corrosion and contamination), have a

detrimental effect on the nuclear performance of the system. Each addition effectively increases the size of the system, thereby increasing the effective prompt-neutron lifetime and lowering the maximum neutron fluence for a given neutron yield.

The introduction of voids by division of the fuel into small components results in a decrease in the effective density of the system. The critical size and the prompt-neutron lifetime of a bare homogeneous spherical uranium (enriched to 93% ^{235}U) system as a function of the effective density of the uranium is illustrated in Fig. 12. The
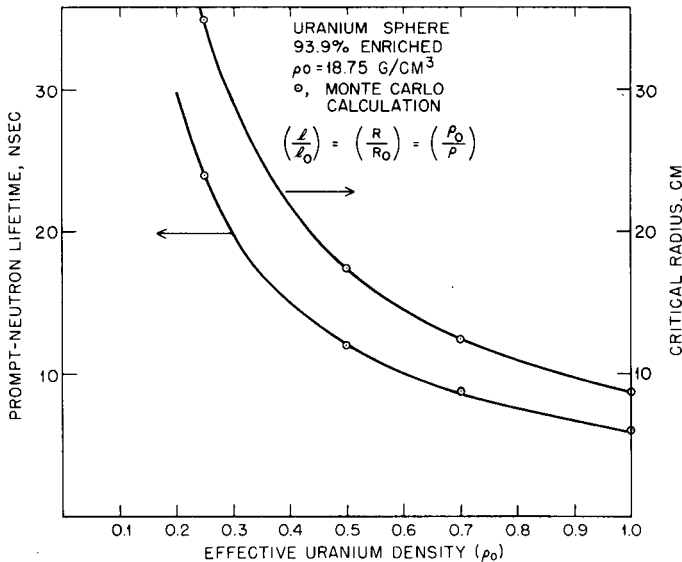
Fig. 12—*Critical radius and prompt-neutron lifetime as function of uranium density.*

circles represent the results of a 58-energy-group Monte Carlo calculation. Over the range of densities examined by Monte Carlo techniques, the critical radius and the prompt-neutron lifetime were found to be inversely proportional to the density of the system. It is of interest that this result is identical to that predicted by a simple one-energy-group diffusion-theory analysis.

The maximum packing fraction obtainable with uniform spheres is 0.74, which corresponds to a face-centered cubic structure. From Fig. 12 we see that reducing the density of a bare spherical 93.9%-enriched spherical system to $0.74\rho_0$ increases the critical radius from 8.72 to 11.8 cm and the prompt-neutron lifetime from 6 to 8.1 nsec. Using Eq. 3 and holding all other parameters constant, we see that such a change in the prompt-neutron lifetime would result in a 26%

loss in total neutron yield. A 0.905 packing fraction can be achieved with uniform-diameter rods; this would, according to Fig. 12, result in a minimum prompt-neutron lifetime of 6.6. The use of spheres or cylindrical rods of two different radii would result in increased packing fractions.

Fuel Assembly Configuration

The design of the EDNA fuel assembly must result in a small compact assembly with cavities for electron or gamma-radiation entry, for the neutron-producing target, and for experiment irradiation. In addition, the fuel assembly design must incorporate mechanisms for normal slow reactivity control and for fast-scram capability.

TARGET AND BEAM-ENTRY CONSIDERATIONS.   The size and depth of the beam (gamma or electron)-entry cavity required depends strongly on the beam—target concept employed for neutron production. In any event the incorporation of a beam-entry cavity in the design will result in a less than optimum fuel-assembly geometry. As part of Sandia's target study program, two basic beam—target schemes were investigated using the APFA. By varying the depth of the radial $3/4$-in.-diameter APFA beam-entry cavity, we could study the relative multiplied neutron production as a function of cavity depth. The 17-Mev electron beam was impinged on $235U$ at the end of the cavity. The results are shown in Fig. 13; they indicate that electrons impinging near the center of the assembly are approximately three times as efficient in overall neutron production as electrons applied to the outside surface. No allowance has been made for degradation of the electron beam as it is transmitted in air over the distances of concern.

The high forward peaking of the bremsstrahlung radiation suggests the possibility of placing a target outside the assembly and using the beam-entry cavity for transmission of the bremsstrahlung radiation to a point near the center of the assembly. Such a scheme would allow most of the electron-beam energy to be deposited in a material external to the fuel assembly. Again using the APFA facility, we investigated the effect of such a scheme; the results indicated that a 40% reduction in yield would result from placing the electron target at the outside surface rather than near the center of the assembly. This result is, of course, tied to the particular characteristics of the beam delivered to the APFA fuel assembly. It may be possible to increase the multiplied yield of the system by filling the cavity with a low-Z material. The low-Z material would have the effect of increasing the effectiveness of the gamma-produced neutrons and of decreasing the critical size of the fuel assembly. However, some loss will occur in the amount of bremsstrahlung radiation delivered to the uranium.

Furthermore, the addition of a large amount of low-atomic-mass material will certainly result in an increase in the effective prompt-neutron lifetime of the system. The net effect of such a target configuration will be determined in future experiments.

The interplay between the beam-entry cavity size, depth, and location and the source-neutron effectiveness is quite complicated.
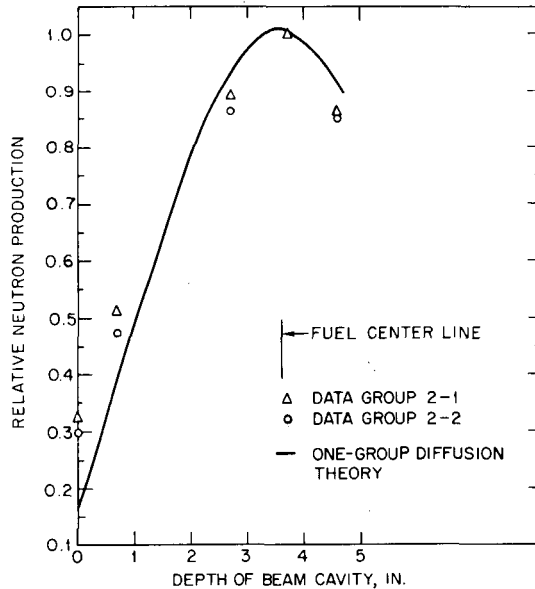
Fig. 13 — Relative neutron production as a function of beam-entry depth for APFA. No correction for gamma penetration.

Ideally, the neutrons would be produced at the center of a solid assembly by an electron beam traveling through an infinitesimally small beam-entry cavity. As the size of the beam-entry cavity and effective target surface area increase, the effectiveness of the neutrons decreases, owing to the increase in solid angle for leakage and the increase in the mean distance of neutron production from the center of the assembly. Furthermore, to provide a beam-entry cavity and non-fissile materials in the target, fuel material must be displaced. The critical size and prompt-neutron lifetime are then increased, resulting in an overall reduction in performance.

IRRADIATION CAVITY. The maximum neutron fluence in a bare fast metal assembly occurs near the center of the system. Removal of fuel material from this region to provide an irradiation cavity constitutes

a reactivity loss which, when adjusted for, results in a dispropor-
tionately larger addition of mass on the outside surface. Furthermore,
the larger and hence the more usable the irradiation cavity, the lower
will be the average neutron fluence in the cavity for a given peak neu-
tron fluence in the system. The net result of incorporating an irradia-
tion cavity at the point of maximum neutron fluence is an overall
reduction in total neutron yield and a corresponding reduction in the
neutron fluence for a given neutron yield. As the size of the cavity in-
creases, so does the degradation of the assembly performance. In
selecting the location and size of an irradiation cavity, one must also
consider the relative intensities of the bremsstrahlung and neutron
radiations. The SPR II can and will be used to study the effect of beam-
entry cavity size for cavity diameters up to 1.5 in. Limited neutron
effectiveness studies can also be performed using SPR II. These
experiments, though limited, will provide useful checks on calcula-
tional models.

REACTIVITY CONTROL.   For the provision of slow reactivity control
without an excessive number of control elements, schemes other than
those used in fast burst reactor design must be incorporated into the
fuel assembly design. Excessive stress levels would be produced in
solid fissile control rods, such as those used in SPR II (10 in. in length,
$7/8$ in. in diameter). For preserving the compactness of the system,
nonfissile materials should not be used internally. Indications are that
the best mechanism for control is nonmoderating reflecting materials
external to the main fuel assembly. Such reflectors, having a total
reactivity worth of a few dollars, would not result in a significant in-
crease in the effective prompt-neutron lifetime. Moderating materials,
however, could result in a significantly increased effective prompt-
neutron lifetime. Studies of various means of reflector control using
SPR II are now in progress.

SAFETY.   One aspect of booster operation which must not be over-
looked in striving to meet the design objectives is operational safety.
A fast burst reactor and a booster assembly have much in common:
they are both compact systems with rapid dynamic response to reac-
tivity changes. The operation of a fast burst reactor, however, re-
quires both high reactivity addition rates and a weak-source condition
just prior to the superprompt critical excursion. Booster operation
requires neither rapid reactivity additions nor a weak-source condi-
tion. Furthermore, the most desirable operational reactivity level
from a physics point of view is far below prompt critical. Even with
the added complexity of a high-voltage generator—fuel assembly com-
bination, the safety of a booster assembly can be assured to a degree
not possible with fast burst reactors.

CONCLUSIONS

No definite conclusions can be reached at this time as to the like-lihood of either failure or success in meeting the design objectives of the EDNA program. No single limitation of the target design or the fuel-assembly design studies constitutes a tragic reduction in system performance from that of the ideal system described previously. Collectively, however, the effect of beam-entry cavities, irradiation-cavity segmentation, diluent materials, and cladding can result in 50% or more less neutron fluence for a given pulse width and source pro-duction than that specified in the design objective. Even with such a reduction in the performance of the system, a neutron fluence of 10^{15} neutrons/cm^2 can still be attained through either an increase in the pulse width or an increase in performance of the high-voltage genera-tor. The final design of the EDNA fuel assembly will represent a com-promise between that which is desirable and that which is acceptable in each of the design areas. Studies in the target-fuel assembly design are far from completion. Many conceptual designs have yet to be stud-ied in detail, as have obvious assembly physics parameters, such as reactivity feedback.

The ability to develop and transmit a high-voltage beam specified for the EDNA program remains uncertain. Much work will be con-centrated in the area of the generator design and in beam-transport studies.

There is no doubt that, even if the EDNA program should fall short of the stated design objective, the information gathered in the design studies will extend the technology of single-burst neutron and fission-gamma sources far beyond that which presently exists.

ACKNOWLEDGMENT

REFERENCES

1. K. L. Crosbie and J. L. Russell, Jr., Hazards Summary for The Accelera-tor Pulsed Fast Assembly, USAEC Report GA-6078, General Atomic Div., General Dynamics Corp., February 1965.
2. M. J. Poole, The Harwell Neutron Project, *New Sci.*, 5(131): 1142 (May 21, 1959).
3. J. L. Russell, Jr. et al., Feasibility Study of the Accelerator Pulsed Fast Assembly, USAEC Report GA-4873, General Atomic Div., General Dynam-ics Corp., December 1963.
4. D. E. Groce, Feasibility Study of an Accelerator-Booster, Fast, Pulsed Research Reactor. Neutron Yield Studies, USAEC Report GA-8087, Gulf General Atomic, Inc., June 1967.

5. W. T. Link and D. H. Sloan, Pulsed Accelerator for Electron Beams, in *Record of the IEEE 9th Annual Symposium on Electron, Ion, and Laser Beam Technology, Berkeley,* May 9-11, 1967, R. F. W. Pease (Ed.), San Francisco Press, Inc., San Francisco, 1967.
6. R. E. Peterson and G. A. Newby, *Nucl. Sci. Eng.,* 1: 112-125 (1956).
7. G. A. Jarvis et al., Two Plutonium-Metal Critical Assemblies, *Nucl. Sci. Eng.,* 8: 525-531 (1960).
8. L. B. Engle et al., Reactivity Contributions of Various Materials in Topsy, Godiva, and Jezebel, *Nucl. Sci. Eng.,* 8: 543-569 (1960).
9. W. S. Gilbert, F. A. Kloverstrom, and F. Rienecker, Jr., Safety Analysis Report for the Super KUKLA Prompt Burst Reactor, USAEC Report UCRL-7695, University of California, 1964.
10. K. L. Crosbie, Gulf General Atomic, Inc., private communication, December 1968.

DISCUSSION

KRONENBERG: What do you expect the ratio to be between the gamma and the neutron dose outside of such a device as compared with a regular Godiva reactor?

COATS: I should think it would be roughly the same as we get now for a Godiva system — Godiva I or Godiva II.

KRONENBERG: Do you not believe that there is some contribution from the scattering of the incident beam in the reactor assembly which contributes to additional gamma radiation?

COATS: You are certainly going to have a contribution from the bremsstrahlung that is produced in the target. I believe, however, that by proper location of the irradiation cavity you can keep this to a minimum. The bremsstrahlung radiation produced in the target is highly directional. If you locate the irradiation cavity at some large angle to the direction of the electron beam and at such a distance to provide shielding by the reactor fuel, the contribution from the bremsstrahlung can be kept to tolerable values.

DONNERT: Have you considered going to electron energies higher than 25 Mev? It would appear on the surface that if you increase the electron beam energy you favor the energy fraction going to bremsstrahlung production; hence, if you dump the same total amount of energy you get more bremsstrahlung and less ionization and thus less heat to dissipate.

COATS: That is certainly a point that I cannot argue with you. If you go to higher voltages you will get a much more efficient transfer of the energy into neutrons. The 25 Mev is a bit arbitrary in the sense that a 25-Mev device was chosen simply because it appears reasonable to produce. If we could go for higher voltages with more assurance of success, I am sure that we would do it.

DONNERT: Do you think that it would work quite a bit better if you could just get to about 50 Mev?

COATS: I am sure that it would.

JOHNSON: Have you looked at what kind of penalties you would pay in terms of increased pulse width if you tried to increase the output just by increasing the multiplication of your assembly?

COATS: Certainly you can increase the multiplication and therefore increase the yield in the system. The one specified parameter that we are trying to hold to is the 1-μsec pulse width. We can, of course, get higher yields at a sacrifice in pulse width.

JOHNSON: What are the penalties in yield in doing this?

COATS: Suppose that we do have a fission yield that produces a neutron fluence of 10^{15}. Temperature rises on the order of $500°C$ will result. Uranium alloyed with 10 wt.% molybdenum has a melting point slightly above $1000°C$. If we doubled the yield of the system, we would be quite close to the melting point. This factor and stress considerations constitute the limitations in yield.

5-3 DISPOSABLE-CORE FAST BURST REACTORS

L. D. P. KING
Los Alamos Scientific Laboratory, Los Alamos, New Mexico

ABSTRACT

A possible means for producing very large fast-neutron bursts appears feasible through the use of a mobile fuel in an unconfined geometry. The fuel is dispersed by internal energy into a large cavity for reuse without damage to the main facility.

A study of such a potential system has been made using a design concept designated Liquid Excursion Pulsed Reactor (LEPR). Calculations and some preliminary experiments for such a system when using a uranyl sulfate fuel solution look promising. Burst intensities of 10^{19} to 10^{20} may be achievable with minimum pulse widths at half maximum of 35 μsec.

Two schematic designs of such a device are illustrated.

The attainment of the highest neutron burst intensities has always been associated with self-destructive excursions. Such excursions have been disruptive owing to the inability of the fuel materials to dissipate the energy released in the fission process with sufficient rapidity to prevent excessive thermal stresses.

On the other hand, the usefulness of such very high intensity sources, even though destructive, has been well documented. As part of the Los Alamos Rover Flight Safety Program, for example, it became desirable to establish the threshold for breakup of a number of different new fuel materials. All available burst facilities were used for these tests but always with negative results since the peak fluxes were too low. It was only in the SNAPTRAN 10A-3 excursion[1] and the Kiwi-TNT experiment[2] that sufficient neutron intensities became available. These were both deliberate destructive excursions.

The need for such very high neutron burst intensities initiated work at Los Alamos to explore the feasibility of making a repetitive

427

device that would permit higher peak fluxes through actual core dispersal during the burst, without facility destruction, however. Destruction of the fuel itself, in the sense of requiring complete refabrication, was arbitrarily excluded as too costly and too difficult operationally to be useful on any repetitive basis.

Fuels that might be applicable to a disposable and reusable core mode of operation include various types of mobile fuel particles or pellets, liquid metals, molten salts, uranyl phosphate, or one of the various types of aqueous fuel solutions.

Aqueous uranyl sulfate was chosen as the most suitable fuel for an initial study of the disposable-core mode of operation because of its large heat capacity and probable ease of dispersal and reassembly. Furthermore, considerable information on the chemical and nuclear properties of this fuel is known from the homogeneous reactor work at Los Alamos and Oak Ridge. Information is also available on the transient response characteristics of this fuel from the Kinetic Experiment on Water Boilers (KEWB)[3] and calculations[4] performed by Atomics International. Since the proposed operating conditions will be in a new regime of temperature and pressure, however, fuel stability limitations are not known without further experimentation.

Considerable information is also available about uranyl phosphate fuel.[5] Although this fuel has a high-temperature nuclear stability, it is less suited to very short pulses since the uranium solubility is relatively low. It has a higher viscosity, and it poses more difficult containment problems. Some calculations were made using this kind of fuel to investigate its nuclear potential for fast burst use.

LIQUID EXCURSION PULSED REACTOR CONCEPT

The idea of a disposable-core pulsed reactor using a liquid fuel led to the concept of the Liquid Excursion Pulsed Reactor (LEPR).[6]

The basic new feature of this concept is the creation of an environment in which a slug of unreflected liquid fuel finds itself in a highly supercritical nuclear condition while being physically unconfined. Immediately following the achievement of this situation, the liquid can be rapidly dispersed into a relatively large void region as a result of its internal heat energy. This void region acts as a containment shell for the fuel and for any heat-exchanger requirements. Inertial-pressure limitations are avoided owing to the geometry and very small fuel volume relative to the containment shell volume.

The following inherent advantages for such a system appear to remove previous peak-power limitations: (1) The size of the excursion is limited only by the excess reactivity available and the total heat

capacity of the fuel solution rather than by normal mechanical-strength considerations. (2) The large amount of heat energy generated by the pulse does not have to be extracted within the core but can be removed by an external system within the containment cavity. (3) The background intensity will be less than in any present fission-source system since the core region is completely dispersed by the fission pulse. This leads to a minimum delayed-neutron and gamma-ray activity and a maximum signal-to-noise ratio. (4) The device is repetitive even though the core region is dispersed. The repetition rate is determined by the time required to assemble another supercritical liquid-fuel geometry.

Data Required To Prove Concept

The following questions must be answered before proceeding confidently with this liquid-fuel concept. (1) Is a large energy generation possible in a fluid-fuel system that is not physically confined in a fixed geometry? (2) Can reactivity additions be made sufficiently large and rapid; and, are there any problems of preinitiation? (3) Does the fuel remain in a physical and chemical state following an excursion so that it may be reused in repetitive pulses? The answers to these questions will now be examined.

1. LARGE ENERGY GENERATION. Calculations at Los Alamos have shown that very large energy generations are possible in an unconfined and unreflected slug of liquid fuel if sufficient excess reactivity is made available.

Several neutronic calculations were first made on unreflected spherical and cylindrical geometries of interest to determine the variation of excess reactivity with fuel volume as well as the effect of the hydrogen-to-uranium concentration on the prompt-neutron lifetime.[7,8]

Calculations combining both the hydrodynamic and kinetic neutronic properties of the fuel in an unreflected spherical geometry were then made by means of the LASL Henre code.[9] Table 1 summarizes a few of the results from these latter computations. It is assumed that the excess reactivities shown can be made available instantaneously.

The first column of the table illustrates an example for a typical uranyl phosphate fuel using a nearly maximum uranium concentration. For supplying a suitable excess reactivity, the solution volume chosen was 60 liters. A large pulse is produced, but the pulse width is not as short as is desirable for some applications owing to the limited uranium solubility and hence relatively long prompt-neutron lifetime. Pulse widths at half maximum are probably limited to $\gtrsim 100\,\mu\mathrm{sec}$ for this fuel, even if larger excess reactivities were made available.

Table 1

SOME CHARACTERISTICS OF SPHERICAL UNREFLECTED LIQUID EXCURSIONS

Characteristic	Maximum molarity, uranyl phosphate	Low molarity, uranyl sulfate	Sulfate with excess reactivity of 31%	Sulfate ultimate energy release	Sulfate in a small system	Sulfate device for irradiation of large samples
Large central cavity	No	No	No	No	No	Yes
Uranyl fuel solutions	Phosphate	Sulfate	Sulfate	Sulfate	Sulfate	Sulfate
Uranium molarity	0.42	0.864	1.56	3.12	3.12	3.12
Fuel core radius, cm	24.3	19.45	24.3	24.3	18.45	22.86 to 32.5
Fuel volume, liters	60.0	30.8	60.0	60.0	26.3	94.4
Fuel density, g/cm^3	1.9	1.31	1.48	1.97	1.97	1.97
Reactivity	1.11	1.193	1.31	1.29	1.12	1.058
Hydrogen/uranium	145	128	69	34	34	34
Prompt-neutron lifetime, μsec	27	13	7	3.2	3.2	3.2
Energy release, Mw-sec	33	64	600	4100	116	400
Width at half maximum, μsec	1400	87	60	35	44	73
Period, μsec	243	50	22.7	10.9	26.1	41.7
Total neutron yield	1.4×10^{18}	2.5×10^{18}	2.3×10^{19}	1.4×10^{20}	4×10^{18}	1.4×10^{19}
Max. fuel pressure, psi	10^3	10^5	4.3×10^5	2.5×10^5	2×10^6	1.4×10^5
Max. fuel temp., °C	407	1595	6125	1875	39×10^3	1975
Max. fuel velocity, cm/sec	3×10^3	5.5×10^4	1.4×10^5	10^5	1.97×10^5	1.5×10^4

The second column is an example of an unreflected uranyl sulfate fuel volume of similar composition to that used in the KEWB experiments.[3] A 19% excess reactivity is made available, however, instead of the 3% used in these experiments. It is seen that a very respectable energy release is obtained in a relatively narrow pulse.

The third column indicates what happens with the sulfate fuel when the very large excess reactivity of 31% is made available. This is attained by increasing the fuel volume and the uranium concentration. The shortened prompt-neutron lifetime makes it possible to narrow the pulse further; the large excess reactivity permits a factor of 10 increase in the energy release.

The fourth column indicates about the ultimate which can be achieved neutronically in the sulfate fuel. The high uranium concentration used has maintained the available reactivity and further shortened the prompt-neutron lifetime. This has resulted in a Godiva-like pulse width with an enormous energy release.

The fifth column indicates what can be done with the high uranium concentration sulfate fuel when used in a small system with an easily achievable reactivity.

The last column in the table shows the results of a calculation for a device designed for the irradiation of large samples in an 18-in.-diameter central cavity. It is evident that with only a modest excess reactivity large narrow pulses are obtained. Very little heating of the cavity pressure shell was found. The peak fuel pressure does not exceed the elastic limit of modern high-strength steels.

Additional calculations were made with this cavity geometry to see what was neutronically possible. The use of 105 and 126 liters of fuel increased the available excess reactivity to 11% and 19%, respectively. The corresponding pulse periods and energy releases were found to be 30 μsec with 1400 Mw-sec and 18 μsec with 3900 Mw-sec. It therefore appears that cavity and noncavity geometries behave similarly neutronically. A considerably larger fuel volume and a different reactivity insertion arrangement may be required, however.

These computational results show that the answer to the first question concerned with the physical and neutronic feasibility of creating large-energy bursts by highly supercritical liquid-fuel geometries can be answered in the affirmative.

2. LARGE EXCESS REACTIVITY. It has been possible, either accidentally or deliberately, to produce large excess reactivities by the rapid removal of poisons from, and the rapid fuel additions to, a critical or nearly critical geometry. In particular, very rapid reflector poison removal rates have been achieved in several destructive excursions by special techniques. The SNAPTRAN 10A-3 excursion mentioned previously introduced $3.6 at an average rate of $400/sec by

means of a pyrotechnic actuator. The period was 0.65 msec with a pulse width at half maximum of about 2.2 msec. The total number of fissions was 1.2×10^{18}. Similarly, the Kiwi-TNT excursion[2] introduced $8.3 at an average rate of $210/sec by means of hydraulic actuators. The period here was 0.6 msec with a pulse width at half maximum of 1.8 msec and a total energy release of 3.1×10^{20} fissions. Reactivity additions of this type are not expected to be destructive in a LEPR-type system since in this system the liquid-fuel core is free to disperse for later reassembly. The KEWB experiments removed $5 of central poison at an average rate of 290 $/sec. The minimum period was 0.57 msec.

Another technique for obtaining large excess reactivities was suggested by experiments concerned with the ejection of H_2O from cylindrical containers. The experiments showed that velocities of 7.5 cm/sec can be achieved in a 30-cm-diameter slug with a fairly simple pneumatic device. Higher velocities can undoubtedly be achieved by more advanced hydraulic or explosive techniques. Such experiments indicate that it will be possible to produce highly supercritical and unconfined slugs of liquid fuel by either projecting the fuel from a region held subcritical by poisons and geometry or by the rapid simultaneous removal of poisons and fuel restraints.

Other methods for achieving large excess reactivities with liquid fuels have been suggested which do not require the removal of poisons. One such scheme proposes to project two subcritical liquid-fuel slugs at each other within a large cavity.[10] Supercriticality is attained on impact of the two masses. An alternative method, which avoids direct impact and optimizes the geometry, is to make one of the fuel slugs in the form of a cylindrical annulus and the second slug a smaller cylinder which can just pass through the annulus. Maximum supercriticality is achieved as the two fuel samples are passing each other.

The second question on the feasibility of providing sufficient excess reactivity to an unconfined fuel slug to produce a large nuclear burst can also be answered in the affirmative.

3. FUEL STABILITY.   The third question requiring an affirmative answer to make the LEPR concept possible is whether the uranyl sulfate fuel maintains its chemical and physical properties to permit reuse. Experimental data from the KEWB experiments[3] indicate that peak burst powers up to about 170 Mw/liter and fuel and energy densities of about 580 kw/sec/liter do not lead to fuel degradation when suitable additives are used in the fuel. The observed temperature rise and maximum pressure for such peak-power conditions were found to be only 88°C and 317 psi, respectively.

Laboratory measurements on the other hand indicate that over an order of magnitude less energy density is permissible if there is to be

no risk of UO_4 precipitation in the fuel. This is based on room-temperature measurements of the solubilities of hydrogen peroxide in the fuel.[11]

The cause of this large discrepancy is unknown. Presumably, the rapid dynamic energy source of a pulse is not directly comparable to a static laboratory measurement. The pulse nature of the energy release, furthermore, permits a long rest period for back reactions to reduce the peroxide concentration.

The energy-density conditions shown in Table 1 are also one to two orders of magnitude higher than have been experimentally used, and therefore there is considerable uncertainty as to fuel stability. Work at Oak Ridge, however, showed that high temperature produces rapid thermal decomposition of H_2O_2. High pressures may also be beneficial. The pulse conditions of Table 1 will produce very high-temperature and internal-pressure conditions precisely at the time of maximum energy release.

Meaningful measurements concerning fuel stability and energy-density limitations can only be made if the fuel is subjected to similar conditions to those existing in a nuclear burst. The combination of high temperature, pressure, and fission density is difficult to achieve experimentally except in an actual fissioning test device. Some measurements that simulate energy deposition rates similar to those in a LEPR device have been achieved, however, by means of a laser.[12] A laser pulse was used to completely vaporize a small fuel sample in a quartz container. It was estimated that the microliter fuel sample absorbed 4 to 6 joules and reached a maximum temperature of about 1800°C and a pressure of 1200 psi. The condensed solution was centrifuged back to its original configuration; no change in the solution was detectable.

It is evident that at the present time one cannot give a completely affirmative answer to the question of solution stability at the highest proposed LEPR operating conditions. Present indications are promising, however. Further experimental work is required to establish the power-density limitations for this type, or other possible, mobile fuel. Critical experiments of the Kinetic Intense Neutron Generator reactor[13] in progress at LASL may be able to supply additional information on the stability of uranyl sulfate type fuel.

Neutron-Source Considerations

The kind of neutron source that is acceptable in a fast burst liquid reactor can be visualized by considering the time t for the occurrence of the burst (composed of two parts, $t_i + t_0$) and the time $\Delta k/a$ required for reactivity insertion, where t_i is the mean initiation time, sec; t_0 is time from burst initiation to peak power, sec; a is reactivity ramp rate, \$/sec; and Δk is total reactivity available, \$.

An unacceptable condition for pulse size arises if the neutron source is of such a magnitude that pulse initiation occurs during the ramp ($\Delta k/a > t_i$) since the yield can then fluctuate orders of magnitude.

An acceptable situation for reproducibility in pulse intensity, but not necessarily for reproducible timing of the peak pulse, arises if $t_i + t_0 \gg \Delta k/a$. This means the source is either so weak that all the reactivity can be inserted before disassembly will occur or, alternatively, the reactivity insertion is so rapid the existing background source does not prevent full reactivity insertion before disassembly.

An acceptable situation for reproducibility in both the time of peak power and yield can be produced by means of a pulsed source with a low fuel background, i.e., the background must be low enough to avoid preinitiation and the pulsed source must be designed to give initiation at the optimum position of the fuel slug.

Some inherent-neutron-background measurements have been made on a potential LEPR uranyl sulfate solution with a 3.12 uranium molarity. Principal neutron backgrounds in such a solution are produced by (α,n) reactions on the oxygen isotopes ^{17}O and ^{18}O and by (γ,n) reactions due to delayed fission-product gamma rays.

Measurements were made[14] to determine the inherent neutron background in uranyl sulfate fuel solutions. In one experiment a normal oxygen composition in the water was used, and in another the ^{17}O and ^{18}O isotopes were depleted. These results indicated that this inherent background is primarily due to the ^{18}O since a depletion factor of about a factor of 10 in this isotope reduced the background neutron count by the same factor. Greater depletion factors can be achieved, if necessary, by an established isotope separation method. The neutron contribution from ^{17}O relative to ^{18}O for the 4.33 average alpha energy from ^{235}U is known to be only about 8.5% in normal water.[15]

Any solution that is reused shortly after an excursion can have a relatively large delayed-gamma-ray background from the fission products, and hence it has the potential for producing neutrons by (γ,n) reactions with beryllium or deuterium. In a LEPR-type pulsed reactor, no reflector is used, and other structural materials are not present in the core; so, no sources of beryllium should be present. Any deuterium present in the fuel solution, however, can produce an appreciable neutron background that will vary with the running history of the solution. Measurements indicate the total neutron release in pure heavy water from this source to be 16% of that of the delayed neutrons but with periods ranging from 2.5 sec to 53 hr.[16] These background neutrons have substantially longer periods than the normal delayed neutrons and can therefore be a problem in the pulse initiation of a repetitive-burst device that reuses its fuel.

Fortunately, this source of neutrons can be decreased many orders of magnitude by reducing the normal 150 ppm of heavy water by the

usual separation methods. A fuel solution using as its hydrogen source the distillate from liquid hydrogen would essentially completely remove this source of neutrons by eliminating deuterium from the fuel.[17]

It would therefore appear that sources of neutron background can be adequately reduced to avoid any preinitiation problems in a LEPR burst facility.

Reactor Configurations

Two possible LEPR configurations have been considered: (1) a minimum-core-size arrangement of interest primarily as a strong neutron source for external applications and (2) a design for the irradiation of large samples in the peak internal flux.

Figures 1 and 2 illustrate schematically the minimum size and the type of configuration used in the calculations of Table 1. A hydraulically actuated piston (9) rigidly connected to a fuel piston (1) by means of a shaft (12) is used to project a slug of liquid fuel (2) from the subcritical geometry of Fig. 1 to the highly supercritical position shown in Fig. 2. The fuel in Fig. 1 is maintained subcritical by a central poison rod (3) and poison vanes (4). In the up position the fuel piston projects into a large cavity (16) so that the cavity gas can have easy access to the piston fuel interface to aid in the release of the fuel slug. As the fuel leaves the piston, the poison rod and vanes exert less and less effect so the fuel slug abruptly becomes highly supercritical. At this point a pulsed-neutron source initiates a rapid excursion. The energy of the excursion disrupts the fuel slug by vaporizing its center. Fuel is thrown outward against the water-cooled containment walls (17) of the cavity. The fuel then runs by gravity into a fuel reservoir, which is not shown, for later reuse. A small radiation and neutron glory hole (25) is aligned with the poison rod (3) so that the fuel-slug geometry can be maintained in its upward travel. A pressurized inert gas is used to prevent any fuel loss through the hydraulic seal (23). A typical hydraulic actuating system, shown in the lower portion of Figs. 1 and 2, is used to propel the fuel slug to a high velocity. For achieving high piston velocities ($\sim$250 ft/sec), a high-pressure sump pump is used to supply hydraulic fluid to multiple accumulators and large headers. The upward velocity of the piston system is brought to a controlled stop by the tapered upper surfaces (14) of the hydraulic cylinder (15) and piston (9).

The second configuration is shown in Fig. 3. A somewhat different arrangement is used to permit the presence of a large central irradiation facility. The liquid fuel fills an open-ended cylinder (2) placed on a pedestal (3). Fuel leakage out the bottom is prevented by the sliding seal (9). The containment shell (2) can be jerked off vertically, along with the internal poison sleeve (7), by a rod (8) connected to a hydraulic
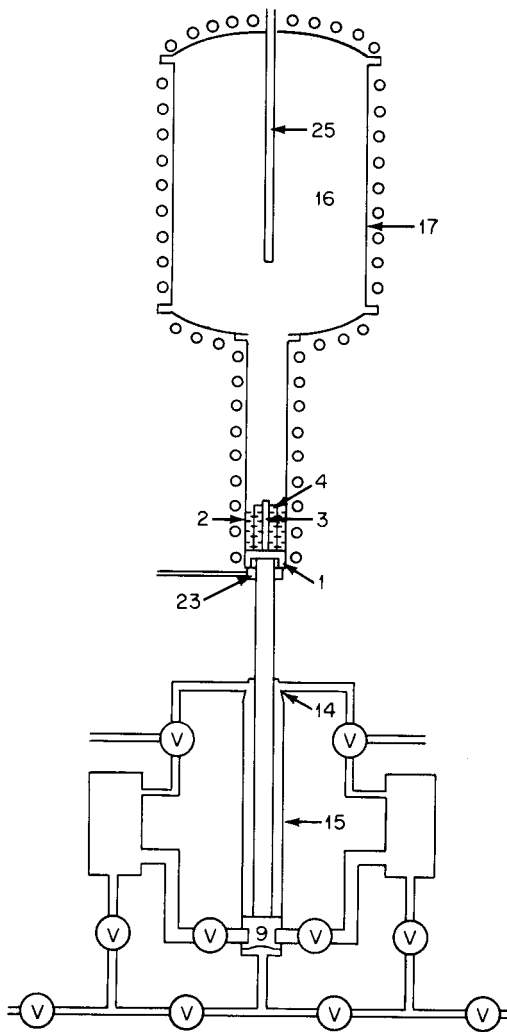
Fig. 1 — Cross section of subcritical configuration of minimum-core-size LEPR.

1, Fuel piston.
2, Slug of liquid fuel.
3, Central poison rod.
4, Poison vanes.
9, Hydraulically actuated piston.
12, Connecting shaft.
14, Hydraulic cylinder,
    tapered upper surfaces.

15, Hydraulic cylinder.
16, Large cavity.
17, Water-cooled
    containment walls.
23, Hydraulic seal.
25, Glory hole.

Fig. 2—Cross section of supercritical configuration of minimum-core-size
LEPR.
1, Fuel piston.
2, Slug of liquid fuel.
3, Central poison rod.
4, Poison vanes.
9, Hydraulically actuated piston.
12, Connecting shaft.
14, Hydraulic cylinder,
    tapered upper surfaces.

15, Hydraulic cylinder.
16, Large cavity.
17, Water-cooled containment walls.
23, Hydraulic seal.
25, Glory hole.

Fig. 3—Cross section of LEPR configuration for the irradiation of large samples in the peak internal flux.

1, Liquid-fuel level.   7, Neutron poison sleeve.
2, Fuel-containment shell.   8, To jerk mechanism.
3, Main support pedestal.   9, Sliding seal.
4, Stationary fuel-pressure shell.   10, Fuel fill tube.
5, Sample-irradiation space.   11, Free-run extension.
6, Sample-support cylinder.   12, Outer-containment shell.

or explosive actuator placed above the view in the figure. The stationary pressure shell (4) provides an inner fuel boundary as well as providing the containment shell for the irradiation cavity (5). Samples for irradiation can be inserted and removed by means of a movable piston (6) made of graphite or other neutronically suitable material. Fuel solution can be added to the core region through a fill pipe (10).

The fuel containment cylinder and poison sleeve are made longer (11) than the fuel region to permit a free-run time in the actuator. In

this manner a high velocity can be achieved before fuel confinement and poison removal takes place. After removal of the poison sleeve and fuel cylinder, the fuel is in a supercritical unconfined geometry. If a neutron pulse now initiates the system, fuel will be dispersed outward by the fission heating of the fuel against the water-cooled walls of the large containment vessel. The fuel is collected in a reservoir, not shown in the figure, for later reuse.

CONCLUSIONS

Present nuclear burst yields are limited by stress limitations imposed on core materials. It appears that these limitations can be circumvented by the use of mobile fuels in novel core designs. The heat capacity of the fuel is sufficient to absorb the desired energy yield. The fuel can be harmlessly dispersed by internal energy from the core region into a heat-exchanger region. Liquid fuels seem particularly suitable. The fuel core can be reconstituted for reuse. The lack of a high repetition rate is not thought detrimental owing to the magnitude of the potential burst yields (10^{19} to 10^{20} fissions).

ACKNOWLEDGMENTS

REFERENCES

1. W. E. Kessler, O. L. Cordes, G. A. Dinneen, R. D. Fletcher, and G. F. Brockett, SNAPTRAN 2/10A-3 Destructive Test Results, USAEC Report IDO-17019, Phillips Petroleum Company, January 1965.
2. L. D. P. King, D. Ackworth, W. V. Geer, C. A. Fenstermacher, B. W. Washburn, and J. F. Weinbrecht, Description of the Kiwi-TNT Excursion and Related Excursions, USAEC Report LA-3350, Los Alamos Scientific Laboratory, July 1966. (Classified).
3. M. S. Dunenfeld and R. K. Stitt, Summary Review of the Kinetics Experiments on Water Boilers, USAEC Report NAA-SR-7087, Atomics International, Feb. 1, 1963.
4. M. Silverberg, P. Speigler, and R. Cordy, An Advanced Solution Pulsed Reactor, *Trans. Amer. Nucl. Soc.*, 7(2): 497-498 (November 1964).
5. B. J. Thamer et al., The Properties of Phosphoric Acid Solutions of Uranium as Fuels for Homogeneous Reactors, USAEC Report LA-2043, Los Alamos Scientific Laboratory, March 1956.
6. L. D. P. King, Program Status Report, Weapons Research and Development. Part I. July to September 1967, pp. 23-27, USAEC Report DIR-2103, Los Alamos Scientific Laboratory, 1967.
7. M. E. Battat, internal LASL memos, June and August 1967.
8. W. R. Stratton and L. B. Engle, Neutronic Calculations Apropos the Pulsed Solution Reactor, internal LASL memo N-2-8118, May 1967.
9. R. J. Lazarus, internal LASL memos, March to November 1967.

10. W. R. Stratton, internal LASL memo N-2-8117, August 1966.
11. B. J. Thamer, internal LASL K Division report, June 1968.
12. B. J. Thamer, The Laser Testing of a Fluid Hydrogeneous Fuel, internal LASL K Division report K-2-4367.
13. L. D. P. King, Liquid Jet Super Flux Reactor, USAEC Report LADC-9413, Los Alamos Scientific Laboratory, 1967. (This reactor was renamed Kinetic Intense Neutron Generator Reactor or KING Reactor.)
14. E. H. Plassman and A. L. Connor, Neutron Counting of an Enriched UO_2SO_4 Solution That Is Low in ^{18}O, internal LASL report W-7-68-611, August 1968.
15. L. F. Hansen et al., The (α,n) Cross Sections on ^{17}O and ^{18}O Between 5 and 12.5 MeV, *Nucl. Phys.*, *A*, 98: 25-32 (1967).
16. S. Bernstein et al., Yield of Photo-Neutrons from Heavy Water, *Phys. Rev.*, 71: 573 (1947).
17. E. S. Robinson, Los Alamos Scientific Laboratory, private communication.

DISCUSSION

HETRICK: One of the surprises we found in the KEWB experiment was that the shorter the period, the more efficient the shutdown from radiolytic gas bubbles. Maybe you could improve the performance of your system by starting out with a highly pressurized system.

KING: One of the ideas of the LEPR concept is that you reduce the high pressures normally produced in a large burst system; you let the fluid create its own internal high pressures, but you do not need a high-pressure containment system. The only high-pressure requirements were in the design with the large internal cavity where we would need something that would take an external pressure when the fuel is dispersed radially outwards.

HETRICK: Let me ask if your excursion calculations included a model of the radiolytic gas effect.

KING: The gas bubbles were not included, but almost everything else was. The equation of state of the fuel was combined with the known neutronic properties in the calculations.

HETRICK: Marvin Dunenfeld derived a model in 1960 which matched very well the empirical observations. The gas became very efficient as a shutdown mechanism around a 1-msec period; I wonder if that might be a severe limitation on the yield that you want. You might be overestimating the yield by an appreciable amount.

KING: The gas bubbles you refer to can play only a very minor role since an appreciable portion of the fuel is vaporized during the fission pulse. Vapor pressure provides the major disassembly force. It turns out that the inertial forces in the very short pulses, which you saw went down to a 35-μsec pulse width at half maximum, are apparently sufficient to prevent disassembly until a very large internal energy has been released. Initially the worry was, of course, whether this could be done.

SHAFTMAN: What about some newer version of the famous old King Push—Pull to do your reassembly?

KING: This is a possibility, of course, but I do not believe it is suitable for the very large bursts shown in the table. I think if you want to get extremely short pulses in an aqueous solution, you need very large excess k's, which must be put in very rapidly, and the LEPR method is superior to any other I know. I did not mention that there are several exotic ways of greatly increasing the rate of reactivity addition without the requirement of poison removal. This can be done by shooting two slugs of liquid at each other. When one projects a slug of liquid rapidly enough, it looks like a piece of ice and maintains its geometry completely for a short time. You can use an annular cylinder as one part of the assembly, and project it at a solid cylinder that forms the center portion of the assembly. A maximum reactivity is attained when these two parts try to pass each other. This is certainly feasible in liquid systems, and dispersal would take place very much as I have indicated.

SHAFTMAN: I am thinking of a situation such as an ejection of a solid absorber from your one system. This initiates the pulse, kicks the fluid out, and goes into another system that looks very much like the first with the solid absorber.

KING: You have the high-pressure problem here of containment, which I have tried to avoid in this concept and I believe must be avoided in very large bursts. Pressures were already beginning to be the limitation in the KEWB experiments. The lack of confinement permits the partially vaporized fuel to expand freely into a larger cavity, which is advantageous for two reasons: first, it reduces the pressures in the containment cavity to reasonable values, and, second, it disperses the fission products, and, as I indicated, this will result in a greatly increased signal-to-noise ratio.

BRUNSON: Have you considered using deuterium instead of hydrogen in this to achieve a higher spectrum and a shorter lifetime?

KING: I think the deuterium would be very detrimental in that it would create preinitiation problems of the type encountered in the Molten Salt Burst Reactor described in the first paper of this session. We can avoid all preinitiation problems in the aqueous solution by making the water for the fuel from liquid hydrogen, which has no deuterium I am told. This would eliminate the $(\gamma-n)$ background produced by fission products. Any $(\alpha-n)$ background inherent in the fuel can be removed, if necessary, by using oxygen depleted in ^{18}O.

5-4 MAXIMUM BURST YIELDS FROM COATED-PARTICLE REACTORS

F. T. ADLER
Physics Department, University of Illinois
Urbana, Illinois

ABSTRACT

In view of the performance of coated-particle fuels (uranium carbide coated by pyrocarbon and imbedded in a graphite matrix) in various reactor systems, it appears of interest to consider qualitatively the ultimate potential of such fuels in terms of attainable burst widths and maximum energy depositions. Limitations inherent in the characteristics of the pyrocarbon shell are discussed.

INTRODUCTION

Fuel bodies that contain the fissile material as small particles have been used or considered for various reactor systems. Coated-particle fuels [uranium oxide or carbide coated by pyrocarbon (PyC) layers and imbedded in a solid graphite matrix] have shown great strength in destructive testing;[1,2] thus a qualitative investigation of the potential and the limitations of such fuels for burst reactor applications appears to be of interest.

By correlating some of the experimental data,[1,2] thresholds for the energy deposition rate have been deduced[1] at which damage to the coating is likely to occur for a given pulse length and a prescribed geometric configuration, i.e., radius of fuel core, thickness of PyC layer, and volume fraction of particles in the matrix. These thresholds agree qualitatively with values obtained by analyzing the effects of reactivity excursions[3] on coated fuel particles in terms of simple models that account for the competing effects of the energy deposition rate, of the pulse lengths, and of the stresses induced by thermal expansion and by temperature gradients in the PyC shells. The results of

443

this analysis and the available experimental information[1] will be used to estimate the order of magnitude of bursts and of the burst widths potentially attainable with coated-particle fuel bodies containing uranium carbide cores coated by representative PyC coatings.

The potential capability of such fuels for burst reactor applications may perhaps first be gauged by considering some of the relevant parameters of existing or proposed reactor systems. Table 1 summarizes representative performance parameters of several operating or proposed burst reactors, together with pulse characteristics in large excursions achieved in destruct-type experiments.

Pulse width, repetition rate, and maximum power attainable in a burst may be considered the prime performance criteria for a pulsed reactor. It is obvious that a reactor core incorporating a substantial amount of graphite, e.g., a Kiwi-TNT-type core, provides a much wider pulse than those attainable with fast assemblies where the burst widths may be in the microsecond range, or, with accelerator pulsing, even in the nanosecond range (see R. G. Fluharty, Session 3, Paper 3). On the other hand, the large heat capacity of graphite fuel bodies makes a very large energy deposition, and therefore a high peak power, feasible. In this respect, however, the energy depositions attainable during a burst will be smaller than those anticipated for the disposable-core fast burst reactors like the LEPR (see L. D. P. King, Session 5, Paper 3).

Thus, it is apparent that a solid reactor core consisting of coated fuel particles will not reach the capabilities envisaged for other systems. On the other hand, the coated-particle fuel body may present advantages when compared, for example, with existing homogeneous reactors of an improved TREAT type. Better fuel and fission-product containment at high operating temperatures may be a possible advantage. A more relevant advantage of the coated-particle fuel bodies may arise from the much narrower pulse width and from the harder spectrum that apparently could be obtained. Pulse widths between 0.5 and 1 msec appear possible; the flux spectra may have a very small thermal and low epithermal component, in contrast with the TREAT-type reactors which are basically thermal reactors.

Both aspects could be important for fuel-testing applications and possibly also for investigation of the propagation of failure in fuel-element assemblies.

MECHANISM OF FUEL BREAKUP PROCESSES

It has been observed that for comparable excursions a fuel matrix containing coated oxide particles can be fragmented; however, a similar matrix containing coated carbide particles remains intact,

Table 1

COMPARISON OF REPRESENTATIVE BURST REACTOR PERFORMANCES

Device	Peak power, Mw	Total energy deposition, Mw-sec	Pulse width, msec	Shortest period, msec	Repetition rate	Δk, %
KEWB	4000	7	1 to 3	0.57	1/hr	3.0
TREAT	6000	1000	150	40	2/day	3.25
TRIGA F	1200	20	10.0	3.0	12/hr	2.4
Godiva II	1.5×10^4	0.26	35 μsec			
Super KUKLA	$\sim 10^5$	100	0.7		3/day	
PBF	3.5×10^5	2000	1.0	1.0	2/day	4.0
RPTF	300	3.0	5 μsec		20 to 200/sec	
SPERT	2400	33		3.3	Destruct	
SNAPTRAN-3	1.37×10^4	40	2.2	0.65	Destruct	3.0
Kiwi-TNT	3.3×10^6	10000	2.5	0.6	Destruct	6.2

showing only such microscopic changes as partial dissolution of the shell surrounding the individual particles or migration of the material forming the particle into the shell, although sufficient heat is developed in some excursions to allow the fuel particle to melt and, potentially, to vaporize.

The breakup of the fuel bodies containing PyC-coated uranium oxide particles can be understood qualitatively as follows: during the initial stage of the reactivity excursion, the fuel particles melt; at high ambient temperature, which may well exceed 2500°C, the oxide reacts with the surrounding carbon to form CO or CO_2. Since these gases are not absorbed, a great pressure rise occurs that may rupture the particles and eventually fragment the graphite matrix. In this event, the response of the fuel body to the excursion is dominated by the formation of gases and vapors which produce the mechanical stresses that are responsible for the breakup process.

For uranium carbide particles, a more intricate interplay between heat transfer and thermomechanical processes occurs; this interplay depends on the physical characteristics of the PyC shell. As long as the shell is intact, heat losses to the matrix are small because of the low conductivity, $k_\perp$, in the crystallographic c-direction, which corresponds to the radial direction in the PyC shell of carbide particles tested.[1] During the initial stage of a reactivity excursion, the temperature in the uranium carbide core of a coated particle therefore increases rapidly. At the same time, the graphite matrix outside the PyC shell remains near its initial temperature. This condition leads to the expansion of the uranium carbide core relative to the shell, which may then be affected by strong hydrostatic pressures as well as thermal stresses arising from the large temperature difference between the uranium carbide core inside and the graphite matrix outside the shell. If the resulting stresses in the shell are sufficiently large, it will crack, and some uranium carbide will enter these cracks when the uranium carbide liquefies. At this stage, however, the heat-transfer characteristics change radically: the uranium carbide is now in contact with a good conductor (the heat conductivity $k_\parallel$, in the crystallographic a-direction, i.e., the tangential direction in the PyC shell, being much larger than $k_\perp$ by perhaps two orders of magnitude), and the uranium carbide loses heat rapidly. Therefore the further pressure buildup in the uranium carbide core is delayed, and matrix damage only occurs if sufficient energy is available to heat not only the uranium carbide sufficiently to create a sizeable vapor pressure but also all the PyC beyond the melting point of the uranium carbide.

It appears therefore that for fuel bodies containing carbide particles the pressure buildup, and thus the effects of an excursion on the coated particles and on the fuel matrix, depends directly on the local changes of the temperature profile in the core and the shell during the

reactivity pulse and on the resulting thermomechanical effects. The temperature profile, in turn, is determined by the combined effects of the rate of energy deposition by fission in the uranium carbide, by the rate of conductive heat losses through the shell, and by the energy absorbed in the phase changes at the moving-phase boundaries. At high temperatures, radiative losses may also become relevant. Because the response of the particles depends on the details of the heat transfer, the response also is strongly affected by irregularities of particle size or shape due to fabrication and the effects of irregular spacing of particles in the graphite matrix. It is therefore necessary to consider idealized simple models for the response of the carbide particles to obtain a qualitative insight into the role of the relevant physical and geometric parameters: specific heat, heat of fusion, coefficient of linear expansion, coefficients of heat conductivity, radius of uranium carbide core, thickness of the shell, and fuel loading of the matrix.

The interplay between these parameters, their experimental uncertainties, and their influence on the energy balance and heat conduction, as well as thermomechanical effects, has been described elsewhere;[3] threshold values for the different phases of the breakup process (melting of fuel core, cracking of PyC shell, and matrix damage) have also been obtained which agree with the experimental data.[1]

The principal results of these considerations are:

1. A large reactivity pulse normally leads first to the cracking of the shell; the threshold for this cracking depends primarily on thermomechanical and hydrostatic pressure effects.

2. After the shell cracks, the heat loss from the uranium carbide increases, and a pause in the temperature rise may be expected.

3. Matrix damage occurs only if sufficient energy is deposited in a short enough time. The energy requirement for matrix damage depends markedly on the pulse length and the volume fraction of the particles in the fuel body.

ULTIMATE POTENTIAL CAPABILITIES
OF COATED-PARTICLE FUEL BODIES

The usefulness of the coated-particle fuel bodies for burst reactor applications will be limited by the possibilities of fuel migration and, more generally, of damage to the PyC shells. For avoiding such damage, the following limitations appear necessary as a minimum:

1. The maximum temperature reached in the uranium carbide core should be below the melting point of UC_2. Therefore the maximum temperature rise permitted in the particle cores should be 2300°C or less.

2. The stresses across the PyC should be well below the fracture stress of about 6×10^4 psi, and the maximum strain should be less than the fracture strain, which, in turn, depends on the specific mode of the formation of the shells.

Shock effects, however, do not appear to play a role in the breakup of the fuel bodies. As an illustration of the order of magnitudes involved, consider a free shell of radius R and thickness d; let c be the velocity of sound in the shell and τ be the duration of heating due to the reactivity pulse. It is customary to consider three regimes: (1) The shock region, where $\tau < d/2c$; (2) The fast-heating region, where radial, but no circumferential, shock effects are expected: $d/2c < \tau < \pi R/2c$; and (3) The slow-heating region, where $\tau > \pi R/2c$.

Assuming that c is of the order of 10^5 cm/sec, R is, at most, 2000 μ, and d is less than 300 μ, one has for the case of fast heating $6 \times 10^{-8} < \tau < 3 \times 10^{-6}$ sec. Thus, it is obvious that even for extremely large particles the heating time would have to be in the microsecond range for shock effects to occur; currently realized reactivity pulse lengths are of the order of 0.1 msec or longer, which rules out shock effects.

The requirement that the carbide core does not melt puts an immediate limitation on the burst size possibly achievable. From a simple heat-balance argument, one obtains for the maximum energy deposition ΔE permissible for a carbide core

$$\Delta E = [C_1 \rho_1 V_1 + K(C_2 \rho_2 V_2 + C_3 \rho_3 V_3)] \, \Delta T \tag{1}$$

where ΔT is the maximum permissible temperature rise, C is the specific heat, ρ is the density, and V is the volume. The indices 1, 2, and 3 refer to the carbide core, the PyC layer, and the matrix region which can be associated with a particle that is obtained by assigning to each particle a spherical graphite shell of an outer diameter corresponding to the average spacing between the centers of the fuel particles.

The constant K is a measure of the fraction of energy which can be dissipated by conductive heat transfer from the core to the PyC shell and the graphite matrix during the reactivity pulse. From Eq. 1 one obtains for F (the maximum number of fissions per cubic centimeters compatible with a temperature rise of 2300°C in the carbide core) the relation

$$F = 1.2 \times 10^{15} \, \frac{1 + 0.1 \, K[(N_c/N_u) - 2]}{1.5 + (N_c/N_u)} \tag{2}$$

where N_c and N_u are the number of carbon and uranium atoms per cubic centimeter, respectively. The following parameter values have

been assumed: $\rho_1 = 11.7$ g/cm^3, $\rho_2 = \rho_3 = 1.9$ g/cm^3, $C_1 = 0.4$ joule/g°C, and $C_2 = C_3 = 1.0$ joule/g°C, which may be appropriate for the relevant orders of magnitude. Illustrative values of F as a function of the carbon-to-uranium ratio are given in Table 2.

It is obvious that the burst performance of such fuels will depend critically on the value of the constant K, which, in turn, depends primarily on the heat-transfer characteristics of the PyC shell and on the geometric configuration. Smaller core radii and thinner PyC shells will greatly improve the heat transfer.

Table 2

MAXIMUM ALLOWABLE ENERGY DEPOSITION RATES, FISSIONS/CM^3*

N_c/N_u †	K‡ = 0.0	K‡ = 0.1	K‡ = 0.5	K‡ = 1.0
2	3.5			
10	1.07	1.16	1.54	2.01
30	0.39	0.51	0.98	1.59
100	0.12	0.25	0.77	1.43
400	0.03	0.16	0.70	1.37
1,000	0.01	0.15	0.69	1.36
10,000	0.001	0.14	0.68	1.35

*Units: 10^{14} fissions/cm^3.

†N_c/N_u = carbon to uranium-235 atomic ratio.

‡K = fraction of heat capacities of PyC shell and matrix usable during excursion as heat dump.

It seems therefore that the fuel bodies already tested[1] may not be optimal for use in burst reactors. Extrapolating from experimental evidence and from the use of simple models, one may conjecture that fuel bodies containing particles with smaller fuel cores (perhaps with diameters in the 30- to 50-μ range) and covered with composite shells may tolerate much higher energy depositions and deposition rates than fuel bodies that have already been tested. Double shells with an inner layer of graphite covered with a thin PyC shell may have particular advantages: the inner layer could help in inhibiting fuel migration, acting as a protective coating; at the same time it provides a readily accessible heat sink since its conductivity may be much higher than that of PyC. The possible reduction of the thickness of the outer PyC shell would, of course, greatly reduce its thermal resistance and thus increase the value of K. Moreover, the stresses in a thin PyC shell could be greatly reduced because of the presence of an inner buffer zone.

This conjecture is, of course, highly speculative: the whole heat-transfer mechanism of a double or multiple coating depends on the production method; laminations may occur which reduce the heat-transfer capability of the shell, and too thin a shell may not withstand

repetitive pulsing. Moreover, small core particles may not be obtainable by large-scale commercial production methods.

   For these reasons one can merely indicate the ultimate range of potential fuel performance. A more quantitative statement based on a combined study of thermomechanical and heat-conduction effects would therefore be quite premature.

   It may, however, be of some interest to consider ultimately attainable burst widths. Again, the values presented in Table 3 are speculative; they are based on simple survey calculations assuming reactivity insertion and withdrawal rates that are on the border line of those already attained. Possible modification could occur, e.g., by suitable pulse shaping or using not fully enriched fuel to increase the reactivity coefficients, which, at the cost of reducing maximum power densities, could lead to such short power bursts.

Table 3

PULSE WIDTHS IN AN EXTREME EXCURSION ($\Delta k = 0.05$)

N_c/N_u*	$t_{1/2}$†
10	0.01
30	0.025
100	0.10
400	1.2

*N_c/N_u = carbon to uranium atomic ratio.
†$t_{1/2}$ = half-width of pulse, msec.

CONCLUSIONS

   Pyrocarbon-coated uranium carbide particles imbedded in a graphite matrix have shown high resistance to breakup in reactivity excursions. It appears conceivable that particles with a modified coating could lead to a better utilization of the inherent advantages of the high heat capacity of such fuel bodies. Although solid fuels containing an appreciable amount of carbon will not be competitive with disposable-core devices to attain maximum burst yields, it appears possible that they could provide much shorter pulse lengths and harder spectra than TREAT-type reactor fuels and thus be of interest for fuel-testing applications.

ACKNOWLEDGMENTS

The author is indebted to L. D. P. King for his continuing interest in this work. Many stimulating discussions with L. D. P. King, W. R. Stratton, M. Bowman, J. C. Rowley, and others at the Los Alamos Scientific Laboratory are also gratefully acknowledged, as well as the help of N. H. Krikorian, J. F. Kerrisk, and W. U. Geer in evaluating material parameters and discussing experimental results and of C. B. Mills with a survey calculation.

REFERENCES

1. W. U. Geer, C. G. Hoffman, and J. F. Kerrisk, The Behavior of Coated Particles in a Large Nuclear Transient (Kiwi-TNT), USAEC Report LA-3367, Los Alamos Scientific Laboratory, September 1965.
2. L. D. P. King, Description of the Kiwi-TNT Experiment and Related Experiments, USAEC Report LA-3350-MS, Los Alamos Scientific Laboratory, in preparation.
3. F. T. Adler, Effects of Reactivity Excursions on Coated Fuel Particles, USAEC Report LA-3547, Los Alamos Scientific Laboratory, January 1968.

DISCUSSION

GLASGOW: Is there any possibility that we could marry these last two concepts and come up with a fluidized-bed concept of pyrocarbon fuel particles?

ADLER: I would not like to speculate about that.

GLASGOW: I was thinking of an added advantage that came up in one of the earlier sessions, of using some type of coolant as your moderating medium.

PERRY: Felix, I missed a point. When you quoted energy deposition figures per centimeter cubed, were those per centimeter cubed of uranium carbide or of the entire matrix?

ADLER: The entire matrix.

Safety
and Diagnostic
Instrumentation

Session 6

6-1 A SURVEY OF SAFETY INSTRUMENTATION AND INTERLOCK REQUIREMENTS

FREDERICK J. SHON
U. S. Atomic Energy Commission

ABSTRACT

Criteria for burst-reactor safety systems are examined critically. Systems usually called "safety" systems are found to have only a small influence on safe operation of burst reactors. Devices that reduce the change of an oversized burst, more properly considered safety systems, are reviewed, and the coincidence and redundancy requirements for all systems are noted. It is concluded that the prime safety factors in the operation of a fast burst reactor are care and intelligence on the part of the operators, that these factors can be aided by properly designed safety systems, and that the need for redundancy and coincidence logic in these systems is inextricably bound up with the operating procedures in use.

INTRODUCTION

The history of fast burst reactor technology, from the early Godiva assembly on, has been one of continual improvement and adaptation. The power of these machines, measured either in terms of peak fission rate or burst size, has grown, and, particularly since the introduction by Haynes, O' Brien,[1] and others of the forced-burst-initiation technique, their usefulness as controlled sources of neutrons has increased.

The idea of deliberately assembling fissile material to a state in excess of prompt criticality is, from the viewpoint of those who operate other types of fissile assemblies, rather hair-raising. Attempting such an assembly without the presence of a source seems a further bit of daring. As Wimett[2] has said: "... there is a basic incompatibility between absolute safeguards against unplanned prompt excursions and the reproducible generation of prompt bursts."

GENERAL PURPOSE OF SCRAM CIRCUITS

Let us consider the safety system of a generalized fissile assembly as shown in the block diagram, Fig. 1. The assembly could be a critical assembly, a research reactor, a power reactor, or any of several fast burst reactors. It has what we will call a "last-stage motion" for in-
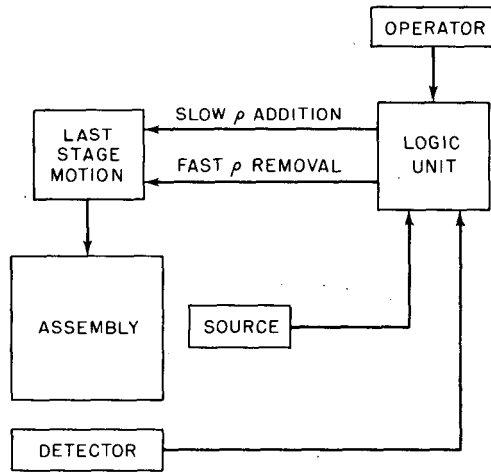
Fig. 1 — *Schematic diagram of a typical safety circuit for a fissile assembly.*

creasing reactivity. By this we mean there is some remotely controlled system for increasing reactivity in the neighborhood of delayed criticality. Such a mechanism is used in the approach to criticality at a time after gross fuel additions have made it possible to complete the approach with one or more simply controlled remote motions.

In the diagram the last-stage motion has two capabilities: Slow reactivity addition and quick reactivity removal.

In most cases the logic unit follows a scheme given in Table 1. The source can be present or absent; the detector can read below some minimum, within a selected range, or above a maximum; the operator can demand reactivity addition, removal, or nothing (ρ is reactivity). Basically, the logic system is intended: (1) to reduce reactivity rapidly when a maximum fission rate is exceeded and (2) to forbid addition of reactivity when no source is present. (Both the source interlock and the minimum detector reading serve this purpose.)

All the systems for fast burst reactors have carried these features also. They have usually been justified as being intended only for steady-state operation. Let us see exactly what these logic conditions mean and what basic troubles they are intended to forestall.

Table 1

SCHEMES FOR LOGIC UNITS

Operator demand	Source condition	Detector reading	Resulting motion
ρ removal	Any	Any	ρ removal
ρ addition	Present	Below min.	None
ρ addition	Absent	Below max.	None
Any	Any	Above max.	ρ removal
ρ addition	Present	Between min. and max.	ρ addition

First, as has been noted by earlier system philosophers,[3,4] even for relatively slow assemblies the system cannot really terminate an excursion. A review[5] of damaging excursions in all sorts of systems, even ones with relatively long neutron lifetimes, indicates that these incidents take place in times far too short for electromechanical systems to react.

Note that the following concept is almost universally true: If an excursion is violent enough to be physically damaging, its time scale is short enough to preclude safety-system action. If, on the other hand, a safety system can terminate the excursion, the excursion could not have been catastrophic anyway.

It must be, then, that the object of such safety and interlock systems is not the termination of excursions. What, then, is its purpose?

Consider what happens if we add reactivity to such a system at a relatively slow rate. Provided, as the interlocks assure, there is a source present and an appreciable fission rate, the fission rate will rise slowly as delayed criticality is approached and will generally exceed the maximum detector reading and cause a scram if an attempt is made to continue reactivity addition to the region near prompt criticality.

Viewed in this fashion, then, the entire system is simply an augmented, nonlinear, negative reactivity feedback, meant to function in a deliberate preinitiation situation. That is, the safety and interlock system of the usual fissile assembly is meant (1) to provide a strong nonlinear negative reactivity feedback and (2) to assure that this mechanism functions by deliberate preinitiation. Thus this type of safety system can prevent (but not terminate) an excursion during a slow approach to delayed criticality. The actual requirements of such a system are not severe. In general, the slow reactivity addition rate is such that the time between passing a high neutron level and arrival at prompt critical is many seconds. A system of the type described needs only to be capable of removing a substantial amount of reactivity in a second or so. This is, of course, true only under conditions where the rate of reactivity addition is low, generally of the order of cents per second, as it is when steady-state

reactors or critical assemblies are being operated or when delayed
critical approaches are being made with burst reactors.

Safety systems, such as that of Fig. 1 or some slight variation
thereof, also perform one other true safety (trouble prevention) func-
tion: They limit power to a value such that the heat generated in steady-
state operation of the assembly never exceeds that which can be carried
off without damage. In assemblies that lack high-capacity cooling sys-
tems, and most burst reactor systems are of this type, the maximum
detector level for scram may be set to limit the power to give non-
damaging temperatures at thermal equilibrium.

Thus the safety and interlock system of Fig. 1 is intended (1) to
prevent excursions under conditions of slow reactivity addition by
preinitiating a strong artificial reactivity feedback and (2) to preclude
steady-state operation at levels such that equilibrium temperatures may
be damaging. Note that both these functions are inherently concerned
with steady-state operation or with operation substantially below prompt
criticality. Neither is directly concerned with safety when the reactor is
burst, although, as we shall see later, some modifications of these func-
tions are indirectly applicable to burst reactor safety. Nonetheless, sys-
tems of the type of Fig. 1 were included in the earlier burst machines
(which were primarily critical assemblies run under special conditions),
and we also observe that this type of system has been carried over into
the safety and interlock systems of typical second-generation fast burst
reactors. Thus in the case of the FRAN reactor, recently set up at
the National Reactor Testing Station[6] either of two picoammeters
driven by ion chambers will cause a scram when driven off scale, and
scrams can be reset only with the source inserted. (Several other
scram and interlock features discussed later are present. They relate
to other requirements more directly innate in the nature of a fast burst
reactor.) The Army Pulse Radiation Facility at Aberdeen, Maryland[7] has
a scram on temperature as well as flux level. These devices are rela-
tively slow in their action; they are therefore protective systems es-
sentially like that of Fig. 1.

During or immediately following a burst, a system of the type of
Fig. 1 can also prevent a second unwanted excursion and prevent the
reactor from levelling off at some undesired power. Both these func-
tions involve responses on a time scale comparable with that required
for the reactor to cool off under normal conditions. They therefore
impose no stringent speed requirement on the system.

BURST REACTOR SAFETY SYSTEMS

For reasons that appear to me to be primarily a matter of habit,
the systems attached to burst reactors to perform the functions de-

scribed in the preceding section are often called "safety systems" in safety analysis reports. As we have noted, these systems actually have little to do with fast burst reactor safety as such. To begin with, they are primarily concerned with preinitiation or steady operations, and neither of these matters is directly concerned with fast burst safety.

As fast burst systems are generally run, the primary purpose of a true safety feature should be to prevent an oversized burst. For examining the possible cause of an oversized burst, let us first investigate a typical fast burst reactor operating sequence and try to pick those places in the sequence where errors or miscalculations could cause such an occurrence. The usual sequence in general terms is:

1. Starting with the reactor in a shutdown condition, with the major safety block and all control rods in their lowest reactivity position, a source is inserted.

2. A large change of reactivity in the positive direction is made (usually by inserting the safety block) at a rate of the order of several dollars per second. The reactor remains well below delayed criticality, but appreciable neutrons are detected because of the source, and the change in multiplication from step 1 is clearly noticeable.

3. The control rods are inserted slowly, one at a time, corresponding to the last-stage motion of Fig. 1, reactivity being added at the rate of a few dollars per minute.

4. The motions of step 3 are continued until the reactor reaches some low power at delayed criticality or nearly delayed criticality. If any departure from delayed criticality is present at this point, its magnitude must be measured carefully.

5. The reactivity is dropped to several dollars below delayed criticality, and the source is removed.

6. A waiting period elapses during which delayed-neutron precursors are allowed to decay until the fission rate has dropped to the point where the source in the reactor may be considered a weak one by Hansen's definition.[8]

7. The reactor is returned rather rapidly to the delayed critical configuration.

8. A known amount of reactivity, sufficient to bring the reactor above prompt criticality by the desired amount, is inserted.

9. The burst occurs either due to the statistically fortuitous initiation of a persistent chain by the natural source present or due to a programmed pulse of neutrons inserted into the assembly by an artificial source.

10. The burst is terminated in its prompt aspect by the inherent negative feedback characteristics of the system. That is, it is terminated by heating and the subsequent expansion, which reduces reactivity below prompt criticality.

11. The slowly decaying tail of fission activity is reduced by withdrawal of the safety block.

There are several places in this sequence where an action can be taken or where an incident could occur which would tend to cause a burst larger than one desires. We note that it is not the so-called "safety system" that determines the burst size in any sense. Burst size is entirely a function of the characteristics of the reactor. The prime variables are the amount of reactivity added during the period just before the burst occurs and the reactivity-feedback coefficients of the design.

It is generally accepted that the most probable cause of an oversized burst is an unintended preburst change in reactivity during step 6; that is, during the time between establishment of delayed criticality and the actual occurrence of the burst. Another possible cause of an oversized burst is a failure to establish exactly the delayed critical condition; i.e., a failure to estimate exactly the reactivity above delayed criticality at the time when that measurement was made. A third possible cause is a failure to properly measure or estimate the amount of reactivity added in step 8 when the burst rod or mass adjustment rod is inserted.

The first of the above troubles can be due to a change in physical configuration (perhaps something falling against the reactor during the decay period), a change in composition (perhaps something being removed or inserted during that period), and so forth. The most likely cause of a failure to properly establish delayed criticality would, of course, be operator error. Similarly, the most likely cause of failure to properly establish the amount of reactivity desired to be added for the burst would also be operator error. One can guard against unwanted changes in reactivity during the decay period only to a limited extent. As the neutrons decay from the assembly and the level drops with no source present, it becomes increasingly difficult to keep exact track of the reactivity. Further, the reactivity of the assembly during this period is usually so far below criticality that practical means of measurement cannot establish the exact base value to within the accuracy required to properly limit burst size. Considering the time period and the fact that the neutron population in the system will remain very low until after the burst reactivity insertion (step 8), we cannot be certain that delayed criticality has again been exactly achieved in step 7. In general, then, we must consider interlocks which prevent an undesirable positive reactivity change during the decay period or which preclude a large operator error in establishment of delayed criticality or in measuring the reactivity addition to be made.

Some systems, such as the FRAN Reactor, incorporate devices intended to guard against gross error in determining delayed criticality. That system has a period-meter scram in operation during the time

when delayed criticality is being established. The scram is set at a value such that it will shut down the system if the period resulting from any preburst configuration could lead to an oversized burst upon the addition of the burst rod. Such a device, because of its action in bringing abnormal behavior to the attention of the operator, is indeed a guard of sorts against an oversized burst.

Figure 2 shows the sequence of operational steps described previously; the points at which a safety system might be expected to function have been indicated, and the type of action such a system should take is noted. Thus in the third step, the safety system of Fig. 1 is operative to prevent an undesired excursion during the approach to delayed criticality. In step 4, a short-period scram is in operation to assure that operator neglect will not result in periods unsafely far from true delayed criticality. In the time period immediately following step 5, one could conceive of a reactivity meter that would at least signal to the operator if the withdrawal of the safety block did not drop the reactivity as far below delayed criticality as had been expected.

This last safety device is, of course, more difficult to construct, especially since the pertinence of such a measurement would, in general, increase as the waiting period progressed; the accuracy of any measurement based on neutron counting, however, would fall off rapidly as the neutron population decreased.

The next device mentioned in Fig. 2, the motion-detector scram, is one which, to my knowledge, has not been incorporated in any sophisticated form on present burst reactors. It is an interlock meant to function if a physical change takes place during the decay period. In some cases a very specialized sort of motion detector has been incorporated in a burst system. The APRFR, for example, which has a movable reactor structure, has a scram that functions if the reactor is moved during the decay period. But it appears that no one has tried to preclude difficulties of the sort that damaged Godiva I; that is, motion of some object in the vicinity of the reactor in such a way as to change the reflection characteristics of the reactor environment. It is rather surprising that this has not been tried since there are several commercially available devices that could do this. There are electromagnetic Doppler-motion detectors (such as the Johnson Control Co. Model G-1 Motion Detector) which can readily sound an alarm when a small mass moves in their field of view. Also available are information storage and comparison devices for closed-circuit television systems (such as the Sutter Co. VMD-2 Video Motion Detector) which will alarm if the sampled area in a picture changes.

The next safety device mentioned in Fig. 2 is the programmed-burst system used with forced initiation. Calling this system a safety feature is rather foreign to the thinking of most designers; but, since
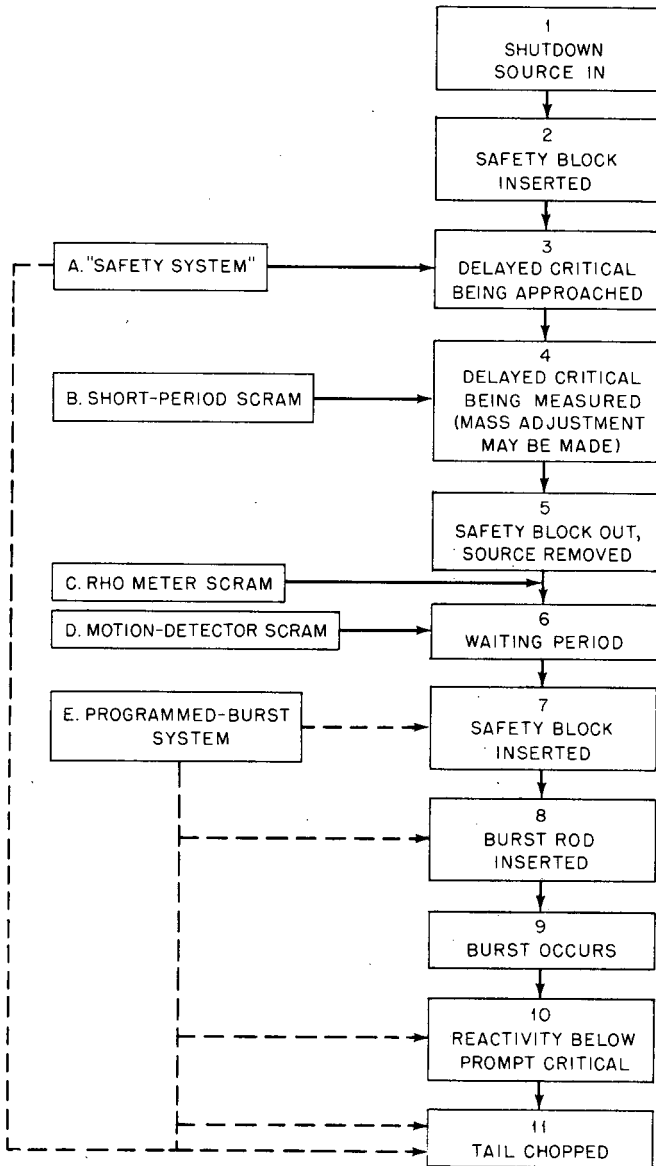
Fig. 2—*Fast burst reactor sequence with effective points of action of safety systems.*

it does indeed originate a signal that will act to prevent either a re-
peated burst or a continued run at finite power after a burst, it serves
at least one function of the system of Fig. 1 and may thus also be
legitimately considered a safety system.

Table 2 lists the safety systems identified thus far, together with
the incident against which each is effective and the speed requirements

Table 2

SAFETY SYSTEMS

System of Fig. 2	Safety functions	Backup	Reaction time required
A, "safety" system	(1) Prevents excursion during d-c approach; (2) Prevents steady-state operation at too high power level; (3) Prevents secondary burst or steady state after burst	Manual scram	Few tenths of a second
B, period scram	Prevents oversized burst due to gross error in delayed critical	Procedures	Few tenths of a second
C, rho meter scram	Prevents oversized burst due to gross error in delayed critical	Procedures	Few tenths of a second
D, motion detector	Prevents oversized burst due to change in reactor environment	Operator observation	Few tenths of a second
E, programmed initiation and scram	Prevents secondary burst or steady state after burst	Manual scram system A	Time fixed by operational rather than safety requirements

of each. Note that, in general, even those meant to protect against an
oversized burst need not be especially quick-acting. In general, if these
systems can act within a time of the order of a few tenths of a second,
they can successfully perform their safety functions.

We might now investigate what the other requirements of these
systems may be. How much redundancy is desirable? To what parts
of the system should a single-failure criterion similar to that of the

Institute of Electrical and Electronics Engineers, Inc. (IEEE)[9] apply?
What coincidence logic is desirable?

REDUNDANCY REQUIREMENTS

All the systems of Fig. 2 are in some sense redundant to the
operating procedures of the burst reactor system. By this we mean that
if all operations are carried out perfectly and no deviations from the
plan occur none of these systems needs to function to assure that no
injury or damage will occur. In this respect the system is like those
developed for other types of reactors.

However, in the case of the fast burst reactor, the converse of
the above statement is much less likely to be true. That is, although
for other reactor types, a failure in operating plans will be readily
caught by the reactor safety system, such is not necessarily the case
for the fast burst system. The burst reactor is, despite the ingenuity
of control-system designers, an inherently unforgiving device, prone to
do the wrong thing in the hands of the careless.

Such errors as the failure to properly measure burst-rod worth
under changed conditions can not only set the stage for an overburst
but can simultaneously vitiate a device, such as system B, meant to
protect against an overburst; nor would a degree of redundance in
system B correct this trouble. Further, undesired changes in the con-
figuration during the decay period can be of a nature not readily discern-
ible either by closed-circuit television or by motion detectors.

It would seem, however, that prudence would dictate at least one
operating independent spare for those systems that are intended to pre-
clude overbursts. That is, systems B, C, and D of Fig. 2 should be
double. One recognizes that redundancy in these systems does not as-
sure their functioning. Indeed, their most likely reason for failure to
function is the occurrence of an event they cannot be designed to meet.
And it has been remarked[10] that safety-system redundancy protects
only against statistical component failure, not against design gaps.

Nonetheless, it does not seem unreasonable to require a double
independent system for each of systems B, C, and D.

System A is also often made redundant, chiefly, it seems, because
of its function to limit power during steady-state operation. Considered
as a device to preclude repeated bursts or unwanted steady operations,
it is in itself redundant to the tail-chopping functions of the programmed-
burst system. And the completely different principles on which these two
systems, A and E, function assure that whatever benefit can be gained
from redundancy is maximized.

Directly involved in the redundancy question is the question of
coincidence logic, which will be treated next.

SINGLE-FAILURE ANALYSES

It is evident from the preceding discussion that we can examine the systems A, B, C, D, and E to assure that no single failure will prevent their functioning. By a single failure we mean: (1) one component that failed or a circuit that faulted, (2) multiple failures resulting from a single external cause, (3) multiple failures resulting from a single internal cause, and (4) the accumulation of undetected failures until they cause a malfunction on test.

The meanings of these four kinds of single failures, extracted from the proposed IEEE Guide to the Application of the Single-Failure Criterion[9] are self-explanatory, with the possible exception of the fourth type mentioned. That type is meant to classify as single any failure that results from several successive failures, each of which would not be individually detectable until the last failure occurred. For example, if either of two redundant safety chains can give a desired signal and if the tests run are such that only one chain need function to give an affirmative result, then, since the failure of one chain would go undetected until the other failed, the failure of both is considered a single failure. It is important to note that the fourth failure class makes certain assumptions about the testing program as well as certain assumptions about the coincidence logic of safety circuits.

If, then, we wish to apply single-failure analysis to the circuits we have identified as preventing accidents in fast burst reactors, we will need to assess the coincidence-logic requirements of burst reactor circuitry.

COINCIDENCE LOGIC

There is a distinct dichotomy of view regarding the coincidence logic that is desirable for the rather special applications represented by fast burst reactor protective circuits. Figure 2 points out several types of protection which are desired.

Further, we have implied that some degree of redundancy is desirable in these circuits. There exists a question as to whether, if redundant, the protective circuits should be completely independent in their action; i.e., whether their coincidence logic should be one-out-of-n or n'-out-of n, where $1 < n' < n$.

Some fast burst reactors, e.g., the APRFR, have been built with two-out-of-three logic in the system designated A in Table 2. There is considerable difference of opinion about the advisability of such a design. Briefly, the arguments are: Independent scrams (one-out-of-n logic) are clearly less likely to fail when needed. Since a burst reactor spends most of its time shutdown anyhow and since its continuity of operation

is never crucial, the false-scram penalties implied by one-out-of-n logic are minimal. Requiring more than one-out-of-n is simply inviting failure under stress.

On the other hand, as we noted earlier, one-out-of-n logic merely assures that an unsafe component failure in one channel will not stop the protective action. It does not guard against underdesign or against occurrence of an unforeseen situation. The probability of unsafe component failure in a properly designed and analyzed system is extremely small, and most protective-system failures in practice are the result of the inherent inability of the system to respond to an unexpected situation. The assurance gained by one-out-of-n is therefore negligible. Using two-out-of-n logic will not only afford some slight advantage in operability during steady-state runs, it will also afford a positive safety advantage. By making it possible to insert a checking signal in one channel at any time during operation, the more complex logic allows one to carry out more frequent checks of the sensitivity of the system without completely interrupting operations.

One could, for example, arrange three motion-detecting systems in two-out-of-three coincidence for system D of Table 2; then, require that just at the end of the decay period some small motion signal be fed to each detector individually to assure that each would have responded if something had moved.

Note, however, that any safety advantage to be gained through a coincidence logic involving more than n'-out-of-n can be achieved only through increased testing capacity. In this sense it hinges upon operational procedure.

CONCLUSIONS

Our primary conclusion regarding the safety and interlock systems for burst reactors is rather a negative one. To wit: these systems neither substitute for, nor substantially enhance, careful and knowledgeable operation. For many types of reactors other than fast burst types, clever interlocking can aid in assuring that operator error will simply be met by refusal to perform. Here, however, the errors most likely to be destructive are ones that no interlock prevents.

Some protection can be gained against excessive temperatures in the steady-state mode by a system like that of Fig. 1. Such a system also affords protection against undesired excursions during the approach to criticality.

Rather little design ingenuity appears to have gone into interlock systems to prevent oversized bursts. In particular, devices are available to alarm or scram on a change in reactor environment during the

decay period. Protection of that sort seems the only type that could supplement careful operation to a substantial degree.

Redundancy in interlock and scram systems seems desirable, and a review of all safety systems for conformance with the IEEE Single Failure Criterion is a fairly simple and desirable step in safety analysis.

Coincidence logic is largely a matter of the designer's own personal preference. A properly constructed system can add safety to the extent to which mechanical systems can do so, irrespective of the coincidence logic employed. Some additional protection seems available through multiple coincidence when combined with a carefully planned testing schedule, but the cost involved in such systems would usually be more than the additional assurance would justify.

REFERENCES

1. K. L. Haynes and P. D. O'Brien, Precisely Timed Initiation of a Fast Burst Reactor, *Trans. Amer. Nucl. Soc.*, 6: 284 (1963).
2. T. F. Wimett, Fast Burst Reactors in the USA, USAEC Report LADC-6786, Los Alamos Scientific Laboratory, 1965.
3. R. S. Stone, Control Systems of Pulse Reactors, *Nucl. Safety*, 3: 43-46 (1962).
4. L. C. Oakes, The Control and Safety of Pulse Reactors, *Nucl. Safety*, 9: 363-371 (1968).
5. W. R. Stratton, A Review of Criticality Incidents, USAEC Report LA-3611, Los Alamos Scientific Laboratory, 1967.
6. S. R. Gossmann and V. B. Gottschalk, Safety Analysis Report for the FRAN Prompt Burst Machine, USAEC Report IDO-17231, Phillips Petroleum Co., 1967.
7. R. W. Dickenson et. al., Safety Analysis Report for Army Pulse Radiation Facility Fast Pulse Reactor, Report BRL-1356, U. S. Army Ballistic Research Laboratories, 1967.
8. G. E. Hansen, Assembly of Fissionable Material in the Presence of a Weak Neutron Source, *Nucl. Sci. Eng.*, 8: 709-719 (1960).
9. Guide to the Application of the Single Failure Criterion to Nuclear Power Protection Systems, fourth draft, prepared by Institute of Electrical and Electronics Engineers, Nuclear Science Group (IEEE/NSG), Standards Subcommittee WGi.
10. S. H. Hanauer and C. S. Walker, Design Principles of Reactor Protection Instrument Systems, USAEC Report ORNL-NSIC-51, Oak Ridge National Laboratory, 1968.

DISCUSSION

MURPHY: It strikes me on listening to your safety procedures that much of the work is relatively straightforward; it simply involves detailed checking of the reactor characteristics to ensure that certain safety interlocks are present, and so on. Nowadays high-speed digital computers are available at a price that is not much different from that of a good multichannel analyzer. I am wondering if there are any laboratories now using small computers, e.g., something on the order

of a PDP-8, to give a real-time check of not only the condition of your interlocks but also to give real-time checking of the reactor operator's verification of delayed critical.

(During the LASL tour that followed the conference, it was found that the Los Alamos UHTREX reactor is controlled by such a computer system. Of course, UHTREX is not a fast burst reactor, but the differences in a computer-control system for a burst reactor should not be very great.)

SHON: To my knowledge there are no burst reactors that are doing this; of course, other types of reactors are doing it. I might say though that ever since the days of Frankenstein men have been inherently afraid of their own creations. So, on the reactors where real-time computers are used to establish reactor characteristics and respond to them, designers have been remarkably reluctant to trust the computers to add reactivity. They will let the computer take reactivity away anytime, but to add it, the computer always just tells the operator. I am not sure that this is a good idea. It might be good to have a programmed-burst sequence that is completely controlled by a computer.

CLACK: It seems to me that in your talk and in previous ones it has been implicit that you can always rely on a negative temperature coefficient. Is this in fact guaranteed under all circumstances?

SHON: The reactor is designed to have this.

CLACK: Could the characteristics change so that you got a positive temperature coefficient?

SHON: I think it could happen. I cannot think offhand of exactly what parameters would have to change, but I suppose if you had some sort of reflector that the reactor could expand into or something like that you might get a positive coefficient under some conditions.

6-2 TIME-DEPENDENT DOSIMETRY AND SPECTROSCOPY

S. KRONENBERG and R. A. LUX
Institute for Exploratory Research, U. S. Army Electronics Command,
Fort Monmouth, New Jersey

ABSTRACT

Requirements for instrumentation to measure dose rate and time-dependent neutron and gamma-ray spectra from fast burst reactors are discussed. Specific dose-rate measuring systems are compared. Techniques for obtaining time-dependent spectra are discussed.

In the intense radiation environment of a pulsed reactor, many physical properties of exposed equipment show strong changes that have a potential use in time-dependent dosimetry and gamma-ray and neutron spectrometry. In the design of a system to study the environment, the main difficulty, in fact, is to select from these properties the most suitable ones for extracting the desired information. A useful system should satisfy the following requirements:

1. Its readout should be interpretable in well-defined units of the measured parameter; for example, when dose is being measured as a function of time, the readout should be proportional to rads (in terms of the irradiated material), roentgens, or neutrons per square centimeter (nvt). This can be done only if the response of the detector is independent of energy or if both its energy response and the energy distribution of the incident radiation are known.

2. The resolving time of the system (including the recorder) should be short compared with the pulse duration. For a typical 40-μsec burst length, the resolving time should be less than 1 μsec, including both the buildup and decay of the signal, so that small intensities immediately following high intensities can be monitored reliably.

3. The system should be able to operate without saturation between 4×10^{12} rads/sec in the glory hole of a modern burst reactor and a few

rads per second for large distances. In practice this can be accomplished by the use of two or more detector systems with different operational ranges.

4. If desired, the system should be able to yield separate information on neutron and gamma-ray dose rates. This can be done by using two different detectors having different neutron and gamma-ray sensitivity ratios. The ideal situation would be to have one detector sensitive only to neutrons and the other only to gamma rays. Although detectors with high gamma-ray-to-neutron sensitivity ratios can be made, the reverse is difficult.

DOSE-RATE MEASURING INSTRUMENTS

The most straightforward approach is calorimetry, in which total heating produced by the radiation is measured. Classical calorimeters are integrating devices with a response time on the order of seconds, making them suitable only for total dose measurements. Recently a detector using the pyroelectric effect in a ferroelectric material has been developed[1,2] with a time resolution of about 30 nsec.

Scintillators and photomultipliers or photodiodes are frequently used to measure the dose rate of a fast burst reactor. Inorganic crystals are not useful because of the long decay time of the fluorescence, about[3] 250 nsec for NaI(Tl) and 1.5 μsec for CsI(Tl). Systems with organic scintillators are quite satisfactory and are commonly used. Organic scintillators are sensitive to gamma rays, and those containing hydrogen (some do not, e.g., hexafluorobenzene) are sensitive to fast neutrons. Their light output is directly proportional to gamma-ray energy absorbed for energies above 20 kev. However, the output per unit energy for neutrons is not linear until recoil-proton energies[4] approach 20 Mev. So, for the energies encountered in pulsed reactors, their neutron response is nonlinear.

The time resolution of organic scintillators is limited by the decay of fluorescence. Typical decay curves[5] are shown in Fig. 1. For most applications this decay is no problem.

Saturation effects in organic scintillators are not well understood. There is some indication that high dose rates may saturate the scintillator,[6] and permanent degradation of output at total doses of 10^6 to 10^8 rads is well known for some scintillators.[4] Recovery of the permanent effect is seen with aging or heating.

Diffused-junction silicon diodes are frequently used to measure dose. Their output is proportional to the absorbed silicon dose and independent of the type of incident particle. Although these silicon diodes are sensitive primarily to gamma rays, sensitivity to neutrons may be obtained by coating them with an appropriate material (e.g.,
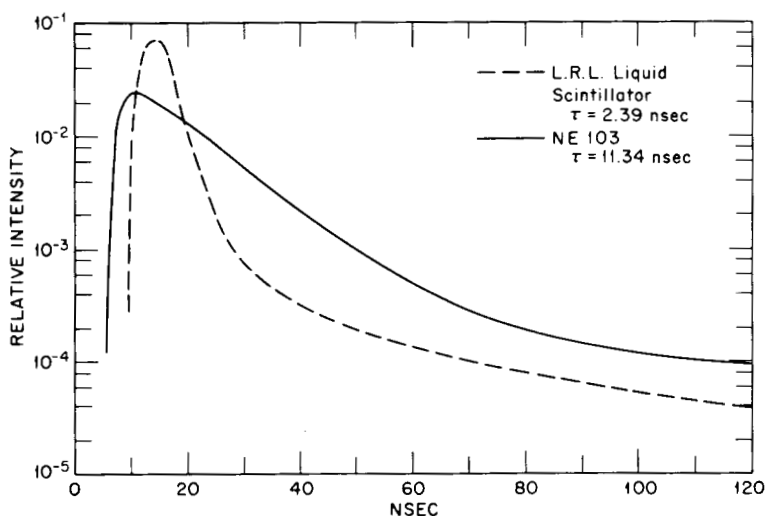
Fig. 1 — *Light output as a function of time following an exposure of a scintillator to a short pulse of gamma rays from a linear accelerator.*

hydrogenous material for fast neutrons, ^{6}Li for almost-energy-independent response, or ^{235}U for thermal neutrons). These detectors are linear up to 10^{12} rad/sec, and their resolving time is 1 to 2 nsec. Typical sensitivity is 3 microcoulombs/rad/g of junction volume, with junction volumes ranging from 0.002 to 1 g.

The secondary-electron–mixed-radiation dosimeter (SEMIRAD) is also used to measure reactor pulses at high dose rates.[7] Its signal depends on the absorbed dose in the layer of wall adjacent to the vacuum chamber. It has a flat energy dependence for gamma rays above 80 kev. Figure 2 shows a typical gamma-ray SEMIRAD. Neutron-sensitive versions have been made using either hydrogenous wall ma-
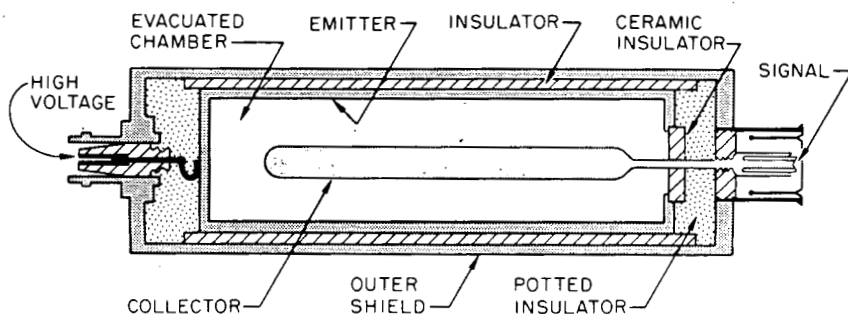
Fig. 2 — *Cross section through a SEMIRAD diode.*

terial (protected by an evaporated metal coating) for fast neutrons or fissionable materials for total neutron measurements. The hydrogenous wall instrument has an output proportional to rads in the wall material for both gammas and neutrons.

Resolving times on the order of 3 nsec are readily obtained; no saturation is seen at dose rates of 10^{12} rads/sec. The major disadvantage of the SEMIRAD is its low sensitivity (typically 3×10^{-12} coulomb/rad which prohibits its use except near the reactor and necessitates great care to avoid radiation-induced cable effects.

Compton diodes have been repeatedly tried for gamma-ray measurements. Their sensitivity is less than that of the SEMIRAD (about 10^{-12} coulomb/rad). The major disadvantage is a very complicated energy response for both gammas and neutrons, which is also a function of the direction of the incident radiation.[8,9]

A new method for dose-rate measurement is now under development at Nuclear Defense Laboratories (NDL).[10] The system uses the radiation-produced ions in a solution of perchloric acid to absorb light. The loss of transparency of the solution is proportional to the radiation intensity. Using a He−Ne laser beam and a system of mirrors and optical filters, personnel can remotely monitor the transparency of the radiation cell without the use of signal cables. Figure 3 shows the arrangement of this dose-rate meter. This method is usable for total doses of 500 to 20,000 rads. The signal is proportional to water rads per unit time. Time resolution of 10^{-9} sec has been reported.
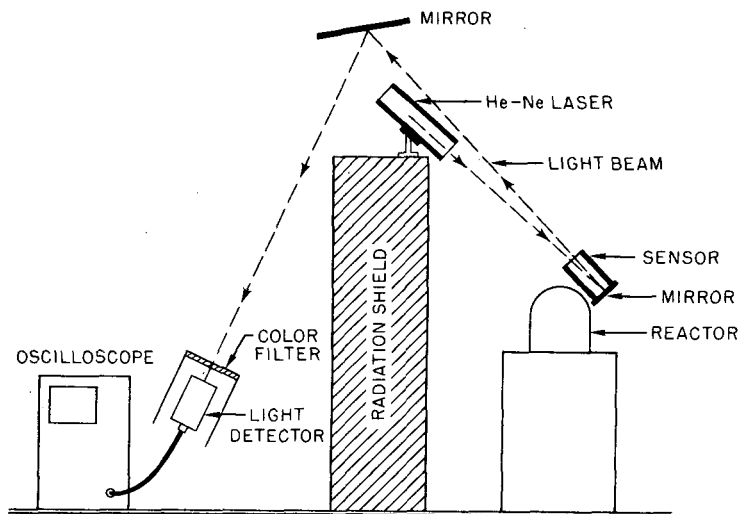
Fig. 3 — *Experimental arrangement of the transient-ion sensor and its system at a fast burst reactor.*

NEUTRON AND GAMMA-RAY SPECTROSCOPY

Two basic types of instruments are used to determine time-dependent neutron or gamma spectra: (1) a monochromator, such as a bent crystal diffraction grating for gamma rays or a recoil-proton magnetic spectrometer for fast neutrons, with an array of detectors at the image plane of the monochromator, and (2) an array of detectors, each with a different energy response. The spectrum is then unfolded from the combined output.

Both types share some characteristics. Readout of all the detectors must be in parallel; the number of channels of energy resolution equals the number of detectors. For a high-resolution system, the parallel electronics and display become quite cumbersome. A frequently used expedient is to assume constancy of spectra from burst to burst and to examine only a limited portion of the spectrum on each burst.

The time resolution of either type depends on the detectors used.

Monochromators have several advantages: The readout gives the spectrum either directly or after a minimum correction for the energy response of the detectors. The energy resolution is limited only by collimation of the incident beam and the detector size; several hundred channels of energy resolution are feasible. Both crystal and magnetic spectrometers can be calibrated absolutely.

The major disadvantage of monochromators is their very low sensitivity. Since good energy resolution requires very tight collimation at both input and output, the radiation seen by an individual detector is very small compared with what would be seen in the free radiation field. Therefore the shielding requirements and cable-effect problems are magnified. A further consequence of the tight collimation is that the monochromator measures only radiation from a particular direction. This can lead to severe errors if scattered radiation makes a significant contribution to the total dose.

The energy-dependent array principle has been applied in several ways to both neutron and gamma spectrometry. For gamma spectrometry the simplest is an array of detectors with different absorbers. Below 100 kev excellent discrimination can be obtained by varying the Z value of the absorbers, making use of the sharp K edge. Above 100 kev the thickness is varied; lower energy gamma rays are more selectively absorbed. A spectrometer of this type has been built using ferroelectric detectors.[2] Figure 4 shows the spectrum obtained from a flash X-ray pulse.

Two types of neutron spectrometers have been developed. One type developed at NDL uses solid-state detectors coated with various elements in which neutrons induce reactions. The response of an individual detector depends on the reaction cross section of the coating element;

hence, it can change very rapidly as a function of energy. Through the use of fissionable coatings, spectra can be measured down to thermal energies. Solid-state detectors with ^{235}U and ^{6}Li coatings are commercially available.
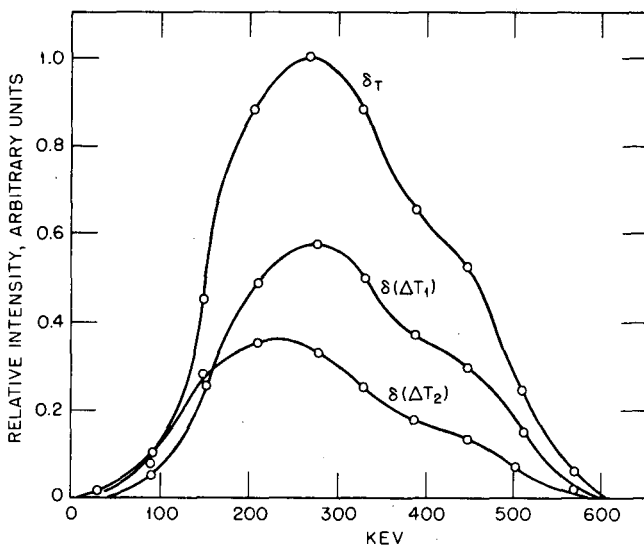
Fig. 4—*Gamma spectrum from a flash X-ray machine taken by means of fer-roelectric materials.* σ_T = *spectrum averaged over the pulse length;* $\sigma(\Delta T_1)$ = *between 0 and 30 μsec; and* $\sigma(\Delta T_2)$ = *between 30 μsec and the end of the pulse.*

A second kind of spectrometer uses proton recoils in a thin sheet of plastic scintillator.[10] Owing to edge effects the output per incident neutron at a given energy is not a linear function of sheet thickness; so such an array allows recovery of the original neutron spectrum. The lower energy limit of this system is set by the requirement of good scintillator response to proton recoils, about 0.5 Mev. Figure 5 shows the response of scintillators of various thicknesses as a function of incident neutron energy.

The major disadvantage of all the energy-dependent array systems is the requirement for unfolding the spectrum from the detector signals. The calculation required is the numerical solution of a Fredholm integral equation:

$$S_n(t) = \int_0^\infty dE \ R_n(E) \ F(E, t) \tag{1}$$

where S_n and $R_n(E)$ are the signal output and the response function of the nth detector, respectively, and $F(E,t)$ is the neutron flux. For

computer solution this equation is usually written as a matrix equation:

$$S_n(t) = R_{nE} F_E(t) \qquad (2)$$

This equation is then solved at increments of t. In general the matrix R is ill behaved and cannot be directly inverted; hence, iterative ap-
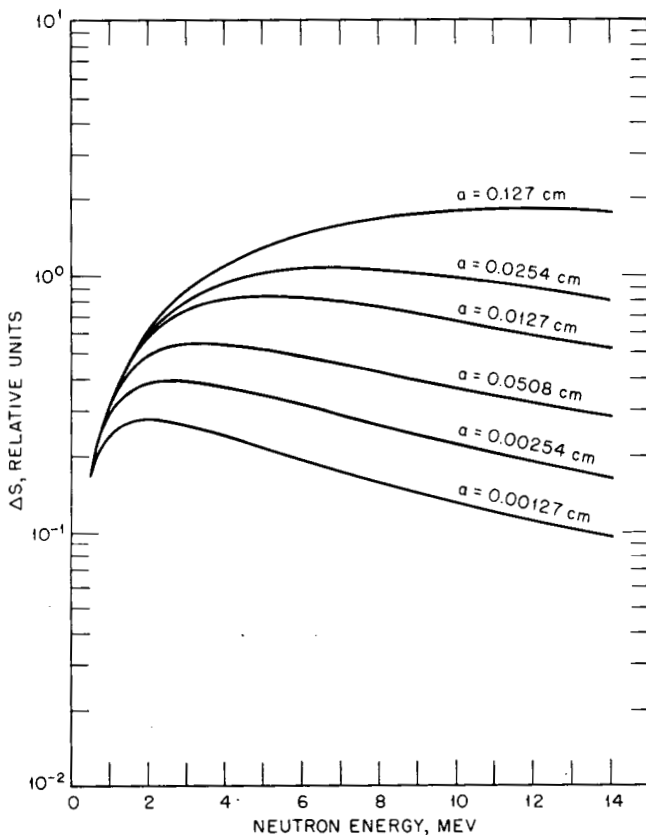
Fig. 5—*Normalized sensitivity of organic scintillators of varying thicknesses (a) to neutrons (nvt) as function of neutron energy.*

proximation schemes have evolved. Two such schemes are outlined below.

The first, by Gold,[11] assumes a trial solution $F_E^{(0)}$. Then the signal corresponding to this trial solution is calculated:

$$S_n^{(0)} = R_{nE} F_E^{(0)} \qquad (3)$$

The next trial solution is generated by the relation

$$F_i^{(1)} = \frac{F_i^{(0)} S_i}{S_i^{(0)}} \qquad (4)$$

Iteration stops when some $S_n^{(k)}$ is sufficiently close to the experimental signal S_n.

This algorithm is very sensitive to the correct choice of the trial solution. For a trial solution greatly different from the correct spectrum, the algorithm can go into unstable oscillation.

The second algorithm involves more calculation per iteration but converges more quickly and is very insensitive[12] to the initial choice of $F_E^{(0)}$. In fact, $F_E^{(0)}$ can be chosen as a null vector. The basic algorithm is given as

$$P_n^{(0)} = r_n^{(0)} = S_n - R_{nE} F_E^{(0)} \qquad (5)$$

$$\alpha^{(0)} = \frac{\sum_i (P_i^{(0)} r_i^{(0)})}{\sum_i (P_i^{(0)} R_{ij} P_j^{(0)})} \qquad (6)$$

$$F_E^{(k+1)} = F_E^{(k)} + \alpha^{(k)} P_E^{(k)} \qquad (7)$$

$$r_i^{(k+1)} = r_j^{(k)} - \alpha^{(k)} R_{ij} P_j^{(k)} \qquad (8)$$

$$P_i^{(k+1)} = r_i^{(k+1)} - \frac{\sum (r_i^{(k+1)} R_{ij} P_j^{(k)})}{\sum (P_i^{(k)} R_{ij} P_j^{(k)})} P_i^{(k)} \qquad (9)$$

Owing to the rapid convergence computer, running time is not excessive.

CALIBRATION TECHNIQUES FOR DETECTORS

Detectors can be calibrated by preexposure to a steady-state neutron or gamma source in the laboratory. This procedure yields mediocre results. Its lack of reliability is caused by the large difference in intensities encountered at the burst compared with the calibration source. However, this type of calibration can be used to compute sensitivity settings of the recording apparatus. Much more accurate is the calibration obtained during the burst itself by attaching reliable integrating dosimeters at the sensor and by expressing the integrated time vs. intensity recording in terms of the independently obtained total dose.

REFERENCES

1. D. L. Hester, D. D. Glower, and L. J. Overton, Use of Ferroelectrics for Gamma Ray Dosimetry, Transactions of a Professional Group on Nuclear Engineering, *IEEE (Inst. Elec. Electron Eng.)*, *Trans. Nucl. Sci.*, 11(6): 145 (1964).
2. D. Miller, P. Schlosser, J. Burt, D. D. Glower, and J. M. McNeilly, A Pulsed Radiation Energy Spectrometer Using Ferroelectrics, *IEEE (Inst. Elec. Electron. Eng.)*, *Trans. Nucl. Sci.*, 14(6): 245 (1967).
3. J. B. Birks, *The Theory and Practice of Scintillation Counting*, Chap. 11, The Macmillan Company, New York, 1964.
4. J. B. Birks, *The Theory and Practice of Scintillation Counting*, Chap. 6, The Macmillan Company, New York, 1964.
5. J. Kirkbride, E. C. Yates, and D. D. Crandall, Measurement of the Decay Time of Organic Scintillators, *Nucl. Instrum. Methods*, 52: 293 (1967).
6. J. Stevens and R. B. Knowlen, Transient Nonlinear Response of Plastic Scintillators, *IEEE (Inst. Elec. Electron. Eng.)*, *Trans. Nucl. Sci.*, 15(3): 136 (1968).
7. S. Kronenberg, High-Intensity Radiation Dosimetry with SEMIRAD, U. S. Army Research and Development Monograph Series, No. 3, 1966.
8. J. G. Kelly, Compton Diodes: Theory and Conjectures, USAEC Report SC-RR-67-855, Sandia Corporation, 1968.
9. P. J. Ebert and A. F. Langon, *Rev. Sci. Instrum.*, 38: 1747 (1967).
10. N. Klein, J. E. Fenning, Jr., and T. L. Smith, Measurement of X-Ray Pulses by Chemical Means, Report NDL-TR-115, Nuclear Defense Laboratories, 1968.
11. R. Gold, An Iterative Unfolding Method for Response Matrices, USAEC Report ANL-6984, Argonne National Laboratory, 1964.
12. F. S. Bechman, *Mathematical Methods for Digital Computers*, A. Ralston and H. S. Wilf, (Eds.), Chap. 4, John Wiley & Sons, Inc., New York, 1960.

DISCUSSION

DONNERT: I would like to comment on the detection system that has been tried out by the Nuclear Defense Laboratory (NDL) using the laser beam. What is actually observed is the change in the concentration of the solvated electron. The system, as was pointed out, has several advantages; the disadvantage, as the system now stands, is that it responds to neutrons and gamma radiation. Several years ago, before I left NDL, there was some serious discussion about getting differentiation between neutrons and gamma rays by using two detectors—one essentially a hydrogenous system and the other an essentially deuterated system. By getting both concentration–time traces, one ought to be able to distinguish between neutrons and gamma rays. Is there anything along those lines being done?

LUX: I do not know; I have seen nothing on the deuterated system.

6-3 DIGITAL REACTOR PERIOD COMPUTATIONS

E. S. KENNEY and M. A. SCHULTZ
Department of Nuclear Engineering, The Pennsylvania State University,
University Park, Pennsylvania

ABSTRACT

Three methods of digitally extracting reactor period are discussed for pulse-detector inputs. One of the methods discussed in this paper is explored in detail to investigate the limits of accuracy for pulse-detector input systems. Also, a simulation of the device proposed has been set up on a large digital computer to optimize the selectable parameters. Hybrid period systems for pulsing reactors are introduced with a limited treatment of their function.

INTRODUCTION

This paper reviews digital techniques of reactor-period computation and describes instruments developed by the authors and others which compute period by digital techniques. The object of this paper is not to discuss the use of large digital computers interfaced to conventional reactor information transducers; our interest lies rather in the area of reactor instrumentation channels that would replace conventional analog functions, unit by unit. We envision digital count-rate meters, digital linear power channels, and digital period meters which eventually would replace presently used analog units.

DIGITAL COUNT-RATE METERS

A very impressive paper on a wide-range digital count-rate meter was published by Vincent and Rowles[1] in 1963. By an ingenuous manipulation of data accumulated in a binary scaling system, they achieved the effect of an analog-circuit "smoothing" time constant.

Figure 1(a) shows the conventional linear analog count-rate meter (CRM) circuit with pulse-standardizing univibrator and diode pump. Figure 1(b) shows the additional circuitry required to produce a simple log count-rate meter (LCRM). Figure 1(c) shows a somewhat more precise multidecade log count-rate meter that takes advantage of the

(a)

(b)

(c)
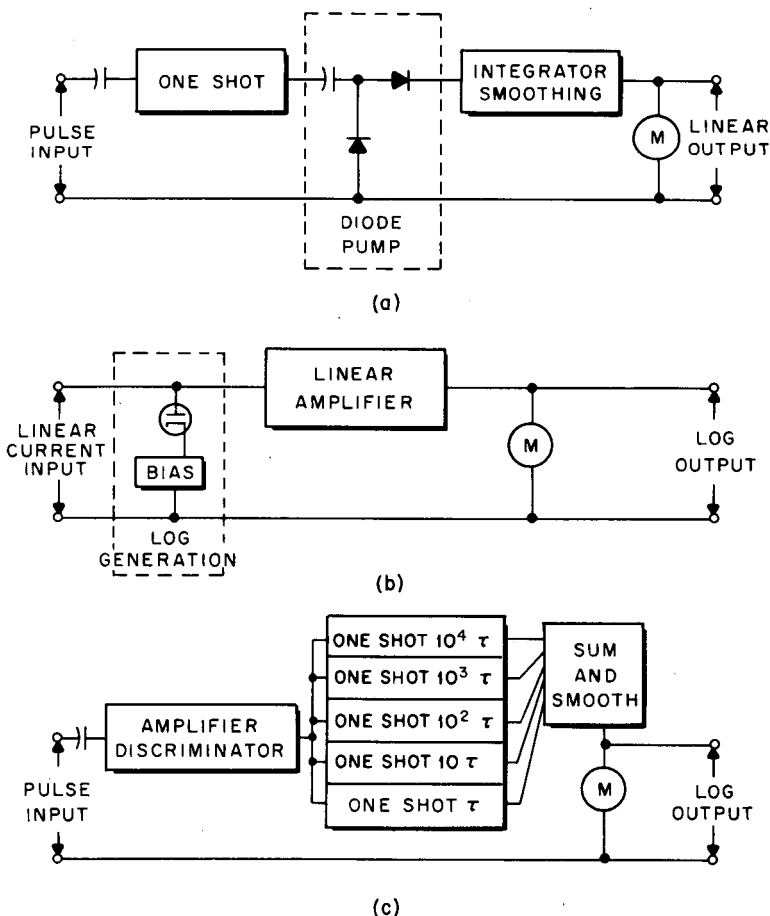
Fig. 1 — Analog count-rate meters. (a) Conventional analog count-rate meter. (b) Log count-rate meter. (c) Multidecade count-rate meter.

saturation characteristics of several single-stage systems. This last system can confine LCRM errors to a small fraction of a decade over five decades.

The digital CRM system of Vincent and Rowles is shown in simplified block-diagram form in Fig. 2. The operation of this unit illustrates the design of both a practical CRM and the ultimate function of a precise

logarithm-extraction period computer. Digitally, to simulate the effect of a time constant, one wishes to produce the behavior shown in Eq. 1:

$$C = C_\infty (1 - e^{-\alpha t}) \qquad (1)$$

This can be done by accumulating counts over a set period of time and then subtracting a constant fraction of the total accumulated counts.
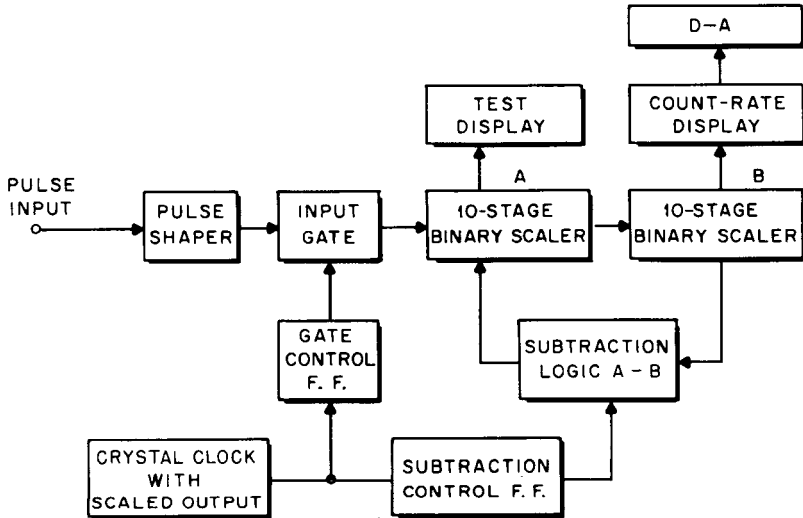
Fig. 2—Simplified block diagram of the digital CRM of Vincent and Rowles.

This procedure is cycled continuously, adding C_r counts each cycle and subtracting a fraction $\alpha C(t)$ of the total accumulated counts. In fact, one recognizes the analogy to the basic differential equation

$$dC(t) = [C_r - \alpha C(t)] \, dt \qquad (2)$$

which has Eq. 1 as its solution. Performing this manipulation with binary scaling equipment is simple in concept, but it does require a sizeable amount of basic digital hardware. However, with modern integrated circuits the implementation of this concept is quite practical.

An additional comment is needed to clarify the operation of Vincent and Rowles' system. Specifically, a constant fraction of a number is automatically available in any scaler to the base upon which the scaler operates, i.e., the base 2 for a binary scaler. In the system described in Fig. 2, the fraction used was 2^{-10} or 1/1024; it was obtained by interrogating stages 11 through 20 of the scaler.

It is worthwhile to mention that recorder outputs and analog meter indications are readily available by simple D—A conversion. Moreover, punched paper tape, printer, or other digital records are also available for direct computer input or permanent files.

Another interesting approach to digital count-rate meters and period extraction was reported by Fuan, Furet, and Kaiser,[2] in 1966. These authors addressed themselves to the problem of the large power and consequent count-rate changes which occur during normal reactor start-up and operation. They developed a rate meter with an automatic change of counting time corresponding to changes of input rate. They thereby achieved a control of the statistical error. Their system also used a logic-switching circuit to select one of two different sensitivity amplifier—detector assemblies to expand the overall dynamic range of operation. A detailed description of their period computation method will be presented later.

BACKGROUND OF DIGITAL PERIOD COMPUTATION

Figures 3(a) and (b) show the usual simplified analog reactor power-period system and a digital system of the same format. In designing a digital period system, the first thought that might occur to the engineer is to reproduce the functions of the analog system directly on a one-for-one basis. Knowing that the conventional determination of period is based on first extracting a voltage proportional to the logarithm of power and then differentiating this signal, designers have first looked for ways of digitally extracting the logarithm of a signal. Fuan, Furet, and Kaiser[2] and Vincent, Rowles, and Steels[3] have done this by very clever utilization of binary logic. In the work of Fuan, Furet, and Kaiser, about 200 transistors and 200 diodes were required for the period computer.

In Fig. 4, the basics of the process of extracting a logarithm with binary logic are illustrated based on the Vincent approach. Recalling how a time-constant effect was achieved by subtraction of a constant fraction of the total of the stored counts each cycle, one can easily make the small step to the formation of a logarithm. Instead of one subtraction at the end of a count, the subtraction process is repeated until the count accumulated in the scaler is reduced to some preselected level. The number of subtractions necessary to reach the preselected level is the logarithm of the stored number to a precision dictated by the fractional value selected in the subtraction process, plus a constant.

From Fig. 4 it is clear that an exponential decrease of the original count is occurring; that is, in any time Δt, the count is reduced by a constant fraction of the remaining count. This process leads to an approximation of a decreasing exponential. If one chooses to stop the sub-
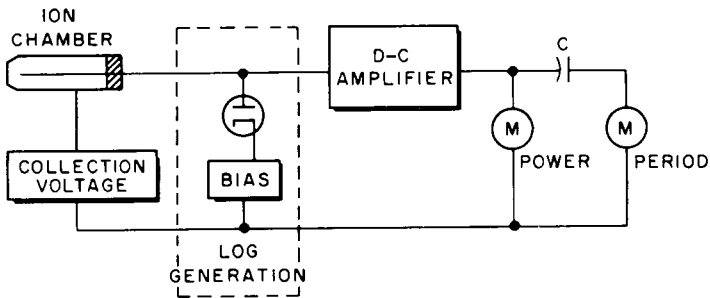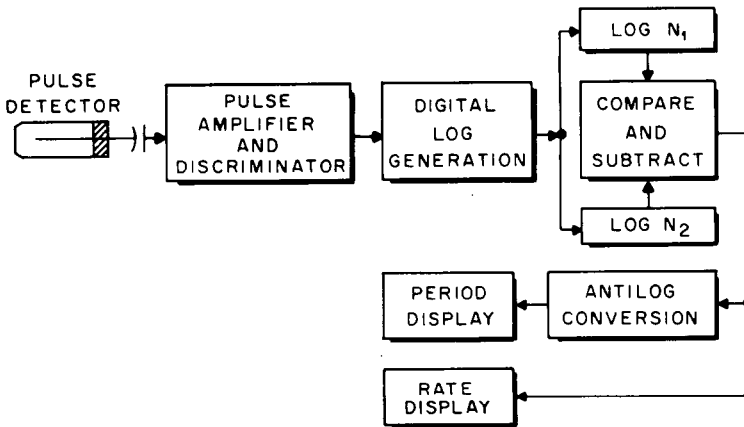
Fig. 3—(a) Conventional analog reactor-period system and (b) the digital counterpart.

traction process at some minimum count, C_0, the number of subtractions, N, is a direct measure of the logarithm of the original count as shown in Eq. 3, where the increments are reduced to the differential limits,

$$\ln C_r = \ln C_0 + \alpha N \tag{3}$$

From Fig. 3(b) reactor period is computed by subtracting two sequential logarithms. Note that the logarithm of the constant C_0 is eliminated.

A reactor increasing in power on a constant period follows the simple exponential expression

$$P = P_0 \, e^{t/T} \tag{4}$$

NUMBER OF SUBTRACTIONS (N)
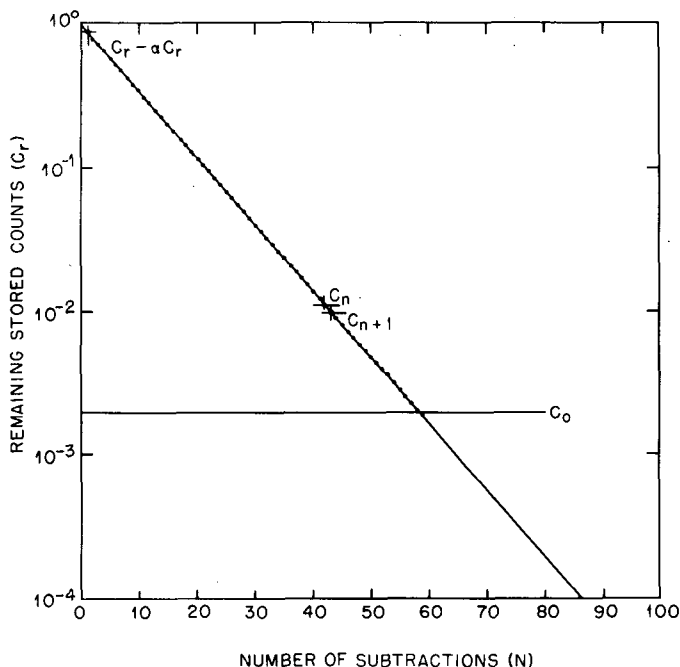
Fig. 4—Digital generation of the logarithm of a number C_r.

where T is the reactor period. Taking logarithms of power at two se-
quential times yields

$$\ln P_1 - \ln P_2 = \frac{\Delta t}{T} \qquad (5)$$

An increment of N from Eq. 3 and Δt in Eq. 5 are obviously related by
the clock frequency in the computer. Power and counting rate are here
considered to be equivalent.

From Eq. 5 it is clear that both analog and digital period meters of
conventional design compute the inverse period or the rate of change of
power with time. On an analog period meter the inversion to period units
in seconds is taken care of by calibrating the readout meter backward,
reading from infinity to something like 1 sec as a maximum indication.
Fuan produced the necessary inversion for the digital system by com-
puting the logarithm of the difference of the logarithms of the counts
and then executing an antilogarithm computation to obtain T. From the
standpoint of the operation of a reactor, the inverse period or rate of
reactor power change is a perfectly usable quantity, and the extra com-
putation to obtain the period appears to be quite unnecessary in prac-

tice. In fact many power reactors use inverse-period meters calibrated in such units as decades per minute.

Even though the logarithm approach is satisfactory, it is not the only means of producing a usable digital period computation. In fact, this approach appears unnecessarily complicated for certain applications. For example, one can write the equation for period as

$$\frac{1}{T} = \frac{1}{P}\frac{dP}{dt} \tag{6}$$

In finite difference notation, this equation becomes

$$\frac{1}{T} = \frac{1}{P}\frac{\Delta P}{\Delta t} \tag{7}$$

Since Δt can be fixed by a computer clock, the computation becomes

$$\frac{1}{T} = \frac{1}{\Delta t}\frac{\Delta P}{P} \tag{8}$$

The minimum digital computation necessary appears to require a subtraction of two counts equivalent to power at a fixed difference in time and then a division by a count also equivalent to power. The computation implied by Eq. 8 is restricted to small changes in power, and consequently, as will be shown later, is subject to a compromise between errors arising from counting statistics and those relating to the computing approximation.

Although additions and subtractions are easily performed digitally, a division requires some type of iteration or other multiple manipulation. To an additional degree of approximation, Eq. 8 can be written as

$$\frac{1}{T} = \frac{1}{\Delta t}\left[\frac{P_{n+1} - P_n}{P_n}\right] = \frac{1}{\Delta t}\left[\frac{P_{n+1}}{P_n} - 1\right] \tag{9}$$

Fuan used this latter form in an actual computer where only a division of two numbers had to be worked out. Figure 5 represents this computer in block diagram form. His procedure for division was simply to multiply P_n by a factor k and then find, by repeated subtractions, the number of times kP_n could be removed from P_{n+1}. Clearly k is some small convenient fraction of 1, i.e., 1/100 or 1/1000. The result of the division must be multiplied by k to obtain the quotient, but, with the proper choice of k, this is only a simple display manipulation. Further, if the computer were set to operate with Δt equal to 1 sec and if it were desired to display rate of power change in percent per second,
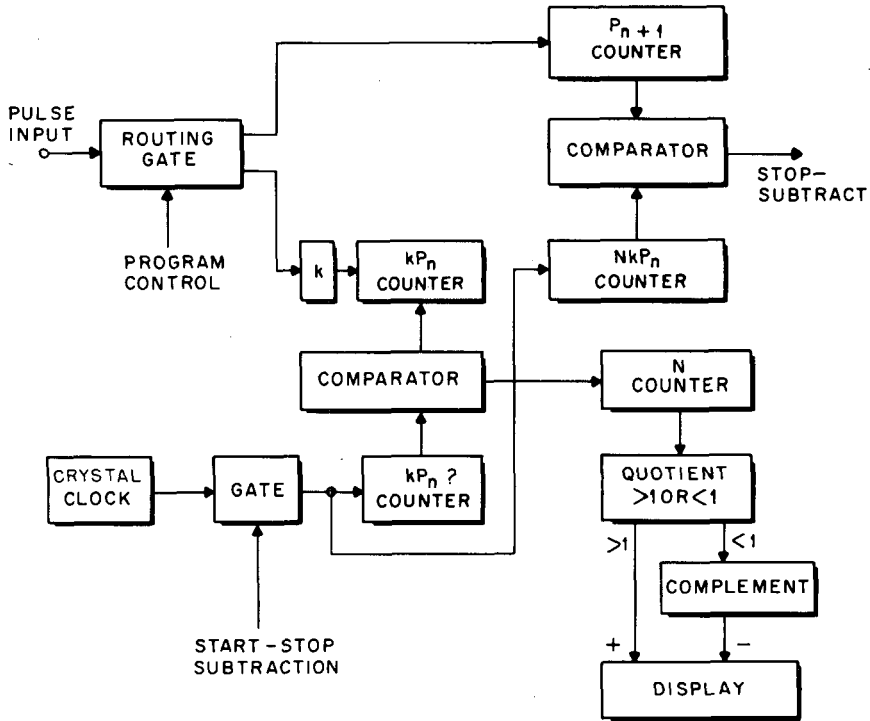
Fig. 5—Digital rate computer that divides by successive subtraction.

an interesting choice for k is 1/100. Then the result of the division is exactly the quantity wanted (percent of power change per second) after the computer subtracts the equivalent of (-1) in accordance with Eq. 9.

For this type of period computer, a negative period is sensed by a logic detection of a quotient of less than 1. When this situation occurs, the quotient is complemented before display. This sensing process also permits the selection for display of a plus or minus sign on the readout panel. Fuan, Furet, and Kaiser stated an accuracy of between 2000 and 50% for this computer, depending upon input signal rate.

MILLETRON PERIOD COMPUTER

Although Fuan's computer was simpler than Vincent's, it was felt that further investigation would prove worthwhile in three basic areas. First, it was determined that period rather than rate of change could be computed directly without complex manipulations. Second, it was believed that the accuracy of the Fuan system could be substantially improved by a study of the controlling parameters. Finally, it was be-

lieved that a system could be devised which would have a shorter dead time for sensing immediately a rapid power change (See Ref. 4.)

Figure 6 illustrates the basic principle of operation of a period computer as indicated in Ref. 4. This computer reads out period directly
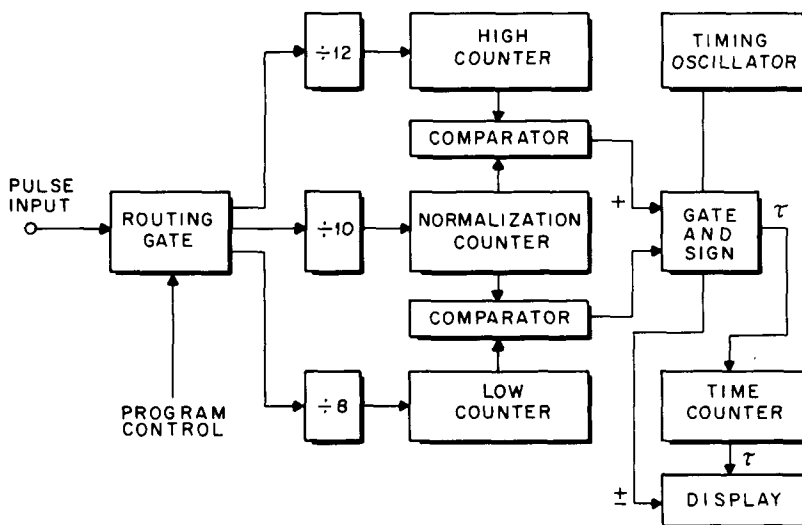
Fig. 6 — Period computer that measures time to achieve preset power change.

by simply counting the time required for the reactor power to increase or decrease by a set percentage. The principle of operation is based on another interpretation of the period equation

$$\ln P = \ln P_0 + \frac{t}{T} \tag{10}$$

or

$$\ln \frac{P}{P_0} = \frac{t}{T} \tag{11}$$

If we select P to be KP_0, then

$$\ln K = \frac{t}{T} \tag{12}$$

and

$$T = \frac{t}{\ln K} \tag{13}$$

The logarithm in Eq. 13 creates no problem in a computer since it is a fixed constant: a scale factor or an oscillator setting. The problem of computing period is thereby reduced to simply counting a scaled oscillator frequency while the reactor experiences a preselected power change. A division must still be performed in the computer but only by a fixed number. This process is very simple, as can be seen in Fig. 6.

Equation 13 must also be considered for negative periods. In this case, since t is always positive, ln K must take on a different fixed value. It must, of course, represent a power decrease, and therefore it is numerically less than zero. It is also of slightly greater absolute magnitude. From Fig. 6 it can be seen that positive and negative periods are computed by simultaneously checking for power increases or decreases. Comparators are used to sense the time increment during which the power has decreased or increased to preselected factors.

In operation, as indicated in Figs. 6 and 7, a period computation starts with a normalization count that is prescaled by a factor of 10. This count is equivalent to P_0 and is stored until one of the comparators senses that the power has increased or decreased by 20%. At the end of the normalization count, the period clock counter is started. This clock will accumulate pulses from a master oscillator until one of the comparators fires. When a comparator fires, it causes the period clock counter to display its contents, and it also selects a plus or minus sign as required.

In the interest of simplicity, the difference in the $|1/\ln K|$ factors for positive and negative periods can be ignored for most practical work. For the described computer, the oscillator was adjusted to yield the proper positive periods whereas the negative periods were in error by a small, but known amount. Using dual clock counters and separate oscillators, one could eliminate this error. It could also be eliminated by a manipulation during transfer to display.

Note that the indicated prescale factors of 8, 10, and 12 are used for illustration to set up K values of K = 0.8, K = 1, and K = 1.2. Any other related combination may be wired in to adjust computation speed or accuracy. A second point worth emphasizing is that the $\div 8$ and $\div 12$ counters function as rate meters, starting at zero and accumulating counts over a preselected gate time to check for a comparison. If a comparison is not reached, the counters are reset to zero, and a new count is initiated. Counting and resetting would then be continued until comparison is achieved in either the $\div 8$ or $\div 12$ scalers. Clearly the precision of time resolution is limited to the width of a counting-gate interval as can be seen in Fig. 7. For example, if a gating time of 0.1 sec were used and $|1/\ln K| = 5$, a 30-sec period would be computed in 6 sec. This computation would require 60 gating intervals; it would result in a time resolution of 1 part in 60.
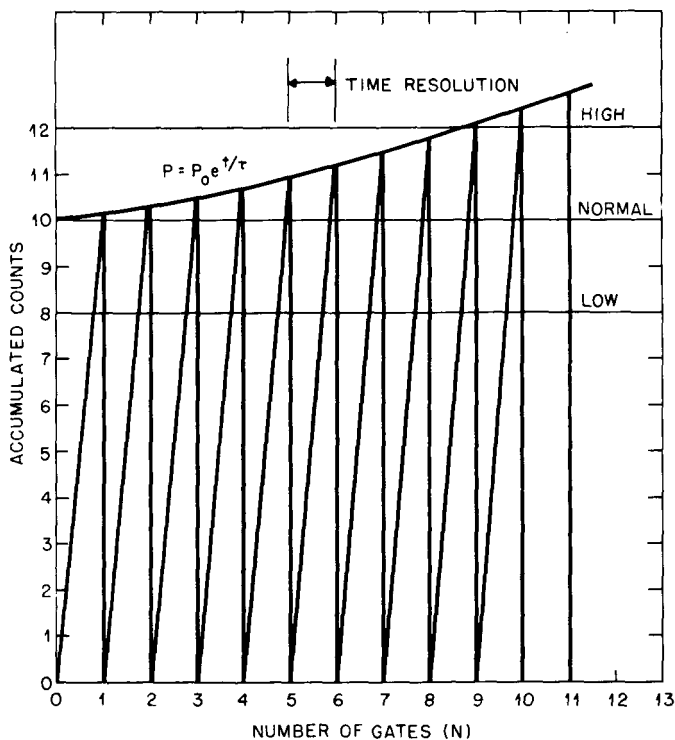
Fig. 7—Relative counts scaled into the high and low counters during an exponential reactor-power increase.

FACTORS INFLUENCING PERIOD COMPUTATION ERROR

The digital period computer just described is quite simple; this simplicity is gained at the sacrifice of some accuracy. Since the comparison counters continuously discard data until a comparison is achieved, the available information on reactor power is not used to maximum efficiency. On the other hand, one cannot compute period to any respectable precision in any similar system using consecutive short gating times with ordinary counting tubes. For example, a BF_3 counter can be operated up to about 1 megahertz pulse output rate. In a time interval of $1/10$ sec, if a reactor is on a long period, it may only change power by a small fraction of 1%. Clearly one could not reliably distinguish such a power change above the statistical fluctuations of the detector output. Because of the quality of the information available from conventional pulse counters, the reactor must be allowed to change power level by several percent before period can be computed to an acceptable precision.

Figure 8 shows a model used to investigate the effect of the allowed power change in digital period computation. Also shown in this figure is a linearized representation of an increasing reactor-power trace and the $\pm 1\sigma$ error band expected for a count-rate sensing of the power level. Using the -1σ deviation for a possible normalization count and a $+1\sigma$ deviation for a subsequent comparison count, we may devise a measure of timing or period error in computation. The timing error, ϵ, can be shown to be

$$\epsilon = \frac{T - t_1}{T} = 1 - \frac{t_1}{T} = 1 - \frac{K(N_0 - \sqrt{N_0}) - \sqrt{N_0} - N_0}{K \ N_0 - N_0} \tag{14}$$

which reduces to

$$\epsilon = \frac{1}{\sqrt{N_0}} \left(\frac{K + 1}{K - 1} \right) \tag{15}$$

In these equations, N_0 represents the expected counting rate at $t = 0$, K is the power increase being sensed, T is the time the power increase should require, and t_1 is the possible shorter time measured under the assumptions of $\pm 1\sigma$ counting fluctuations noted previously.

Equation 15 shows that one can reduce error with high counting rates. However, Fig. 8(b) shows that within the limits of present-day counters, power changes of the order of 20% are necessary for reasonable computation error. For example, a counting rate of 10^6/sec using 1-sec accumulation times would yield 1% accuracy in the computation of period for 20% power change. This accuracy could be improved by taking longer counts or demanding a larger power change. If $K = 2$, 10^6 accumulated counts per sample would yield 0.3% period-computation accuracy.

The functions of the device shown in Fig. 6 were programmed at Pennsylvania State University on an IBM 360 to examine more completely the problem of accuracy in a digital period meter. Figure 9 illustrates the errors observed for a set of fixed periods as the simulated reactor power was increased. Various periods were selected, as were several values of K, the power-change factor. The results clearly substantiate, in principle, the predictions of Eq. 15.

In the digital simulation, the reactor-power increase was taken to follow the expected exponential behavior. The data used to compute power as observed by a BF_3 counter were generated in the computer by a method used for function generation in Monte Carlo computations. A Gaussian statistical distribution was entered with 1000 increments of dispersion. For a given true power, a random-number selection of a possible count-rate determination provided a simulation of the situation
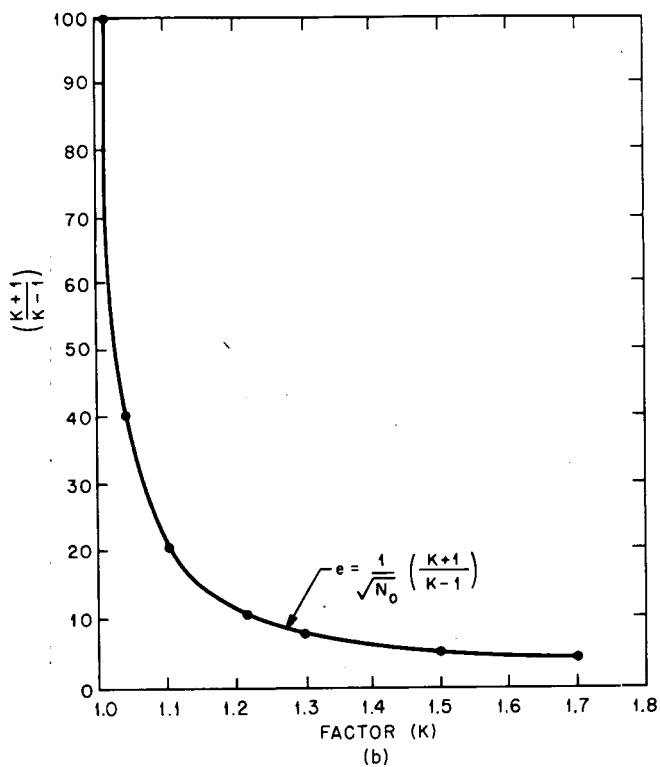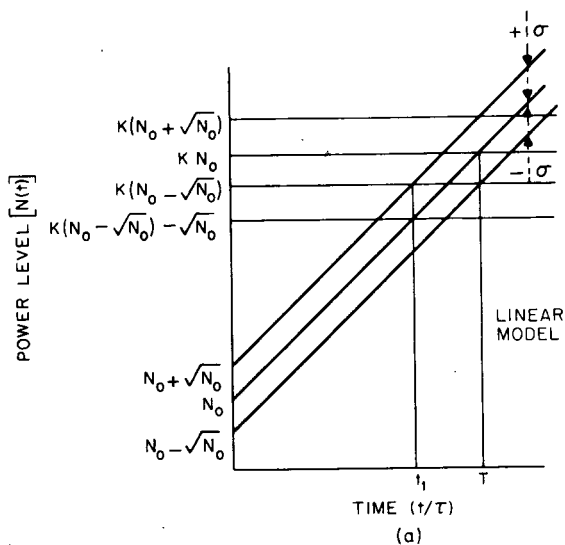
Fig. 8— (a) Model for investigating the effect of selected power-change factor on digital computation of period. (b) Linearized representation of an increasing reactor-power trace.
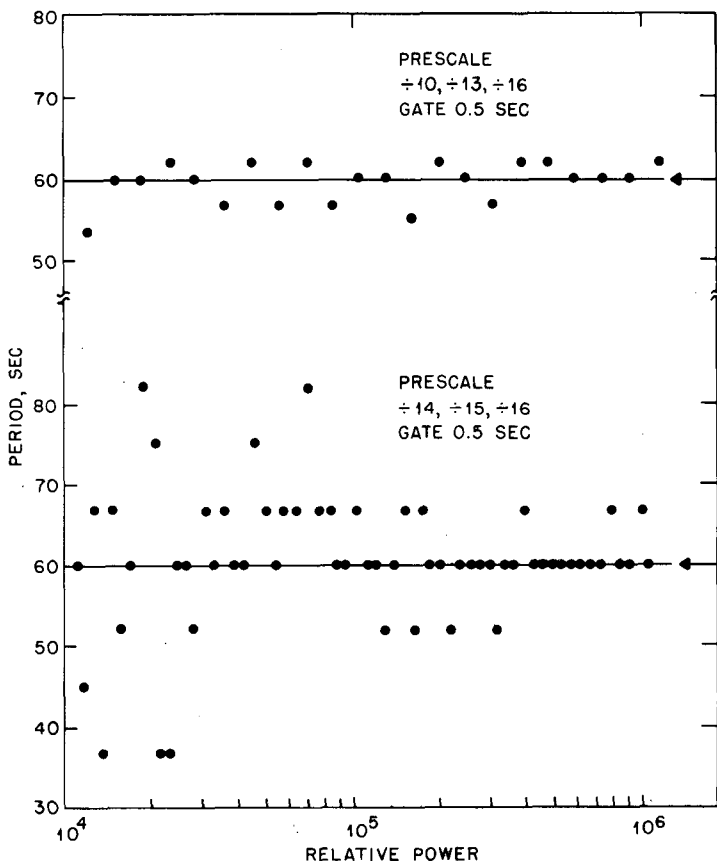
Fig. 9— Output of period-computer simulation for constant positive 60 period.

the digital period meter would experience with the BF_3 pulse-counter input. The IBM 360 then proceeded to compute period exactly as the actual period computer would.

DIGITAL PERIOD COMPUTATION IN PULSING REACTORS

Using pulse-counter inputs, digital computation of power and period in pulsing reactors is difficult. For a slow pulsing machine, such as a TRIGA, time resolution on the order of 1 msec is necessary to define the power as a function of time. Within 1 msec even a counter delivering a 1-megahertz rate will only accumulate 1000 events. Such a counter will be useful only over about the top decade of a reactor pulse. Systems using BF_3 or fission-chamber counters are thus very restricted in use for pulsing reactors.

Figure 10 shows a hybrid system that can measure reactor period in fast pulsing reactors.[5] The circuit was originally developed for the White Sands Fast Burst Reactor, and the block diagram of Fig. 10 is from an Oak Ridge National Laboratory schematic modified by Mille-tron, Inc., for use on the Army Pulse Radiation Facility Reactor. The
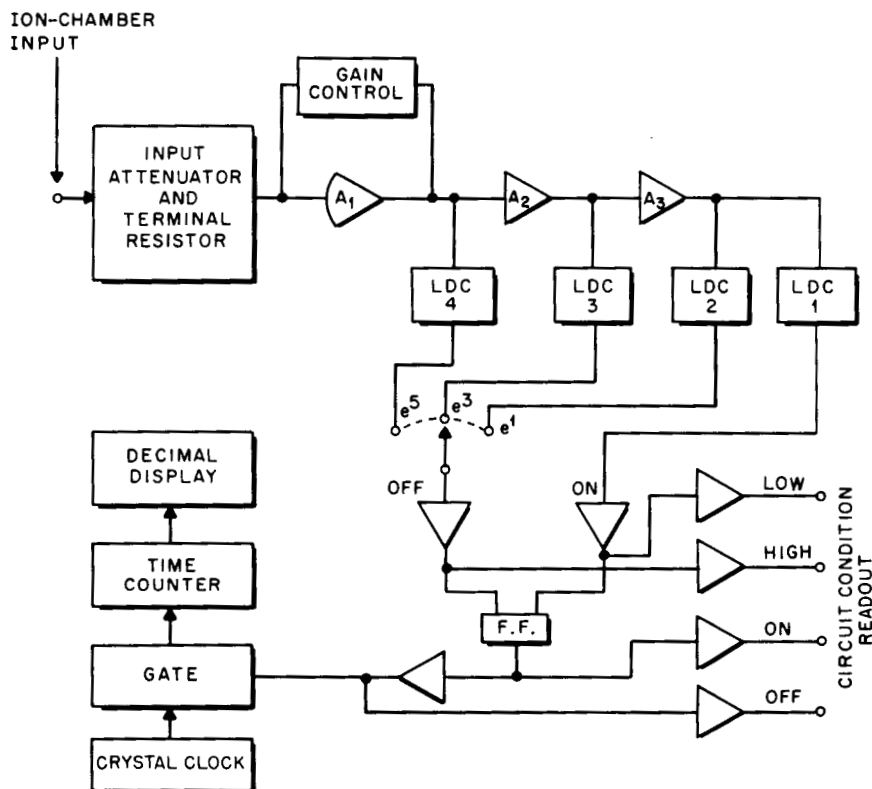
Fig. 10—Hybrid prompt-period meter.

circuit simply finds the e-folding time of a reactor. When a predeter-mined power level is sensed in LDC-1 (LDC stands for level-detection circuits), a clock is started which runs until LDC-2, 3, or 4 senses that the power has increased by e, e^3, or e^5. The accumulated time is a direct measure of period. This period computer uses current input signals and can function over a wider range of power than a pulse input system. It can work with very fast periods, being restricted only by the frequency response of the amplifiers and comparators.

Current input systems appear to have a substantial advantage over pulse input systems in respect to the information content of the in-

coming signals. A boron-lined reactor-power-detecting ion chamber will experience more than 10^{11} events/sec when providing an output signal of 1 ma. The maximum resolvable event rate in a fast BF_3 counter is only about 10^6/sec. The signal from a current chamber is clearly better than that from a pulse counter, as far as the statistical fluctuation of the signal is concerned. For fast pulsing reactors, some form of hybridizing appears necessary to produce a practical digital period meter.

In Fig. 11 the concept of the device in Fig. 10 is expanded. Rather than using a number of amplifiers, the comparison voltage or the level-
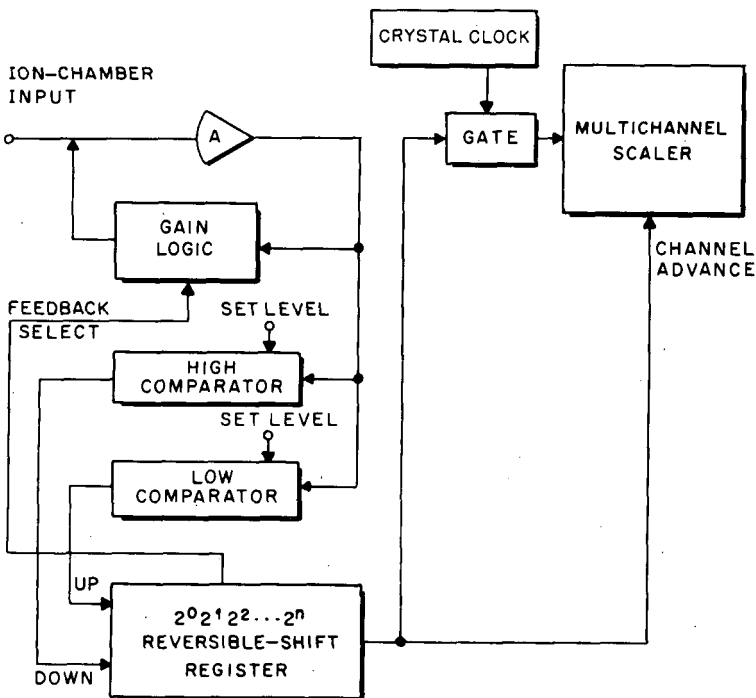
Fig. 11 — Proposed hybrid prompt-period meter providing sequential readings.

amplifier gain is increased or decreased by a factor of 2 each time comparison is achieved. In this way a continuous record of doubling time is accumulated in the multichannel scaler. This type of doubling-time presentation was mentioned very early by Schmidt, Eriksen, and Peil.[6] The multichannel scaler is moved to the next channel each time a power doubling is sensed. Dead time is encountered in shifting channels, particularly if a magnetic memory is used in the multichannel scaler. However, this dead time is known, and it can be added to the accumu-

lated time. Using 1-megahertz logic, this system should be quite adequate to follow a TRIGA reactor. With 100-megahertz logic, it should be usable with prompt burst reactors.

CONCLUSIONS

In view of the satisfactory performance that digital count-rate meters have achieved, they should now be seriously reviewed by instrument suppliers for incorporation into reactor start-up channels. Digital period meters operating on pulse counters can be made to provide usably accurate readings; however, their range is restricted, and the use of ion chambers with $D-A$ converters presently promises superior accuracy. At today's stage of development, pulse digital period meters appear to be of most use in reactor calibration and research. In this use one can tolerate factor of 2 power changes during period computation and still obtain outstanding accuracy. In routine reactor operation, periods must be computed for very small power changes where the pulse-counter method has difficulty generating usable accuracy.

For pulsing reactors a system that provides a single period reading for each pulse has been designed and constructed. A proposed system based on an expansion of the same concept illustrates that by hybridizing the period computer and using ion-chamber input, one should be able to compute period continuously with digital readout during a reactor pulse in the microsecond domain.

REFERENCES

1. C. H. Vincent and J. B. Rowles, A Digital Linear Rate Meter, *Nucl. Instrum. Methods*, 22: 201-220 (1963).
2. J. Fuan, J. Furet, and J. Kaiser, The Use of Digital Techniques for Nuclear Instrumentation, *IEEE (Inst. Elec. Electron Eng.), Trans. Nucl. Sci.*, 14(1): 233-240 (1967).
3. C. H. Vincent, J. B. Rowles, and R. A. W. Steels, A Precise Digital Period Meter for a Nuclear Reactor, *Nucl. Instrum. Methods*, 26: 221-237 (1964).
4. M. A. Schultz, T. Matty, and E. S. Kenney, Wide Range Digital Nuclear Instrumentation Channel. Phase I Study, USAEC Report NYO-3738-7, Milletron, Inc., May 30, 1967.
5. Thomas Matty, Milletron, Inc., personal communication.
6. J. O. Schmidt, B. K. Eriksen, and W. Peil, A Digital Start-up Control Unit for Nuclear Reactors, *IRE (Inst. Radio. Eng.) Trans. Nucl. Sci.*, 8(3): 1-12 (July 1961).

DISCUSSION

JOHNSON: I assume that this system is really only for information. You would never use it as part of a control circuit on a reactor would you?

KENNEY: You mean the last one or all the circuits I was describing?

JOHNSON: The general idea.

KENNEY: The idea? Well, we had hoped really to develop a digital device that would be satisfactory for use in controlling a reactor. We really had hoped to do it.

JOHNSON: It seems to me it would always be inherently inferior to an analog system because you would have to look at two points (in time).

KENNEY: Yes, I think the obvious deficiency of a pulse detector is here. As long as you try to work with a megacycle input, or even if you go to something more sophisticated and work with a 100-Mc input, you just have not improved the error situation that much; 10^8 events/sec compared with 10^{11} in an ionization chamber, and you still are not home free. So it seems to me that hybridization would be the only answer if you want to have digital readout.

6-4 A REVIEW OF SOME PASSIVE DOSIMETRY METHODS USED IN RADIATION-EFFECTS STUDIES WITH FAST BURST REACTORS

K. C. HUMPHERYS
Weapons Measurements Department, EG&G, Inc., Santa Barbara Division, Goleta, California

ABSTRACT

Some of the more important instruments and methods used to determine neutron fluence, neutron energy spectra, and gamma-ray dose during radiation-effects experiments with fast burst reactors are described and evaluated. General radiation-measurement problems encountered by radiation-effects investigators are summarized, and the fundamental principles on which various measurement techniques are based are outlined.

INTRODUCTION

Over the past decade, the fast burst reactor has won widespread acceptance as a convenient pulsed source of neutrons and gamma rays by investigators studying the effects of radiation on materials, components, and biological systems. In such studies the neutron fluence, neutron energy spectrum, and gamma-ray dose throughout the materials being irradiated must be known during any given pulse of the reactor. The time history of the radiation pulse is also important but is not considered to be within the scope of this paper.

The unique dosimetry requirements for radiation-effects experiments arise from the perturbations created in the free-field environment by the test samples and ancillary apparatus. Because of these perturbations, the investigator must measure the various dosimetric parameters on the actual experiment array or on a mock-up of it. In practice this involves making dosimetric and radiation measurements at many points on, in, and around the various items being irradiated. This necessity for large numbers of measurements during every experiment contrasts sharply with the requirements for mapping the

497

free-field radiation environment, in which case a single set of mea-
surements is usually sufficient to permanently define the neutron
fluence and gamma-ray dose throughout the reactor test cell.

Although numerous dosimetry methods, both dynamic and passive,
can be used to measure radiation environments, owing to the large
numbers of measurements required in radiation-effects experiments,
methods that use the comparatively smaller and less-complex passive
detectors have been and still are preferred. Typically, passive detec-
tors are easy to set up and handle during the experiment, and they can
be read out by the investigator at his convenience.

The review that follows summarizes some of the basic passive
dosimetry methods that have been used or considered for use in
radiation-effects experiments with fast burst reactors. Although the
treatment is by necessity somewhat cursory, the instruments and
methods described are well documented for the convenience of those
readers interested in more detailed information.

NEUTRON-FLUENCE MEASUREMENT

Most neutron-fluence and energy-spectra measurements on fast
burst reactors are made with neutron threshold foil techniques.[1-26]
Other passive techniques that may be applied in characterizing the
neutron environment include the use of nuclear emulsions[27-32] and
condenser-type ionization chambers.[33-35] In addition to these passive
techniques, a variety of dynamic-readout systems can also be used,
including proton-recoil counters,[36-40] solid-state spectrometers,[39-43]
intrinsic thermocouples,[44] and proportional LET chambers.[45,46] Al-
though these dynamic systems are not considered to be within the
scope of this review, it should be noted that even though they are
superior to the passive detectors in certain respects, because of the
complexity of dynamic-readout instrumentation, they are not expected
to replace passive techniques where large numbers of measurements
are required.

Threshold Foils

Many nuclear reactions of the types (n, particle) or (n, fission)
exhibit a threshold energy, E_t, below which the reaction does not occur
and above which it does. Materials that exhibit such a threshold energy
for some nuclear reaction represent a means of detecting the neutron
fluence above that energy. Hence, by using a series of such materials
as threshold detectors and by taking the differences in measured
fluences above various threshold energies, one can determine the
fluences in several energy increments and thus obtain information on
neutron energy spectra.

The cross section for the nuclear reaction rises from zero at the threshold energy and varies as a function of neutron energy above it. Furthermore, the threshold energy and cross section as a function of neutron energy are peculiar to each particular reaction. Many of the isotopes formed by these reactions are radioactive. In such cases, the quantity of radioisotope is obtained by measurement of the induced radioactivity of the foil. The neutron fluence above the threshold energy is then related to this value by the following expression:

$$\Phi_{E_t} = \int_{E_t}^{\infty} \phi(E) \, dE = \frac{A_0}{N} \frac{\int_{E_t}^{\infty} \phi(E) \, dE}{\int_0^{\infty} \sigma(E)\phi(E) \, dE} \tag{1}$$

where Φ_{E_t} = neutron fluence above threshold energy E_t (neutrons/cm^2)
$\phi(E)$ = differential neutron fluence as a function of energy [(neutrons/cm^2)/Mev]
A_0 = radioactivity induced in foil (dis/sec at zero decay time)
N = number of atoms in the foil subject to the reaction
$\sigma(E)$ = cross section for the reaction as a function of neutron energy (cm^2/atom)

The activity of a foil expressed in practical terms is

$$A_0 = \frac{CPM\epsilon}{e^{-\lambda t}} \tag{2}$$

where CPM is counts/min at time t, ϵ is counter efficiency, and $e^{-\lambda t}$ is correction for decay to time t. The number of atoms in the foil subject to the reaction is

$$N = \frac{WN_0 I}{M} \tag{3}$$

where W = foil weight (g)
N_0 = Avogadro number (atoms/mole)
I = isotopic purity in fractional weight
M = isotopic weight (g/mole)

Combining Eqs. 1, 2, and 3, we have

$$\Phi_{E_t} = \left(\frac{CPM}{\epsilon \, w \, e^{-\lambda t}} \frac{M}{N_0 I} \right) \frac{\int_{E_t}^{\infty} \phi(E) \, dE}{\int_0^{\infty} \sigma(E)\phi(E) \, dE} \tag{4}$$

In practice, for most neutron-fluence measurements, the threshold energy and the cross section as a function of neutron energy are replaced with an effective threshold energy, $E_{t_{eff}}$, and a constant effective

cross section, σ_{eff}, weighted by the expected neutron energy spectrum. Table 1 lists several nuclear reactions used as threshold detectors, along with their effective threshold energies and average cross sections, based upon a Watt fission spectrum. Because of the range of neutron energies of interest with a fast burst reactor, only the first four of the listed threshold reactions are customarily used.

Table 1

NEUTRON THRESHOLD DETECTORS

Material	Reaction	Effective threshold energy ($E_{t_{eff}}$), Mev	Effective cross section, 10^{-24} cm^2
^{239}Pu	^{239}Pu(n,f) F.P.	0.010	1.7
^{237}Np	^{237}Np(n,f) F.P.	0.60	1.6
^{238}U	^{238}U(n,f) F.P.	1.5	0.55
^{32}S	^{32}S(n,p)^{32}P	3.0	0.30
^{58}Ni	^{58}Ni(n,p)^{58}Co	3.0	0.29
^{31}P	^{31}P(n,p)^{31}Si	2.5	0.08
^{28}Si	^{28}Si(n,p)^{23}Al	5.5	0.05
^{24}Mg	^{24}Mg(n,p)^{24}Na	6.3	0.05
^{27}Al	^{27}Al(n,α)^{24}Na	8.1	0.11
^{127}I	^{127}I(n,2n)^{126}I	11.0	0.98
^{75}As	^{75}As(n,2n)^{74}As	12.0	1.30
^{90}Zr	^{90}Zr(n,2n)^{89}Zr	14.0	1.60

The true cross section, which varies with neutron energy, is related to a constant idealized cross section above an effective threshold energy as follows:

$$\sigma_{eff} \int_{E_{t_{eff}}}^{\infty} \phi(E)\ dE = \int_0^{\infty} \sigma(E)\phi(E)\ dE \qquad (5)$$

where σ_{eff} is effective cross section and $E_{t_{eff}}$ is effective threshold energy.

Figure 1 shows the idealized cross sections for ^{237}Np and ^{238}U along with their true cross sections. The effective cross section and effective threshold energy are normally specified for a particular neutron spectral distribution, such as a Watt fission spectrum. Figures 2 through 5 are graphs of the effective cross section vs. effective threshold energy for a Watt fission spectrum, a Godiva reactor spectrum, and several assumed extreme spectra for the four most widely used threshold foils. Also shown are the effective cross sections and threshold energy values recommended by the American Society for Testing and Materials.

Although there have been no recent developments in the basic threshold foil technique, additional threshold reactions have been found, and improvements have been made in data-handling techniques.
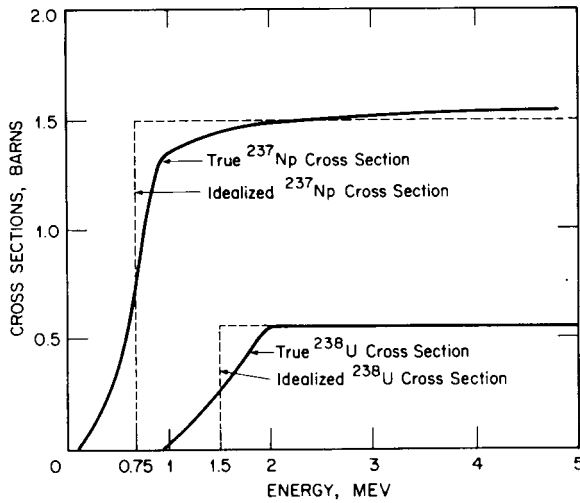
Fig. 1 — *Idealized approximations to cross sections of* ^{237}Np *and* ^{238}U.
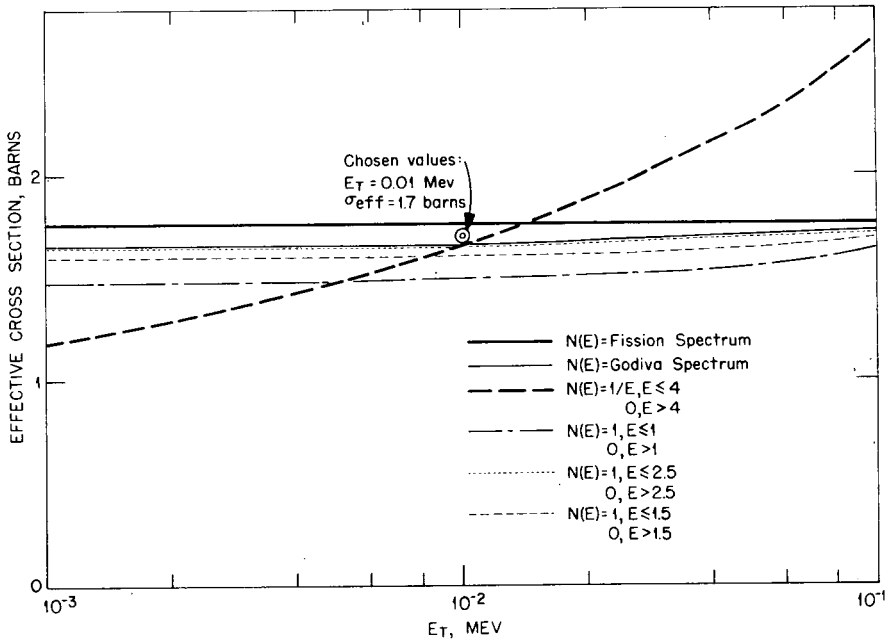
Fig. 2 — *Effective cross section vs. threshold energy for various spectra,* ^{234}Pu *covered with 1.65 g/cm^2 of* ^{10}B. *(Taken from Ref. 18.)*

EFFECTIVE CROSS SECTION, BARNS

Chosen values:
E_T = 0.6 Mev
σ_{eff} = 1.65 barns

N(E) = Fission Spectrum
N(E) = Godiva Spectrum
N(E) = 1/E, E ≤ 2
        0, E > 2
N(E) = 1/E ≤ 1.25
        0, E > 1.25
N(E) = 1, E ≤ 3
        0, E > 3
N(E) = E, E ≤ 1.25
        0, E > 1.25

E_T, MEV
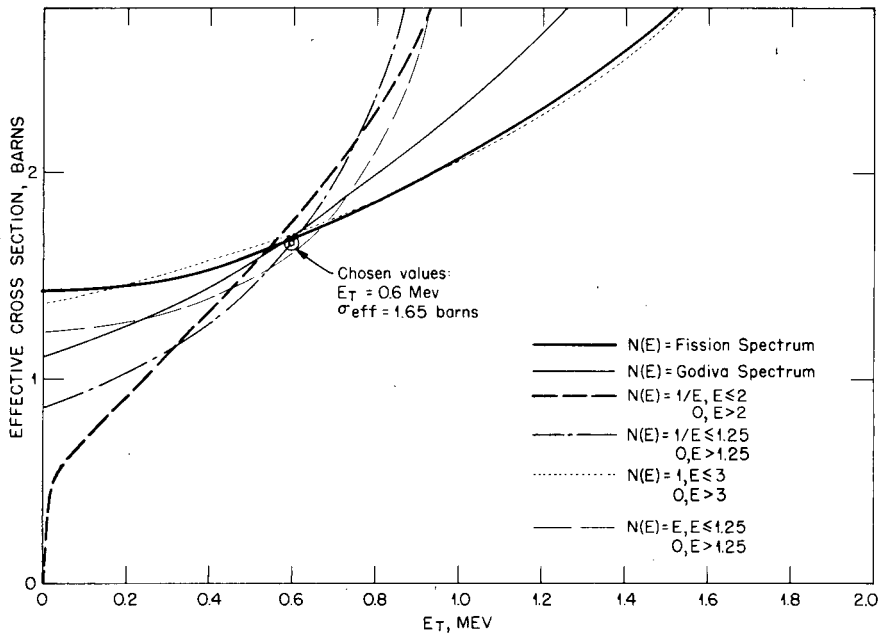
Fig. 3—*Effective cross section vs. threshold energy for various spectra,*
^{237}Np.[18]

EFFECTIVE CROSS SECTION, BARNS

N(E) = Fission Spectrum
N(E) = Godiva Spectrum
N(E) = 1/E, E ≤ 3
        0, E > 3
N(E) = 1, E ≤ 2
        0, E > 2
N(E) = 1, E ≤ 3
        0, E > 3
N(E) = E, E ≤ 3
        0, E > 3

Chosen values:
E_T = 1.5 Mev
σ_{eff} = 0.55 barns

E_T, MEV
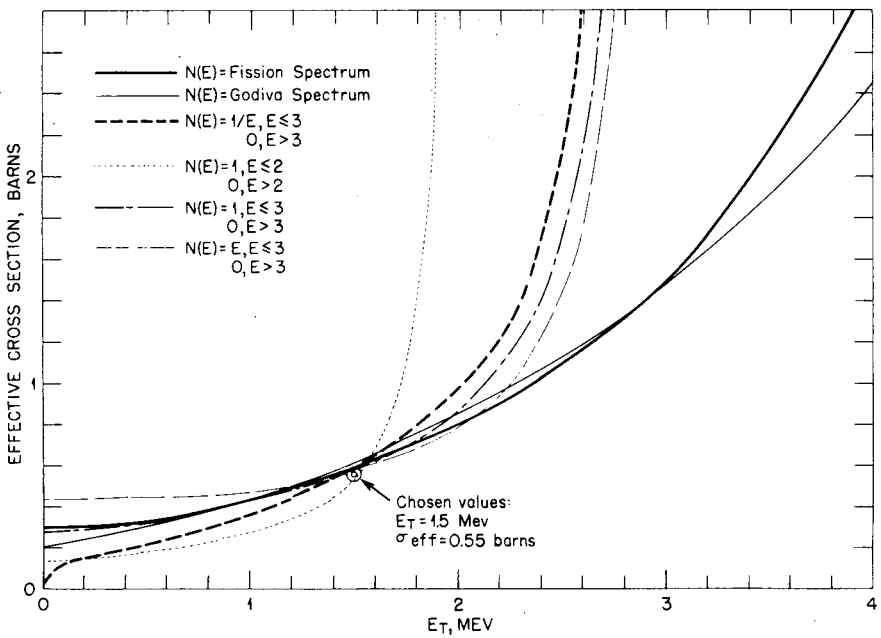
Fig. 4—*Effective cross section vs. threshold energy for various spectra,* ^{238}U.[18]
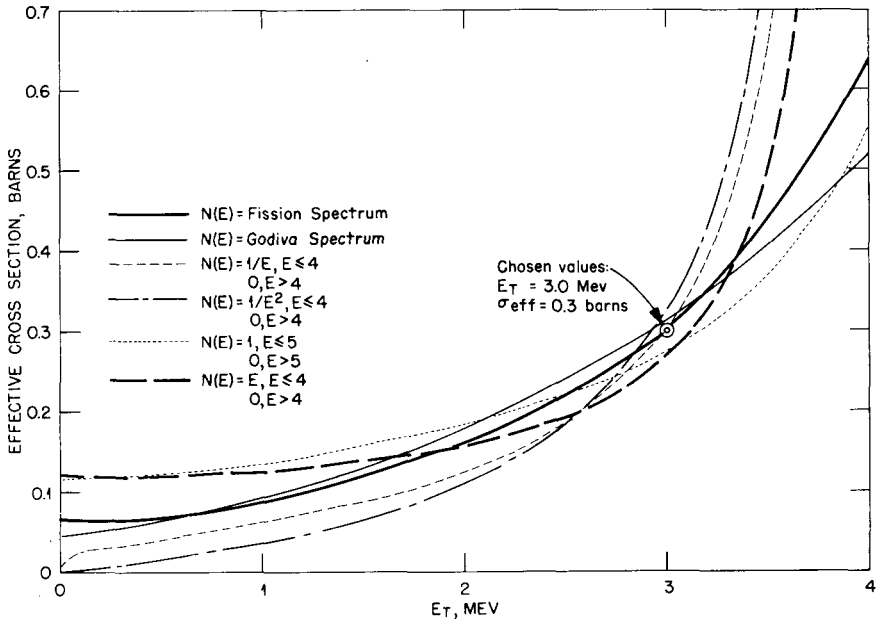
Fig. 5—Effective cross section vs. threshold energy for various spectra, ^{32}S.[18]

Several computer codes have been developed to allow true cross sections as a function of neutron energy for the threshold foils to be used rather than an effective or idealized constant value. In this way one can obtain a complete differential neutron energy spectrum instead of the usual limited breakdown of the spectrum into several energy increments. The technique essentially involves forming a set of simultaneous equations, expressing threshold foil activities as functions of differential spectra, and obtaining a spectrum for which calculated activities agree with the measured activities of the foils. The spectral shape is determined only to the extent that the response functions, or cross sections, of the various threshold foils are linearly independent. At least three computer codes have been developed for this purpose: SAND-II,[47-49] SPECTRA,[50] and RDMM.[51,52]

Nuclear Emulsions

A recoil proton moving through a film emulsion causes ionization along its path, which results in a blackened track in the developed emulsion. The proton energy can be determined from the track length and known range-energy relations. If the neutron direction is known, the neutron energy can then be calculated by

$$E_p = E_n \cos \theta \tag{6}$$

In practice, the nuclear emulsion is usually placed at an angle of 10° with respect to the neutron beam, and all tracks that fall within a 15° cone are accepted for analysis. Thus Eq. 6 simply becomes $E_p = E_n$ to within approximately 4% for those tracks measured.

Significant use of nuclear emulsions has been made for absolute measurement of reactor neutron energy spectra inside fast reactors.[28-32] The nuclear-emulsion measurement of the Godiva I neutron spectrum by Frye, Gammel, and Rosen[27] in 1951 stands as classic among the neutron-spectrum measurements of fast burst reactors. The handling of emulsions is, however, complex and time consuming. Special processing is required, emulsion shrinkage occurs and must be accounted for, and visual microscopic track measurements take many hours of painstaking effort. Therefore, although this method does represent, and has been used for, basic absolute neutron energy spectral measurements, it is not generally used in radiation-effects and radiobiological programs.

Ionization Chambers

Many radiation effects of a biological or physical nature are related to the energy that charged particles impart to material. A historically preferred method of determining this energy deposition involves measuring the ionization of a gas in a small cavity within the material and inferring from this measurement the energy deposition in the surrounding medium. Such ion-chamber measurements, which are based upon the Bragg–Gray principle and the Spencer–Attix theory, can be made with the condenser type of ionization chamber shown in Fig. 6.

This method of dosimetry does not by itself distinguish between energy deposition in a material from the neutron and gamma rays. Instead, it simply gives the total energy deposition by both neutron and gamma rays in the particular material from which the ion chamber is constructed. Although this detection characteristic limits the usefulness of the method in materials studies, it does not affect its application in radiobiological studies, where ion chambers constructed of tissue-equivalent electrically conducting plastic are used extensively for measuring tissue dose.

GAMMA-RAY DOSE MEASUREMENTS

The dosimetry methods most widely used to measure gamma-ray dose in radiation-effects experiments are those which are based on
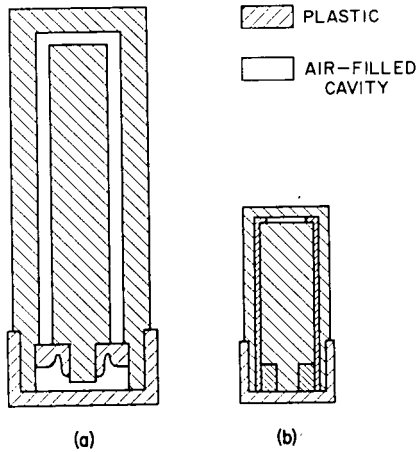
Fig. 6—High-range tissue-equivalent ion chambers. (a) 0 to 10 rads. (b) 0 to 1000 rads.

radiation-induced changes in the luminescent and optical-absorption properties of various glasses and in the luminescent properties of crystalline materials, such as alkali–halide phosphors. Other passive methods that can be used are based on radiation-induced changes in various chemicals. Also available are a number of dynamic-readout-type ionization chambers and scintillation detectors that measure gamma-ray dose rate and pulse shape as well as gamma-ray dose. However, as in the case of neutron-fluence measurement, passive dosimetry methods are preferred where large numbers of measurements are required.

The types of radiation-induced luminescent and optical changes in materials which form the basis for dosimetry measurements are thermoluminescence,[53-56] degradation of natural photoluminescence,[57-60] radiation-induced photoluminescence,[61-66] and variation in optical density.[67-69] Except for the degradation of natural photoluminescence, all these radiation-induced changes are used extensively in gamma dosimetry.

The various radiation-induced chemical reactions that can be used for dosimetry measurements include oxidation–reduction, decomposition, acid formation, optical-density changes, and optical rotation. Chemicals that show oxidation–reduction or decomposition when irradiated have been the most commonly used in chemical dosimeters.

The gamma-ray dosimeters most commonly used in radiation-effects experiments with the fast burst reactor are described in the following sections. Also described are several miscellaneous systems of current or future importance to general gamma-ray dosimetry.

Thermoluminescent Dosimeters

Thermoluminescence, broadly defined as the emission of light when a solid is heated to a temperature below that of incandescence, is not new. In fact it is only a special case of phosphorescence. Since 1883 when Becquerel[53] published his first report on work in this field, a variety of thermoluminescent materials have been investigated, and a wealth of information on the subject is available in the literature. The bibliography compiled by Angino, Grogler, and McCall[54] is an excellent guide to the literature on thermoluminescence, and Refs. 55 and 56 are of specific interest as an introduction to the entire field of luminescence.

Of the many thermoluminescent phosphors available, manganese-activated calcium fluoride (CaF_2: Mn) and lithium fluoride (LiF) have proven most practical for dosimetry applications. Ionizing radiation raises bound electrons into the conduction band in these phosphors. The electrons are stored in the metastable state until the application of thermal energy at some later time allows them to return to the ground state, accompanied by the emission of visible light. The intensity of the emitted light is directly related to the radiation exposure received by the phosphor.

These thermoluminescent dosimeter (TLD) materials are available as a powder, as small phosphor-filled glass needles, and as hot-pressed chips or rods (see Fig. 7). Below approximately 200 kev, energy-correction shields are necessary for the CaF_2: Mn dosimeters but not for the LiF dosimeters. However, in high-thermal-neutron environments, suitable neutron shields must be used with both dosimeters. Figure 8 shows the energy response for both TLD materials. The usable range of these TLD's varies slightly according to the form of the material. The overall range is, however, on the order of 10^{-2} to 10^5 r.

Glass Dosimeters

At radiation exposure levels below about 10^3 r, changes occur in the luminescent properties of certain glasses; at higher levels, changes occur in their absorption spectrum. Based on these changes in luminescence and absorption, a number of glasses have been developed specifically for dosimetry applications.[61-66] Two of the most widely used of these are silver-activated phosphate glass and cobalt glass. A recently developed bismuth glass is expected to receive wide acceptance as a dosimeter material for measuring very high dose levels. In general, these glasses form sturdy, simple, relatively accurate dosimeters that are easy to handle and analyze, and they are reusable. However, since glass generally has a higher Z value than tissue, air,
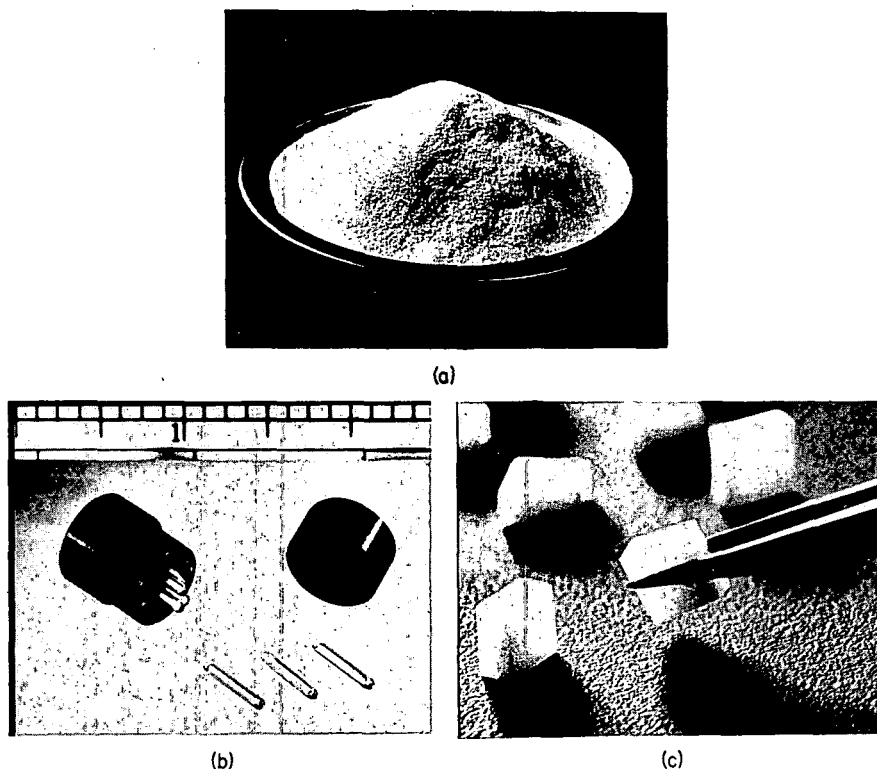
Fig. 7 — Thermoluminescent dosimeters. (a) Phosphor powder. (b) Glass needles filled with phosphor powder. (c) Phosphor chips.

or water, it will usually exhibit an over-response relative to these materials at low gamma-ray energies. Energy shields are therefore required with these dosimeters to obtain a flat or uniform response. Table 2 lists the dosimeters and their characteristics. Figure 9 shows the various forms of the dosimeters and their energy shields, and Fig. 10 shows the shielded and unshielded energy response of the silver-phosphate and cobalt-glass dosimeters.

Use of the silver-activated phosphate-glass dosimeter[65,66] is based on the production of ultraviolet-excited luminescent centers by ionizing radiation. The exact photochemical reaction is not known, but it is presumed that a positive ion traps an electron at some preferred energy level. An exponential buildup of luminescence for a short time after irradiation indicates that other electron levels are also filled but soon decay to the final state in the region of interest. Illumination by ultraviolet light raises these bound electrons to a higher state from which they return to the ground state with emission of their charac-
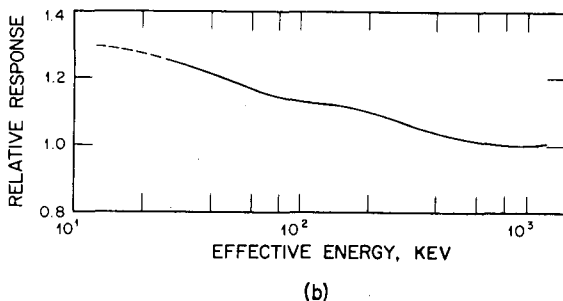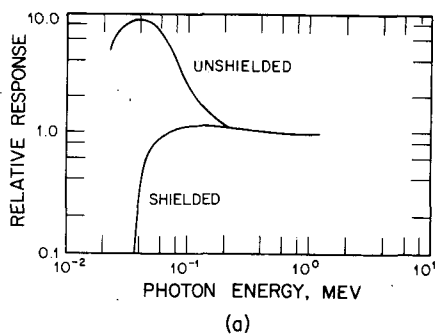
Fig. 8 — Thermoluminescent-dosimeter energy response. (a) Calcium fluoride.
(b) Lithium fluoride. (Taken from R. K. Durkee et al., Energy and Rate Dependence Studies, Report S-237-R, EG&G, Inc., July 1963.)

Table 2

GLASS-DOSIMETER CHARACTERISTICS

Dosimeter	Exposure range, r	Accuracy, %	Rate dependence, r/sec	Fast-neutron response, r/neutron/cm^2
High-Z silver phosphate rods	10^1 to 2×10^4	±10	None to 10^9	<$3 \times 10^{-10+}$
Low-Z silver phosphate	10^1 to 2×10^4	±~10	None to 10^9	~6×10^{-9}
Cobalt glass	10^4 to 4×10^6	±10	None to 10^9	<3×10^{-10}
Bismuth glass	10^6 to 10^{10}	±10		Negative

teristic orange luminescence, which peaks near 615 to 640 mm. Energy-compensation shields and thermal-neutron shields have both been developed for this glass composition. The exposure range of this dosimeter is about 10^1 to 2×10^4 r.

Exposure of cobalt-glass plates to ionizing radiation results in formation of color centers in the glass.[67,68] The major induced absorp-
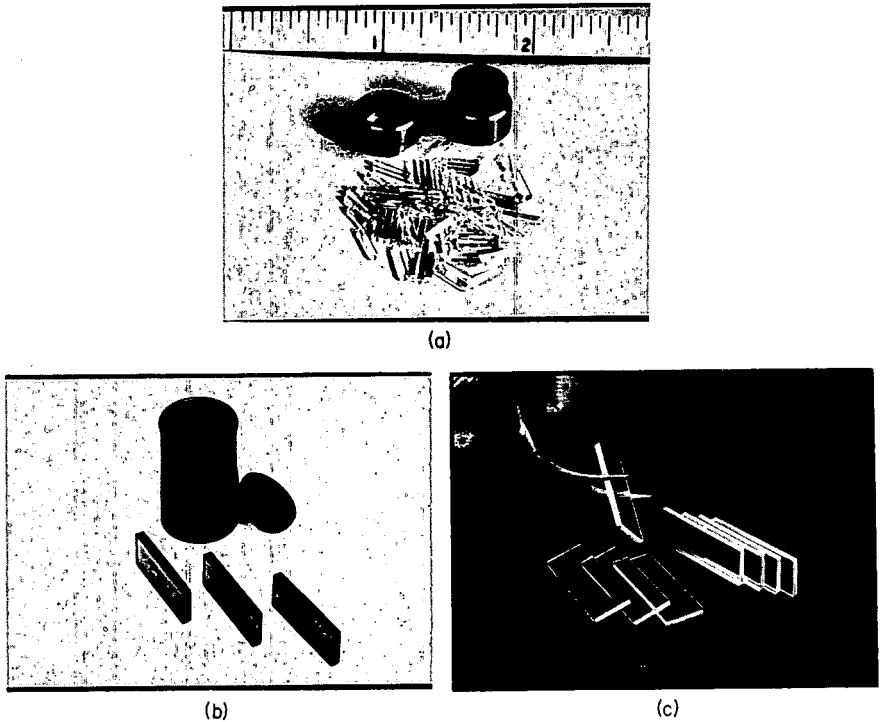
Fig. 9—Glass dosimeters. (a) Silver-activated glass rods. (b) Cobalt-glass plates. (c) Bismuth-glass plates.
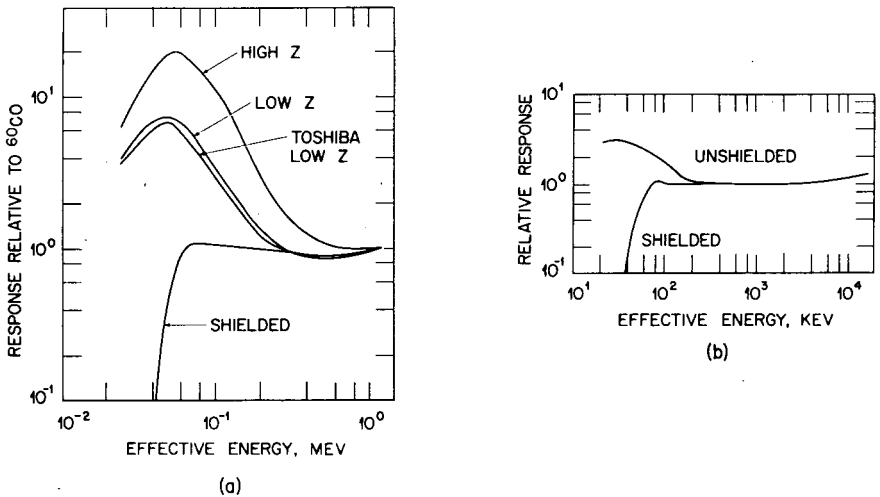
Fig. 10 — Glass-dosimeter energy response.[60] (a) Glass rods. (b) Cobalt glass.

tion band occurs at 400 nanometers. This glass exhibits considerably greater color stability than most glasses, and it has a low-energy over-response somewhat smaller than that of silver-activated phosphate glass. However, an energy-compensation shield and a thermal-neutron shield are both required. The useful exposure range of this glass is from 10^4 to 4×10^6 r.

A bismuth–lead–borate glass[69] has been developed as a high-level gamma dosimeter, specifically for use in mixed gamma–neutron environments. This glass has a wider sensitivity range and much less fading of induced coloration than the other dosimeter glasses. The absorption band is induced at about 480 nanometers. It has been postulated that a photochemical reaction in which Bi_2O_3 is reduced to bismuth by As_2O_3 is responsible for the induced coloration. The useful exposure range of this dosimeter is about 10^6 to 10^{10} r.

Chemical Dosimeters

A wide variety of chemical systems has been studied for dosimeter application, with the readouts ranging in complexity from a simple visual evaluation of color change to complex chemical–analytical methods. However, systems that employ spectrophotometric analysis are the most commonly used. Chemical dosimeters can be used to measure radiation dose from millirads to thousands of megarads, and they are probably the most accurate laboratory dosimeters available. However, they also require rather elaborate preparation. The chemicals must be very pure to obtain good reproducibility, and it is often necessary to seal the solutions under special atmospheres. Also, since the chemicals usually consist of water or some organic liquid, they normally show a very high neutron response.

The three most important chemical systems are ferrous sulfate, ceric sulfate, and oxalic acid. Another system that shows great promise for high-dose-range dosimetry applications employs radiochromic materials. Table 3 lists the characteristics of these chemical-dosimeter systems.

Table 3

CHEMICAL-DOSIMETER CHARACTERISTICS

Dosimeters	Exposure range, r	Accuracy to within, %	Rate dependence, r/sec	Fast–neutron response, r/neutron/cm^2
Ferrous sulfate	10^3 to 4×10^4	~3	None to 10^8	2 to 3×10^{-9}
Ceric sulfate	10^4 to 10^6	~5	None to 10^8	2 to 3×10^{-9}
Oxalic acid	10^5 to 10^{10}	±15	None to 10^{10}	2 to 3×10^{-9}
Radiachromic materials	10^5 to 10^9		None to 10^{11}	

The ferrous sulfate, or Fricke,[70-73] dosimeter has been studied extensively. Because of its desirable characteristics, it has been accepted as the standard against which other dosimeter systems are calibrated. The standard Fricke dosimeter is based on the oxidation of ferrous ions in $0.8N$ H_2SO_4. The exposure is determined by photometrically measuring the ferric-ion concentration. The ferric ion has a broad absorption peak at 305 nanometers. This dosimeter has a satisfactory response in the range of 10^3 to 4×10^4 rads, and it has no rate dependence up to 10^8 rads/sec when properly used. It is accurate to within about $\pm 1\%$, and the range can be extended to about 10^5 rads in an oxygen-saturated atmosphere.[74]

The ceric sulfate dosimeter is similar to the Fricke dosimeter, but it has a higher range. It is based on the reduction of ceric ions in H_2SO_4 to cerous ions. The concentration of ceric ion is measured photometrically at 320 nanometers, the ceric-ion absorption peak in H_2SO_4. The response is linear with exposure up to about 10^6 rads, but the solution is very susceptible to photoreduction by ordinary light, which limits its reliability unless special precautions are taken.[75]

The oxalic acid dosimeter[76-78] is a solution of oxalic acid in distilled water. Radiation decomposes the oxalic acid into CO_2 and small amounts of aldehydes. The radiation dose is related to the amount of decomposed oxalic acid. The concentration of the remaining acid is determined either by NaOH titration or spectrophotometric analysis with copper benzidine. The oxalic acid-cupric benzidine complex has an absorption band at 248 nanometers, which is proportional to the oxalic acid concentration. The dosimeter system is essentially linear with dose in the range of 10^5 to 10^{10} r.

Recent research with radiachromic materials indicates that they are potentially very useful as high-dose-range dosimeters. These dosimeters consist of colorless cyanide salts of the aminotriphenylmethane dyes in appropriate activator solvents. These solutions become deeply colored when exposed to ionizing radiation. This phenomenon was originally noted by Lyman Chalkley.[79] In recent years various films, gels, impregnated papers, and liquid solutions of these dye-cyanides have been studied as dosimeters by W. L. McLaughlin[80-82] and Humpherys.[83] Typical response curves (optical density vs. exposure) for several of these materials are given in Fig. 11. These materials have a very long shelf life, small temperature dependence, oxygen insensitivity, negligible fade, linear response, and no need for ultrapure materials. The neutron response is not known but is currently under investigation at the University of Arizona by M. Wacks.

There are a great number of other chemical and miscellaneous dosimeters,[78-106] both inorganic and organic, suitable for dosimetry measurements from 1 to 10^9 r. These dosimeters range in development from the relatively untested optically active organic compounds
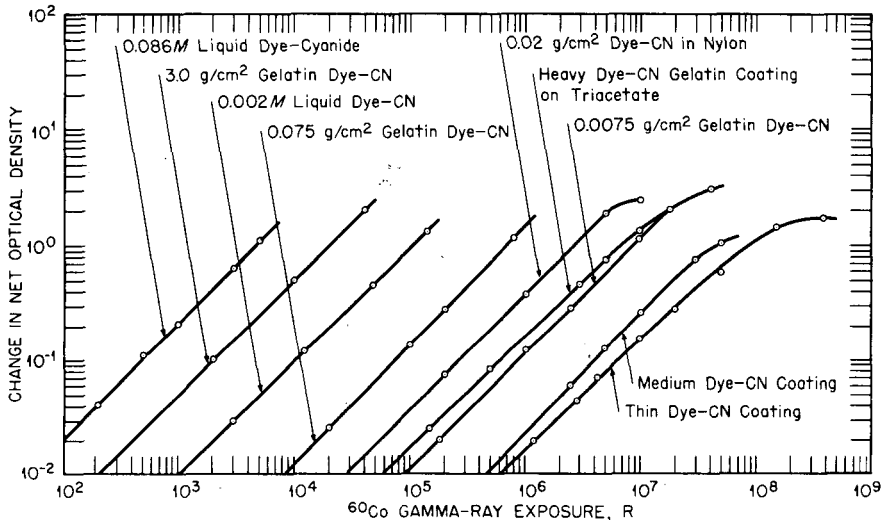
Fig. 11 — Typical response curves for various radiachromic materials. (From W. L. McLaughlin, National Bureau of Standards, personal communication, 1968.)

to the fully developed chlorinated hydrocarbon dosimeter. However, none are satisfactory for present application.

REFERENCES

1. G. S. Hurst et al., Techniques of Measuring Neutron Spectra with Threshold Detectors — Tissue Dose, Determinations, *Rev. Sci. Instrum.*, 27: 153 (1956).
2. S. R. Hartman, A Method for Determining Neutron-Flux Spectra from Activation Measurements, USAEC Report WADC-TR-57-375, Wright Air Development Center, 1957.
3. P. W. Reinhardt and F. J. Davis, Improvements in the Threshold Detector Method of Fast Neutron Dosimetry, *Health Phys.*, 1: 169 (1958).
4. J. A. Sayeg, P. S. Harris, and J. H. Larkins, Experimental Determination of Fast- and Thermal-Neutron Tissue Dose, USAEC Report LA-2174, Los Alamos Scientific Laboratory, 1958.
5. G. S. Hurst and R. H. Ritchie, Radiation Accidents: Dosimetric Aspects of Neutron and Gamma-Ray Exposures, USAEC Report ORNL-2748 (Pt. A), Oak Ridge National Laboratory, 1959.
6. J. B. Trice, Techniques for Measuring Reactor Neutron Spectra, Report 186, General Electric Aircraft Nuclear Propulsion Department, 1959.
7. P. S. Harris, E. F. Montoya, and W. H. Schweitzer, Dose and Flux Measurements on Godiva Radiation-Effect Experiments, USAEC Report LA-2355, Los Alamos Scientific Laboratory, 1959.
8. J. A. Sayeg, The Godiva II Critical Assembly: Dosimetry for Biological Research, USAEC Report LA-2435, Los Alamos Scientific Laboratory, 1960.
9. J. H. McNeilly and J. W. Kinch, Neutron-Flux Mapping for the KUKLA Facility April 5 to 11, 1961, Report NDL-TR-8, Nuclear Defense Laboratory, 1961.

10. J. H. McNeilly and J. W. Kinch, Neutron-Flux Measurements of the TRIGA Mark F Reactor, Report NDL-TR-12, Nuclear Defense Laboratory, 1961.
11. W. H. Buckalew, Neutron-Flux and Spectra Measurements in the Sandia Pulsed Reactor Facility (SPRF), USAEC Report SCR-463, Sandia Corporation, 1962.
12. K. C. Humpherys, Neutron-Flux and Spectra Measurements in the Void Tank of the TRIGA Mark F Reactor, USAEC Report SCR-480, Sandia Corporation, 1962.
13. K. C. Humpherys, Some Standardization Efforts of the American Society for Testing and Materials, in *Neutron Dosimetry*, Symposium Proceedings, Harwell, England, 1962, Vol. 2, pp. 487-496, International Atomic Energy Agency, Vienna, 1963 (STI/PUB/69).
14. J. A. Sayeg and K. C. Humpherys, The Measurement of Neutron Tissue Dose in Small Volumes, EG&G, Inc., Santa Barbara Division, 1963. (Talk presented at a Health Physics Meeting, June 1963.)
15. J. A. Sayeg et al., Neutron and Gamma Dosimetry Measurements at the AFRRI-DASA TRIGA Reactor, Report S-260-R, EG&G, Inc., Santa Barbara Division, 1964.
16. R. C. Barrall and W. N. McElroy, Neutron-Flux Spectra Determination by Foil Activation. Volume II. Experimental and Evaluated Cross-Section Library of Selected Reactors, Report AFWL-TR-65-34 (Vol. 2), Air Force Weapons Laboratory, 1965.
17. W. L. Zijp, Review of Activation Methods for the Determination of Fast Neutron Spectra, Dutch Report RCN-37, 1965.
18. Calculation of Neutron Dose to Polymeric Material and Application of Threshold-Foil Measurement, Report D2365-65, American Society for Testing and Materials, 1965.
19. S. B. Field and C. J. Parnell, The Use of Threshold Detectors to Determine Changes in a Fast Neutron Energy Spectrum with Depth in a Phantom, *Brit. J. Appl. Radiology*, 38: 618-621 (1965).
20. W. N. McElroy, L. Baurmash, C. Bingham, F. Franklin, and J. Kinzer, First Status Report. Interlaboratory Cooperative Study on Neutron Flux Spectral Measurements, Calculations, and Data Correlation for Reactor Irradiation and Physics Studies, USAEC Report NAA-SR-Memo-11816, Atomics International, 1966.
21. J. A. Sayeg, W. M. Quam, and K. C. Humpherys, Neutron and Gamma Dosimetry Measurements at Walter Reed Army Institute of Research, Report S-324-R, EG&G, Inc., Santa Barbara Division, 1966.
22. R. E. Dahl et al., Neutron Dosimetry Studies in EBR II for Radiation Damage Experiments, *Trans. Amer. Nucl. Soc.*, 10: 485 (1967).
23. W. N. McElroy et al., A Computer-Automated Iterative Method for Neutron Flux Spectra Determination by Foil Activation, Volumes 1-4, Report AFWL-TR-67-41, Air Force Weapons Laboratory, 1967.
24. J. A. Halbleib, J. V. Walker, and C. L. Greer, Neutron Spectroscopy by Foil Activation in Radiation-Effects Studies, USAEC Report SC-DC-67-1572, Sandia Corporation, 1967.
25. J. L. Jackson and J. A. Ulseth, Neutron Dosimetry Studies in EBR II, *Nucl. Appl.*, 5: 275-282 (1968).
26. K. C. Humpherys and J. A. Sayeg, Nuclear Accident Dosimetry: Depth Dose Considerations, Report S-394-R, EG&G, Inc., Santa Barbara Division, 1968.
27. G. M. Frye, Jr., J. H. Gammel, and L. Rosen, Energy Spectrum of Neutrons from Thermal-Neutron Fission of ^{235}U and from an Untamped Multiplying Assembly of ^{235}U, USAEC Report LA-1670, Los Alamos Scientific Laboratory, 1954.
28. N. Nereson and F. Reines, Nuclear Emulsions and the Measurement of Low Energy Neutron Spectra, *Rev. Sci. Instrum.*, 21: 534-545 (1950).

29. E. R. Graves and L. Rosen, Distribution in Energy of the Neutrons from the Interaction of 14-Mev Neutrons with Some Elements, *Phys. Rev.*, 89: 343-348 (1953).

30. L. Rosen, Nuclear Emulsion Techniques for the Measurement of Neutron Energy Spectra, *Nucleonics*, 2: 32-38 (1953).

31. J. H. Roberts, Absolute Flux Measurements of Anisotropic Neutron Spectra with Proton Recoil Tracks in Nuclear Emulsions, *Rev. Sci. Instrum.*, 28(9): 677-680 (1957).

32. W. C. Redman and J. H. Roberts, Some Current Techniques of Fast Neutron Spectrum Measurements, in *Proceedings of the Second United Nations International Conference on the Peaceful Uses of Atomic Energy, Geneva, 1958*, Vol. 12, p. 72, United Nations, New York, 1958.

33. H. H. Rossi and G. Failla, Tissue-Equivalent Ionization Chambers, *Nucleonics*, 14: 32 (1956).

34. F. R. Shonka, J. R. Rose, and G. Failla, Conducting Elastic Equivalent to Tissue, Air, and Polystyrene, in *Proceedings of the Second United Nations International Conference on the Peaceful Uses of Atomic Energy, Geneva, 1958*, Vol. 21, p. 184, United Nations, New York, 1958.

35. J. A. Sayeg et al., Neutron and Gamma Dosimetry Measurements at the AFRRI-DASA TRIGA Reactor, Report S-260-R, EG&G, Inc., Santa Barbara Division, 1964.

36. E. F. Bennett, Fast Neutron Spectroscopy by Proton-Recoil Proportional Counting, *Nucl. Sci. Eng.*, 27: 16-27 (1967).

37. E. F. Bennett, Neutron Spectrum Measurement in a Fast Critical Assembly, *Nucl. Sci. Eng.*, 27: 28-33 (1967).

38. J. A. Auxier et al., Dosimetry Applications, in Health Physics Division Annual Progress Report for Period Ending July 31, 1961, USAEC Report ORNL-3189, pp. 172-179, Oak Ridge National Laboratory, 1961.

39. E. F. Bennett, R. Gold, and R. J. Huber, Spectrum Measurements in a Large Dilute Plutonium-Fueled Fast Reactor, in *Proceedings of the International Conference on Fast Critical Experiments and Their Analysis, Argonne, October 1966*, USAEC Report ANL-7320, pp. 477-480, Argonne National Laboratory, 1966.

40. R. B. Moler and W. E. Zagotta, Development of Neutron Spectrometry for Critical Assemblies, USAEC Report IITRI-578, Illinois Institute of Technology Research Institute, 1968.

41. T. A. Love and R. B. Murray, Use of Silicon Surface-Barrier Counters in Fast-Neutron Detection and Spectroscopy, USAEC Report CF-60-5-121, Oak Ridge National Laboratory, 1960.

42. J. A. Auxier et al., Dosimetry Applications, in Health Physics Division Annual Progress Report for Period Ending July 31, 1964, USAEC Report ORNL-3697, pp. 155-159, Oak Ridge National Laboratory, 1964.

43. M. R. Raju, The Use of the Miniature Silicon Diode as a Radiation Dosimeter, *Phys. Med. Biol.*, 2(3): 371-376 (1966).

44. R. G. Morrison, Application of Miniature Intrinsic Thermocouples for Reactor-Transient Diagnostics, USAEC Report LA-3313-MS, Los Alamos Scientific Laboratory, June 1965.

45. H. H. Rossi and W. Rosenzweig, A Device for the Measurement of Dose as a Function of Specific Ionization, *Radiology*, 64: 404 (1955).

46. A. C. Lucas, Characteristics of a 2-inch Spherical Proportional Counter, Report S-70-TN, EG&G, Inc., Santa Barbara Division, October 1968.

47. W. N. McElroy, S. Berg, T. Crockett, and R. Hawkins, A Computer-Automated Iterative Method for Neutron-Flux Spectra Determination by Foil Activation. A Study of the Iterative Method, Report AFWL-TR-67-41 (Vol. 1), Air Force Weapons Laboratory, 1967.

48. S. Berg and W. N. McElroy, A Computer-Automated Iterative Method for Neutron-Flux Spectra Determination by Foil Activation. SAND-II (Spectrum

Analysis by Neutron Detectors II) and Associated Codes, Report AFWL-TR-67-41 (Vol. 2), Air Force Weapons Laboratory, September 1967.

49. S. Berg, Modification of SAND-II, in preparation.

50. C. R. Greer, J. A. Halbleib, and J. V. Walker, Technique for Unfolding Neutron Spectra from Activation Measurements, USAEC Report SC-RR-67-746, Sandia Corporation, December 1967.

51. G. Di Cola and A. Rota, Calculation of Differential Fast-Neutron Spectra from Threshold-Foil Activation Data by Least-Squares Series Expansion Methods, *Nucl. Sci. Eng.*, 23: 344-353 (1965).

52. G. Di Cola and A. Rota, RDMM: A Code for Fast-Neutron Spectra Determination by Activation Analysis, EURATOM Report EUR-2985.e, 1966.

53. H. Becquerel, *Ann. Chem. Phys.*, 30: 1-68 (1883).

54. E. E. Angino, N. Grogler, and R. McCall, Thermoluminescence. Bibliography, USAEC Report TID-3911 (Rev. 2), Texas A&M University, February 1965.

55. G. R. Fonda and F. Seitz (Eds.), *Preparation and Characteristics of Solid Luminescent Materials*, John Wiley & Sons, Inc., New York, 1948.

56. H. P. Kallman and G. M. Spruch, *Luminescence of Organic and Inorganic Materials*, in *Proceedings, International Conference*, John Wiley & Sons, Inc., New York, 1962.

57. F. H. Attix, High-Level Dosimetry by Luminescence Degradation, *Nucleonics*, 17: 142 (April 1959).

58. F. H. Attix, Dosimetry by Solid State Devices, Report NRL-5777, Naval Research Laboratory, June 15, 1962.

59. J. H. Schulman, H. W. Etzel, and J. G. Allard, Application of Luminescence Changes in Organic Solids to Dosimetry, *J. Appl. Phys.*, 28: 792 (July 1957).

60. C. G. Weis, Some Luminescent Properties of the Mixed Phenyl- and p-Biphenyl-Substituted Silanes Under Ultra-violet, Gamma, and Beta Excitation, Report AD-259662, Air Force Institute of Technology, March 1961.

61. J. Paymal, M. Bonnaud, and P. LeClerc, Radiation Dosimetry Glasses, *J. Amer. Ceram. Soc.*, 43: 430 (August 1960).

62. W. A. Hedden, J. F. Kircher, and B. W. King, Investigation of Some Glasses for High-Level Gamma Radiation Dosimeters, *J. Amer. Ceram. Soc.*, 43: 413 (August 1960).

63. R. G. Bauman, Glass Slides Help Map Gamma Fields, *Nucleonics*, 14: 90 (June 1956).

64. J. F. Kircher, B. W. King, M. J. Oestmann, P. Schall, Jr., and G. D. Calkins, Recent Research in High-Level Gamma Dosimetry, in *Proceedings of the Second United Nations International Conference on the Peaceful Uses of Atomic Energy, Geneva, 1958*, Vol. 21, p. 199, United Nations, New York, 1958.

65. S. Davison, S. A. Goldblith, and B. E. Proctor, Glass Dosimetry, *Nucleonics*, 14: 34 (January 1956).

66. R. K. Durkee, Silver-Activated Phosphate Glass Microdosimeters for Gamma-Ray Dose Measurements, in *Manual of Radiation Dosimetry Experiments*, Experiment No. 7, K. C. Humpherys, Ed., Report S-305-MN, EG&G, Inc., Santa Barbara Division, (July 1964).

67. J. H. Schulmann, C. C. Klick, and H. Rabin, Measuring High Doses by Absorption Changes in Glass, *Nucleonics*, 13: 30 (February 1955).

68. N. J. Kreidl and G. E. Blair, A System of Megaroentgen Glass Dosimetry, *Nucleonics*, 14: 56 (January 1956).

69. N. J. Kreidl and G. E. Blair, Recent Developments in Glass Dosimetry, *Nucleonics*, 14: 82 (1956).

70. J. Weiss, A. O. Allen, and H. A. Schwartz, Use of the Fricke Ferrous Sulfate Dosimeter, in *Proceedings of the International Conference on the Peaceful Uses of Atomic Energy, Geneva, 1955*, Vol. 12, p. 179, United Nations, New York, 1956.

71. R. H. Schuler and A. O. Allen, Yield of the Ferrous Sulfate Radiation Do-
simeter: An Improved Cathode-Ray Determination, *J. Chem. Phys.*, 24: 56
(January 1956).

72. M. J. Oestmann, J. F. Kircher, and P. Schall, Jr., A Survey of Current
Research and Developments in the Field of Dosimetry, USAEC Report
REIC-6, Radiation Effects Information Center, May 31, 1958.

73. S. I. Taimuty, A Review of Dosimetry Field. Report No. 1, Report AD-
296591, Stanford Research Institute, Sept. 1, 1962.

74. F. J. Haasbroek, Extending the Range of the "Fricke" Dosimeter up to
10^6 Rads, USAEC Report BNL-763, Brookhaven National Laboratory,
April 1962.

75. S. W. Nicksic and J. R. Wright, Effect of Light on Ceric–Cerous Dosim-
etry, *Nucleonics*, 13: 104 (November 1955).

76. I. G. Draganic, N. W. Holm, and J. E. Maul, Laboratory Manual for Some
High-Level Chemical Dosimeters: Ferrous Sulphate, Oxalic Acid, Ceric
Sulphate, Polyvinyl-Chloride Foils, Danish Report RISO-22, July 1961.

77. M. Matsui, Studies on Chemical Change in Radiolysis. III. The Action of
Gamma-Rays on Aqueous Solution of Oxalic Acid, *Sci. Pap. Inst. Phys.
Chem. Res. (Jap.)*, 53: 292 (December 1959).

78. I. G. Draganic, B. B. Radak, and V. M. Markovic, Measurement of Absorbed
Dose of Mixed-Pile Radiation in Aqueous Radiation Chemistry, *Int. J. Appl.
Radiat. Isotop.*, 16: 145 (March 1965).

79. L. Chalkley, Photometric Papers Sensitive Only to Short-Wave Ultraviolet,
J. Opt. Soc. Amer., 42: 387 (1952).

80. W. L. McLaughlin and L. Chalkley, Low Atomic Number Dye Systems for
Ionizing Radiation Measurement, *Photogr. Sci. Eng.*, 9: 159 (1965).

81. W. L. McLaughlin and L. Chalkley, Measurement of Radiation Dose Distri-
butions with Photochromic Materials, *Radiology*, 84: 124 (1965).

82. W. L. McLaughlin and L. Chalkley, Versatile Chemical Dosimetry Systems
for Radiation Processing, *Trans. Amer. Nucl. Soc.*, 10(1): 52 (June 1967).

83. K. C. Humpherys and R. L. Wilcox, High Dose Range X-Ray and Gamma-
Ray Dosimeter, Report No. S-424-R, EG&G, Inc., Santa Barbara Division,
1968.

84. T. R. Johnson and J. J. Martin, Benzene in Water is Simple, Reliable
Gamma Dosimeter, *Nucleonics*, 20: 83 (July 1962).

85. T. J. Hardwick, On the Radiolysis of Aqueous Sodium Formate Solutions,
Radiat. Res., 12: 5 (January 1960).

86. T. J. Hardwick and W. S. Guentner, On the Use of Aqueous Sodium Formate
as a Chemical Dosimeter, *J. Phys. Chem.*, 63: 896 (June 1959).

87. L. Wiesner, The Use of Polyisobutylene in Solutions for Measuring Doses
from 10^3 Rad up to About 10^{10} Rad, in *Selected Topics in Radiation Dosim-
etry*, Symposium Proceedings, Vienna, 1960, pp. 361-370, International
Atomic Energy Agency, Vienna 1961 (STI/PUB/25).

88. M. J. Day and G. Stein, The Action of Ionizing Radiations on Aqueous Solu-
tions of Methylene Blue, *Radiat. Res.*, 6: 666 (June 1957).

89. S. C. Sigoloff, Chemical and Colorimetric Dosimetry: The Tetrachloro-
ethylene Chemical Dosimeter System, in *Selected Topics in Radiation Do-
simetry*, Symposium Proceedings, Vienna, 1960, p. 337, International
Atomic Energy Agency, Vienna, 1961 (STI/PUB/25).

90. S. M. Dec, Optically Active Organic Compounds as High-Level Gamma
Dosimeters, USAEC Report WADC-TR-59-711, Wright Air Development
Center, November 1959.

91. J. Weiss, A Survey of Chemical Dosimetric Systems, *Int. J. Appl. Radiat.
Isotop.*, 4: 89 (December 1958).

92. F. E. Hoecker, Characteristics of the Radiation Polymerization Dosim-
eter, *Health Phys.*, 8: 381 (August 1962).

93. J. W. Boag, G. W. Dolphin, and J. Rotblat, Radiation Dosimetry by Trans-
parent Plastics, *Radiat. Res.*, 9: 589 (December 1958).

94. K. K. Harris and W. E. Price, A Thin Plastic Radiation Dosimeter, *Int. J. Appl. Radiat. Isotop.*, 11: 114 (September 1958).
95. V. H. Ritz, A Note on Mylar Film Dosimetry, *Radiat. Res.*, 15: 460 (October 1961).
96. I. Kuegler and A. Scharmann, Dosimetry of Ionizing Radiation Using Plastics, USAEC Report AERE-Trans-932, translated from *Atomkernenergie*, 4(1): 23-27 (January 1959).
97. C. Artande and A. A. Stonehill, Polyvinyl Chloride — New High-Level Dosimeter, *Nucleonics*, 16: 118 (May 1958).
98. E. J. Henley and D. Richman, Cellophane — Dye Dosimeter for 10^5 to 10^7 Roentgen Range, *Anal. Chem.*, 28: 1580 (October 1956).
99. A. M. Bishay, A Bismuth Lead Borate Glass Dosimeter for High-Level Gamma Measurements, *Phys. Chem. Glasses*, 2: 33 (April 1961).
100. P. Harteck and S. Dondes, Nitrous Oxide Dosimeter for High Levels of Betas, Gammas, and Thermal Neutrons, *Nucleonics*, 14: 66 (March 1956).
101. R. C. Von Borstel and R. W. Rogers, Alpha-Particle Bombardment of the Habrobracon Egg. II. Response of the Cytoplasm, *Radiat. Res.*, 8: 248 (March 1958).
102. M. J. Oestmann and J. F. Kircher, A Survey of Current Research and Developments in the Field of Dosimetry, USAEC Report REIC-6(Add.), Radiation Effects Information Center, Battelle Memorial Institute, Mar. 31, 1959.
103. R. K. Mortimer, Radiobiological and Genetic Studies on a Polyploid Series (Haploid to Hexaploid) of Saccharomyces Cerevisiae, *Radiat. Res.*, 9: 312 (September 1958).
104. P. B. Fairand and E. N. Wyler, A Survey of Current Research and Developments in the Field of Dosimetry, USAEC Report REIC-33, Radiation Effects Information Center, Battelle Memorial Institute, Sept. 30, 1963.
105. S. I. Taimuty, R. A. Glass, and B. S. Deaver, Jr., High-Level Dosimetry of Gamma and Electron Beam Sources, in *Proceedings of the Second United Nations International Conference on the Peaceful Uses of Atomic Energy, Geneva, 1958*, Vol. 21, p. 204, New York, 1958.
106. S. I. Taimuty, *Recent Developments in Gamma-Ray Dosimetry*, American Society for Testing and Materials Special Publication No. 276, 1959.

DISCUSSION

KRONENBERG: You mentioned a very low response of the TLD's to neutrons. Does this number include or exclude the gamma rays produced by inelastic scattering of fast neutrons within the detector?

HUMPHERYS: The gamma rays produced in the dosimeter itself by the neutrons are included as part of the neutron response.

KRONENBERG: In a pure neutron environment would there still be some response by the dosimeter?

HUMPHERYS: Yes.

KRONENBERG: Would this response be larger than the number you quoted in your paper?

HUMPHERYS: No, if indeed you had a pure neutron environment. That is one of the reasons I said "is probably" about that value. If a reactor designer would design us a reactor with a gamma switch that we could turn off, we could define the exact neutron response for you. The big problem in trying to measure neutron sensitivity is to get a

pure neutron source with no gamma contamination. Some of the early measurements of neutron response of TLD materials and of glass rods yielded a much much higher value. As a matter of fact, if you were to make a gamma-dose measurement on a Godiva-type reactor and then correct for the neutron response by some of the early information available, you would end up with a negative gamma dose for the reactor. Over the years these neutron-response values have become smaller and smaller, and they possibly reflect the degree of capability of getting a gamma-free neutron field for the measurements.

DONNERT: There is one difficulty with those gamma-radiation dosimetry systems which has not been alluded to and which also to some extent can explain the observation of a "negative" gamma-radiation dose. That is the possibility that the response of several of the gamma-radiation dosimeters depends on dose-rate as well as dose, if the dose rate is high enough. Dose-rate effects have been observed in lithium fluoride thermoluminescent dosimeters, in silver-activated borosilicate glass, as well as in the ferrous sulphate chemical dosimeters.

HUMPHERYS: Yes, dose-rate problems have always existed too. We are currently in the process of further defining and delineating the response of CaF_2: Mn and LiF to very high rates of radiation and, as yet, find no dependence at the rates encountered in pulsed reactors.

McTAGGART: We have measured total doses of LiF dosimeters in and around the VIPER reactor. By exposing the LiF dosimeters inside lead blocks, which attenuate the gamma flux more than the neutron flux, we deduce that the neutron sensitivity of our dosimeters is about 10^{-10} r/neutrons/cm^2.

6-5 DEVELOPMENT AND APPLICATION
OF FISSION-COUPLES

R. G. MORRISON
Phillips Petroleum Company, Atomic Energy Division, Idaho Falls, Idaho

ABSTRACT

During the past several years a form of intrinsic thermocouple, called a fission-couple, has been used by a number of experimenters to monitor fast temperature transients on reactor fuels.

In this application a small piece of fuel is used as the sensing device. The temperature of the sensor is monitored by attaching very fine thermocouple wires to the fuel. This technique has demonstrated that actual reactor periods as short as 10 μsec can be measured accurately. The device is being adapted to neutron-flux measurement problems by normalizing the observed temperature rise to known neutron fluxes. The normalization is dependent on the validity of standard flux measurements determined by activation or radiochemical analysis.

This paper discusses the enthalpy of the fissile element in the sensing part of the detector and develops a mathematical model for determining heat losses due to the various mechanisms present in the particular geometric application.

The paper also describes several specific applications now being used and refers to available data from these experiments.

INTRODUCTION

The dependable use of thermocouples in reactor environments has been established for many years. Basic thermocouple materials withstand radiation environments as well as any sensing materials and the performance and reliability of the device has been established.[1]

This paper is addressed to the use of a type of intrinsic thermocouple in reactor diagnostics. The understanding of transient temperatures is of fundamental importance in determining the physical behavior of materials during reactor excursions. This technique offers a method of determining transient and steady-state temperatures accurately.

519

The term "intrinsic" is used to identify the thermocouple application in which two separate thermocouple sensing leads are attached to a third material, and the third material becomes an integral part of the sensing circuit. The application described here can be considered as a form .of intrinsic thermocouple; however, the heat-transfer mechanisms are somewhat different than those encountered in conventional thermocouple measurements. This device, called a fission-couple, is identified for the unique characteristic of having the heat source as an integral part of the sensing mechanism. For this reason, only heat losses are considered in determining the performance characteristics since the heat is generated within the sensing mechanism.

It is important to consider all the conditions that this technique will encounter in steady-state and transient conditions. Once reasonable models of performance are developed and understood, the technique becomes a valuable tool, not only for temperature measurements, but also for direct neutron-flux and neutron-spectra measurements.

MODEL DEVELOPMENT

The signal measured in a thermocouple circuit has a number of sources. In the steady-state situation, the signal can be mainly attributed to the Seeback effect, which produces a current in a circuit comprised of two metals with one junction hotter than the other. Other effects, such as the Peltier effect, which tends to heat or cool the thermoelectric junction according to the' direction of current flow, or the Thompson effect, which develops a potential gradient along a differentially heated conductor, are relatively minor in this application but must be considered if the temperature differentials become very high (>600°C). In a rapidly changing condition, several other voltage sources appear which can seriously degrade the signal. The piezo-electric effect from mechanical displacement and the paramagnetic properties of the measurement hardware all tend to contribute to signal generation in an electromagnetic field. The magnitude of this signal is influenced by the geometry of the measurement device and electrical and mechanical coupling to other parts of the circuit hardware. The decoupling of the sensing element from massive structures is extremely important in that it eliminates the electrical path for these stray signals.

The model developed is comprised of a pair of thermocouple leads and a piece of fissile material. The thermoelements are welded to the fissile material to form an electrical circuit. In the event that a gamma-compensated device is desired, one of the thermoelements is then welded to a separate element that has gamma-absorption characteristics similar to the fissile element, as well as similar thermal

and thermoelectric properties. This compensating element is designed to heat from gammas only; the fissile element heats from fissions and gammas. By connecting the sensing leads in a bucking configuration, we can consider the signal output to be due to fissioning only.
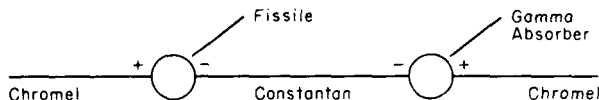
The accuracy and response of the circuit are improved by selecting thermoelement materials that have low thermal conductivity, thermal capacitance, and small cross-sectional area. It is also important to choose thermocouple sensing materials with thermal properties that match each other. Uneven heat flow from the fissile element in contact with the sensing material can create a sizeable temperature gradient and thus form an intermediate thermal electromotive-force junction in the circuit which will give erroneous temperature indications (e.g., uranium has a contact potential of ~20 $\mu v/°C$).

Having considered these possible effects, we have concluded that the most compatible materials for a fission-couple using enriched uranium as the driving sensor are Chromel and Constantan. A search of the physical properties of conventional thermocouple materials will reveal that Chromel—Constantan is the best candidate since the relationship of heat capacity, density, and thermal conductivities of the two materials is within 1%.*

The energies released by various mechanisms in a fissile material are listed in Table 1.

The heat generated in the sensor is assumed to be ~180 Mev/fission. A portion of the fission fragment, neutrons, and gamma rays escape from the surface of the sensor. Further testing is required to determine if the beta particles offer a significant contribution.

Assuming that ^{235}U is chosen as the sensing material, the approximate fission mean free path for thermal neutrons can be found from

$$\frac{1}{N\sigma} = \lambda \qquad (1)$$

where σ is the cross section (thermal), N is the atom density, and λ is the thermal mean free path (fission). The standard "barn book"[3] for cross sections lists a value of ~0.015 in. for thermal neutrons. It is of interest to consider the relation between λ and size for a ^{235}U element.

---

*The $k\rho C_p$ of Chromel vs. Constantan is 647 vs. 642 [Btu²/(ft⁴/hr/°F)²] determined from handbook values.

Table 1

LIBRATION OF HEAT DUE TO FISSION*

	Mev
Instantaneous:	
Energy of fission fragments	168
Energy of fission neutrons	5
Instantaneous gamma rays	5
Capture gamma rays	7
	185
Delayed:	
Beta particles from fission products	7
Gamma rays from fission products	6
Radiation from capture products	2
	15
Total	200

*From S. Glasstone, *Principles of Nuclear Reactor Engineering*, p. 24, D. Van Nostrand Company, Inc., Princeton, N. J., 1956.

The energy spectra of the neutron fluxes in which the fission-couples will have to operate may range from quite well thermalized fluxes to fluxes with energy spectra approaching the fission spectrum, as in the case of fast burst reactors. Fission-spectrum neutrons from ^{235}U have an average energy of $\sim$2 Mev. Since the ^{235}U fission cross section[4] for neutrons of this energy is in the order of 1 barn, the value of λ for 2-Mev neutrons is quite large ($\sim$8 in.). A ^{235}U element of 0.015 in. in diameter would be rather insensitive to 2-Mev neutrons. On the other hand, the same element would be expected to have relatively good sensitivity for thermal neutrons. Stillman[5] of Los Alamos is conducting a series of experiments aimed at determining the optimum size of the fissile element. In monitoring the temperature rise obtained from Super KUKLA bursts (average energy = 0.67 Mev), his data indicate that elements with diameters ranging from 0.015 to 0.023 in. are satisfactory and, essentially, provide the same output. The proper diameter can be estimated as $\geq$0.023 in. by shielding the energies below 0.4 ev. For a totally thermalized spectrum, the diameter of the sensing element becomes more critical, and present empirical results indicate the dimension should be less than 0.015 in. but greater than 0.008 in.

From these results the proper size of a ^{235}U sensing element is seen to be of the order of 0.015 in., λ for thermal neutrons; but, the optimization appears to be complicated by other phenomena, such as self-shielding effects and loss of fission fragments, neutrons, and gamma rays from the surface of the sensor. The application of the

device must also be considered with respect to the flux source, e.g., anisotropic fluxes will require a smaller diameter than isotropic fluxes.

Referring to Fig. 1 for a model of the fission-couple, we can estimate certain properties of the device from fairly simple considera-
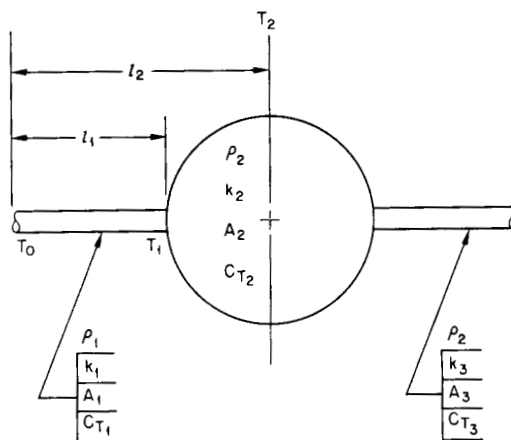
Fig. 1 — Fission-couple model.

ρ, density
k, thermal conductivity
C, thermal capacity
A, cross-sectional area

T_0, ambient temperature
T_1, junction temperature
T_2, elevated temperature due to fissioning

tions. For example, the temperature drop along the leads can be obtained by using Fourier's law of heat conduction:

$$\frac{Q}{A} = -k \frac{dt}{dx} \tag{2}$$

where Q/A is heat flux into thermoelement junction and Q is rate of flow of energy into junction. This is a steady-state relation neglecting radial heat conduction in the lead and neglecting radiative losses, a reasonable approximation for very thin wires in the temperature range of interest. Also, assuming that the thermal conductivity is a constant, the temperature at any point x in the region $0 \le x \le l_1$ is

$$T(x) = \frac{Qx}{k_1 A_1} + T_0 \tag{3}$$

(Note the frame of reference for x in Fig. 1.)

Using Eq. 2 and assuming a linear temperature dependence of conductivity $k = k_0 + C(T - T_0)$ (valid in the range of 20 to 500°C),

$$T(x) = -\frac{Qx}{\left[k_0 + \frac{C(T - T_0)}{2}\right] A_1} + T_0 \tag{4}$$

The drop from junction temperature T_1 to T_0 is then given by

$$T_1 - T_0 = -\frac{k_0}{C} + \frac{1}{C}\ (k_0^2 + 2aCQ)^{\frac{1}{2}} \tag{5}$$

where a is the geometry factor of l_1/A_1 of the thermocouple leads, T_0 is the reference temperature, and C is a constant over the range of measurement.

If heat is flowing through A_1, then a temperature gradient also exists in the fissile material. The temperature distribution can be obtained from the more general heat-diffusion equation

$$0 = q + k_2 \nabla^2 T$$

The term q represents the energy generation rate per unit volume in the material, and, in general, it will depend upon the neutron-flux distribution in the material and upon the neutron-energy distribution. The form of the Laplacian ∇^2 will depend upon the choice of the co-ordinate system used. Suitable boundary conditions must be specified to couple the solution of this equation to the solution of the equations for the temperature of the leads.

The heat H generated by the fission process is determined by

$$H = \rho V M_F\ \frac{N_a}{A}\ \sigma_f \phi\ EK \tag{6}$$

where ρ = density of element
 V = volume of element
 M_F = mass fraction of fissionable atoms
 N_a = Avogadro's number (6.025×10^{23} atoms/gram atom)
 A = atomic weight
 σ_f = spectral average cross section
 ϕ = integrated neutron flux
 E = constant (energy released/fission)
 K = conversion factor (cal/Mev)

Assuming that the temperature rise of the fissile material is an adiabatic process, we can derive the following heat quantity (H) as

$$H = \int_{T_1}^{T_2} \rho V C_p \, dT \tag{7}$$

where C_p = specific heat of fissile material
V = volume of fissile material
T_1 = initial temperature
T_2 = final temperature·
ρ = fissile material density

(Note: The temperature range of measurement is picked where C_p is in a linear region of fissile-material property and is represented by the equation

$$C_p = C_1 + C_2 T \; (cal/g°K) \tag{8}$$

where C_1 is specific heat at zero temperature, C_2 is the rate of change of specific heat with temperature, and T is absolute temperature.)

Combining Eqs. 7 and 8 and integrating yields

$$H = \rho V \left[C_1 T + \frac{C_2 T^2}{2} \right]_{T_1}^{T_2} \tag{9}$$

and evaluating Eq. 9,

$$H = \rho V \left[-\left(C_1 T_1 + \frac{C_2 T_1^2}{2} \right) + \left(C_1 T_2 + \frac{C_2 T_2^2}{2} \right) \right]$$

Let $\Delta T = T_2 - T_1$ and $C_{p_1} = C_1 + C_2 T_1$ which makes Eq. 9

$$H = \rho V \left(C_{p_1} + \frac{C_2}{2} \Delta T \right) \Delta T \tag{10}$$

By making Eq. 6 equal to Eq. 10, we can determine that the temperature of the element should be

$$\rho V \left(C_{p_1} + \frac{C_2}{2} \Delta T \right) \Delta T = \rho V M_F \frac{N_a}{A} \sigma_f \phi \; EK$$

Let

$$M_F \frac{N_a}{A} \sigma_f \; EK = C_4$$

then

$$\Delta T = \frac{-C_{p_1} + (C_{p_1}^2 + 2 C_2 C_4 \phi)^{\frac{1}{2}}}{C_2} \tag{11}$$

which is the temperature rise of the fissile material for the adiabatic condition.

Assuming that a very rapid fission burst raises the fissile-material temperature by 500°C adiabatically, then the maximum rate of heat transfer from the fissile material to the thermocouple leads will occur immediately following the burst. For 0.0005-in. thermocouple leads and a 0.015-in. ^{235}U sphere, this maximum rate can be shown to be quite small using Eq. 2 (considering only one of the leads)

$$Q \simeq k_1 A_1 \frac{T_1 - T_0}{l_1}$$

$$\simeq \frac{(0.046)(1.26 \times 10^{-6})(500°C)}{0.254} = 1.15 \times 10^{-4} \; cal/sec$$

This assumes that under 500°C temperature differential the only heat loss of significance is along the thermocouple leads. Since the two materials of the sensing leads have been picked for matching thermal properties, the total loss from the 0.015-in. sphere of uranium is equal to 2.30×10^{-4} cal/sec. If we assume the heat capacity of ^{235}U at 500°C as 0.0426 cal/(g/°C), the corresponding maximum rate of loss in temperature can be determined as

$$\frac{dT}{dt} = \frac{Q}{C_p m} = \frac{2.30 \times 10^{-4}}{(0.0426)(6.41 \times 10^{-4})} = 8.3°C/sec$$

(For the sake of simplicity, k_1 and C_p were considered as constants in the above evaluations, and m is the mass of the fissile material.) In transient tests of duration less than 100 msec and of temperatures approaching 500°C, this loss is probably smaller than the resolution of the recording system.

Considerable thought has been put into a method of determining the amount of heat loss due to fission fragments leaving the surface of the fissile material. Since the idealized model has sensing metal at the surface of the fuel, it is postulated that the loss is partially compensated for by the fragments being absorbed in the metal.

APPLICATIONS

A number of experiments have used this technique; available reports are listed in the bibliography. In addition to those listed, P. G. Salgado of K-5, Los Alamos, is completing a series of experiments aimed at determining the thermal conductivity of buffer materials and of isotropic carbon coating of kernels of enriched uranium carbide.

One of the most recent applications of this technique has been the determination of the angular distribution of thermal neutrons in the Special Power Excursion Reactor Test No. 4 (SPERT-4). For this requirement M. L. Stanley has designed a device that uses cadmium as a thermal-neutron shield with a 15° aperture. The thermal neutrons incident to the sensing element then determine the source geometry. Preliminary tests indicate that reliable and repeatable data are being obtained. Figure 2 shows a graph of observed values from 19 SPERT-4 excursions. The burst periods ranged from 10 to 3.0 msec (see
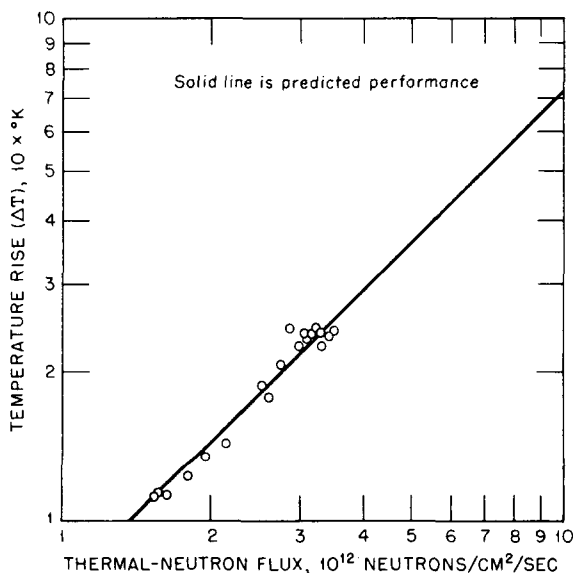
Fig. 2— *Comparison of predicted performance of 71 wt.% Al−29 wt.% U (93% enriched uranium) angular dependent fission thermocouple. (Points are data points for thermocouple output in circuit 5.)*

Table 2). The solid line represents the calculated value using Eq. 11. The fissile alloy in this case is 71 wt.% Al−29 wt.% U. The uranium is 93% enriched.

This particular experiment is still in progress. The fission-couple devices have been installed in the reactor for approximately five months and have recorded approximately 200 excursions.

SUMMARY AND CONCLUSIONS

This measurement offers a number of important advantages over the standard neutron-measurement tools. The ideal instrument for

Table 2

FISSION-THERMOCOUPLE OUTPUT FOR 3- TO 10-MSEC PERIOD
SERIES IN SPERT-4

Run number	Predicted ΔT, °C	Temperature differential, °C					Standard deviation
		TC-2*	TC-3*	TC-4*	TC-5*	Average	
420	23.0	28.0	26.8	25.8	24.4	26.3	±0.9
421	24.0	28.2	26.8	26.4	24.4	26.4	±0.9
422	23.5	28.0	26.4	26.0	24.0	26.1	±1.0
423	22.8	27.6	26.6	25.6	23.4	25.8	±1.0
424	26.0	27.6	26.0	25.8	23.6	25.8	±0.9
425	22.8	27.8	26.4	26.0	23.8	26.0	±0.8
426	22.9	27.4	26.0	25.8	23.8	25.8	±0.8
427	24.0	27.6	26.0	26.2	23.8	25.9	±0.9
428	22.9	27.6	26.2	26.2	23.6	25.9	±1.0
429	23.5	27.4	26.2	26.0	23.6	25.8	±0.9

*TC is thermocouple circuit number.

reactor diagnostics and control should be capable of detecting neutrons in the presence of strong gamma radiation, should be accurate, should respond rapidly to changes in neutron flux, and should offer minimum perturbation to the measured parameter. The device discussed in this paper meets these requirements in flux levels from 10^9 to 10^{15} neutrons/cm²/sec. The entire detector can be made small (<0.125 in. in diameter), and it has low impedance (<100 ohms for 10-unit thermopiles). The sensitivity of a single-element fission-couple is about 60 μv/°C using Chromel and Constantan leads. The rise time is quite small. Comparison of fission-couple response with photodiode response has shown the rise time to be <5 μsec. Proper selection of materials can eliminate gamma-heating effects and shock or transient signals from paramagnetic properties. The impedance characteristics of the transducer make the measurement as simple and economical as any thermocouple measurement circuit. Continued use and evaluation of the technique should provide experience for experimenters to determine which applications are most suitable. Normalization of the thermal electromotive force generated in the circuit to conventional measuring techniques for neutron flux is being established. The applications now in use indicate that a cheap, rugged, and dependable tool is available. Further development in packaging will provide a fairly universal instrument for all reactor applications where fuel temperature or neutron flux is the desired measurement.

REFERENCES

1. M. J. Kelley, W. W. Johnson, and C. D. Baumann, Effects of Nuclear Radiation on Thermocouples, in *Temperature Measurements and Control for Sci-*

ence and Industry, Vol. 3, Pt. 2, p. 655, American Institute of Physics, New York, 1962.
2. S. Glasstone, *Principles of Nuclear Reactor Engineering,* p. 24, D. Van Nostrand Company, Inc., Princeton, N. J., 1956.
3. D. J. Hughes and R. B. Schwartz, Neutron Cross Sections, USAEC Report BNL-325, Brookhaven National Laboratory, 1958.
4. S. Glasstone, *Nuclear Reactor Engineering,* p. 808, D. Van Nostrand Company, Inc., Princeton, N. J., 1963.
5. D. B. Stillman, Proposed Fission-Couple Experiments, internal Report J8-67-67, Los Alamos Scientific Laboratory, 1967.

BIBLIOGRAPHY

Dittbenner, G. R., Development and Application of the Intrinsic Thermocouple for Fast Response, USAEC Report UCRL-14593, University of California, Lawrence Radiation Laboratory, 1966.
Morrison, R. G., Application of Miniature Intrinsic Thermocuples for Reactor Transient Diagnostics, USAEC Report LA-3313-MS, Los Alamos Scientific Laboratory, 1965.
Morrison, R. G., Instrument Development Branch Annual Report, USAEC Report IDO-17269, Idaho Operations Office, 1968.
Morrison, R. G., and D. B. Stillman, Fission-Couples Applied Toward Reactor Diagnostics and Safety, USAEC Report LA-3470-MS, Los Alamos Scientific Laboratory, 1966.
Stanley, M. L., Fission-Couple Cryogenic Applications Feasibility Study, USAEC Report IDO-17268, Idaho Operations Office, 1968.
Stillman, D. B., Summary of Fission-Couple Experiments at the Super KUKLA Reactor, internal Report J8-67-385 (plus *continuing reports*), Los Alamos Scientific Laboratory, 1967.

DISCUSSION

FREEMAN: I am wondering about the effects of burn-up on these fission-couples. To put it another way, what application do you see for monitoring conditions in and around an operating power reactor?

GOSSMAN: I do not know. I am not an expert on this subject.

STILLMAN: We have used them in the Omega West Reactor in a steady-state radiation environment; however, we have not had too much success with them. We used a fission-couple with a junction of 80% niobium and 20% uranium (of which 93.5% is ^{235}U). This gave temperatures like 600 to 700°C. I think we will have to go to lower enrichments of uranium. The fission-couple stayed in the reactor for five days while the temperature output steadily decreased. This decrease in output did not tie in with the ^{235}U depletion of the bead. The decrease in output was much too great for fuel depletion. But this application around a power reactor is one which we wanted to try.

We have done flux monitoring, radially and vertically, with these detectors in different prompt burst reactors. This type of measurement seems to be a real use for these detectors. The detector is quite small; so there is a minimum perturbation from the detector itself

when monitoring the neutron flux. We are still trying to develop the fission-couple for steady-state radiation conditions.

McTAGGART: I have two questions. One concerns the rate of heat loss from these beads. You quoted a figure of 8°/sec down the wires. Have you a comfortable figure for the radiation heat loss from the bead itself?

STILLMAN: It does not really become too important until you get to high temperatures like 1000°C. Then it becomes important as the thermal radiation goes as T^4. If you stay at low temperatures, by placing them in the appropriate neutron flux, the heat loss due to thermal radiation appears to be negligible. The numbers we have calculated are in Report LA-3470-MS. If you are looking at a rate change, which is what we use them for in monitoring reactor periods, the time scale is such that temperature losses have not bothered us.

McTAGGART: The other question is have you any experience with using plutonium as the source material?

STILLMAN: No, but Sandia has. They have used plutonium to measure fission spectra. They use neptunium oxide, plutonium oxide, ^{238}U, and ^{235}U to look at the fission spectrum.

BARTON: What sort of periods do you find these thermocouples can measure effectively? What is their time response?

STILLMAN: We used them on the White Sands Missile Range burst reactor and every other prompt burst reactor we could use. We always accurately followed their period measurement. For some time, this was our only means of checking their time response. For determining any limitations in response time, fission-couples were placed 3 m from a nuclear weapon in a recent underground nuclear-weapons test at the Nevada Test Site. The detector accurately followed the change in neutron population (alpha measurement) as the weapon exploded. The rapid change in neutron population has an e-folding time of 20 nsec.

Fast Burst Reactor
Safeguards Analysis

Session 7

7-1 THE ESSENTIALS OF FAST BURST REACTORS SAFEGUARDS ANALYSIS

ROBERT L. SEALE
University of Arizona, Tucson, Arizona

ABSTRACT

A review of the reactor safeguards analysis methods for fast burst reactors emphasizes the essential difference between fast burst reactors and the power reactors that have a dominant influence in the safeguards analysis literature. This difference is the much smaller fission-product inventory present in the fast burst reactor. The objective of safeguards analysis is usually stated as verifying the protection of the public from any exposure to radiation produced by the reactor. Present criteria established for operating facilities meet this objective.

Considering a more restrictive requirement, mainly the protection of personnel at the facility, the record of recent years shows that the concept of remote operation has provided the means of meeting this objective.

Finally, there is hope that the establishment of an appropriate set of operating limits can provide the vehicle by which protection of the reactor itself may be attained. Whether or not this hope is fulfilled depends very strongly on the definition of a realistic set of operating limits and on the measures taken when operating limits are violated.

Operating limits should be defined such that a violation is a clear indication of unsatisfactory performance. Under these circumstances the management of the facility could then take action to analyze the cause of exceeding the operating limits and to assure the future observance of operating limits, greatly reducing the chances of an incident that could damage the reactor. In effect, it is suggested that a violation of the operating limits be treated as an administrative incident of relatively serious proportions. It is important that the spirit of the operating limit not be diluted by the inclusion of trivial restrictions that do not bear on the safety of reactor operation. The operating limits should be clearly and unambiguously stated, and their enforcement should be a prime responsibility of the facility management.

The first step in determining the essential features of the safeguards analysis for a fast burst reactor is to define the objectives of the safeguards analysis. Traditionally the stated function of safeguards analysis has been to provide an engineering evaluation of the anticipated

operating procedures for a reactor to show that normal operation will result in no adverse effect on the radiological environment of the general public and that the radiological exposure of operating personnel falls within the criteria set forth in the appropriate regulations (*Code of Federal Regulations,* Title 10, Chapter I, Part 20, hereafter abbreviated 10 *CFR* 20, for U. S. Atomic Energy Commission controlled facilities).[1] Further, the mechanism by which various accidents might occur and the severity of those accidents are evaluated, ultimately in terms of the effect these accidents might have on the general public. In performing these analyses recourse to the large body of literature on reactor safeguards must be made with care. The large fission-product inventories encountered in large power reactors have influenced the criteria that have been established in the form of guidelines for reactor safeguards analysis. Certainly the Atomic Energy Commission Manual Volume 8401, "A Guide for the Organization and Contents of Safety Analysis Reports," intended as a guide for the analysis of power reactors, has marginal utility as a suggested guide of factors to be considered in analyzing the safeguards requirements for fast burst reactors.

In spite of the preoccupation of AECM 8401 with central-station power reactors, safeguards analysis for fast burst reactors is an art that has been practiced with increasing regularity in recent years. This increase is due to the increased number of fast burst reactors being built to meet the needs of various programs. The need to review and in some cases supplement the safeguards analysis for facilities that have been in operation for some time has also contributed to this activity. These reviews have been the result of the desire to increase the size of the operational bursts at a given facility, the occurrence of incidents at an operating facility, or the questioning of practices or design by the operating staff or the appropriate safety-review groups concerned with the particular facility. The documented results of some of these safeguards analysis activities have been examined in an attempt to determine the significant features of a fast burst reactor safeguards analysis.[2-9]

Although there is not a specified set of questions to be answered or a table of contents for fast burst reactor safeguards analysis, a more or less traditional format has been established for these reports. Typical contents of these reports include introduction, site description, facility description, reactor, reactor analysis, instrumentation and control, organization and operation, and accident analysis. There are some variations from this format; however, the items shown in this tabulation are generally included. Incidentally, a safeguards analysis report contains more information than that required to meet the nominal safeguards analysis requirements. The report usually includes a

broad justification for the construction and operation of the facility. Also, the report is written in a style that allows it to be used as a preliminary training manual for operating personnel. With these additional objectives in mind, a brief summary of the various sections of a safeguards analysis report is in order.

First there is a description of the site, including the geology and climatology of the immediate site and the location of centers of population in the vicinity of the reactor. Second, the facility is described, including the reactor building and the control building. Then the reactor itself is rather comprehensively described. This description includes information regarding the fuel material, the geometry and mass of the various core components, the safety block, the control-rod drive system, and fast-rod actuator systems. Other features may include a description of the start-up source, the burst-initiating source, the reactor cooling system, and special equipment for handling or positioning the reactor in the operating cell.

At this point it is possible to evaluate the extent to which the normal operation of the reactor constitutes a significant radiation source as far as the general public and the operating crew are concerned. We must recognize that the acceptable exposure to the operating crew resulting from the burst operation of the reactor is considerably less than the limits set forth in 10 *CFR* 20. The reason is very simply that the majority of the radiation exposure allowed the operating crew is received between bursts during the performance of duties associated with the routine inspection and maintenance of the reactor core, including such tasks as the tightening of bolts, resetting of limit switches, and the like. As a result the design of the facility is such as to limit the exposure from burst operation to the operating crew to the order of 1% of the 10 *CFR* 20 limit. The exposure limit for unmonitored personnel in 10 *CFR* 20 is approximately one-third that imposed on monitored personnel; consequently, the nominally acceptable exposure to unmonitored personnel from burst operation is higher than the actually acceptable dose to the operating crew since unmonitored personnel do not have access to the reactor and hence are not exposed between bursts. This argument has significance when we consider that there are three ways in which the environment resulting from normal burst operation can be brought within the limits desired. One is by the shielding of the reactor; the second is by the imposition of separation distance between the reactor and the operating personnel. Under either of these circumstances, as long as unmonitored personnel are at distances greater than that of the operating personnel, the requirements of 10 *CFR* 20 have been more than met. If on the other hand the shielding requirement for operating personnel is met by placing them within a shielded room, then the establishment of a large exclusion area

around the reactor is necessary to provide protection of unmonitored personnel. In any event the safeguards requirements to protect both operating personnel and the public from the effects of normal operation are straightforward, and they pose no particular difficulties or even inconvenience in the design of the facility.

The safeguards analysis report also includes an investigation of the control system of the reactor, including a description of the man—machine interface and the various instrumentation channels.

A very important requirement is the outlining of the administrative and operating procedures for the facility. This includes a description of the qualifications of the operating staff, a delineation of responsibilities for operational safety, a statement of the procedures necessary to assure proper design and control of various experiments to be placed in the vicinity of the reactor, and a preliminary statement of the inspection and operating procedures for the reactor. This statement of the operating procedures includes a sequential cataloging of the steps necessary to perform the normal burst in a safe manner and, insofar as is possible at the time of the safeguards analysis, a statement of the consequences of that normal burst.

At this point in the safeguards analysis, we have accumulated the information necessary to understand the normal operation of the reactor; it is at this point that we finally arrive at what is usually regarded as the safeguards analysis for the reactor, that is, the analysis of the consequences of some accidental operation of the reactor. Traditionally this accident analysis has been made on the basis of something called the maximum credible accident (MCA), or more recently, the design-basis accident. Considerable disagreement has arisen regarding the definition of the size of this accident, as evidenced by the information shown in Table 1.

Table 1

BURST SIZES FOR VARIOUS FAST BURST REACTORS

Reactor mass of fuel, kg		Operational burst size, fissions	MCA burst size, fissions
Enriched ^{235}U fuel			
SPR	~57	2×10^{16}	10^{18}
KUKLA	~60	2×10^{16}	10^{18}
FRAN (NRTS)	~63	5.6×10^{16}	1.5×10^{17}
Enriched ^{235}U $-$ 10 wt. % Mo fuel			
HPRR (ORNL)	115	10^{17}	10^{19}
FBR (WSMR)	103	10^{17}	10^{19}
APRF (BRL)	132	1.5×10^{17}	10^{19}
SPR II	105	1.7×10^{17}	10^{18}

For enriched-uranium-fueled reactors, the MCA is a factor 50 times larger than the operational burst. The list of reactors shown in Table 1 is not complete; however, the reactors shown are generally representative of the uranium-metal systems, and the 10^{18} fission MCA is the largest estimated for that system. With ^{235}U − 10 wt. % Mo-fueled fast burst reactors, there is some disagreement regarding the size of the burst classified as the MCA. Incidentally, the operational burst for these systems is from 5 to 10 times larger than for the uranium-fueled systems. The maximum credible accident for the ^{235}U − 10 wt. % Mo reactors is variously set at 10^{18} fissions or 10^{19} fissions. The 10^{18} fission MCA assumed for the Sandia Pulse Reactor II (SPR II) is the same[7] as was assumed for the enriched-uranium-fueled SPR I.[3] Establishing 10^{19} fissions as the MCA corresponds to limiting the energy available from an excursion to that amount necessary to vaporize the core of the reactor.[8] On the basis of the adjustment of the data of Wimett et al.[10] made by Lundin[4] for the ^{235}U − 10 wt. % Mo systems, 10^{19} fissions would be achieved for a reactivity addition of approximately 50¢ above prompt critical. The original calculations of Wimett et al. were based on a coupled neutronic − hydrodynamic model that used a gas equation of state. Parameters in this equation of state were adjusted to give results that agreed through the range of reactivity additions that were achieved in Godiva I. A simple extrapolation of these results is somewhat questionable. Possibly a more cogent argument regarding the establishment of an MCA can be based on the results of the various incidents that have occurred to date in which bare-metal fast burst reactors have been involved. A summary of the documented incidents is given in Table 2. In all instances the fission yield involved in the incident has been well below the 10^{18} fission level, even though in some cases the yield was large enough to cause extensive damage to the fuel of the assembly. Under the circumstances it seems unlikely that the 10^{19} fission MCA is in fact realistic. Quibbling about variations smaller than a factor of 10 is a frustrating mental exercise. In any event the radiological release associated with the occurrence of the MCA does not impose severe limitations with regard to exclusion areas for a fast burst facility. This, of course, is primarily due to the low fission-product inventory associated with these reactors.

Assuming that a competent criticality monitoring system has been designed for the assembly operation, the possibility of a stacking accident is removed by the requirement that all actual approaches to critical be carried out in the remote-assembly mode. Typically incidents occurring during assembly of a reactor are the result of personnel being unaware of the actual geometry of the reactor components (due to improper indication of control-rod or safety-block locations) or

Table 2

CRITICALITY ACCIDENTS FOR METAL SYSTEMS[11]

Incident	Date	Fissions	Cause	Physical damage to assembly
Plutonium core, tungsten-carbide reflector	Aug. 21, 1964	$\sim 10^{16}$	Hand stacking of reflector	None
Plutonium core, beryllium reflector	May 21, 1946	$\sim 3 \times 10^{15}$	Hand stacking of reflector	None
Jemina	Apr. 18, 1952	1.5×10^{16}	Computation error	None
Godiva I	Feb. 3, 1954	5.6×10^{16}	Incorrect positioning of fuel	Slight warping of core pieces
Godiva I	Feb. 12, 1957	1.2×10^{17}	Shift of experimental equipment	Warping, oxidation, near melting of a core center
Uranium core, beryllium reflected	Mar. 26, 1963	3.7×10^{17}	Improper alignment of components	15 kg of uranium burned, 10 kg of uranium melted onto floor
Fast Burst Reactor, White Sands Missile Range	May 28, 1965	1.5×10^{17}	Unprogrammed burst due to error in estimated reactivity	Failure of assembly bolts, coating chipped, two rings thrown from assembly
Aberdeen Pulsed Reactor Facility, Ballistic Research Laboratory	Sept. 6, 1968	$\sim 6 \times 10^{17}$	Burst rod in seated position not at maximum reactivity position in travel	Plastic flow in safety block, fusing of some core parts

an improper assessment of the reactivity worth of experimental assemblies, which act as reflectors placed in the vicinity of the reactor. Analysis of the characteristics of the assembly greatly limits the consequences of such an incident by requiring the presence of a source of neutrons during the assembly operation and limiting the rate at which reactivity is added to the assembly as the components are brought together. Hansen's[12] classic analysis of this problem has been applied to the SPR II reactor by Coats and O'Brien.[7] Their results indicate that the chances of having an inadvertent burst that would exceed the operational burst of about 2×10^{17} fissions during the assembly of SPR II in the presence of an effective source of 4×10^5 neutrons/ sec is less than 1 in a 1000 if the ramp rate of the reactivity addition is kept less than \$4/sec. Accordingly the safety-block speed has been adjusted to never exceed a reactivity addition of \$4/sec. The result of this procedure is not to prevent an inadvertent burst but to provide assurance that the size of an inadvertent burst during start up will be limited to a value within the capability of the assembly. This ramp rate is made satisfactory for the rapid assembly of the reactor when a programmed burst is desired by the simple expedient of removing the source and allowing the background neutron population to decay, reducing the chances of preinitiation to an acceptably small value for the programmed burst. Thus a compromise between the desire to limit the unprogrammed burst and to have an acceptably low incidence of preinitiated bursts is achieved.

The conclusion from this example is not that all burst reactors should be designed to have a ramp rate of reactivity addition that is less than \$4/sec; rather, the use of ramp rate of insertion of reactivity as a design parameter instead of as an independent variable in the safety analysis is to be commended. Little is contributed to safety to make detailed analyses of the consequences of extremely high rates of reactivity addition to predict the occurrence of paper incidents that reach the limit of the so-called maximum credible accident. Rate of reactivity addition is, in fact, a variable that can be controlled during the assembly of the reactor, and methods of analysis of the influence of rate of reactivity addition as a function of the source strength of neutrons in the reactor are available.

The programmed burst in which an excessive amount of reactivity is introduced to the machine is a result of improper evaluation of the desired reactivity to be inserted above delayed critical to get the desired burst size. Presumably if the calibration of the reactor control rods and burst rod has been properly carried out and the evaluation of the adjustment necessary to get the desired reactivity above delayed critical is properly made, this incident does not occur. Unfortunately this incident has occurred in the past, and one can only conclude that,

when it has occurred, it has been the result of (1) a gross error in interpretation of the calibration curves by the operator, (2) unfamiliarity with or misunderstanding of the characteristics of the reactor on the part of the operator, or (3) undetected movement or unexpected effects from experimental equipment. It is difficult to see how a formal safeguards analysis performed prior to the construction of the reactor can provide any great measure of assurance against the occurrence of the latter type of incident. However, the safeguards analysis can set the stage for the proper climate for the management of the facility. Ultimately administrators of the facility have the responsibility to motivate personnel to discharge competently the responsibility for reactor operation.

In summary, the safety analysis of a fast burst reactor satisfies its limited objective, namely, documenting the measures to protect the public from radiation exposure resulting from the normal operation of the reactor or the occurrence of incidents. Indeed, in many instances, the exclusion areas that have been provided around operating facilities are actually greater than those required to satisfy the needs of the safeguards analysis, and one can only speculate on whether considerations of privacy and prestige associated with large exclusion areas may or may not enter the issue.

In imposing a more restrictive requirement on the safeguards analysis, namely, verifying the protection of personnel at the operating facility, it seems obvious that the concept of remote operation has proven to be more successful than anyone had ever hoped. The eminent safety record of operating personnel at fast burst reactor facilities in the last 20 years attests to this.

Having speculated about real estate and pointed with pride to the success of the concept of remote operation in protecting operating personnel, it seems only appropriate to turn to the challenge of the future. The hope is that modern safeguards analysis can provide a vehicle by which a significant measure of protection of the fast burst machine can be attained. This goal may be reached through the definition of a set of operating limits that defines a standard of performance against which the operation of the facility can be judged. The requirement for operating limits for various reactors has been imposed in this country in the last few years. There has been some question as to the proper definition of an operating limit relative to the normal operation of a machine. It seems appropriate that operations that exceed the operating limit should be treated as an administrative incident even though no significant damage to the fast burst reactor machine has taken place. Assuming the proper attitude on the part of the management of the facility, analysis of the cause of exceeding operating limits, and action taken to assure the future observance of operating

limits could greatly reduce the possibility of an incident occurring that would damage the reactor. To be an effective administrative tool, operating limits should be uncluttered by trivial points that do not bear upon the safety of the reactor operation. The operating limits themselves should be clearly and unambiguously defined, and the enforcement of their intent should be a primary responsibility of the administration of the facility, which brings us to probably the most important point of all. In the operation of a fast burst reactor facility, there can be no ambiguity regarding responsibility for the safety of the operation of the facility. Lines of communication should be clear-cut, review procedures for various experiments should be unambiguously defined, and any deviation from this review procedure should be seriously reprimanded.

REFERENCES

1. *Code of Federal Regulations*, Title 10, Chapter I, Rules and Regulations, Part 20, U. S. Atomic Energy Commission.
2. E. R. Christie and B. W. Mar, The KUKLA Prompt Critical Assembly, Hazards Summary Report, USAEC Report UCRL-6105, Lawrence Radiation Laboratory, 1960.
3. P. D. O'Brien, Hazards Evaluation of the Sandia Pulsed Reactor Facility, USAEC Report SC-4357A (RR), Sandia Corporation, 1961.
4. M. I. Lundin, Health Physics Research Reactor Hazards Summary, USAEC Report ORNL-3248, Oak Ridge National Laboratory, 1962.
5. K. B. Carver and T. G. Taxelius (Eds.), Fast Burst Reactor Facility. Final Safeguards Report, U. S. Army Report KN-685-63-1, Kaman Nuclear Division, Kaman Aircraft Corp., 1963.
6. W. S. Gilbert, F. A. Kloverstrom, and F. Rienecker, Jr., Safety Analysis Report for the Super KUKLA Prompt-Burst Reactor, USAEC Report UCRL-7695, Lawrence Radiation Laboratory, 1964.
7. R. L. Coats and P. D. O'Brien, SPR II Safety Analysis Report, USAEC Report SC-RR-66-2706, Sandia Corporation, 1967.
8. R. W. Dickinson et al., Safety Analysis Report for Army Pulse Radiation Facility Fast Pulse Reactor, U. S. Army Report BRL-1356, Ballistic Research Laboratory, 1967.
9. S. R. Gossman and V. B. Gottschalk, Safety Analysis Report for FRAN Prompt Burst Machine, USAEC Report IDO-17231, Phillips Petroleum Company, 1967.
10. T. F. Wimett, R. H. White, W. R. Stratton, and D. P. Wood, Godiva II—An Unmoderated Pulse Irradiation Reactor, *Nucl. Sci. Eng.*, 8: 691-708 (1960).
11. W. R. Stratton, Review of Criticality Accidents, USAEC Report LA-3611, Los Alamos Scientific Laboratory, 1967.
12. G. E. Hansen, Assembly of Fissionable Material in the Presence of a Weak Neutron Source, *Nucl. Sci. Eng.*, 8: 709-719 (1960).

7-2 SOME ASPECTS OF RISK ASSESSMENT IN RELATION TO A BURST REACTOR

F. R. FARMER
Authority Health and Safety Branch, United Kingdom Atomic Energy Authority,
Risley, Warrington, Lancs, England

ABSTRACT

The quantitative technique previously proposed[1] by the author is used selectively to discuss some aspects of burst reactor safety. It is concluded that, subject to certain provisos, a fast burst reactor can, in principle, be designed and operated within the safety targets proposed. In addition, the author points out that, apart from safety considerations, the need to "protect investment" leads to criteria of the same order as those derived from safety requirements.

All reactors carry some risk of releasing fissile material and fission products to the atmosphere, and a burst reactor is no exception. This risk can be made acceptable by incorporating various features into the design and by adopting special procedures in operation. The extent of these protective measures is obviously a matter of opinion which reflects past experience and current practices in the industry.

This paper does not set out to establish the safety of a specific reactor, nor is it a justification of one method of assessment against another. Its purpose is to illustrate some aspects of the probabilistic approach. In essence, this approach is quite simple, even if difficult to apply. It recognizes that there is some risk in building and operating reactors as, indeed, there is risk in most human activities.

The type of risk and the extent of public involvement is fairly clear for most common industrial or social activities; however, nuclear energy is seen as a new risk and one carrying a greater potential for public involvement. This factor has led to more interest in safety than is usual in technological development and to a search for a definition of "undue risk"—a search which, up to date, has been largely illusory.

During the last 20 years, the consideration of risk from nuclear activities has passed through many stages. One, which is easily assimilated and superficially attractive, aims at establishing a limit of risk from all credible occurrences at a level at which there would be no harm to people, or more correctly, that the potential harm would be below the level of statistical observation. But, as time passes, the framework of credibility becomes more complex; additional and more unusual situations are examined, such as the effect of crashing aircraft, earthquakes, or typhoons, and early assumptions are reexamined, bringing again into question the possibility of pressure-vessel or large-pipe failure or the effectiveness of spray or flooding systems.

This question may seem far removed from a fast burst reactor, but what accidents should a designer assume? What should he deem credible or incredible when he enters a field with no established case history? Should he assume the potential failure of any stressed steel by analogy of pipe failure? Should he assume that control systems will operate and that valves will close? Should he consider externally impacting loads, such as aircraft?

The answers do not emerge clearly from a study of past rulings; the designer may be forced to obtain new rulings from safety committees and licensing groups. Consultative processes are obviously desirable in setting up safety standards, but clearly consultation should lead to criteria that are reasonably stable and unambiguous and capable of common interpretation whether applied by designer, operator, or assessor.

In an attempt to generate discussion of basic risk criteria, an earlier paper[1] discussed an extreme example of siting a large reactor in the middle of a populated area of four million people. Assuming ^{131}I as an indicator of hazard, a boundary line was proposed relating the upper limits of iodine releases and their corresponding frequencies of occurrence; for example, limiting 10^3 curies at 10^{-3}/year, reducing to 10^{-6}/year for 10^5 curies. Reactors may not be capable of reaching this target for some time to come; but in a development phase a somewhat higher risk may be acceptable, and on other less-populated sites a less-restrictive target would still maintain risk at the same level.

Considerations of this type when applied to a fast burst reactor involve the following stages:

1. Determine the Potential Hazard. The reactor may contain plutonium in addition to fission products. The limit of hazard will depend very much on size and fuel, but it is likely that the extreme limit is comparable to that of a 1- to 10-Mw power reactor, i.e., in the range of 10^4 to 10^5 curies of ^{131}I. For this release the target frequency proposed[1] for a populated site is 10^{-5} to 10^{-6} per year.

2. Consider the Site. On a fairly remote site, the public risk can be reduced by at least 2 orders of magnitude to give a target of 10^{-3} to

10^{-4} per year. The protection of people on the site and the effect on other facilities needs consideration but is unlikely to modify the target specification in the low-frequency region.

3. Consider the Reactor. An early safety assessment will indicate some of the ways in which accidents might occur. Unlike most power reactors, the safety of a fast burst reactor is unlikely to depend on the heat-removal circuits; and the reactor is unlikely to work under high pressure and is therefore not dependent on the integrity of a primary pressure envelope.

The main areas of concern are likely to be:
(a) Errors in prediction of the core performance, i.e., uncertainty in parameters.
(b) Errors in operator action.
(c) Failure in the control system designed to shut down the reactor after a burst.

The electrical and mechanical gear provided to shut down the reactor will have some chance of failure which might be as low as 10^{-3} to 10^{-4} per demand but is unlikely to be lower, particularly in an experimental facility, even with the provision of alternative and redundant systems. If there are 100 operations per year, a chance of failure is in the range of 10^{-1} to 10^{-2} per year, quite a significant risk.

Although a failure does not necessarily lead to a peak of energy liberation and core dispersion, uncontrolled excursions are difficult to analyze and expensive to test. It is unlikely then that the designer will attempt to show that the risk of a severe excursion is less than 10^{-2} (within the family of all possible excursions); rather, he will seek means for containing the consequences by providing containment local to the hazard (e.g., plutonium) or as an enveloping enclosure with or without filters.

These protective measures are likely to ameliorate the consequences of a wide range of accidents and are more likely to succeed for small excursions than for large ones. There is some risk of partial or complete failure through faults in valves, switchgear, joints, or filters, or in passive systems through incomplete appreciation of the consequences of the accident (pressure, temperature, missiles, etc.).

For reasonably simple systems, a failure rate approaching 1 in 100 is achievable and capable of fair, if not precise, confirmation by vigilant inspection. A significantly lower rate is difficult to achieve, and it brings into question the validity of the accident analysis. Hence, at the conceptual design stage, it seems possible to reach the target in the respect of accidents stemming from malfunction of the shutdown system.

Mechanical and electrical equipment can be routinely tested, and performance based on or compared with a considerable amount of

parallel and relevant information. In contrast, the possibility of human error in loading or in evaluation of core performance is far less amenable to comparative numerical evaluation—partly on emotional grounds, partly through lack of systematic study. This subject has received attention in aircraft safety, and recently J. F. Ablitt has discussed some implications of human error in reactor operations. It remains for the designer or assessor to recognize that failure is possible, to identify areas of particular safety significance, and to state his own views on failure rate.

The production of a burst will require adjustment of the reactor controls by the operators. It is intended that such operations should be scrupulously vetted and double checked, but, even so, I believe that mistakes may arise at a rate between 1 per 100 to 1 per 1000 per operation.

Recognizing the possibility of error, some designers will attempt to limit consequences by ensuring that the maximum foreseeable error leads only to fuel damage and not to violent disruption. Limitations of this sort imposed by design undoubtedly reduce risk, but at some lower frequency they are circumvented by intent or mischance. On balance, it is hard to believe that the risk of severe accident from error in control settings can be much less than 10^{-3} per event. If the control settings are adjusted 10 to 100 times per year, this again gives a predicted accident frequency of 10^{-1} to 10^{-2} per year.

These arguments have been presented in generalized form; however, any specific proposal for a reactor would be treated in considerable detail, and the best use made of all available and relevant information on plant and operator performance. In summary, an assessment might conclude that a fast burst reactor can be designed and operated within the safety targets proposed, provided that:

(a) The reactor site is reasonably remote.

(b) The control system has adequate diversity and redundancy and is subject to planned maintenance and performance checks.

(c) The core evaluation and control setting is carried out by competent staff and double checked.

(d) Containment shall be provided to limit the escape of hazardous material to less than 1%. This containment shall be shown by routine tests to have a chance of failure of less than 10^{-2} per event.

Even so, on a provisional judgment, the risk of severe damage to the facility might be 10^{-1} to 10^{-2} per year, and the risk of releasing a substantial fraction of the core material might be 10^{-4} per year.

Apart from safety, considerable emphasis must always be placed on the protection of investment. The present estimate of risk to the facility of 10^{-1} to 10^{-2} per year is probably as high as could be tolerated. This is the range predicted for malfunction of the control system

or operator error (for the assumptions made). Hence, sustained effort is needed to reduce the accident frequency, effort apart from any later protection that may be credited to containment.

This paper illustrates a general theme, the numbers used are indicative only; they are used to amplify the theme. If the fast burst reactor contained no plutonium (or equivalent), the estimated hazard might be reduced by a factor of 100; consequently, either containment might be omitted or more populated sites might be used. Conversely, if the reactor contained large amounts of plutonium, the overall hazard might be increased by a further factor of 10 and even more stringent containment might be required or limitations might be placed on the frequency of operation or times of operation. Essentially, this approach recognizes that man-made objects may fail and that operators may fail and that estimates of failure potential derived from perceptive and critical use of comparative data, systematically assembled, will give a better appreciation of the potential weaknesses of the reactor system. This approach does not lead to the indefinite chase of the infinitesimally small ("to reduce the possibility of failure to nil to the sixth power"), provided that there is agreement on the degree of risk currently considered reasonable in relation to consequences. Agreement on this score is likely to develop in time as most countries at a comparable stage of development carry risks from social and industrial activities that differ only by small factors from country to country. There may be arguments about the interpretation of evidence, but, if considered constructively, these arguments will in time lead to a convergence of opinion, as future safety can only be based on past and present experience.

REFERENCE

1. F. R. Farmer, Siting Criteria—A New Approach, in *Containment and Siting of Nuclear Power Plants,* Symposium Proceedings, Vienna, 1967, pp. 303-323, International Atomic Energy Agency, Vienna, 1967 (STI/PUB/154).

7-3 A STANDARD FOR FAST BURST REACTORS

A. DE LA PAZ
Department of the Army, White Sands Missile Range,
New Mexico

ABSTRACT

The accumulated experience and continued development and use of fast burst reactors make it essential that a standard be developed for the operation of these reactors. The efforts of American Nuclear Society subcommittee N14 have led to the development of a standard based on the full use of the experience gained to date. This standard, when formalized and issued, should be of considerable use to personnel involved in the design, operation, and regulatory review of fast burst reactors.

The use of fast burst reactors in a variety of experimental programs has resulted in a wealth of accumulated experience. Further, the demonstrated versatility of fast burst reactors has led to their continued development and application in support of new experimental requirements. The projected development of this field of reactor technology, coupled with the availability of operational experience, has made the development of a standard for the operation of fast burst reactors highly desirable. Recognizing this, the Standards Committee of the American Nuclear Society established a subcommittee whose objective is the preparation of such a standard. It was considered that development of a standard on operation of fast burst reactors would provide a basic set of general guidelines aimed at the safe and proper operation of these reactors in accordance with the benefit of past experience. The availability of these general guidelines would benefit those persons involved in the operation, design, and regulatory review of these reactors. The availability of the standard will also strengthen the basis of understanding between operational and regulatory review organizations.

The subcommittee, designated as N14, was organized in 1968; it consists of the following members:

A. De La Paz, White Sands Missile Range, Chairman

D. P. Wood, U. S. Atomic Energy Commission, Albuquerque Operations Office

P. D. O'Brien, Sandia Laboratories

T. F. Wimett, Los Alamos Scientific Laboratory

L. B. Holland, Oak Ridge National Laboratory

R. L. Long, University of New Mexico

Effort on developing a standard for operation of fast burst reactors was initiated by the subcommittee in August 1968 primarily as a result of the work of H. Paxton at Los Alamos Scientific Laboratory. The starting point for the standard was a list of general guidelines developed as a result of discussions between H. Paxton and some of the members of the subcommittee (Wimett, O'Brien, and Long). A draft standard was developed and sent out for review and comment by members of the subcommittee and others working in fast burst reactor technology. Extensive discussions and communications on this draft standard were then used in the development of the current form of the standard being acted upon by the subcommittee. This current form of the standard is presented as Appendix A of this paper.

OBJECTIVES

The standard, as proposed, has as its primary objective the specification of general criteria to be applied to the operation of fast burst reactors to ensure the safety of the general public and operating personnel. Other general objectives in addition to this basic safety requirement include the identification and emphasis of the role of the administrative procedures and the definition of basic reactor system performance requirements. The latter areas, for example, are of considerable importance since they significantly affect the safety of the overall operation. The combination of the basic objective and the supporting general requirements is aimed at development of a standard that, in general, applies to all fast burst reactors.

The standard is not intended to specify design requirements or otherwise limit or infringe upon design efforts in fast burst reactor technology. This aspect is necessary since preparation of a standard cannot be based upon projected developments in the field, and it must rely primarily on the use of past experience and present technology. The standard is therefore primarily directed at the operation of fast burst reactors. The requirements noted in the standard may, of course, be used by the reactor designer for general guidance but should not be considered as limiting his effort.

The standard as developed is divided into two essential areas: (1) those considerations which should be adhered to for compliance with the standard and (2) those factors which are recommended but do not need rigid compliance. The word "shall" defines the former considerations whereas the word "should" covers the latter. In this connection, the subcommittee did not pass or otherwise make a judgment regarding the requirement and enforceability associated with compliance with the standard. It was considered that this area was beyond the purview of the subcommittee, whose function was primarily the technical development of the standard. The matter of enforceability of the standard is the same as that which applies to all standards developed by the American Nuclear Society (ANS). In all cases, further formalization and legal action beyond the scope of ANS are required.

The following parts of this paper present the principal considerations associated with the basic areas of coverage of the standard.

ADMINISTRATIVE PROCEDURES

The general administrative procedures that are necessary to the safety of fast burst reactors are presented in terms of: (1) the definition of responsibilities, (2) the review procedures that apply to proposed experiments, (3) the requirements on the availability and presence of properly certified personnel during reactor operation and maintenance, and (4) the availability of written procedures governing the operation of the reactor.

The requirement that management define the responsibilities involved in reactor operations is aimed at ensuring that all personnel fully understand their commitment to the safety of reactor operations within the scope of the duties and responsibilities of their position. If this is not accomplished, a lack of communication among the personnel involved, for example, could lead to a possibly hazardous condition. Moreover, if an ambiguity exists in this area, it would be greatly emphasized if something did go wrong. The clear definition of duties and responsibilities is an essential part of the overall selection, training, and certification of reactor personnel, and it must be effectively carried out by management.

The state of the reactor systems must be properly monitored by the reactor staff personnel any time that an actual or potential change in the condition of these systems takes place. The requirement that (1) two certified personnel be present in the control area during reactor operations and (2) one certified reactor operator be present in the control area during any maintenance or experimental setup effort involving the reactor systems is aimed at providing this coverage.

The need to provide for the review of proposed experiments prior to their irradiation is essential to the safety of the reactor operations.

This need is particularly significant in view of the different types of experiments that may be irradiated and their effect on the burst characteristics of the reactor. The proper evaluation of these effects is essential to the safety of the reactor since its reactivity state and the value of the prompt reactivity inserted to achieve the burst may be changed by the location, size, and mass characteristics of the reactor. In addition, experiments having unique characteristics, such as fluids or explosive materials, may be proposed for irradiation. The established review procedures should provide for the evaluation of the safety of the reactor under all proposed experimental arrangements.

FACILITY LAYOUT

A section covering the general requirements applicable to the fast burst reactor facilities is included in the standard. The initial part of the section deals with the requirements covering access to the reactor and the provisions that must be provided to ensure the safety of the general public and operating personnel during all phases of operation of the reactor. This includes shielding, fencing, and any other physical provision that may be employed to accomplish the proper degree of safety.

General factors that should be considered in the design of the facility are also presented. Attention is directed at the provisions that are required to prevent accidental criticality resulting from maloperation of facility auxiliary systems, such as cranes and elevators. Reference is also made to the need for having emergency procedures and provisions for preventing flooding of the reactor cell.

The inclusion of these factors in the standard is aimed at ensuring that the overall reactor facility is provided with appropriate provisions not directly associated with the reactor system but nevertheless necessary to the protection of operating personnel and the general public.

REACTOR CHARACTERISTICS

Characteristics covered in the standard basic to fast burst reactors are aimed at establishing the safety necessary to permit operation. The major areas covered are the requirements that apply to the provisions made for the control and termination of the reactor operation. The major safety device is defined as the safety-block movement; it reflects the condition that this movement be the primary mechanical shutdown mechanism of the reactor. In addition, the standard calls for at least two independent safety devices (such as movement of the safety block and control rods) having fail-safe features.

A primary requirement included in the standard is that the reproducibility of the reactivity-control components shall be such that variations in burst yield do not exceed plus or minus 20%. This provision is of vital importance since the degree of repeatability of burst yields at equivalent conditions is an excellent means of monitoring the operational condition of the reactor. If the variation is high or otherwise not in line with previous data and experience, it may indicate that there is looseness in the control elements, thus resulting in different positioning conditions prior to the burst. Corrective action must then be taken to prevent any further deterioration of the system involved which would result in still greater variations in burst yields.

This section on reactor characteristics in the standard also includes the general provisions that should be available in reactor-system interlocks to prevent resetting of the reactor scrams or insertion of the safety block unless the control elements are at their position of minimum effectiveness. The section also notes that an interlock should be included to prevent the addition of reactivity after the start of the neutron-decay period. These requirements have been included to ensure that the sequence of reactor operation is carried out such that additions of reactivity are made under carefully controlled conditions that permit a proper evaluation of the effects of these additions on the overall reactivity state of the reactor.

EQUIPMENT CRITERIA

General requirements have been included to ensure that provision is made for the prevention of any unauthorized operation of the reactor. In addition, guidelines have been included noting that manual scram capabilities should be provided which can be actuated from any location that requires the exclusion of personnel during reactor operation. These general requirements are expanded to include the need to ensure communication between personnel at the reactor control console and others at various locations in the facility, particularly the reactor cell. Provisions for ensuring that the reactor is scrammed upon loss of power to any safety device have also been included.

OPERATING PROCEDURES

General procedures considered to be necessary in the safe operation of fast burst reactors are also included in the standard. These procedures include the clearing of the reactor exclusion areas and the satisfactory check-out of newly installed or modified equipment prior to reactor operations. In the standard particular attention is paid to the

need for suspending operations if an unexplained behavior of the reactor takes place. The general opinion of the subcommittee was that such situations should not be left unresolved since the unexplained behavior could be a preliminary indication of an uncontrolled operation. The reliance placed upon proper operation of the reactor systems to terminate the burst and the fact that once the burst is initiated it proceeds to a termination based on the performance of the reactor systems make it essential that routine operations be suspended under these circumstances. The subcommittee did, however, recognize that reactor operations could be required to evaluate the cause of malfunctions or system deficiencies.

This section of the standard on operating procedures concludes with a presentation of the general requirements of the burst-production cycle and the operations that should be performed prior to initial burst operation of a reactor. Requirements for the daily check-out of the reactor systems prior to operation are also presented.

APPENDIX A: TENTATIVE STANDARD FOR FAST BURST REACTORS

Scope

This standard is for the guidance of those persons involved in the design, operation, and review of fast burst reactors. It has been formulated in general terms to be applicable to all current fast burst reactors and is intended to be used only for general guidance in design effort for future reactors.

Definitions

LIMITATIONS

The following definitions should not be regarded as encyclopedic. Other terms with definitions accepted by usage and by standardization in the nuclear field are not included.

GLOSSARY OF TERMS

Shall, should, and may: The word "shall" is used to denote a requirement; the word "should" to denote a recommendation; and the word "may" to denote permission, neither a requirement nor a recommendation. To conform to this standard, all operations shall be performed in accordance with its requirements but not necessarily with its recommendations.

Fast burst reactor: An essentially unmoderated assembly of fissionable material designed to be operated to produce short-duration high-intensity bursts of fission radiation.

Scram: A rapid reduction of reactivity to subcriticality.

Control elements: As used herein the term "control elements" includes those reactor-core components whose movement increases or decreases the reactivity of the reactor, and it includes the control rods, burst rod, and safety block, or equivalent.

Safety block: The safety block is that control element having a reactivity worth such that its movement following a burst is the primary mechanical means of terminating the operation.

Safety device: A mechanism or system designed to reduce the reactivity of a fast burst reactor by movement of one (or more) of the control elements.

Administrative Procedures

Responsibility for the safety of operation shall be assigned unambiguously by management.

An experiment plan shall be reviewed and approved in accordance with procedures established by management prior to the start of each experiment.

At least two persons properly certified in accordance with procedures established by management shall be present in the reactor-control-console area during burst operation of the reactor.

At least two properly certified persons shall be present during reactor maintenance or experimental setup operations involving potential changes in reactivity of the reactor. One of these two persons shall be present at the reactor control console.

Written procedures incorporating safety features shall govern all operations. There shall be provision for keeping procedures current.

Facility Layout

Procedures shall be established for the control of access to the reactor area.

Physical provision (e.g., shielding, fencing, and distance) shall be provided for the protection of the general public and operating personnel from the effects of a burst an order of magnitude greater than the planned limit.

The following shall be considered in planning a fast burst reactor facility:

a. The prevention of accidental criticality that might result from failure or maloperation of supporting equipment, such as cranes, elevators, or other handling devices.

b. The prevention of unauthorized entry into hazardous areas during nonworking hours.

c. Convenience of reactor operations and feasibility and ease of reactor-systems maintenance procedures.

d. Prevention of flooding.

e. Emergency procedures.

A permanently installed radiation area-monitoring system with appropriate alarm indication shall be provided which is designed to monitor and indicate the radiation levels at selected points.

Reactor Characteristics

Inherent prompt-reactivity quenching (negative temperature coefficient) shall be a fundamental characteristic of the reactor.

There shall be at least two independent safety devices (such as a safety block and control rods), and both shall have fail-safe (with respect to electrical power) scram features.

The major safety device (such as safety-block movement) shall be capable of shutting down the reactor to subcritical under the most reflective conditions for any possible experimental arrangement. The rate of reactivity reduction upon scram shall be greater than the normal rate of addition.

Reproducibility of the effect of the reactivity-control components shall be such that burst yield variation shall not exceed $\pm 20\%$.

A shroud to limit neutron reflection by experiment should be available and used as deemed appropriate.

There should be control rod(s) with total reactivity worth greater than the excess reactivity (with the reactor fully assembled and all control rods in) for the bare (unreflected) reactor.

There should be interlocks to prevent the following:

a. Resetting of the scrams unless the control elements are at positions of minimum effectiveness.

b. Insertion of the safety block unless the other control elements are at positions of minimum effectiveness, except at the end of the neutron-decay period.

c. Reactivity addition by control-rod movement after the start of the neutron-decay period.

Equipment Criteria

There shall be physical safeguards against unauthorized operation of the reactor.

There shall be means of communication between personnel at the reactor control console and others in the reactor area.

Provisions for manual scram actuation shall exist at the reactor control console and in those general locations in the reactor area which require the exclusion of personnel during reactor operation.

Loss of power to any safety device shall initiate a scram.

Operating Procedures

Procedures for ensuring that the reactor exclusion areas are cleared of all personnel shall be established and carried out prior to the start of any reactor operation.

The satisfactory mechanical performance of newly installed or significantly altered control-element systems or safety devices shall be established before achieving initial criticality following the system or component installation or modification.

Reactivity additions shall not be made unless the effects of preceding additions have been observed and understood.

Any unexpected behavior of the reactor or its associated equipment shall be evaluated promptly.

The proper functioning of the required number of safety devices shall be established prior to starting operations each day. In the course of these tests or early in each day's operation, the response of each required detector system to a change in neutron or gamma-ray level, as applicable, shall be confirmed.

Consideration of the influence of peripheral experimental equipment on reactivity and the calibration of all control elements shall be guided by prior experimental information and calculation.

Additions of reactivity shall not be made simultaneously by two or more types of control elements.

The following operations should be performed as part of the initial operations conducted following first assembly of the reactor fuel. These preliminary operations should be conducted in accordance with formally approved written procedures.

a. A visual and mechanical check of the reactor fuel assembly.

b. Verification of reactor-shutdown margin and determination of the rate of shutdown associated with safety-block movement.

c. Detailed calibration of the control rods, including a check of the reproducibility of the reactivity effects of cycling the control rods.

d. Calibration of the burst rod with sufficient detail to govern adjustment to the desired worth, if applicable.

e. Calibration of incremental reactivity adjustments, such as those required to compensate for reactivity effects of peripheral experimental equipment.

The burst-production cycle shall include the following:

a. A reference reactivity check at delayed criticality or by means of a positive period no shorter than 10 sec.

b. Adjustment of the control-rod positions, taking into account the reactor-fuel temperature and the effects of the experimental arrangement on the reactivity worth of the burst rod so that actuation of the burst rod will give the desired reactivity.

c. Adjustment in reactivity by control-rod movement to compensate for temperature variations during the neutron-decay period, if required.

DISCUSSION

McENHILL: I think I missed the objectives of the exercise, yet the objectives must, I feel, be eminently clear. There was a compound of principle and procedure in the presentation, whereas I personally feel there is a need to divorce the two. It is a very salutary exercise for each operator to sit down and carefully delineate the safety principles upon which his reactor and his total facility depend. Having set down all the principles on which safety depends, he can then delineate the full detailed operating procedures, and at this stage he can use codes of practice, etc., to help him. I was concerned that with a compound of principle and practice such as that proposed there is just a danger that this could become a checklist for operators who thought that if they went through all these things they might have a safe facility. I am not wholly sold on the idea of standardized encyclicals. I like general principles and I like illustrations, but I get a little worried about detailed codes of practice taking the place of thinking and experience. I admit I may be quite wrong in the objectives.

DE LA PAZ: The objective of the standard is not to provide details of operational procedures. The standard would not replace the basic safety documents of the facilities, such as the technical specifications, operating limits, procedures, or the safeguards analysis report. It does, however, in a general way, hopefully provide some basis of understanding between the regulatory review agency personnel and the reactor-operations personnel. For example, if the standard were completed we would not have any possibility of an unexpected imposition of new safety requirements. So the standard provides a definition of requirements which form the basis of, hopefully, some understanding. Only in that respect do I think that it has merit.

ZITEK: Are you saying that the Atomic Energy Commission will accept this standard in lieu of a technical specification?

DE LA PAZ: No. I said that the standard does not replace the technical specification. This stage in operational considerations deals with safety, and it is apart from technical specifications.

CALLIHAN: The disposition of this proposed standard has not been entirely established. I cite a similar document, prepared a number of years ago, dealing with critical experiments that exists today not as a USA standard but as an ANS standard. Nonetheless, following the process by which a draft is first developed and after the subcommittee action when they have prepared what they believe to be a final document, the

availability of that document will be announced in *Nuclear News* and will be available for comment. There is still that opportunity to take a crack at it. This present draft is an effort, at any rate, as was the one with critical experiments, to get into print that on which experienced people in the field had agreed. Obviously there is no legal connotation in any industry-developed standard until a regulating body, a municipality for example, adopts it as a part of a code, as a part of a building code for example.

Throughout these papers a thread of experience has run which leads me to a very hackneyed remark: we have a score or more years now of exciting and progressive experience in nuclear energy, but they have been frightfully costly because of safety factors piled on top of ignorance factors, and ignorance factors piled on top of safety factors. Now one can at least express the hope that some return can be gleaned from the experiences of these costly years.

Wider Applications
of
Fast Burst Reactors

Session 8

8-1 NEUTRON DIFFRACTION USING REPETITIVELY PULSED SOURCES

R. M. BRUGGER* and K. H. BECKURTS†‡
*Idaho Nuclear Corporation, Idaho Falls, Idaho; †Brookhaven National
Laboratory, Upton, New York

ABSTRACT

The methods of neutron diffraction and possible experiments are outlined.
The advantages of such methods are established, and the ability to increase
the effective experimental capabilities is demonstrated. The mentioned ex-
periments demonstrate the need for a continued effort to increase the effec-
tiveness of slow-neutron-scattering experiments.

INTRODUCTION

Thermal neutrons have advantages compared with other types of
particle probes in revealing the positions[1] and motions[2] of atoms in
solids, liquids, and gases. In this paper thermal-neutron research
with repetitively pulsed neutron sources leading to structural infor-
mation will be discussed; in the following paper (K. H. Beckurts and
R. M. Brugger, Session 8, Paper 2), the inelastic-scattering experi-
ments leading to dynamical information will be presented.

The first of the advantages neutrons have over other methods
is that neutrons are penetrating particles for most samples, which
allows them to see the atomic structure in bulk and not on the surface.
One example of the exploitation of this penetrability is in studies of
samples at high pressures in which the neutron passes through a
relatively thick sample holder and observes the pressurized sample
inside. The second advantage is that the neutrons most desirable for

---

diffraction studies are nondestructive because they have too little energy to break chemical bonds. It has been shown that powder diffraction patterns for samples that disintegrate during an X-ray exposure can be obtained by neutrons without excessive damage. The third advantage is that neutrons have a different sensitivity of interaction to atoms than do the other probes. This allows different combinations of atoms to be studied, i.e., neutrons can locate the positions of hydrogen atoms in the presence of heavy elements and the ordering of atoms in compounds composed of neighboring elements in the periodic table. The fourth advantage is that, since the neutrons have magnetic moments, they interact with atoms having magnetic moments to reveal magnetic ordering in materials. Neutron diffraction has contributed the bulk of our knowledge about magnetic ordering in antiferromagnetic materials, spiral magnetic structures, spin density waves, and magnetic density distribution per unit cell. Because of these many advantages, thermal neutrons have become an important probe for the researcher to ascertain atomic structures.

As with most particle probes, the advantages of neutrons in certain situations are disadvantages in others. For example, the fact that neutrons are penetrating probes means that they are poor for studying surface phenomena. In addition to such inherent disadvantages, neutron diffraction has always lagged behind X-ray diffraction in developments of experimental techniques and the availability and intensity of sources. Because of the advantageous qualities of neutrons, a need exists for more sources to pursue pulsed-neutron studies. Many of their disadvantages will be overcome when intense repetitively pulsed neutron sources become available and techniques are developed to exploit them. The following sections will briefly outline some of the changes in techniques and the experiments that are possible now or will become possible when more-intense sources are realized.

PRESENT DIFFRACTION TECHNIQUES

Neutron diffraction is based on the Bragg relation $\lambda = 2d \sin \theta_B$, where λ is the wavelength of the neutrons, d is the plane spacing of the crystal, and θ_B is the Bragg angle (which is one-half the scattering angle). The conventional neutron-diffraction approach was an outgrowth of X-ray diffraction; neutrons having one wavelength λ are scattered from a sample, and a search is made of $2\theta_B$ for a preference in scattering. The values of θ_B at which there is preference for scattering allows a set of d values to be calculated, as illustrated in Fig. 1 along with an example of data. With the background of experience from X-ray diffraction and the availability of steady-state reactors, this conventional technique has proved very successful.
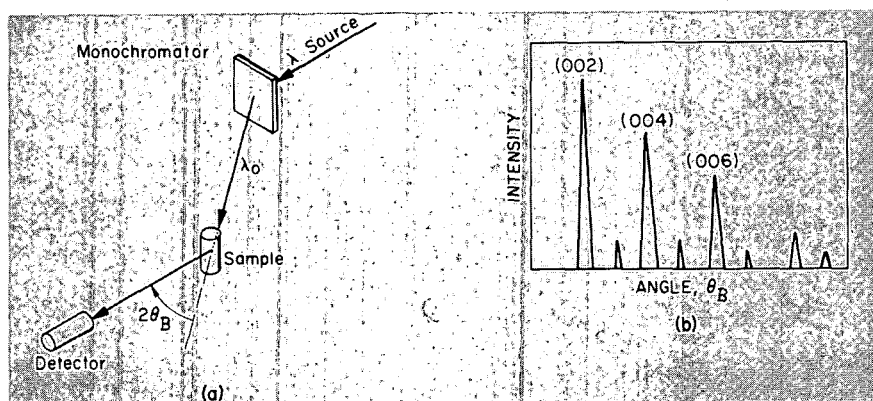
Fig. 1 — (a) Conventional fixed-wavelength neutron-diffraction experiment and (b) an example of the data.

Because of the desire to increase the capabilities of diffraction methods and because of the anticipation of repetitively pulsed sources as more-intense sources, new approaches to diffraction have begun to be developed in the last several years. These methods depend on time-of-flight measurements; Fig. 2 is an example. Here pulses of polychromatic neutrons are produced either by chopping a beam from a steady source or by pulsing the source itself. The bursts of neutrons impinge upon a sample, and the wavelengths of those that are preferentially scattered by the sample at a fixed scattering angle are determined by measuring their time of flight to the detector. These λ's measured at fixed θ_B allow a set of d values to be calculated from the Bragg equation. It has been shown that for powdered samples with a steady source of neutrons, comparable resolution and intensity to the conventional technique can be obtained with the time-of-flight technique. Time-of-flight experiments in which $2\theta_B$ is near 180° should yield extremely good resolution.
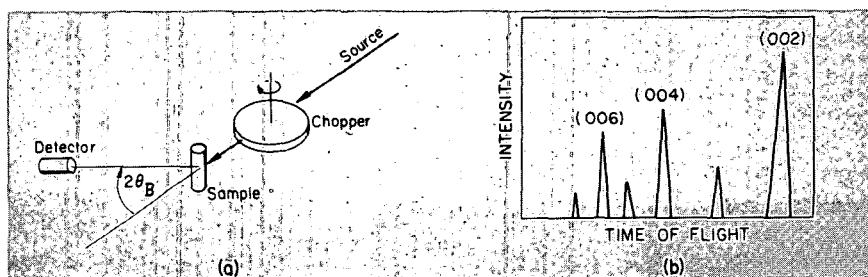
Fig. 2 — (a) Time-of-flight fixed-angle neutron-diffraction experiment and (b) an example of the data.

Because of the backlog of experience, the conventional method is more convenient and desirable for most experiments. However, the time-of-flight technique with steady sources has certain advantages, i.e., its use with pressurized samples, with very cold samples, and for the study of transient effects. This technique is being developed, but it probably accounts for less than 5% of the effort at this time. With the advent of intense repetitively pulsed sources, however, the time-of-flight technique promises to increase the experimental capabilities by several orders of magnitude, and its application will be greatly expanded.

An example of a time-of-flight neutron-diffraction experiment is the one now operating at the Materials Testing Reactor (MTR).[3] The experimental arrangement is shown in Fig. 3. A beam of thermal neutrons is taken from the steady-flux reactor and chopped into bursts by a mechanical chopper. These bursts of neutrons impinge
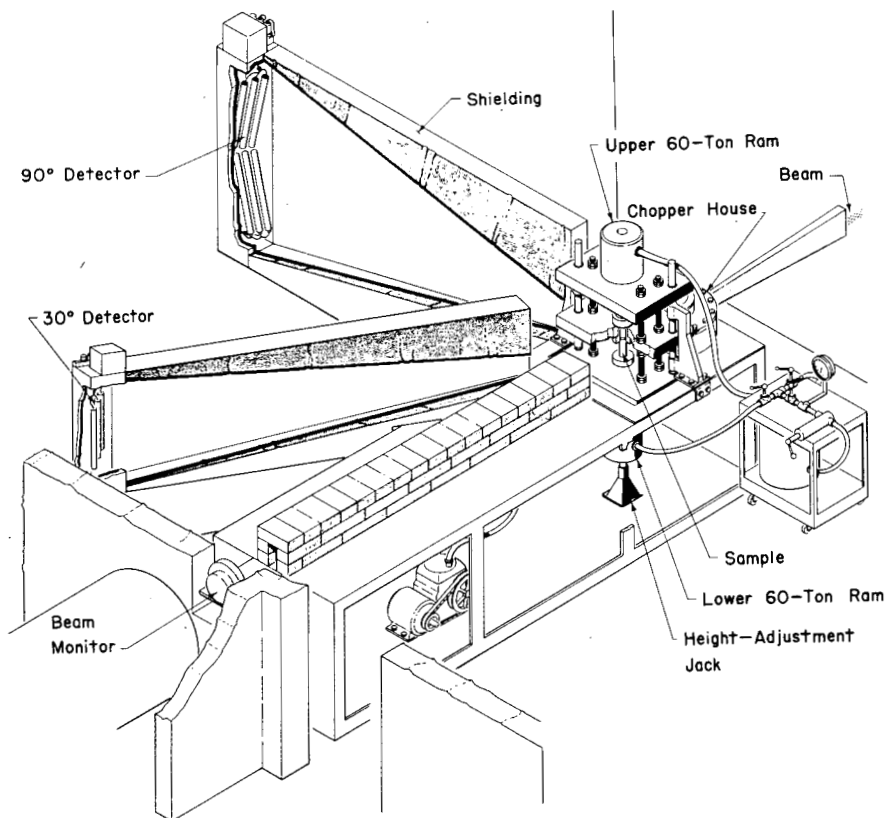
Fig. 3—A cutaway of the MTR time-of-flight neutron-diffraction instrument used for studying samples at high pressures.

upon a powdered sample, and a small percentage are diffracted toward the detectors. The detectors are located at scattering angles of 90° and 60° at flight paths of 2 m. The flight time or wavelength of the scattered neutrons is determined by multichannel time analyzers associated with each detector.

The time-of-flight method was developed for these experiments because it is more compatible with the pressure chambers required to hold the pressurized samples. The exertion of large pressure upon the sample requires that it be surrounded by a massive pressure cell. But to allow the neutrons to enter and exit from the sample requires that not too much material interfere with the beam. The use of a conventional diffraction system would have required that the strength of a large area of the cell, that area needed to scan the Bragg angle, would be limited.

On the other hand, by using the time-of-flight method, only narrow cracks were cut into the sample cylinder to allow the beam to enter and exit at the fixed angles. Figure 4 shows one of the pressure cells which has held a sample $\frac{1}{4}$ in. in diameter and 1 in. long to pressures of 40 kbars. The alumina cell is hard and thick enough when supported to hold this pressure, yet thin enough to pass a large fraction of the neutrons. The binding ring provides the strength, and its strength is only slightly compromised by the narrow beam cracks.

Figure 5 is an example of diffraction data obtained with this system when the sample was bismuth pressurized until it transformed into a different phase. About 40 Bragg peaks were obtained, from which the crystal structure of bismuth in phase II was indexed for the first time.

FUTURE DIFFRACTION TECHNIQUES

The time-of-flight technique is very wasteful of neutrons when a steady reactor is the source; the duty cycle is less than 1%. But the time-of-flight technique comes into its own with the advent of repetitively pulsed sources whose peak power is very high but whose average power is equivalent to present reactors. With repetitively pulsed sources the neutrons are produced only when they are needed. With the proper design of the pulsed source and the tailoring of experiments, effective increases in capability of 100 to 1000 should be realized.

Although some latitude and personal preference are considered in the parameters of the repetitively pulsed source, the characteristics outlined in Table 1 give one possible set. For the neutrons to have a wavelength compatible with the atomic spacings of the samples under study, their energies need to span the range from 0.001 to 1 ev. This

Upper Ram Extension

Upper Tungsten Carbide Pin

Binding Ring (R/C 45)

Hardened Steel Wedge (R/C > 60)

Aluminum Oxide Cell

Sample

Diffracted Beam to -30° Detector

To Beam Monitor

Incident Beam

Diffracted Beam to 90° Detectors

Lower Tungsten Carbide Pin

Tungsten Carbide Pin Support

Lower Ram Extension

5 cm
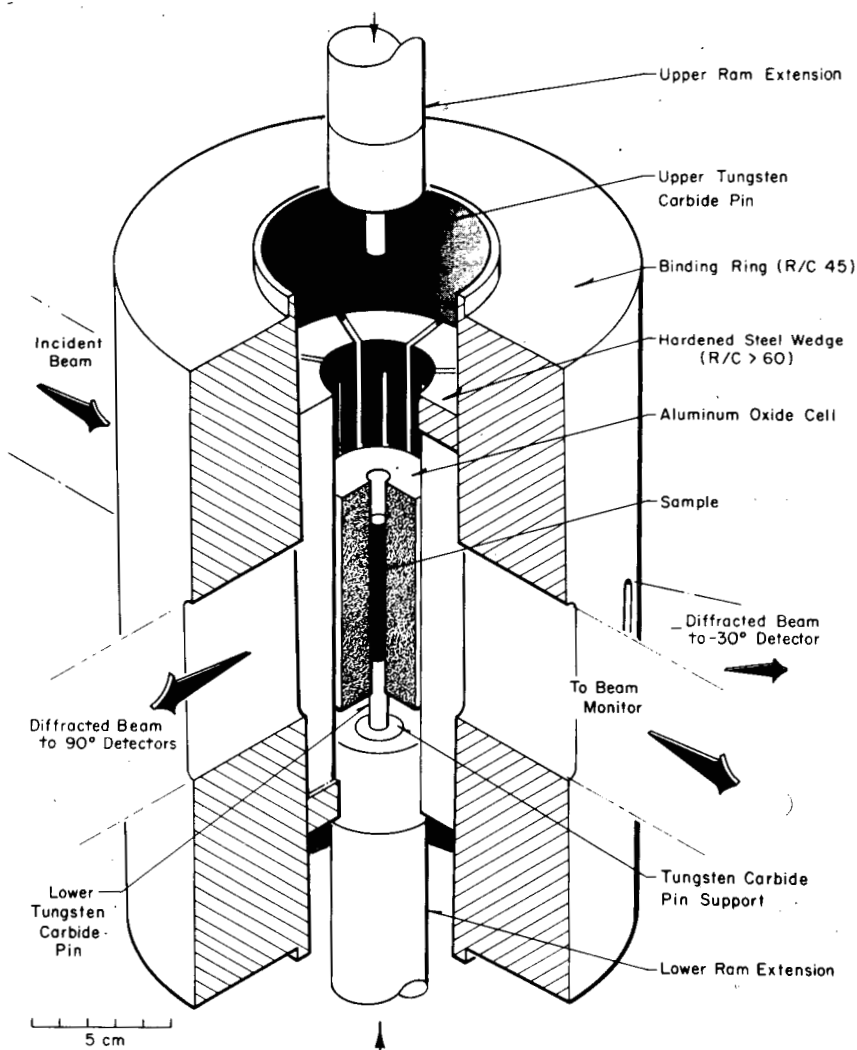
Fig. 4—A cutaway of the cell used in the high-pressure experiments.

range can be obtained easily from a cold moderator placed near the source. Fluharty[4] has shown that the burst times of the thermal neutrons emitted from a cold moderator can be as low as 10 μsec. For cold neutrons the bursts will be wider, possibly as wide as 50 μsec. This burst time or less is desired to give the desired resolution in the experiments. Moderators or radiators as large as 10 by 10 cm are also quite compatible with these burst times. They are large enough to give good intensity and small enough that the time resolution
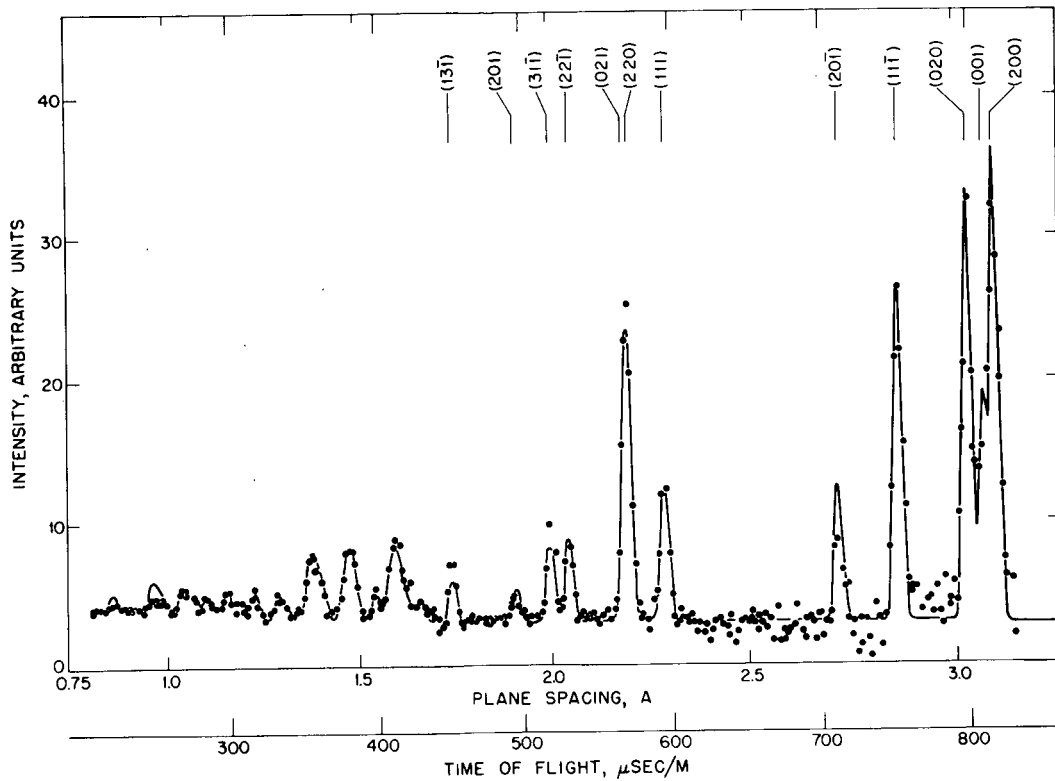
Fig. 5 — An example of the neutron-diffraction pattern of bismuth in phase II. $2\theta = 60°$

Table 1

DESIRABLE CHARACTERISTICS OF REPETITIVELY PULSED
NEUTRON SOURCE

Energy range, ev	0.001 to 1.00
Burst width, μsec	~10 (hot neutrons) to 50 (cold neutrons)
Repetition rate, pulses/sec	5 to 100
Beam radiator size, cm^2	~10 × 10
Intensity, neutrons/cm^2/sec	Equivalent to 10^{17} neutrons/cm^2/sec steady state
Backgrounds	Low
Beam tubes	Multiple

is not smeared. Such a pulsed source can also be made compatible
with low neutron generation between bursts which appears as back-
ground. Several beam tubes can be designed around the source to
service at least 10 experiments. From 5 to 100 pulses/sec will yield
the maximum intensity by having the maximum repetitive rate while
not allowing overlap in the experiments. Having selected these limits
on the source, a repetitively pulsed source is conceivable with an
average power of 1 to 10 Mw and an equivalent experimental capability
of a steady-state reactor of the order of 10^{17} neutrons/cm^2/sec.
This source can be built within the present limits of engineering
capability.

The time-of-flight techniques must be expanded to use these
pulsed sources effectively. For powdered and amorphous solids,
liquids, and gases, the present time-of-flight techniques will only
have to be made compatible with the pulsed sources. This is straight-
forward. For single-crystal diffraction studies the instrumentation
must be extended. One approach is to construct a space- and time-
sensitive detector. Then the equivalent of Laue patterns will be
obtained but with additions. Where the Laue techniques with X rays
only observe diffraction spots of mixed order, the time-of-flight
system with neutrons incorporating a space- and time-sensitive
detector will observe all these spots but determine magnitudes for
each order contributing to a spot. Thus a complete single-crystal
diffraction pattern will be obtained in a single setting. Ideally these
space and time detectors would be spherical and centered on the
samples; but, planar or cylindrical detectors may be acceptable.

One possible experimental arrangement, depicted in Fig. 6,
expands the idea of this type of time-of-flight Laue diffraction experi-
ment. Polychromatic neutrons from the pulsed source are diffracted
by the single-crystal sample. A large multiwired spark chamber
located behind the sample detects the diffracted neutrons. The chamber
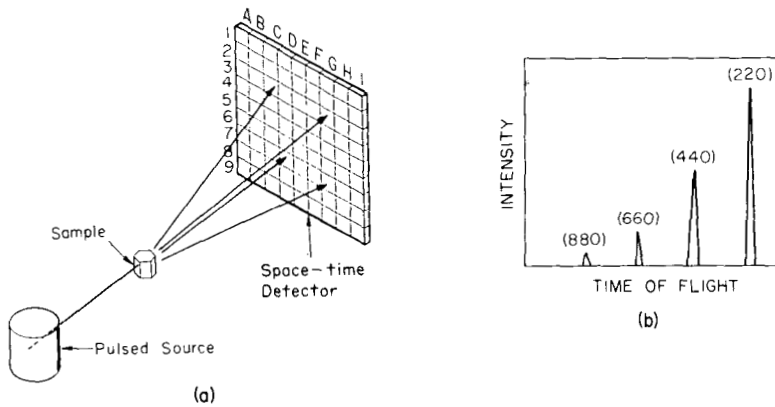
Fig. 6 — (a) A possible arrangement for single-crystal diffraction using time-of-flight methods and (b) an example of the data at the point indicated as C-3 in (a).

is filled with ^{3}He to increase its sensitivity. The position in space at which each neutron interacted with the chamber is determined by coincidence of signals from vertical and horizontal wires if a crossed-wire system is used or by signal transmission time along the wire if parallel wires in only one direction are used. These data are stored in a large memory data storage – processing system. At a later time the memory is scanned to reveal a time-of-flight spectrum for each area of the detector, an area which would be determined by the spacing of the wires. From these spectra the location of the Laue spots could be determined. For each spot the time-of-flight spectrum would separate all orders. No uncertainty would remain between the contributions to the (00n) spot by neutrons having wavelength λ diffracted from planes d apart as compared with neutrons contributing to the same spot but with wavelengths of 2λ, 3λ, etc., diffracted from planes 2d, 3d, etc., apart. Having once accepted the concept of time-of-flight diffraction, one realizes that many permutations of the experiments become possible. Brainstorming of experimental capabilities has only begun.

FUTURE EXPERIMENTS

Much information about the physical properties of nature is determined through a measurement of the microscopic structure of materials. In fact, crystallography, which is this determination, is now recognized as an independent discipline of science. Crystallography has gained such status because of the vast amount of research that has occurred in this discipline, and the amount projected in the future seems unbounded. Neutron-diffraction research has contributed

its fair share to the growth of crystallography even though neutrons were latecomers; their share of the future studies appears at least as large as that of neutron-diffraction research. Pulsed-neutron diffraction can carry a fair share of this load.

The advent of more-intense sources or sources with unique characteristics always opens up new vistas of research. This has been quite apparent recently in optics. Although the old sources certainly were not considered to be weak, the coming of the lasers has made possible radical and exciting new experiments. The same will happen in slow-neutron physics when the experimental flux is increased.

Although much of the future research in crystallography, such as studies of organic crystals, magnetic crystals, and alloys, can and will be made with pulsed sources having fluxes no higher than the existing reactors, many important future studies will only be feasible or possible when more-intense sources are available. The experiments mentioned in this section will emphasize the latter.

Many materials having the simpler crystalline structure have been analyzed, but even more materials with complicated structure have not been analyzed. As the structures of the simpler materials have been determined, the interest has been extended to more complicated cases. But impeding this extension is the increasing difficulty of the experiments. Thus the focus of neutron diffraction with present experimental capabilities might be roughly represented as a bell-shaped curve centered around a dozen atoms per unit cell but with wings extending on the low side to very difficult to measure unstable compounds of a few atoms per unit cell and on the high side to the simpler biological molecules of a few thousand atoms per unit cell. An attempt to depict this is given in Fig. 7. On the basis of past progress of neutron diffraction and the feasibility of performing experiments, one might expect the median of such a curve to shift toward 100 atoms/unit cell when effective fluxes of about 10^{17} neutrons/ cm^2/sec become available. Here neutrons will make major contribu-
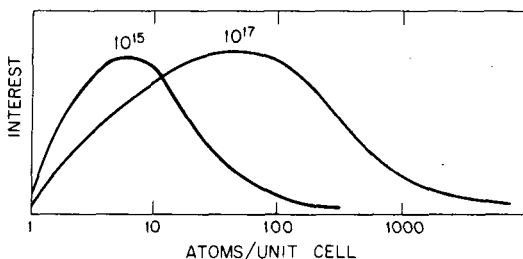
Fig. 7—An attempt to depict the shift of interest as more-intense sources become available.

tions by locating the positions of hydrogens particularly after X rays have located the $C-N-O$ backbone of these molecules. A major share of the information about biological processes is held in hydrogen locations and in the change of location as biological processes progress.

Studies of magnetic structure, which require polarized beams, can be made with time-of-flight methods. One approach would be polarizing filters, such as the $La_2Mg_{12}(NO_3)_{12}24(H_2O)$, which would be placed in the beams both to polarize the incident beam and to analyze the scattered beam. Many magnetic ordering studies would then become accessible.

Besides the need for more-intense sources to progress to more-complicated molecules, more-intense sources are also needed for experiments in which the sample is exposed to extreme conditions. The neutron-diffraction experiments on samples pressurized to >100 kbars is one example of these extremes. At present the extreme of pressure is 40 kbars with initial experiments just starting on samples at 100 kbars. But these measurements are on powdered samples of relatively simple structure. Experiments with single-crystal samples are desirable, but none have yet been attempted at high pressures. Because of the small samples that must be employed, the maximum initial intensity will be required.

Great interest exists in studying samples to 1 megabar because these pressures are representative of the core of our earth. But a static pressure system which will reach 1 megabar has yet to be designed for X rays, much less for neutrons; the X-ray devices are now straining toward 300 to 500 kbars. When these devices are designed for neutrons, they will certainly entail a quite small sample deeply embedded in the pressure system.

Besides the extremes of pressure, samples under other extreme conditions are also of interest. Such parameter variables as temperature (both low and high), magnetic field, electric fields, tension forces, and sheer forces are examples. In many of these extreme environments, only small samples will be possible. These experiments will then require the maximum flux to guarantee success. One interesting set of conditions is the measurement of samples at constant volume, which requires adjustment of both pressure and temperature.

Megabar pressures have been reached in transient systems, and intense pulsed X-ray systems are now available for studying these transient systems. A similar approach can also be followed in neutron diffraction when pulsed sources that are intense enough are available. The transient approach demonstrates two advantages of pulsed systems. First, one has the ability to extend the limit of forces acting on the sample, in this case pressure, by applying a transient force. Besides pressure, other forces might be applied transiently, such as electric or magnetic field, shock waves, and so forth. The second

advantage is the ability to study the change in structure of the material as the transient force is building up and decaying.

Neutron and X-ray diffraction have determined the structures of many pure systems. Although knowledge of the pure system is important and often dominant, nature provides few solids that are pure. In fact, the impurities often radically change the nature of the material, and this change provides the interesting study. Although neutrons are not well adapted to observe small amounts of impurities in materials, some success has been had in these experiments when the impurity atoms are in a concentration greater then 1%. These experiments are usually conducted at small scattering angles where good resolution is required; more-intense sources of thermal neutrons would allow the experiments to be refined. Observation of the modification of the host lattice of as little impurity as 0.1% should be feasible in the future.

Because of our poor understanding of the liquid state, experiments on liquids are difficult to project. However, neutron diffraction from liquids has shed some light in this area, and more experiments probably lie ahead. Of particular interest is the "crystal like" nature of a liquid and the range or extent of this correlated structure. Very long wavelength neutrons may be needed to observe the size of these crystal globules. The intensity of long wavelength or cold-neutron beams is quite restricted at present. More experiments will probably be forthcoming when more-intense sources are made available.

Neutron radiography can be considered to be a form of neutron diffraction or scattering. Recent emphasis has been directed toward the efficient use of weaker sources; however, needs can be projected for experimentation along at least two additional paths. Very high resolution and better definition are desirable in some experiments. The definition can be obtained by tailoring the energies of the neutrons to be most sensitive to the element of interest. This can be achieved with steady-state reactors through monoenergetic beams, but it can also be achieved through time-of-flight neutron radiography with pulsed sources. The second path is to use the pulsed capabilities to take motion pictures — motion neutron radiographs of a rapidly changing sample. Such pictures would complement X-ray motion pictures.

Neutron diffraction with repetitively pulsed sources has several other possibilities. Studies of radioactive samples too hot for X-radiography are possible. Change of lattice spacing with neutron dose is an example of the information to be gained. As the research capabilities expand, analytical methods of using these developments should be forthcoming. Any one of the different experimental techniques is a possibility. So far little progress along this line has been achieved because of limited source strength. This discussion indicates

the need for continued effort to increase the effectiveness of slow-neutron-scattering experiments.

ACKNOWLEDGMENT

REFERENCES

1. G. E. Bacon, *Neutron Diffraction*, Oxford University Press, Inc., New York, 1962.
2. P. A. Egelstaff (Ed.), *Thermal Neutron Scattering*, Academic Press Inc., New York, 1965.
3. T. G. Worlton, Ph. D. Dissertation, Brigham Young University, 1967, unpublished.
4. R. G. Fluharty, F. B. Simpson, G. J. Russell, and J. H. Menzel, Moderator Studies for a Repetitively Pulsed Test Facility, *Nucl. Sci. Eng.*, 35: 45-69 (1969).

DISCUSSION

KRONENBERG: Toward the end of your paper you mentioned that much higher intensity sources are needed. In your opinion, what is the importance of higher intensity at the cost of increased pulse length?

BRUGGER: For these experiments that I have mentioned, I think we need pulses of 10 μsec or less. For many of the experiments that have been done by pulsed methods, the time-of-flight equipment produced pulses of about 10 μsec. In contrast, the IBR reactor in Russia produces longer pulses, and these are used. I think these longer pulses are a less desirable way to operate. Dr. Fluharty has shown that we can get short pulses out of pulsed sources; we should not settle for anything less. Certainly we would desire shorter pulses if the same number of neutrons were in each pulse; but, if we have to sacrifice neutrons for shorter pulses, I would not want to do it. As far as I am concerned, 10 μsec is a nice compromise.

KRONENBERG: Does not the length of pulse influence very strongly your time-of-flight measurements?

BRUGGER: Yes, of course, the pulse length does influence the time-of-flight measurements. I think we can get adequate resolution at 10 μsec; at 50 μsec we do not have good resolution. At the present time 1 μsec would be better than I would efficiently use.

GOSSMAN: Are these fluxes that you quoted, 10^{14} to 10^{17}, incident on the experiment, or is this the pulsed-reactor flux?

BRUGGER: No, these fluxes are not incident on an experiment. I had to pick some reference so I picked essentially the source flux back at the core or at the pulsed reactor. They are effective fluxes; they are not total fluxes. A pulsed reactor is not going to produce 10^{17} average flux, but it produces 10^{17} effective flux. For example, the IBR reactor at about 6 kw is as effective as a 10^{14} neutrons/cm^2/sec steady-state reactor in the data that are produced. This is an estimate from looking at their experimental data.

GOSSMAN: What about the energies? Is there any preference for thermal over fast?

BRUGGER: Yes, for solid-state physics one would like fluxes between 1 mv and 1 ev. We heard earlier in the conference that the Russians are going down to 1 m/sec. I am not sure what that is in energy, but it is such an extreme case on the low-energy side that I do not think we appreciate how to use it. On the other hand, neutrons above 1 ev are so energetic or their wavelengths are so short that there is not a great use for them in solid-state physics.

GOSSMAN: On these repetitively pulsed reactors do you think you can get such low energies with the necessary high intensities?

BRUGGER: The reactor that Fluharty proposed had about a 10^{17} equivalent flux. It would give this equivalent flux because it is a pulsed reactor. If you cut out the repetition rate, you are back to a mediocre source. It was pointed out earlier this afternoon that the average radioactivity produced by a single-burst reactor was very low whereas a repetitively pulsed reactor is very high. This factor demonstrates that the average flux out of the single-pulsed device is low; one only gains flux if one pulses it very often.

McENHILL: I wonder if I might ask a question in relation to your space—time detector? In the United Kingdom there has been the usual argument about the relative merits of a high-flux continuous reactor and something like a pulsed-neutron booster for the study of condensed matter, the net result being that no new facility is yet approved. One of the things that would be particularly interesting, since to some extent it compensates for low-neutron fluence in certain experiments, is to develop a space—time detector with a very good spatial resolution. Since this detector would be useful in the type of inelastic-scattering experiments and the type of neutron-diffraction experiments you discussed, I wondered if you were developing such a device at Idaho. You said the data processing facility is available, but is there any active work being done to develop a big counter matrix?

BRUGGER: "Is there any development being done in our laboratory?" Our answer to this question is the same as to why England does not settle on a design; we do not have the money. I have heard of one space-sensitive detector being developed at Oak Ridge, but I have not seen it yet.

McENHILL: I know Dr. Beckurts is going to answer, but I would just like to say that we are doing a very small feasibility study on such a counter at Aldermaston. We have looked at spark counters and dismissed them; we have looked at solid-state lithium-drifted germanium counters, and, although we are using them for medical applications, we are not going to use them for this. We have settled for plastic scintillators, but we are not moving very fast due to lack of money and effort.

BECKURTS: In the context of the Grenoble high-flux reactor project, we are trying to develop such space–time detectors. We are following several routes: one is based on scintillators, and the other on using crossed-wire proportional counters. It is interesting to note that high-energy physicists have recently discovered the usefulness of cross-wire proportional counters in contrast to spark chambers, and there is important work going on at European Organization for Nuclear Research (CERN) and also at Brookhaven National Laboratory from which I think neutron physicists could really profit very much.

8-2 REPETITIVELY PULSED REACTOR APPLICATIONS TO NEUTRON INELASTIC-SCATTERING EXPERIMENTS

K. H. BECKURTS*† and R. M. BRUGGER‡
*Brookhaven National Laboratory, Upton, New York; ‡Idaho Nuclear Corporation, Idaho Falls, Idaho

ABSTRACT

The possibilities for using a repetitively pulsed reactor as a neutron source for inelastic-scattering time-of-flight studies with slow neutrons are reviewed. A rough comparison between steady-state reactors and repetitively pulsed reactors for a simple experiment is carried out in some detail, and the implications of the recently introduced method of statistical chopping are reviewed. It is concluded that very advanced repetitively pulsed reactor systems, yielding short bursts and peak fluxes in the range of 10^{16} to 10^{17} neutrons/cm^2/sec, could result in considerable progress in the field of inelastic-scattering studies.

INTRODUCTION

Inelastic scattering of near-thermal neutrons has become one of the main research applications of thermal-neutron beams from reactors. Started about 15 years ago, these experiments had the initial objective of ascertaining scattering behavior of materials to be used as reactor moderators. This inelastic-scattering technique was quickly realized to be a most powerful tool for the study of dynamical properties of matter, and the effort subsequently shifted in that direction. The intent of this paper is not to give a detailed account of the various possible applications of inelastic neutron scattering (for detailed surveys see Refs. 1 to 3), but the following is a short list of fields where neutrons have been applied successfully or where their application seems promising.

---

†On leave of absence from Institut fur Angewandte Kernphysik, Kernforschungszentrum, Karlsruhe, Germany.

1. Dispersion laws of phonons in solids.

2. Dispersion laws for magnons in solids; spin waves.

3. Interactions between excitations in solids; phonon–phonon, phonon–magnon, etc.

4. Dynamics of ordering processes near phase transition points.

5. Dynamical structure of liquids; phonons, diffusive motions, etc.

6. Properties of quantum fluids.

7. Vibrational spectra of complex molecules; biological systems, polymer cross linking, etc.

8. Frequency distributions of impurities in host lattices.

9. Magnetic and electric quadrupole hyperfine interaction.

10. Studies of electronic levels in solids.

11. Investigations of the properties of dense gases.

Inelastic-scattering experiments require a double neutron spectrometer as schematically shown in Fig. 1(a). The measured quantity is the scattering law $S(\kappa, \omega)$, in which $\hbar\vec{\kappa} = \vec{P} - \vec{P}_0$ is the change in neutron momentum and $\hbar\omega = E - E_0$ is the change in neutron energy in the scattering event. Obviously, and as seen in Fig. 1(b), the resolution in the determination of $S(\vec{\kappa}, \omega)$ is directly related to the size of the volume elements $d\vec{P}^3$ and $d\vec{P}_0^3$, which, in turn, are determined by the angular and energy resolution of the double spectrometer. Since in a scattering ex-

(a)

(b)
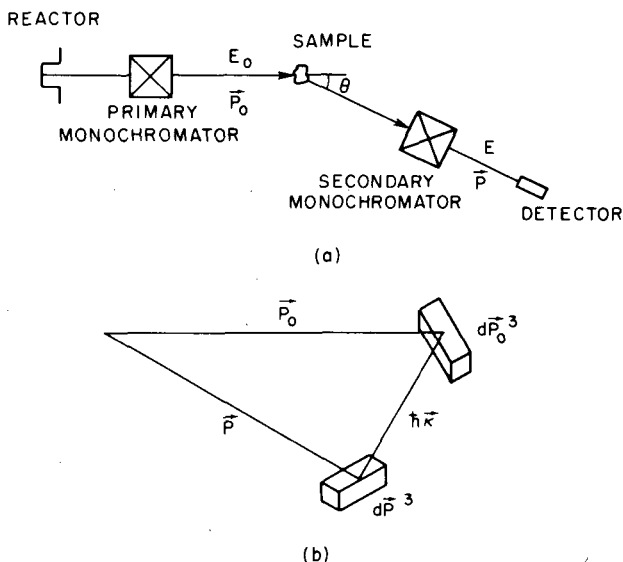
Fig. 1 — (a) Principal arrangement for inelastic-scattering experiments. Energy transfer is $\hbar\omega = E_0 - E$; momentum transfer is $\hbar\vec{\kappa} = \vec{P}_0 - \vec{P}$. (b) Relations for scattering experiment in momentum space. Counting rate is $R \sim nfS(\vec{\kappa}, \omega) \, d\vec{P}_0^3 \, d\vec{P}^3$.

periment the counting rate* is $R \sim nfS(\vec{\kappa},\omega)\,d\vec{P}^3 d\vec{P}_0^3$, it becomes obvious that, as the resolution is increased, the counting rate drops sharply. Here n is the neutron density of the source reactor, and f is the beam-utilization factor that expresses which portion of the impinging neutrons is actually used in the spectrometer. As a matter of fact, almost all scattering experiments require a high resolution, and to obtain acceptable counting rates and signal-to-background ratios, we need (1) reactors with very high useful neutron fluxes and (2) instruments that make highly efficient use of these fluxes.

In the past, experimenters have used steady-state reactors with flux levels in the range of 10^{12} to 10^{14} neutrons/cm^2/sec. They used instruments which, though often ingenious, were far from making optimum use of the available flux. Many valuable results have been obtained, but the attainable counting rates and signal-to-background ratios have seriously limited the accuracy of many investigations and have ruled out some of the previously mentioned applications completely. Recently, further progress became possible with the successful operation of the very high flux reactors at Brookhaven National Laboratory and at Oak Ridge National Laboratory and the construction of the Grenoble high flux reactor, all three of which provide flux levels close to or above 10^{15} neutrons/cm^2/sec. Simultaneously, several new experimental techniques are being developed which promise a very efficient utilization of the neutron flux. We can thus expect rapid growth of inelastic-scattering techniques during the next few years.

There is, however, a completely different approach to the problem than larger steady-state reactors. Many neutron spectrometers employ time-of-flight (TOF) methods, either for primary or for secondary energy selection or for both. In any case their performance depends essentially on the peak reactor flux during a short time interval rather than on the time-averaged flux. These spectrometers can therefore take advantage of the high peak fluxes available from repetitively pulsed reactors. At the same time, they can take additional advantage of the low average flux levels in repetitively pulsed reactors; the high-flux region becomes more easily accessible, and radiation loads on crucial parts of the experiments (like cold moderators, in-pile collimators, etc.) are much lower. This repetitively pulsed reactor approach was first carried out by the Dubna group, members of which have written many fine research papers on inelastic-scattering measurements performed with their IBR reactor.[5-7] The potential of this approach has been investigated thoroughly by the Ispra group in the context of the SORA development program.[8-9] Major parts of two international meetings during the year 1966 were devoted to discussions

---

*This relation is very plausible. It is derived in Ref. 4.

of repetitively pulsed reactor application to inelastic-scattering studies.[10,11]

TIME-OF-FLIGHT EXPERIMENTS

Let us investigate this repetitively pulsed reactor approach a little closer: Fig. 2 shows schematically the four principal types of double neutron spectrometers used for inelastic-scattering studies on steady-
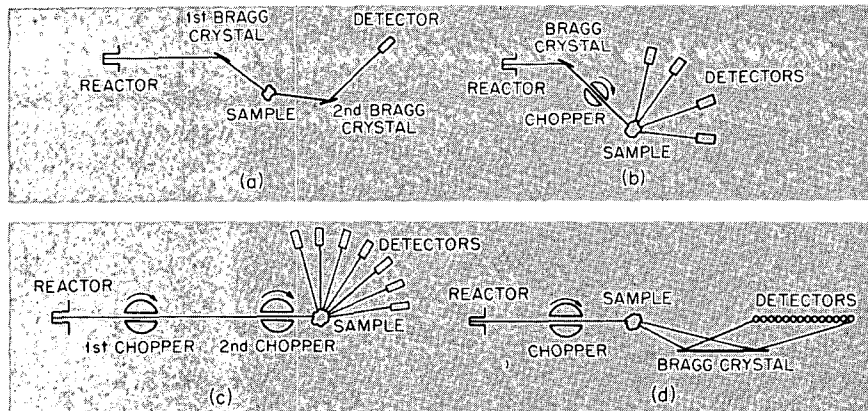
Fig. 2—*Four basic types of double spectrometers. (a) Triple axis spectrometer. (b) Crystal—chopper spectrometer. (c) Phase chopper system. (d) Chopper— crystal spectrometer.*

state reactors. They represent all the four possible combinations of the two basic techniques for neutron monochromatization, i.e., crystal diffraction and TOF selection. Using crystal diffraction for the energy analysis on both the primary and the scattered-neutron beam leads to the well-known triple-axis spectrometer. This instrument is ideal for experiments where only narrow and well-defined regions of the $\vec{\kappa}, \omega$ space have to be scanned; in fact, most of our knowledge about phonon and magnon dispersion relations stems from experiments with triple-axis spectrometers. Selecting the primary energy by crystal diffraction and the secondary energy by TOF can be achieved in several ways: a mechanical chopper in combination with a stationary crystal can be used or the crystal can be rotated at a high angular speed so that the Bragg condition is fulfilled only for short time intervals. Such rotating crystal spectrometers have certain advantages over crystal—chopper combinations since a certain amount of intensity bunching is possible. Another possibility, presently under investigation at Oak Ridge, is to use magnetic reflections from ferrites which can be

switched by pulsed magnetic fields. In any case, the crystal – TOF combination is a good technique for measurements where large regions in $\vec{\kappa}, \omega$ space have to be scanned simultaneously since many secondary detectors and flight paths can be used. The combination is thus very suitable for studies of incoherent scattering; however, it has also been used successfully for phonon-dispersion relation measurements.

Using TOF methods for both primary- and secondary-energy measurements yields the double chopper whose applicability is similar to that of the crystal – TOF combination. Over most of the range of incident energies, the intensity at a given resolution would be lower than that obtainable with a crystal – TOF combination; however, at very low energies ($\sim 10^{-3}$ ev) suitable monochromatization crystals are difficult to find, and at high incident energies ($\sim 10^{-1}$ ev) the crystal reflectivities drop sharply.

The remaining possibility is to use TOF for primary-energy selection and crystal diffraction for the secondary. Crystal diffraction is a very powerful device which has probably not been exploited to its full potential. By proper arrangement of several secondary monochromating crystals, the $\vec{\kappa}, \omega$ space can be scanned along preset $\vec{\kappa}$ direction simultaneously. If only downscattering to low energies is of interest, a beryllium filter between the sample and the crystals can be used to reduce backgrounds and eliminate higher order reflection corrections. [In a simpler version of this method, only a beryllium filter is used, and all downscattering below the beryllium cutoff energy is measured (inverse beryllium-filter method). There is also a simpler version of the crystal – TOF combination in which only a beryllium filter is used to roughly monochromatize the primary beams (beryllium-filter – chopper method).]

It is obvious that all these spectrometers, with the exception of the triple-axis spectrometer, can also be used in combination with a repetitively pulsed reactor. At the same time they can be simplified since one of the choppers can be eliminated. Figure 3 shows a crystal – TOF facility at the Dubna IBR reactor.[5] The neutron burst from the fast core is thermalized in an H_2O moderator and monochromatized by a zinc single crystal, and the scattered neutrons traverse a 10-m flight path. The setup was mainly intended for phonon-dispersion relation measurements. Figure 4 shows a double TOF facility at the IBR reactor which was built by the Obninsk group.[6] After thermalization, the primary neutron bursts travel for about 11.3 m before they hit a chopper that has a defined phase relation to the reactor pulse. A nearly monochromatic pulse is thus obtained which is scattered by a sample very close to the chopper. Energy after scattering is measured using 11 flight paths at different scattering angles with lengths up to 11 m. As an example of the data obtained with this instrument, Fig. 5 shows flight
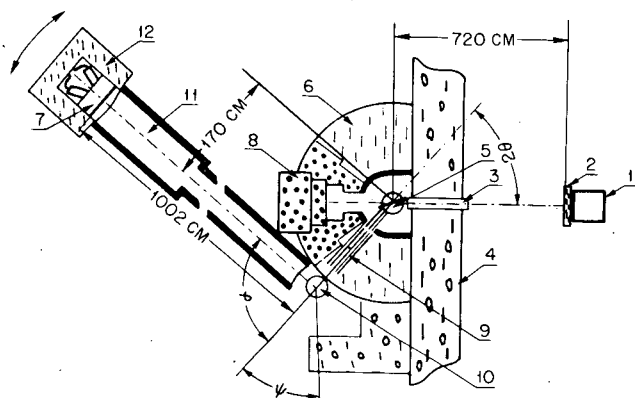
Fig. 3 — Crystal—TOF spectrometer at the IBR Reactor.

1, Reactor core
2, Moderator
3, 11, Neutron flight tube
4, 6, 8, Shielding
5, Zinc single crystal
7, Detector
9, Collimator
10, Sample
12, Detector shield
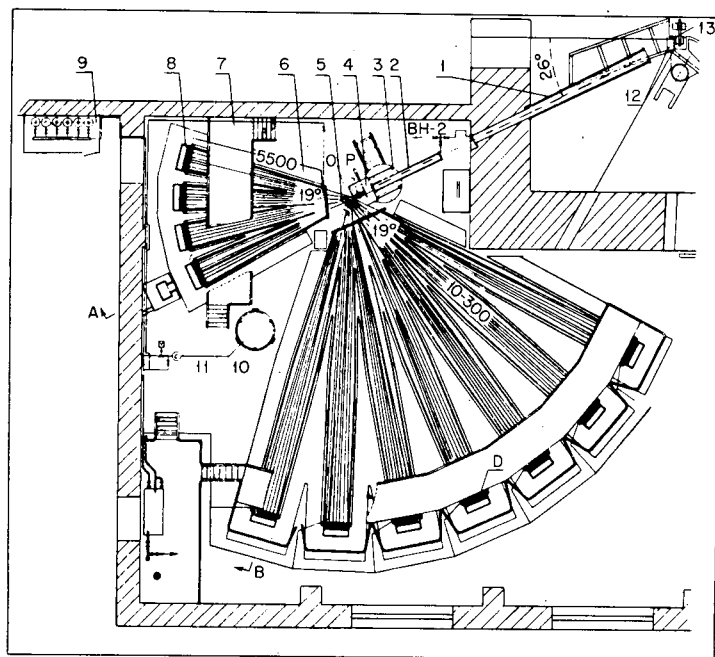
Fig. 4 — Double TOF spectrometer at the IBR reactor. P, Chopper. Q, Sample. D, Detectors. 1,2,4, Collimators and flight paths. Other numbers and letters are not defined.
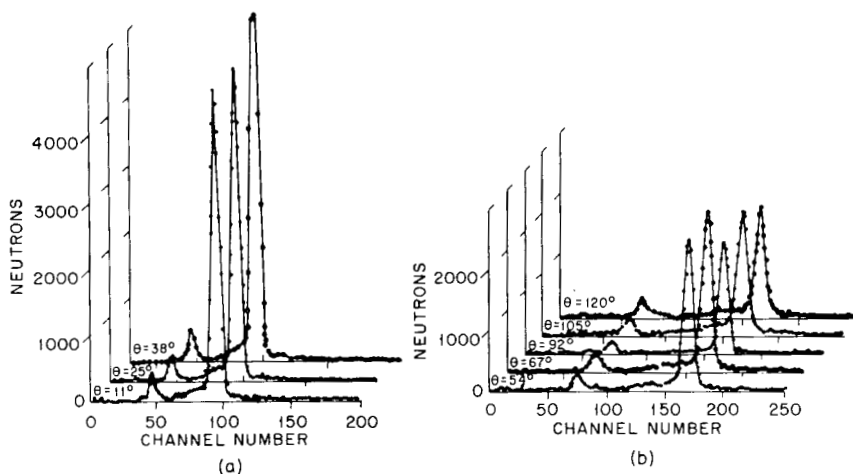
Fig. 5—Spectra of neutrons scattered by $ZrH_{1.46}$ for various angles ($E_0 = 0.024$ ev, $T = 400°C$) observed by Liforov et al. at the IBR reactor. (a) Secondary flight path 5.5 M. (b) Secondary flight path 10.5 M.

time distributions of 24-Mev incident neutrons scattered by $ZrH_{1.46}$ at various angles. The elastic peak and the peak for one-phonon gains from the well-known 0.13-ev optical level can be very well separated, and the contributions of acoustic modes are well discernible. Finally, Fig. 6 shows a TOF—crystal diffraction double neutron spectrometer at the IBR reactor.[7] A beryllium filter is used for the scattered neutrons to remove higher order reflections. The primary flight path is of the order of 20 m. Figure 7 shows the TOF spectrum recorded with poly-
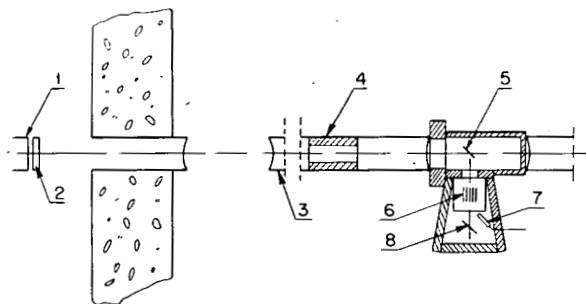
Fig. 6—Crystal—TOF spectrometer at the IBR reactor.

1, Reactor core   5, Sample
2, Moderator   6, Beryllium filter with collimating cadmium insert
3, Vacuum tube   7, BF_3 counters
4, Collimator   8, Sample
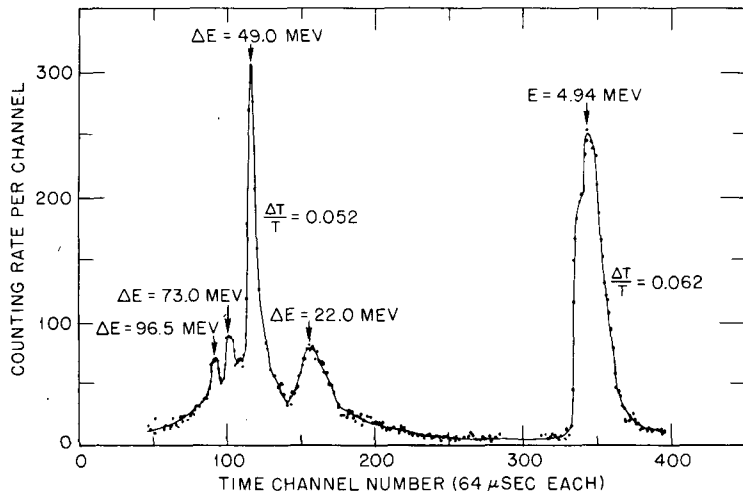
Fig. 7—Spectrum of neutrons scattered by polycrystalline NH₃Cl at T = − 75°C observed by Parlinski et al. at the IBR reactor.

crystalline NH_4Cl as the scattering substance and gives an idea of very good resolution obtainable with this instrument.

REPETITIVELY PULSED VS. STEADY-STATE EXPERIMENTS

The spectrometers described in the preceding section do not represent the only, nor the optimized, instruments that can be built; in fact, many kinds of improvements and modifications have been used or proposed, e.g., use of additional filters, neutron-conducting tubes, advanced multidetector arrangements employing multiwire proportional chambers, etc. However, these more basic instruments are convenient for comparing the potential of steady-state and repetitively pulsed reactors. Such comparisons depend strongly on the type of experiment to be conducted, and they can be made only within rather wide limits. Of course, the experiments also depend strongly on the characteristics of the repetitively pulsed reactor under consideration, and they may help to establish the desirable characteristics for the repetitively pulsed reactor.

Let us consider, as in Fig. 2(d), a very simple experiment in which the primary energy selection is by TOF, the secondary by crystal diffraction, and let the secondary spectrometer be exactly the same in both cases. We then have to compare the attainable intensities of the two setups for the same primary energy resolution $\Delta E/E$. According to Kley,[8] this can be done by introducing a figure of merit M which is de-

fined in the following way: M is the number of neutrons/cm^2/sec/ΔE hitting the scattering sample for a repetitively pulsed reactor setup divided by the number of neutrons/cm^2/sec/ΔE hitting the scattering sample for a steady-state reactor.

For experiments on coherent scattering which require a good angular resolution of the incident beam, Kley proposes a modified quantity: M^1 is the number of neutrons/cm^2/sec/ΔE/steradian hitting the scattering sample for a repetitively pulsed reactor divided by the number of neutrons/cm^2/sec/ΔE/steradian hitting the scattering sample for a steady-state reactor.

It can be shown very easily that the following relations hold:

$$M = \left(\frac{\phi_1}{\phi_2}\right) \frac{F_1}{F_2} \frac{\Delta t_1}{\Delta t_2} \frac{\nu_1}{\nu_2} \left(\frac{l_2^2}{l_1^2}\right)$$

$$M^1 = \left(\frac{\phi_1}{\phi_2}\right) \frac{\Delta t_1}{\Delta t_2} \frac{\nu_1}{\nu_2} \left(\frac{l_2^2}{l_1^2}\right)$$

where ϕ_1 = peak flux in repetitively pulsed reactor

Δt_1 = effective width of thermalized burst from repetitively pulsed reactor

F_1 = usable area at the source of the beam hole in the repetitively pulsed reactor

ν_1 = burst repetition rate of repetitively pulsed reactor

l_1 = distance between beam-hole source and scattering sample

ϕ_2 = flux in steady-state reactor

Δt_2 = burst width produced by the chopper

F_2 = effective beam cross section of the chopper

ν_2 = repetition rate of the chopper

l_2 = distance between chopper and scattering sample

Owing to the request for equal resolution, we have $\Delta t_1/l_1 = \Delta t_2/l_2$. Assuming further that the repetition rate is dictated by frame-overlap conditions, we have $\nu_1/\nu_2 = l_2/l_1 = \Delta t_2/\Delta t_1$ and thus

$$M = \frac{\phi_1}{\phi_2} \frac{F_1}{F_2} \left(\frac{\Delta t_2}{\Delta t_1}\right)^2$$

$$M^1 = \frac{\phi_1}{\phi_2} \left(\frac{\Delta t_2}{\Delta t_1}\right)^2$$

These relations show the advantage of a high peak flux in a repetitively pulsed reactor. Furthermore, in the case of incoherent scattering experiments where the angular resolution of the primary neutrons does not matter, the repetitively pulsed reactor receives a considerable

benefit since the full primary-beam cross section defines the usable solid angle; however, in a steady-state-reactor experiment, the beam cross-section area is seriously restricted by the chopper — F_1/F_2 may be as large as 10. The last factor, however, appears to be a very serious disadvantage of the repetitively pulsed reactor. With the chopper, Δt is limited by mechanical design considerations; Δt_2 as low as 10 to 20 μsec appears feasible and has been achieved in operating systems. The effective burst width of the thermalized pulse from a repetitively pulsed reactor depends on many parameters, especially the actual width of the fast burst and the size, shape, composition, and temperature of the moderator. The above relation indicates that the quantity $\Phi_{max}/\Delta t_2$ has to be optimized in a repetitively pulsed reactor. The result of this optimization, of course, depends also very strongly on the neutron energy range.

For very cold neutrons (E < 0.01 ev), the width of the neutron burst is essentially determined by the thermalization and diffusion time in the moderator, and the burst width cannot be reduced much below ~100 μsec without excessive losses in peak flux. This would make repetitively pulsed reactors less attractive for cold-neutron studies. (An obvious way to reduce Δt_1 would be to use an additional chopper close to the repetitively pulsed reactor. One then loses, of course, the F_2/F_1 advantage; also, the resulting loss in duty cycle can hardly be compensated by increasing the repetition rate.) Fortunately, neutron-conducting tubes offer a very elegant way out of this difficulty: The $(\Delta t_2/\Delta t_1)^2$ factor arises due to the effective solid angle which extends from the sample to the source and which decreases as the flight path increases. However, if a neutron-conducting tube with totally reflecting walls[12] is used, there is no reduction in intensity and the $(\Delta t_2/\Delta t_1)^2$ factor drops out completely. The critical angle for a nickel surface is 23 min at 4 Å $\cong$ 0.006 ev. This is reasonable for coherent scattering experiments using cold neutrons.

At higher neutron energies shorter burst widths may be obtained by reasonably tailored moderation, and in the epithermal range the limiting element may be the primary fast-neutron burst rather than the moderation process. Accelerator-injected operation of a reactivity-modulated booster system may prove advantageous over the repetitively pulsed reactor operation mode to obtain short bursts. The possibility of obtaining short pulses is discussed in papers by Russel, Crosbie, and Stevens,[13] Fluharty,[14] and Poole;[15] we shall not go into more detail here. It appears possible to obtain near-maximum peak fluxes at burst widths that do not exceed those obtainable from choppers. This is indicated in particular by the recent results of Fluharty et al.[14] which showed that optimized $\Phi_{max}/\Delta t^2$ values can be obtained at widths of $\approx$10 μsec at neutron energies as low as 0.005 ev using solid NH_4 at liquid-nitrogen temperatures as a moderator.

The decisive figure of merit for comparing the performance of scattering experiments using repetitively pulsed reactors and steady-state neutron sources is the ratio of the peak flux in the repetitively pulsed reactor to the time-averaged flux in the steady-state reactor, perhaps with a certain but not too serious disadvantage factor for the repetitively pulsed reactor due to burst width and with some beam-area advantage factors for certain types of experiments. It is thus the potential for high peak fluxes which makes repetitively pulsed reactors attractive to neutron inelastic-scattering studies. The IBR yields a peak flux of around 5×10^{13} neutrons/cm^2/sec and thus cannot give data of basically higher quality than existing medium or high flux reactors. The SORA reactor with a plutonium core would yield a peak flux of about 4×10^{15} neutrons/cm^2/sec which is higher than the peak flux in existing high flux reactors. Indeed, some experiments could be expected to perform better with SORA than with other existing sources. But the true progress would arise if repetitively pulsed reactors with peak flux values well above 10^{16}, which are probably unattainable to steady-state reactors at reasonable operation costs, could be built.

THE STATISTICAL CHOPPER

The preceding considerations have shown that in TOF measurements a repetitively pulsed reactor with a given peak flux performs about as well as a steady-state reactor with the same average neutron flux, i.e., with an average power that may be as much as 100 or even 500 times higher than that of the repetitively pulsed reactor. Time-of-flight spectrometers thus make an extremely inefficient use of the neutrons from a steady-state reactor. Only a fraction $\Delta t/T$ of the neutrons is used where Δt is the chopper burst width and $T = 1/\nu$, the recurrence time which is normally set by frame-overlap considerations. If a broad neutron spectrum is chopped, the duty cycle becomes worse the higher the resolution is pushed.

Recently a new concept of chopper construction has been developed[16,17] which may lead to considerable improvement in time utilization. Although at present it is applicable to steady-state reactors only, this technique deserves close examination in this paper since it may affect the evaluation of steady-state vs. repetitively pulsed systems. This technique is the so-called "statistical chopper," which is schematically shown in Figs. 8 to 10. The chopping wheel consists of such an array of slits and absorbing masks that the transmitted neutron beam forms a pseudonoise sequence [S(t)] of bursts with varying length and intervals. These pseudonoise sequences, which have been investigated thoroughly in the context of error-correcting codes,[18] have the particular property that their autocorrelation function is very similar
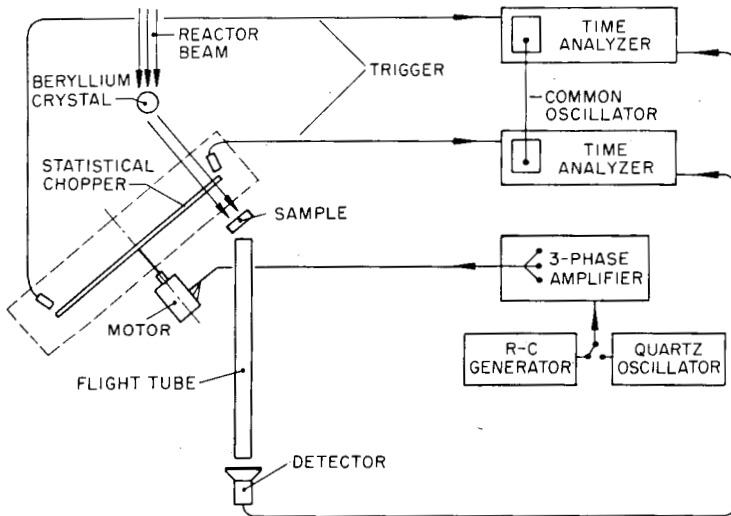
Fig. 8— General layout of TOF system at the statistical chopper at Karlsruhe.
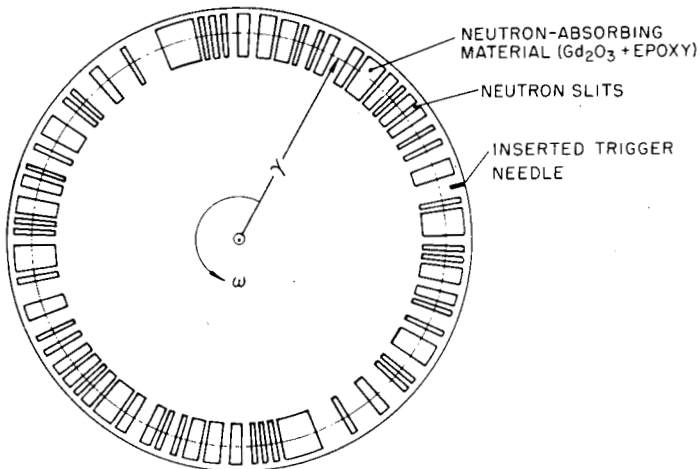
Fig. 9— Disk with two pseudorandom binary sequences (diameter 51 cm, angular velocity 7382 rpm, and $\Delta t = 32$ μsec) at the statistical chopper at Karlsruhe.

to the resolution function of a simple chopper running with the same speed as the statistical wheel and having just one slit of about the same width as the smallest one within the pseudonoise sequence. If measurements using the statistical chopper are considered in the usual manner and if a cross correlation between the measured TOF distribution and the source function is performed, the same result $[\varphi(t)]$ as with a nor-
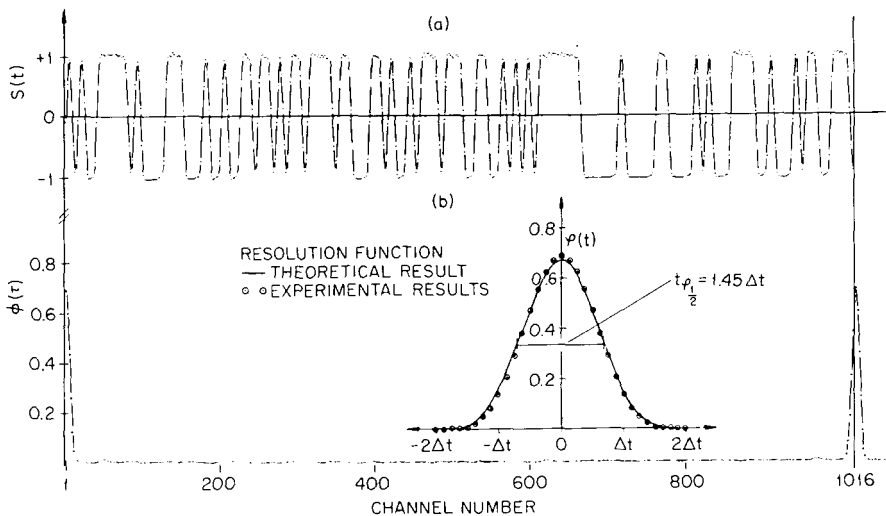
Fig. 10—(a) Experimentally observed signal function [S(t) = 2T(t)-1, where T(t) is the transmission] at the statistical chopper at Karlsruhe. (b) Experimentally observed autocorrelation function at the statistical chopper at Karlsruhe.

mal chopper is obtained. Without sacrificing resolution and at the same overlap conditions, the duty cycle has thus been increased from ≈1% to about 50%. This looks very surprising at first view, and a closer inspection of the statistical error appearing in this type of measurement shows that the gain in statistical accuracy in the determination of the neutron TOF distribution is in general much smaller than the gain in total transmitted intensity. If F(t) is the actual neutron TOF distribution to be observed, the ratio of the statistical error in a given measuring time interval for the two methods is[16,17]

$$\frac{\delta F_{\text{statistical chopper}}}{\delta F_{\text{normal chopper}}} \approx \sqrt{\frac{2\left[\overline{F} + (4u/N)\right]}{F(t) + 2u}} \quad .$$

where u is the time-uncorrelated counter background, $N = T/\Delta t$ is a number characterizing the number of elementary steps in the pseudo-noise sequence, and $\overline{F}$ is the average of the TOF distribution taken over the recurrence period T of the chopper. This relation shows the tremendous potential of the statistical chopper method as far as background rejection is concerned; in this respect almost full advantage of the increased duty cycle is taken. But, even if there is no uncorrelated background, the statistical method yields higher accuracy in those regions of the TOF spectrum where $F(t) > 2\overline{F}$. Fortunately, in many cases, e.g., TOF diffraction, phonon and magnon studies, and detailed analysis

of quasielastic scattering lines, this region is the one in which worth-while information appears in a time spectrum.

So far, the technique has been used successfully by the group at Argonne National Laboratory[16] and Karlsruhe for TOF diffraction studies and by the Karlsruhe group[17,19] for phonon-dispersion-law measurements on platinum and silver. Investigators at Idaho recently constructed a correlation chopper, and they are exploring its usefulness. Judging from the experience gathered at Karlsruhe, the statistical technique increases the effective neutron flux for certain investigations by a factor that may be as high as 10.

We believe that this powerful technique has to be further exploited before any final conclusions can be drawn. Its applicability can be extended to other types of experiments; it appears promising, for instance, to build a double chopper based on this principle which would simultaneously scan the whole range of primary and secondary energies. Chopping schemes other than the simple binary pseudonoise sequences may be found which, at some sacrifice in duty cycle, lead to a higher gain in statistical accuracy for certain types of problems. The Oak Ridge electromagnetic chopper that was mentioned previously may turn out to be an almost ideal pseudonoise modulator.

There is still another approach to the high-duty cycle chopper, i.e., sinusoidal modulation of the continuous reactor beam and subsequent measurement of the Fourier transform of the TOF distribution function.[20,21] This has probably not yet been developed to the same state of the art as the statistical pulsing technique, but it also appears promising for certain, though more restricted, classes of problems.

CONCLUSIONS

The preceding remarks by no means imply that these new high-duty cycle systems rule out repetitively pulsed reactors. On one hand there are many problems where the high-duty cycle systems cannot be used advantageously and where only a higher peak flux can help (a typical example would be very weak peaks in a TOF distribution next to very strong ones which would be overshadowed). Furthermore, strong repetitively pulsed reactors may be used for the study of time-dependent phenomenon in solids or liquids which is not possible when statistical pulsing on steady-state beams is used. Finally, there is no doubt that some statistical features can be used to improve the performance of repetitively pulsed reactors. It would probably be feasible to design double TOF spectrometers combining a repetitively pulsed reactor and a statistical chopper. Statistical concepts may eventually be used to increase the repetition rate of a pulsed reactor (by a factor of 2 to 5) beyond those rates normally set by frame-overlap conditions.

In any case, however, a repetitively pulsed reactor has to be well advanced to compete with or to surpass our present-day high-flux reactors using optimized instruments. Peak flux levels in the 10^{16} to 10^{17} range should be obtained at very short bursts and high repetition rates. Some more specific data for a desirable system are given in the preceding paper (see R. M. Brugger and K. H. Beckurts, Session 8, Paper 1). The number of available beam holes should be large (10 to 15), and there should be very flexible facilities to install various kinds of moderators to match the spectrum and the time spread of the neutrons to the individual experiment. We are aware that these parameters represent an enormous extrapolation over presently attainable figures. They are, however, in the same range as those considered in the framework of the present Brookhaven National Laboratory (see J. Hendrie et al., Session 3, Paper 2) and Idaho[14] proposals.

Although this system is desirable, it would be extremely worthwhile to actually build a system with less ambitious specifications in the near future. A system with specifications in the range of SORA would represent a very useful intermediate step between IBR and the very advanced system mentioned previously. Actually operating a system of this size would initiate many new experimental techniques that may give additional momentum to the repetitively pulsed reactor approach.

ACKNOWLEDGMENT

REFERENCES

1. P. A. Egelstaff (Ed.), *Thermal Neutron Scattering,* Academic Press, Inc., New York, 1962.
2. R. M. Brugger, Studies of Condensed Matter Using Neutrons, in *Intense Neutron Sources,* Seminar Proceedings, Sante Fe, N. Mex., Sept. 19-23, 1966, USAEC Report CONF-660925, 1967.
3. *Inelastic Scattering of Neutrons from Solids and Liquids,* Proceedings Series, Chalk River, 1962, International Atomic Energy Agency, Vienna, 1963, (STI/PUB/62); *Inelastic Scattering of Neutrons,* Proceedings Series, Bombay, 1964, International Atomic Energy Agency, Vienna, 1965 (STI/PUB/92); and *Neutron Inelastic Scattering,* Proceedings Series, Copenhagen, 1968, International Atomic Energy Agency, Vienna, 1968 (STI/PUB/187).
4. H. Maier-Leibnitz, *Nukleonik,* 8: 61 (1966).
5. K. Parlinski et al., in *Research Applications of Nuclear Pulsed Systems,* Panel Proceedings, Dubna, 1966, International Atomic Energy Agency, Vienna, 1967 (STI/PUB/144).
6. V. G. Liforov et al., in *Research Applications of Nuclear Pulsed Systems,* Panel Proceedings, Dubna, 1966, International Atomic Energy Agency, Vienna, 1967 (STI/PUB/144).

7. L. B. Pikelner and V. T. Rudenko, in *Research Applications of Nuclear Pulsed Systems,* Panel Proceedings, Dubna, 1966, International Atomic Energy Agency, Vienna, 1967 (STI/PUB/144).

8. W. Kley, in *Research Applications of.Nuclear Pulsed Systems,* Panel Proceedings, Dubna, 1966, International Atomic Energy Agency, Vienna, 1967 (STI/PUB/144).

9. W. Kley, The Use of Pulsed Reactors in the Field of Neutron and Solid-State Physics, Euratom Report EUR-2538e, 1965.

10. *Research Applications of Nuclear Pulsed Systems,* Panel Proceedings, Dubna, 1966, International Atomic Energy Agency, Vienna, 1967 (STI/PUB/144).

11. *Intense Neutron Sources,* Seminar Proceedings, Sante Fe, N. Mex., Sept. 19-23, 1966, USAEC Report CONF-660925, 1967.

12. H. Maier-Leibnitz and T. Springer, *Reactor Sci. Tech.,* 17: 217 (1963).

13. J. L. Russel, K. L. Crosbie, and C. A. Stevens, in *Research Applications of Nuclear Pulsed Systems,* Panel Proceedings, Dubna, 1966, International Atomic Energy Agency, Vienna, 1967 (STI/PUB/144).

14. R. G. Fluharty, F. B. Simpson, G. J. Russell, and R. H. Morris, A Proposal for a Repetitively Pulsed Test Facility (RPTF), USAEC Report IN-1149, Idaho Nuclear Corp., 1967.

15. M. Poole, in *Research Applications of Nuclear Pulsed Systems,* Panel Proceedings, Dubna, 1966, International Atomic Energy Agency, Vienna, 1967 (STI/PUB/144).

16. K. Sköld, *Nucl. Instr. Methods,* 63: 14 (1968).

17. F. Gompf et al., in *Neutron Inelastic Scattering,* Proceedings Series, Copenhagen, 1968, International Atomic Energy Agency, Vienna, 1968 (STI/PUB/187).

18. W. Golomb, *Shift Register Sequences,* Holden—Day, Inc., San Francisco, 1966.

19. W. Drexel and W. Glaeser, in preparation.

20. W. L. Whittemore et al., in *Neutron Inelastic Scattering,* Proceedings Series, Copenhagen, 1968, International Atomic Energy Agency, Vienna, 1968 (STI/PUB/187).

21. K. H. Beckurts, Institut fur Angewandte Kernphysik, Kernforschungszentrum, Karlsruhe, unpublished, 1966.

8-3 FISSION-NEUTRON PULSE RADIOLYSIS

L. M. THEARD and J. L. RUSSELL, JR.
Gulf General Atomic Incorporated, San Diego, California

INTRODUCTION

Radiation chemistry, which concerns chemical effects induced in matter by ionizing radiation, is studied by various techniques.[1] Stable chemical products, e.g., hydrogen gas and hydrogen peroxide generated in aqueous solutions, can be detected subsequent to the irradiation and studied as a function of various parameters, such as radiation dose, dose rate, and additive concentration. Unstable transient chemical products, such as free radicals and ions, can be detected also, and the information obtained is very useful in determining the mechanisms by which radiation induces chemical transformations in matter.

Pulse radiolysis is one of the techniques which permits the direct study of radiation-produced transient chemical species.[2] The technique is usable under conditions of such practical importance as with liquids at room temperature. Of further importance the time dependence of various short-lived (less than 10^{-3} sec) chemical transients can be determined, following pulse irradiation, thus providing information pertinent to mechanisms of reactions. The detection method is fast-response optical absorption or spectrophotometry. The required radiation source must provide high-intensity pulses of radiation with short pulse duration compared with the lifetime of the transients to be studied.

In the past only pulsed electrons and X rays have been used in pulse radiolysis. However, certain fast burst reactors generate neutron pulses that are usable for pulse radiolysis studies. The data that might be obtained from such studies on biochemical systems have an important relevance to radiobiology and radiation therapy. This paper discusses the proposed use of the Accelerator-Pulsed Fast Critical Assembly (APFA-III) for fission-neutron pulse radiolysis studies.

SOME ASPECTS OF RADIATION CHEMISTRY AND RADIATION BIOLOGY

A principal step in the radiation-induced decomposition of molecular systems is the formation of ions, free electrons, and free radicals.[1,2] For the irradiation of water, these processes may be represented as follows. Ionization,

$$H_2O \rightsquigarrow H_2O^+ + e^- \qquad (1)$$

is followed by electron hydration

$$e^- \xrightarrow{ n\,H_2O } e_{aq}^- \qquad (2)$$

and OH formation via ion−molecule reaction

$$H_2O^+ + H_2O \rightarrow H_3O^+ + OH \qquad (3)$$
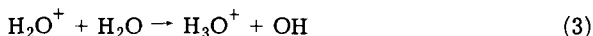
Formation of H and OH free radicals may occur also via electronic excitation of water by the radiation

$$H_2O \rightsquigarrow H_2O^* \qquad (4)$$

to produce an excited water molecule, H_2O^*, which decomposes

$$H_2O^* \rightarrow H^\cdot + OH \qquad (5)$$
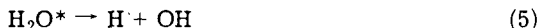
The free radicals e_{aq}^- (hydrated electron), OH (hydroxyl radical), and H (hydrogen atom) are all very reactive and will react with each other or with impurities and solutes present in the water.

In biological systems, reactions 1 through 5 will occur to a significant extent since water comprises a large fraction (approximately 80% in many cases) of the living cell. The free radicals generated from water decomposition in the cell may react with biomolecules. This process is called the radiobiological indirect effect. Biomolecules in irradiated cells are also damaged by direct absorption of energy from the radiation; this effect is called the direct effect.

Decomposition of biomolecules by both indirect and direct effects proceeds via free-radical intermediate forms of the biomolecule.[3] For example, hydroxyl radicals add on to various portions of the important giant molecule deoxyribonucleic acid (DNA) to form free radicals[4] which, in turn, are reactive with other free radicals and with oxygen. Alternatively, direct excitation of DNA can lead to loss of a hydrogen atom which leaves a free-radical form of DNA that also reacts further with other free radicals or with oxygen.

Radiation chemical studies of dilute aqueous solutions of bio-chemicals pertain primarily to the indirect effect since most of the radiation energy is absorbed by water. Information pertaining to the direct effect can be obtained in solutions of sufficiently high biochemical concentration for which direct absorption by the biochemical is significant. Direct effects may be studied also with dry biochemicals, of course, but this approach is of limited applicability in pulse radiolysis since the sample must be optically transparent in the visible and ultraviolet spectral regions.

Charged particles deposit energy inhomogeneously in condensed media.[1,5] The loss of energy per unit distance traveled is a function of the particle speed and the magnitude of its charge. The slower the speed and the greater the charge, the greater the energy loss per unit distance. Thus the energy loss per unit distance increases in the order electrons, protons, and alpha particles for these particles at equal initial energy.

As a result of inhomogeneous energy deposition by ionizing radiation, free radicals are generated inhomogeneously, and their chemistry is a function of their spacial distribution. Electrons with energy of the order of 1 Mev lose about 100 ev average per loss event. The average energy loss per unit distance traversed, $(-dE/dt)$ or LET (linear energy transfer), is 0.02 ev/Å. Therefore the average separation of energy-deposition events[5] is 5000 Å. For each deposition of energy of the order of 100 ev, an ion and a secondary electron are produced; the secondary electron, which carries most of the energy deposited, can further ionize and excite molecules. These additional ionizations and excitations will occur in close proximity to the first ionization, however, since the range of the low-energy secondary electron is very low. As a result several ionizations, excitations, and subsequent decompositions will occur in a volume of small diameter, generally a few tens of angstroms.

The situation is quite different for high-LET particles. The average LET for fission neutrons in water is about 4 ev/Å. In this case energy is deposited primarily by energetic protons generated through collision between fission neutrons and hydrogen atoms bound in water molecules. An average LET of 4 ev/Å indicates that the average energy deposited for each water molecule traversed is sufficient to dissociate one of the hydrogen–oxygen bonds in water. Further, the amount of energy deposited for each two adjacent molecules traversed is sufficient to ionize one of the molecules. The result then is that a cylindrical volume containing closely spaced ions, electrons, and free radicals is generated along the proton track. Nuclei of oxygen, carbon, and other atoms generated in solution by neutron collisions will produce cylinders of reactive chemical intermediates in even greater concentrations.

Macromolecular biomolecules present in a fission-neutron-irradiated medium are likely to undergo multiple bond breakage from direct effects because of the large amount of energy imparted to the molecule even if the ionizing particle traverses the smallest dimension of the molecule. Irradiation of surrounding aqueous regions can lead to multiple bond breakage by the indirect effect where free radicals are generated sufficiently close to the biomolecule. The specific chemical bonds broken by fission neutrons may differ from those broken by fast electrons since the energy imparted to molecules generally is higher for the former.

It has been found that radiation-induced damage of cells and tissues may be much greater (up to a factor of 3) in the presence of oxygen than in the absence of oxygen.[3] However, this effect is observed only for radiations of low LET, such as gamma rays and fast electrons. This observation has practical importance to radiation therapy. Thus in tumors with poor vascular systems, the oxygen content may be lower than in the surrounding normal tissue. As a result the tumor tissue is less sensitive to gamma-ray therapy than is the surrounding tissue. Efforts to overcome this differential in tissue sensitivity to radiation have included patient treatment in a hyperbaric oxygen environment which enhances the radiation sensitivity of the tumor by increasing its oxygen content although not affecting the radiation sensitivity of the normal tissue.[3] Alternatively, if high-LET radiation can be used, the radiation sensitivities of normal and anoxic tissue are equal, and no undesirable differential effect prevails. The technology of neutron therapy has not yet permitted the widespread use of hyperbaric oxygen environments. Another of its characteristics of interest is its high penetrability along with high LET as opposed to the low penetrability of a direct source of high-LET particles. Analogously, low-LET gamma rays are employed often in radiation therapy for their high penetrability in preference to fast-electron beams having the same LET.

Characteristics of the observed radiobiological oxygen effect suggest that its mechanism involves free-radical reactions. It is known that e_{aq}^-, H, and various free-radical forms of biomolecules generated by the direct and indirect effects react readily with oxygen. Thus it is plausible that reaction of these species with oxygen for low-LET radiations leads to more damage (e.g., through peroxide formation) than that which occurs in the absence of oxygen. For high-LET radiations, which tend to be more damaging than low-LET radiations, it is likely that the reactions of oxygen with damaged biomolecules simply result in a type of overkill. The chemical effect induced in cells by high-LET radiation in the absence of oxygen may be as biologically damaging as that which results in the presence of oxygen. Important to this ex-

planation is the requirement that the biochemical effect of high-LET radiation is different from that of low-LET radiation. Such a difference may be detectable by a comparison of neutron and electron pulse radiolysis studies in which free radicals generated in identical systems by the different radiations may be detected and distinguished by their optical absorption spectra and reaction kinetics.

Principle of Pulse Radiolysis

The various free radicals generated in a sample by ionizing radiation may disappear by a variety of mechanisms. During irradiation the free-radical concentration will attain a value called the steady-state concentration for which the rate of free-radical formation equals the rate of disappearance. Optical absorption of many free radicals occurs in the ultraviolet and visible spectral regions. Thus when generated in media transparent in these spectral regions, these free radicals are potentially detectable by optical absorption spectrophotometry. The steady-state free-radical concentration generated by low-intensity radiation sources, however, is usually too low for detection by this method. Very high intensity radiation sources, such as the electron linear accelerator, generate detectable concentrations of free radicals, and, of added importance, the irradiation time required is short compared to the lifetime of many of the free radicals generated. Therefore by using a fast-response spectrophotometric system, one can observe free-radical concentration as a function of time as reaction occurs. Information obtained includes absorption spectra that indicate the type of free radicals formed, the intensity of absorption that relates to the free-radical yield, and the time dependence of free-radical concentration from which mechanisms of reaction often can be determined. Free-radical reactions presently can be time-resolved down to the order of 10^{-8} sec.

A schematic representation of an experimental setup used at Gulf General Atomic Incorporated is shown in Fig. 1. The optical components shown are fixed on a portable table that can be oriented to permit passage of a 15-Mev electron beam through spherical mirror 4 (SM 4), the sample cell, and SM 5. Alternatively, the table can be positioned so that the electron beam traverses the sample cell from the side perpendicular to the direction shown. The focusing and reflecting elements of the optical system are front-surfaced aluminum mirrors. From a lamp, light that is reinforced by reflection from spherical mirror SM 1 is imaged through flat mirror 1 (FM 1) by SM 2 on an entrance window in SM 3. Spherical mirrors (SM 4) (split vertically into two identical halves), SM 3, and the sample cell constitute a multiple-traverse absorption array that can be set for up to 28 passes of light (in units of four passes) through samples as long as 4 cm.
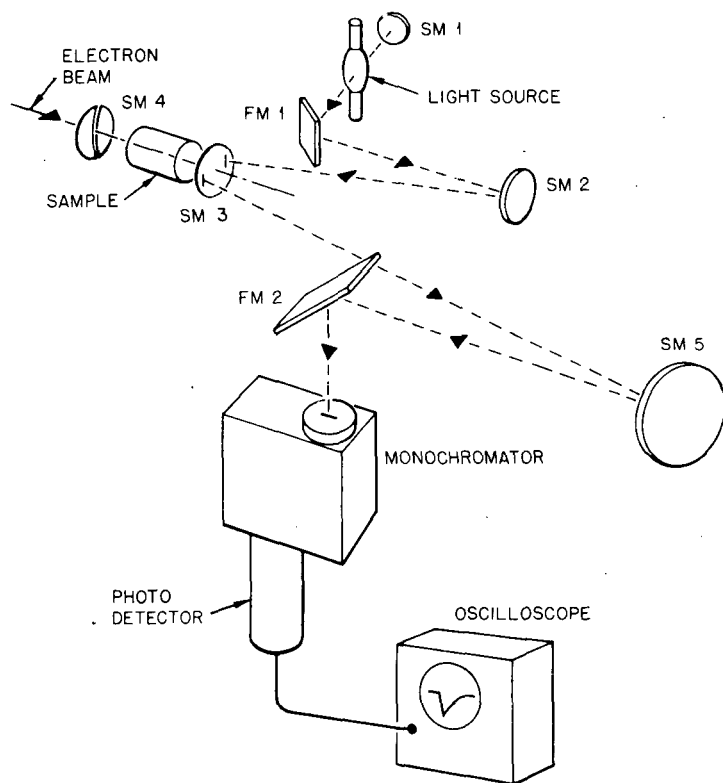
Fig. 1—Schematic of Gulf General Atomic pulse radiolysis apparatus. SM is spherical mirror; FM is flat mirror.

After the final traversal of the light beam through the sample, an image of the light source is focused on an exit window in SM 3. The light is reimaged by SM 5 through FM 2 onto the entrance slit of the monochromator. The exiting monochromatic light is detected by a photomultiplier tube whose response is displayed on an oscilloscope screen.

Figure 2 is a photograph of oscilloscopic display of photomultiplier response to light at a wavelength of 335 mμ. The irradiated sample is an aqueous solution of thymine, a constituent of the nucleic acid DNA, with ethanol added to suppress the reaction of OH and H with thymine. The reaction product, which absorbs light, is formed by the addition of e_{aq}^- to thymine to give a negatively charged product T^-. The oscilloscope sweep is triggered 60 μsec before the firing of a 0.1-μsec electron pulse. When the pulse is fired, reaction of e_{aq}^- with thymine is complete in about 0.2 μsec. Thus the decrease in light intensity shown at a sweep speed of 50 μsec per horizontal division appears to

50 μSEC/DIVISION
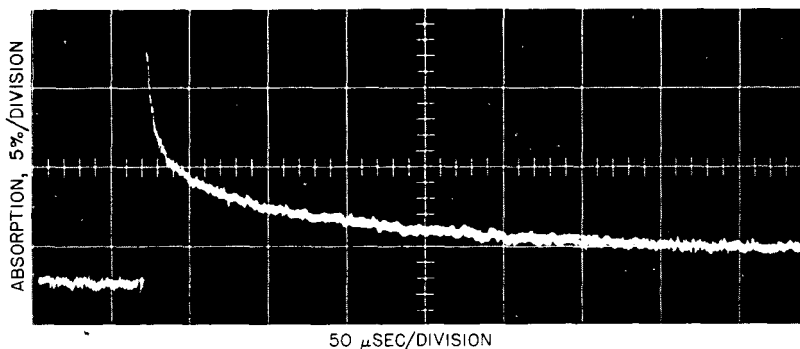
Fig. 2—Oscilloscope trace showing the decay of T^- in an aqueous solution of thymine ($4.6 \times 10^{-4}M$) and ethanol (0.1M); pH 5.5, wavelength 335 mμ, and dose ~1600 rads.

be instantaneous at the point where the radiation pulse is fired. The decrease of light absorption with increasing time is a function of the decrease of the concentration of T^- as a result of its subsequent reaction. The signal decay is interpretable in terms of two processes. The first, indicated by the initial sharp decrease of signal, is attributable to neutralization of T^- by hydrated protons to form a product TH which also absorbs light at 335 mμ. The second process is the slower disappearance of TH by reaction with itself and possibly other free radicals. Figure 3 shows absorption spectra taken from a series of photographs similar to that shown in Fig. 2 for varying wavelength.

Fission-Neutron Pulse Radiolysis

The Accelerator Pulsed Fast Critical Assembly (APFA) generates pulsed neutrons; it is suitable for use in neutron pulse radiolysis studies. The APFA, shown in Fig. 4, is a 7-in.-diameter uranium (93 wt.% ^{235}U) unreflected fast reactor. With the reactor in a sub-prompt critical configuration, the electron beam from the Gulf General Atomic 50-Mev or 94-Mev Linac is injected into the core through a beam-entry hole $^3/_4$-in. in diameter. The beam is stopped near the center of the core, resulting in bremsstrahlung and providing a gross neutron source through (γ,n) and (γ,f) reactions with the uranium nuclei. This source is subsequently multiplied by the reactor, producing a short-time-duration (~7×10^{-6} sec) intense pulse of neutrons from the reactor with a uniform neutron leakage over 4π steradians.

The peak fast-neutron flux inside the cavity is 5×10^{17} neutrons/cm^2/sec, whereas, at closest approach outside the cavity, it is an order of magnitude lower. The resultant neutron dose in water outside the cavity is about 600 rads, which is adequate to produce a spectrophoto-

0.14

T⁻

0.12

0.10

OUTSIDE DIAMETER, IN.

0.08

0.06

TH

0.04

0.02

0

300 325 350 375 400 425 450

λ, Mμ

○—○ T⁻ SPECTRUM TAKEN AT END OF 0.1 μSEC PULSE

●—● TH SPECTRUM TAKEN 50 μSEC AFTER PULSE
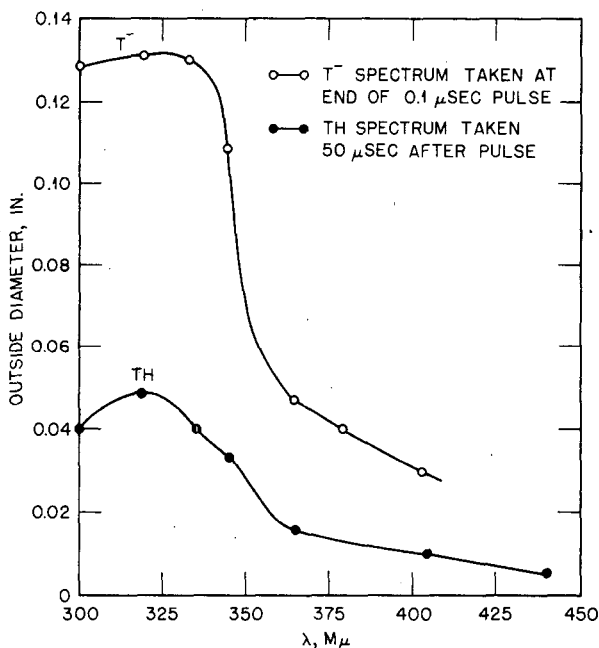
Fig. 3—Spectra determined from data on aqueous solutions of thymine (4.6 × 10⁻⁴M) and ethanol (0.1M); pH 5.5, wavelength 335 mμ, and dose ~1600 rads. T⁻ and TH from T⁻ + H₃O⁺ₐq → TH + H₂O.

metrically observable concentration of hydrated electrons and other free radicals in aqueous solution. Modifications of the Gulf General Atomic pulse radiolysis optical system will permit its use with APFA-III. The 7-μsec half-width of the pulse is sufficiently short for time resolution of certain free radicals, as indicated in Fig. 2. The gamma dose is about one-fourth the neutron dose. Effects attributable to gamma irradiation for APFA-III pulse radiolysis studies can be estimated by effects of hydrogenous shielding materials and by comparison to electron-pulse radiolysis results.

Data on both the indirect and direct effects for aqueous systems will be sought. For pure water the determination of the yield and time dependence of e_{aq}^- (detectable by absorption of red light) will be of interest. This information along with data on effects of additive reactants may provide a means for determining track dimensions. Studies of biochemical solutes are of interest over a concentration range up to where direct effects are important. Free radicals distinguishable in spectral characteristics and reactivity from those generated by energetic electrons will be sought.
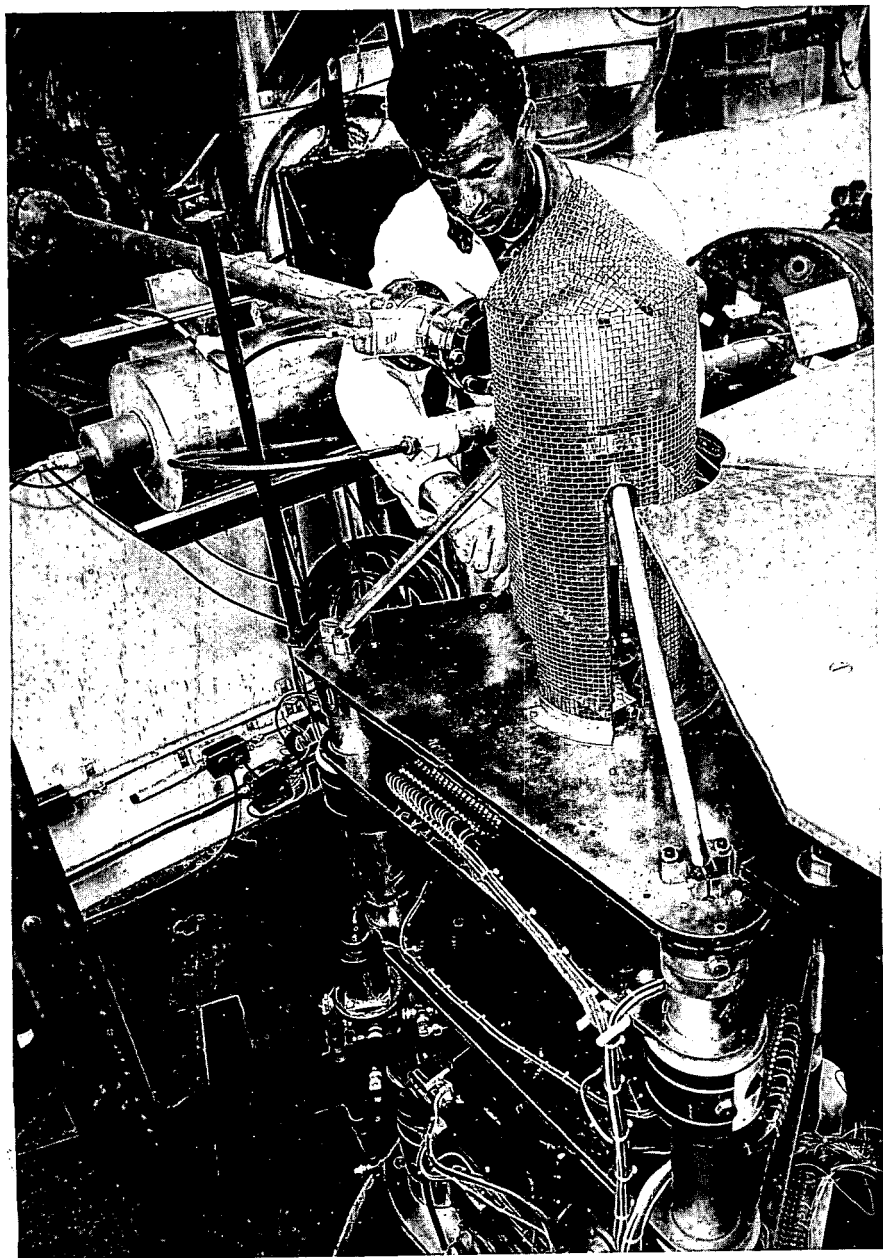
Fig. 4—The APFA-III.

ACKNOWLEDGMENT

REFERENCES

1. M. Burton, Radiation Chemistry, *Chem. Eng. News,* 47: 88 (1969).
2. L. M. Dorfman and M. S. Matheson, Pulse Radiolysis, in *Progress in Reaction Kinetics,* Vol. 3, p. 237, G. Porter, Ed., Pergamon Press, Inc., New York, 1965.
3. Z. M. Bacq and P. Alexander, *Fundamentals of Radiobiology,* Pergamon Press, Inc., New York, 1961.
4. L. S. Myers, Jr., M. L. Hollis, and L. M. Theard, in *Radiation Chemistry,* p. 345, Advances in Chemistry Series No. 81, American Chemical Society, Washington, D. C., 1968.
5. A. O. Allen, *The Radiation Chemistry of Water and Aqueous Solutions,* D. Van Nostrand Company, Inc., Princeton, N. J., 1961.
6. L. M. Theard and F. C. Peterson, Pulse Radiolysis Study of Protection of Pyrimidine-Base Components of Nucleic Acid by Aminothiols in Aqueous Solutions, USAEC Report GA-8872, Gulf General Atomic, Inc., 1968.

DISCUSSION

GOTTSCHALL: Considering your time resolution possible right now as well as the LET effect, would you comment on possible direct observation of intratrack reactions?

THEARD: I think that it is very unlikely. Perhaps I should clarify your question a little bit for those who might not be familiar with radiation chemistry in that much detail. The question pertains to intratrack free-radical reactions as opposed to free-radical reactions occurring outside the track. A significant point is that the high density of free radicals within the track of high-LET radiation leads to considerable radical−radical reaction. Indeed, the intratrack chemistry is more probable in the case of these densely ionizing radiations than is diffusion away from the track. So you can consider that free radicals generated in the track have an alternative to either react with themselves or diffuse away and react with free radicals generated from neighboring tracks or with solutes. The speed of these reactions occurring inside the track, I think even in the case of gamma rays, is on the order of nanoseconds. Consequently, for the extremely high-LET radiations, these processes would probably be much too fast for actual observation at present. What one could hope, which I think would be of importance, is to identify and determine the concentrations of various free radicals which ultimately do migrate from the track.

SMATHERS: Are you bothered at all by the radiolytic-gas production leading to gas bubble formation within the cell and scattering of the light within the time frame that you are working?

THEARD: We have never had any difficulty with that, which I think would pretty much depend on the dose delivered to the sample; in the case of the electron pulse radiolysis where we can deposit very high doses at present, we have never had a problem along those lines.

RUSSELL: The developments at Sandia with plans for a flash X-ray pulsed reactor operating at microsecond or less pulses should have considerable impact on the number of free radicals that can be studied by neutron pulse radiolysis.

THEARD: I agree. As a matter of fact, the history of development of electron pulse radiolysis is one which includes, first, the study of reactions on the time scale of tens of microseconds, and now we are looking at reactions occurring on the order of nanoseconds. I think that similar improvements in neutron pulse radiolysis might be expected, particularly since now there is clearly the prospect for improving the intensity and pulse characteristics of neutrons.

Conference
on
the Use of
Fast Burst Reactors
in
University Programs

This conference was held on Jan. 31, 1969, following the National Topical Meeting on Fast Burst Reactors. It was sponsored by the Department of Nuclear Engineering of the University of New Mexico and the Associated Western Universities with funds provided by the United States Atomic Energy Commission.

Chairman A. E. Wilson, Idaho State University
Panel Moderator G. V. Beard, Director, Associated
  Western Universities
Panel Members   J. C. Cera, Division of Nuclear
                    Education and Training, U. S. Atomic
                    Energy Commission
             R. G. Fluharty, Los Alamos Scientific
                    Laboratory
             D. L. Hetrick, University of Arizona
             J. L. Russell, Gulf General Atomic Inc.

TEACHING APPLICATION OF FAST BURST REACTORS IN UNIVERSITY PROGRAMS

GLENN A. WHAN
The University of New Mexico, Albuquerque, New Mexico

This paper specifically discusses teaching applications of fast burst reactors. There are a great number of ways in which these small bare fast systems can be incorporated into both classroom calculations and laboratory demonstrations. I shall not attempt to relay all these possibilities to you but shall describe only a few of the ways in which we have incorporated these reactors into our teaching program at The University of New Mexico. I hope that the comments I make, as well as the comments made by the authors of the following papers, will stimulate additional ideas.

First, let me make a few comments about calculational problems. In general, these fall into four categories particularly suitable for classroom homework assignments. The first area could be criticality calculations. This type of reactor is an extremely simple clean model which can be used for the calculation of critical mass. You can use almost any degree of complexity, starting with the simple one group up through two groups, S_n, P_n, Monte Carlo, etc. Any of these techniques are applicable to this reactor model, and I do not believe I have to dwell on this idea to any extent.

The second obvious calculational area is kinetics. Here again the system is extremely simple with only a few feedback mechanisms to complicate the kinetics model. One can begin initially with a very simple isothermal point reactor and extend this into the nonisothermal case using one or two dimensions — just as complicated as you wish to be to describe the dynamic behavior of these reactors.

A third area that fits beautifully into classroom exercises is worth calculations. Calculations of control-rod worth, reflector worth, importance functions, and perturbation effects are easily handled for this system, and there are enough experimental data available for these

609

reactors to evaluate just how well calculational results agree with actual experimental measurements.

The fourth area that I will discuss briefly is that of radiation shielding. Some of the radiation problems encountered during the design, construction, and initial start-up of the burst reactor at Sandia gave me a number of very interesting problems that I have passed along to our students. Dosimetry measurements during the initial start-up of the reactor pointed out quite clearly that there were intense fields of radiation outside the reactor building. With these experimental measurements available, I have asked the students to calculate the dose at the side of the building from radiation coming directly through the walls, from radiation scattered off the metal beam-catcher walls, and from air scatter between the reactor building and the beam catcher. Surprisingly, the students come up with calculational values that are correct within an order of magnitude, which is an accomplishment in shielding calculations. Another example that lends itself nicely to calculational models in the classroom is concrete activation inside the reactor building. Air activation inside the building has also caused some trouble. One can give the students a typical burst of 10^{16} or 10^{17} neutrons/burst and ask them to predict the activity of the concrete walls and the activity of the air inside the enclosure. Their results again come within an order of magnitude, and they seem to get some satisfaction out of comparing their theoretical calculations with actual experimental measurements.

Next, I would like to share with you experiences which we have had with instructional laboratory experiments using the Sandia Pulsed Reactor. Each year we conduct these instructional experiments with our laboratory class at the Sandia Laboratory on Saturdays, usually with small groups of six or seven students per class. This fall, because of the increasing enrollments, we had two sections performing the experiments—one section of seven students in the morning and one section of seven students in the afternoon. I shall describe these experiments in more detail later, but first let me talk briefly about three experiments which we have not done routinely with the students, but ones which we are thinking of developing for use in the very near future: reflector-worth measurements, prompt-neutron decay lifetimes, and the time response of radiation detectors and dosimetry.

The reflector-worth experiment should be easy to carry out with this bare uncluttered reactor core. One can position various thicknesses of reflector around the reactor; or, at some distance from the core, one can vary the position of the reflector. It is then a simple matter to measure how much reactivity worth has been added or subtracted. Again this is a very simple calculational model and something that the students can compare with experimental results. A

second experiment that we are considering is one dealing with statistical techniques for the measurement of prompt-neutron decay constants. Again this small compact reactor is very accessible for experimental measuring equipment. It has a very short prompt-neutron lifetime, and there is good separation between the prompt and delayed neutrons. The short decay chains allow for rapid gathering of data. One of our doctoral students is working on this particular problem for his dissertation research, and I am almost certain that out of this research we shall develop an experiment appropriate for our laboratory classes.

The last experiment that I wish to mention is the time response of radiation detection and dosimetry measurements. In most cases radiation detection and dose measurements can best be demonstrated in the laboratory with small steady-state sources. If one wishes to show the time response of active detectors, however, this reactor is particularly useful for producing short bursts of neutrons. A flash X-ray machine can then be used to obtain short bursts of gamma radiation. Also, for short-term changes in passive dosimetry materials, such as changes in optical density and thermoluminescence, studies are best performed with pulsed radiation sources.

One experiment that might be considered a natural for the burst reactor is one demonstrating step insertions of reactivity. The design and instrumentation of the Sandia reactor, however, leaves no simple way to insert step changes of reactivity from delayed critical. The reactor could, of course, be modified, but this modification would not be practical.

In the results of some of the experiments that we have conducted recently with our students, experimental data were taken by one of the laboratory groups which showed the complete calibration of a control rod. Now you might say that one can calibrate a control rod with any reactor so why use a fast burst reactor? This calibration can be done very rapidly with the burst reactor because we can measure periods in the range of 3 to 5 sec. It takes very little time to get each experimental point. The students can calibrate an entire control rod in something like an hour. Another advantage is that since the reactor has so much excess reactivity we can calibrate one entire control rod with little adjustment to the other control rods. Finally, because of the small fast system, there is essentially no interaction between control rods for this core. Interaction is often a difficulty encountered with the calibration of control rods in a thermal core.

The next experiment is a comparison between the experimental results and the theoretically predicted curve for an approach to prompt critical on the Sandia Pulsed Reactor. The experimental points are taken by the students as they approach prompt critical, measuring shorter and shorter periods. This is exciting for the students. Students cannot

very often do an experiment demonstrating the approach to prompt critical. They use their own control-rod calibration data to determine the incremental insertions of control rod for the approach of prompt critical. They take the whole business seriously, and it turns out to be one of our most popular experiments.

Once the prompt critical point has been determined, the students then go through a normal burst sequence for the reactor by inserting 2 or 3¢ worth of excess prompt reactivity. The integrated neutron-flux response is normalized to the steady-state temperature measured in the reactor at some time relatively long after the burst. The students then calculate the dynamic temperature coefficient based on the average temperature in the reactor at the time the core drops below prompt critical. They also measure the static temperature coefficient for the reactor by changing the core temperature 10 to 15°C and then measuring the change in reactivity. It is often difficult in thermal water-cooled reactors to change the temperature over a very large range, and certainly difficult to do it rapidly.

The experiments that I have described involve just two experimental days. The first day we introduce the students to the instrumentation associated with the reactor, let them become familiar with the system, and then perform the control-rod calibration. On the second day we carried out the approach to prompt critical and measured the dynamic and static temperature coefficients.

In summary, I think it is correct to say that the fast burst reactor has played an important part in the teaching activities at The University of New Mexico, in addition to the role it has played and will continue to play in our research program.

UNIVERSITY RESEARCH
USING FAST BURST REACTORS

GEORGE H. MILEY* and HAROLD A. KURSTEDT †
*Nuclear Engineering Program, University of Illinois, Urbana, Illinois;
†Nuclear Engineering Program, Ohio State University, Columbus, Ohio

ABSTRACT

Past university research involving fast burst reactors is reviewed. Several studies related to reactor kinetics and reactor development are discussed. Use of the reactor as a pulsed source to study neutron pulse propagation and radiobiological studies requiring both a pulsed and a steady-state fast-neutron source are also reviewed. A surprising lack of university involvement in studies of radiation effects on materials and electronics is discussed.

On the basis of this review, as well as research reported by nonuniversity investigators, some promising future research areas are suggested along with a discussion of possible means of carrying out off-campus research of this type.

INTRODUCTION

University utilization of fast burst reactors has proceeded over the years on a relatively small scale but with some significant results. There is every reason to believe that such activities will expand in scope and importance in the future. In this paper we review past uses and then examine some future possibilities. Our attention is restricted to single-burst systems. Possible uses of repetitively pulsed fast reactors have been reviewed extensively by others (see R. M. Brugger and K. H. Beckurts, Session 8, Papers 1 and 2, and D. I. Blohkintsev, Session 3, Paper 1). For this reason, and also because such systems are not now generally available, they are not considered in this paper.

University uses of thermal pulsed reactors, such as the TRIGA, were discussed at an earlier American Nuclear Society conference.[1] In contrast, the work described in this paper has been selected because

it specifically requires, for one reason or another, a fast reactor system.

It is estimated that some 15,000 bursts have been recorded with fast burst reactors to date (see P. D. O'Brien, Session 4, Paper 6). If it is assumed that roughly 10 bursts are required for a particular type of experiment, this represents some 1500 different experiments. It will be shown shortly that universities were involved in only a few of these. This raises several questions, e.g., will university involvement increase in the future? How many of the experiments carried out by others might have been suitable for university research? Hopefully answers to these questions will become clear as we proceed.

Fast burst reactor research generally falls under two broad areas: studies aimed at reactor development and studies that use the reactor as a radiation source. The former may be further subdivided into reactor kinetics, materials studies, and instrumentation. Source studies include neutron-beam physics, radiobiological studies, and studies of radiation effects on both materials and electronic components. The following discussion will be organized according to these categories.

REACTOR DEVELOPMENT: STUDIES TO DATE

Reactor Kinetics

A major advantage of the fast burst reactor for kinetics studies is that the absence of reflectors, coolant channels, etc., presents an exceptionally simple geometry and hence a relative "clean" situation for comparing experiments and analysis. Although the actual feedback mechanisms are complicated, they are well defined, and, in contrast to the typical reactor system, the neutronics can be conveniently isolated from other components.

University-related reactor kinetics studies reported to date have largely involved the fast burst reactors at Sandia, the Sandia Pulsed Reactor (SPR) and Sandia Pulsed Reactor II (SPR II). In 1967, Coats' doctoral thesis, based on research[2,3] at SPR, was mainly directed at developing simple analytic methods for analyzing experiments that require the placement of moderating materials near the reactor during a burst. (Moderators may vary and have been varied from polyethylene to monkeys!) Coats developed and experimentally verified a kinetics model applicable to this situation, i.e., to a reflected fast burst reactor. His experiments represent an extension of earlier studies by Long[4] using the White Sands Fast Burst Reactor. This work is continuing through a cooperative program between Sandia and the University of New Mexico (UNM) (see R. L. Long and R. L. Coats,

Session 4, Paper 4). A further extension of the research is underway through the efforts of C. C. Price, a UNM doctoral student, who is investigating techniques for applying statistical analysis (e.g., Rossi-alpha) to determine the prompt-neutron decay constant to predict the burst behavior of SPR II in the presence of a reflector.[5]

Also, Long[6] recently completed an experimental study of reactivity contributions in the glory hole of SPR II. He is currently developing a calculational model for predicting reactivity worths, which will be tested against these data. The result should be most useful for planning reactor experiments.

Sandia and UNM have also cooperated on thermomechanical shock studies reported by Reuscher of Sandia who serves part time on the UNM staff (see J. A. Reuscher, Session 1, Paper 3). To date these studies have largely involved measurements of the shock effects, but work is now underway to develop a coupled thermomechanical neutron-kinetics model for use in burst calculations involving the shock region.

McTaggart[7] reports that there are several studies in progress at the VIPER reactor in England which involve universities. These include an investigation of a multipoint spatial model by Vaughan of Birmingham University; analysis of the inertial stress problem for an idealized geometry and extending to plastic deformation by Carter of Cambridge University; and a remeasurement of delayed-neutron data in a variable spectrum environment by Clifford of Imperial College.

Materials

The prime university involvement in this area to date is the study of stress-corrosion cracking of uranium – molybdenum alloys by Hoenig and Sulsona of the University of Arizona.[8] Their research was done under contract with the U. S. Army in connection with development of the Army reactor at Aberdeen. Results were used in Sulsona's Ph. D. thesis.

Instrumentation

The main university involvement in instrumentation to date comes through a cooperative program between Sandia and Glower's investigators at Ohio State University involving the development of ferro-electric element causes a release of electrical charge by the element. The linearity of this system, as well as its response in high-intensity neutron and gamma fields, has been studied using the SPR. Although such detectors may find applications with a variety of sources, certainly one motivation for their development is their use with burst reactors.

THE REACTOR AS A RADIATION SOURCE: STUDIES TO DATE

Neutron Beam and Neutron Pulse Experiments

Miley and his students[10,11] have used the Oak Ridge Health Physics Research Reactor (HPRR) as a pulsed source of neutrons to study neutron-pulse propagation through a large graphite stack located near the reactor.[10,11] This study represents an extension of earlier work of this nature which used a TRIGA reactor.[11] The HPRR offers several advantages over the thermal system. The relatively narrow pulse ($\sim$60 μsec at full width and half-maximum as opposed to $\sim$10 msec for the TRIGA) affords a more precise determination of the neutron dispersion law at higher frequencies. The slowing down and approach to thermal equilibrium can also be conveniently studied; and, since the reactor is not located in a pool, the propagating medium is easily accessible, and a variety of arrays and geometries can be envisioned.

An important advantage of the burst reactor over typical accelerator neutron sources is the high intensity available. (The time-integrated intensity from a high repetition rate accelerator is competitive, but the signal-to-noise ratio is not as good as for a single high-intensity burst operation.) Miley and coworkers have carried out some preliminary studies involving highly absorbing heterogeneous arrays designed to exploit this advantage. They have shown that such measurements are possible using the HPRR, but an extensive measurement and theoretical development is required before meaningful results are obtained.

Radiobiological Studies

Universities have perhaps been involved to a larger extent in radiobiological studies than any other area. The bulk of this work has been centered at the HPRR.

Constantin and coworkers at the University of Tennessee Agriculture Research Laboratory have reported extensive studies of fast-neutron effects on seeds, seedlings, and plants.[12-16] Love, now associated with the Horticulture Department of Louisiana State University, is also actively involved in this work.

It is interesting to note that most of these irradiations involve low-power steady-state runs rather than burst operation. Constantin and Love[12] list three reasons for using the HPRR: the fast-neutron energy spectrum is well known; dosimetry is accurate and reproducible; and thermal-neutron and gamma-ray contaminations are low.

Various animal irradiations have been studied, and Willhoit[17] received his Ph.D. from the University of Pittsburgh for studies at the HPRR involving rats. Now at the University of North Carolina, he has continued similar studies.[18] The advantages of HPRR cited

previously for seed irradiation are equally significant here. In addition, Russell[19] showed that fast neutrons offer a higher mutation-to-sterilization ratio than gammas; so the breeding period over which significant mutation data can be collected is extended. Also he notes that dose-rate effects are smaller than for gamma rays; these factors may be quite significant in animal studies.

Radiation Effects on Materials and Electronics

It appears that a bulk of the studies to date requiring burst operation of the various fast burst reactors fall under this heading. Surprisingly, however, the authors were not able to find any instances where universities have been directly involved.

FACILITY UTILIZATION BY UNIVERSITIES

From the preceding discussion it is clear that two facilities, Sandia's SPR and SPR II and Oak Ridge's HPRR, have been involved in most university studies to date. Two students, one from the University of Virginia and one from the University of Arizona, have just recently begun reactor kinetic oriented studies at White Sands,[20] but none of the other facilities are similarly involved. The Army burst reactor facility at the Ballistics Research Laboratory is not yet operational, but there is an indication that cooperative university programs would be welcomed.[21] However, such programs would not be easily introduced elsewhere. The Godiva IV facility at Los Alamos is mainly intended to explore the possible development of improved fast burst reactors, and this program does not lend itself well to simultaneous use by others (see T. F. Wimett, R. H. White, and R. G. Wagner, Session 2, Paper 2). Kloverstrom[22] is pessimistic about possible use of the Super KUKLA at the Nevada Test Site. He stresses that its location in a restricted area is a real disadvantage. Further he fears that "the repetition rate of a fast burst reactor is far too low for most (nuclear physics) applications to compare favorably with other pulsed neutron sources. Hence he feels that such reactors are "not a promising tool in university-type research with the possible exception of special areas like radiation damage, biomedical studies, and property studies of fissile materials." (Although we essentially agree with this idea, we contend, however, that the number and importance of these "special areas" are such that fast burst reactors are a promising tool for university research.) Little information is available about attitudes at the one remaining facility, FRAN, recently relocated at the reactor test site in Idaho.

In review it would appear that more-extensive university use of these facilities has been hampered by such factors as their remoteness

and sometimes classified nature, their service orientation and difficulties in scheduling, the expenses involved in off-campus research, and a general lack of knowledge of the facilities by university faculty. However, none of these obstacles is insurmountable, and the studies cited earlier demonstrate that if well-thought-out research is developed by faculty, methods can be found to do it. In such situations the reactor staff members have almost always been very encouraging, cooperative, and helpful.

We might next consider some specific forms for carrying out future programs. One possibility would be to locate a fast burst reactor on a university campus. There are, however, a number of obvious problems with this approach, including questions related to safety, money, and flexibility. Thus it appears that continued and expanded cooperative programs with existing and new facilities represent the most reasonable path to follow. A number of opportunities exist. Summer work at the facilities involving both faculty and students is often feasible. Students may be assigned to the facility during the period required to carry out their thesis research. If the reactor is not too distant from a university, it may be possible to commute for short periods of time to carry out specific experiments. (As noted earlier, George Miley and several of his students have made a number of short visits to the HPRR, a distance of 520 miles from campus.) Finally, it might be noted that a summer institute designed to acquaint faculty with potential research with fast burst reactors has been proposed by Robert Long, but no definite arrangements have been made yet.

Financing such studies is a problem common to all research. In this case, however, in addition to the usual support from government agencies, support can be obtained directly from the facility or from organizations like Associated Western Universities or Oak Ridge Associated Universities.

SOME POTENTIAL RESEARCH AREAS

It would indeed be difficult and dangerous to attempt to predict the research areas which will or should receive attention in the future. Rather, the present comments are merely intended to list a few areas that might be considered by interested persons. Extension of the various university studies cited earlier represent one starting point. In addition, extensions of some of the studies reported by nonuniversity investigators would appear to be appropriate for university research.

Reactor kinetics and the associated thermomechanical shock problem are excellent examples. Some progress has been made in the development of accurate analytic models that incorporate the effect

of the shock on the reactor kinetics; however, considerably more work and verification by comparison with experiment appears warranted. A growing university interest in this area was noted earlier, and several other studies have been reported recently.[23-25] Kurstedt and Kazi have described the development of the computer code SAKIMO, which is based on a spatial average (point reactor) model for both the neutronics and inertia effects. The latter is effectively represented as the displacement of a thin cylindrical shell. Appropriate reactivity coefficients to represent this effect are determined by normalizing the model to low-yield bursts; it then can be applied to the high-yield region, where shock effects are important, and it allows a study of the resulting pulse shapes and temperature history. Several extensions of this model might be considered, e.g., spatial effects might be included, coupled with an explicit calculation of the reactivity coefficients.

The calculation of reactivity coefficients for these small fast reactors remains a challenging problem. In addition to the shock feedback problem, the accurate evaluation of reactivity coefficients is quite critical in the design of repetitively pulsed reactors. Along these lines, Takahashi[26] recently described a series of Monte Carlo calculations to determine the reactivity change due to a moving reflector. He was forced to use rather elaborate technique because the perturbation involved truly represents a three dimensional problem, for which Monte Carlo methods are well suited. He notes difficulties were encountered when similar calculations were attempted with S_N and first-flight collision-probability methods.

The thermal-shock studies by Reuscher were noted earlier, and additional information is given in Refs. 27 and 28. He suggests several unsolved problems remain. Studies to date have generally been restricted to one-dimensional problems. Some two-dimensional studies have been considered; however, a proper definition of boundary conditions at corners has not been found. Ultimately it is hoped that a full three-dimensional representation can be solved. Another extension is suggested by a possible design proposed for future reactors which involves coated-particle fuel pellets, e.g., see F. T. Adler, Session 5, Paper 4. The importance of thermal shock on the pellets themselves can be alleviated by proper selection of pellet size; however, the effect of the induced vibrations on the container must be considered. This suggests studies of the response to a temperature pulse for cylindrical or hexagonal containers or hexagonal containers filled with elastic spheres or rods.

There are also equally important problems associated with thermal-shock-measurement technique. Most of the measurements to date have employed the traditional Bentley gauge. However, this gauge suffers from interference from the radiation field and, in fact, may

ultimately suffer permanent damage. In an effort to get around this problem, Ellis[29] recently developed a gauge based on an eddy-current measurement. This instrument avoids radiation interference, but in its present state it appears to suffer from sensitivity and accuracy problems. Alternately Miley[30] has suggested the use of a laser for this measurement. Deflection from mirrors attached to the core would offer one means of detection. Another scheme would be to make the mirror on the core a part of the laser's optical cavity, in which case observation of fringe patterns would provide a very sensitive detector that would be free of radiation effects.

Some important practical extensions of the neutron pulse studies mentioned earlier are also possible. Neutron diffraction and time-of-flight studies anticipated for future repetitively pulsed reactors require a moderator block to thermalize neutrons before they enter the flight tube. This problem has only recently been discussed in detail by Fluharty[31] (see also Session 3, Paper 3). The moderator block must be designed to meet very stringent requirements. It must neither widen the pulse too much nor attenuate its amplitude excessively. A comprehensive theoretical treatment has not been published, and, since experimental data are scanty, it is doubtful that an optimum block design has been achieved. Experimental studies to date have employed the Rensselaer Polytechnic Institute linear accelerator. However, a fast burst reactor might be used, and it would offer the advantages of a realistic energy spectrum and geometry. Physically the experiment would be quite similar to the propagation experiment described by Miley, Tsoulfanidis, and Doshi,[10,11] except that appropriate moderator materials and sizes would be used instead of a graphite stack. This problem is especially intriguing because it combines advanced research in neutron thermalization with an immediate practical application.

Areas suggested up to this point have been directly related to reactor kinetics or reactor development. Actually, even more opportunities appear to exist in the areas of radiation effects in biology, materials, and electronics. As discussed earlier university involvement in biological studies has been strong, but practically no involvement has been developed in the other areas. The reason is not clear. Universities are involved in such studies using other radiation sources. Yet fast burst reactors offer some important advantages for these studies, e.g., dose-rate range and fast-neutron intensity, and, in fact, several of the reactors have been justified largely on this basis. One possible explanation is that university staff views the nature of these studies as too empirical or applied. If so, this point of view would appear to be shortsighted. True, many of the studies reported to date were designed to yield specific data for immediate applications. Still,

we must remember that the basic underlying mechanisms are often poorly understood and worthy of academic study.

The phenomenon of radiation-induced electrical conductivity in insulating materials is an excellent example. Studies at Sandia using SPR have established extensive empirical data that can be used in design studies, etc.;[32-34] however, the detailed mechanisms involved in the phenomenon remain ambiguous.

Early investigators studying polyethylene proposed that the proton ion acted as a charge carrier. This model slowly gave way to a trapping model in which electronic conduction dominated. Then it was suggested that a hopping model, attributed to unpublished studies by S. H. Glarum, was more suitable. Others have shown that the interaction of Compton and delta-ray electrons and trapped electrons may have a significant role. In retrospect, it is clear that the mechanisms are indeed complicated and require much more study before a definitive theory is possible. Coppage and Peterson[34] state that they avoid the use of a model "as much as possible in the belief that insufficient knowledge exists concerning the transport properties of polymeric materials to warrant the use of any 'conventional' models."

This situation is not uncommon in other radiation-effect studies. It is not surprising either since radiation interactions with matter are typically complex. A wealth of fundamental research appears possible in these areas which would be most appropriate for university involvement.

ACKNOWLEDGMENTS

REFERENCES

1. G. H. Miley, Utilization of a Pulsed Reactor for Research and Irradiation, in Proceedings of the International Conference on the Utilization of Research Reactors and Reactor Mathematics and Computation, Mexico City, May 2–4, 1967, Vol. 3, pp. 1646-1656, Report CNM-R-2, May 1967.
2. R. L. Coats, Neutron Kinetics of a Fast Burst Reactor, Ph. D. Thesis, University of Oklahoma, 1967.
3. R. L. Coats, Neutron Kinetics of a Reflected Fast Burst Reactor, USAEC Report SC-RR-67-802, Sandia Corporation, December 1967.
4. R. L. Long, Effects of Reflectors on the Burst Characteristics of the WSMR Fast Burst Reactor, Trans. Amer. Nucl. Soc., 8(2): 451 (1965).

5. R. L. Long, University of New Mexico, personal communication, December 1968.
6. R. L. Long, Reactivity Contributions in the Glory Hole of the Sandia Pulsed Reactor-II, *Nucl. Appl.*, 6: 8-15 (1969).
7. M. H. McTaggart, Atomic Weapons Research Establishment, personal communication, February 1969.
8. S. A. Hoenig and H. Sulsona, A Field Emission Microscopic Investigation of the Effects of Ambient Atmosphere on the Stress-Corrosion Cracking of Uranium—Molybdenum Alloys, U. S. Army Ballistics Research Laboratory Report, Aberdeen, Md., Mar. 9, 1968.
9. D. L. Hester, D. D. Glower, and L. J. Overton, Use of Ferroelectrics for Gamma-ray Dosimetry, *IEEE (Inst. Elec. Electron. Eng.), Trans. Nucl. Sci.*, 145 (1964).
10. G. H. Miley and P. K. Doshi, Pulse Propagation Experiments Using a Fast Burst Reactor, *Trans. Amer. Nucl. Soc.*, 8: 37 (1965).
11. G. H. Miley, N. Tsoulfanidis, and P. K. Doshi, Pulse Propagation Experiments Using a Reactor Source, in *Neutron Noise, Waves, and Pulse Propagation*, Gainesville, Fla., Feb. 14-16, 1966, pp. 117—134, R. E. Uhrig (Coordinator), AEC Symposium Series, No. 9 (CONF-660206), 1967.
12. M. J. Constantin and J. E. Love, Seedling Responses of Vigna Sinensis. II. Savi to Gamma and Neutron Seed Irradiation, *Radiat. Bot.*, 7: 497-506 (1967).
13. M. J. Constantin and T. S. Osborne, The RBE of Fast Neutrons in Seed Radiosensitivity, *Genetics*, 52: 437 (1967).
14. T. S. Osborne and M. J. Constantin, Predicting Seed Radiosensitivity to Gamma Rays and Fast Neutrons, *Genetics*, 52: 464 (1965).
15. J. E. Love and M. J. Constantin, The Induction of Bud Sports in *Coleus Blumei* by Fast Neutrons, *Proc. Amer. Soc. Hort. Sci.*, 88: 617-630 (1966).
16. J. E. Love and M. J. Constantin, Shoot Morphogenesis of *Chrysanthemum Morifolium*: Effects of Neutron and Gamma Radiation at Various Intervals after Photo-Induction, *Proc. S. Sect. Amer. Soc. Plant Physiol.*, 284-285 (1966).
17. D. G. Willhoit, Radiation Dose-Response Relationship Based on Neutron-Induced Hematologic Changes in Rats, Ph. D. Thesis, University of Pittsburg, 1964.
18. D. G. Willhoit, *Acute Intestinal Radiation Death in the Guinea Pig*, University of North Carolina, Department of Environmental Science and Engineering, Publication No. 132, 1966.
19. W. L. Russell, Effect of the Interval Between Irradiation and Conception on Mutation Frequency in Female Mice, *Proc. Nat. Acad. Sci. U. S.*, 54: 1552-1557 (1965).
20. A. De La Paz, White Sands Missile Range, private communication, January 1969.
21. A. H. Kazi, U. S. Army Ballistic Research Laboratory, personal communication, January 1969.
22. F. A. Kloverstrom, Lawrence Radiation Laboratory, personal communication, January 1969.
23. H. A. Kurstedt, A. H. Kazi, and V. E. Gazillo, The Core-Displacement Reactivity Coefficient of a Fast Pulse Reactor, *Trans. Amer. Nucl. Soc.*, 11: 583 (1968)
24. H. Kurstedt and A. Kazi, Analysis of the Inertial Effect on Fast-Pulse Reactor Behavior, *Trans. Amer. Nucl. Soc.*, 11: 219 (1968).
25. J. Randles, Feedback Due to Elastic Waves and Doppler Coefficient During the Excursions of a Pulsed Fast Reactor, *J. Nucl. Energy, Parts A and B*, 20: 1-16 (1966).

26. H. Takahashi, Monte Carlo Method for Reactivity Change Due to Geometrical Perturbation, *Trans. Amer. Nucl. Soc.*, 11: 533 (1968).
27. J. A. Reuscher, Thermal Shock Measurements on the White Sands Missile Range Fast Burst Reactor, USAEC Report SC-RR-65-587, Sandia Corporation, August 1966.
28. J. A. Reuscher, Thermal Stress Analysis for the Sandia Pulse Reactor II, *Trans. Amer. Nucl. Soc.*, 10: 242 (1967).
29. J. F. Ellis, An Instrument for Measuring Mechanical Vibrations in Fast-Pulse Reactor Cores, *Trans. Amer. Nucl. Soc.*, 11: 342 (1968).
30. G. H. Miley, University of Illinois, unpublished, January 1969.
31. R. G. Fluharty, F. B. Simpson, and G. J. Russell, Moderator Studies for a Repetitively Pulsed Test Facility (RPTF), *Nucl. Sci. Eng.*, 35: 45-69 (1969).
32. F. N. Coppage and A. W. Snyder, Neutron Effectiveness in Producing Photoconductivity in Dielectric Materials, USAEC Report SCDC-3125, Sandia Corporation, June 1963.
33. S. E. Harrison, F. N. Coppage, and A. W. Snyder, Gamma-Ray and Neutron-Induced Conductivity in Insulating Materials, *IEEE (Inst. Elec. Electron. Eng.) Trans. Nucl. Sci.*, 118-130 (November 1963).
34. F. N. Coppage and F. C. Peterson, Some Properties of Conductivity Induced in Polystyrene by Pulsed Gamma Rays, USAEC Report SC-R-65-943, Sandia Corporation, July 1965.

DESIGN PROBLEMS

PAUL D. O'BRIEN
Sandia Laboratories, Sandia Corporation, Albuquerque, New Mexico

I never felt that Glenn Whan and I agreed completely on what the subject of design problems entails. I would prefer to go beyond the scope of problems concerned strictly with the mechanical design of fast burst reactors and generally discuss design, analytical, and even operational problems that are amenable, at least, to partial solution at universities.

Specifically I am going to discuss problems associated with the three reactor programs of current interest at Sandia Corporation: (1) Although the Sandia Pulsed Reactor II (SPR II) has been in operation for over a year and a half, it would be naive to suggest that all its problems have been dealt with satisfactorily. (2) In Session 5, Paper 2 Dick Coats described the booster. Although we have made some progress, we are only at the beginning of a long list of problems that will have to be solved during the next 3 or 4 years. (3) Still farther down the road is a very high yield burst reactor capable of delivering a fast-neutron fluence of 10^{16} in a single burst — perhaps a reactor like one of those described by King or Perry (see L. D. P. King, Session 5, Paper 3, and A. M. Perry, Session 5, Paper 1). With these reactors we are talking about energy releases of the order of thousands of mega-watt-seconds per burst; clearly, difficult problems will be associated with this design — lots of them!

The problems I will consider fall into these three areas. I do not know the answers or even, in some cases, how to begin finding the answers; nobody does. But the problems can be solved through the mutual effort of people in the laboratory and people at universities. They can be solved as thesis problems for M.S. or Ph. D. degrees. They can be solved by faculty members working as consultants. Some

of them might be solved by an academic task force like the one proposed by Bob Long for the investigation of neutron-wave propagation.

These problems are almost impossible to try to categorize according to discipline. S. A. Hoenig, at the University of Arizona, for example, is a physicist working in the Electrical Engineering Department on metallurgical problems. Fast burst reactor problems, like most nuclear-engineering problems, cross many interdisciplinary boundaries.

I am well aware that most of you work at universities at which there simply is no easy access to a fast burst reactor. That factor is not necessarily a barrier to your participation in the solution of fast burst reactor problems. Sooner or later there must be some laboratory work in the practical application of the solution to a particular problem; but, the work leading to that solution can be carried out by two people, one at the laboratory working in conjunction with one, either a student or faculty member, at the university. In general, I think it is fair to say that, timewise, the more remote the practical application of the solution to a problem is, the more amenable that solution is to work done largely on campus. Then as the time for application approaches, the greater the percentage of the work that must be done at the laboratory. George Miley (see preceding paper) has already alluded to one of the difficulties that arises in this situation: the reactors that are already in operation are usually so heavily scheduled that it is virtually impossible to plan a careful, methodical, long reactor experiment. And, to have any hope of approval at all, any experiment must have at least a remote application to work in which the laboratory is interested; we simply cannot accommodate some of the flights of fancy that occasionally cross the professorial mind.

After that long-winded introduction, let us consider a few of the problems of current interest at Sandia.

(1) Ever since the original SPR became operational in 1961, interest in varying the neutron-to-gamma ratio has continued. The reason for this interest is obvious: varying the neutron-to-gamma ratio of a single radiation source is the most convenient way to determine which component of the radiation, neutrons or gammas, is responsible for producing some observed effect. Sporadic attempts have been made to shield, selectively, neutrons or gammas (a slab of lead or polyethylene is easy to place between the reactor and an experiment). But a systematic analysis has never been developed which would allow the neutron-to-gamma ratio to be tailored to the experimenter's requirements. This problem is of considerable interest at all fast burst reactor facilities, and one which could be solved with only a modest amount of experimental verification.

(2) Gordon Hansen referred to the problem of burst initiation probability as a function of source level in the reactor (see Session 1,

Paper 4). In our early operational experience with SPR II, we have experienced a higher incidence of preinitiation than would be expected on the basis of Hansen's or George Bell's work at Los Alamos. Although the problem now appears to be unique to SPR II (undoubtedly due to the relatively high residual gamma activity of the core), it will certainly become important at other facilities as they move toward high reactor performance. We do not understand the problem, and we simply do not have the time to pursue it. This aspect would make an interesting M.S. or Ph. D. thesis.

(3) From Coats' description of the booster, we are aware of the reason for considering finely divided cores: massive fuel components just will not accommodate the very rapid deposition of fission energy that is characteristic of booster operation. For example, if we were to use SPR II as a multiplying assembly in a booster, we would be dumping 6 or 7 megajoules of energy in a nearly solid 100-kg mass of fuel — in 1 μsec. This would clearly be a one-shot device! One of the problems associated with a finely divided core is reactivity feedback: how does one calculate the temperature coefficient of reactivity? Intuitively we can argue that the center of mass of each individual fuel particle remains fixed in space during a burst; the mass of the fuel does not change, so the overall density does not change. Is there a reactivity feedback mechanism? How big is it? Could it possibly be positive? (That possibility would certainly be an undesirable situation!)

In connection with the problem of reactivity feedback, until now no one has ever considered the contribution of Doppler broadening to the shutdown coefficient of a Godiva-type reactor because of the very low ^{238}U content of the fuel. It could be very important in a finely divided booster core.

(4) A worthwhile problem for a mechanical engineer would be a definitive study of the distribution of energy deposition in a core during a burst. As operators we are primarily interested in the relative fission (or energy) yield from burst to burst. For this purpose the temperature rise of any point in the core serves as a convenient and adequate measure of relative yield. But we really have not taken the trouble to analyze the thermodynamics of a burst so that we can realistically relate the temperature rise at some point in the core to the absolute energy release during the burst.

I will simply enumerate some of the other problems that might provide a basis for closer cooperation between fast burst reactor laboratories and universities. George Miley mentioned instrumentation; certainly there is lots of room for improvement of the diagnostic instrumentation used in conjunction with fast burst reactors. Among the more obvious needs are radiation-insensitive high-frequency strain

gauges, displacement transducers, accurate period-measuring devices, and reactivity meters.

He also mentioned the need for research with materials. This area is one in which universities can play, and have played, an important role. We need better alloys; we do not even know very well what physical properties make a material good or bad for application in a fast burst reactor. We need to know the relation between the strength of a material measured under static conditions and its strength at the very high strain rates that arise during a burst. We need to know more about the failure mechanisms of fast burst reactor fuels, and we obviously need to know more about the problems associated with the use of fluid fuels, which appear as interesting possibilities for application in a very high yield burst reactor.

Then there are chemistry problems, e.g., corrosion, material compatibility, and so forth; and kinetics problems, e.g., an analytical treatment of the effect of experiments on the neutronics of the reactor; and health-physics problems, e.g., we have had some problem with the release of fission products during high-level bursts of SPR II. This problem is going to be exaggerated in a finely divided core. Other health-physics problems that will undoubtedly arise during the booster program are those associated with the use of ^{239}Pu or, more likely, ^{233}U. In metallurgy we need insight into the importance of phase stability in solid metal fuels. A lot of work is yet to be done in the field of transformation kinetics under fast transient conditions.

In summary, we have no dearth of problems of mutual interest to universities and fast burst reactor laboratories. As the designs of these reactors become more and more sophisticated, the associated problems become more and more challenging. The professional competence of the people at the laboratories is constantly being upgraded; so excellent guidance is available for graduate students doing thesis research in absentia. Close cooperation between laboratories and universities is advantageous since we have more problems to solve than we have people to solve them. In short, fast burst reactor technology provides an ideal medium for interaction between universities and government-operated laboratories.

SUMMARY OF CONFERENCE ON THE USE OF FAST BURST REACTORS IN UNIVERSITY PROGRAMS

WESLEY K. FOELL
University of Wisconsin, Madison, Wisconsin

This paper briefly summarizes the one-day conference on The Use of Fast Burst Reactors in University Programs held at the University of New Mexico, Albuquerque, N. Mex., on Jan. 31, 1969. The conference, held in conjunction with the Fast Burst Reactors National Topical Meeting, was sponsored by the Department of Nuclear Engineering of the University of New Mexico and the Associated Western Universities with funds provided by the U. S. Atomic Energy Commission. The observations presented in this paper represent my views and a partial consensus derived from informal discussions with a limited number of attendees.

The design and use of fast burst reactors are areas of the nuclear field which have received little attention from nuclear science and engineering educators. However, this special class of reactors has some unique features which make it very useful for academic training and research. The objective of the conference was to define the extent to which fast burst reactor technology should be incorporated into university teaching and research programs. The National Topical Meeting had 163 attendees, including 44 university people. At the university conference, almost all the university-associated attendees were present.

Although teaching applications were discussed, the majority of time was devoted to research applications and the mechanics of university—industry collaboration which could best involve the universities in this research. Consequently this summary is divided into three sections: (1) teaching applications, (2) research applications, and (3) university—industry—government laboratory collaboration in fast burst reactor research.

The types of fast burst reactors discussed at the Topical Meeting fell somewhat naturally into two categories: (1) single-burst reactors of

the Godiva type and (2) repetitively pulsed reactors of the Russian IBR type. The former were the primary object of the educational conference discussions, and the conclusions in this paper for the most part refer to this type.

Teaching Applications

The University of New Mexico is apparently the only university having enough access to fast burst reactors to permit their use for teaching. The oral presentation and ensuing discussion on this subject did illustrate that this class of reactors possesses some unique aspects for instruction. The most salient of these are: (1) the simplicity of analysis of its static and kinetic behavior, e.g., a one-group diffusion theory analysis often suffices; (2) unique versions of reactivity measurements are possible, e.g., 3- to 5-sec periods can be used in control-rod calibrations; (3) the simplicity of the system as a neutron and gamma-ray source lends itself to interesting shielding experiments; and (4) it is well suited for experiments dealing with the kinetic response of radiation detectors and dosimetry.

Research Applications

The research applications discussed were also limited primarily to the single-burst reactor although considerable interest was evident for use of a repetitively pulsed fast reactor, if and when such a device is constructed in the United States.

George Miley's excellent review of past and present research applications (see paper by Miley and Kurstedt) identified several areas in which universities were, or more importantly, could be, involved. The majority of these research applications involve the study of phenomena which are (1) strongly rate dependent and take place on a time scale of the order of the reactor burst width and (2) require a very hard neutron spectrum. A simple example is the propagation of a fast-neutron pulse through a small metallic assembly. All these applications fall into two broad categories: (1) reactor development and (2) research requiring short intense bursts of fast neutrons or gamma radiation, designated here as burst-source experiments. Subclasses were identified within these categories.

APPLICATIONS OF FAST BURST REACTORS

Reactor development experiments	Burst-source experiments
Reactor physics and kinetics	Neutron-beam experiments
Engineering mechanics	Biological effects
Materials	Radiation effects
Radiation effects	Materials
Instrumentation	Electronics

A few universities are presently involved in research in one or more of the above areas. However, for the most part, these few are located within a reasonable distance from a fast burst reactor facility. For example, the University of New Mexico and the University of Arizona apparently are heavily involved in research on SPR II at Sandia. Neither the Health Physics Pulsed Reactor (HPPR) at Oak Ridge National Laboratory nor the Army Pulse Radiation Facility Reactor (APRFR) at the Ballistic Research Laboratories is presently being utilized to any great extent for university-initiated research.

The discussion on research applications indicated one aspect of the previous Fast Burst Reactor conference that apparently frustrated several attendees; this was the failure to identify and discuss broad research areas whose needs are met by fast burst reactors. It is reasonable, though perhaps overly optimistic, to hope that the understanding of fast burst reactors gained from this conference and the resulting publicity may generate new attempts at better research utilization within a much broader group of scientific disciplines.

The research applications of the repetitively pulsed fast reactors received extensive attention previous to the conference, and their potential for university use was reiterated here. Such research areas as space- and time-dependent detectors, solid-state physics, accelerator booster systems, and time-dependent transport theory would be associated with such systems and would certainly have academic respectability.

Several of the attendees expressed strong sentiment for a follow-up conference aimed exclusively at users and applications of fast burst reactors.

University-Industry-Government Laboratory Collaboration

It appears extremely unlikely that a fast burst reactor will be located on a university campus in the near or foreseeable future. There was strong agreement among the participants that the vitality of university research in this area would consequently depend upon the degree of collaboration between universities and industrial and government laboratories. Paul O'Brien of Sandia very eloquently described Sandia's interest in university collaboration, and he even went so far as to suggest several areas of possible research. These included problems in reactor physics, materials, health physics, and engineering mechanics. Representatives from the FRAN staff at the National Reactor Testing Site also displayed strong interest in cooperative ventures. The suggested mechanisms by which this could be accomplished are (1) graduate students' theses, (2) faculty task forces at the universities, and (3) faculty consulting activities. (Some enthusiasm was also shown by a few faculty members who suggested that the IBR reactor in

Dubna should be made available to their students.) A few universities located near fast burst reactor facilities might well serve as liaisons or as clearinghouses for this type of research collaboration. On the debit side of the ledger, it was observed that some of the fast burst facilities may not have enough staff and experience to tolerate the presence of initially inexperienced graduate students.

CONCLUSIONS

A brief and certainly not all-inclusive interpretation of the conclusions derived from the conference is:

1. Fast burst reactors possess several unique pedagogical characteristics, making them attractive for university teaching applications. This factor has had limited educational impact, however, since the reactors are readily accessible only to a few universities located near the facilities.

2. Fast burst reactors are well suited for research in several areas, but universities, with a few notable exceptions, are not heavily involved in their use. The consensus, however, was that universities could and should be more involved.

3. A much stronger mode of university – industry – government laboratory interaction is necessary to permit effective university research in this area. Industry, the university associations, and government strongly supported this view.

4. A conference or institute devoted primarily to users and research applications of fast burst reactors might be an appropriate follow-up of this conference. Tentative Atomic Energy Commission interest in such a conference was expressed.

5. The conference organizers, sponsors, and speakers deserve the unanimous commendation and appreciation of the attendees for providing a format and an atmosphere conducive to a very informative and valuable discussion on the educational uses of this class of reactors. The successful creation of contacts between the universities and the staffs associated with the fast burst reactor facilities was due primarily to the enthusiasm and the generosity of all those responsible for the conference.

LIST OF PARTICIPANTS

ADLER, F. T.
Physics Department
University of Illinois
Urbana, Ill.

BACA, JOSE R., Capt.
U. S. Air Force
Albuquerque, N. Mex.

BANFIELD, THOMAS V.
Reactor Operations Division
Argonne National Laboratory
Argonne, Ill.

BANKES, WALTER J.
White Sands Fast Burst Reactor
    Facility
Tucson, Ariz.

BARRACLOUGH, EDMUND L.
U. S. Atomic Energy Commission
Albuquerque Operations Office
Albuquerque, N. Mex.

BAUER, ARTHUR A.
Battelle Memorial Institute
Columbus, Ohio

BEARD, G. V.
Associated Western Universities
Salt Lake City, Utah

BECKURTS, K. H.
Brookhaven National Laboratory
Upton, N. Y.

BISCHOFF, JOHN
University of New Mexico
Albuquerque, N. Mex.

BLACKBURN, EDWARD, Lt. Col.
Surgeon General's Office
Department of the Army
Washington, D. C.

BLOKHINTSEV, D. I.
Joint Institute for Nuclear Research
Dubna, USSR

BONZON, LLOYD L.
Sandia Corporation
Albuquerque, N. Mex.

BOWER, CHARLES
Battelle Memorial Institute
Columbus, Ohio

BRIDGES, HERBERT
University of New Mexico
Albuquerque, N. Mex.

BRONSON, G. S.
Argonne National Laboratory
Idaho Falls, Idaho

BROWN, WILBUR K.
Los Alamos Scientific Laboratory
Los Alamos, N. Mex.

BRUGGER, ROBERT M.
Idaho Nuclear Corporation
Idaho Falls, Idaho

CALLIHAN, DIXON
Union Carbide Corporation,
    Y-12 Plant
Oak Ridge, Tenn.

CARLSON, BENGT
Los Alamos Scientific Laboratory
Los Alamos, N. Mex.

633

CAROSSINO, CARLOS
University of New Mexico
Albuquerque, N. Mex.

CARPENTER, JOHN M.
Department of Nuclear Engineering
University of Michigan
Ann Arbor, Mich.

CERA, JOHN C.
U. S. Atomic Energy Commission
Washington, D. C.

CHARYULU, V.
Department of Engineering
Idaho State University
Pocatello, Idaho

CHIEN, JI-PENG
Institute of Nuclear Energy Research
Lung-Tan, Taiwan.

CLACK, ROBERT W.
Department of Nuclear Engineering
Kansas State University
Manhattan, Kans.

COATS, RICHARD L.
Sandia Corporation
Albuquerque, N. Mex.

COCHRAN, R. G.
Nuclear Engineering Department
Texas A & M University
College Station, Tex.

CONANT, J. C.
Sandia Corporation
Albuquerque, N. Mex.

DE LA PAZ, A.
Chief, Fast Burst Reactor Division
Nuclear Effects Directorate
White Sands Missile Range, N. Mex.

DeMASTRY, JOHN A.
Battelle Memorial Institute
Columbus Laboratories
Columbus, Ohio

DITTO, STEPHEN J.
Oak Ridge National Laboratory
Oak Ridge, Tenn.

DIXON, DWIGHT R.
Brigham Young University
Provo, Utah

DONNERT, HERMANN J.
Department of Nuclear Engineering
Kansas State University
Manhattan, Kans.

ELDRIDGE, H. B.
University of Wyoming
Laramie, Wyo.

ELLETT, D. MAXWELL
Sandia Corporation
Albuquerque, N. Mex.

ENNIS, W. D.
U. S. Atomic Energy Commission
Idaho Operations Office
Idaho Falls, Idaho

EPTING, GLENDA S.
Division of Technical Information
   Extension
U. S. Atomic Energy Commission
Oak Ridge, Tenn.

ESTES, BERRY F.
U. S. Atomic Energy Commission
Albuquerque Operations Office
Albuquerque, N. Mex.

EVERETT, WILLIS L.
University of New Mexico
Albuquerque, N. Mex.

FARKAS, M. S.
Battelle Memorial Institute
Columbus, Ohio

FARMER, F. R.
United Kingdom Atomic Energy
   Authority
Risley Warrington
Lancs, England

FITZGERALD, CHRIS
Managing Editor
Nuclear News
Hinsdale, Ill.

FLUHARTY, REX G.
Los Alamos Scientific Laboratory
Los Alamos, N. Mex.

FOELL, WESLEY K.
Nuclear Engineering Department
University of Wisconsin
Madison, Wis.

FREEMAN, DARRELL D.
General Electric Company
Advanced Products Operation
Sunnyvale, Calif.

FRISCH, O. R.
Nuclear Physics Section
University of Cambridge
Cavendish Laboratories
Cambridge, England

GERHARD, HOWARD J.
U. S. Air Force
Albuquerque, N. Mex.

GLASGOW, DAVID E.
Ohio State University
Columbus, Ohio

GOSSMANN, S. R.
Phillips Petroleum Company
Idaho Falls, Idaho

GOTTSCHALK, V. B.
Phillips Petroleum Company
Idaho Falls, Idaho

GOTTSCHALL, W. CARL, Jr.
Chemistry Department
University of Denver
Denver, Colo.

GRAHAM, KINGSLEY F.
University of Michigan
Ann Arbor, Mich.

GRAVES, GLEN A.
Los Alamos Scientific Laboratory
Los Alamos, N. Mex.

GRIFFITH, JERRY D.
U. S. Army
Rockville, Md.

GRUNDL, JAMES A.
Los Alamos Scientific Laboratory
Los Alamos, N. Mex.

GUTHRIE, ARTHUR
University of New Mexico
Albuquerque, N. Mex.

HALLINAN, EDWARD J., Capt.
1101 Madeira Drive, S.E. Room 130
Albuquerque, N. Mex.

HANSEN, GORDON E.
Los Alamos Scientific Laboratory
Los Alamos, N. Mex.

HASENKAMP, ARTHUR
Sandia Corporation
Albuquerque, N. Mex.

HELFER, PAUL G.
U. S. Geological Survey
Denver, Colo.

HELMS, STEVEN A.
U. S. Army
Stafford, Va.

HENDRIE, JOSEPH M.
Brookhaven National Laboratory
Upton, N. Y.

HENNIES, H.
Interatom, Internationale
   Atomreaktororbau G.m.b.h.
Cologne, West Germany

HETRICK, DAVID L.
University of Arizona
Tucson, Ariz.

HILL, JERRY L.
University of New Mexico
Albuquerque, N. Mex.

HOFFMAN, KENNETH
Brookhaven National Laboratory
Upton, N. Y.

HOLLAND, LEO B.
Oak Ridge National Laboratory
Oak Ridge, Tenn.

HOLM, ARLEE
University of New Mexico
Albuquerque, N. Mex.

HORAK, JAMES A.
Los Alamos Scientific Laboratory
Los Alamos, N. Mex.

HUMPHERYS, KENT C.
Weapons Measurements Department
EG&G, Inc.
Goleta, Calif.

JEFFERSON, ROBERT M.
Sandia Corporation
Albuquerque, N. Mex.

JOHNSON, BRYCE W.
U. S. Atomic Energy Commission
Idaho Operations Office
Idaho Falls, Idaho

JONES, GERALD M.
U. S. Atomic Energy Commission
Albuquerque Operations Office
Albuquerque, N. Mex.

KAZI, A. H.
U. S. Army
Ballistics Research Laboratory
Aberdeen, Md.

KEEPIN, G. R.
Los Alamos Scientific Laboratory
Los Alamos, N. Mex.

KELLEY, ROBERT E.
University of California
Lawrence Radiation Laboratory
Mercury, Nev.

KENNEY, EDWARD S.
Nuclear Engineering Department
Pennsylvania State University
University Park, Pa.

KING, JOHN S.
University of Michigan
Ann Arbor, Mich.

KING, L. P. D.
Los Alamos Scientific Laboratory
Los Alamos, N. Mex.

KRONENBERG, STANLEY
U. S. Army Electronics Command
Fort Monmouth, N. J.

KUROSU, TATSUO
Atomic Power Development
   Associates, Inc.
Detroit, Mich.

KURSTEDT, HAROLD A., Jr.
Nuclear Engineering Department
Ohio State University
Columbus, Ohio

KUWABARA, JUN
Atomic Power Development
   Associates, Inc.
Detroit, Mich.

LARRIMORE, JAMES A.
EURATOM
Ispra, Italy

LOCHNER, JERRELL R.
University of New Mexico
Albuquerque, N. Mex.

LONG, ROBERT L.
Nuclear Engineering Department
University of New Mexico
Albuquerque, N. Mex.

LUERA, THEODORE F., Jr.
White Sands Missile Range
El Paso, Tex.

LUNDIN, M. I.
Oak Ridge National Laboratory
Oak Ridge, Tenn.

LUX, ROBERT
U. S. Army Electronics Command
Fort Monmouth, N. J.

McENHILL, JOHN J.
Atomic Weapons Research
   Establishment
United Kingdom Atomic Energy
   Authority
Aldermaston, England

McTAGGART, M. H.
Atomic Weapons Research
   Establishment
United Kingdom Atomic Energy
   Authority
Aldermaston, England

MADDOX, JACK
University of New Mexico
Albuquerque, N. Mex.

MAKENS, R. F.
U. S. Atomic Energy Commission
Idaho Operations Office
Idaho Falls, Idaho

MANHART, ROBERT A.
Electrical Engineering Department
University of Nevada
Reno, Nev.

MIHALCZO, JOHN T.
Union Carbide Corporation, Nuclear
   Division, Y-12 Plant
Oak Ridge, Tenn.

MIKULAS, JOHN
University of New Mexico
Albuquerque, N. Mex.

MILEY, GEORGE H.
Nuclear Engineering Laboratory
University of Illinois
Champaign, Ill.

MOAK, DONALD P.
Battelle Memorial Institute
Columbus, Ohio

MOORE, M. S.
Los Alamos Scientific Laboratory
Los Alamos, N. Mex.

MORRISON, R. G.
Phillips Petroleum Company
Idaho Falls, Idaho

MUEHLHAUSE, CARL O.
National Bureau of Standards
Bethesda, Md.

MURPHY, HARRY M., Jr.
3912 Hilton Avenue, N.E.
Albuquerque, N. Mex.

NELSON, PAUL
Sandia Corporation
Albuquerque, N. Mex.

NEWBY, GLEN A.
Space Nuclear Systems Division
U. S. Atomic Energy Commission
Washington, D. C.

NORTON, BOYD
Phillips Petroleum Company
Idaho Falls, Idaho

O'BRIEN, PAUL D.
Sandia Corporation
Albuquerque, N. Mex.

ORNDOFF, JOHN D.
Los Alamos Scientific Laboratory
Los Alamos, N. Mex.

PAULK, J. I.
Mississippi State University
State College, Miss.

PERKINS, DAVID R.
United Nuclear Corporation
Research Engineering Center
Elmsford, N. Y.

PERRY, ALFRED M.
Oak Ridge National Laboratory
Oak Ridge, Tenn.

PETERSON, L. R.
University of California
Lawrence Radiation Laboratory
Mercury, Nev.

PETERSON, ROLF E.
Los Alamos Scientific Laboratory
Los Alamos, N. Mex.

PORTER, L. E.
Physics Department
University of Montana
Missoula, Mont.

PRICE, CHARLES
University of New Mexico
Albuquerque, N. Mex.

REUSCHER, J. A.
Sandia Corporation
Albuquerque, N. Mex.

RIVARD, J.
Sandia Corporation
Albuquerque, N. Mex.

RUSH, WILLIAM A.
U. S. Air Force
Albuquerque, N. Mex.

RUSSELL, GARY J.
Idaho Nuclear Corporation
Idaho Falls, Idaho

RUSSELL, JOHN L., Jr.
Gulf General Atomic, Inc.
San Diego, Calif.

SAILOR, VANCE L.
Brookhaven National Laboratory
Upton, N. Y.

SALGADO, PETER G.
Los Alamos Scientific Laboratory
Los Alamos, N. Mex.

SANDQUIST, GARY
Mechanical Engineering Department
University of Utah
Salt Lake City, Utah

SAUNDERS, CHARLES E.
Department of the Army
Falls Church, Va.

SCRIVNER, GARY I.
University of New Mexico
Albuquerque, N. Mex.

SEALE, ROBERT L.
Nuclear Engineering Department
University of Arizona
Tucson, Ariz.

SECKER, PHILLIP A.
Los Alamos Scientific Laboratory
Los Alamos, N. Mex.

SHAFTMAN, DAVID H.
Reactor Physics Division
Argonne National Laboratory
Argonne, Ill.

SHISHMAN, THOMAS T.
University of New Mexico
Albuquerque, N. Mex.

SHON, FREDERICK J.
U. S. Atomic Energy Commission
Washington, D. C.

SMATHERS, JAMES B.
Nuclear Engineering Department
Texas A & M University
College Station, Tex.

SMITH, DAVID R.
Los Alamos Scientific Laboratory
Los Alamos, N. Mex.

SNYDER, A. W.
Sandia Corporation
Albuquerque, N. Mex.

SNYDER, JOHN A.
Sandia Corporation
Albuquerque, N. Mex.

SOMMAR, JOHN P., Lt.
U. S. Air Force
Albuquerque, N. Mex.

SPANO, ALFRED H.
Phillips Petroleum Company
Idaho Falls, Idaho

SPITZER, JOSEF
University of New Mexico
Albuquerque, N. Mex.

STATHOPLOS, ANTHONY
Nuclear Technology Corp.
White Plains, N. Y.

STEWART, LEONA
Los Alamos Scientific Laboratory
Los Alamos, N. Mex.

STILLMAN, DAN B.
Los Alamos Scientific Laboratory
Los Alamos, N. Mex.

STRATTON, W. R.
Los Alamos Scientific Laboratory
Los Alamos, N. Mex.

SULLIVAN, R. F.
U. S. Atomic Energy Commission
Walnut Creek, Calif.

SUTHERLAND, ROBERT L.
University of Wyoming
Laramie, Wyo.

SWANSON, VERN A.
Atomics International
Canoga Park, Calif.

TASCHEK, R. F.
Los Alamos Scientific Laboratory
Los Alamos, N. Mex.

THAMER, BURTON J.
Los Alamos Scientific Laboratory
Los Alamos, N. Mex.

THEARD, L. M.
Gulf General Atomic, Inc.
San Diego, Calif.

TILLER, ROBERT E.
U. S. Atomic Energy Commission
Idaho Operations Office
Idaho Falls, Idaho

TOLMAN, BERT
Phillips Petroleum Company
Idaho Falls, Idaho

TUTTLE, ROLLAN J.
White Sands Missile Range
El Paso, Tex.

WAGNER, ROBERT G.
University of California
Los Alamos Scientific Laboratory
Los Alamos, N. Mex.

WALTAR, ALAN E.
Battelle Northwest
Richland, Wash.

WELCH, DON L.
Los Alamos Scientific Laboratory
Los Alamos, N. Mex.

WELLS, HAROLD E.
U. S. Army Material Command
Washington, D. C.

WHAN, GLEN A.
Nuclear Engineering Department
University of New Mexico
Albuquerque, N. Mex.

WHITE, ROGER H.
Los Alamos Scientific Laboratory
Los Alamos, N. Mex.

WILKINSON, LARRY
General Electric Company
Pleasanton, Calif.

WILLIAMS, DAVID H.
U. S. Atomic Energy Commission
Albuquerque, N. Mex.

WILSON, ALBERT E.
Department of Engineering
Idaho State University
Pocatello, Idaho

WIMETT, T. F.
Los Alamos Scientific Laboratory
Los Alamos, N. Mex.

WOOD, DAVID P.
U. S. Atomic Energy Commission
Albuquerque, N. Mex.

YAMAMOTO, HISASHI
Atomic Power Development
  Associates, Inc.
Detroit, Mich.

YAO, ELY
University of New Mexico
Albuquerque, N. Mex.

YAO, PAUL
University of New Mexico
Albuquerque, N. Mex.

YASVITSKI, Y.
Joint Institute of Nuclear Research
Dubna, USSR

YEATER, MAX L.
Rensselaer Polytechnic Institute
Troy, N. Y.

YOCKEY, HUBERT P.
Ballistics Research Laboratory
Bel Air, Md.

AUTHOR INDEX

SUBJECT INDEX

AEC SYMPOSIUM SERIES